



National Snow and Ice Data Center  
Advancing knowledge of Earth's Frozen Regions

# The Effective Resolution of CETB Image Products

---

Special report # 21

13 May 2021

---

**D.G. Long**

Brigham Young University  
Provo, UT

**M.J. Brodzik and M. Hardman**

National Snow and Ice Data Center  
Boulder, CO

## **Citation**

Long, David G., Brodzik, Mary J., and Hardman, Molly A. 2021. The Effective Resolution of CETB Image Products. NSIDC Special Report 21. Boulder CO, USA: National Snow and Ice Data Center.

<http://nsidc.org/sites/nsidc.org/files/files/NSIDC-special-report21.pdf>.

# The Effective Resolution of CETB Image Products

David G. Long, Mary J. Brodzik, and Molly Hardman

May 13, 2021

## Abstract

The Calibrated Passive Microwave Daily Equal-Area Scalable Earth (EASE) Grid 2.0 Brightness Temperature (CETB) Earth System Data Record (ESDR) project team creates conventional and enhanced resolution radiometer brightness temperature images on standard, compatible grids from calibrated satellite radiometer measurements. The processing employs the radiometer form of the Scatterometer Image Reconstruction (rSIR) algorithm to create enhanced resolution images, which are posted on fine resolution grids. In this white paper we evaluate the effective resolution of the CETB products using actual sensor data collected over coastline and island crossings. A comparison of the spatial resolution of the rSIR-enhanced and conventionally-processed (gridded) data is presented. We find that the *effective* resolution of daily CETB rSIR images is 30–60% finer than conventionally processed gridded data. Examples for each sensor channel are included. While the analysis presented is for CETB images, the general principles of resolution discussed in this white paper apply to images from any source.

## 1 Introduction

The NASA MEaSUREs Calibrated Passive Microwave Daily EASE-Grid 2.0 Brightness Temperature ESDR (CETB) Earth System Data Record (ESDR) project team has created a single, consistently processed, multi-sensor ESDR of Earth-gridded microwave brightness temperature ( $T_B$ ) images spanning from 1978 to the present based on new fundamental climate data records (FCDRs) for passive microwave observations from a wide array of sensors [1, 2, 3]. The CETB dataset includes both conventional and enhanced resolution  $T_B$  images on standard map projections and is designed to serve the land surface and polar snow/ice communities in studies of climate and climate change [4].

The conventional resolution CETB  $T_B$  images are created using standard drop-in-the-bucket (DIB), also known as gridding (GRD), techniques. To create finer resolution images, reconstruction techniques are employed [4]. The images are produced on compatible map projections and grid spacings [2, 3]. Previous papers have used simulation to compare the resolution enhancement capability for the Scatterometer Image Reconstruction algorithm (rSIR) [4, 5] and the Backus-Gilbert (BG) [6, 7, 8] approach, where it was found that rSIR provided improved performance compared to BG with significantly less computation [4, 9].

The CETB SMAP  $T_B$  images are created on fine resolution grids [2] to meet signal processing requirements of the rSIR algorithm [4]. The effective image resolution, defined by the 3 dB width of the pixel spatial response function (PSRF), is coarser than the grid spacing. This enables the images to be subsampled in order to reduce data volume if desired, but also leads to the question: what is the *effective* resolution of the rSIR images and what data resampling can be done? Simulation was previously employed to validate the resolution enhancement [4, 9]. More recently, [10] used coast and island crossings to evaluate the effective resolution of SMAP enhanced resolution compared to GRD images on standard SMAP project grids.

In this white paper we adapt the coast and island crossing methodology described in [10] and apply it to actual CETB rSIR products to measure the effective spatial resolution of the CETB enhanced resolution products. The results are compared to the effective resolution of conventionally processed gridded images, i.e., GRD images. We find that the enhanced resolution images are, as expected, oversampled, but have finer resolution than the GRD images by as much as 30-60%.

Parameter(s):	MICROWAVE > BRIGHTNESS TEMPERATURE	Data Format(s):	NetCDF
Spatial Coverage:	N: 90, S: -90, E: 180, W: -180	Platform(s):	Aqua, DMSP 5D-2/F10, DMSP 5D-2/F11, DMSP 5D-2/F13, DMSP 5D-2/F14, DMSP 5D-2/F8, DMSP 5D-3/F15, DMSP 5D-3/F16, DMSP 5D-3/F17, DMSP 5D-3/F18, DMSP 5D-3/F19, Nimbus-7
Spatial Resolution:	3.125 km to 25 km	Sensor(s):	AMSR-E, SMMR, SSM/I, SSMIS
Temporal Coverage:	25 October 1978 to 1 July 2017 (Updated 2018)	Version(s):	V1
Temporal Resolution:	12 hour	Metadata XML:	<a href="#">View Metadata Record</a>
Data Contributor(s):	Mary Brodzik, David Long, Molly Hardman, Aaron Paget, Richard Armstrong		

Figure 1: CETB sensors and their characteristics. SMAP, launched in 2015 and currently operating as of Apr. 2021, is not included in this list.

## 2 Background

The theory of radiometer reconstruction and resolution enhancement is provided in [4] and [9]. Figures 1 and 2 identify each of the CETB sensors and the time-line of their available data [3]. Recently, SMAP sensor data [11] was added to the CETB [2, 9]. We note that the SMAP data is available both on SMAP-standard grids and CETB-standard grids. The effective resolution of the former is considered in [10] while the analysis of the latter is included in this report.

For each of the CETB sensors, brightness temperature ( $T_B$ ) image products are created by mapping individual  $T_B$  measurements onto an Earth-based grid using EASE-Grid 2.0 map projections [12, 13]. In the conventional-resolution gridded CETB product (GRD), the center

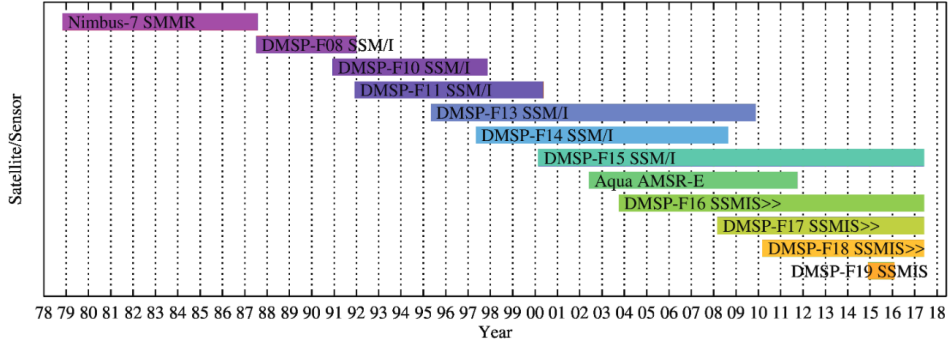


Figure 2: CETB sensor timelines. SMAP, launched in 2015 and currently operating as of Apr. 2021, is not included in this list. Some sensors continue to operate to the present.

of each measurement location is mapped to an output projected grid cell or pixel. All measurements within the specified time period whose center fall within the bounds of a particular grid cell are averaged together. The unweighted average becomes the reported pixel  $T_B$  value for that grid cell. Since measurement footprints can extend outside of the pixel, the effective resolution of GRD images is coarser than the pixel size. We call the spacing of pixels the “pixel posting” or the “posting resolution”, see Fig. 3.

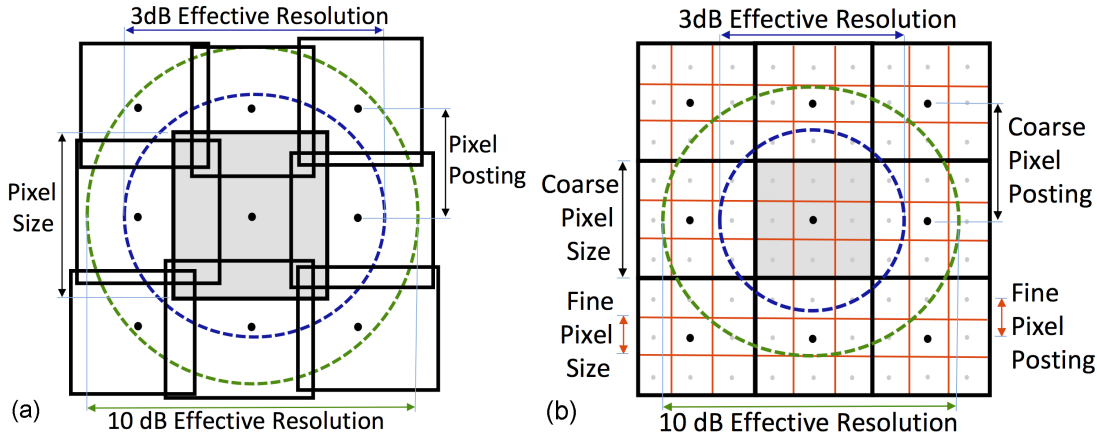


Figure 3: Pixel size versus posting illustrations. (a) Diagram showing irregularly sized and overlapping pixels posted on a uniform grid (discussed later). Due to the processing used to compute the pixel value, the  $-3$ -dB contour of the pixel spatial response function (PSRF) is larger than the pixel area. A  $-10$ -dB contour of PSRF is shown for comparison. (b) Diagram of uniform grids showing both fine and coarse pixels. The effective resolution solution of the PSRF of both coarse and fine pixels is the same, with the fine pixels posted at finer spacing (posting resolution). [10]

Finer spatial resolution CETB products are generated using reconstruction with the rSIR algorithm [4, 5, 14]. The iterative rSIR algorithm employs regularization to trade off noise and resolution by limiting the number of iterations and thereby producing partial reconstruction [9, 14]. The rSIR products are posted on fine resolution grids with an effective resolution that

is coarser than the posting resolution, i.e., they are oversampled, see Fig. 3b. The CETB provides  $T_B$  images on Northern Hemisphere (E2N), Southern Hemisphere (E2S), and Tropical/Temperate (E2T) EASE-2 map projections using DIB gridding at 25 km postings and rSIR  $T_B$  images at finer postings on the same projections using nested EASE-2 grids [3]. SMAP images are also produced on the mid-latitude E2M EASE-2 map projection for DIB at 36 km with finer rSIR postings (9 km and 3 km) on nested EASE-2 grids [9].

### 3 Pixel Spatial Response Function

The key to understanding the *effective* resolution of an image is understanding the *pixel spatial response function* (PSRF). This differs from the *measurement* response function (MRF) that describes the spatial characteristics of an *individual measurement*, i.e., how much the brightness temperature at each spatial location contributes to the measurement. Essentially, this is the antenna pattern<sup>1</sup>, i.e., the temporally integrated antenna pattern of an individual measurement. When individual measurements are mapped onto a grid to create a  $T_B$  pixel *image*, the original measurements are processed in some way. They may be combined (averaged), interpolated, resampled, or processed in another way to create a 2-d array of pixel values.

To understand the effective pixel resolution, we are interested in the PSRF that describes the spatial characteristics of the estimated *pixel*, i.e., how much the brightness temperature at a particular spatial location contributes to the reported brightness temperature of the pixel. In effect, the PSRF is the impulse response of the measurement and image formation system, which includes the image formation from possibly multiple measurements of the same pixel, while the MRF is the spatial response of a single measurement. Analysis of the PSRF validates the effective resolution of the image formation.

Computation of the PSRF can be done with the MRFs of the individual measurements combined into the pixel values. In general, the PSRF varies from pixel to pixel due to the differences in location of the measurement within the pixel area and variations in the MRFs for the measurements [9]. We note that the variation in the MRFs precludes the use of classic deconvolution algorithms that require a fixed response function. Typically, the PSRF is normalized to a peak value of 1.

Note that the pixel value of simple image formation algorithms such as DIB is proportional to the linear sum of measurements included in the pixel value [4]. Thus, the PSRF is proportional to the linear sum of the measurements' MRF included in the pixel value. Similarly, for resampling or interpolation, the PSRF is the weighted linear sum of the measurement MRF's included in the pixel value and combines the effects the offset of the measurements from the pixel center and from each other [4, 17]. For rSIR, the PSRF linear summation approach cannot be used due to the non-linearity in the algorithm. Prior studies have primarily relied on simulation to compute the PSRF using simulated impulse functions [9, 4, 17]. In this paper we estimate the PSRF from actual data.

---

<sup>1</sup>The MRF is really a “smeared” version of the antenna pattern which is the result of the movement of the antenna pattern on the surface over the measurement integration period, see [4].

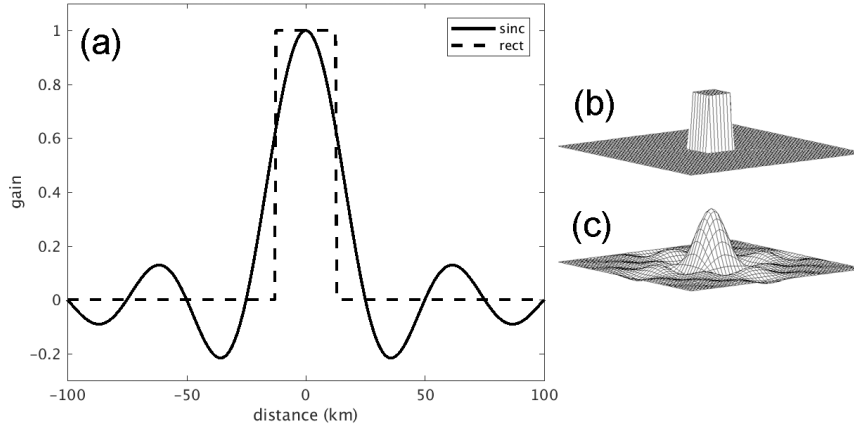


Figure 4: (a) One-dimensional sinc function compared to a rect function. Illustration of two-dimensional (b) rect and (c) sinc functions. [10]

### 3.1 Relationship of the PSRF and the Effective Resolution

Given the PSRF, the effective resolution of the pixel corresponds to the area of the PSRF greater than a particular threshold, typically  $-3$  dB [15, 9], though other values are sometimes used. We often express the resolution in terms of the square root of the area, which we call the “linear resolution” in this paper. For example, the ideal PSRF for a rectilinear image is a two-dimensional “rect” or “box-car” function that is valued at one over the pixel area and zero elsewhere, see Fig. 4. Consider a  $25$  km image grid<sup>2</sup>. The ideal “pixel resolution” of this is  $625$  km<sup>2</sup>, which is a linear resolution of  $25$  km. Note, however, that according to the Nyquist criterion the finest spatial frequency that can be represented with pixel values spaced  $25$  km apart is  $1/50$  km<sup>-1</sup>, i.e., the wavelength of the finest representable spatial frequency is  $50$  km.

Since only a finite number of discrete measurements are available, we *must* assume that the signal and the PSRF are bandlimited in a way that is consistent with the sample spacing [16]. A bandlimited version of such an ideal boxcar PSRF is a two-dimensional sinc function, as seen in Fig. 4. For ideal  $25$  km sampling, this bandlimited PSRF is the best achievable PSRF that is consistent with the sampling. By the Nyquist criterion, signals with frequency higher than one half the sampling rate (posting) cannot be represented without aliasing.

The spacing of the pixels is herein called the “posting resolution”. In general, the pixels can be larger than their spacing (the posting resolution) so that the pixels overlap, as illustrated in Fig. 3a. In this case, the pixel size is larger than the posting resolution. The resulting linear resolution of the PSRF is thus larger than the posting resolution, which means that the *effective resolution* is coarser than the posting resolution. When the posting resolution is finer than the effective resolution the signal is sometimes termed “over sampled” as illustrated in Fig. 3b. While in principle in such cases the image can be resampled to a coarser posting resolution

<sup>2</sup>This is the “base size” used for CETB products. The map projection (EASE-Grid 2.0) is the same for all products, but the pixel size varies depending on the sensor and channel. To ensure that the different product grids are embedded, they are all powers of 2 divisions of this base size, e.g.,  $12.5$  km,  $6.25$  km,  $3.125$  km [4]. SMAP rSIR products are additionally available on  $36$  km,  $9$  km, and  $3$  km grids. This grid embedding scheme restricts the choices for gridding different sized sensor footprints.

with limited loss of information, deliberate oversampling provides flexibility in resampling the data, and is the approach taken by CETB when it reports images on map-standard pixel sizes (posting resolutions). Because rSIR is able to extract finer scale resolution than other approaches, the finer posting preserves as much information as possible.

One way to determine the effective resolution of actual images is based on first estimating the step response of the imaging process. Assuming the PSRF is essentially symmetric, the PSRF can be derived from the observed step response by linear deconvolution. Recall that the step response is mathematically the convolution of the PSRF with a step function. The PSRF can thus be computed from the step response by deconvolution with a step function. In this case the deconvolution product represents a slice of the PSRF. The effective linear resolution is then size or width of the reg the PSRF that is above a -3 dB (1/2) threshold.

## 4 Discussion: Effective Versus Posting Resolution

Regardless of the posting resolution (image pixel spacing), the effective resolution of the reconstructed  $T_B$  image is defined by the PSRF. To avoid aliasing the posting resolution must be smaller (finer) than the effective resolution. We note that as long as this requirement is met, the posting resolution can be arbitrarily set. Thus, the pixel size can be arbitrarily determined based on the the pixel size of a standard map projection such as the EASE-Grid 2.0 system [3, 12].

There are advantages of a finer posting resolution. For example, since the effective resolution can vary over the image due to the measurement geometry, the PSRF is not spatially constant. As a result, because the image has uniform pixel sizes, the image may be over or under sampled in some areas. Fine posting ensures all information is preserved and that Nyquist sampling criterion is met. Furthermore, finer posting provides optimum (in the bandlimited sense) interpolation of the effective information in the image. This interpolation can be better than bi-linear or bi-cubic schemes often used for interpolation. Fine resolution eases adjustment of the image to compensate for small mapping biases. We also note that fine posting resolution is required by the signal processing in reconstruction to properly represent the sample locations and measurement response functions. On the other hand, oversampled images produce larger files and there is potential confusion among users in understanding the effective resolution and correlation between adjacent pixels.

When creating the original CETB dataset Long and Brodzik wanted to ensure that although the different frequency channels have different resolution, which necessitates using different grid resolutions, the grid resolutions are easily related to each other (i.e., powers of 2) to simplify comparison and the use of the data [4]. Hence, grid sizes were chosen such that, based on careful simulation, the RMS error in the reconstructed  $T_B$  images was minimized subject to choosing from a small set of possible sizes. This analysis is why particular channels are on particular resolution posting grids even though their effective resolution may be coarser—the finer grid provides better error reduction [4].

As previously noted, the “ideal” PSRF is 1 over the pixel and 0 elsewhere, i.e. a small box car function. However, since the signal is on a discrete grid, we must assume that the signal is bandlimited so that the samples can represent the signal without aliasing. Thus, the band



limited ideal PSRF is a low-pass filtered rect function, i.e., a two-dimensional sinc function (Fig. 4), though in practice the PSRF has a wider main lobe and smaller side lobes. Because the PSRF is non-zero outside of the pixel area, the signal from outside of the pixel area “leaks” into the observed pixel value. For example, if we have an open ocean pixel where the ocean at 160 K is adjacent to a land pixel where the land is 250 K, a PSRF of that is down 10 dB at the next pixel will contribute approximately 9 K to the observed ocean value, essentially raising the observed value to 169 K from its ideal value of 160 K.

The fact that the PSRF is non-zero outside of the pixel area also means that nearby pixels are statistically correlated with each other. Thus, the pixels are not independent even in the ideal case! The pixel correlation is even stronger when the effective resolution is coarser than the posting resolution. While making the effective resolution the same as the posting resolution can minimize the apparent statistical correlation between adjacent pixels, it also results in a loss of information.

## 5 Resolution Estimation of Actual Data

To illustrate the estimation of the PSRF and the effective resolution, SMAP data is used. The same approach is applied to other CETB sensors in later sections. In this section we evaluate the effective linear resolution of SMAP image data from SMAP CETB daily images at both conventional and enhanced resolution via estimation of the pixel step response. To do this, we arbitrarily select a small 200 km by 200 km region centered at approximately 69N and 49E in the Arctic Ocean to do the analysis, see Fig. 5. The cold ocean/warm land transitions provide sharp discontinuities that can be simply modeled. *Ostrov Kolguyev* is a nominally-flat, tundra-covered island that is approximately 81 km in diameter with a maximum elevation of  $\sim 120$  m. The island is nearly circular. Since there is variability (noise) from pass to pass, average results over a 20-day time period are considered. Figure 6 shows individual CETB subimages over the study period. The data time period was arbitrarily selected using CETB  $T_B$  images so that the  $T_B$  values vary only minimally, i.e., are essentially constant, over the time period with high contrast between land and ocean.

Two horizontal transects of the study region are considered in separate cases. One crosses the island and the coast, while the second crosses a patch of sea ice and the coast, see Fig. 7. Due to the dynamics of the sea ice that is further from the shore, only the near-coast region is considered. We model the surface brightness temperature as essentially constant with different values over land and water.

Fig. 7 compares 20-day averaged daily GRD and rSIR images of the study region. In these images, the cooler (darker) areas are open ocean. Land areas have high temperatures, with sea-ice covered areas exhibiting a somewhat lower  $T_B$ . The GRD images are blocky, while the high-resolution images exhibit finer resolution and more accurately match the coastline. These images were created by averaging 20 days of daily  $T_B$  images in order to minimize noise-like effects due to (1)  $T_B$  measurement noise and (2) the effects of the variation in measurement locations within each pass and from pass-to-pass. The derived PSRF and linear resolution thus represent temporal averages. The derived PSRFs are representative of single-pass PSRFs in other areas.

\*.png

**SMAP 1.4V M rSIR 2015092**

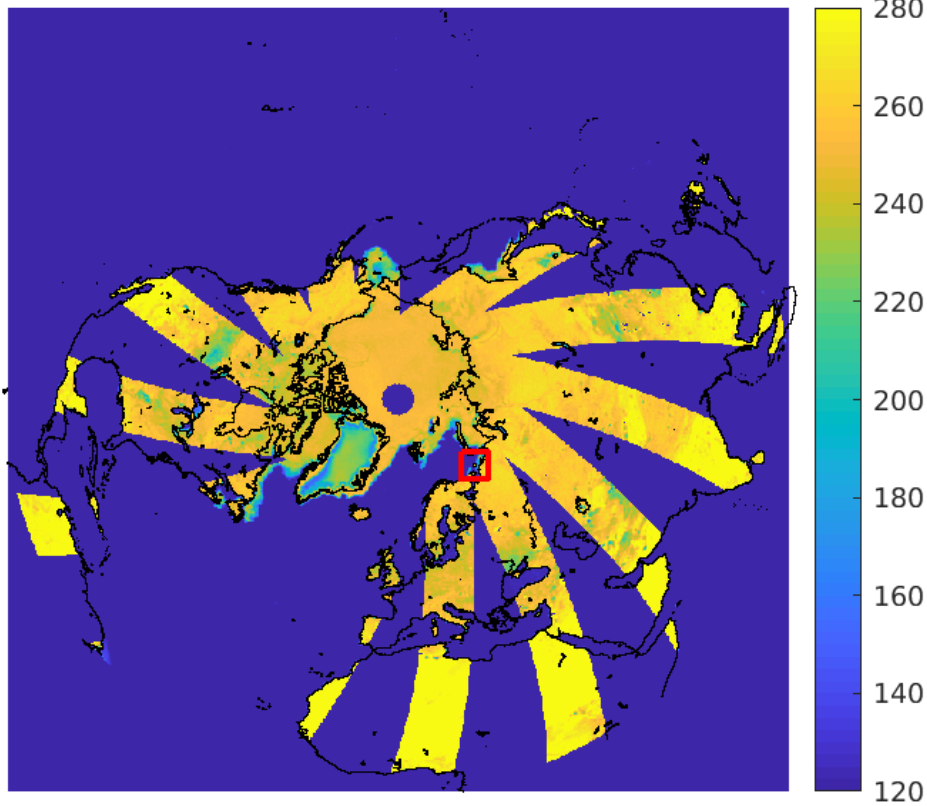


Figure 5: rSIR Northern Hemisphere SMAP Radiometer  $T_B$  EASE-Grid 2.0 1.4 GHz, vertically-polarized (v pol), brightness temperature image, evening (single overpass), on day of year 091, 2015. Open ocean appears cold (low  $T_B$ ) compared to land and sea-ice ice. The thick red box that is right and below center shows the study area.

Examining Fig. 7 we observe that the ocean and land values are reasonably modeled by different constants, with a transition zone at the coastline. It is evident that the GRD images are much blockier than the rSIR images. This is due to the finer grid the rSIR images are computed on and their better effective resolution. Due to the coarse quantization of the GRD image, the island looks somewhat offset downward whereas the rSIR image better corresponds to the superimposed coastline map.

Fig. 8 plots the image  $T_B$  value along the two study transects. Note that rSIR  $T_B$  values have sharper transitions from land to ocean than the GRD images and that the GRD image underestimates the island  $T_B$ . The GRD values also have longer ocean-side transitions than rSIR and overestimate  $T_B$  in the *proliv Pomorskiy* strait separating the island and coastline south (right) of the island. On the other hand, the rSIR curves appear to exhibit a small under- and over-shoot near the transitions. This is not surprising given the bandlimit (low-

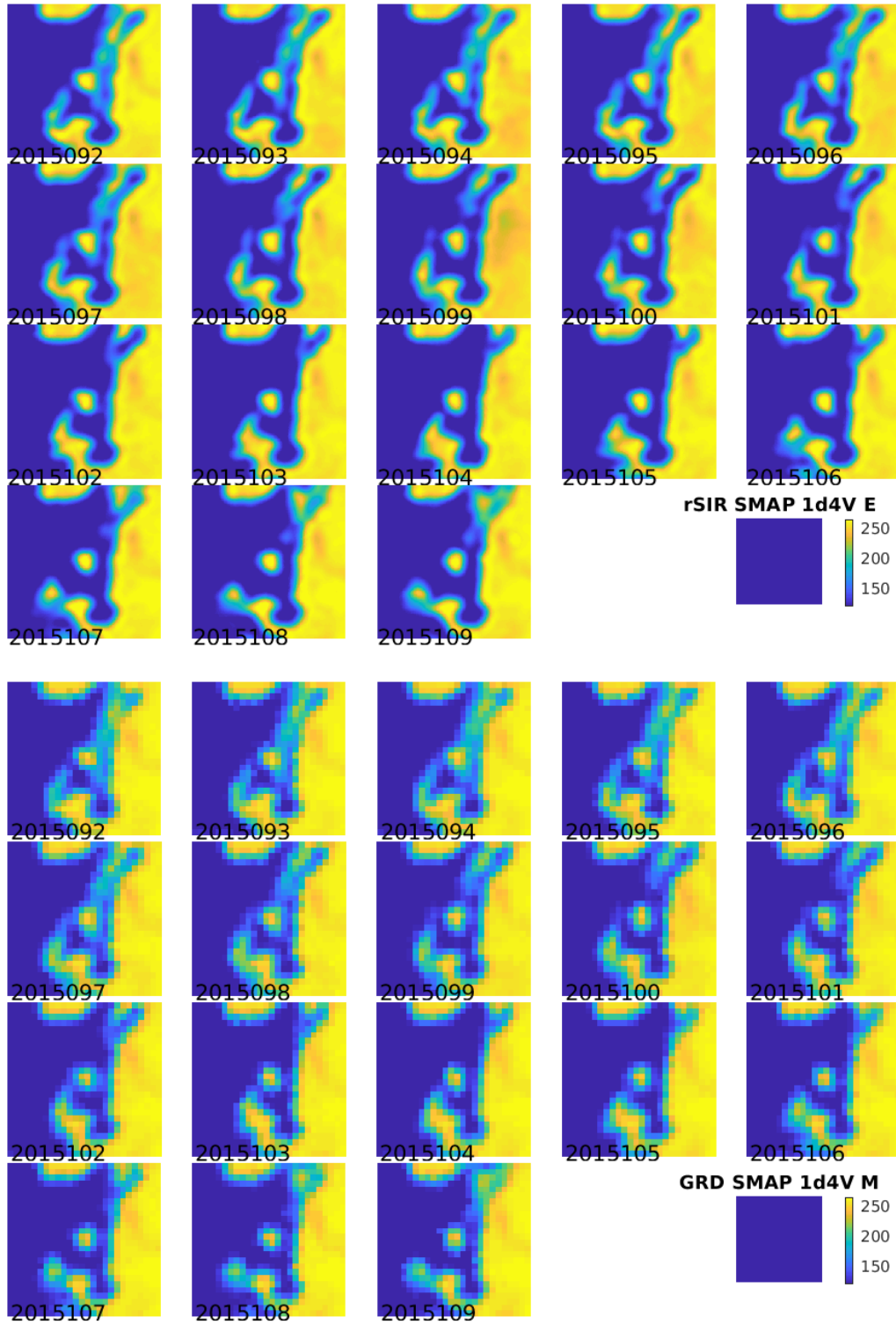


Figure 6: Time series of SMAP (top) rSIR (3.125 km) and (bottom) GRD (25 km)  $T_B$  images over the study area. Image dates are labeled on the image. The purple box in the lower right corner next to the color bar is a plot routine artifact and should be ignored.

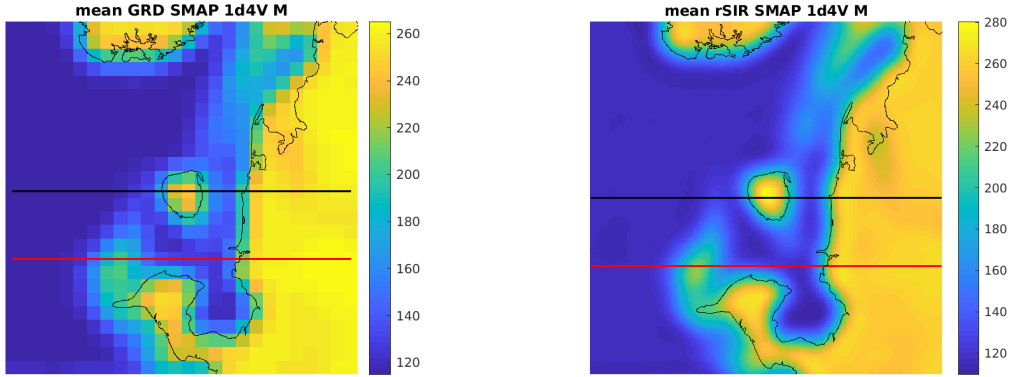


Figure 7: 20-day average of daily SMAP v-pol  $T_B$  images over the study area spanning day-of-year 91-110, 2015 with a coastline overlay. (left) 25-km GRD. (right) 3.125-km rSIR. Note the apparent offset of the island in the GRD, which results from the coarse pixels. The thick horizontal lines show the data transect locations where data is extracted from the image for analysis. The black line is the “island-crossing” case while the red line is the “coastline-crossing” case.

pass) required for digital representation and processing.

Lacking high resolution true  $T_B$  maps, it is difficult to precisely analyze the accuracy and resolution of the images. However, we employ signal processing considerations to infer the expected behavior of the values. For analyzing the expected data behavior along these transects we introduce a simple step model for the underlying  $T_B$ . Noting that the  $T_B$  variation over land near the coast for the coastline case is a nearly constant 260 K with a variation no more than a few K, we model the land as a constant 260 K. Similarly, the ocean  $T_B$  is modeled as a constant 120 K. Slightly different, subjectively chosen values are used for the island case.

The modeled  $T_B$  is plotted in Fig. 7 for comparison with the observed and reconstructed values. The modeled  $T_B$  is filtered with a 25 km Gaussian response filter, shown in green, for comparison. Note that the nominal resolution of antenna pattern of SMAP is  $\sim 36$  km, so this is finer than the nominal SMAP antenna pattern on the surface [9]. The window-filtered model  $T_B$  thus represents something better than “ideal” result, i.e., better than the best than can be achieved from the model.

Examining Fig. 8, we note that the ripple artifacts in the rSIR  $T_B$  transition from ocean to land in both examples are the result of the implicit low pass filtering in the reconstruction. The pass-to-pass variability in the  $T_B$  observations is approximately the same for both GRD and rSIR in most places, suggesting that there is not a significant noise penalty when employing rSIR reconstruction for SMAP.

Insight can be gained by examining the spectra of the signal. Fig. 10 presents the wavenumber spectra of the key signals in Fig. 9. The spectra were computed by zero padding the data. For simplicity, only the Fourier transforms of the average curves are shown. The spectra of the modeled signal peaking at 0 wavenumber, and then tapers off at higher wavenumbers. The filtered model signal represents the best signal that can be recovered. The GRD signal closely

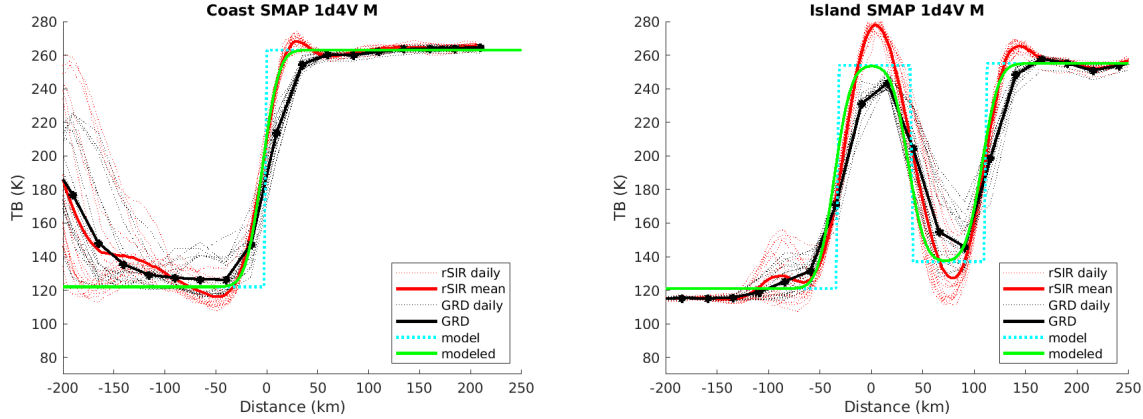


Figure 8: Plots of  $T_B$  along the two analysis transect lines shown in Fig. 7 for the (left) coast-crossing and (right) island-crossing cases. Daily values over the study period are shown for rSIR and GRD as thin blue and yellow lines, respectively. The averages of these lines are shown in red and black. The discrete step and convolved Gaussian step models are also shown. The  $x$  axis is centered on the rSIR-derived coastline or island center for the particular case.

follows the ideal until it reaches the  $1/72 \text{ km}^{-1}$  frequency supported by the antenna pattern, and rolls off slightly as it approaches the  $1/50 \text{ km}^{-1}$  cutoff frequency permitted by the grid, beyond which it cannot represent the signal further. rSIR nicely follows this signal out to the limit of the graph and thus has higher effective resolution than GRD, even though the total energy in the signal is small at this level. Details of the high wavenumber responses differ between the coast-crossing and island-crossing case, but the same conclusions apply.

Deconvolution of the step response is accomplished in the frequency domain by dividing the step response by the spectra of the modeled step function, with care for how zeros and near-zeros in the modeled step function are handled in the inverse operation. The ideal GRD PSRF (blue dashed line) is a rect that cuts off at  $1/50 \text{ km}^{-1}$ . The estimated GRD PSRF spectrum closely matches the ideal. The rSIR PSRF spectrum also matches the ideal in the low frequency region, but also contains additional information at higher wavenumbers, which gradually rolls off. This additional spectral content provides the finer resolution of rSIR compared to the GRD result.

Finally, the estimated one-dimensional PSRFs are computed as the inverse Fourier transform of the PSRF spectra in Fig. 9 as shown in Fig. 10. Table 1 shows the linear resolution for each, computed as the width of the PSRF at the -3 dB point. For comparison, the linear resolution using both -2 dB and -10 dB thresholds is shown. In all cases the resolution of rSIR is better than the observed GRD resolution.

A key observation is that the effective resolution, as defined by the -3-dB width of the derived PSRFs, is very similar for both analysis cases. As expected, the observed GRD PSRFs results are coarser than the ideal GRD PSRFs due to the extension of the MRFs outside of the pixel area. The rSIR curve has a small shoulder on the right side which makes it asymmetric and wider in the coastal case than the island case, but otherwise the rSIR PSRF nearly matches the Gaussian-filtered model over the main lobe. The island crossing rSIR result

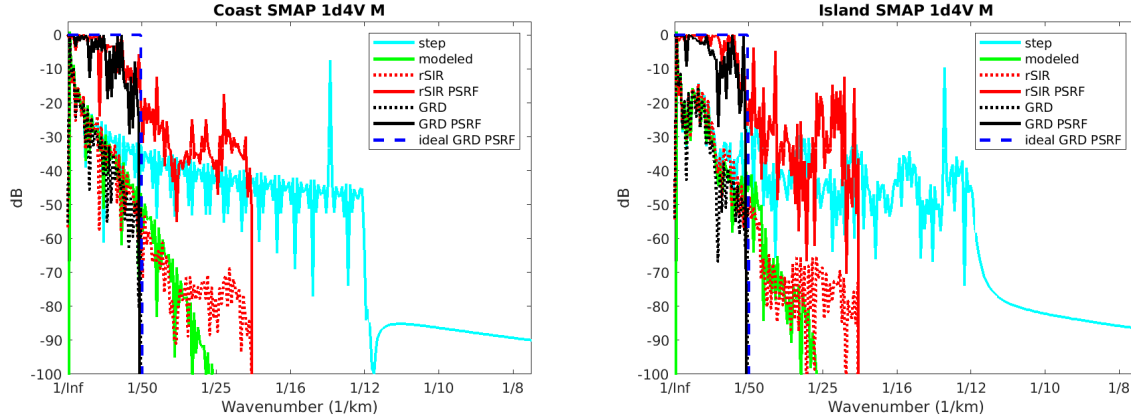


Figure 9: Wavenumber spectra of the  $T_B$  slices, the model, and the PSRF. (left) Coast-crossing case. (right) Island-crossing case. See text.

Table 1: Inferred linear resolutions from Fig. 10 for various thresholds.

Algorithm	-3 dB Thres		-2 dB Thres		-10 dB Thres	
	Coast	Island	Coast	Island	Coast	Island
Gauss	30.0	30.0	24.4	24.4	54.8	54.8
rSIR	36.1	38.8	28.0	33.2	59.2	59.5
ideal GRD	36.2	36.2	30.3	30.3	54.5	54.5
GRD	47.0	46.1	38.8	38.3	75.7	72.7

has finer linear resolution than both the ideal GRD and actual GRD results. The island rSIR resolution represents an improvement of nearly 30% from the observed GRD resolution and 10% from the ideal GRD resolution. We conclude that rSIR does, in fact, provide finer effective resolution than GRD products, with an improvement of nearly 30% for this sensor.

The appendix provides an analysis for each major sensor in the CETB with separate analyses by sensor, sensor channel (frequency and polarization), and local-time-of-day (ltod). For single day images, the improvement in resolution for rSIR versus GRD varies from approximately 30% to 60%, depending on sensor and channel for most cases. The results are similar for different image ltods.

## 6 Conclusion

This white paper considers the effective resolution of conventional and enhanced resolution  $T_B$  image products available from the NASA-sponsored Calibrated Passive Microwave Daily EASE-Grid 2.0 Brightness Temperature (CETB) ESDR project. This project includes a long time series of consistently calibrated  $T_B$  images from SMMR, SSM/I, SSMIS, AMSR-E, and SMAP [3]. The image formation step function response is derived from polar images, from which the effective resolution is determined by computing the pixel spatial response function. As expected, the effective resolution of the images is coarser than the posting (pixel spacing)

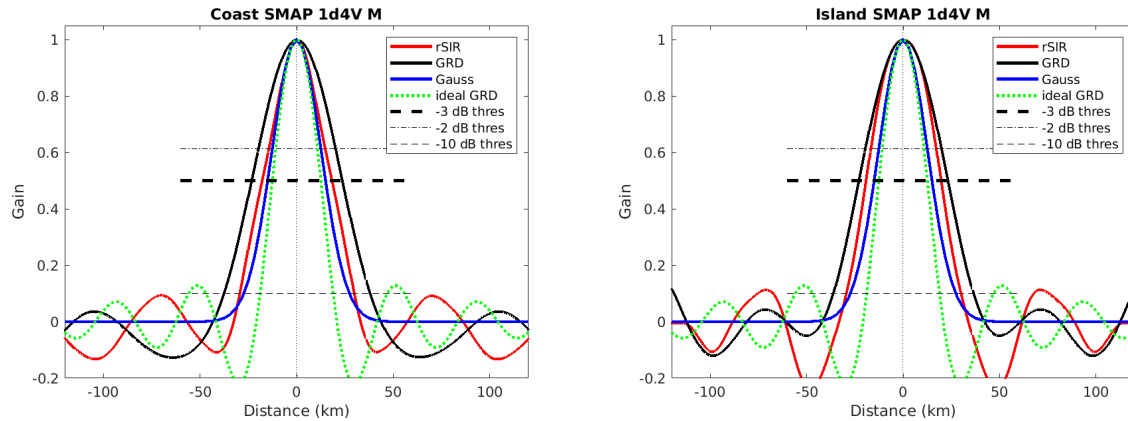


Figure 10: Derived single-pass rSIR and GRD PSRFs from the (left) coast-crossing and (right) island-crossing cases. Shown for comparison are a 36-km wide Gaussian window and a 36-km wide sinc function, which represents the ideal GRD pixel PSRF. The horizontal dashed line corresponds to the -3 dB line. The effective 3-dB linear resolution is the width of the PSRF at this line.

resolution for both conventionally processed (GRD) data and enhanced resolution rSIR images. The rSIR pixel spatial response function exhibits significantly finer spatial resolution than GRD, with a 30–60% improvement in effective resolution for rSIR compared to GRD. The precise resolution improvement of rSIR is sensor and channel dependent.

## References

- [1] M.J. Brodzik, D.G. Long, M.A. Hardman, A. Paget, and R. Armstrong. 2016, Updated 2020. MEaSUREs Calibrated Enhanced-Resolution Passive Microwave Daily EASE-Grid 2.0 Brightness Temperature ESDR, Version 1. Boulder, Colorado USA. NASA National Snow and Ice Data Center Distributed Active Archive Center. doi:10.5067/MEASURES/CRYOSPHERE/NSIDC-0630.001.
- [2] M.J. Brodzik, D.G. Long and M.A. Hardman, 2019. SMAP Radiometer Twice-Daily rSIR-Enhanced EASE-Grid 2.0 Brightness Temperatures, Version 1.0. Boulder, CO: National Snow and Ice Data Center. Digital media. doi:10.5067/QZ3WJNOUZLFK.
- [3] M.J. Brodzik and D.G. Long, 2018. Calibrated passive microwave daily EASE-Grid 2.0 brightness temperature ESDR (CETB): Algorithm theoretical basis document, National Snow and Ice Data Center (NSIDC) publication [Online] Available at: [http://nsidc.org/pmesdr/files/MEaSUREs\\_CETB\\_ATBD\\_v1.0.pdf](http://nsidc.org/pmesdr/files/MEaSUREs_CETB_ATBD_v1.0.pdf).
- [4] D.G. Long and M.J. Brodzik, Optimum image formation for spaceborne microwave radiometer products, *IEEE Trans. Geosci. Remote Sensing*, vol. 54, no. 5, pp. 2763–2779, doi:10.1109/TGARS.2015.2505677, 2016.

- [5] D.G. Long and D.L. Daum, Spatial resolution enhancement of SSM/I data, *IEEE Trans. Geosci. Remote Sensing*, vol. 36, no. 2, pp. 407–417, 1998.
- [6] G.E. Backus and J.F. Gilbert, Numerical applications of a formalism for geophysical inverse problems, *Geophys. J. R. Astron. Soc.*, vol. 13, pp. 247–276, 1967.
- [7] G.E. Backus and J.F. Gilbert, Resolving power of gross Earth data, *Geophys. J. R. Astron. Soc.*, vol. 16, pp. 169–205, 1968.
- [8] A. Stogryn, Estimates of brightness temperatures from scanning radiometer data, *IEEE Trans. Antennas Propagat.*, vol. AP-26, pp. 720–726, 1978.
- [9] D.G. Long, M.J. Brodzik, and M. Hardman, Enhanced Resolution SMAP Brightness Temperature Image Products, *IEEE Trans. Geosci. Remote Sensing*, vol. 57, no. 7, pp. 4151–4163, doi:10.1109/TGRS.2018.2889427, 2019.
- [10] D.G. Long, M.J. Brodzik, and M. Hardman, Evaluating the Effective Resolution of Enhanced Resolution SMAP Brightness Temperature Image Products, *IEEE Trans. Geosci. Remote Sensing*, in review, 2021.
- [11] J. Piepmeier, P. Mohammed, G. De Amici, E. Kim, J. Pen and C. Ruff, Algorithm Theoretical Basis Document: SMAP Calibrated, Time-ordered Brightness Temperatures L1B\_TB Data Product, SMAP Project, Rev. A, 10 Dec 2014, available online at URL [https://smap.jpl.nasa.gov/system/internal\\_resources/details/original/278\\_L1B\\_TB\\_RevA\\_web.pdf](https://smap.jpl.nasa.gov/system/internal_resources/details/original/278_L1B_TB_RevA_web.pdf).
- [12] M.J. Brodzik, B. Billingsley, T. Haran, B. Raup, M. H. Savoie, EASE-Grid 2.0: Incremental but significant improvements for Earth-Gridded data sets, *ISPRS Int. J. Geo-Information*, vol. 1, no. 1, pp. 32–45, 2012.
- [13] M.J. Brodzik, B. Billingsley, T. Haran, B. Raup, M. H. Savoie, Correction: M.J. Brodzik, et al., EASE-Grid 2.0: Incremental but significant improvements for Earth-Gridded data sets, *ISPRS Int. J. Geo-Information*, vol. 1, no. 1, pp. 32–45, 2012, *ISPRS Int. J. Geo-Information*, vol. 3, no. 3, pp. 1154–1156, 2014.
- [14] D.S. Early and D.G. Long, Image reconstruction and enhanced resolution imaging from irregular samples, *IEEE Trans. Geosci. Remote Sensing*, vol. 39, no. 2, pp. 291–302, 2001.
- [15] F. Ulaby and D.G. Long, *Microwave Radar and Radiometric Remote Sensing*, University of Michigan Press, Ann Arbor, Michigan, 2014.
- [16] D.G. Long and R. Franz, Band-limited signal reconstruction from irregular samples with variable apertures, *IEEE Trans. Geosci. Remote Sensing*, vol. 54, no. 4, pp. 2424–2436, 2016.
- [17] D.G. Long, Comparison of SeaWinds Backscatter Imaging Algorithms, *IEEE J. Sel. Topics in Applied Earth Observations*, vol. 10, no. 3, pp. 2214–2231, doi:10.1109/JSTARS.2016.2626966, 2017.



## Appendix: Analysis for All CETB Sensors

In this rather lengthy appendix, the methodology described in the main report for analyzing the effective resolution of  $T_B$  images is applied to the various CETB sensor types, specifically AMSR-E, SMAP, SMMR, SSM/I, and SSMIS. The same time period is used for SSM/I, SSMIS, and SMAP, with different, arbitrarily selected time periods for AMSR-E and SMMR. Some analysis time periods are shorter to minimize temporal variations in the imagery. A separate analysis is provided for each channel for both “morning” (M) and “evening” (E) local-time-of-day (ltod) images provided by the CETB. Some tables and figures are repeated for convenience. For analysis of CETB rSIR images with posting resolutions less than 3.125 km, the images were sinc function interpolated<sup>3</sup> to 3.125 km pixel resolution.

### A General Comments

We note that some channels (most notably the high frequency channels) include strong atmospheric interference and/or may have very little land/ocean/ice contrast. In these cases, the analysis cannot be expected to work as well, though the results are presented anyway. The 6 GHz channels of SMMR and, to a lesser degree, of AMSR-E are so coarse that the coastline edges are not apparent in the images, which limit the accuracy of the results. In some cases, especially for lower frequencies, sea ice or the leakage of land  $T_B$  creates a  $T_B$  rise (i.e., a bump) in the ocean east (above in the image) of the peninsula. Since this is not accounted for in the simple  $T_B$  model employed, the PSRF estimate may be degraded by ripples and/or higher sidelobes. In general, the island PSRFs are considered the most accurate.

The CETB team used the input data as provided by the suppliers, with no modification or adjustment. However, for some sensors (notably SMMR) the reported latitude and longitude of the  $T_B$  measurements are slightly inaccurate. This results in biases in the apparent positions of surface features (e.g., coastlines) in the images. In addition, temporal variations of the position error “jitters” the positions and has the effect of degrading the effective resolution. In performing the analysis, some images were subjectively shifted vertically and/or horizontally a few pixels to ensure that the island position in the image properly lined up with the coastline map. In most cases the shift was no more than one GRD pixel and five rSIR pixels with the largest shifts required only for SMMR, which also showed some temporal variation in location accuracy. Note that the GRD and rSIR “slices” do not precisely align (i.e., they do not cover the same area on the ground) due to the difference in vertical extent of the single row of pixels in each slice: the GRD slices are 25 km tall, while the rSIR slices are 3.125 km tall.

As noted in the main text, the results are sensitive to the locations of the model transitions. In generating the model  $T_B$  values, the transition edges were manually determined for each sensor and channel to be at approximately the halfway point between the high and low (land/ocean) values. Previous simulations [4, 9] suggest that at sharp step-like transitions, GRD undershoots the step, while rSIR slightly overshoots the step. Thus, in selecting the ocean and land  $T_B$  values for the model, a value approximately halfway between the GRD and

---

<sup>3</sup>To do this, the Matlab function ‘periodic.interp’ was used after filling in no-data values in each image with the image mean. This is equivalent to periodic sinc function (Dirichlet function) interpolation [16].

rSIR values was chosen.

## A.1 Sensor Specific Comments

Comments regarding the analysis for each CETB sensor class are provided in this section. Note that in all cases, the CETB product uses the best available data for each sensor.

### A.1.1 AMSR-E

A 20 day period in late summer (244-264) 2005 was arbitrarily selected. The area is free of sea ice during this period. There is some day to day variation in  $T_B$ . The low resolution of the 6 GHz channel causes some leakage from the peninsula into the ocean on the coastline slice, which creates a bump left of the coast line transition that results in “shoulders” and high sidelobes in the PSRF. As the channel frequency increases from 6 GHz to 89 GHz, more and more atmospheric effects can be noted, as is apparent in the increasing standard deviation over the ocean. As expected, the highest frequency (89 GHz) has significant atmospheric variations that reduce the land/ocean  $T_B$  contrast.

### A.1.2 SMAP

Sea ice above and to the left of the peninsula creates a rise in the ocean  $T_B$  to the left of the coastline. There may be some ice between the island and the coast. Both of these adversely affect the resolution estimates somewhat. The low frequency (1.4 GHz) provides surface  $T_B$  measurements with very little atmospheric effects.

### A.1.3 SMMR

In general the SMMR data is of much lower quality than the other sensors with temporally varying location biases. The 6 GHz channels of SMMR are so coarse that the island and coast edges are not apparent in some of the images, which limits the accuracy of the results and precludes estimates in many cases. The narrow coverage of the SMMR over the study area introduces artifacts and filtering effects that also cause issues with the analysis. Unfortunately, the SMMR measurement position accuracy varies, which results in variations in the apparent positions of the islands and coastlines with time. In many cases, the standard analysis approach used in this report fails to provide useful estimates of the PSRF.

### A.1.4 SSMIS

A short (days 100-103,2015), but overlapping time period with SMAP is used for SSMIS due to temporal variations of the surface. The shorter time period is not considered an issue in the resolution estimates. Sea ice above and to the left of the peninsula creates a rise in the ocean  $T_B$  to the left of the coastline. There may be some ice between the island and the coast. Both of these adversely affect the resolution estimates somewhat, giving rise to shoulders and broader rSIR mainlobes for the PSRF estimates in some cases.

As expected, the highest frequency (91 GHz) has significant atmospheric and surface temperature variations that reduce that land/ocean  $T_B$  contrast that in some cases preclude reasonable estimates.

### A.1.5 SSM/I

As in the SSMIS case, a short (days 100-103,2015), but overlapping time period with SMAP is used for SSM/I due to due to temporal variations of the surface. The shorter time period is not considered an issue in the resolution estimates. Sea ice above and to the left of the peninsula creates a rise in the ocean  $T_B$  to the left of the coastline. There may be some ice between the island and the coast. Both of these adversely affect the resolution estimates somewhat giving rise to shoulders and broader rSIR mainlobes for the PSRF estimates in some cases.

Results for SSM/I 22V are not included due to sensor data quality issues in the source data sets over the time period of interest. There are coverage gaps and holes in some of the channels.

As expected, the highest frequency (85 GHz) has significant atmospheric and surface temperature variations that reduce the land/ocean  $T_B$  contrast that in some cases preclude reasonable estimates.

## B Summary of Resolution Comparisons

The following comprehensive list of tables summarize the analysis results for each sensor, channel and ltod. A full set of figures for each case are given in succeeding sections.

Table 2: Resolution estimates for AMSRE channel 06H LTOD E

Algorithm	-3 dB Thres		-2 dB Thres		-10 dB Thres	
	Coast	Island	Coast	Island	Coast	Island
Gauss	30.0	30.0	24.4	24.4	54.8	54.8
rSIR	65.0	40.0	57.8	31.6	139.5	68.8
ideal GRD	36.2	36.2	30.3	30.3	54.5	54.5
GRD	73.8	58.7	61.4	50.1	133.4	83.1

Table 3: Resolution estimates for AMSRE channel 06H LTOD M

Algorithm	-3 dB Thres		-2 dB Thres		-10 dB Thres	
	Coast	Island	Coast	Island	Coast	Island
Gauss	30.0	30.0	24.4	24.4	54.8	54.8
rSIR	48.3	53.0	41.2	45.0	120.4	102.0
ideal GRD	36.2	36.2	30.3	30.3	54.5	54.5
GRD	54.4	72.2	44.5	60.1	103.0	111.6

Table 4: Resolution estimates for AMSRE channel 06V LTOD E

Algorithm	-3 dB Thres		-2 dB Thres		-10 dB Thres	
	Coast	Island	Coast	Island	Coast	Island
Gauss	30.0	30.0	24.4	24.4	54.8	54.8
rSIR	51.9	58.2	40.5	43.7	85.2	110.6
ideal GRD	36.2	36.2	30.3	30.3	54.5	54.5
GRD	72.4	70.3	60.0	59.1	110.8	104.7

Table 5: Resolution estimates for AMSRE channel 06V LTOD M

Algorithm	-3 dB Thres		-2 dB Thres		-10 dB Thres	
	Coast	Island	Coast	Island	Coast	Island
Gauss	30.0	30.0	24.4	24.4	54.8	54.8
rSIR	58.1	49.2	45.4	33.4	86.7	76.6
ideal GRD	36.2	36.2	30.3	30.3	54.5	54.5
GRD	67.3	63.1	57.1	51.7	96.2	110.2

Table 6: Resolution estimates for AMSRE channel 10.7H LTOD E

Algorithm	-3 dB Thres		-2 dB Thres		-10 dB Thres	
	Coast	Island	Coast	Island	Coast	Island
Gauss	30.0	30.0	24.4	24.4	54.8	54.8
rSIR	41.5	37.9	33.3	31.7	77.2	57.2
ideal GRD	36.2	36.2	30.3	30.3	54.5	54.5
GRD	52.1	52.6	43.5	43.6	78.7	83.4

Table 7: Resolution estimates for AMSRE channel 10.7H LTOD M

Algorithm	-3 dB Thres		-2 dB Thres		-10 dB Thres	
	Coast	Island	Coast	Island	Coast	Island
Gauss	30.0	30.0	24.4	24.4	54.8	54.8
rSIR	38.0	36.8	30.9	29.7	67.6	58.1
ideal GRD	36.2	36.2	30.3	30.3	54.5	54.5
GRD	47.2	49.0	39.0	40.6	76.2	77.6

Table 8: Resolution estimates for AMSRE channel 10.7V LTOD E

Algorithm	-3 dB Thres		-2 dB Thres		-10 dB Thres	
	Coast	Island	Coast	Island	Coast	Island
Gauss	30.0	30.0	24.4	24.4	54.8	54.8
rSIR	46.6	32.5	37.3	26.8	83.0	93.6
ideal GRD	36.2	36.2	30.3	30.3	54.5	54.5
GRD	53.9	57.7	44.8	47.8	84.0	91.5

Table 9: Resolution estimates for AMSRE channel 10.7V LTOD M

Algorithm	-3 dB Thres		-2 dB Thres		-10 dB Thres	
	Coast	Island	Coast	Island	Coast	Island
Gauss	30.0	30.0	24.4	24.4	54.8	54.8
rSIR	45.9	28.2	38.7	19.9	84.5	79.1
ideal GRD	36.2	36.2	30.3	30.3	54.5	54.5
GRD	49.4	55.0	40.7	45.4	82.0	89.7

Table 10: Resolution estimates for AMSRE channel 18H LTOD E

Algorithm	-3 dB Thres		-2 dB Thres		-10 dB Thres	
	Coast	Island	Coast	Island	Coast	Island
Gauss	30.0	30.0	24.4	24.4	54.8	54.8
rSIR	31.5	19.9	27.2	16.5	50.1	32.2
ideal GRD	36.2	36.2	30.3	30.3	54.5	54.5
GRD	53.8	40.8	44.9	33.9	84.2	63.8

Table 11: Resolution estimates for AMSRE channel 18H LTOD M

Algorithm	-3 dB Thres		-2 dB Thres		-10 dB Thres	
	Coast	Island	Coast	Island	Coast	Island
Gauss	30.0	30.0	24.4	24.4	54.8	54.8
rSIR	27.0	17.0	22.8	14.1	42.3	27.9
ideal GRD	36.2	36.2	30.3	30.3	54.5	54.5
GRD	44.1	45.8	36.5	37.6	71.8	78.9

Table 12: Resolution estimates for AMSRE channel 18V LTOD E

Algorithm	-3 dB Thres		-2 dB Thres		-10 dB Thres	
	Coast	Island	Coast	Island	Coast	Island
Gauss	30.0	30.0	24.4	24.4	54.8	54.8
rSIR	25.9	20.0	21.2	16.5	46.5	32.3
ideal GRD	36.2	36.2	30.3	30.3	54.5	54.5
GRD	45.3	36.8	36.9	30.7	83.9	55.9

Table 13: Resolution estimates for AMSRE channel 18V LTOD M

Algorithm	-3 dB Thres		-2 dB Thres		-10 dB Thres	
	Coast	Island	Coast	Island	Coast	Island
Gauss	30.0	30.0	24.4	24.4	54.8	54.8
rSIR	23.9	18.7	19.8	15.4	39.1	32.0
ideal GRD	36.2	36.2	30.3	30.3	54.5	54.5
GRD	43.2	41.4	35.8	34.4	70.7	64.6

Table 14: Resolution estimates for AMSRE channel 23H LTOD E

Algorithm	-3 dB Thres		-2 dB Thres		-10 dB Thres	
	Coast	Island	Coast	Island	Coast	Island
Gauss	30.0	30.0	24.4	24.4	54.8	54.8
rSIR	29.6	23.1	24.8	18.9	47.9	39.5
ideal GRD	36.2	36.2	30.3	30.3	54.5	54.5
GRD	44.8	45.6	36.6	37.7	79.2	73.1

Table 15: Resolution estimates for AMSRE channel 23H LTOD M

Algorithm	-3 dB Thres		-2 dB Thres		-10 dB Thres	
	Coast	Island	Coast	Island	Coast	Island
Gauss	30.0	30.0	24.4	24.4	54.8	54.8
rSIR	29.9	24.9	24.2	20.6	53.4	40.2
ideal GRD	36.2	36.2	30.3	30.3	54.5	54.5
GRD	41.9	43.5	34.4	35.9	72.1	71.0

Table 16: Resolution estimates for AMSRE channel 23V LTOD E

Algorithm	-3 dB Thres		-2 dB Thres		-10 dB Thres	
	Coast	Island	Coast	Island	Coast	Island
Gauss	30.0	30.0	24.4	24.4	54.8	54.8
rSIR	25.8	24.8	21.7	20.6	39.8	39.7
ideal GRD	36.2	36.2	30.3	30.3	54.5	54.5
GRD	52.7	41.6	43.7	34.5	84.5	65.5

Table 17: Resolution estimates for AMSRE channel 23V LTOD M

Algorithm	-3 dB Thres		-2 dB Thres		-10 dB Thres	
	Coast	Island	Coast	Island	Coast	Island
Gauss	30.0	30.0	24.4	24.4	54.8	54.8
rSIR	30.5	22.8	24.8	18.8	53.3	38.0
ideal GRD	36.2	36.2	30.3	30.3	54.5	54.5
GRD	44.1	45.6	36.3	37.6	75.2	74.9

Table 18: Resolution estimates for AMSRE channel 36H LTOD E

Algorithm	-3 dB Thres		-2 dB Thres		-10 dB Thres	
	Coast	Island	Coast	Island	Coast	Island
Gauss	30.0	30.0	24.4	24.4	54.8	54.8
rSIR	23.0	32.7	18.6	27.0	46.0	47.4
ideal GRD	36.2	36.2	30.3	30.3	54.5	54.5
GRD	50.0	38.2	41.7	31.8	77.4	59.5

Table 19: Resolution estimates for AMSRE channel 36H LTOD M

Algorithm	-3 dB Thres		-2 dB Thres		-10 dB Thres	
	Coast	Island	Coast	Island	Coast	Island
Gauss	30.0	30.0	24.4	24.4	54.8	54.8
rSIR	20.1	15.1	17.7	12.0	34.9	61.1
ideal GRD	36.2	36.2	30.3	30.3	54.5	54.5
GRD	40.1	38.6	33.0	32.0	67.2	61.0

Table 20: Resolution estimates for AMSRE channel 36V LTOD E

Algorithm	-3 dB Thres		-2 dB Thres		-10 dB Thres	
	Coast	Island	Coast	Island	Coast	Island
Gauss	30.0	30.0	24.4	24.4	54.8	54.8
rSIR	18.0	22.6	14.8	18.6	32.5	37.9
ideal GRD	36.2	36.2	30.3	30.3	54.5	54.5
GRD	53.8	36.1	44.9	30.1	85.1	55.0

Table 21: Resolution estimates for AMSRE channel 36V LTOD M

Algorithm	-3 dB Thres		-2 dB Thres		-10 dB Thres	
	Coast	Island	Coast	Island	Coast	Island
Gauss	30.0	30.0	24.4	24.4	54.8	54.8
rSIR	19.9	17.4	16.6	14.3	31.3	31.5
ideal GRD	36.2	36.2	30.3	30.3	54.5	54.5
GRD	38.1	37.1	31.5	30.8	61.4	58.4



Table 22: Resolution estimates for AMSRE channel 89H LTOD E

Algorithm	-3 dB Thres		-2 dB Thres		-10 dB Thres	
	Coast	Island	Coast	Island	Coast	Island
Gauss	30.0	30.0	24.4	24.4	54.8	54.8
rSIR	18.6	17.0	15.4	13.9	29.8	34.1
ideal GRD	36.2	36.2	30.3	30.3	54.5	54.5
GRD	29.3	28.8	24.5	24.2	43.3	41.7

Table 23: Resolution estimates for AMSRE channel 89H LTOD M

Algorithm	-3 dB Thres		-2 dB Thres		-10 dB Thres	
	Coast	Island	Coast	Island	Coast	Island
Gauss	30.0	30.0	24.4	24.4	54.8	54.8
rSIR	14.8	15.2	12.2	12.5	24.6	27.9
ideal GRD	36.2	36.2	30.3	30.3	54.5	54.5
GRD	39.2	39.2	32.4	32.4	63.8	63.1

Table 24: Resolution estimates for AMSRE channel 89V LTOD E

Algorithm	-3 dB Thres		-2 dB Thres		-10 dB Thres	
	Coast	Island	Coast	Island	Coast	Island
Gauss	30.0	30.0	24.4	24.4	54.8	54.8
rSIR	16.2	13.4	13.3	11.2	28.5	20.8
ideal GRD	36.2	36.2	30.3	30.3	54.5	54.5
GRD	33.3	29.8	28.0	24.9	48.0	45.1

Table 25: Resolution estimates for AMSRE channel 89V LTOD M

Algorithm	-3 dB Thres		-2 dB Thres		-10 dB Thres	
	Coast	Island	Coast	Island	Coast	Island
Gauss	30.0	30.0	24.4	24.4	54.8	54.8
rSIR	14.7	14.6	12.2	12.1	23.8	22.6
ideal GRD	36.2	36.2	30.3	30.3	54.5	54.5
GRD	47.1	48.2	38.9	39.6	75.3	81.6

Table 26: Resolution estimates for SMAP channel 1.4H LTOD E

Algorithm	-3 dB Thres		-2 dB Thres		-10 dB Thres	
	Coast	Island	Coast	Island	Coast	Island
Gauss	30.0	30.0	24.4	24.4	54.8	54.8
rSIR	46.8	35.9	37.8	28.7	74.8	54.7
ideal GRD	36.2	36.2	30.3	30.3	54.5	54.5
GRD	57.4	47.2	48.2	38.9	85.9	75.6

Table 27: Resolution estimates for SMAP channel 1.4H LTOD M

Algorithm	-3 dB Thres		-2 dB Thres		-10 dB Thres	
	Coast	Island	Coast	Island	Coast	Island
Gauss	30.0	30.0	24.4	24.4	54.8	54.8
rSIR	40.9	36.6	30.4	31.2	64.2	57.4
ideal GRD	36.2	36.2	30.3	30.3	54.5	54.5
GRD	46.5	43.1	38.4	35.9	75.5	66.5

Table 28: Resolution estimates for SMAP channel 1.4V LTOD E

Algorithm	-3 dB Thres		-2 dB Thres		-10 dB Thres	
	Coast	Island	Coast	Island	Coast	Island
Gauss	30.0	30.0	24.4	24.4	54.8	54.8
rSIR	39.2	36.7	32.0	29.8	63.2	60.4
ideal GRD	36.2	36.2	30.3	30.3	54.5	54.5
GRD	54.3	49.4	45.4	41.3	81.6	74.7

Table 29: Resolution estimates for SMAP channel 1.4V LTOD M

Algorithm	-3 dB Thres		-2 dB Thres		-10 dB Thres	
	Coast	Island	Coast	Island	Coast	Island
Gauss	30.0	30.0	24.4	24.4	54.8	54.8
rSIR	36.1	38.8	28.0	33.2	59.2	59.5
ideal GRD	36.2	36.2	30.3	30.3	54.5	54.5
GRD	47.0	46.1	38.8	38.3	75.7	72.7

Table 30: Resolution estimates for SMMR channel 06H LTOD E

Algorithm	-3 dB Thres		-2 dB Thres		-10 dB Thres	
	Coast	Island	Coast	Island	Coast	Island
Gauss	30.0	30.0	24.4	24.4	54.8	54.8
rSIR	45.3	28.4	39.8	20.3	107.5	105.5
ideal GRD	36.2	36.2	30.3	30.3	54.5	54.5
GRD	206.7	32.1	89.2	26.7	324.6	49.9

Table 31: Resolution estimates for SMMR channel 06H LTOD M

Algorithm	-3 dB Thres		-2 dB Thres		-10 dB Thres	
	Coast	Island	Coast	Island	Coast	Island
Gauss	30.0	30.0	24.4	24.4	54.8	54.8
rSIR	107.1	57.4	39.7	54.0	136.7	144.2
ideal GRD	36.2	36.2	30.3	30.3	54.5	54.5
GRD	112.3	88.1	104.6	79.5	137.2	113.8

Table 32: Resolution estimates for SMMR channel 06V LTOD E

Algorithm	-3 dB Thres		-2 dB Thres		-10 dB Thres	
	Coast	Island	Coast	Island	Coast	Island
Gauss	30.0	30.0	24.4	24.4	54.8	54.8
rSIR	126.5	139.4	43.1	33.9	152.1	149.0
ideal GRD	36.2	36.2	30.3	30.3	54.5	54.5
GRD	164.7	47.4	40.8	40.8	446.1	62.7

Table 33: Resolution estimates for SMMR channel 06V LTOD M

Algorithm	-3 dB Thres		-2 dB Thres		-10 dB Thres	
	Coast	Island	Coast	Island	Coast	Island
Gauss	30.0	30.0	24.4	24.4	54.8	54.8
rSIR	62.3	19.4	18.8	14.1	150.8	113.6
ideal GRD	36.2	36.2	30.3	30.3	54.5	54.5
GRD	112.7	64.3	49.8	55.2	132.7	93.4

Table 34: Resolution estimates for SMMR channel 10H LTOD E

Algorithm	-3 dB Thres		-2 dB Thres		-10 dB Thres	
	Coast	Island	Coast	Island	Coast	Island
Gauss	30.0	30.0	24.4	24.4	54.8	54.8
rSIR	59.7	53.0	52.0	43.1	110.8	102.6
ideal GRD	36.2	36.2	30.3	30.3	54.5	54.5
GRD	55.5	35.4	45.3	30.1	100.1	50.0

Table 35: Resolution estimates for SMMR channel 10H LTOD M

Algorithm	-3 dB Thres		-2 dB Thres		-10 dB Thres	
	Coast	Island	Coast	Island	Coast	Island
Gauss	30.0	30.0	24.4	24.4	54.8	54.8
rSIR	51.9	31.2	20.7	22.9	102.0	111.6
ideal GRD	36.2	36.2	30.3	30.3	54.5	54.5
GRD	90.9	40.6	82.5	34.0	117.1	60.9

Table 36: Resolution estimates for SMMR channel 10V LTOD E

Algorithm	-3 dB Thres		-2 dB Thres		-10 dB Thres	
	Coast	Island	Coast	Island	Coast	Island
Gauss	30.0	30.0	24.4	24.4	54.8	54.8
rSIR	78.8	88.4	63.7	77.6	143.4	109.5
ideal GRD	36.2	36.2	30.3	30.3	54.5	54.5
GRD	110.3	27.8	93.2	23.4	165.2	40.3

Table 37: Resolution estimates for SMMR channel 10V LTOD M

Algorithm	-3 dB Thres		-2 dB Thres		-10 dB Thres	
	Coast	Island	Coast	Island	Coast	Island
Gauss	30.0	30.0	24.4	24.4	54.8	54.8
rSIR	72.9	58.4	69.3	52.3	88.3	95.6
ideal GRD	36.2	36.2	30.3	30.3	54.5	54.5
GRD	88.8	40.3	75.6	33.0	129.4	158.5

Table 38: Resolution estimates for SMMR channel 18H LTOD E

Algorithm	-3 dB Thres		-2 dB Thres		-10 dB Thres	
	Coast	Island	Coast	Island	Coast	Island
Gauss	30.0	30.0	24.4	24.4	54.8	54.8
rSIR	56.8	60.6	43.1	46.9	101.5	91.8
ideal GRD	36.2	36.2	30.3	30.3	54.5	54.5
GRD	71.8	30.0	56.6	25.2	124.5	44.3

Table 39: Resolution estimates for SMMR channel 18H LTOD M

Algorithm	-3 dB Thres		-2 dB Thres		-10 dB Thres	
	Coast	Island	Coast	Island	Coast	Island
Gauss	30.0	30.0	24.4	24.4	54.8	54.8
rSIR	57.7	39.8	48.4	36.6	89.9	51.0
ideal GRD	36.2	36.2	30.3	30.3	54.5	54.5
GRD	80.8	38.6	72.1	31.9	109.5	62.9

Table 40: Resolution estimates for SMMR channel 18V LTOD E

Algorithm	-3 dB Thres		-2 dB Thres		-10 dB Thres	
	Coast	Island	Coast	Island	Coast	Island
Gauss	30.0	30.0	24.4	24.4	54.8	54.8
rSIR	64.1	62.6	53.8	56.0	107.1	80.9
ideal GRD	36.2	36.2	30.3	30.3	54.5	54.5
GRD	67.0	40.4	56.4	33.1	99.3	91.0

Table 41: Resolution estimates for SMMR channel 18V LTOD M

Algorithm	-3 dB Thres		-2 dB Thres		-10 dB Thres	
	Coast	Island	Coast	Island	Coast	Island
Gauss	30.0	30.0	24.4	24.4	54.8	54.8
rSIR	50.5	53.9	45.1	21.2	92.8	99.7
ideal GRD	36.2	36.2	30.3	30.3	54.5	54.5
GRD	73.3	45.0	63.6	36.7	102.4	141.8

Table 42: Resolution estimates for SMMR channel 21H LTOD E

Algorithm	-3 dB Thres		-2 dB Thres		-10 dB Thres	
	Coast	Island	Coast	Island	Coast	Island
Gauss	35.9	35.9	29.3	29.3	65.5	65.5
rSIR	28.8	26.8	23.3	21.9	48.3	44.7
ideal GRD	43.4	43.4	36.3	36.3	65.4	65.4
GRD	47.1	48.8	39.2	40.9	72.7	71.2

Table 43: Resolution estimates for SMMR channel 21H LTOD M

Algorithm	-3 dB Thres		-2 dB Thres		-10 dB Thres	
	Coast	Island	Coast	Island	Coast	Island
Gauss	35.9	35.9	29.3	29.3	65.5	65.5
rSIR	28.0	34.0	22.9	25.7	74.1	75.4
ideal GRD	43.4	43.4	36.3	36.3	65.4	65.4
GRD	45.4	45.5	37.8	38.1	70.2	68.6

Table 44: Resolution estimates for SMMR channel 21V LTOD E

Algorithm	-3 dB Thres		-2 dB Thres		-10 dB Thres	
	Coast	Island	Coast	Island	Coast	Island
Gauss	35.9	35.9	29.3	29.3	65.5	65.5
rSIR	22.3	16.7	18.4	14.0	52.4	24.8
ideal GRD	43.4	43.4	36.3	36.3	65.4	65.4
GRD	62.1	47.2	50.5	39.4	97.8	72.9

Table 45: Resolution estimates for SMMR channel 21V LTOD M

Algorithm	-3 dB Thres		-2 dB Thres		-10 dB Thres	
	Coast	Island	Coast	Island	Coast	Island
Gauss	35.9	35.9	29.3	29.3	65.5	65.5
rSIR	26.8	39.1	21.2	30.8	65.7	72.7
ideal GRD	43.4	43.4	36.3	36.3	65.4	65.4
GRD	38.0	43.6	31.9	36.4	55.2	66.3

Table 46: Resolution estimates for SMMR channel 37H LTOD E

Algorithm	-3 dB Thres		-2 dB Thres		-10 dB Thres	
	Coast	Island	Coast	Island	Coast	Island
Gauss	30.0	30.0	24.4	24.4	54.8	54.8
rSIR	35.3	26.4	28.5	20.2	56.7	61.4
ideal GRD	36.2	36.2	30.3	30.3	54.5	54.5
GRD	39.5	39.3	32.7	32.7	62.9	61.2

Table 47: Resolution estimates for SMMR channel 37H LTOD M

Algorithm	-3 dB Thres		-2 dB Thres		-10 dB Thres	
	Coast	Island	Coast	Island	Coast	Island
Gauss	30.0	30.0	24.4	24.4	54.8	54.8
rSIR	22.6	34.9	18.0	29.9	60.9	79.9
ideal GRD	36.2	36.2	30.3	30.3	54.5	54.5
GRD	40.1	38.0	33.3	31.7	63.5	58.5

Table 48: Resolution estimates for SMMR channel 37V LTOD E

Algorithm	-3 dB Thres		-2 dB Thres		-10 dB Thres	
	Coast	Island	Coast	Island	Coast	Island
Gauss	30.0	30.0	24.4	24.4	54.8	54.8
rSIR	36.2	28.4	28.3	22.4	55.4	57.4
ideal GRD	36.2	36.2	30.3	30.3	54.5	54.5
GRD	38.5	43.4	31.8	36.3	63.8	64.7

Table 49: Resolution estimates for SMMR channel 37V LTOD M

Algorithm	-3 dB Thres		-2 dB Thres		-10 dB Thres	
	Coast	Island	Coast	Island	Coast	Island
Gauss	30.0	30.0	24.4	24.4	54.8	54.8
rSIR	27.5	29.2	21.8	22.4	59.1	62.4
ideal GRD	36.2	36.2	30.3	30.3	54.5	54.5
GRD	45.7	43.2	37.7	35.2	76.9	117.2

Table 50: Resolution estimates for SSMIS channel 19H LTOD E

Algorithm	-3 dB Thres		-2 dB Thres		-10 dB Thres	
	Coast	Island	Coast	Island	Coast	Island
Gauss	30.0	30.0	24.4	24.4	54.8	54.8
rSIR	54.8	53.8	47.3	45.4	92.3	87.3
ideal GRD	36.2	36.2	30.3	30.3	54.5	54.5
GRD	66.5	73.6	56.9	61.4	96.4	125.0

Table 51: Resolution estimates for SSMIS channel 19H LTOD M

Algorithm	-3 dB Thres		-2 dB Thres		-10 dB Thres	
	Coast	Island	Coast	Island	Coast	Island
Gauss	30.0	30.0	24.4	24.4	54.8	54.8
rSIR	56.5	44.4	49.7	31.3	96.5	76.4
ideal GRD	36.2	36.2	30.3	30.3	54.5	54.5
GRD	52.8	72.2	43.3	60.3	86.4	104.9

Table 52: Resolution estimates for SSMIS channel 19V LTOD E

Algorithm	-3 dB Thres		-2 dB Thres		-10 dB Thres	
	Coast	Island	Coast	Island	Coast	Island
Gauss	30.0	30.0	24.4	24.4	54.8	54.8
rSIR	62.8	52.5	54.5	43.9	99.5	69.0
ideal GRD	36.2	36.2	30.3	30.3	54.5	54.5
GRD	70.4	67.3	60.1	57.0	100.0	102.9

Table 53: Resolution estimates for SSMIS channel 19V LTOD M

Algorithm	-3 dB Thres		-2 dB Thres		-10 dB Thres	
	Coast	Island	Coast	Island	Coast	Island
Gauss	30.0	30.0	24.4	24.4	54.8	54.8
rSIR	57.3	48.3	50.1	30.8	95.9	68.3
ideal GRD	36.2	36.2	30.3	30.3	54.5	54.5
GRD	59.6	60.1	50.2	49.7	87.6	93.9



Table 54: Resolution estimates for SSMIS channel 22V LTOD E

Algorithm	-3 dB Thres		-2 dB Thres		-10 dB Thres	
	Coast	Island	Coast	Island	Coast	Island
Gauss	30.0	30.0	24.4	24.4	54.8	54.8
rSIR	52.7	55.4	43.5	47.8	92.8	97.8
ideal GRD	36.2	36.2	30.3	30.3	54.5	54.5
GRD	61.8	62.0	51.9	50.7	95.2	104.0

Table 55: Resolution estimates for SSMIS channel 22V LTOD M

Algorithm	-3 dB Thres		-2 dB Thres		-10 dB Thres	
	Coast	Island	Coast	Island	Coast	Island
Gauss	30.0	30.0	24.4	24.4	54.8	54.8
rSIR	50.1	55.6	41.1	47.5	93.1	78.8
ideal GRD	36.2	36.2	30.3	30.3	54.5	54.5
GRD	53.3	94.6	43.9	86.8	86.4	116.3

Table 56: Resolution estimates for SSMIS channel 37H LTOD E

Algorithm	-3 dB Thres		-2 dB Thres		-10 dB Thres	
	Coast	Island	Coast	Island	Coast	Island
Gauss	30.0	30.0	24.4	24.4	54.8	54.8
rSIR	32.8	40.3	26.7	34.6	53.5	60.3
ideal GRD	36.2	36.2	30.3	30.3	54.5	54.5
GRD	59.1	41.8	51.2	34.1	81.1	136.9

Table 57: Resolution estimates for SSMIS channel 37H LTOD M

Algorithm	-3 dB Thres		-2 dB Thres		-10 dB Thres	
	Coast	Island	Coast	Island	Coast	Island
Gauss	30.0	30.0	24.4	24.4	54.8	54.8
rSIR	25.4	33.8	21.1	26.2	43.5	56.8
ideal GRD	36.2	36.2	30.3	30.3	54.5	54.5
GRD	36.4	55.4	30.3	44.5	56.8	107.8

Table 58: Resolution estimates for SSMIS channel 37V LTOD E

Algorithm	-3 dB Thres		-2 dB Thres		-10 dB Thres	
	Coast	Island	Coast	Island	Coast	Island
Gauss	30.0	30.0	24.4	24.4	54.8	54.8
rSIR	37.8	46.5	29.6	39.3	66.8	74.2
ideal GRD	36.2	36.2	30.3	30.3	54.5	54.5
GRD	66.8	60.8	52.3	52.1	105.8	85.8

Table 59: Resolution estimates for SSMIS channel 37V LTOD M

Algorithm	-3 dB Thres		-2 dB Thres		-10 dB Thres	
	Coast	Island	Coast	Island	Coast	Island
Gauss	30.0	30.0	24.4	24.4	54.8	54.8
rSIR	22.6	29.7	18.3	23.5	44.6	51.2
ideal GRD	36.2	36.2	30.3	30.3	54.5	54.5
GRD	36.5	47.6	30.8	39.1	52.5	82.6

Table 60: Resolution estimates for SSMIS channel 91H LTOD E

Algorithm	-3 dB Thres		-2 dB Thres		-10 dB Thres	
	Coast	Island	Coast	Island	Coast	Island
Gauss	30.0	30.0	24.4	24.4	54.8	54.8
rSIR	17.4	23.5	14.7	19.5	25.2	36.5
ideal GRD	36.2	36.2	30.3	30.3	54.5	54.5
GRD	35.8	35.4	30.1	28.9	53.1	129.6

Table 61: Resolution estimates for SSMIS channel 91H LTOD M

Algorithm	-3 dB Thres		-2 dB Thres		-10 dB Thres	
	Coast	Island	Coast	Island	Coast	Island
Gauss	30.0	30.0	24.4	24.4	54.8	54.8
rSIR	16.5	13.3	13.5	11.0	28.3	21.1
ideal GRD	36.2	36.2	30.3	30.3	54.5	54.5
GRD	25.5	32.3	21.5	27.2	36.4	47.1

Table 62: Resolution estimates for SSMIS channel 91V LTOD E

Algorithm	-3 dB Thres		-2 dB Thres		-10 dB Thres	
	Coast	Island	Coast	Island	Coast	Island
Gauss	30.0	30.0	24.4	24.4	54.8	54.8
rSIR	10.7	8.4	9.0	7.1	15.6	12.1
ideal GRD	36.2	36.2	30.3	30.3	54.5	54.5
GRD	38.0	107.6	30.9	42.6	75.3	121.4

Table 63: Resolution estimates for SSMIS channel 91V LTOD M

Algorithm	-3 dB Thres		-2 dB Thres		-10 dB Thres	
	Coast	Island	Coast	Island	Coast	Island
Gauss	30.0	30.0	24.4	24.4	54.8	54.8
rSIR	19.6	13.8	16.7	11.5	27.6	21.2
ideal GRD	36.2	36.2	30.3	30.3	54.5	54.5
GRD	31.7	34.9	26.4	29.0	48.0	54.3

Table 64: Resolution estimates for SSMI channel 19H LTOD E

Algorithm	-3 dB Thres		-2 dB Thres		-10 dB Thres	
	Coast	Island	Coast	Island	Coast	Island
Gauss	30.0	30.0	24.4	24.4	54.8	54.8
rSIR	58.1	46.4	45.3	40.7	111.5	73.4
ideal GRD	36.2	36.2	30.3	30.3	54.5	54.5
GRD	72.1	54.2	62.5	44.8	100.0	87.3

Table 65: Resolution estimates for SSMI channel 19H LTOD M

Algorithm	-3 dB Thres		-2 dB Thres		-10 dB Thres	
	Coast	Island	Coast	Island	Coast	Island
Gauss	30.0	30.0	24.4	24.4	54.8	54.8
rSIR	52.6	61.5	47.5	19.4	66.1	78.1
ideal GRD	36.2	36.2	30.3	30.3	54.5	54.5
GRD	49.1	70.7	40.8	65.1	75.9	86.3

Table 66: Resolution estimates for SSMI channel 19V LTOD E

Algorithm	-3 dB Thres		-2 dB Thres		-10 dB Thres	
	Coast	Island	Coast	Island	Coast	Island
Gauss	30.0	30.0	24.4	24.4	54.8	54.8
rSIR	58.6	51.4	44.8	44.1	112.0	68.7
ideal GRD	36.2	36.2	30.3	30.3	54.5	54.5
GRD	70.8	50.4	61.4	42.3	99.0	75.7

Table 67: Resolution estimates for SSMI channel 19V LTOD M

Algorithm	-3 dB Thres		-2 dB Thres		-10 dB Thres	
	Coast	Island	Coast	Island	Coast	Island
Gauss	30.0	30.0	24.4	24.4	54.8	54.8
rSIR	41.7	45.3	34.9	40.5	86.0	87.9
ideal GRD	36.2	36.2	30.3	30.3	54.5	54.5
GRD	60.2	89.3	49.5	81.9	94.1	114.0

Table 68: Resolution estimates for SSMI channel 37H LTOD E

Algorithm	-3 dB Thres		-2 dB Thres		-10 dB Thres	
	Coast	Island	Coast	Island	Coast	Island
Gauss	30.0	30.0	24.4	24.4	54.8	54.8
rSIR	22.2	35.4	17.4	27.0	53.1	57.1
ideal GRD	36.2	36.2	30.3	30.3	54.5	54.5
GRD	44.1	43.2	37.0	36.4	66.5	63.1

Table 69: Resolution estimates for SSMI channel 37H LTOD M

Algorithm	-3 dB Thres		-2 dB Thres		-10 dB Thres	
	Coast	Island	Coast	Island	Coast	Island
Gauss	30.0	30.0	24.4	24.4	54.8	54.8
rSIR	32.2	34.1	28.7	26.9	46.0	60.4
ideal GRD	36.2	36.2	30.3	30.3	54.5	54.5
GRD	53.3	46.1	43.9	38.8	84.4	67.7

Table 70: Resolution estimates for SSMI channel 37V LTOD E

Algorithm	-3 dB Thres		-2 dB Thres		-10 dB Thres	
	Coast	Island	Coast	Island	Coast	Island
Gauss	30.0	30.0	24.4	24.4	54.8	54.8
rSIR	22.8	28.7	17.8	21.9	52.2	50.8
ideal GRD	36.2	36.2	30.3	30.3	54.5	54.5
GRD	42.1	36.7	35.2	30.5	63.8	57.2

Table 71: Resolution estimates for SSMI channel 37V LTOD M

Algorithm	-3 dB Thres		-2 dB Thres		-10 dB Thres	
	Coast	Island	Coast	Island	Coast	Island
Gauss	30.0	30.0	24.4	24.4	54.8	54.8
rSIR	34.8	29.1	31.3	23.8	52.8	48.5
ideal GRD	36.2	36.2	30.3	30.3	54.5	54.5
GRD	70.9	63.9	65.9	57.7	84.4	80.9

Table 72: Resolution estimates for SSMI channel 85H LTOD E

Algorithm	-3 dB Thres		-2 dB Thres		-10 dB Thres	
	Coast	Island	Coast	Island	Coast	Island
Gauss	30.0	30.0	24.4	24.4	54.8	54.8
rSIR	17.5	19.6	14.4	16.0	28.3	39.3
ideal GRD	36.2	36.2	30.3	30.3	54.5	54.5
GRD	43.1	30.8	36.0	25.8	65.7	45.8

Table 73: Resolution estimates for SSMI channel 85H LTOD M

Algorithm	-3 dB Thres		-2 dB Thres		-10 dB Thres	
	Coast	Island	Coast	Island	Coast	Island
Gauss	30.0	30.0	24.4	24.4	54.8	54.8
rSIR	11.2	43.3	9.4	18.7	16.5	53.7
ideal GRD	36.2	36.2	30.3	30.3	54.5	54.5
GRD	24.8	26.4	20.9	22.2	35.9	37.9

Table 74: Resolution estimates for SSMI channel 85V LTOD E

Algorithm	-3 dB Thres		-2 dB Thres		-10 dB Thres	
	Coast	Island	Coast	Island	Coast	Island
Gauss	30.0	30.0	24.4	24.4	54.8	54.8
rSIR	14.7	15.0	12.2	12.4	23.6	24.5
ideal GRD	36.2	36.2	30.3	30.3	54.5	54.5
GRD	31.5	38.6	26.3	32.1	48.0	59.5

Table 75: Resolution estimates for SSMI channel 85V LTOD M

Algorithm	-3 dB Thres		-2 dB Thres		-10 dB Thres	
	Coast	Island	Coast	Island	Coast	Island
Gauss	30.0	30.0	24.4	24.4	54.8	54.8
rSIR	17.5	16.1	14.6	13.4	26.0	25.2
ideal GRD	36.2	36.2	30.3	30.3	54.5	54.5
GRD	36.7	44.3	30.4	36.8	60.7	68.3

## C AMSRE Figures

### C.1 AMSRE Channel 06H E Figures

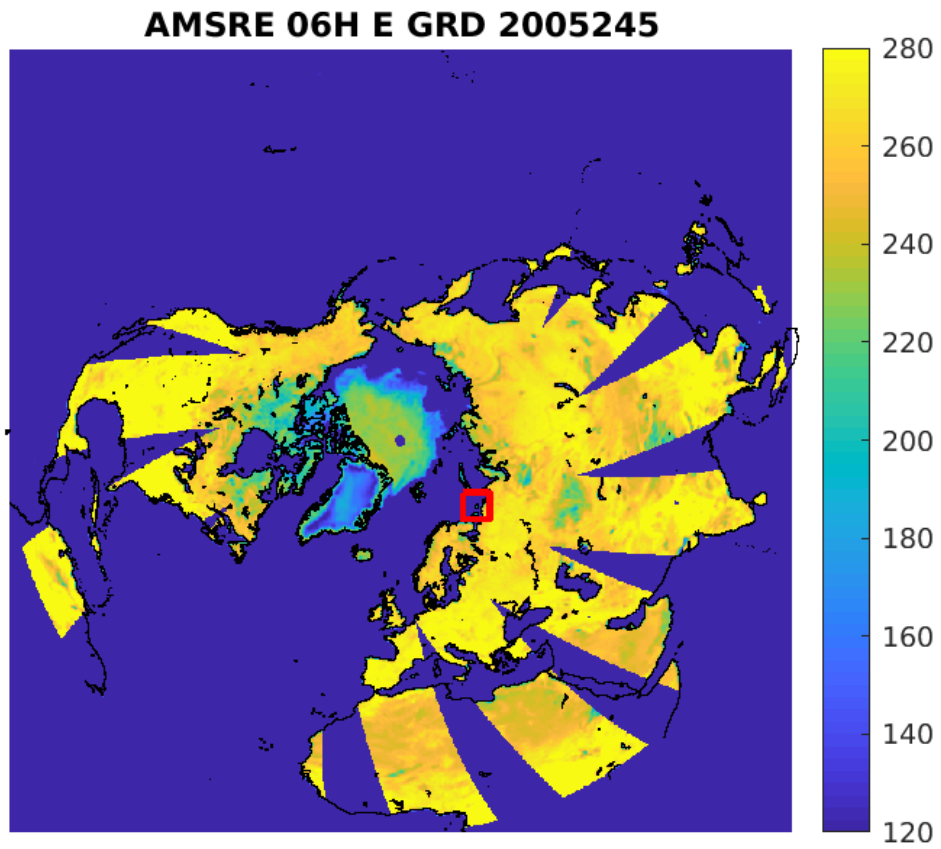


Figure 11: rSIR Northern Hemisphere view.

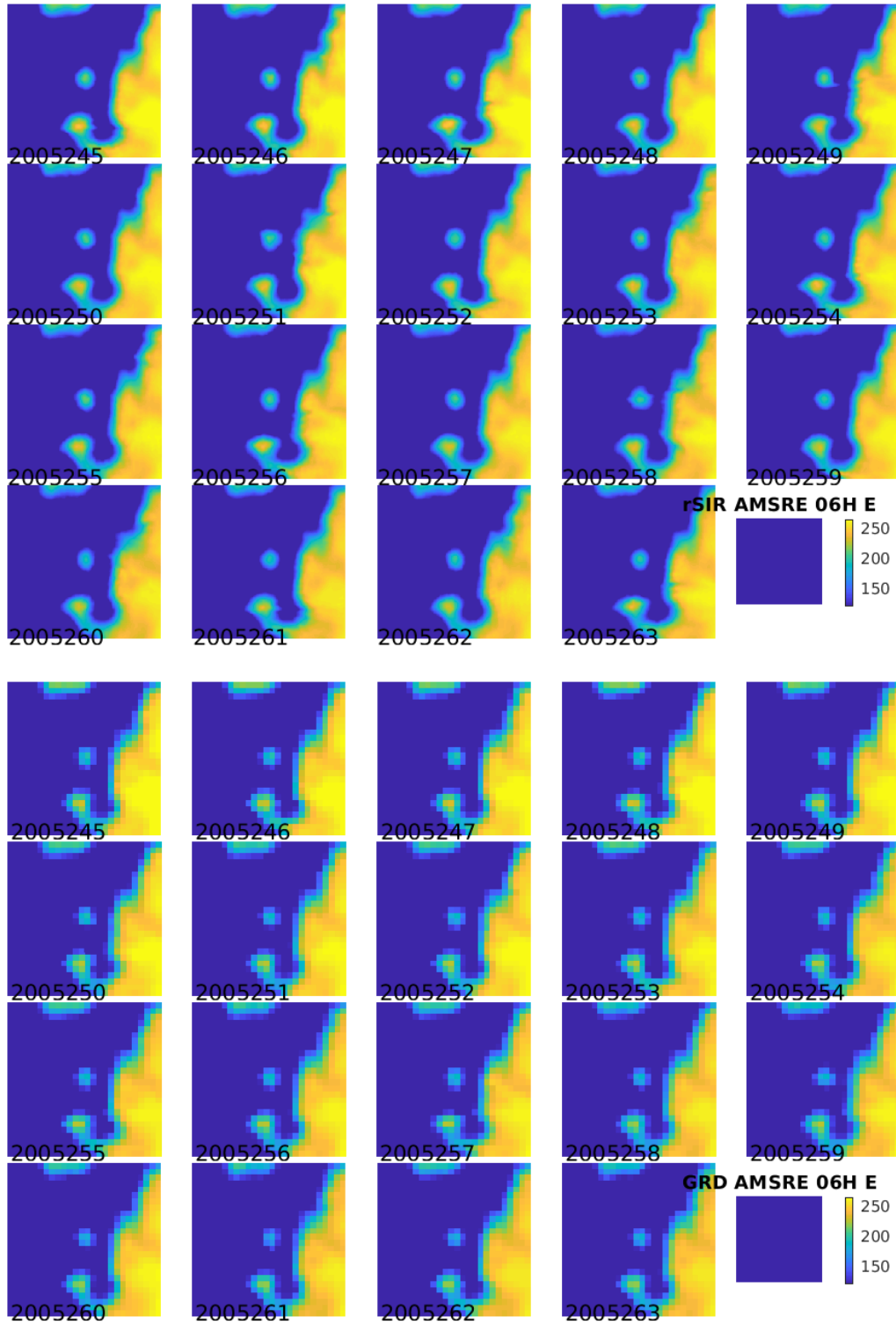


Figure 12: Time series of (top) rSIR and (bottom) GRD  $T_B$  images over the study area. Image dates are labeled on the image.



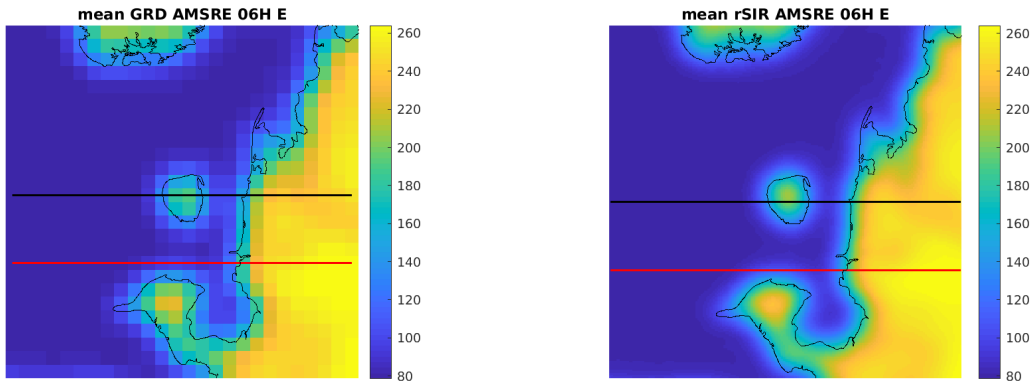


Figure 13: Average of daily  $T_B$  images over the study area. (left) 25-km GRD. (right) 3.125-km rSIR. The thick horizontal lines show the data transect locations where data is extracted from the image for analysis.

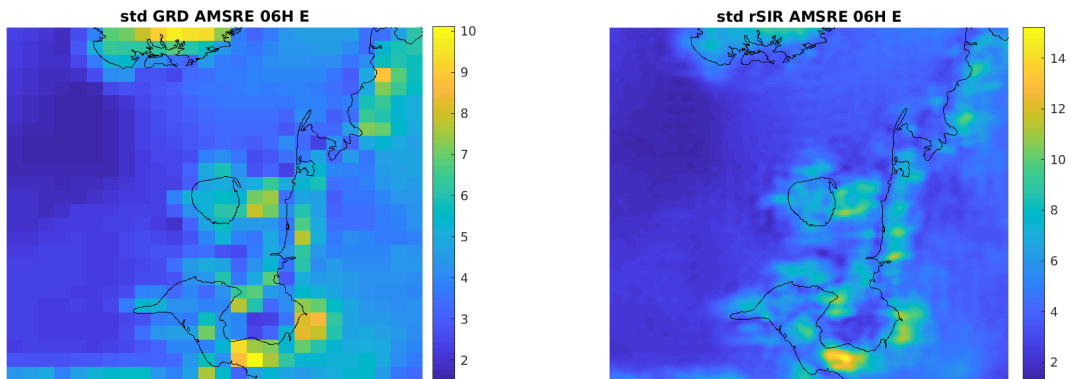


Figure 14: Standard deviation of daily  $T_B$  images over the study area. (left) 25-km GRD. (right) 3.125-km rSIR.

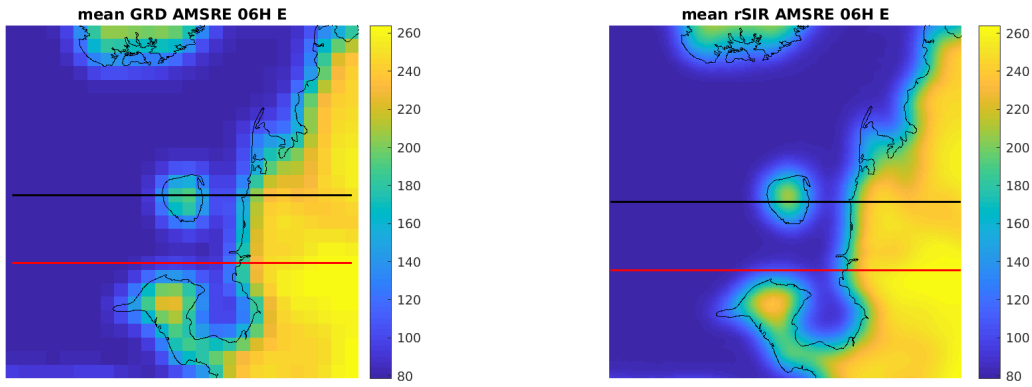


Figure 15: [Repeated] Average of daily  $T_B$  images over the study area. (left) 25-km GRD. (right) 3.125-km rSIR. The thick horizontal lines show the data transect locations where data is extracted from the image for analysis.

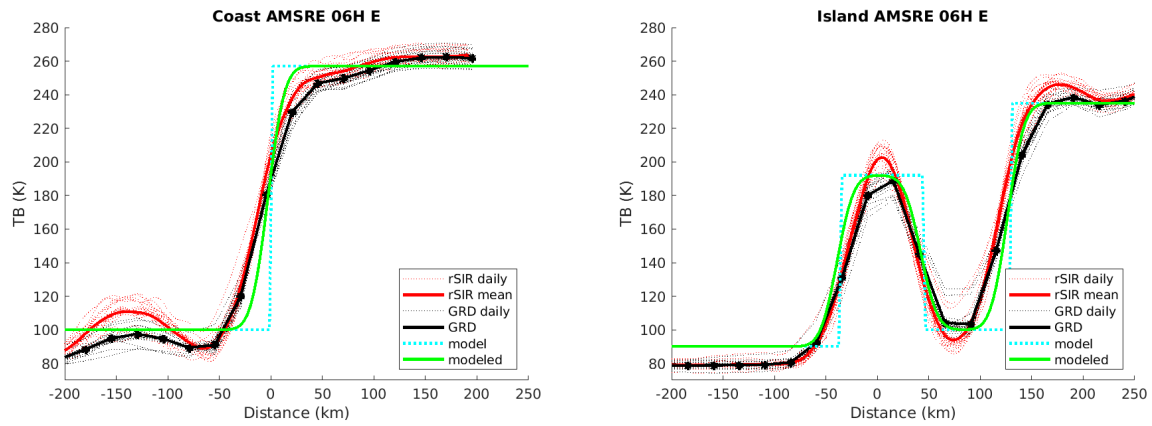


Figure 16: Plots of  $T_B$  along the two analysis case transect lines for the (left) coast-crossing and (right) island-crossing cases.

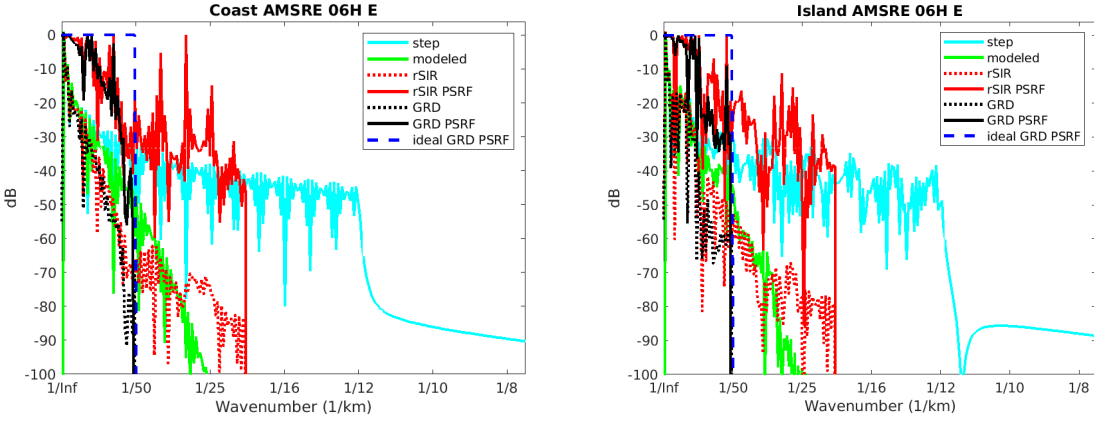


Figure 17: Wavenumber spectra of the  $T_B$  slices, the model, and the PSRF. (left) Coast-crossing case. (right) Island-crossing case.

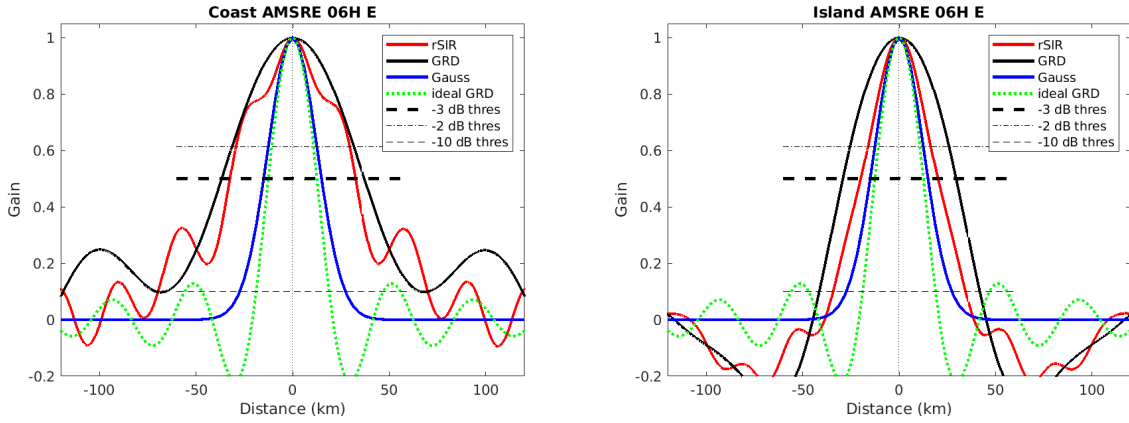


Figure 18: Derived single-pass rSIR and GRD PSRFs from the (left) coast-crossing and (right) island-crossing cases.

Table 76: Resolution estimates for AMSRE channel 06H LTOD E

Algorithm	-3 dB Thres		-2 dB Thres		-10 dB Thres	
	Coast	Island	Coast	Island	Coast	Island
Gauss	30.0	30.0	24.4	24.4	54.8	54.8
rSIR	65.0	40.0	57.8	31.6	139.5	68.8
ideal GRD	36.2	36.2	30.3	30.3	54.5	54.5
GRD	73.8	58.7	61.4	50.1	133.4	83.1

## C.2 AMSRE Channel 06H M Figures

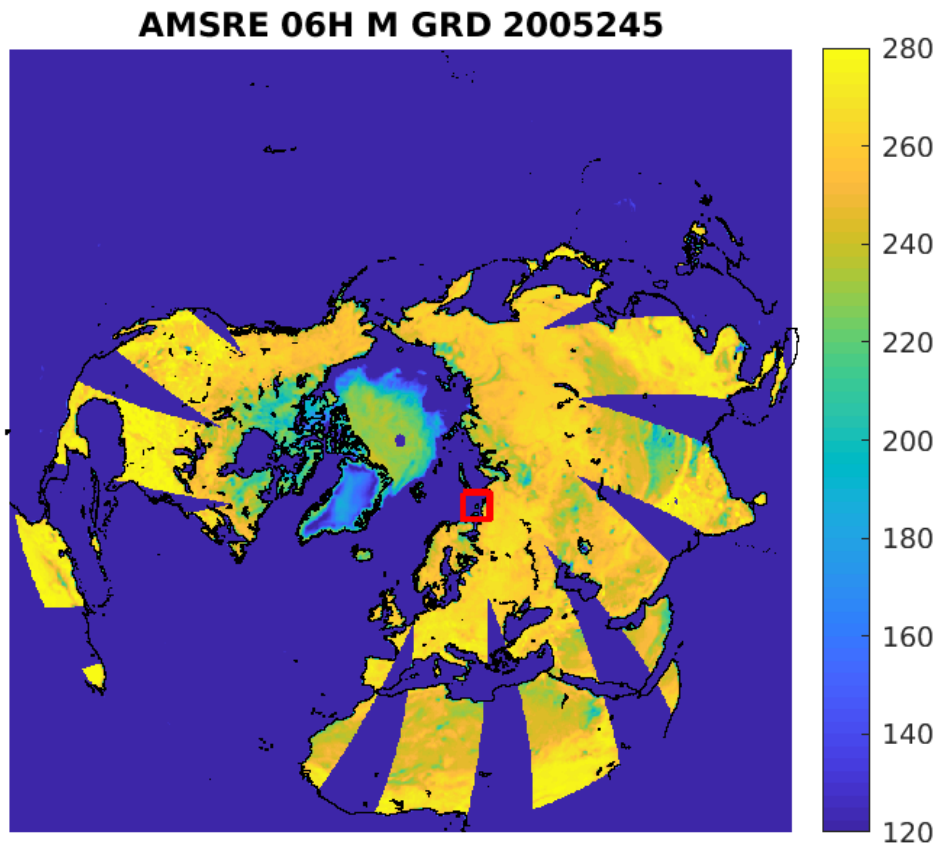


Figure 19: rSIR Northern Hemisphere view.

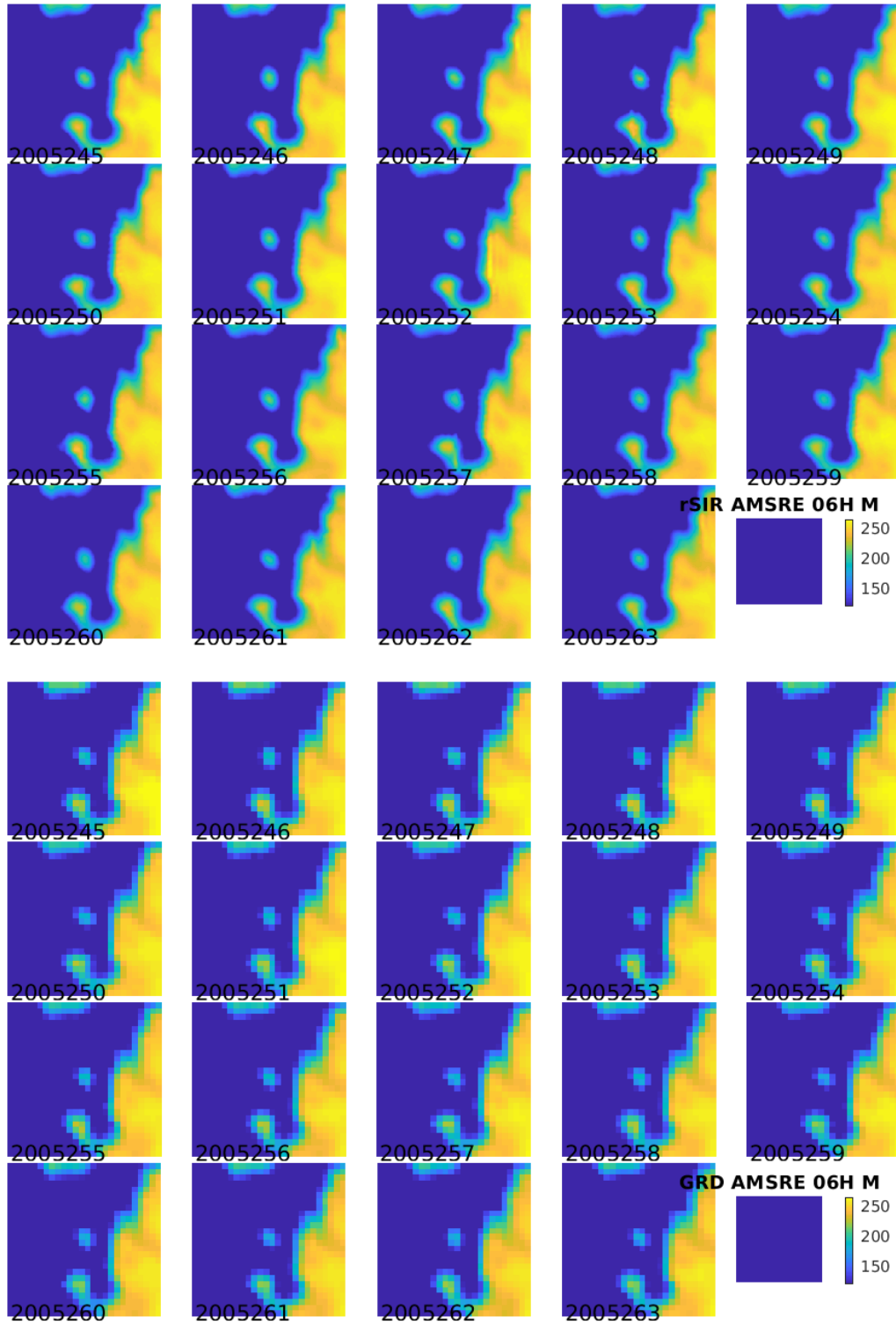


Figure 20: Time series of (top) rSIR and (bottom) GRD  $T_B$  images over the study area. Image dates are labeled on the image.

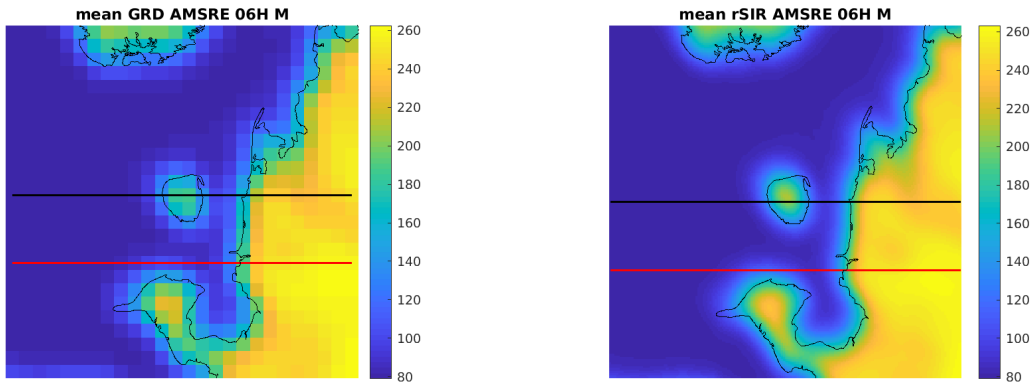


Figure 21: Average of daily  $T_B$  images over the study area. (left) 25-km GRD. (right) 3.125-km rSIR. The thick horizontal lines show the data transect locations where data is extracted from the image for analysis.

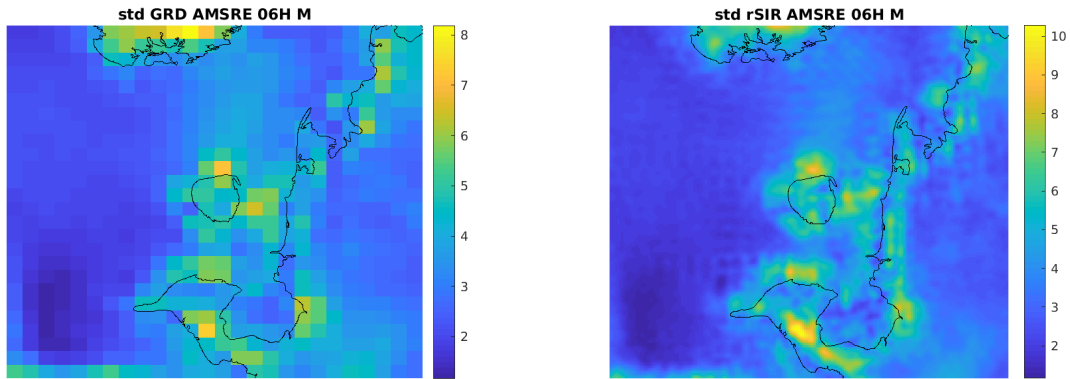


Figure 22: Standard deviation of daily  $T_B$  images over the study area. (left) 25-km GRD. (right) 3.125-km rSIR.

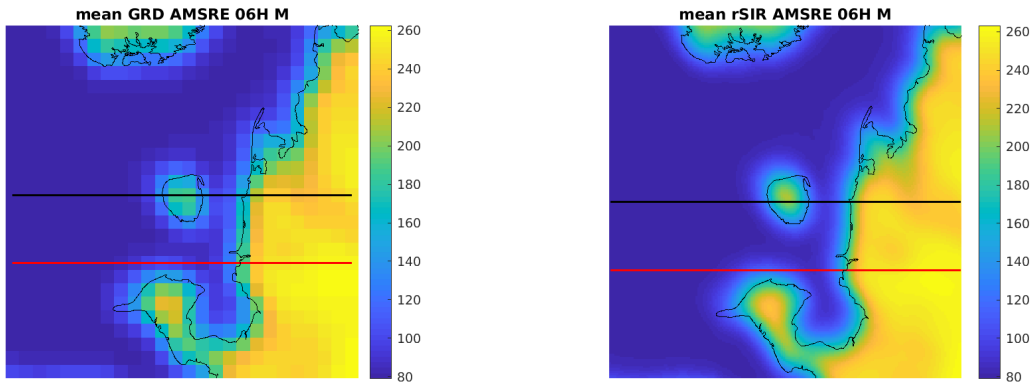


Figure 23: [Repeated] Average of daily  $T_B$  images over the study area. (left) 25-km GRD. (right) 3.125-km rSIR. The thick horizontal lines show the data transect locations where data is extracted from the image for analysis.

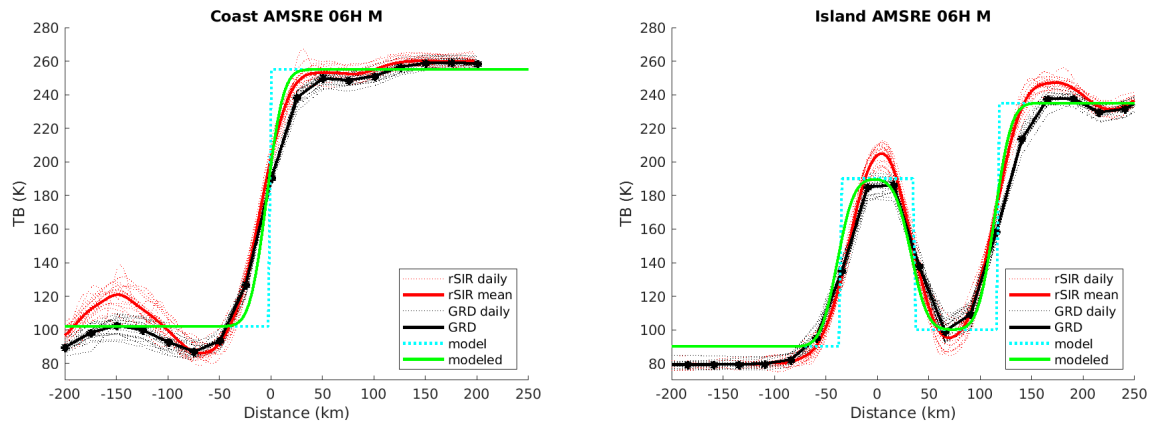


Figure 24: Plots of  $T_B$  along the two analysis case transect lines for the (left) coast-crossing and (right) island-crossing cases.

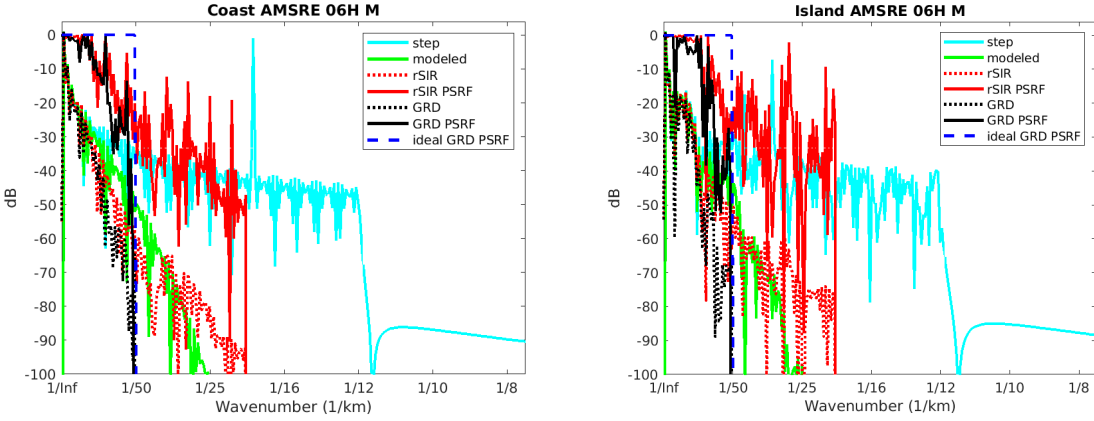


Figure 25: Wavenumber spectra of the  $T_B$  slices, the model, and the PSRF. (left) Coast-crossing case. (right) Island-crossing case.

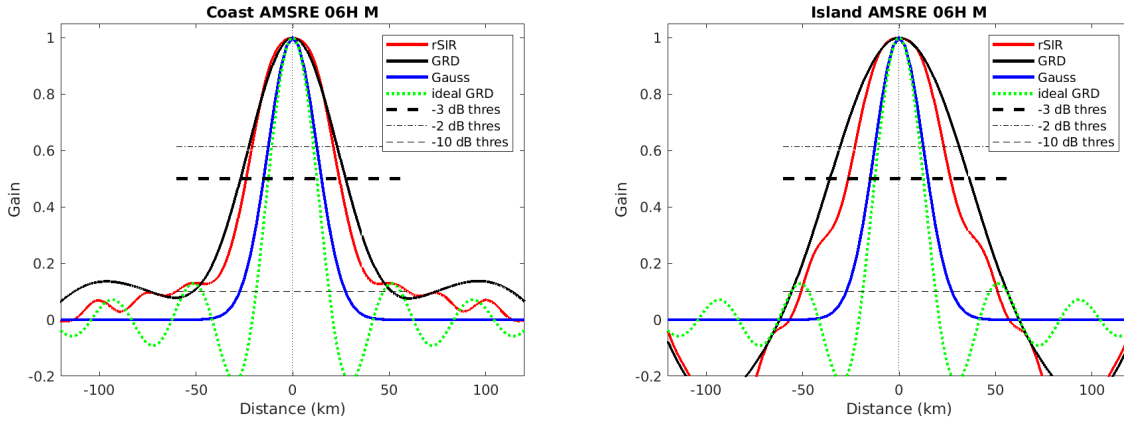


Figure 26: Derived single-pass rSIR and GRD PSRFs from the (left) coast-crossing and (right) island-crossing cases.

Table 77: Resolution estimates for AMSRE channel 06H LTOD M

Algorithm	-3 dB Thres		-2 dB Thres		-10 dB Thres	
	Coast	Island	Coast	Island	Coast	Island
Gauss	30.0	30.0	24.4	24.4	54.8	54.8
rSIR	48.3	53.0	41.2	45.0	120.4	102.0
ideal GRD	36.2	36.2	30.3	30.3	54.5	54.5
GRD	54.4	72.2	44.5	60.1	103.0	111.6



### C.3 AMSRE Channel 06V E Figures

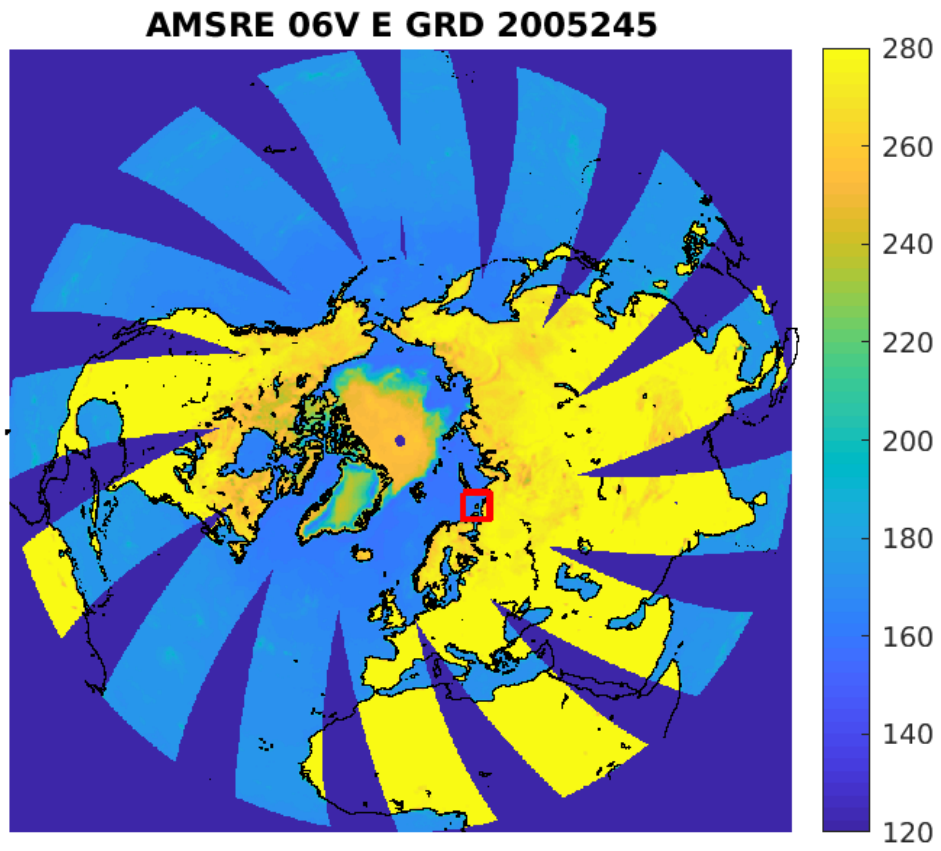


Figure 27: rSIR Northern Hemisphere view.

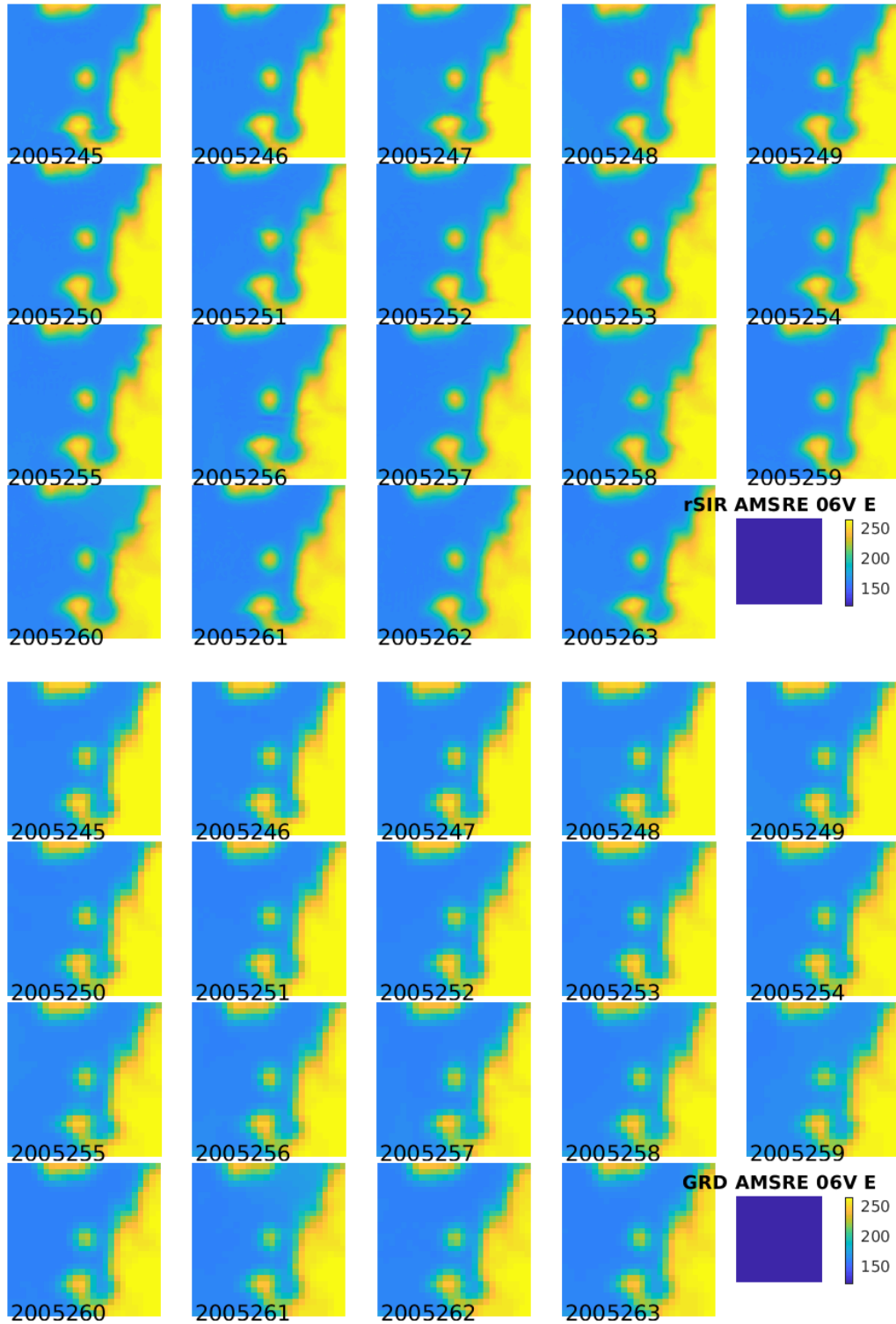


Figure 28: Time series of (top) rSIR and (bottom) GRD  $T_B$  images over the study area. Image dates are labeled on the image.

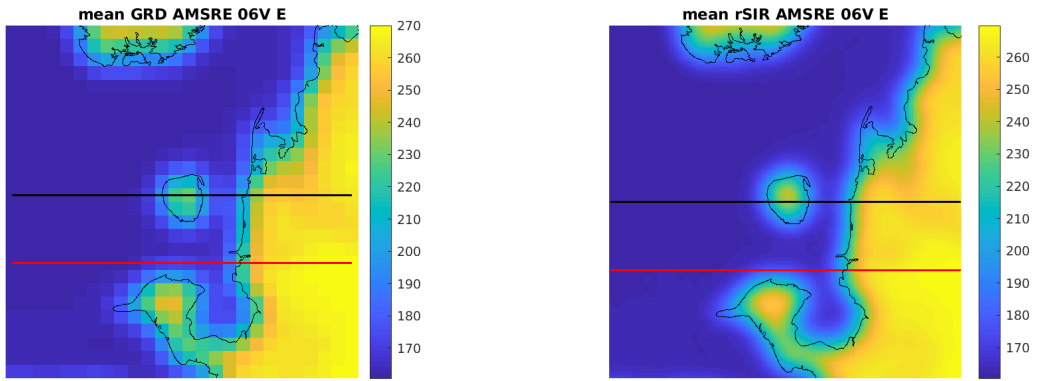


Figure 29: Average of daily  $T_B$  images over the study area. (left) 25-km GRD. (right) 3.125-km rSIR. The thick horizontal lines show the data transect locations where data is extracted from the image for analysis.

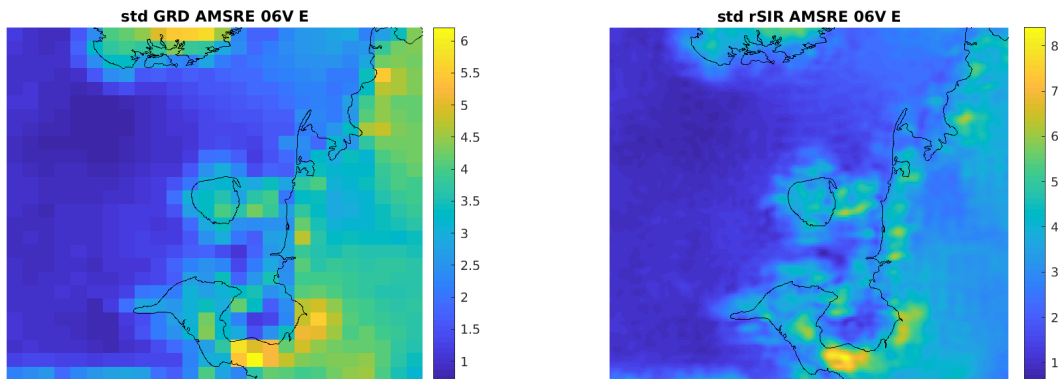


Figure 30: Standard deviation of daily  $T_B$  images over the study area. (left) 25-km GRD. (right) 3.125-km rSIR.

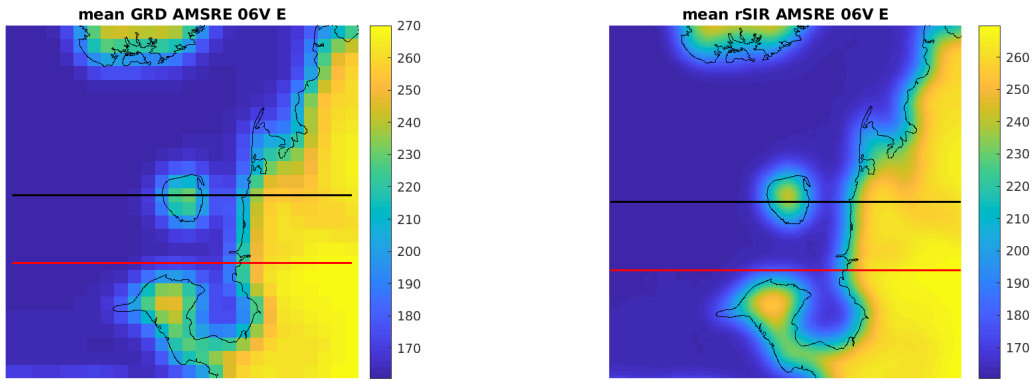


Figure 31: [Repeated] Average of daily  $T_B$  images over the study area. (left) 25-km GRD. (right) 3.125-km rSIR. The thick horizontal lines show the data transect locations where data is extracted from the image for analysis.

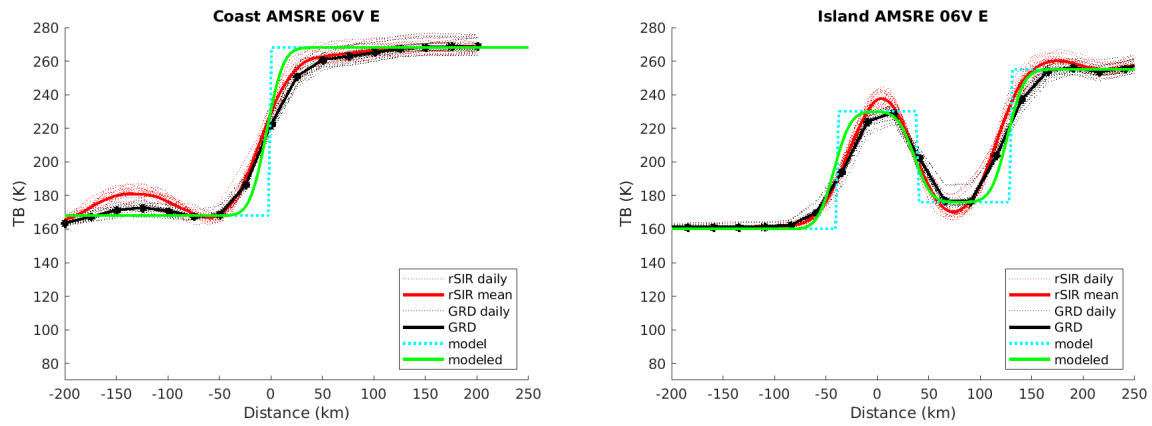


Figure 32: Plots of  $T_B$  along the two analysis case transect lines for the (left) coast-crossing and (right) island-crossing cases.

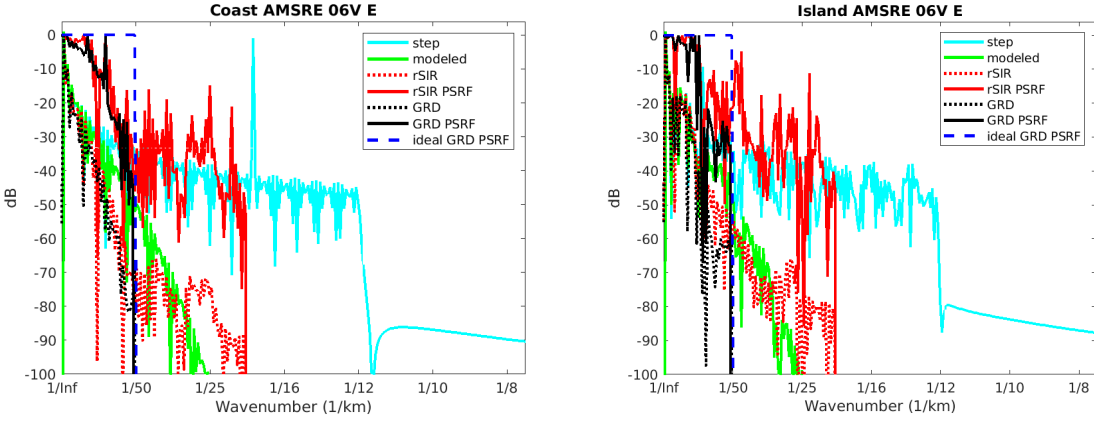


Figure 33: Wavenumber spectra of the  $T_B$  slices, the model, and the PSRF. (left) Coast-crossing case. (right) Island-crossing case.

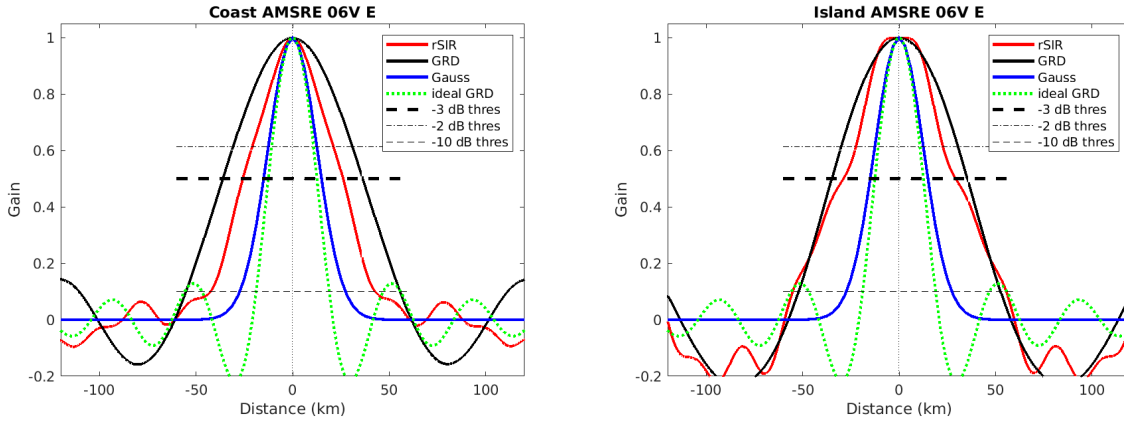


Figure 34: Derived single-pass rSIR and GRD PSRFs from the (left) coast-crossing and (right) island-crossing cases.

Table 78: Resolution estimates for AMSRE channel 06V LTOD E

Algorithm	-3 dB Thres		-2 dB Thres		-10 dB Thres	
	Coast	Island	Coast	Island	Coast	Island
Gauss	30.0	30.0	24.4	24.4	54.8	54.8
rSIR	51.9	58.2	40.5	43.7	85.2	110.6
ideal GRD	36.2	36.2	30.3	30.3	54.5	54.5
GRD	72.4	70.3	60.0	59.1	110.8	104.7

## C.4 AMSRE Channel 06V M Figures

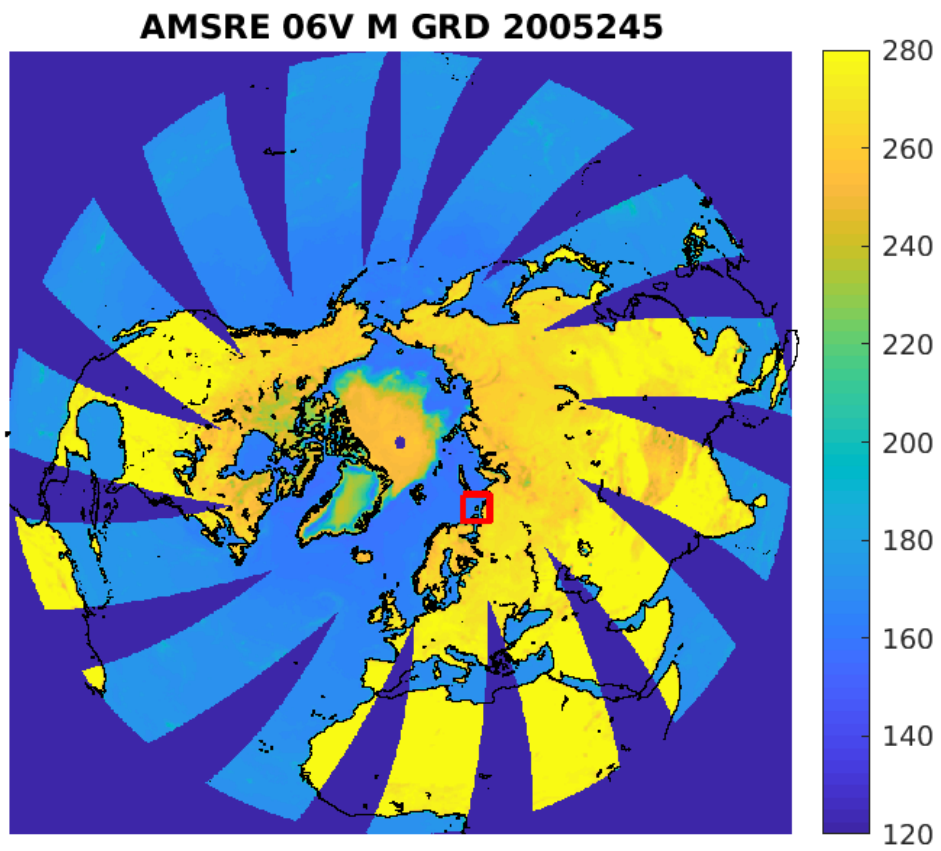


Figure 35: rSIR Northern Hemisphere view.

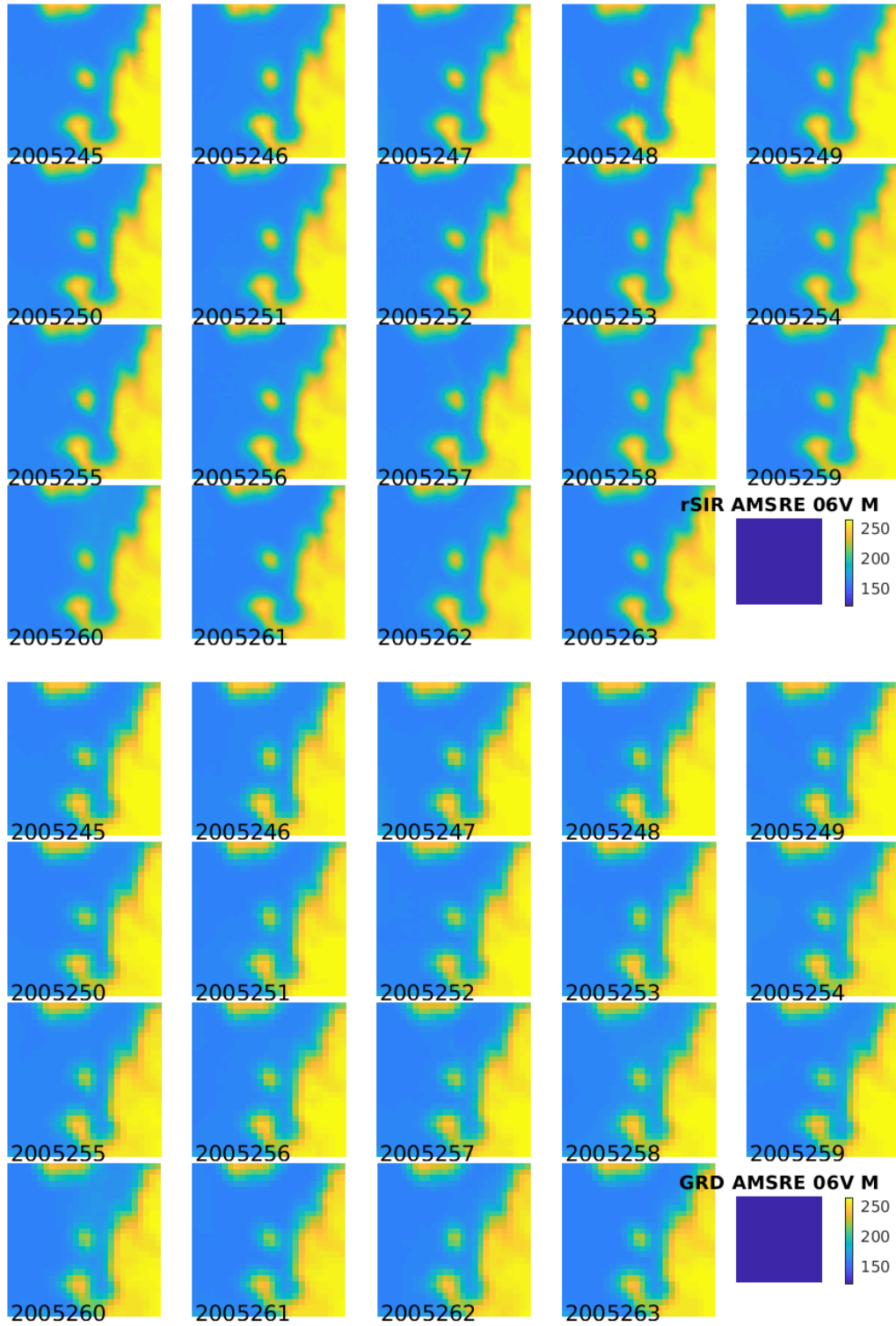


Figure 36: Time series of (top) rSIR and (bottom) GRD  $T_B$  images over the study area. Image dates are labeled on the image.

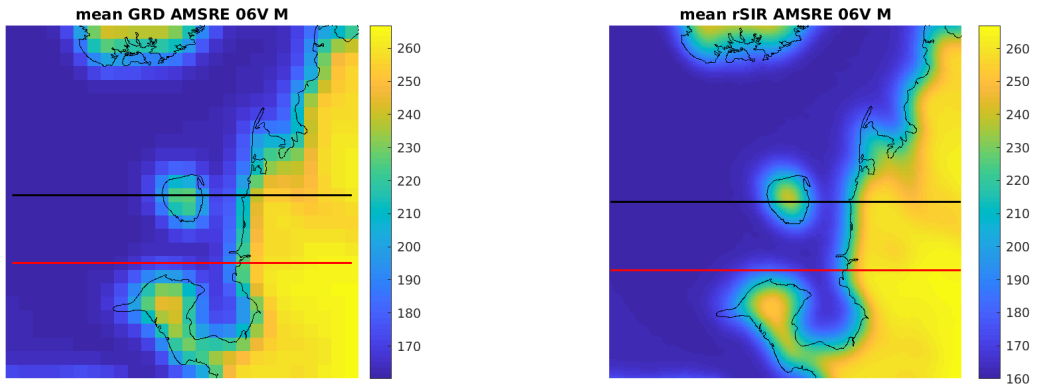


Figure 37: Average of daily  $T_B$  images over the study area. (left) 25-km GRD. (right) 3.125-km rSIR. The thick horizontal lines show the data transect locations where data is extracted from the image for analysis.

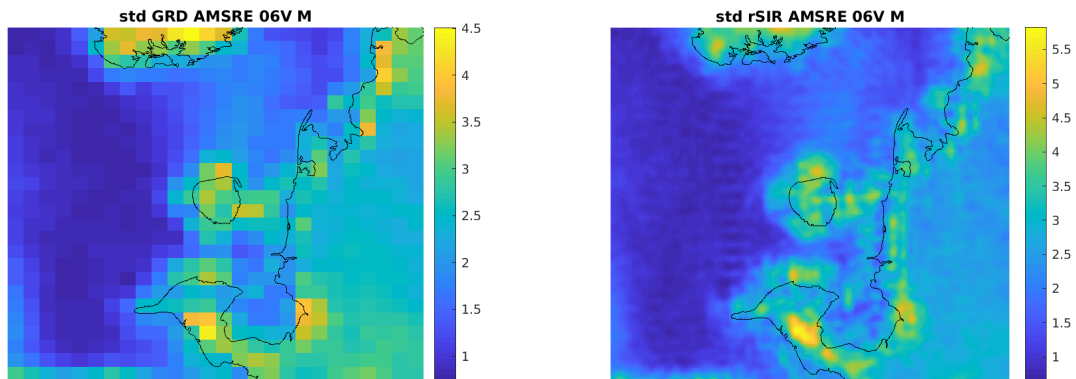


Figure 38: Standard deviation of daily  $T_B$  images over the study area. (left) 25-km GRD. (right) 3.125-km rSIR.



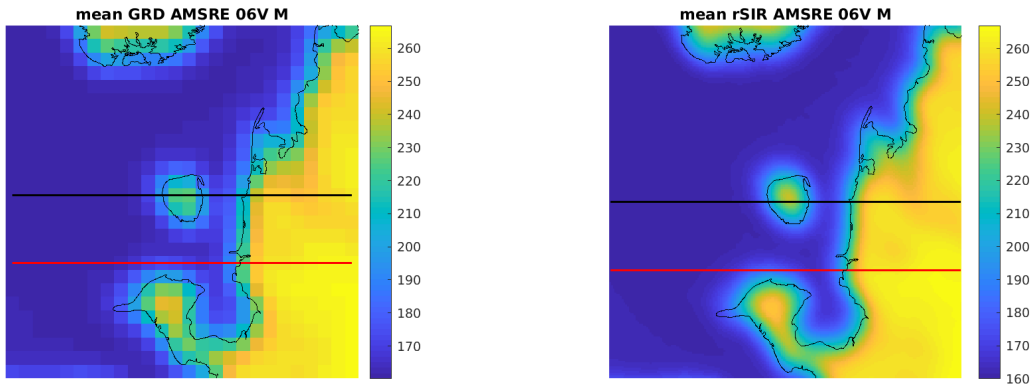


Figure 39: [Repeated] Average of daily  $T_B$  images over the study area. (left) 25-km GRD. (right) 3.125-km rSIR. The thick horizontal lines show the data transect locations where data is extracted from the image for analysis.

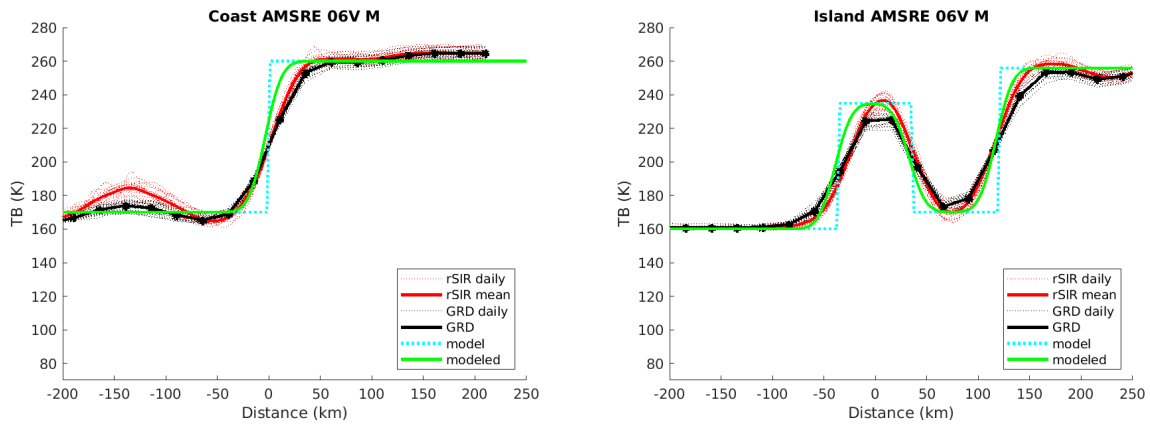


Figure 40: Plots of  $T_B$  along the two analysis case transect lines for the (left) coast-crossing and (right) island-crossing cases.

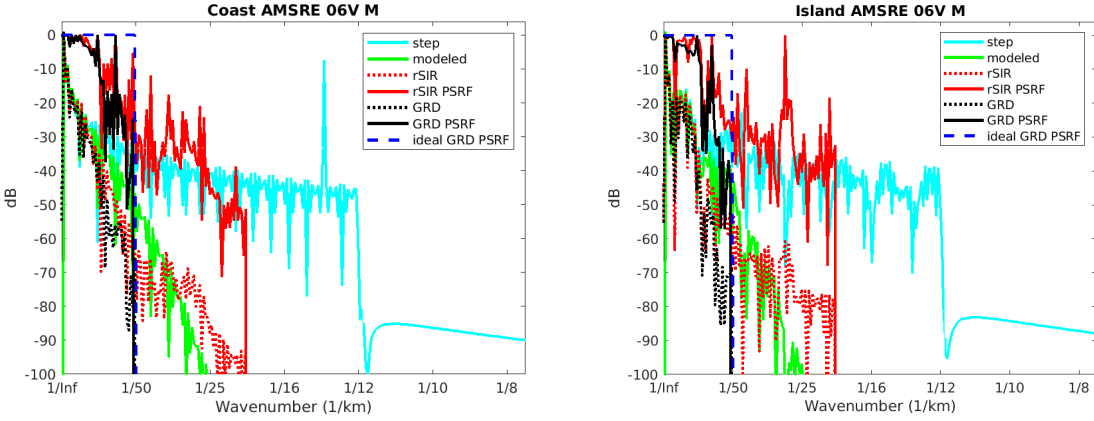


Figure 41: Wavenumber spectra of the  $T_B$  slices, the model, and the PSRF. (left) Coast-crossing case. (right) Island-crossing case.

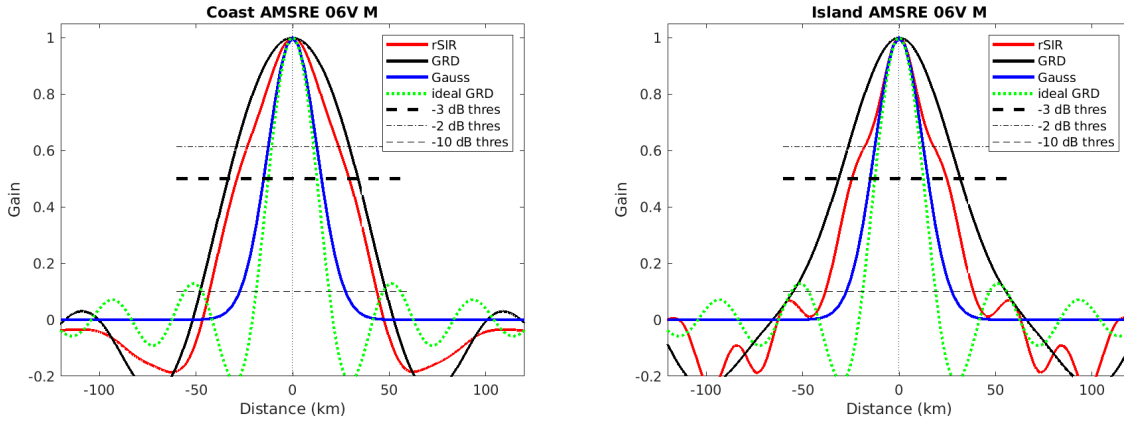


Figure 42: Derived single-pass rSIR and GRD PSRFs from the (left) coast-crossing and (right) island-crossing cases.

Table 79: Resolution estimates for AMSRE channel 06V LTOD M

Algorithm	-3 dB Thres		-2 dB Thres		-10 dB Thres	
	Coast	Island	Coast	Island	Coast	Island
Gauss	30.0	30.0	24.4	24.4	54.8	54.8
rSIR	58.1	49.2	45.4	33.4	86.7	76.6
ideal GRD	36.2	36.2	30.3	30.3	54.5	54.5
GRD	67.3	63.1	57.1	51.7	96.2	110.2

## C.5 AMSRE Channel 10.7H E Figures

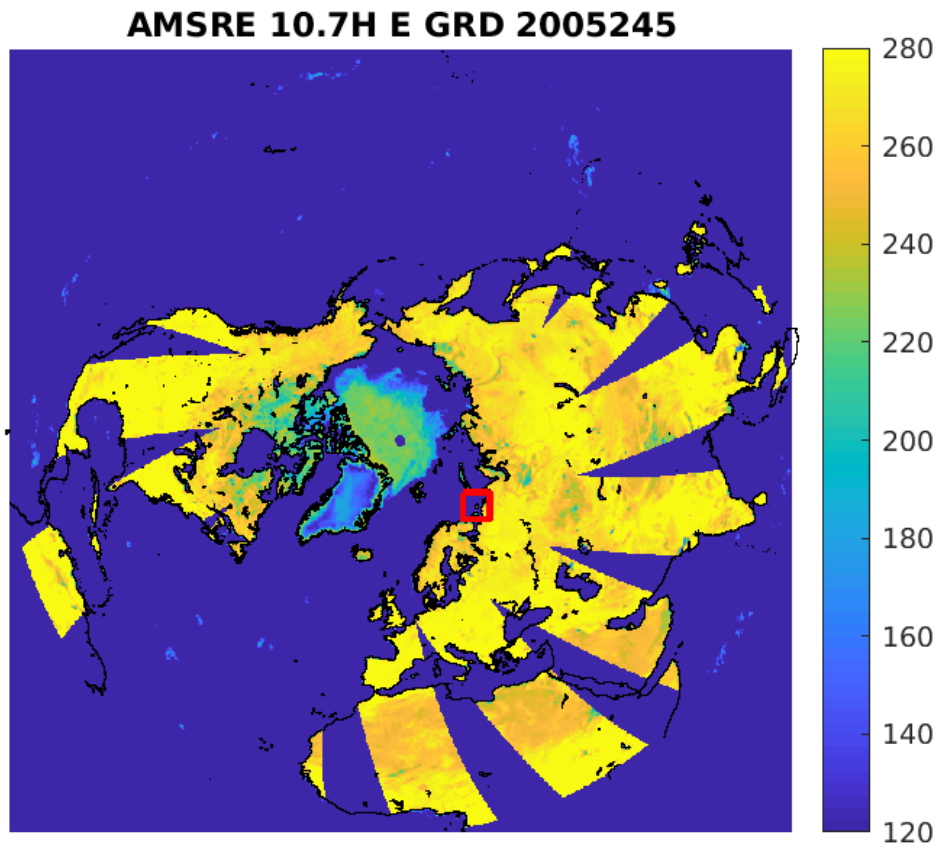


Figure 43: rSIR Northern Hemisphere view.

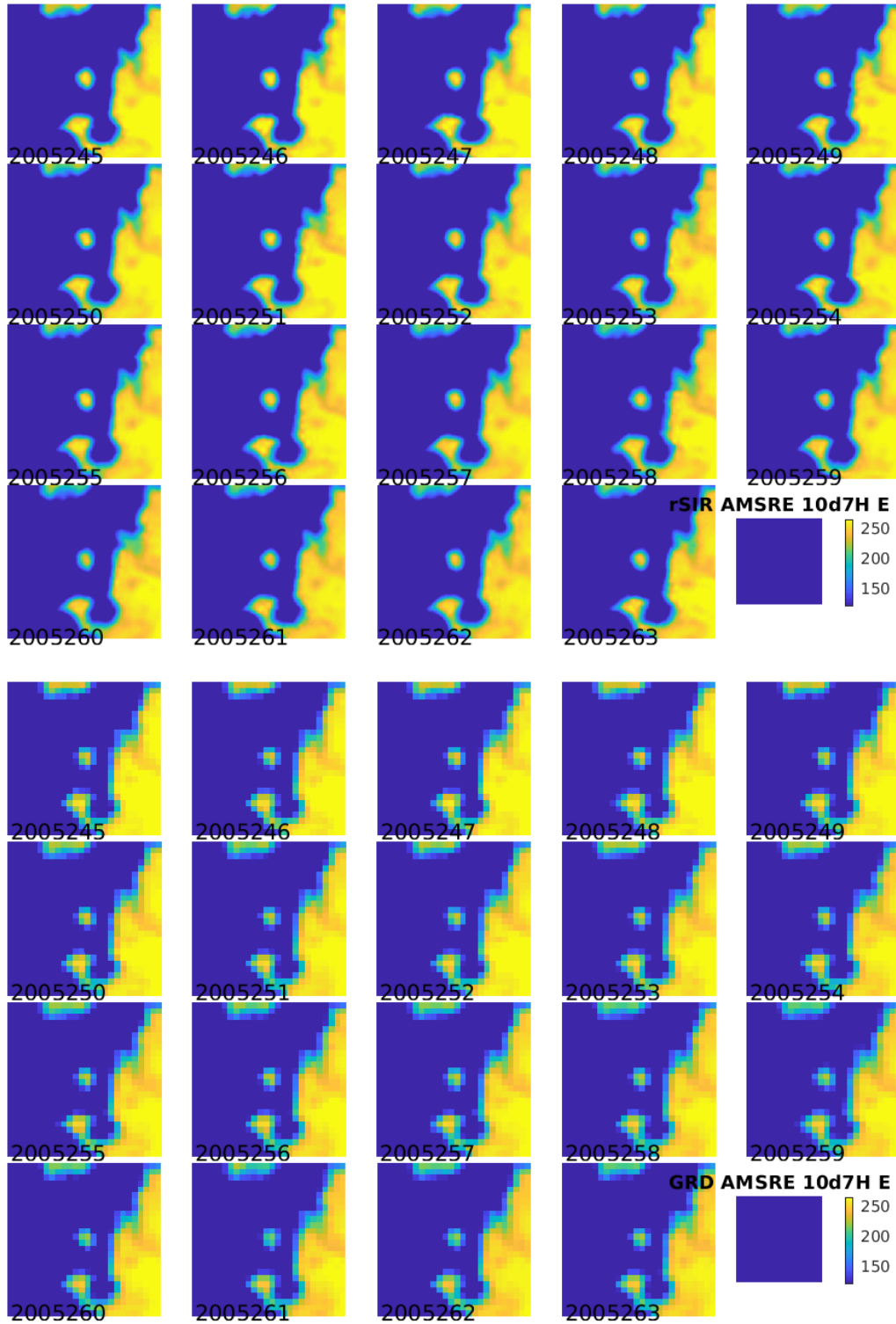


Figure 44: Time series of (top) rSIR and (bottom) GRD  $T_B$  images over the study area. Image dates are labeled on the image.

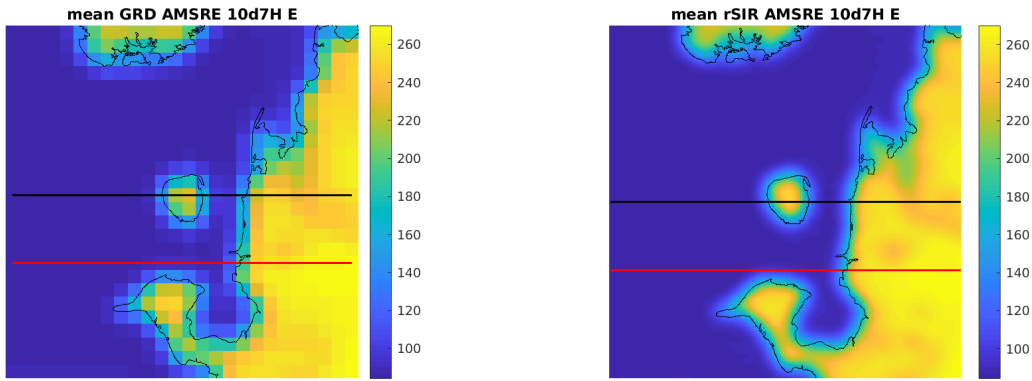


Figure 45: Average of daily  $T_B$  images over the study area. (left) 25-km GRD. (right) 3.125-km rSIR. The thick horizontal lines show the data transect locations where data is extracted from the image for analysis.

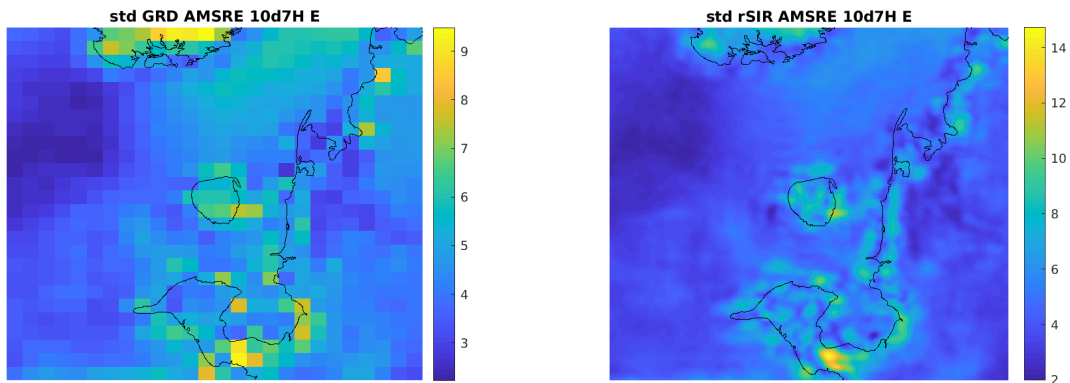


Figure 46: Standard deviation of daily  $T_B$  images over the study area. (left) 25-km GRD. (right) 3.125-km rSIR.

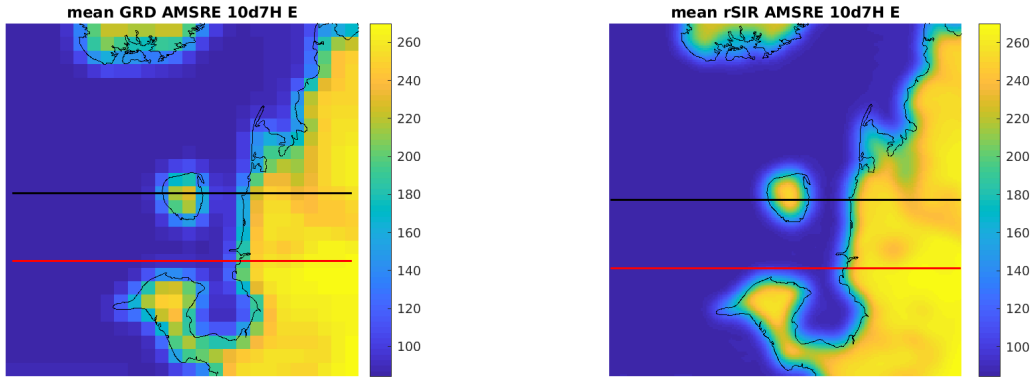


Figure 47: [Repeated] Average of daily  $T_B$  images over the study area. (left) 25-km GRD. (right) 3.125-km rSIR. The thick horizontal lines show the data transect locations where data is extracted from the image for analysis.

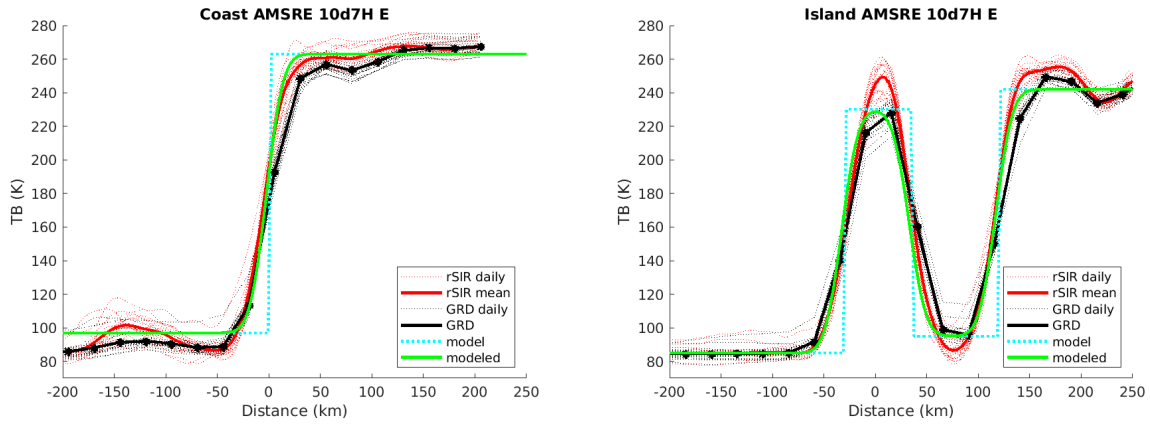


Figure 48: Plots of  $T_B$  along the two analysis case transect lines for the (left) coast-crossing and (right) island-crossing cases.

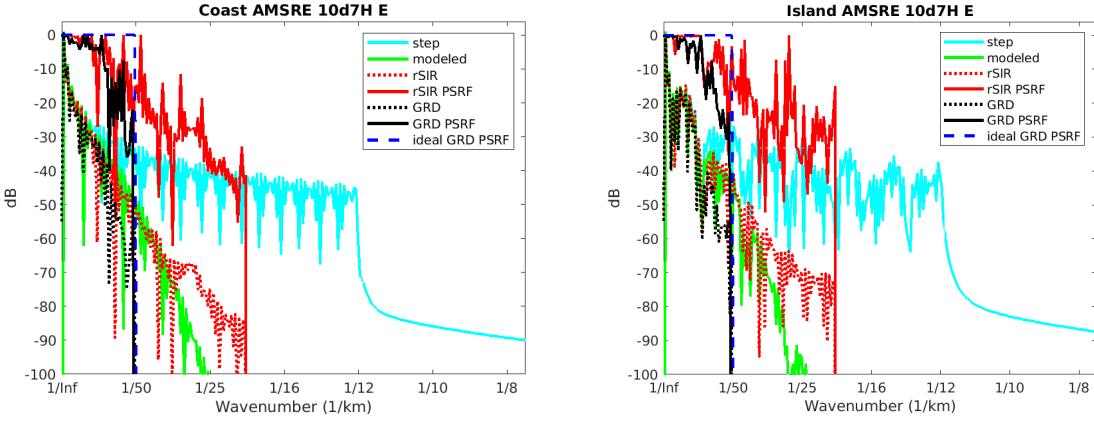


Figure 49: Wavenumber spectra of the  $T_B$  slices, the model, and the PSRF. (left) Coast-crossing case. (right) Island-crossing case.

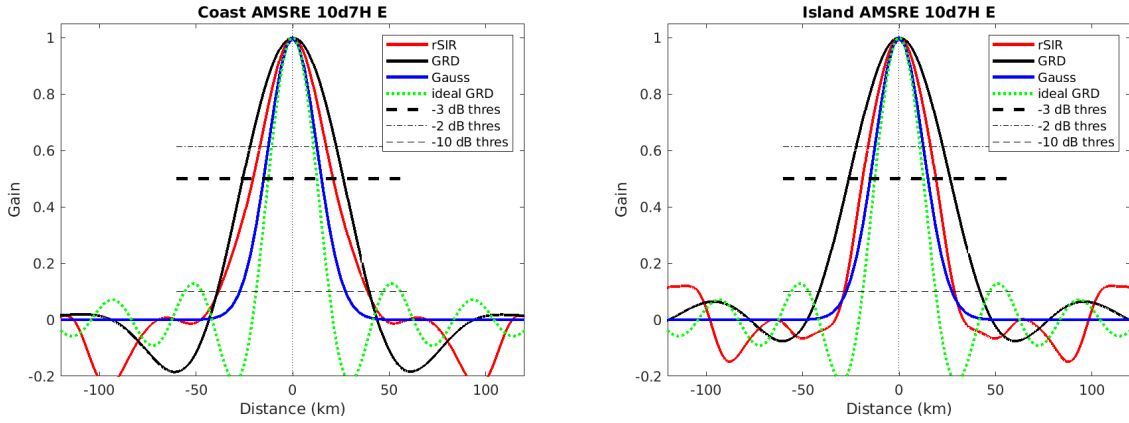


Figure 50: Derived single-pass rSIR and GRD PSRFs from the (left) coast-crossing and (right) island-crossing cases.

Table 80: Resolution estimates for AMSRE channel 10.7H LTOD E

Algorithm	-3 dB Thres		-2 dB Thres		-10 dB Thres	
	Coast	Island	Coast	Island	Coast	Island
Gauss	30.0	30.0	24.4	24.4	54.8	54.8
rSIR	41.5	37.9	33.3	31.7	77.2	57.2
ideal GRD	36.2	36.2	30.3	30.3	54.5	54.5
GRD	52.1	52.6	43.5	43.6	78.7	83.4

## C.6 AMSRE Channel 10.7H M Figures

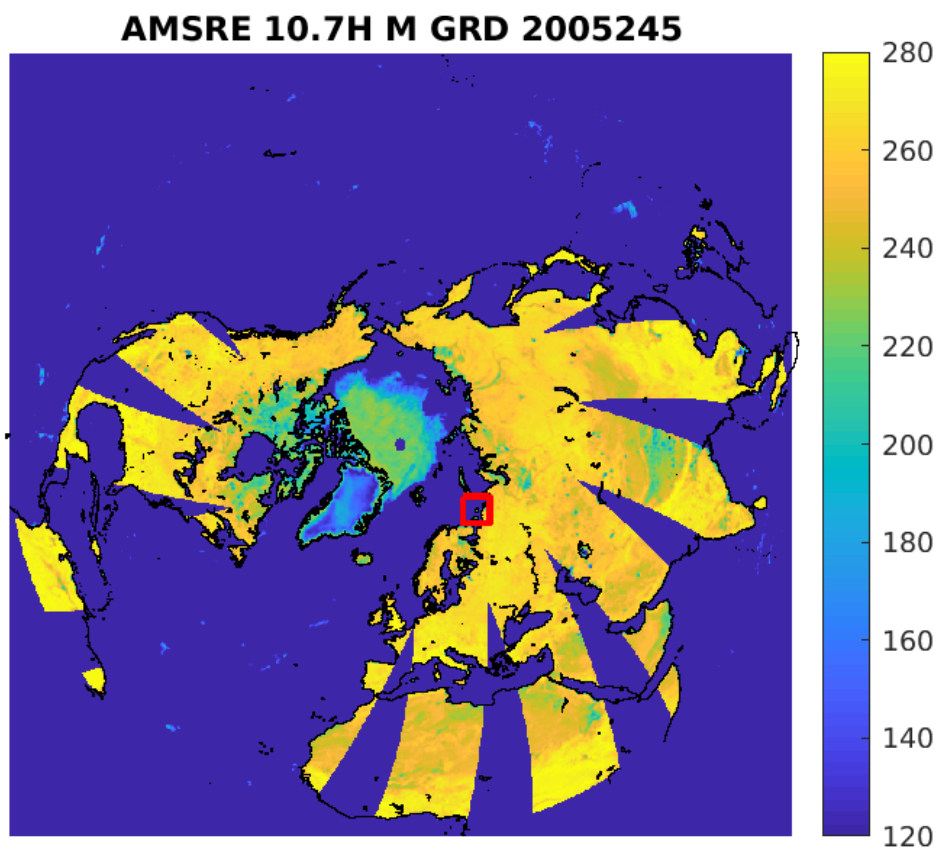


Figure 51: rSIR Northern Hemisphere view.



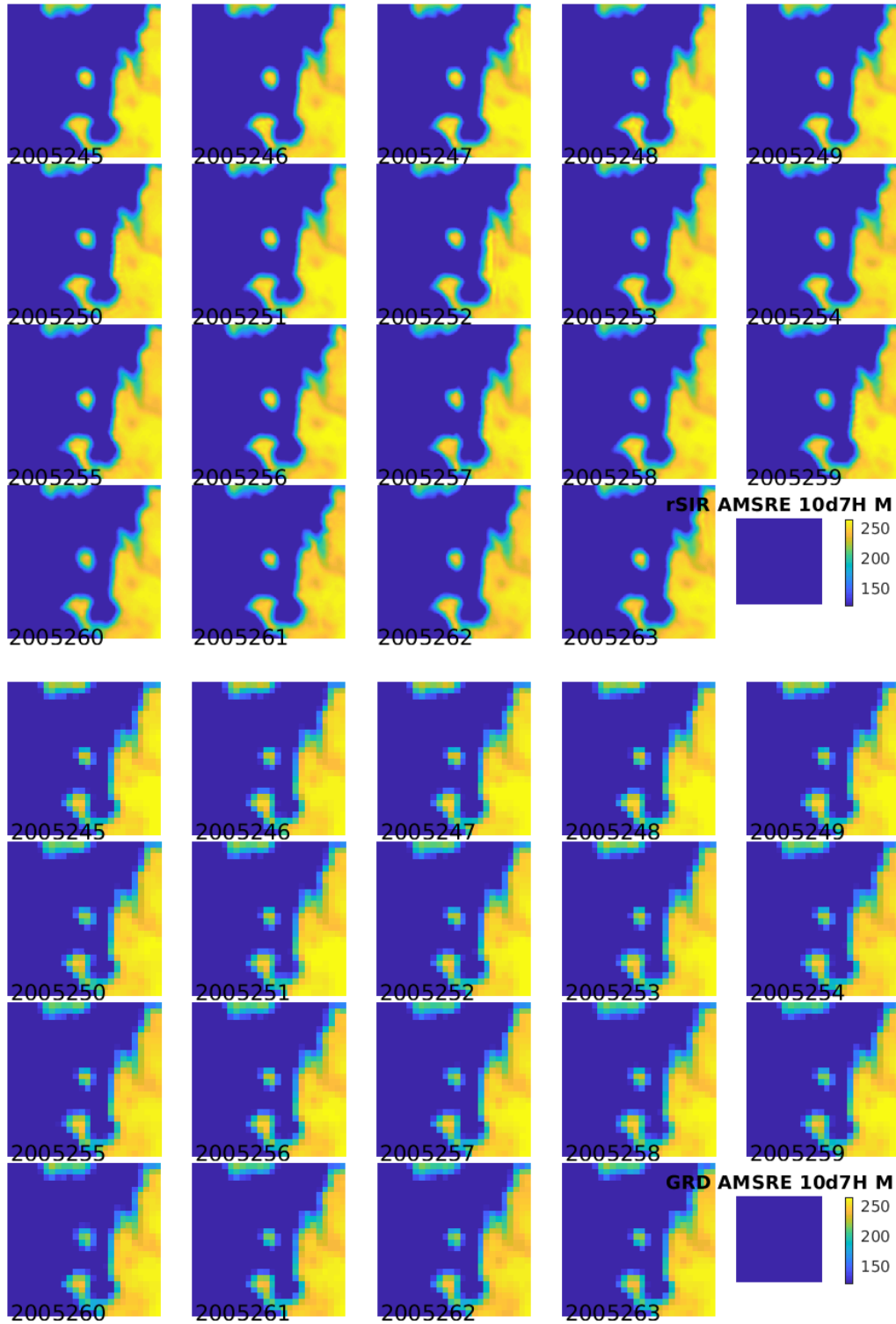


Figure 52: Time series of (top) rSIR and (bottom) GRD  $T_B$  images over the study area. Image dates are labeled on the image.

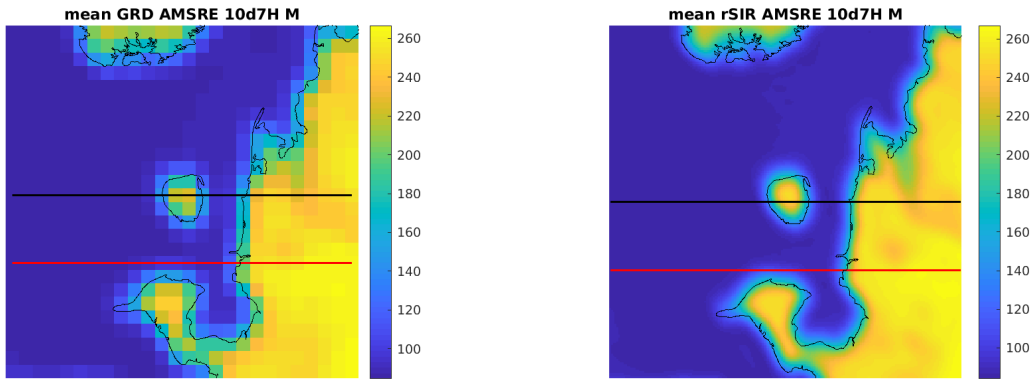


Figure 53: Average of daily  $T_B$  images over the study area. (left) 25-km GRD. (right) 3.125-km rSIR. The thick horizontal lines show the data transect locations where data is extracted from the image for analysis.

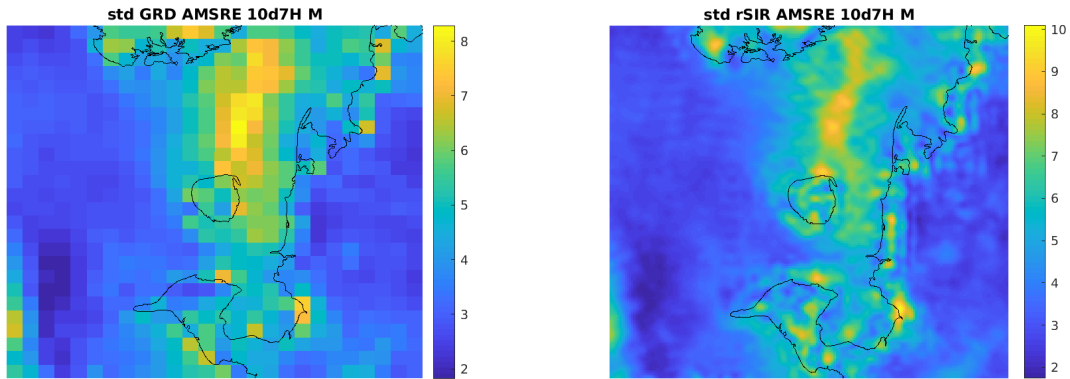


Figure 54: Standard deviation of daily  $T_B$  images over the study area. (left) 25-km GRD. (right) 3.125-km rSIR.

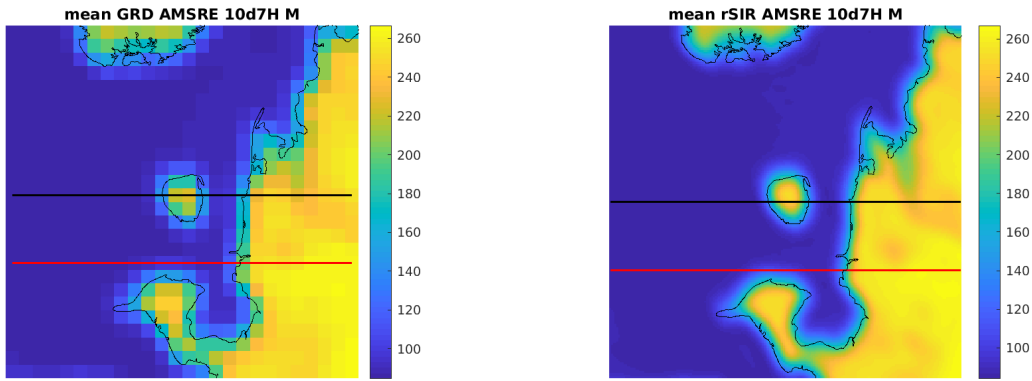


Figure 55: [Repeated] Average of daily  $T_B$  images over the study area. (left) 25-km GRD. (right) 3.125-km rSIR. The thick horizontal lines show the data transect locations where data is extracted from the image for analysis.

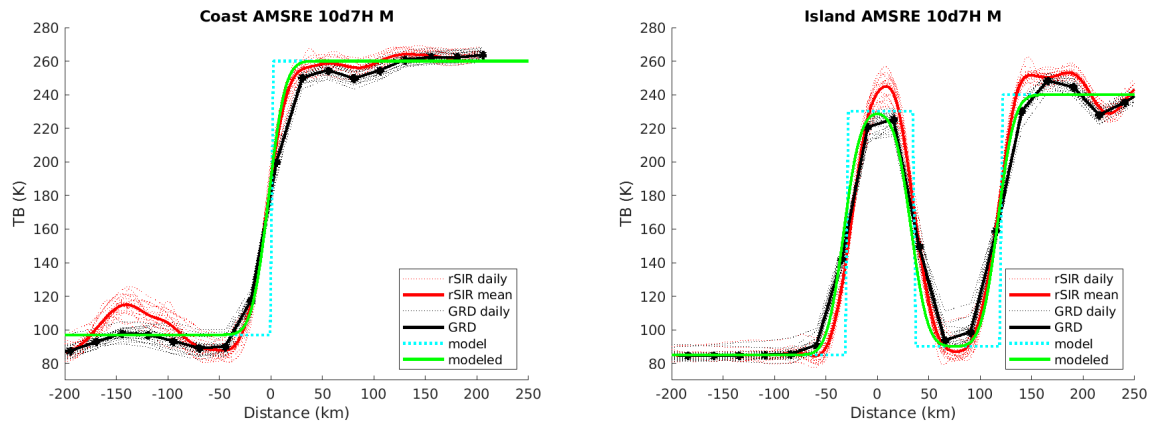


Figure 56: Plots of  $T_B$  along the two analysis case transect lines for the (left) coast-crossing and (right) island-crossing cases.

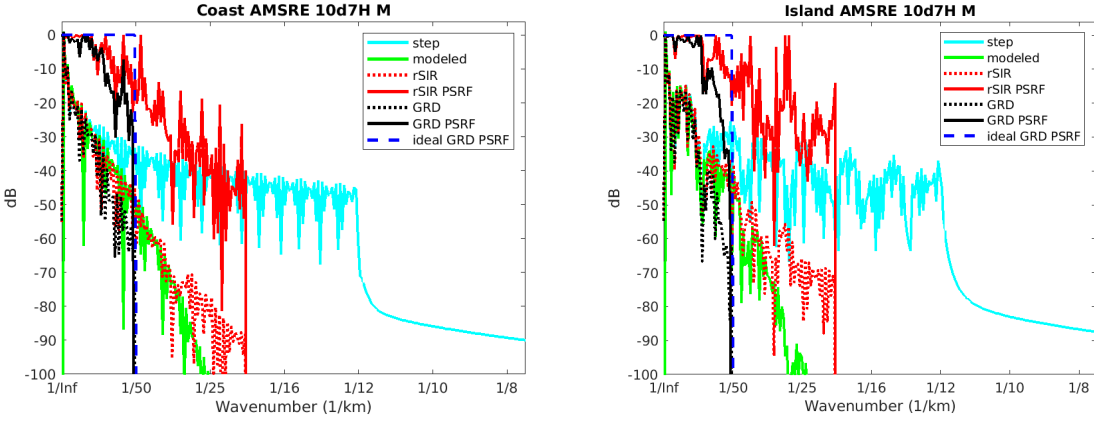


Figure 57: Wavenumber spectra of the  $T_B$  slices, the model, and the PSRF. (left) Coast-crossing case. (right) Island-crossing case.

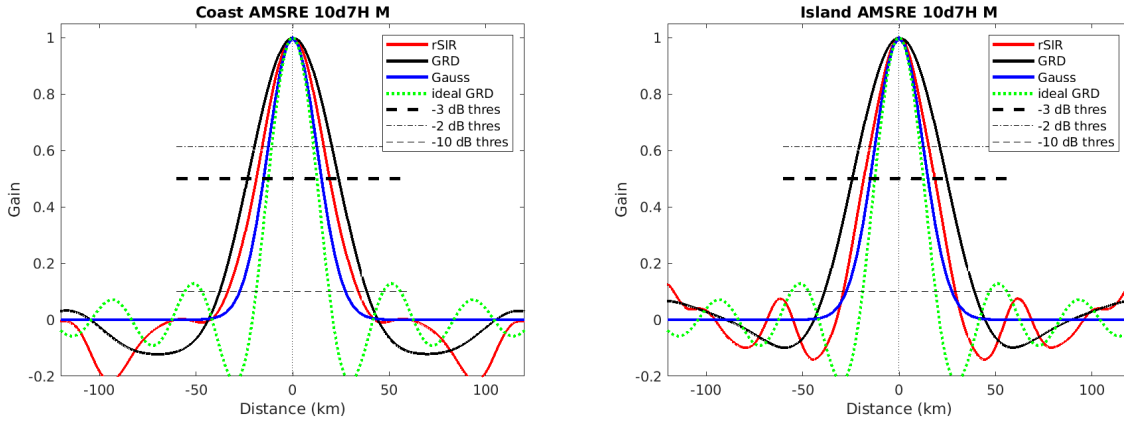


Figure 58: Derived single-pass rSIR and GRD PSRFs from the (left) coast-crossing and (right) island-crossing cases.

Table 81: Resolution estimates for AMSRE channel 10.7H LTOD M

Algorithm	-3 dB Thres		-2 dB Thres		-10 dB Thres	
	Coast	Island	Coast	Island	Coast	Island
Gauss	30.0	30.0	24.4	24.4	54.8	54.8
rSIR	38.0	36.8	30.9	29.7	67.6	58.1
ideal GRD	36.2	36.2	30.3	30.3	54.5	54.5
GRD	47.2	49.0	39.0	40.6	76.2	77.6

## C.7 AMSRE Channel 10.7V E Figures

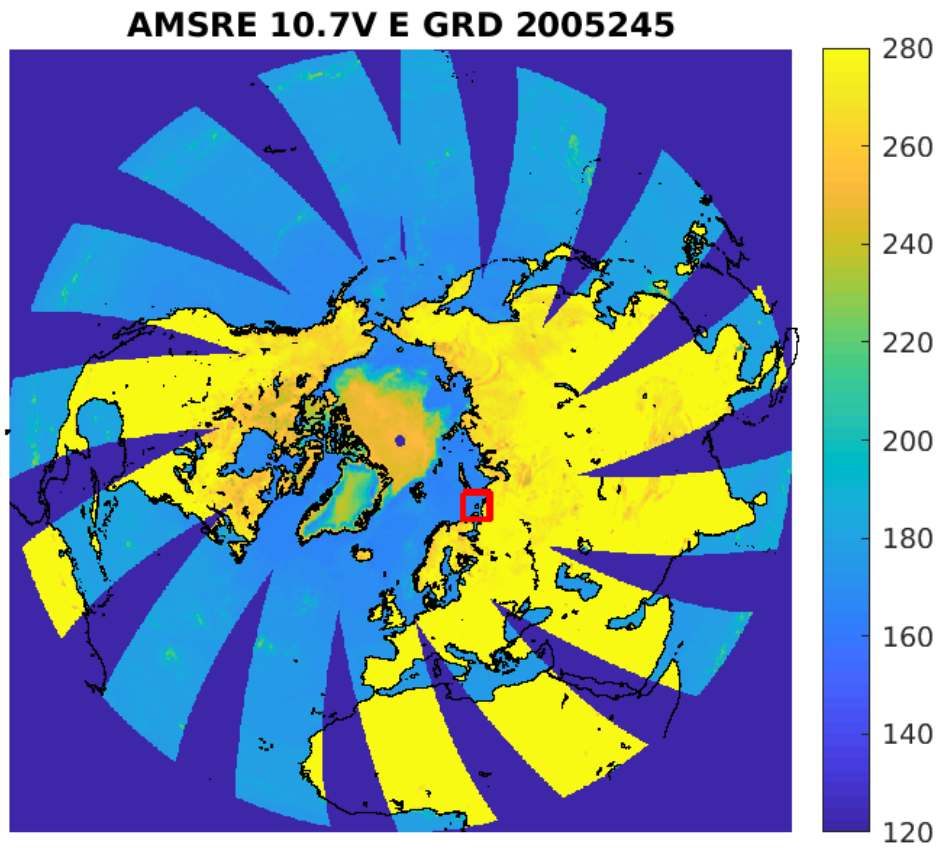


Figure 59: rSIR Northern Hemisphere view.

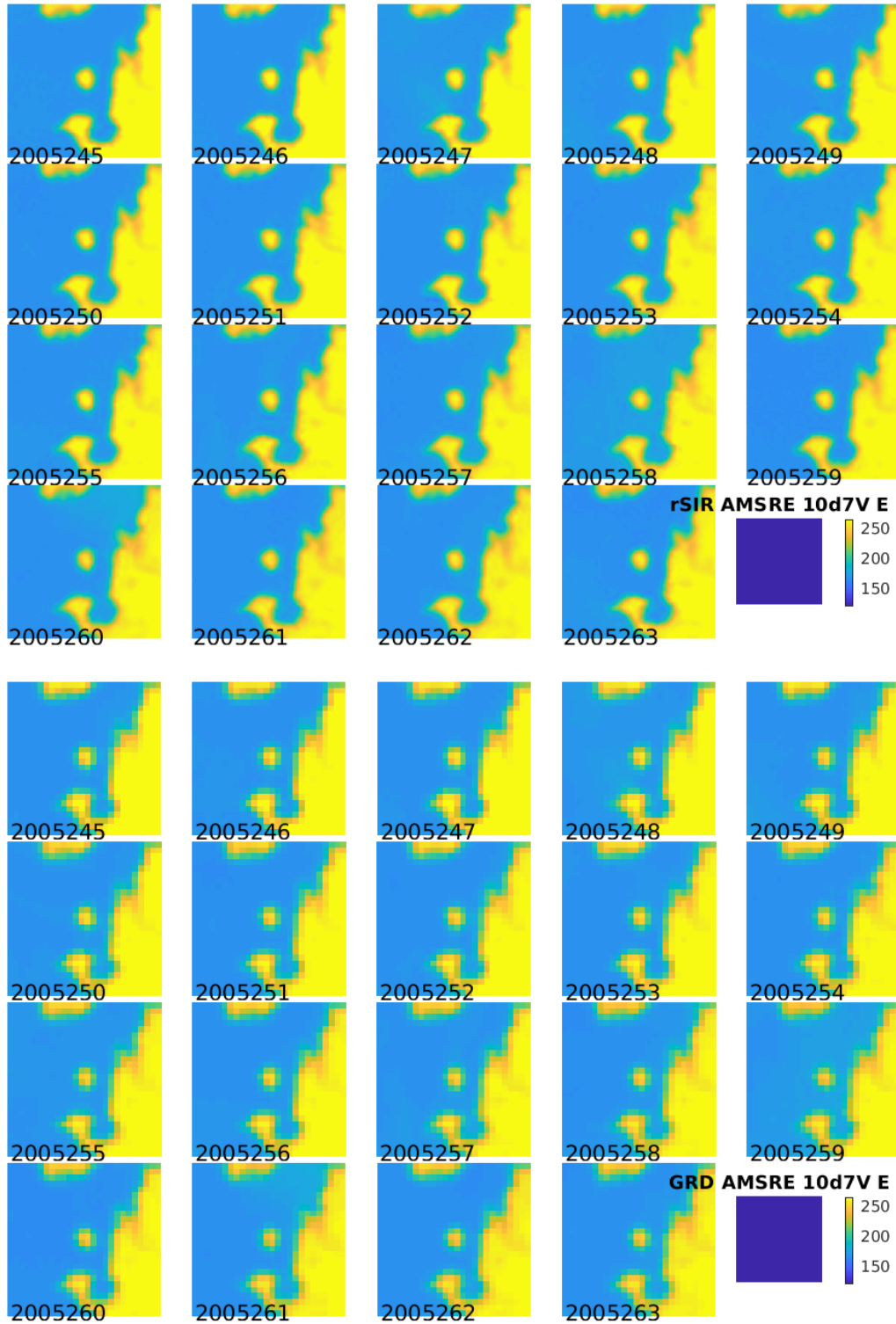


Figure 60: Time series of (top) rSIR and (bottom) GRD  $T_B$  images over the study area. Image dates are labeled on the image.

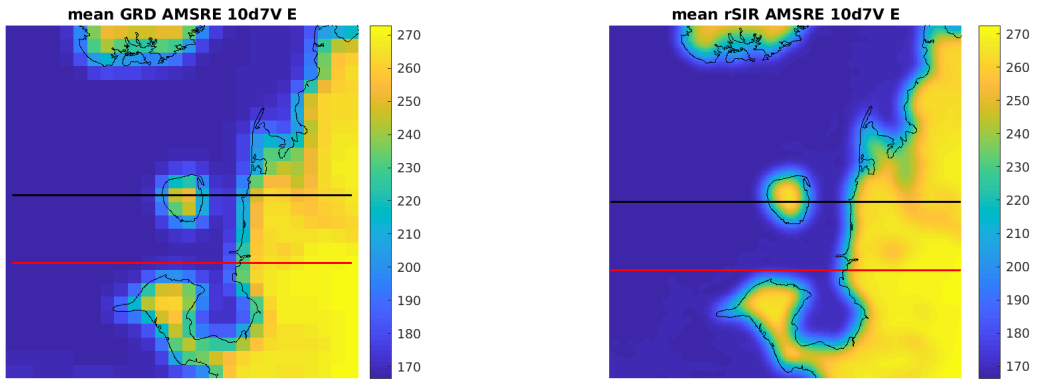


Figure 61: Average of daily  $T_B$  images over the study area. (left) 25-km GRD. (right) 3.125-km rSIR. The thick horizontal lines show the data transect locations where data is extracted from the image for analysis.

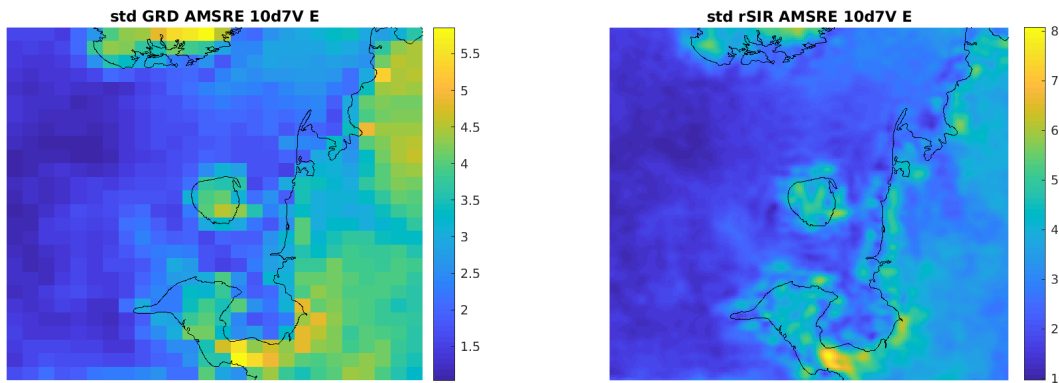


Figure 62: Standard deviation of daily  $T_B$  images over the study area. (left) 25-km GRD. (right) 3.125-km rSIR.

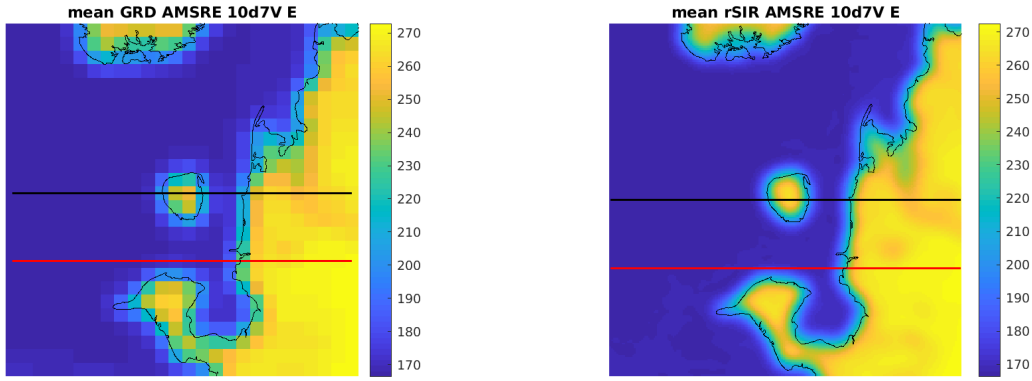


Figure 63: [Repeated] Average of daily  $T_B$  images over the study area. (left) 25-km GRD. (right) 3.125-km rSIR. The thick horizontal lines show the data transect locations where data is extracted from the image for analysis.

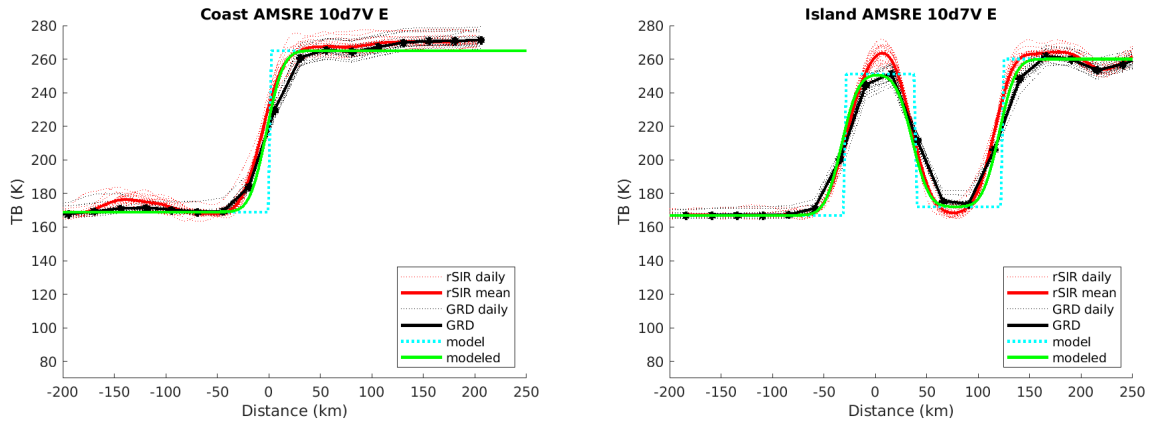


Figure 64: Plots of  $T_B$  along the two analysis case transect lines for the (left) coast-crossing and (right) island-crossing cases.



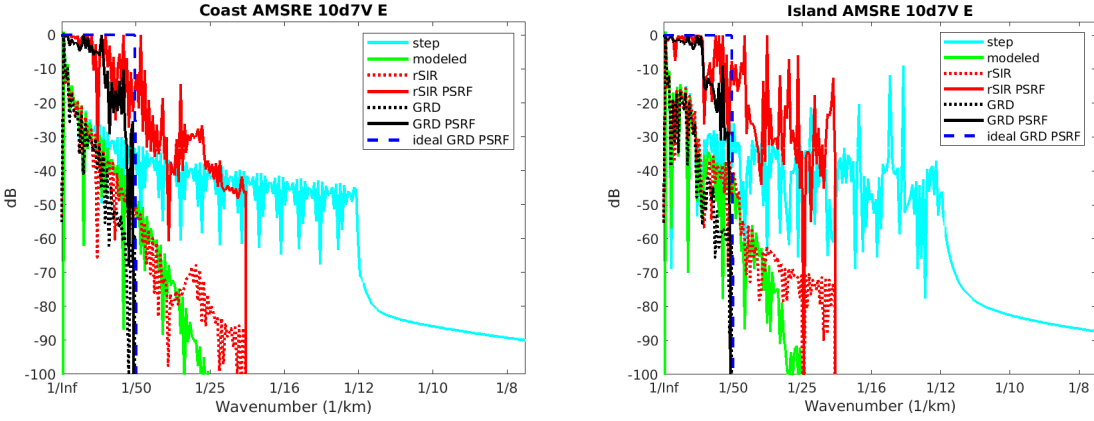


Figure 65: Wavenumber spectra of the  $T_B$  slices, the model, and the PSRF. (left) Coast-crossing case. (right) Island-crossing case.

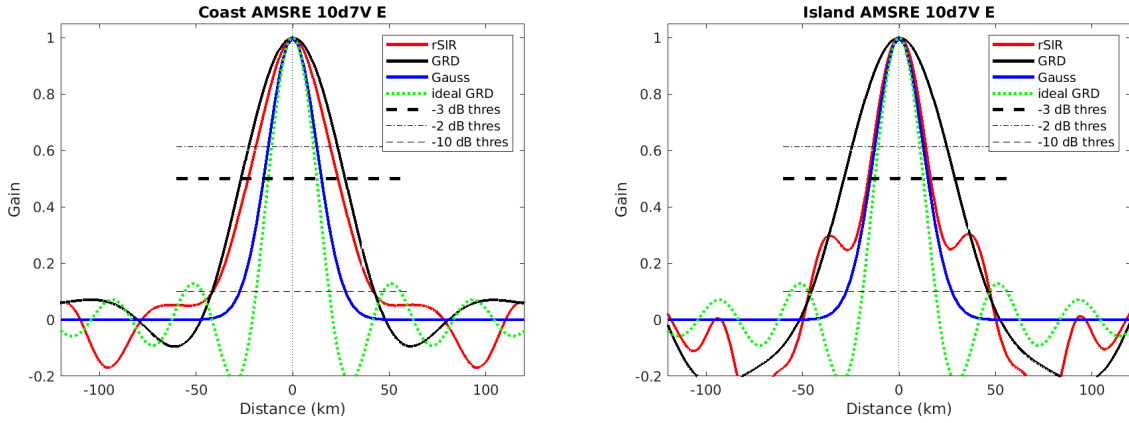


Figure 66: Derived single-pass rSIR and GRD PSRFs from the (left) coast-crossing and (right) island-crossing cases.

Table 82: Resolution estimates for AMSRE channel 10.7V LTOD E

Algorithm	-3 dB Thres		-2 dB Thres		-10 dB Thres	
	Coast	Island	Coast	Island	Coast	Island
Gauss	30.0	30.0	24.4	24.4	54.8	54.8
rSIR	46.6	32.5	37.3	26.8	83.0	93.6
ideal GRD	36.2	36.2	30.3	30.3	54.5	54.5
GRD	53.9	57.7	44.8	47.8	84.0	91.5

## C.8 AMSRE Channel 10.7V M Figures

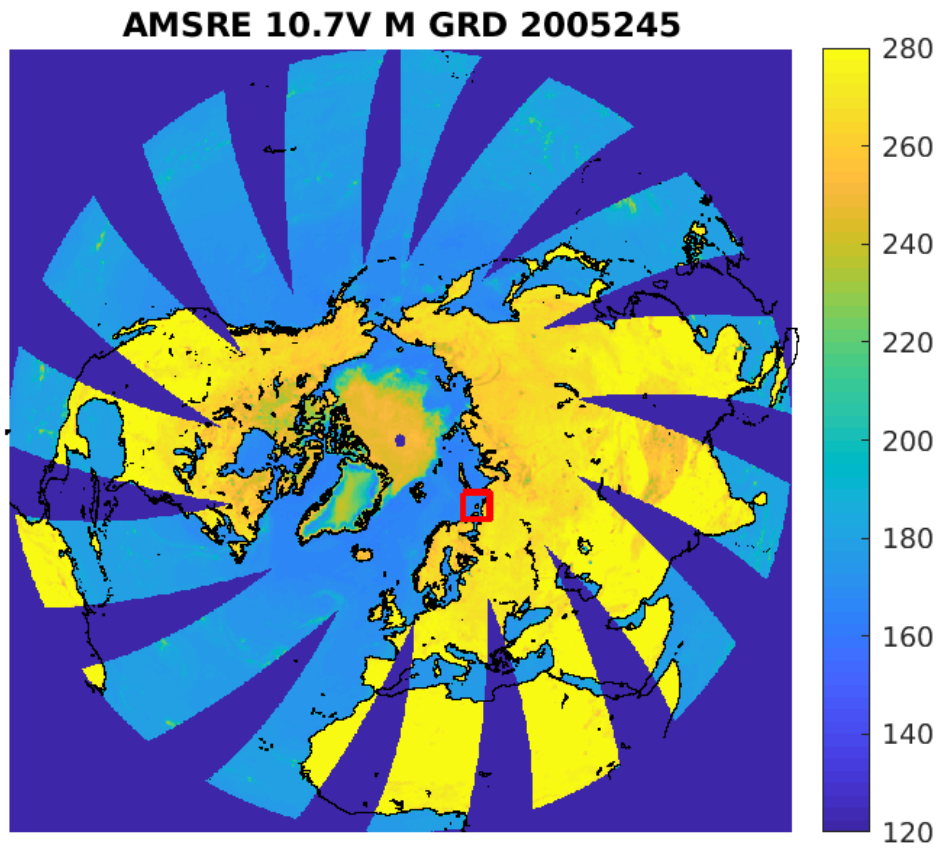


Figure 67: rSIR Northern Hemisphere view.

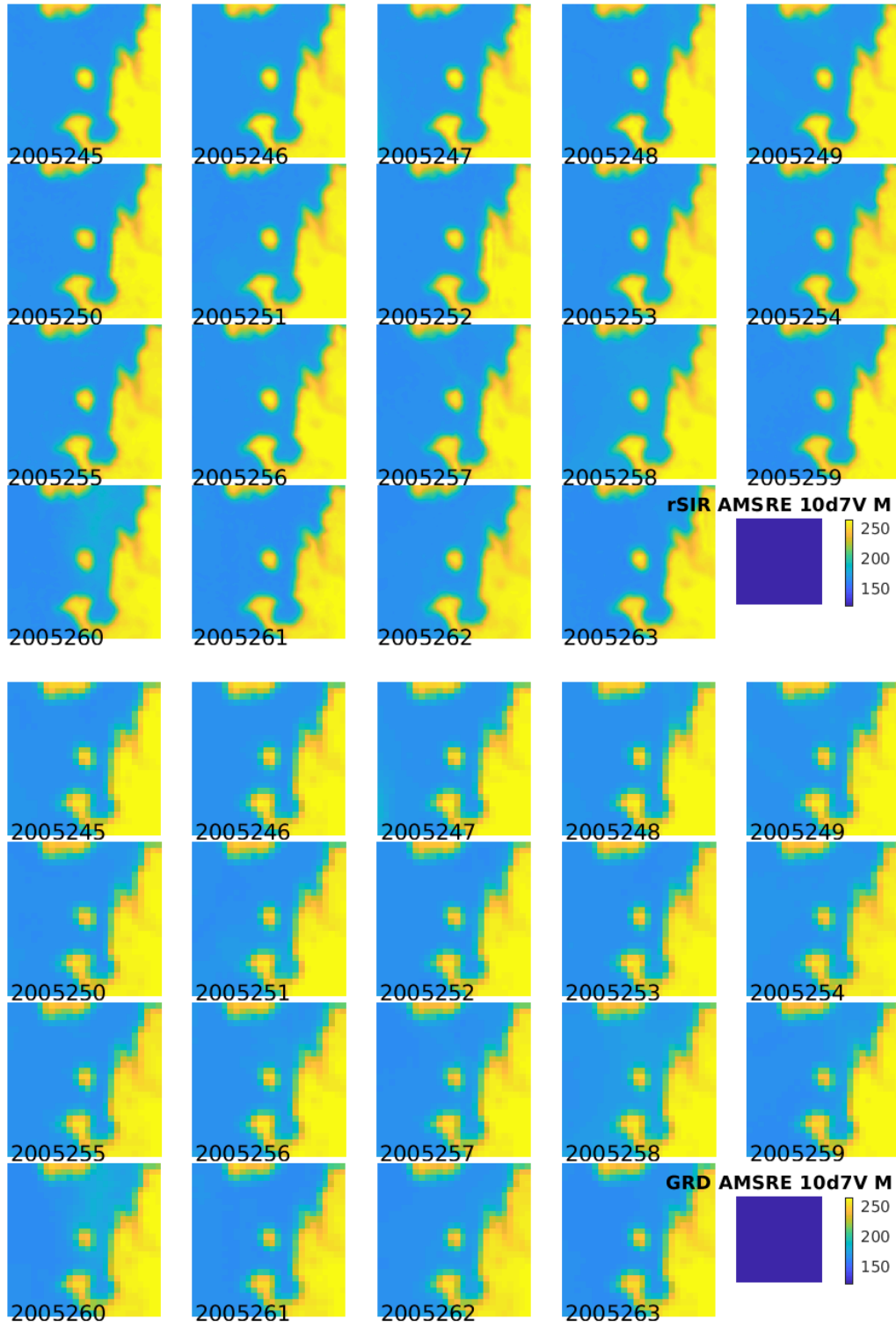


Figure 68: Time series of (top) rSIR and (bottom) GRD  $T_B$  images over the study area. Image dates are labeled on the image.

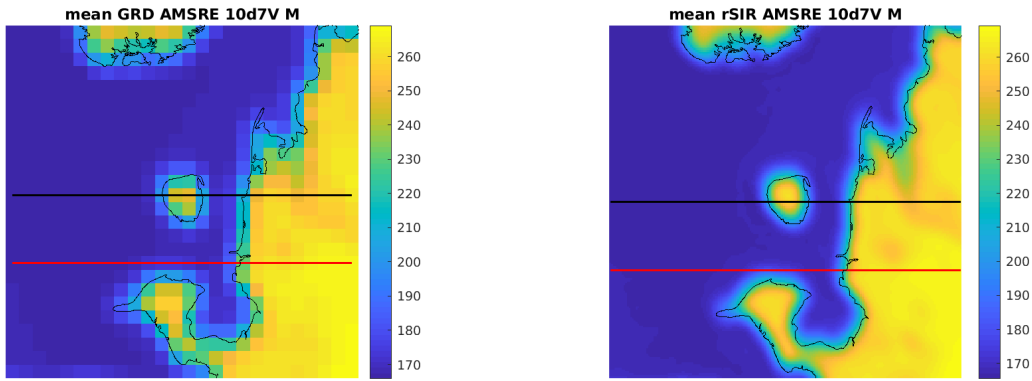


Figure 69: Average of daily  $T_B$  images over the study area. (left) 25-km GRD. (right) 3.125-km rSIR. The thick horizontal lines show the data transect locations where data is extracted from the image for analysis.

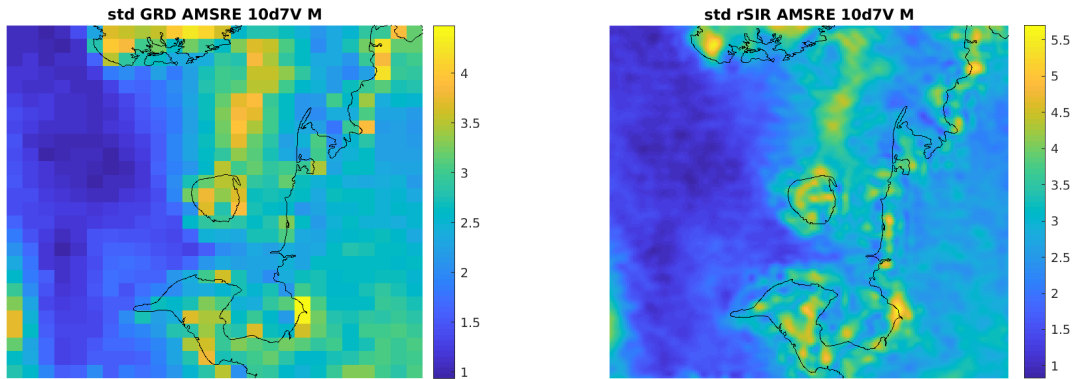


Figure 70: Standard deviation of daily  $T_B$  images over the study area. (left) 25-km GRD. (right) 3.125-km rSIR.

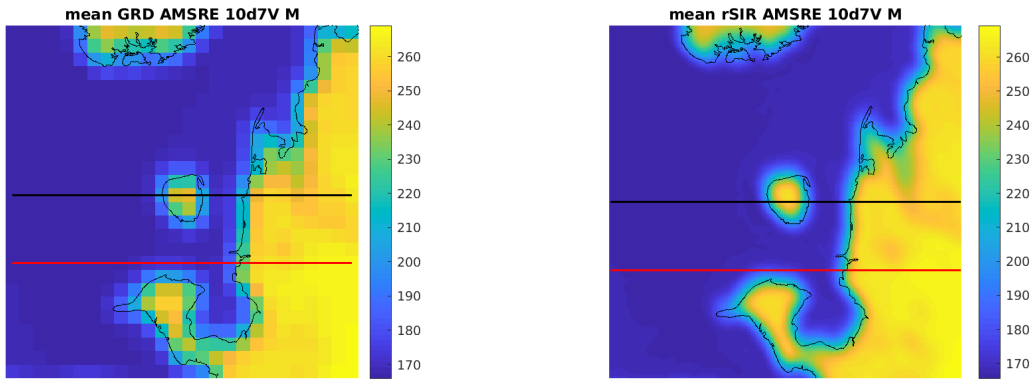


Figure 71: [Repeated] Average of daily  $T_B$  images over the study area. (left) 25-km GRD. (right) 3.125-km rSIR. The thick horizontal lines show the data transect locations where data is extracted from the image for analysis.

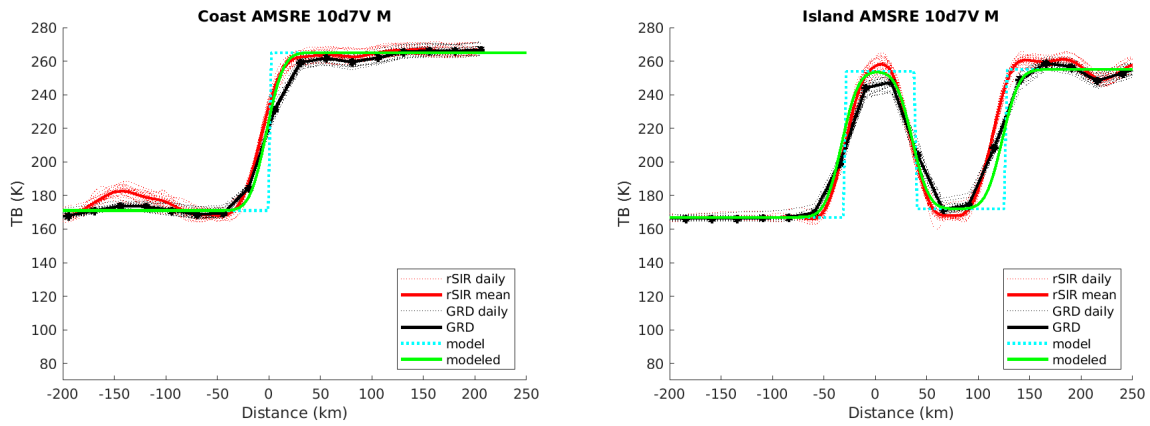


Figure 72: Plots of  $T_B$  along the two analysis case transect lines for the (left) coast-crossing and (right) island-crossing cases.

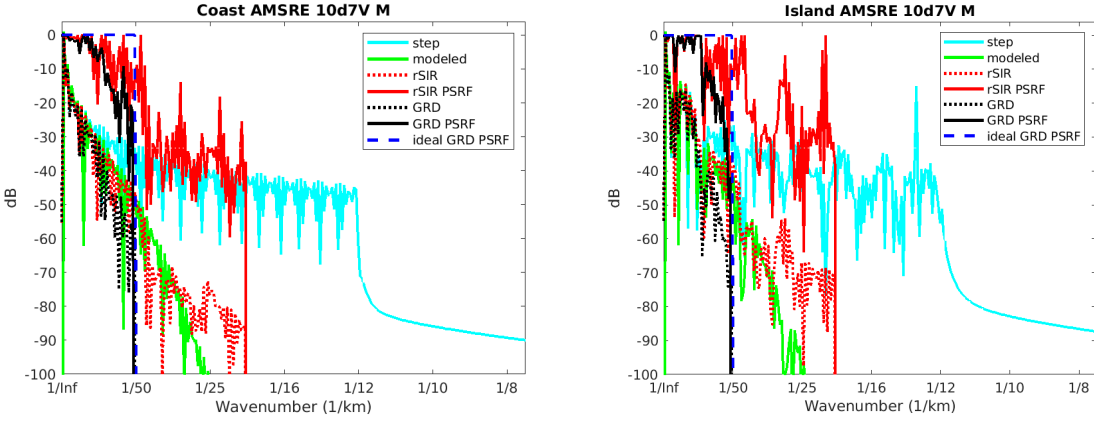


Figure 73: Wavenumber spectra of the  $T_B$  slices, the model, and the PSRF. (left) Coast-crossing case. (right) Island-crossing case.

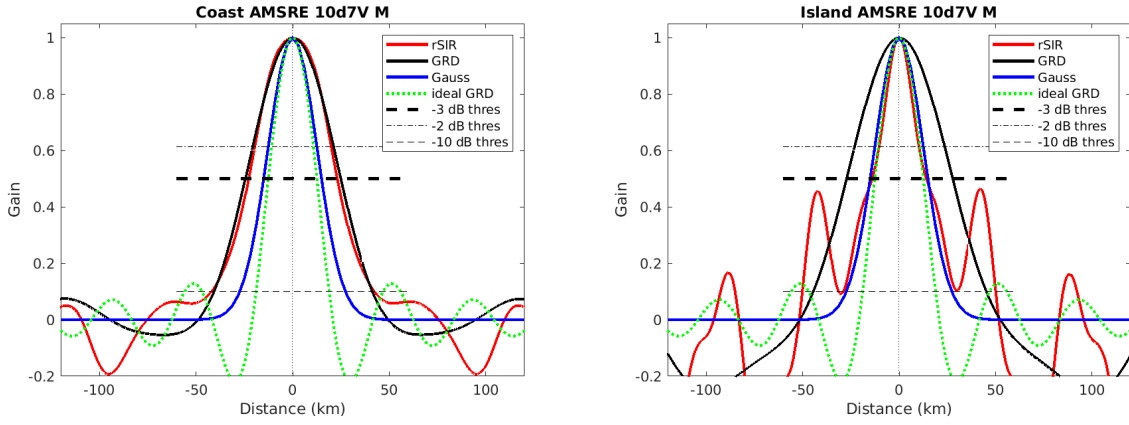


Figure 74: Derived single-pass rSIR and GRD PSRFs from the (left) coast-crossing and (right) island-crossing cases.

Table 83: Resolution estimates for AMSRE channel 10.7V LTOD M

Algorithm	-3 dB Thres		-2 dB Thres		-10 dB Thres	
	Coast	Island	Coast	Island	Coast	Island
Gauss	30.0	30.0	24.4	24.4	54.8	54.8
rSIR	45.9	28.2	38.7	19.9	84.5	79.1
ideal GRD	36.2	36.2	30.3	30.3	54.5	54.5
GRD	49.4	55.0	40.7	45.4	82.0	89.7

## C.9 AMSRE Channel 18H E Figures

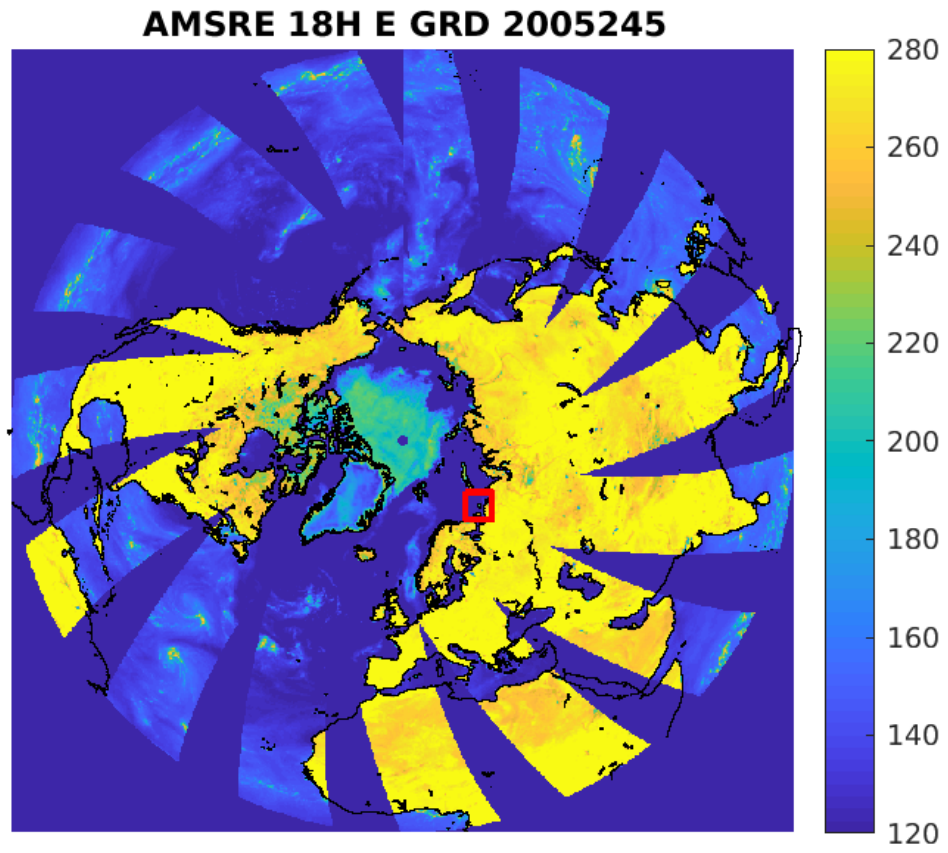


Figure 75: rSIR Northern Hemisphere view.

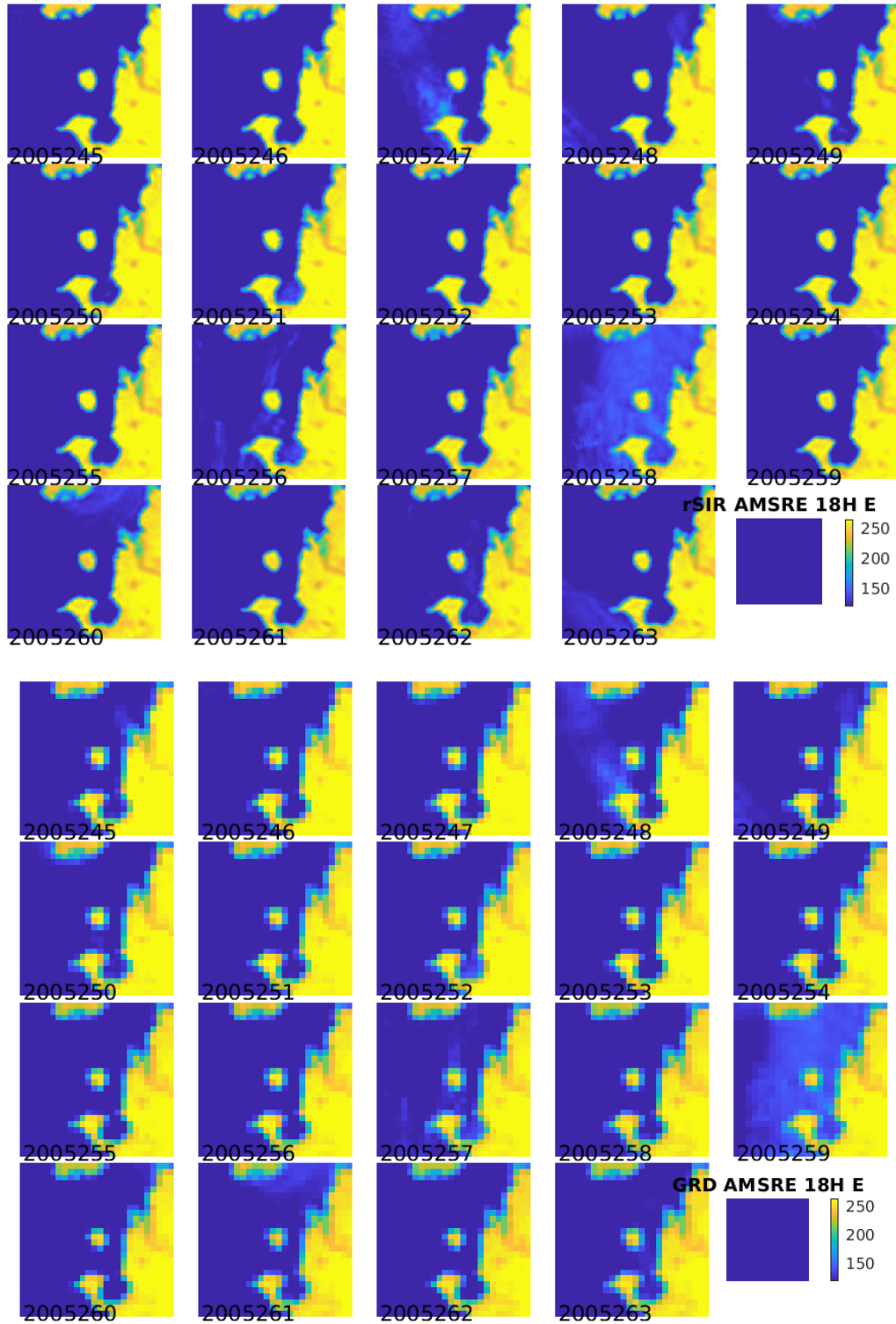


Figure 76: Time series of (top) rSIR and (bottom) GRD  $T_B$  images over the study area. Image dates are labeled on the image.



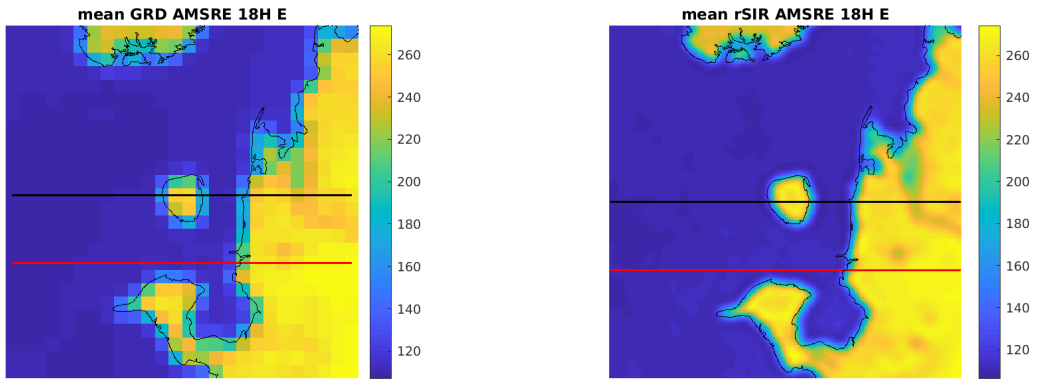


Figure 77: Average of daily  $T_B$  images over the study area. (left) 25-km GRD. (right) 3.125-km rSIR. The thick horizontal lines show the data transect locations where data is extracted from the image for analysis.

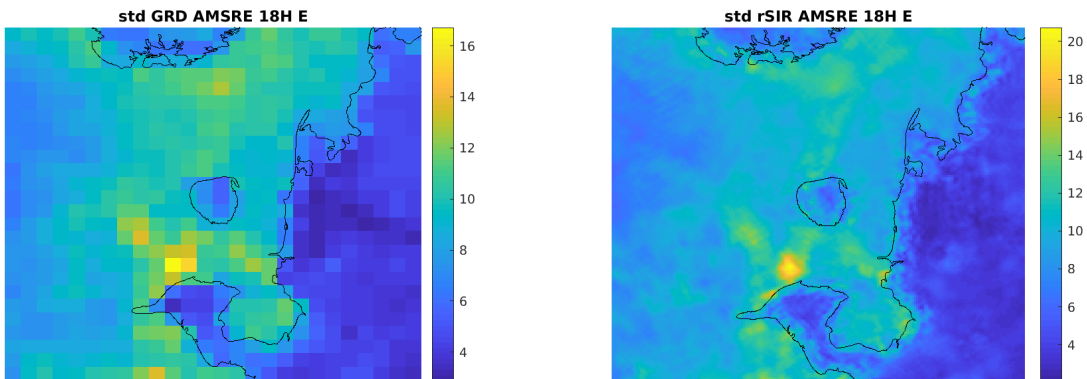


Figure 78: Standard deviation of daily  $T_B$  images over the study area. (left) 25-km GRD. (right) 3.125-km rSIR.

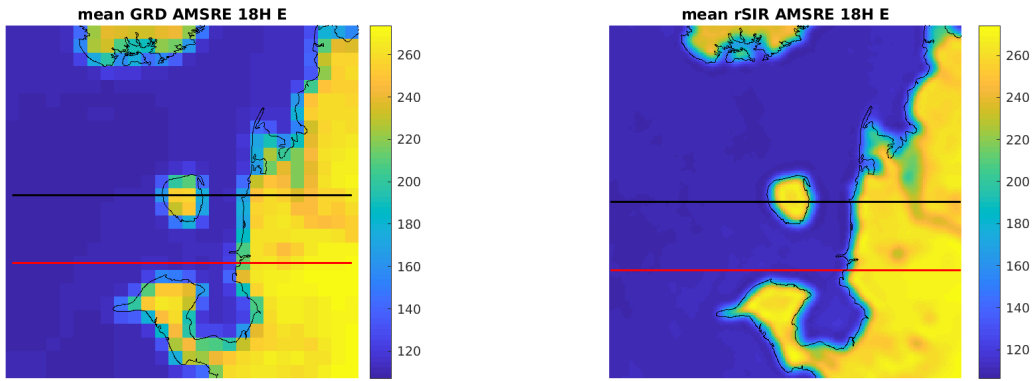


Figure 79: [Repeated] Average of daily  $T_B$  images over the study area. (left) 25-km GRD. (right) 3.125-km rSIR. The thick horizontal lines show the data transect locations where data is extracted from the image for analysis.

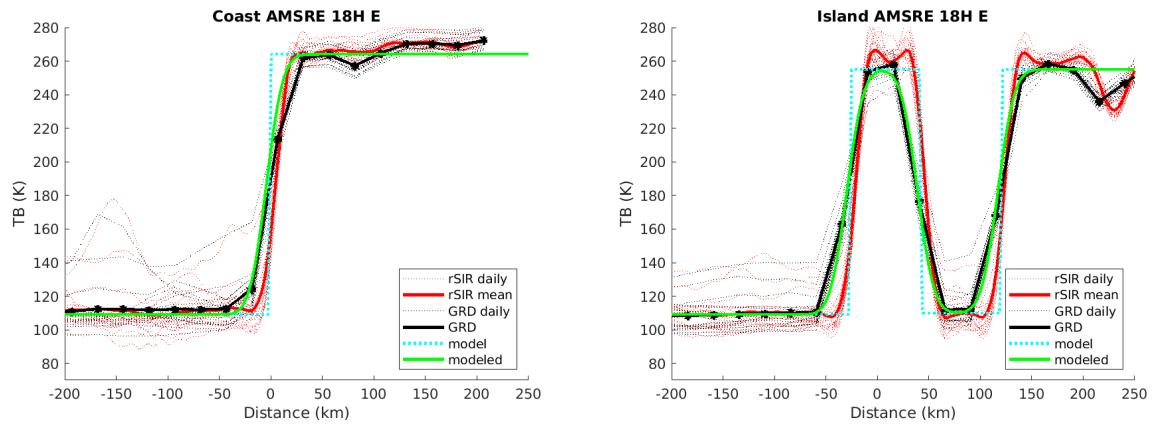


Figure 80: Plots of  $T_B$  along the two analysis case transect lines for the (left) coast-crossing and (right) island-crossing cases.

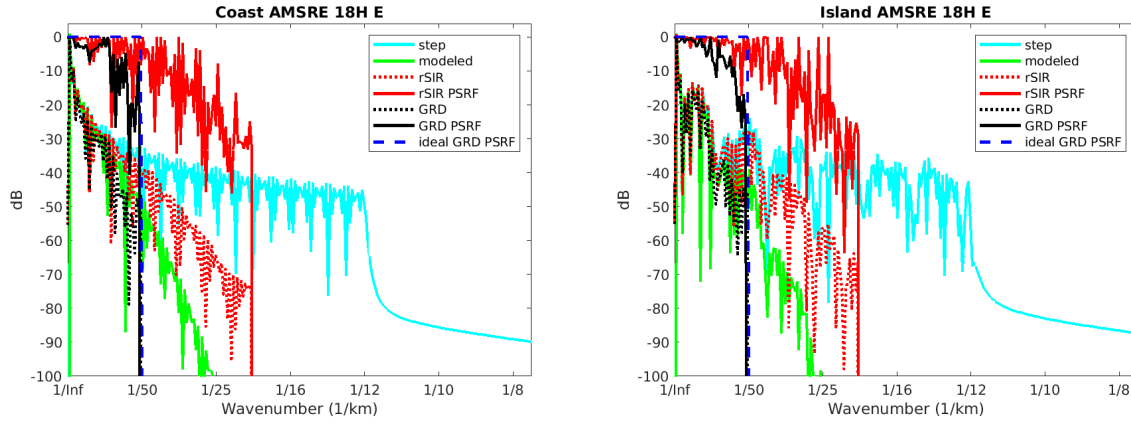


Figure 81: Wavenumber spectra of the  $T_B$  slices, the model, and the PSRF. (left) Coast-crossing case. (right) Island-crossing case.

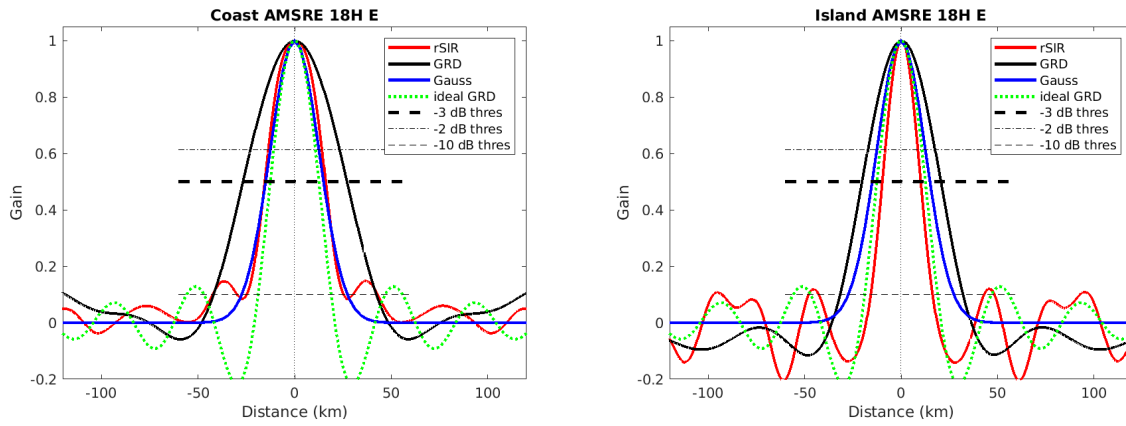


Figure 82: Derived single-pass rSIR and GRD PSRFs from the (left) coast-crossing and (right) island-crossing cases.

Table 84: Resolution estimates for AMSRE channel 18H LTOD E

Algorithm	-3 dB Thres		-2 dB Thres		-10 dB Thres	
	Coast	Island	Coast	Island	Coast	Island
Gauss	30.0	30.0	24.4	24.4	54.8	54.8
rSIR	31.5	19.9	27.2	16.5	50.1	32.2
ideal GRD	36.2	36.2	30.3	30.3	54.5	54.5
GRD	53.8	40.8	44.9	33.9	84.2	63.8

## C.10 AMSRE Channel 18H M Figures

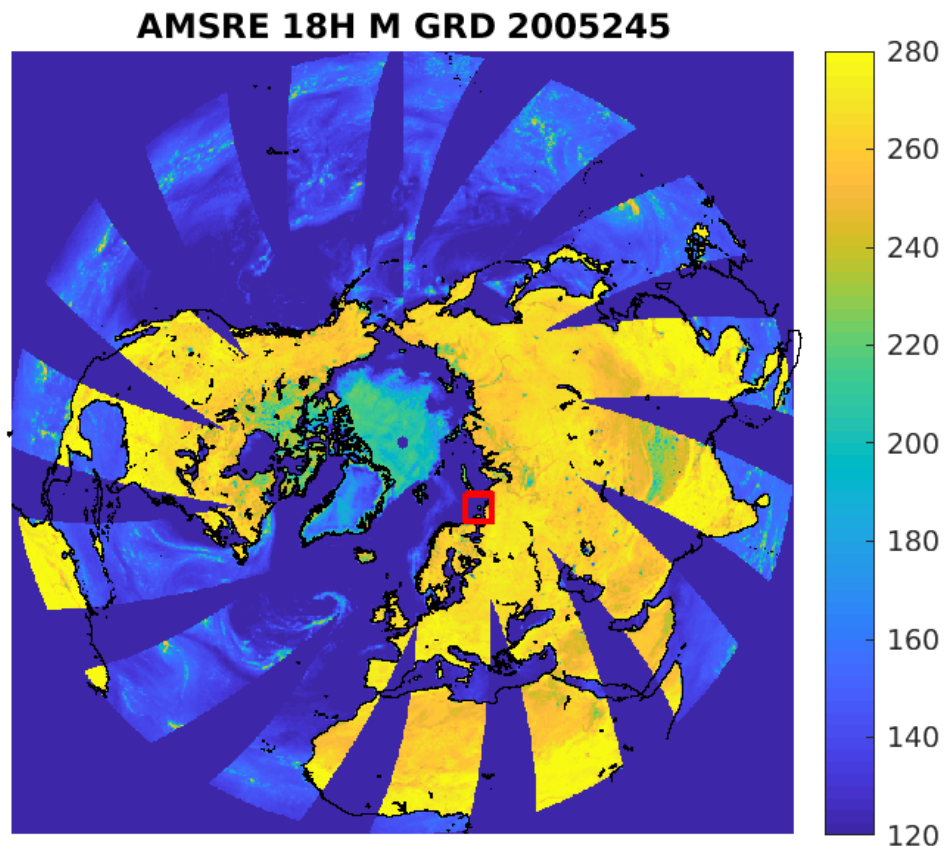


Figure 83: rSIR Northern Hemisphere view.

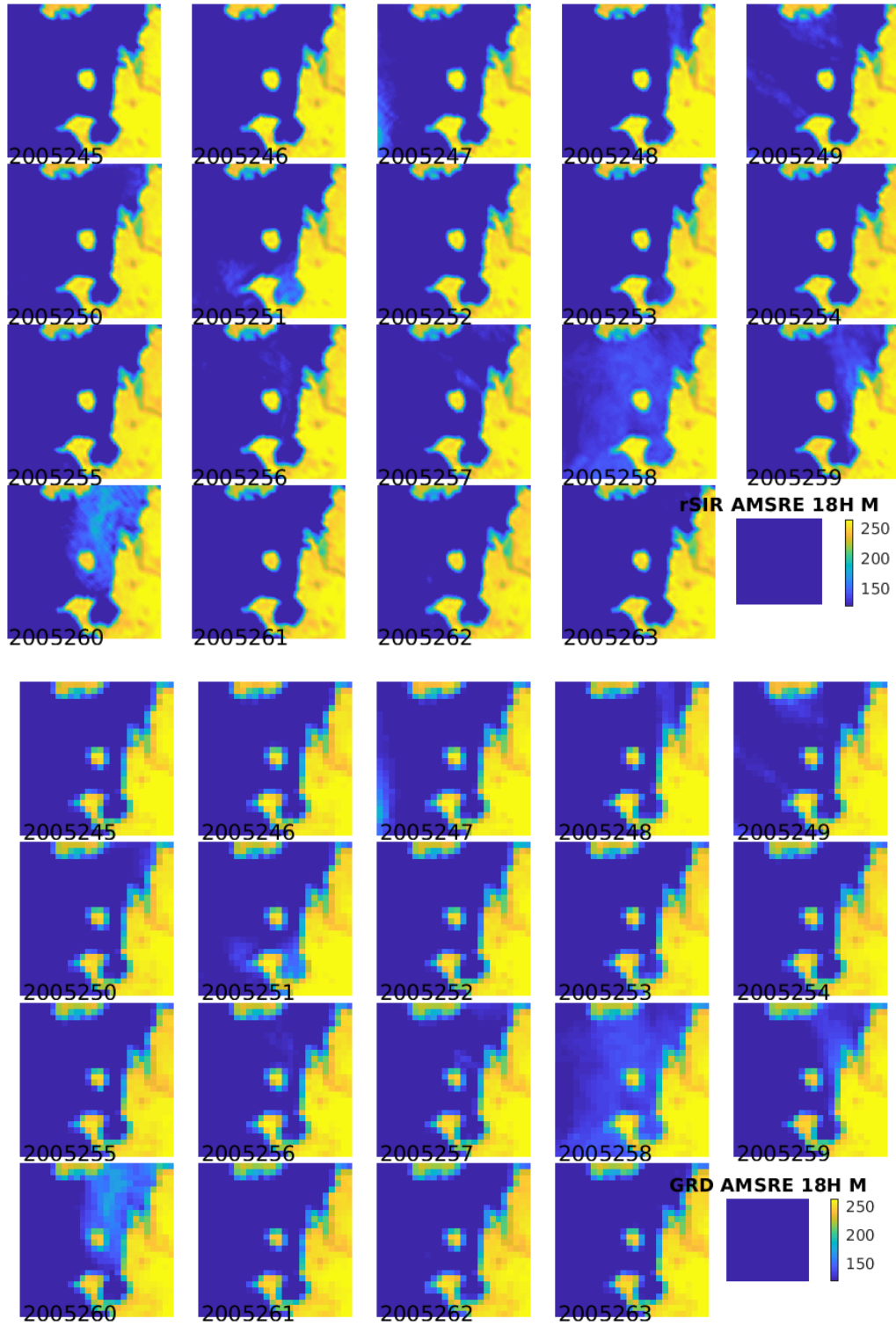


Figure 84: Time series of (top) rSIR and (bottom) GRD  $T_B$  images over the study area. Image dates are labeled on the image.

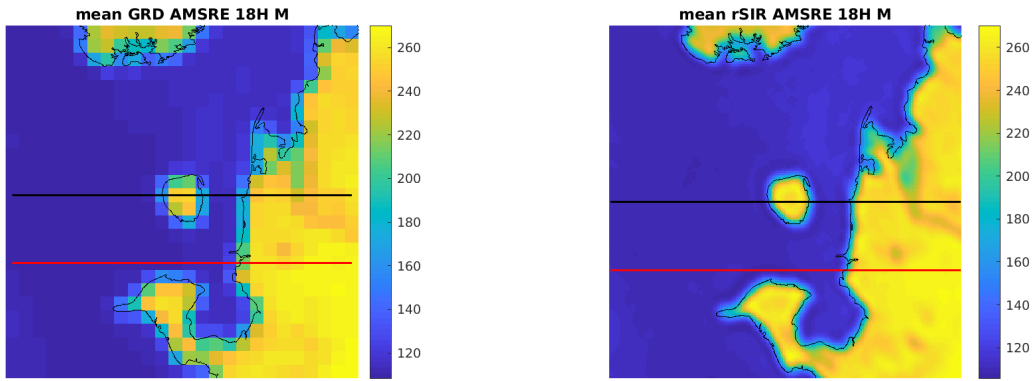


Figure 85: Average of daily  $T_B$  images over the study area. (left) 25-km GRD. (right) 3.125-km rSIR. The thick horizontal lines show the data transect locations where data is extracted from the image for analysis.

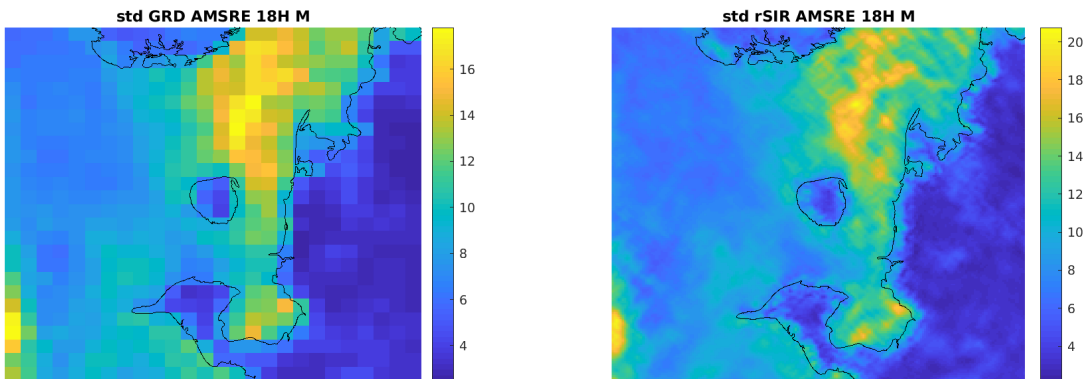


Figure 86: Standard deviation of daily  $T_B$  images over the study area. (left) 25-km GRD. (right) 3.125-km rSIR.

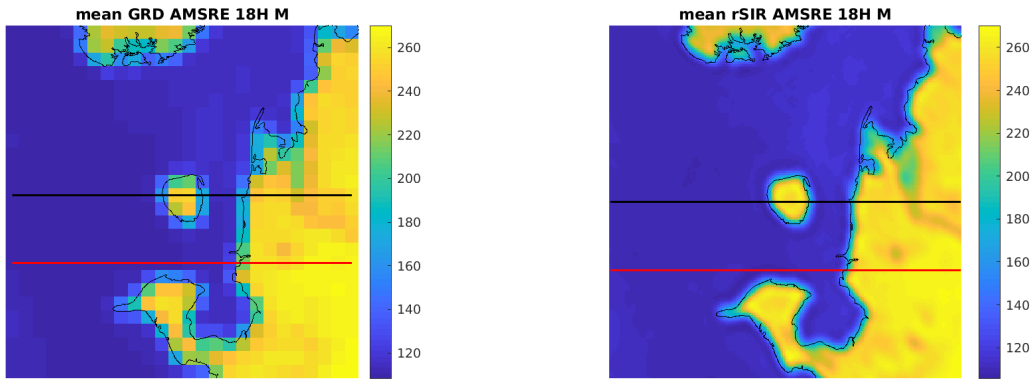


Figure 87: [Repeated] Average of daily  $T_B$  images over the study area. (left) 25-km GRD. (right) 3.125-km rSIR. The thick horizontal lines show the data transect locations where data is extracted from the image for analysis.

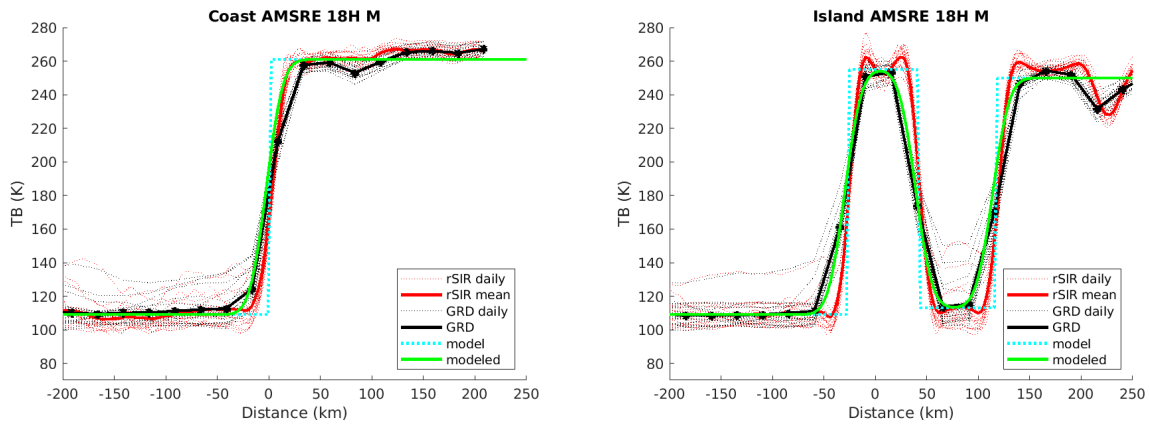


Figure 88: Plots of  $T_B$  along the two analysis case transect lines for the (left) coast-crossing and (right) island-crossing cases.

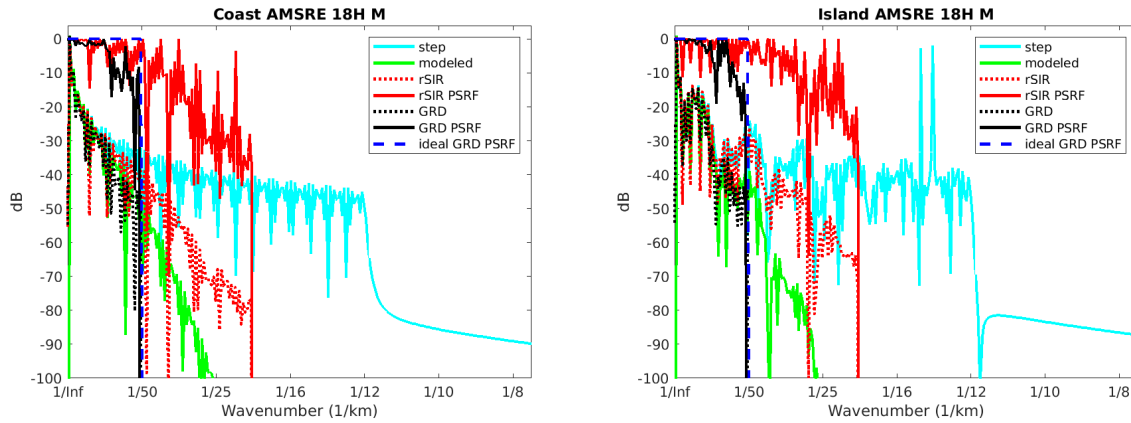


Figure 89: Wavenumber spectra of the  $T_B$  slices, the model, and the PSRF. (left) Coast-crossing case. (right) Island-crossing case.

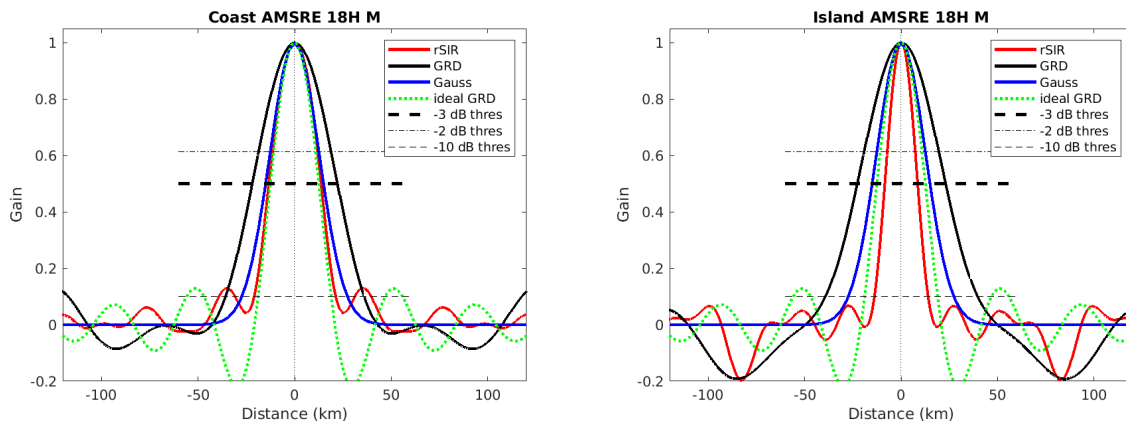


Figure 90: Derived single-pass rSIR and GRD PSRFs from the (left) coast-crossing and (right) island-crossing cases.

Table 85: Resolution estimates for AMSRE channel 18H LTOD M

Algorithm	-3 dB Thres		-2 dB Thres		-10 dB Thres	
	Coast	Island	Coast	Island	Coast	Island
Gauss	30.0	30.0	24.4	24.4	54.8	54.8
rSIR	27.0	17.0	22.8	14.1	42.3	27.9
ideal GRD	36.2	36.2	30.3	30.3	54.5	54.5
GRD	44.1	45.8	36.5	37.6	71.8	78.9



## C.11 AMSRE Channel 18V E Figures

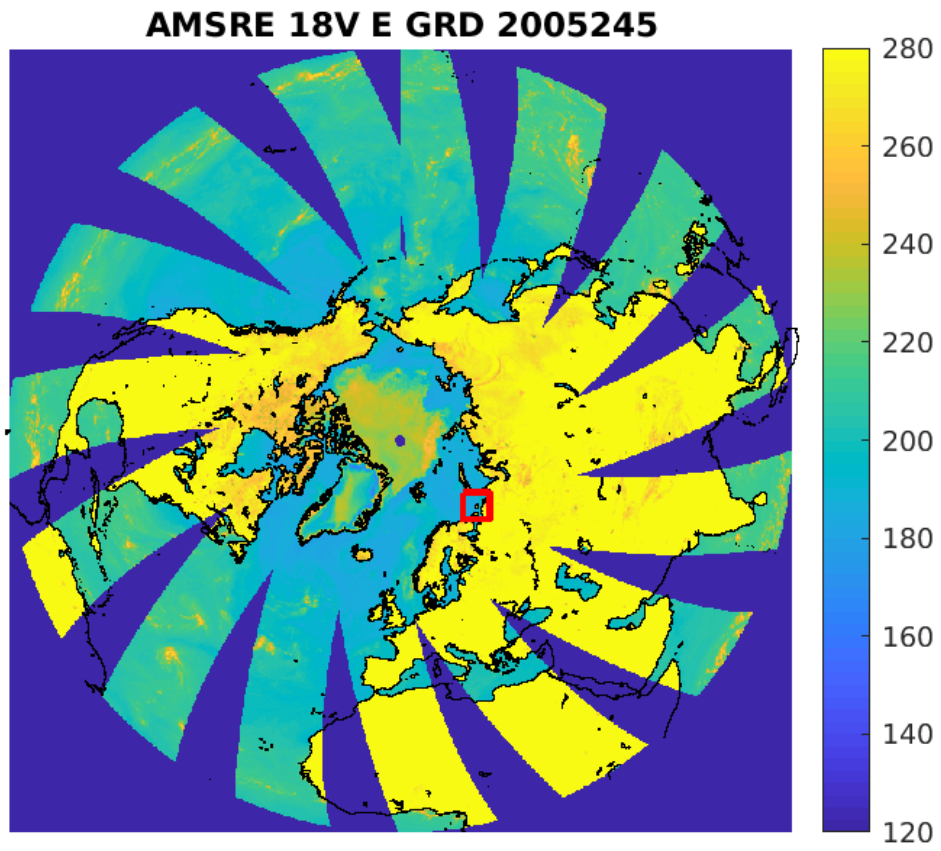


Figure 91: rSIR Northern Hemisphere view.

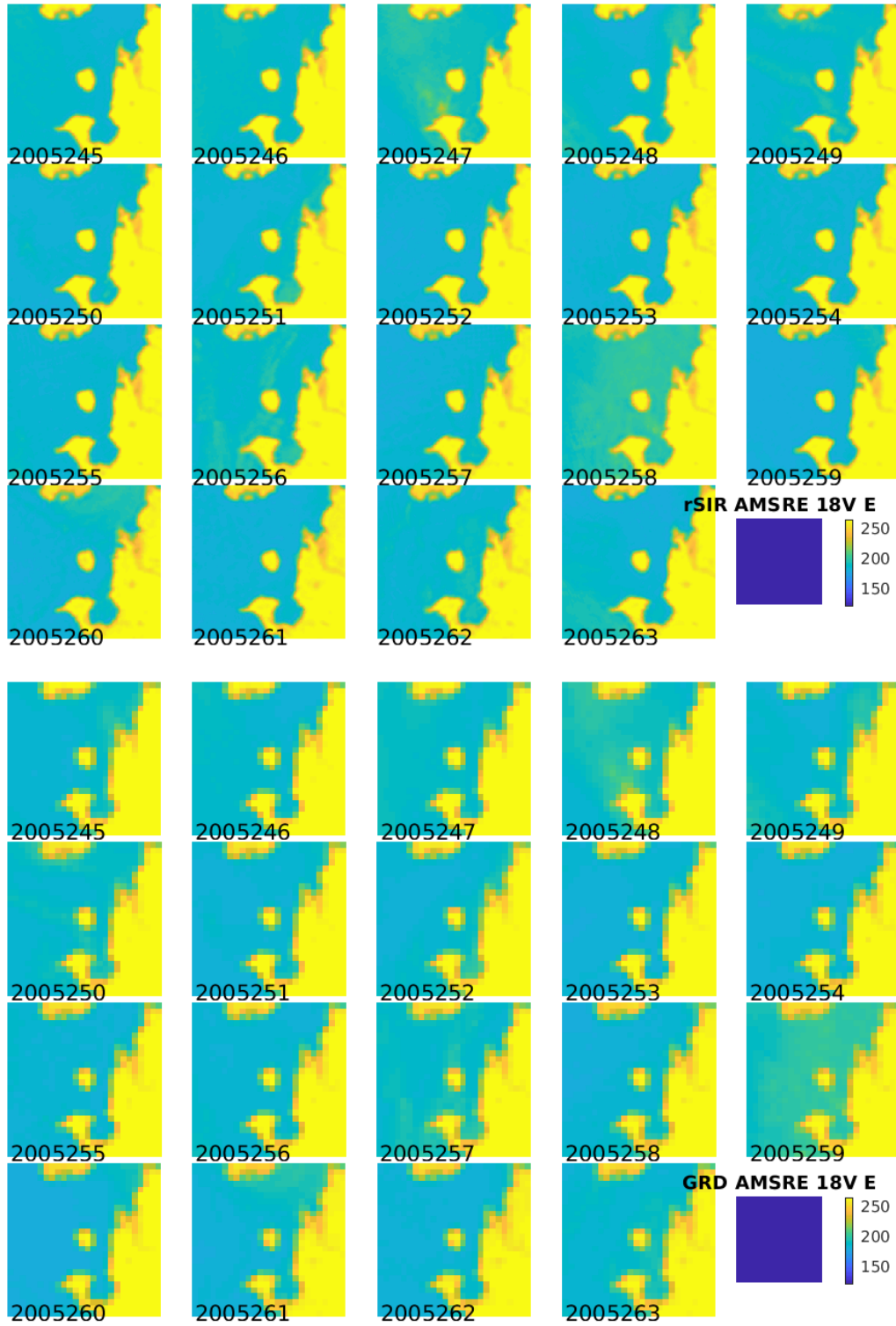


Figure 92: Time series of (top) rSIR and (bottom) GRD  $T_B$  images over the study area. Image dates are labeled on the image.

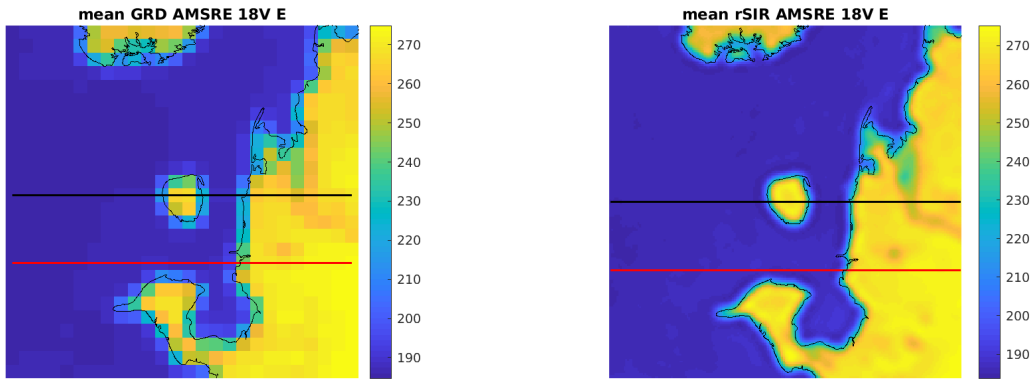


Figure 93: Average of daily  $T_B$  images over the study area. (left) 25-km GRD. (right) 3.125-km rSIR. The thick horizontal lines show the data transect locations where data is extracted from the image for analysis.

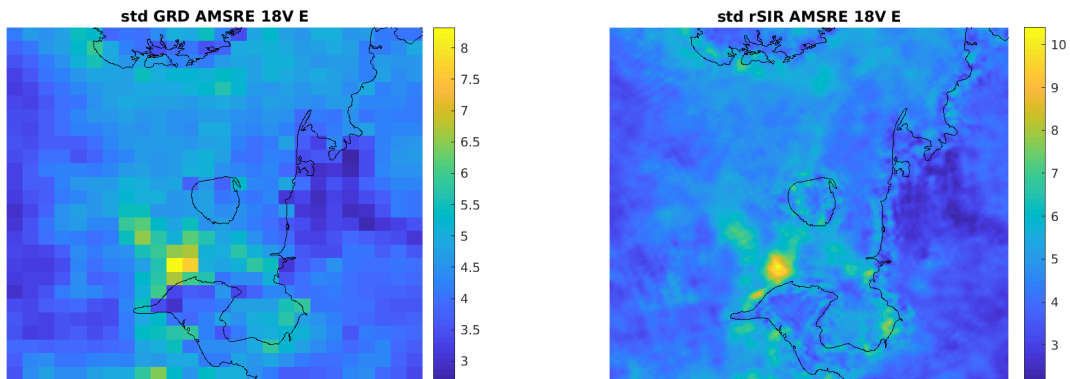


Figure 94: Standard deviation of daily  $T_B$  images over the study area. (left) 25-km GRD. (right) 3.125-km rSIR.

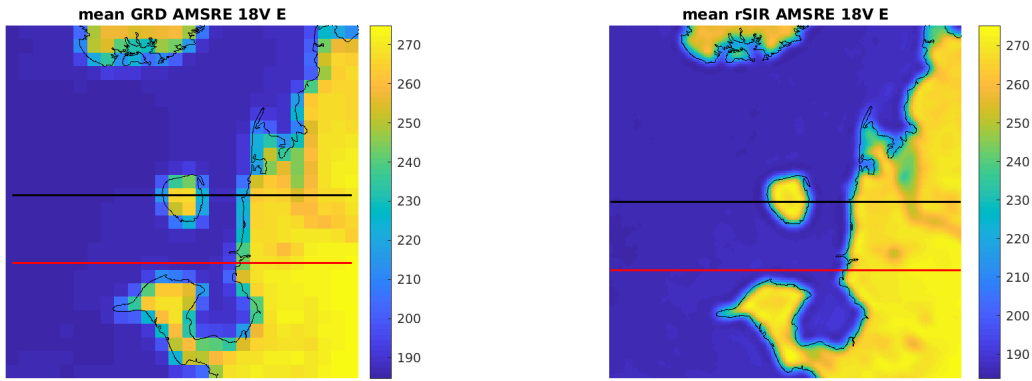


Figure 95: [Repeated] Average of daily  $T_B$  images over the study area. (left) 25-km GRD. (right) 3.125-km rSIR. The thick horizontal lines show the data transect locations where data is extracted from the image for analysis.

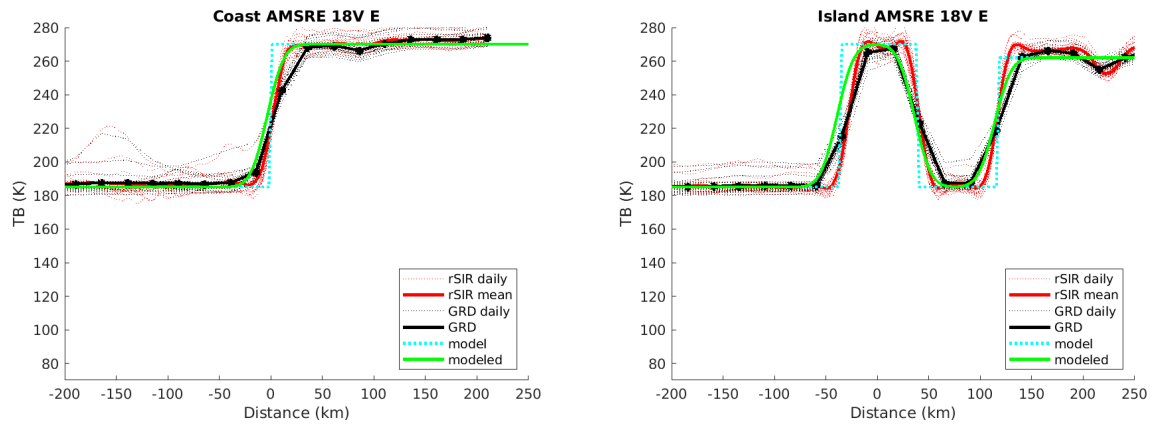


Figure 96: Plots of  $T_B$  along the two analysis case transect lines for the (left) coast-crossing and (right) island-crossing cases.

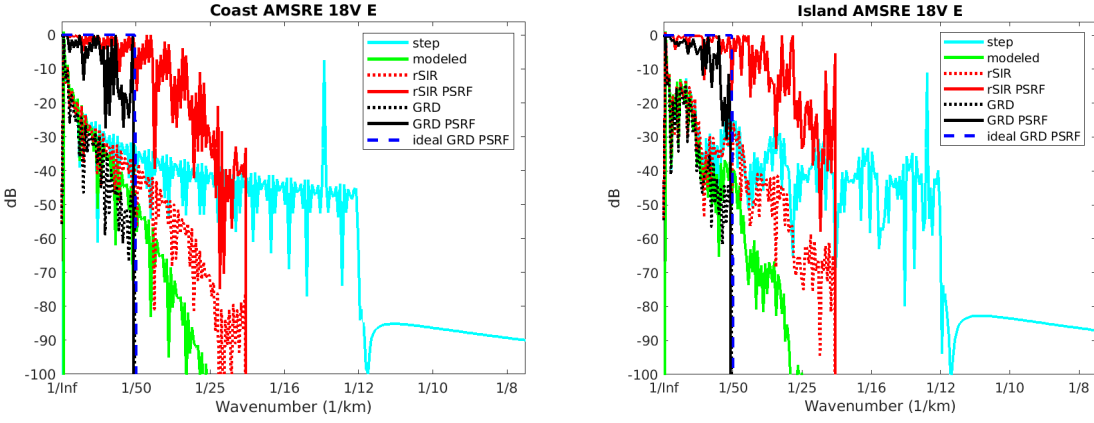


Figure 97: Wavenumber spectra of the  $T_B$  slices, the model, and the PSRF. (left) Coast-crossing case. (right) Island-crossing case.

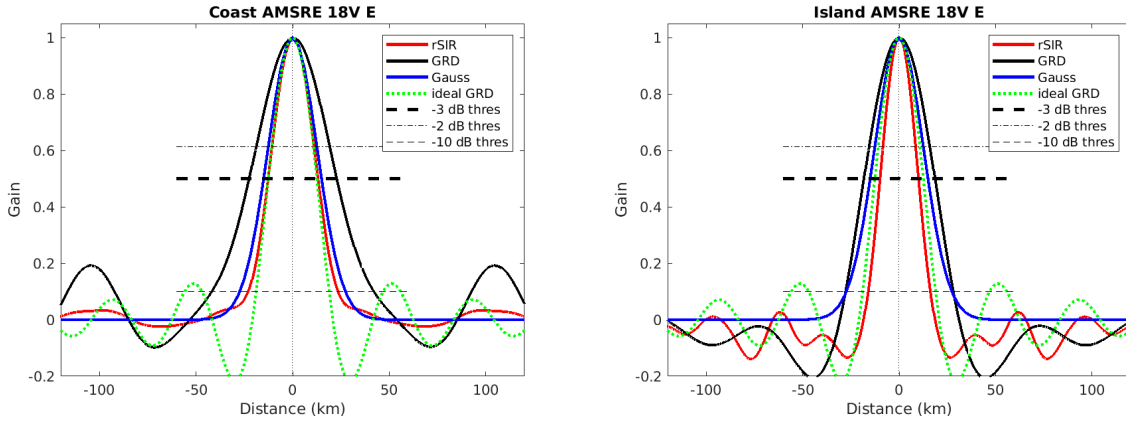


Figure 98: Derived single-pass rSIR and GRD PSRFs from the (left) coast-crossing and (right) island-crossing cases.

Table 86: Resolution estimates for AMSRE channel 18V LTOD E

Algorithm	-3 dB Thres		-2 dB Thres		-10 dB Thres	
	Coast	Island	Coast	Island	Coast	Island
Gauss	30.0	30.0	24.4	24.4	54.8	54.8
rSIR	25.9	20.0	21.2	16.5	46.5	32.3
ideal GRD	36.2	36.2	30.3	30.3	54.5	54.5
GRD	45.3	36.8	36.9	30.7	83.9	55.9

## C.12 AMSRE Channel 18V M Figures

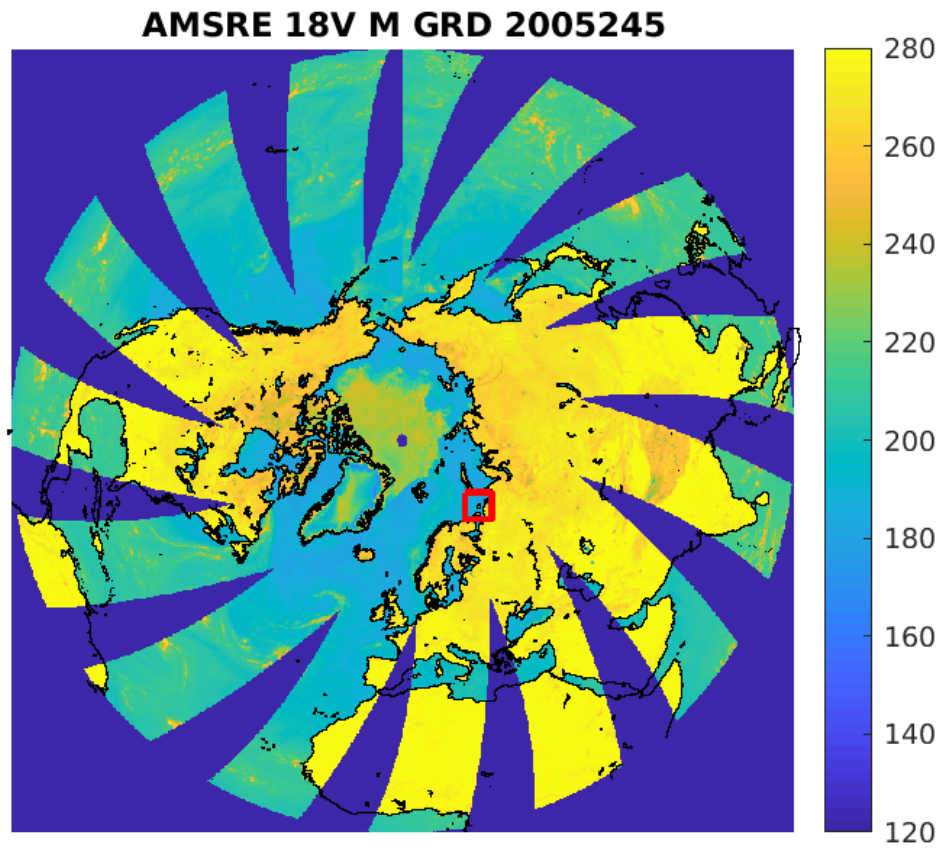


Figure 99: rSIR Northern Hemisphere view.

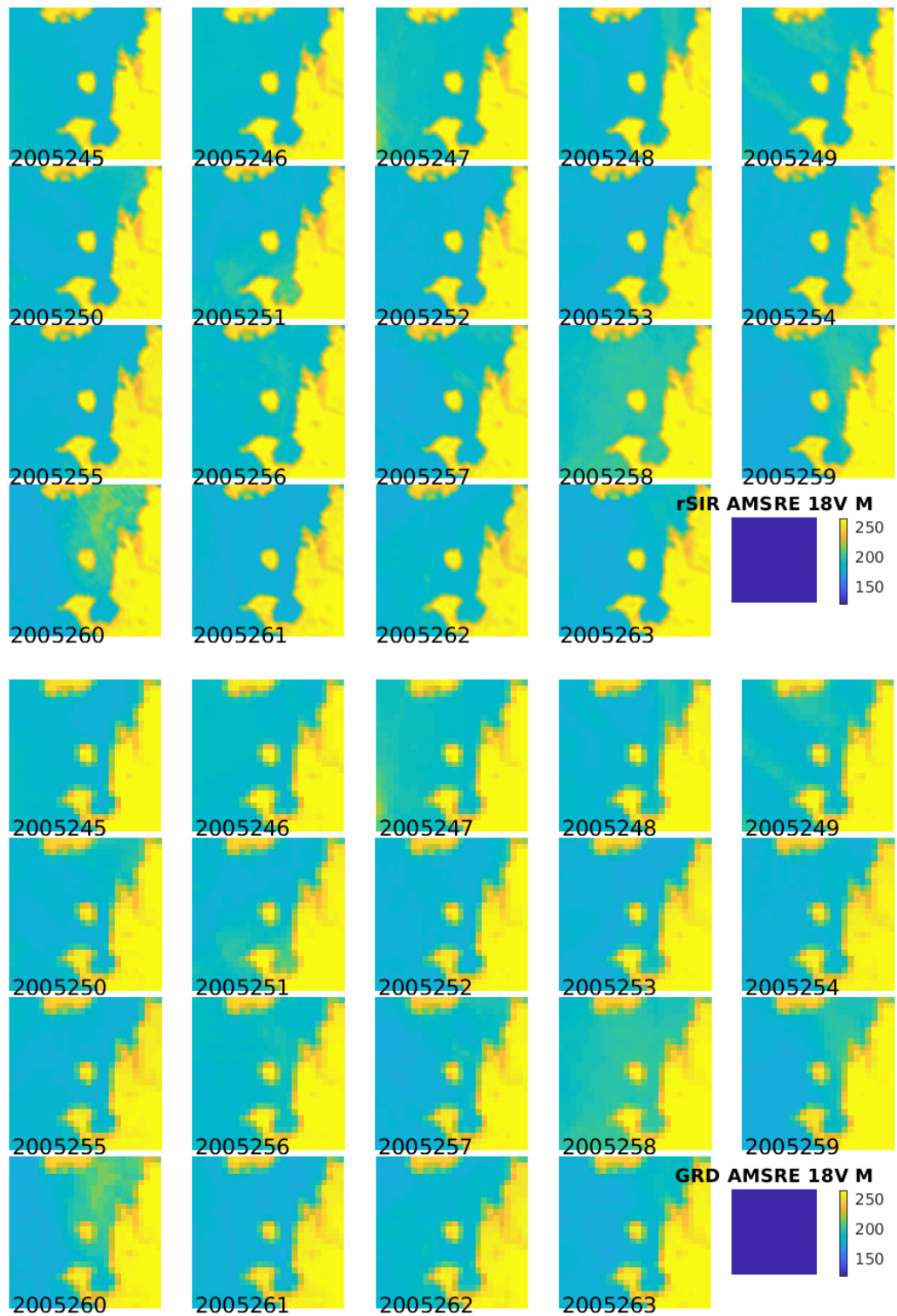


Figure 100: Time series of (top) rSIR and (bottom) GRD  $T_B$  images over the study area. Image dates are labeled on the image.

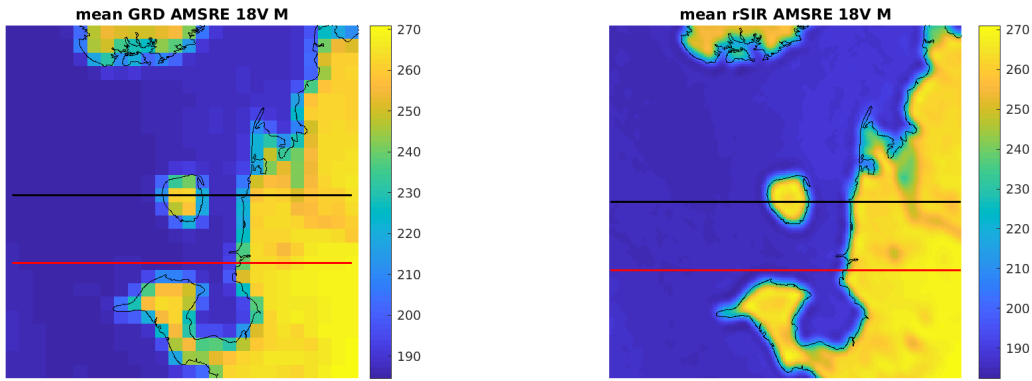


Figure 101: Average of daily  $T_B$  images over the study area. (left) 25-km GRD. (right) 3.125-km rSIR. The thick horizontal lines show the data transect locations where data is extracted from the image for analysis.

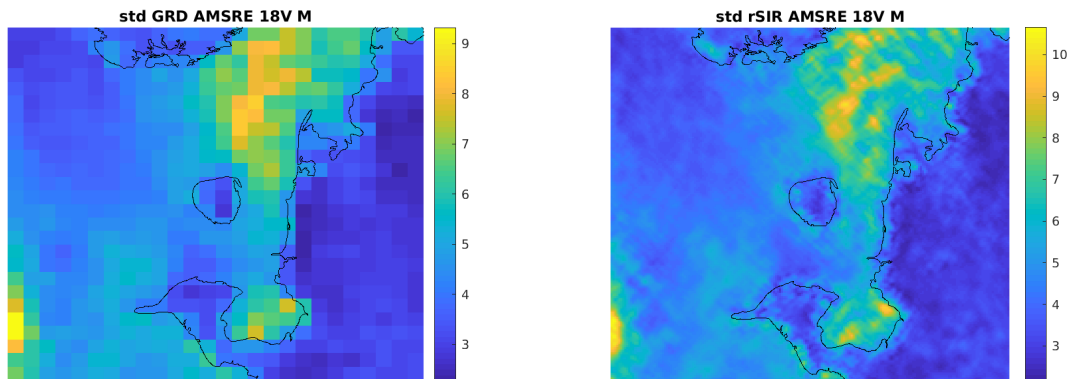


Figure 102: Standard deviation of daily  $T_B$  images over the study area. (left) 25-km GRD. (right) 3.125-km rSIR.



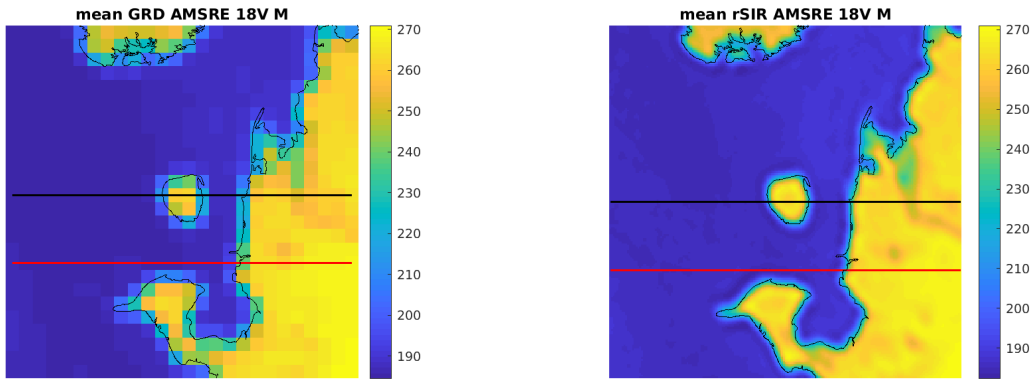


Figure 103: [Repeated] Average of daily  $T_B$  images over the study area. (left) 25-km GRD. (right) 3.125-km rSIR. The thick horizontal lines show the data transect locations where data is extracted from the image for analysis.

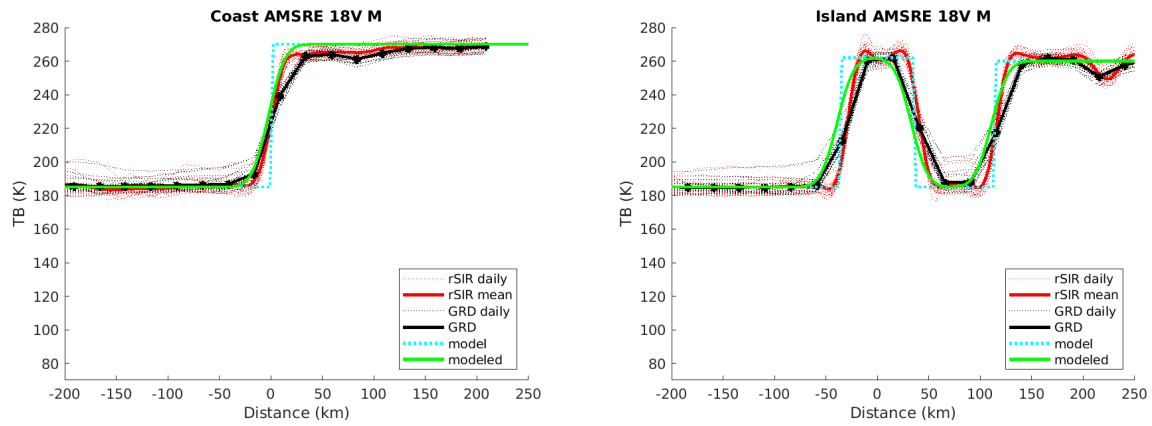


Figure 104: Plots of  $T_B$  along the two analysis case transect lines for the (left) coast-crossing and (right) island-crossing cases.

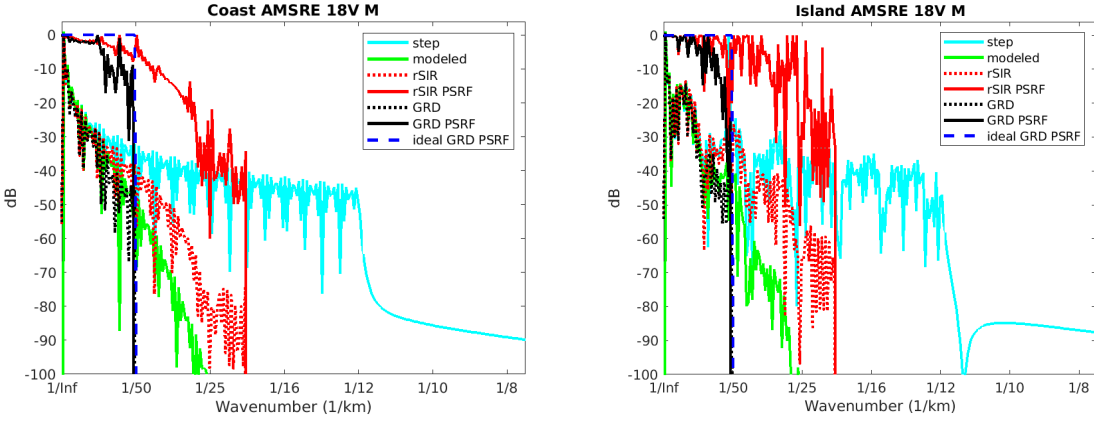


Figure 105: Wavenumber spectra of the  $T_B$  slices, the model, and the PSRF. (left) Coast-crossing case. (right) Island-crossing case.

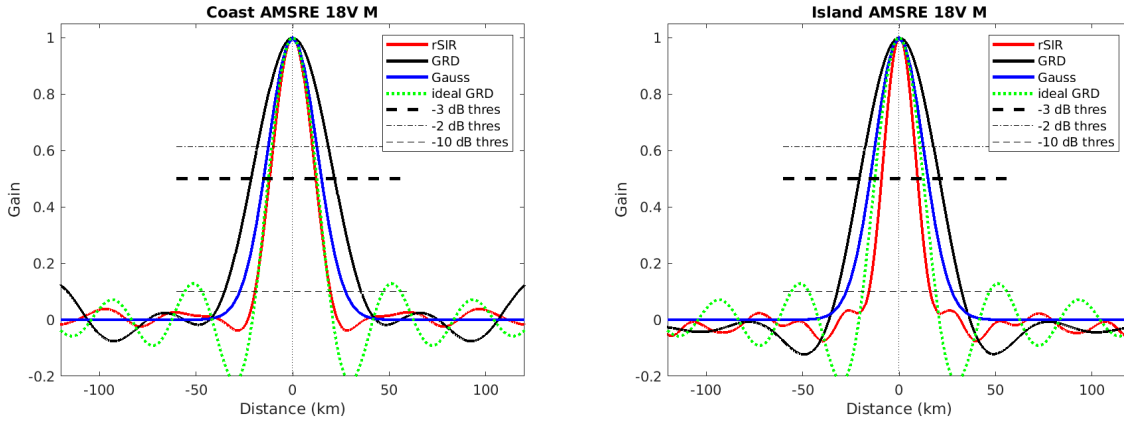


Figure 106: Derived single-pass rSIR and GRD PSRFs from the (left) coast-crossing and (right) island-crossing cases.

Table 87: Resolution estimates for AMSRE channel 18V LTOD M

Algorithm	-3 dB Thres		-2 dB Thres		-10 dB Thres	
	Coast	Island	Coast	Island	Coast	Island
Gauss	30.0	30.0	24.4	24.4	54.8	54.8
rSIR	23.9	18.7	19.8	15.4	39.1	32.0
ideal GRD	36.2	36.2	30.3	30.3	54.5	54.5
GRD	43.2	41.4	35.8	34.4	70.7	64.6

### C.13 AMSRE Channel 23H E Figures

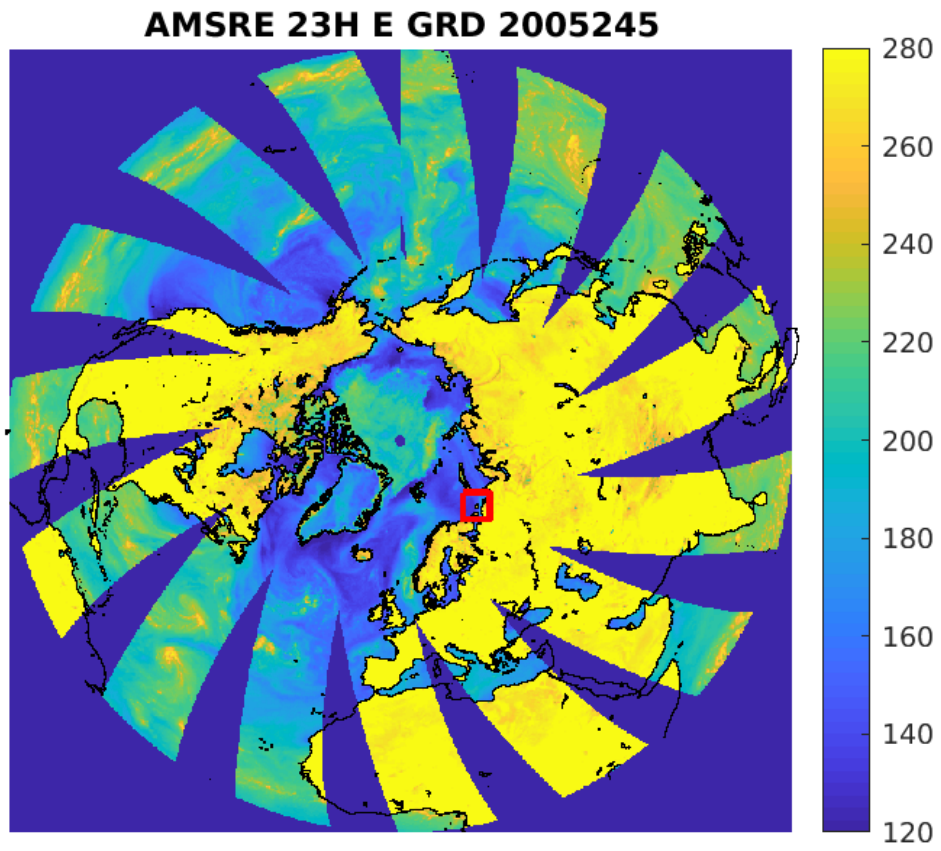


Figure 107: rSIR Northern Hemisphere view.

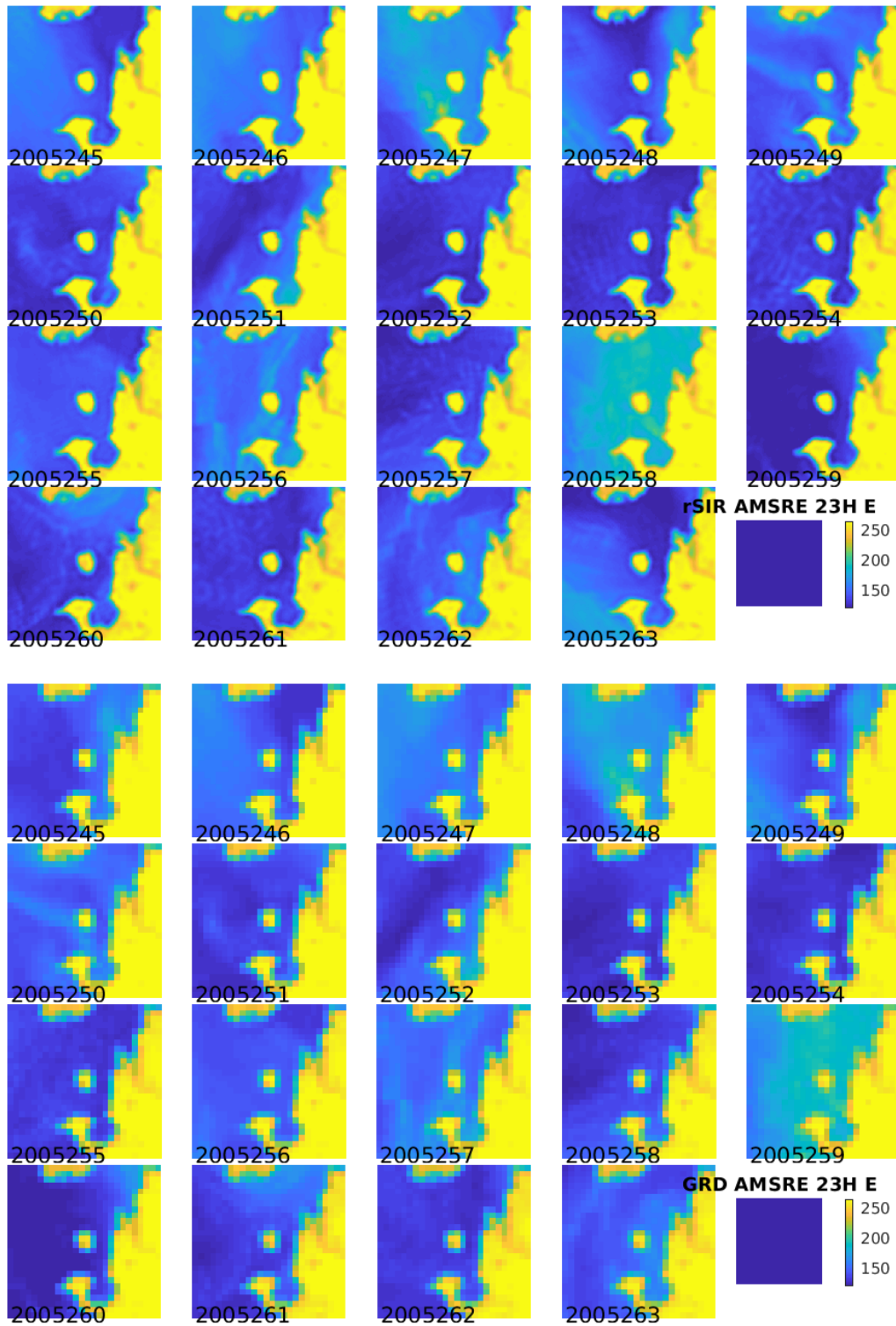


Figure 108: Time series of (top) rSIR and (bottom) GRD  $T_B$  images over the study area. Image dates are labeled on the image.

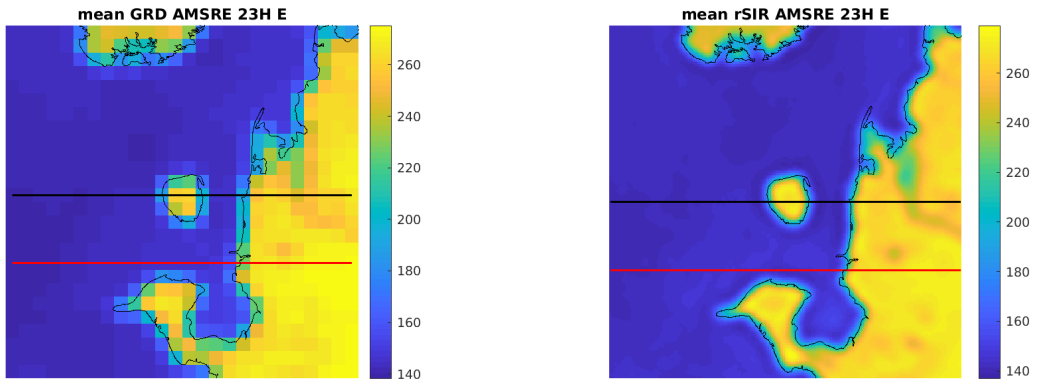


Figure 109: Average of daily  $T_B$  images over the study area. (left) 25-km GRD. (right) 3.125-km rSIR. The thick horizontal lines show the data transect locations where data is extracted from the image for analysis.

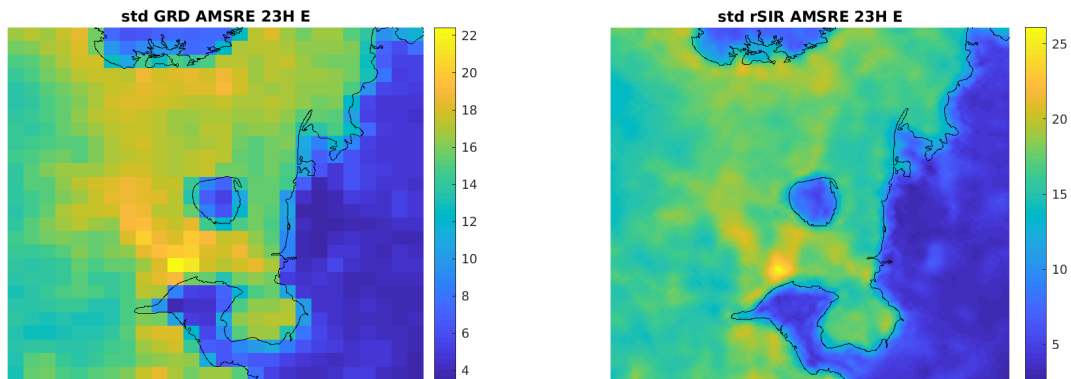


Figure 110: Standard deviation of daily  $T_B$  images over the study area. (left) 25-km GRD. (right) 3.125-km rSIR.

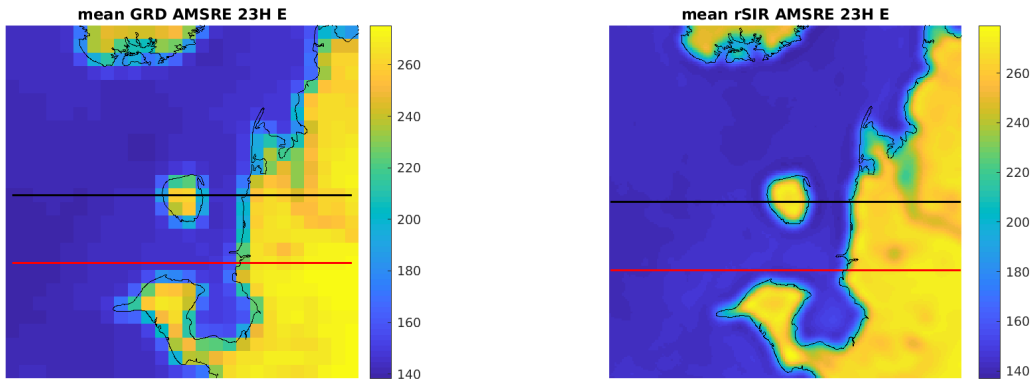


Figure 111: [Repeated] Average of daily  $T_B$  images over the study area. (left) 25-km GRD. (right) 3.125-km rSIR. The thick horizontal lines show the data transect locations where data is extracted from the image for analysis.

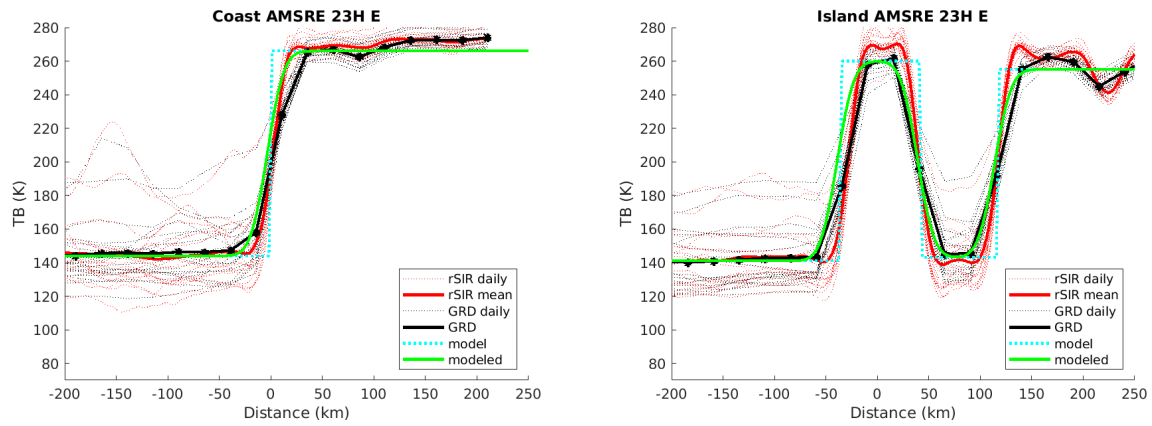


Figure 112: Plots of  $T_B$  along the two analysis case transect lines for the (left) coast-crossing and (right) island-crossing cases.

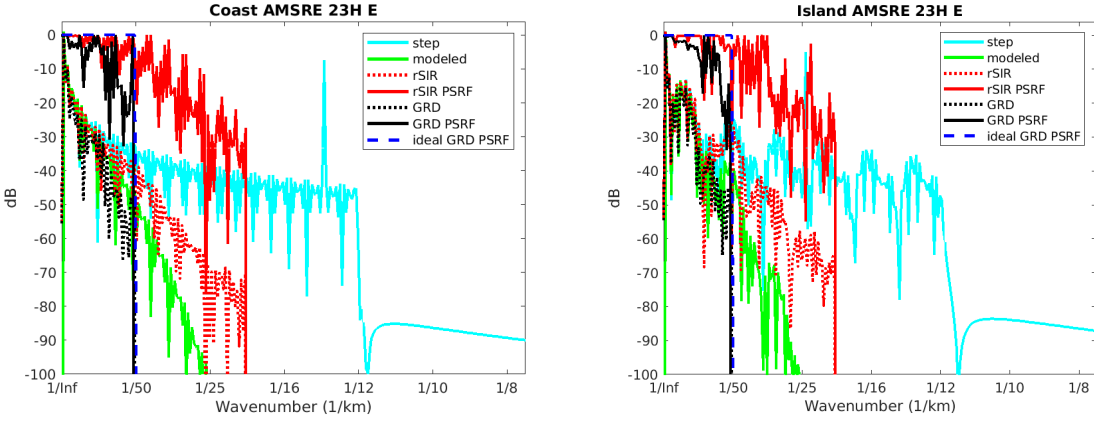


Figure 113: Wavenumber spectra of the  $T_B$  slices, the model, and the PSRF. (left) Coast-crossing case. (right) Island-crossing case.

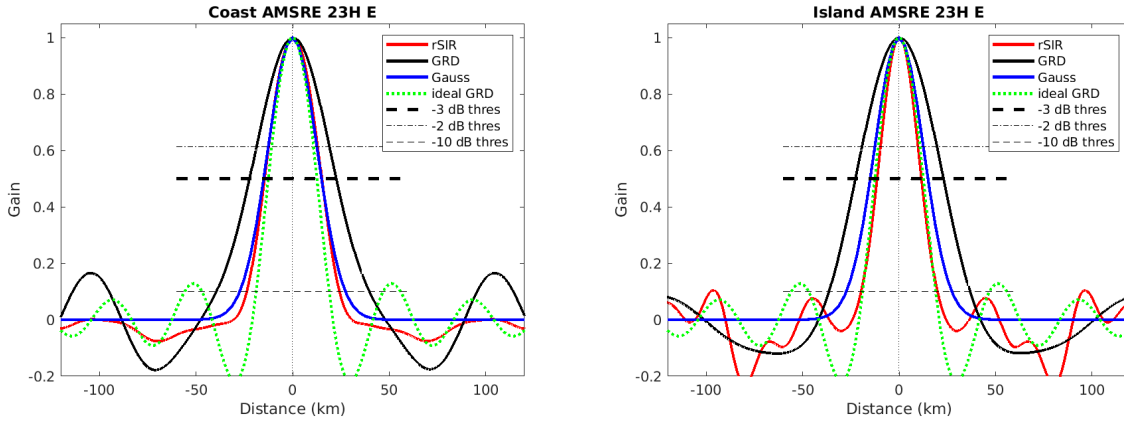


Figure 114: Derived single-pass rSIR and GRD PSRFs from the (left) coast-crossing and (right) island-crossing cases.

Table 88: Resolution estimates for AMSRE channel 23H LTOD E

Algorithm	-3 dB Thres		-2 dB Thres		-10 dB Thres	
	Coast	Island	Coast	Island	Coast	Island
Gauss	30.0	30.0	24.4	24.4	54.8	54.8
rSIR	29.6	23.1	24.8	18.9	47.9	39.5
ideal GRD	36.2	36.2	30.3	30.3	54.5	54.5
GRD	44.8	45.6	36.6	37.7	79.2	73.1

## C.14 AMSRE Channel 23H M Figures

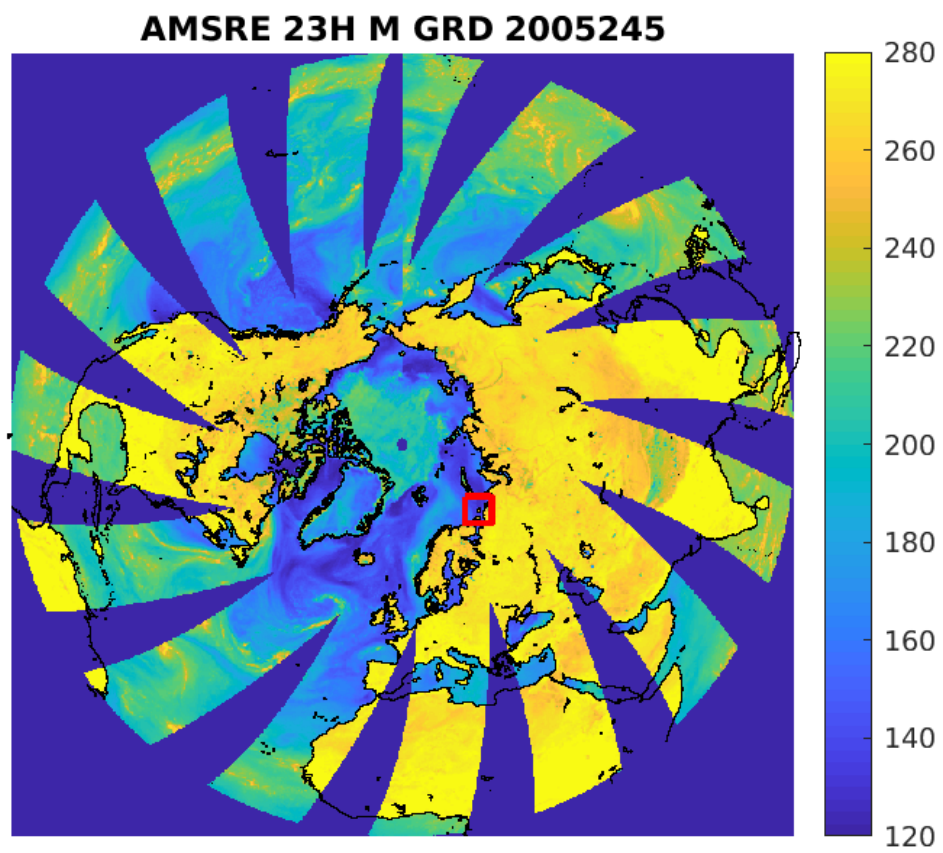


Figure 115: rSIR Northern Hemisphere view.



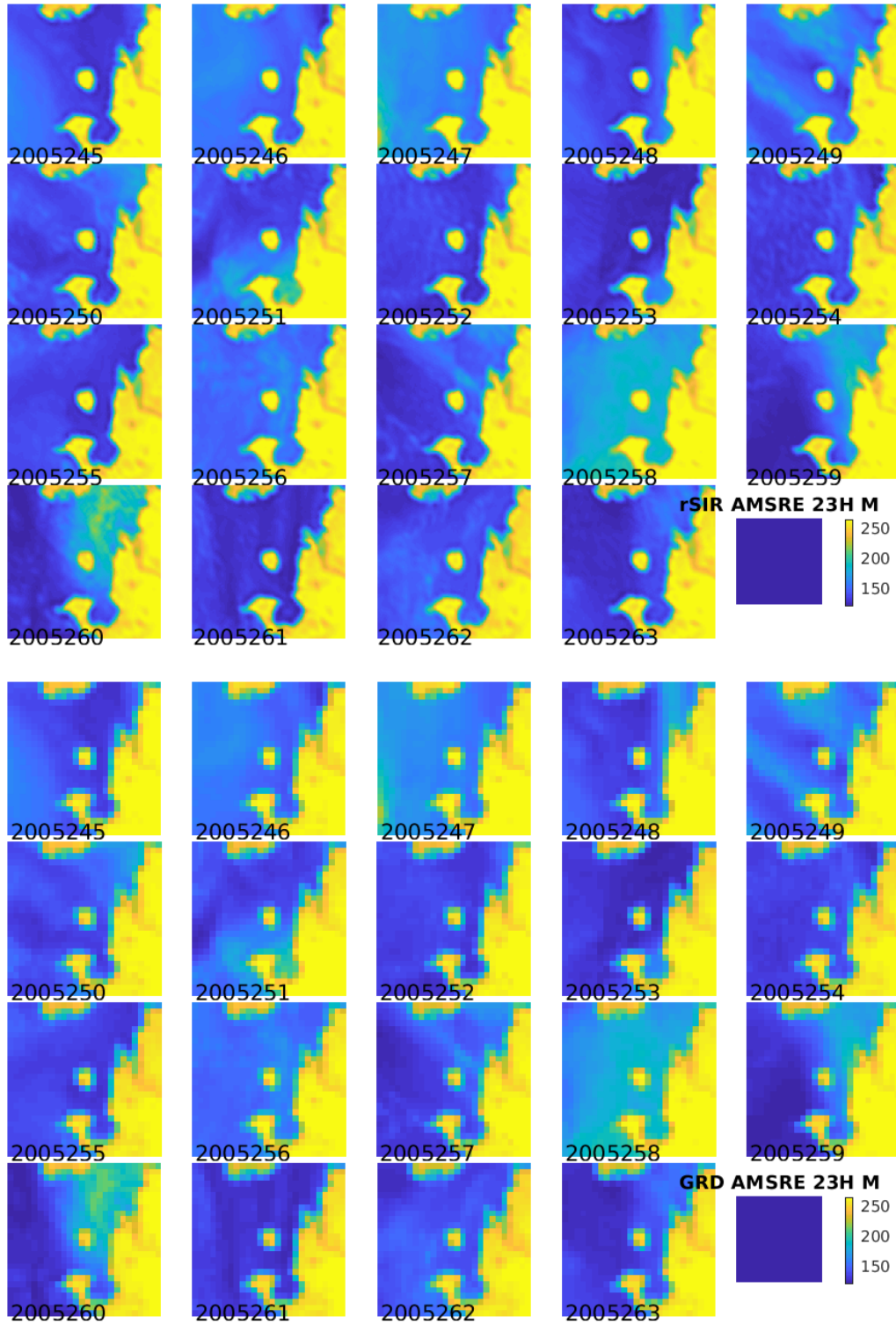


Figure 116: Time series of (top) rSIR and (bottom) GRD  $T_B$  images over the study area. Image dates are labeled on the image.

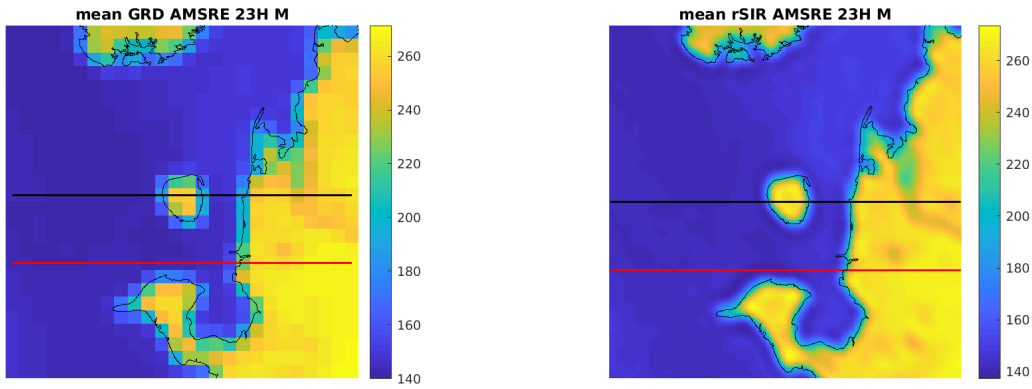


Figure 117: Average of daily  $T_B$  images over the study area. (left) 25-km GRD. (right) 3.125-km rSIR. The thick horizontal lines show the data transect locations where data is extracted from the image for analysis.

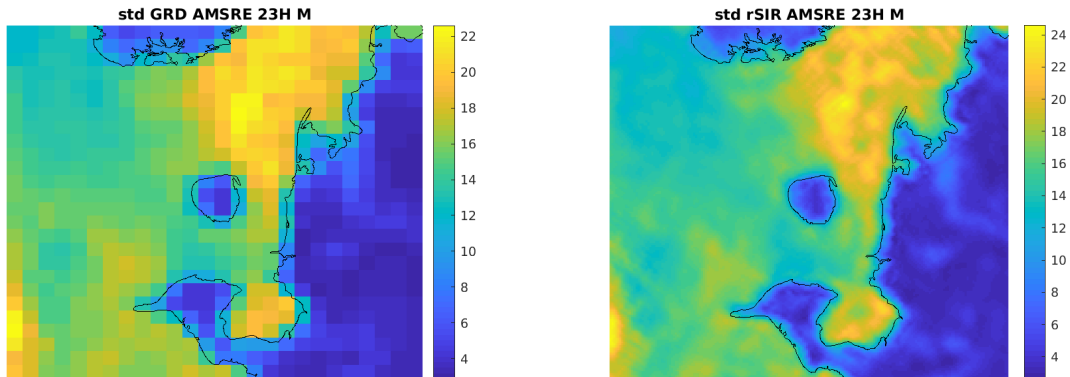


Figure 118: Standard deviation of daily  $T_B$  images over the study area. (left) 25-km GRD. (right) 3.125-km rSIR.

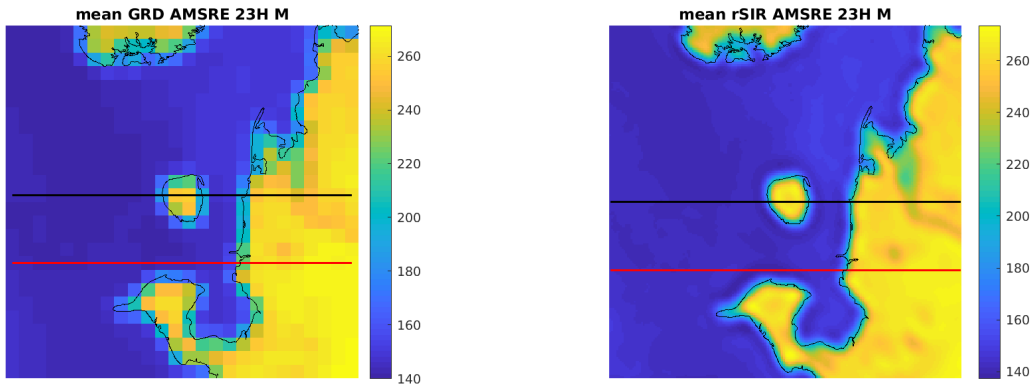


Figure 119: [Repeated] Average of daily  $T_B$  images over the study area. (left) 25-km GRD. (right) 3.125-km rSIR. The thick horizontal lines show the data transect locations where data is extracted from the image for analysis.

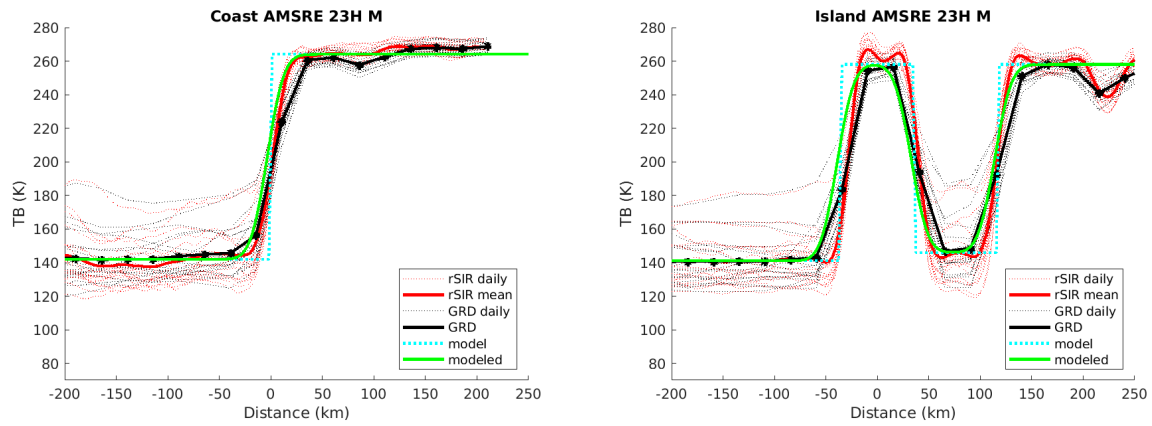


Figure 120: Plots of  $T_B$  along the two analysis case transect lines for the (left) coast-crossing and (right) island-crossing cases.

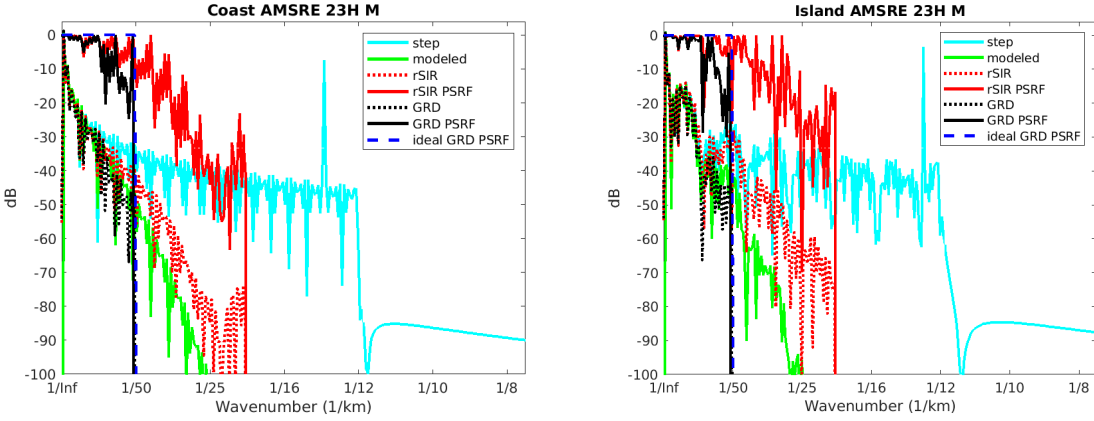


Figure 121: Wavenumber spectra of the  $T_B$  slices, the model, and the PSRF. (left) Coast-crossing case. (right) Island-crossing case.

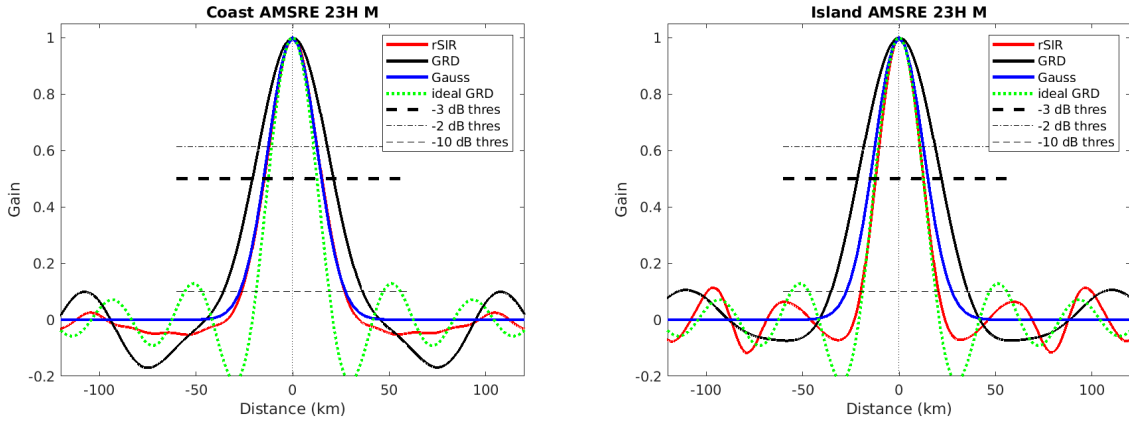


Figure 122: Derived single-pass rSIR and GRD PSRFs from the (left) coast-crossing and (right) island-crossing cases.

Table 89: Resolution estimates for AMSRE channel 23H LTOD M

Algorithm	-3 dB Thres		-2 dB Thres		-10 dB Thres	
	Coast	Island	Coast	Island	Coast	Island
Gauss	30.0	30.0	24.4	24.4	54.8	54.8
rSIR	29.9	24.9	24.2	20.6	53.4	40.2
ideal GRD	36.2	36.2	30.3	30.3	54.5	54.5
GRD	41.9	43.5	34.4	35.9	72.1	71.0

C.15 AMSRE Channel 23V E Figures

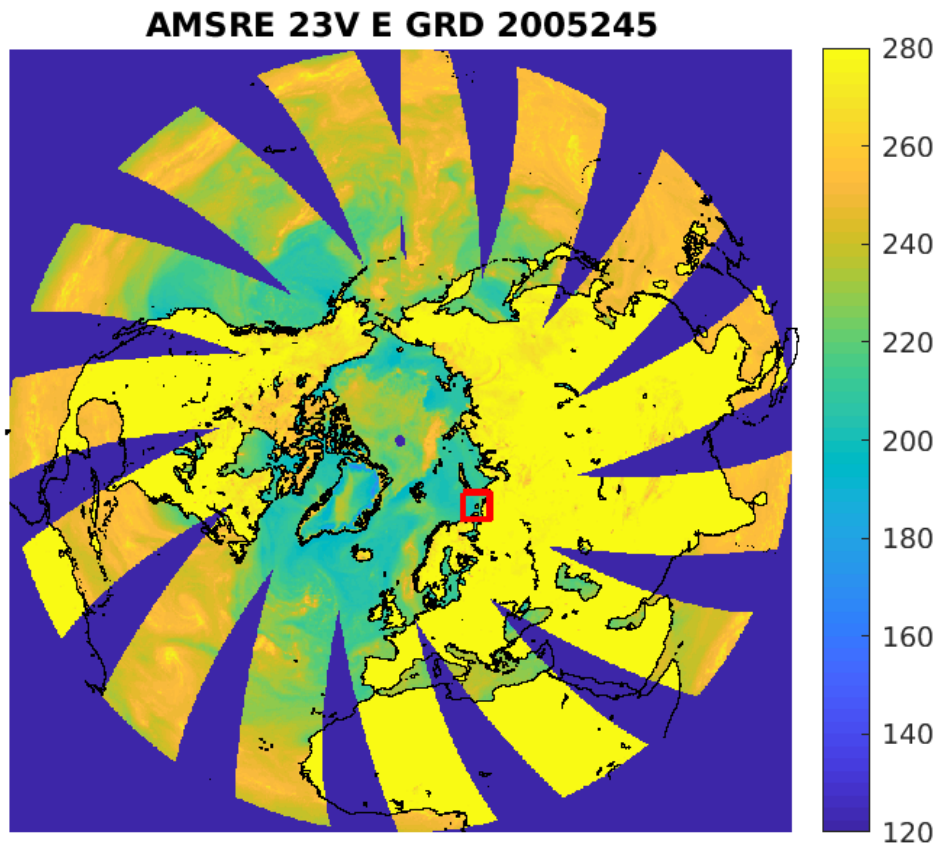


Figure 123: rSIR Northern Hemisphere view.

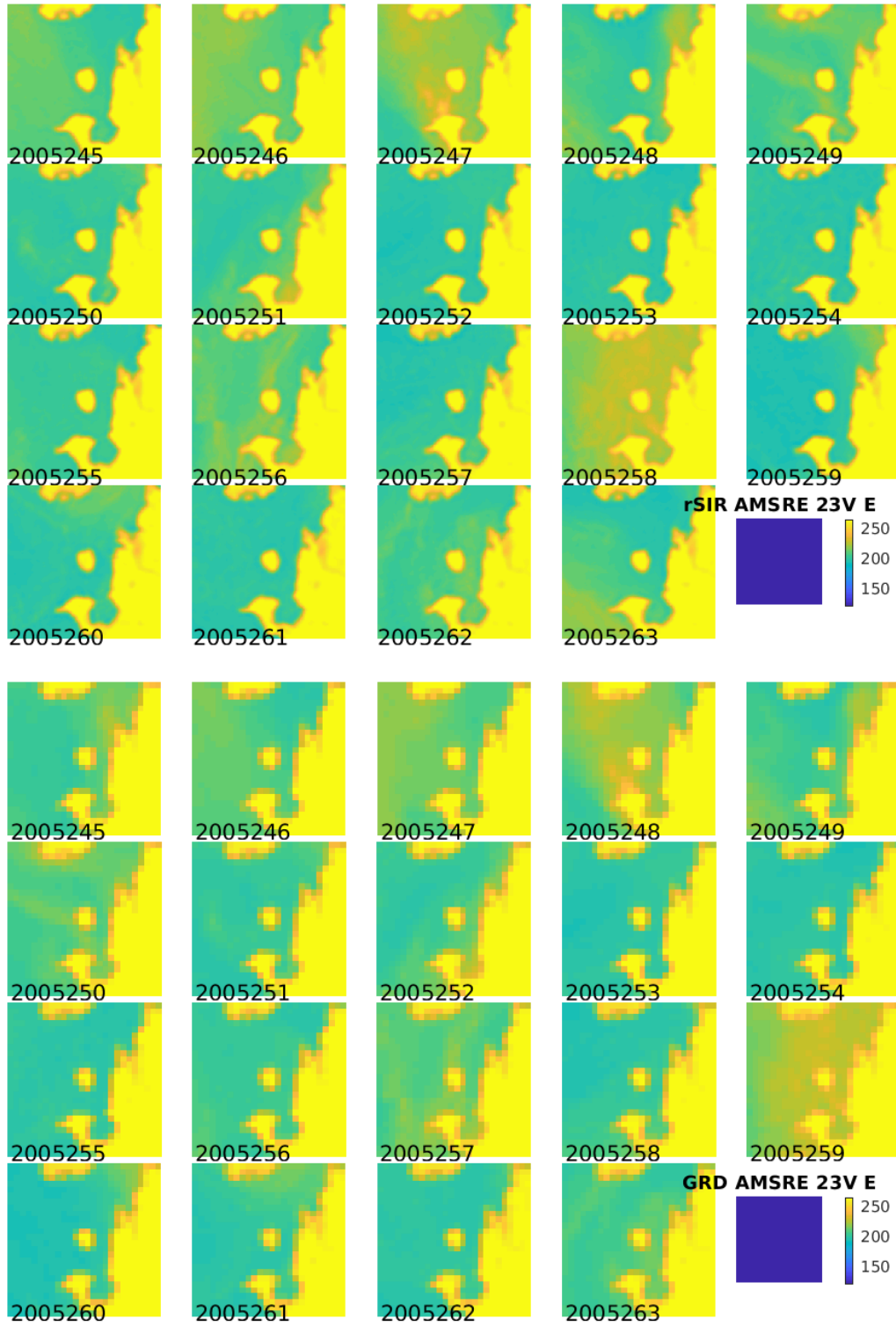


Figure 124: Time series of (top) rSIR and (bottom) GRD  $T_B$  images over the study area. Image dates are labeled on the image.

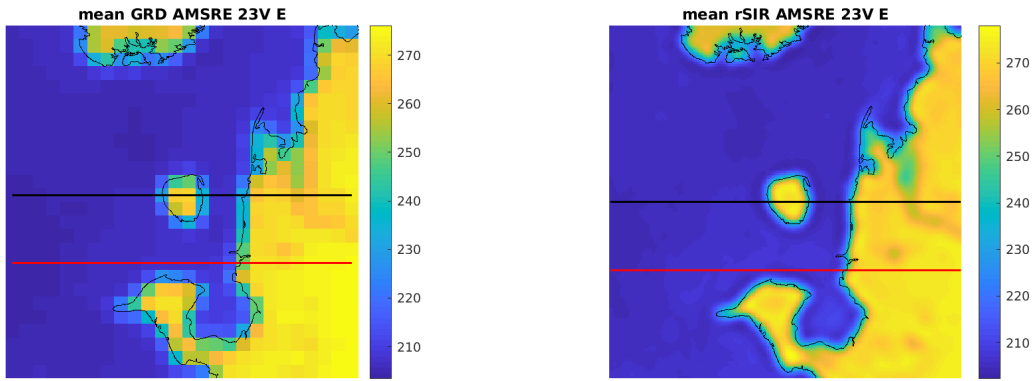


Figure 125: Average of daily  $T_B$  images over the study area. (left) 25-km GRD. (right) 3.125-km rSIR. The thick horizontal lines show the data transect locations where data is extracted from the image for analysis.

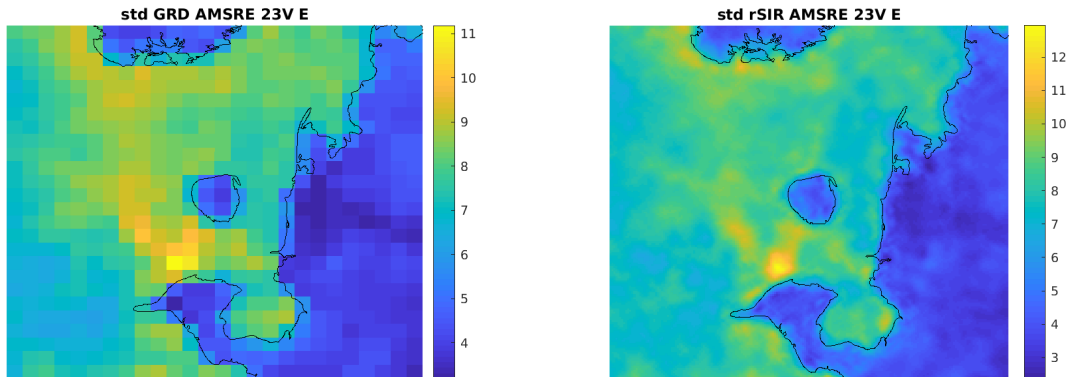


Figure 126: Standard deviation of daily  $T_B$  images over the study area. (left) 25-km GRD. (right) 3.125-km rSIR.

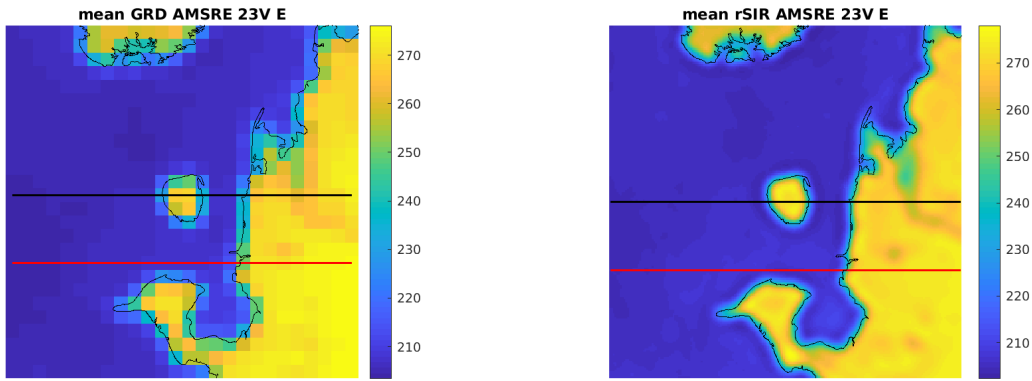


Figure 127: [Repeated] Average of daily  $T_B$  images over the study area. (left) 25-km GRD. (right) 3.125-km rSIR. The thick horizontal lines show the data transect locations where data is extracted from the image for analysis.

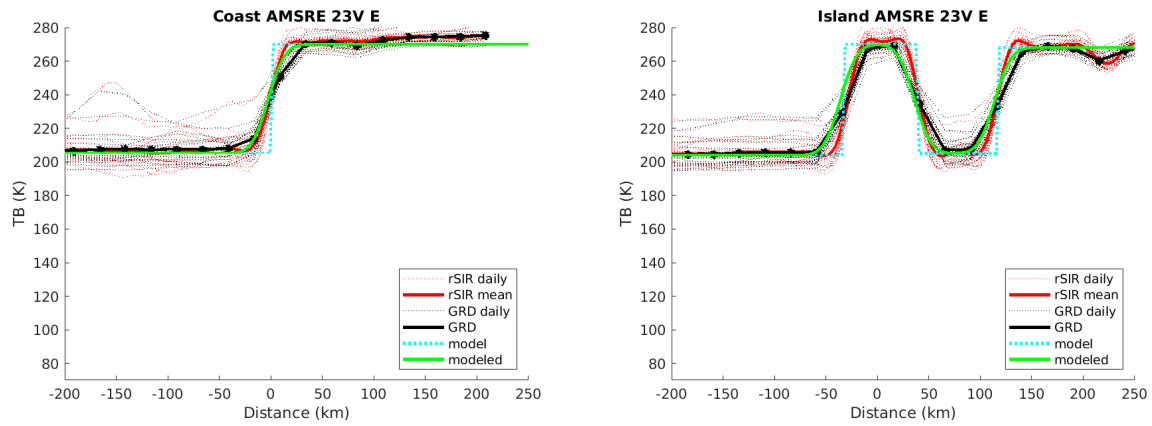


Figure 128: Plots of  $T_B$  along the two analysis case transect lines for the (left) coast-crossing and (right) island-crossing cases.



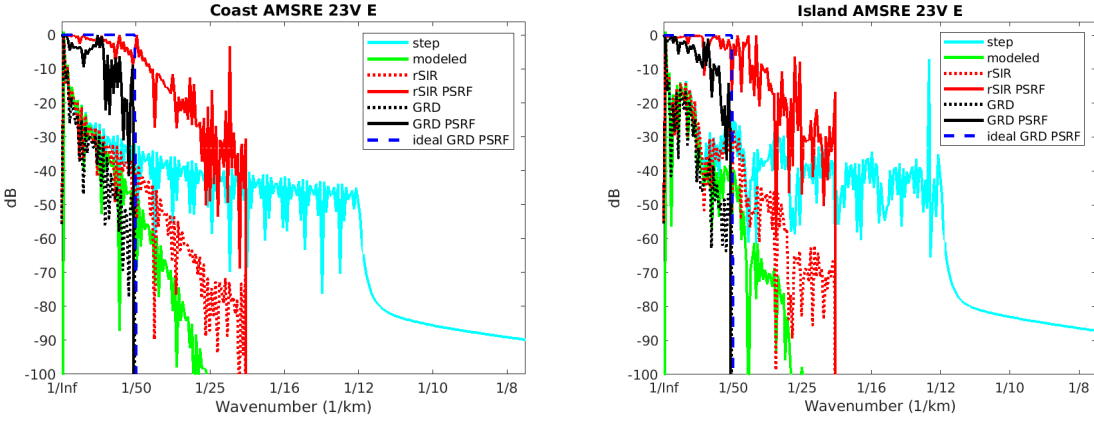


Figure 129: Wavenumber spectra of the  $T_B$  slices, the model, and the PSRF. (left) Coast-crossing case. (right) Island-crossing case.

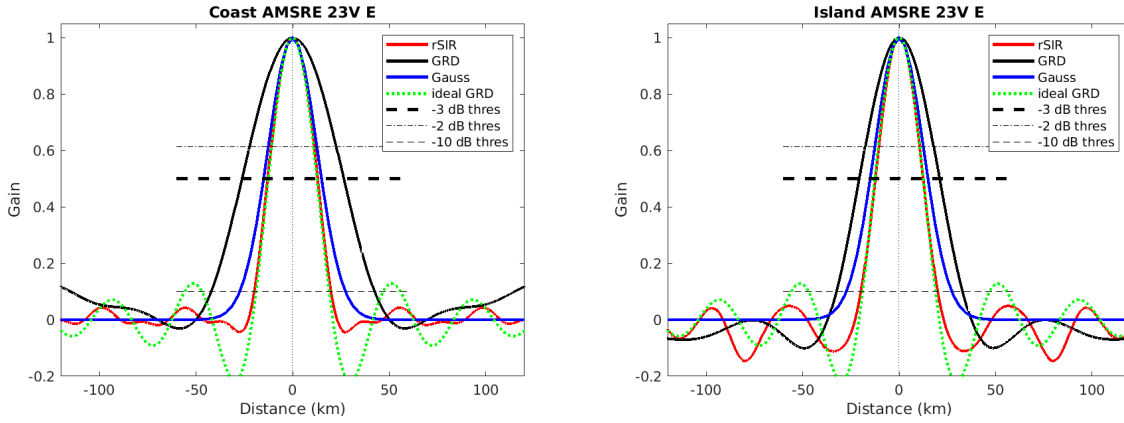


Figure 130: Derived single-pass rSIR and GRD PSRFs from the (left) coast-crossing and (right) island-crossing cases.

Table 90: Resolution estimates for AMSRE channel 23V LTOD E

Algorithm	-3 dB Thres		-2 dB Thres		-10 dB Thres	
	Coast	Island	Coast	Island	Coast	Island
Gauss	30.0	30.0	24.4	24.4	54.8	54.8
rSIR	25.8	24.8	21.7	20.6	39.8	39.7
ideal GRD	36.2	36.2	30.3	30.3	54.5	54.5
GRD	52.7	41.6	43.7	34.5	84.5	65.5

## C.16 AMSRE Channel 23V M Figures

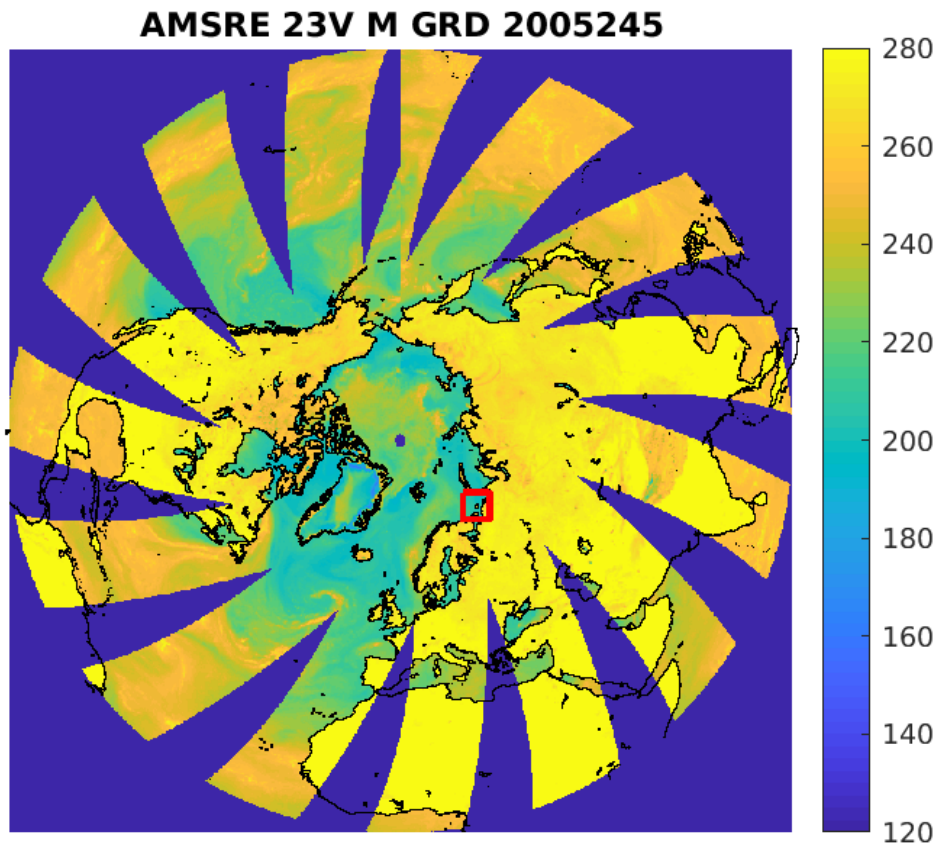


Figure 131: rSIR Northern Hemisphere view.

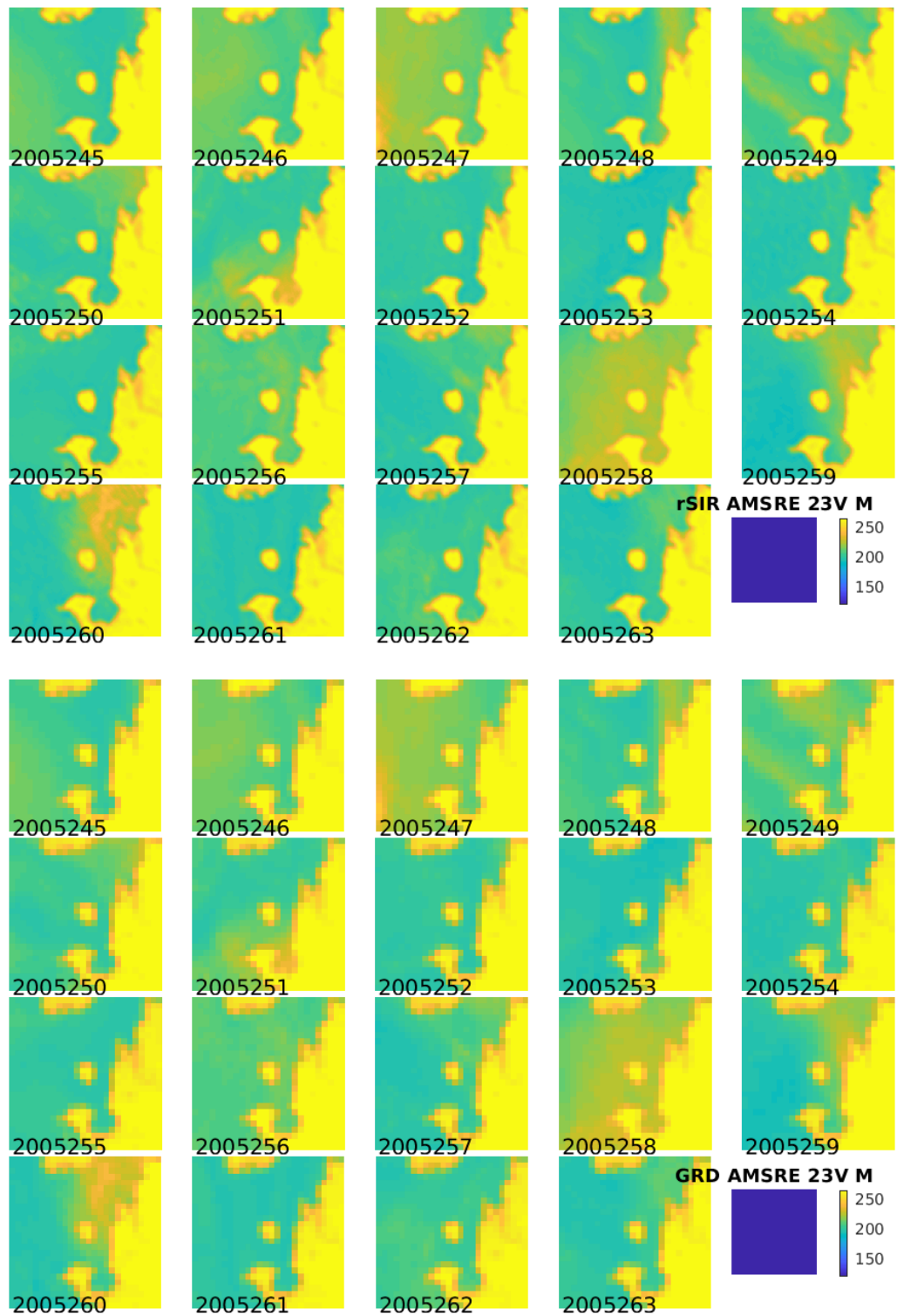


Figure 132: Time series of (top) rSIR and (bottom) GRD  $T_B$  images over the study area. Image dates are labeled on the image.

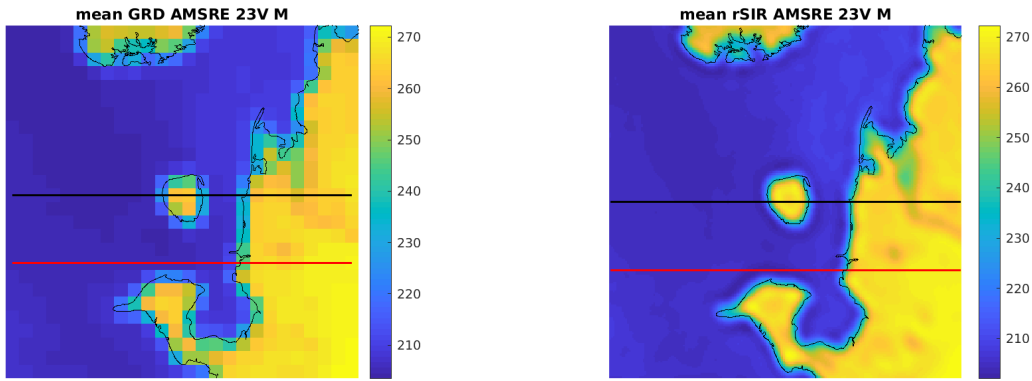


Figure 133: Average of daily  $T_B$  images over the study area. (left) 25-km GRD. (right) 3.125-km rSIR. The thick horizontal lines show the data transect locations where data is extracted from the image for analysis.

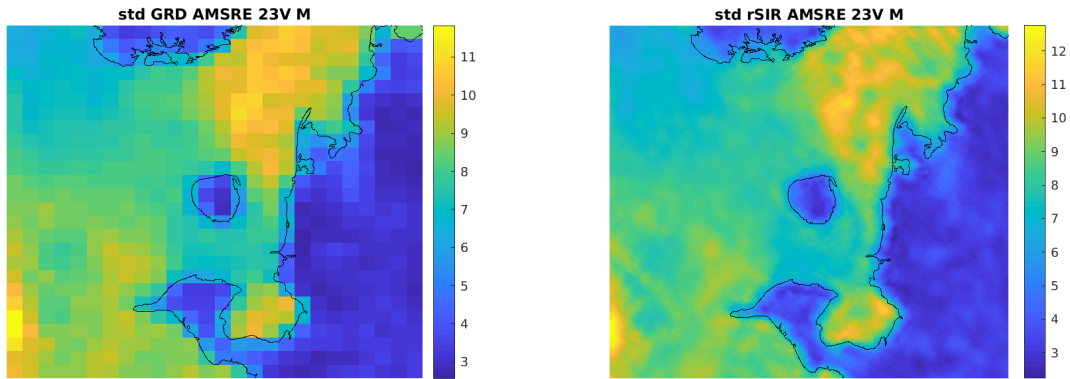


Figure 134: Standard deviation of daily  $T_B$  images over the study area. (left) 25-km GRD. (right) 3.125-km rSIR.

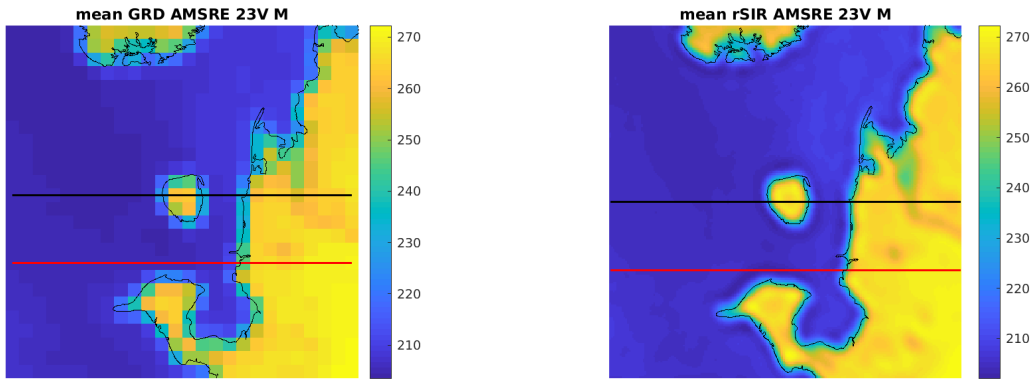


Figure 135: [Repeated] Average of daily  $T_B$  images over the study area. (left) 25-km GRD. (right) 3.125-km rSIR. The thick horizontal lines show the data transect locations where data is extracted from the image for analysis.

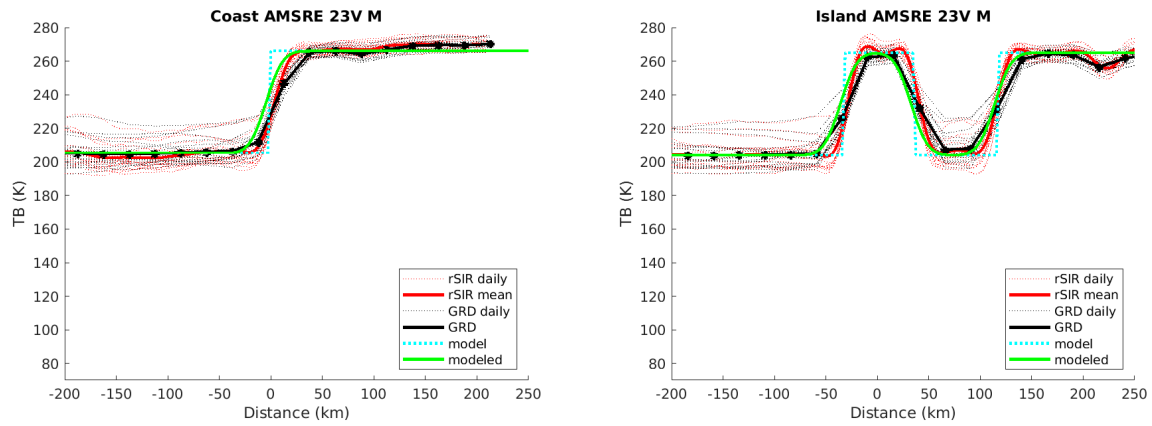


Figure 136: Plots of  $T_B$  along the two analysis case transect lines for the (left) coast-crossing and (right) island-crossing cases.

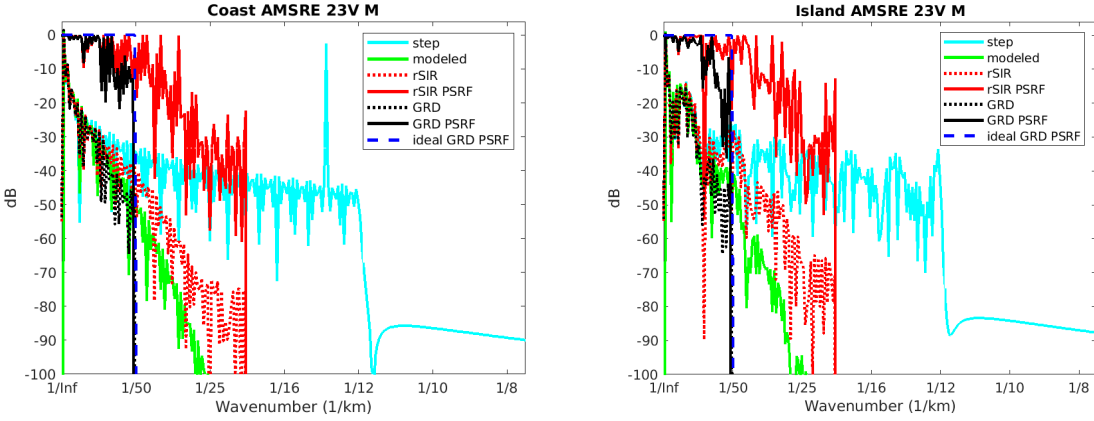


Figure 137: Wavenumber spectra of the  $T_B$  slices, the model, and the PSRF. (left) Coast-crossing case. (right) Island-crossing case.

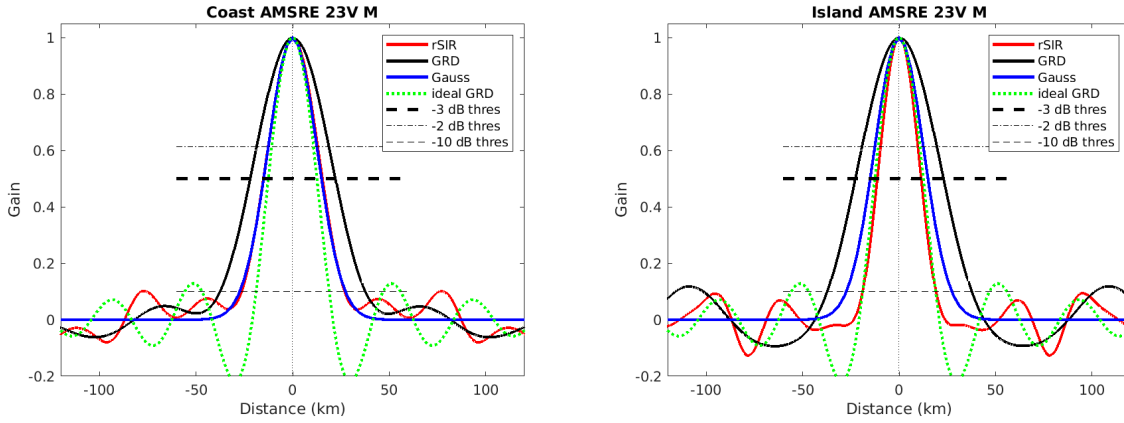


Figure 138: Derived single-pass rSIR and GRD PSRFs from the (left) coast-crossing and (right) island-crossing cases.

Table 91: Resolution estimates for AMSRE channel 23V LTOD M

Algorithm	-3 dB Thres		-2 dB Thres		-10 dB Thres	
	Coast	Island	Coast	Island	Coast	Island
Gauss	30.0	30.0	24.4	24.4	54.8	54.8
rSIR	30.5	22.8	24.8	18.8	53.3	38.0
ideal GRD	36.2	36.2	30.3	30.3	54.5	54.5
GRD	44.1	45.6	36.3	37.6	75.2	74.9

## C.17 AMSRE Channel 36H E Figures

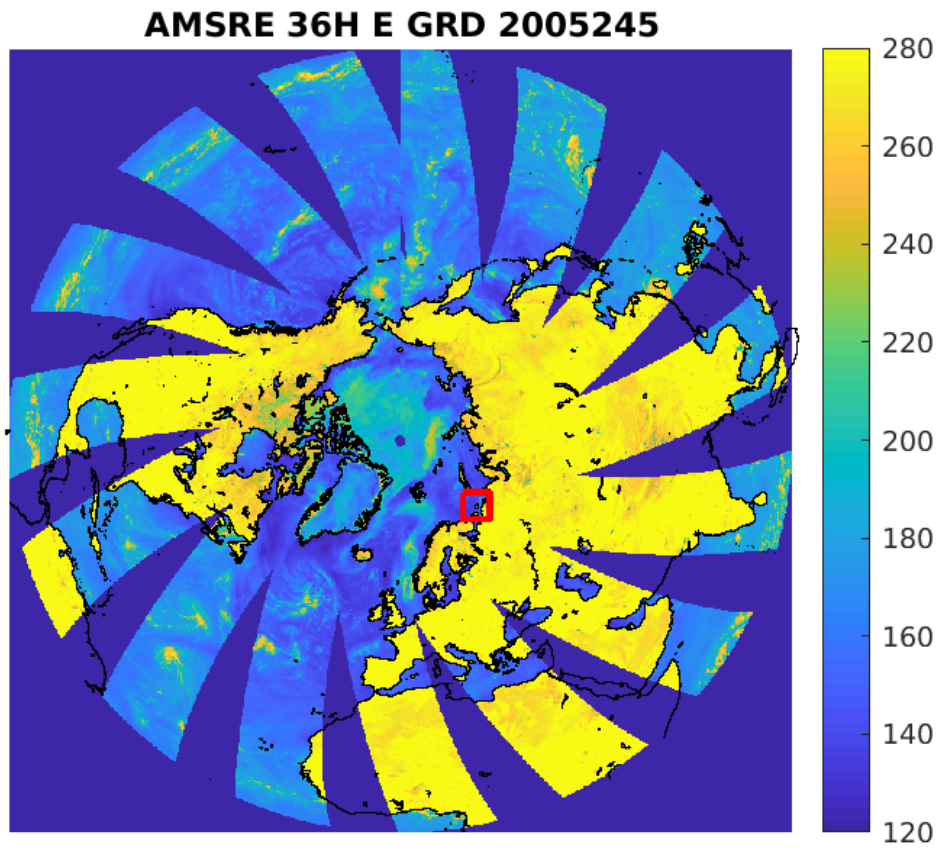


Figure 139: rSIR Northern Hemisphere view.

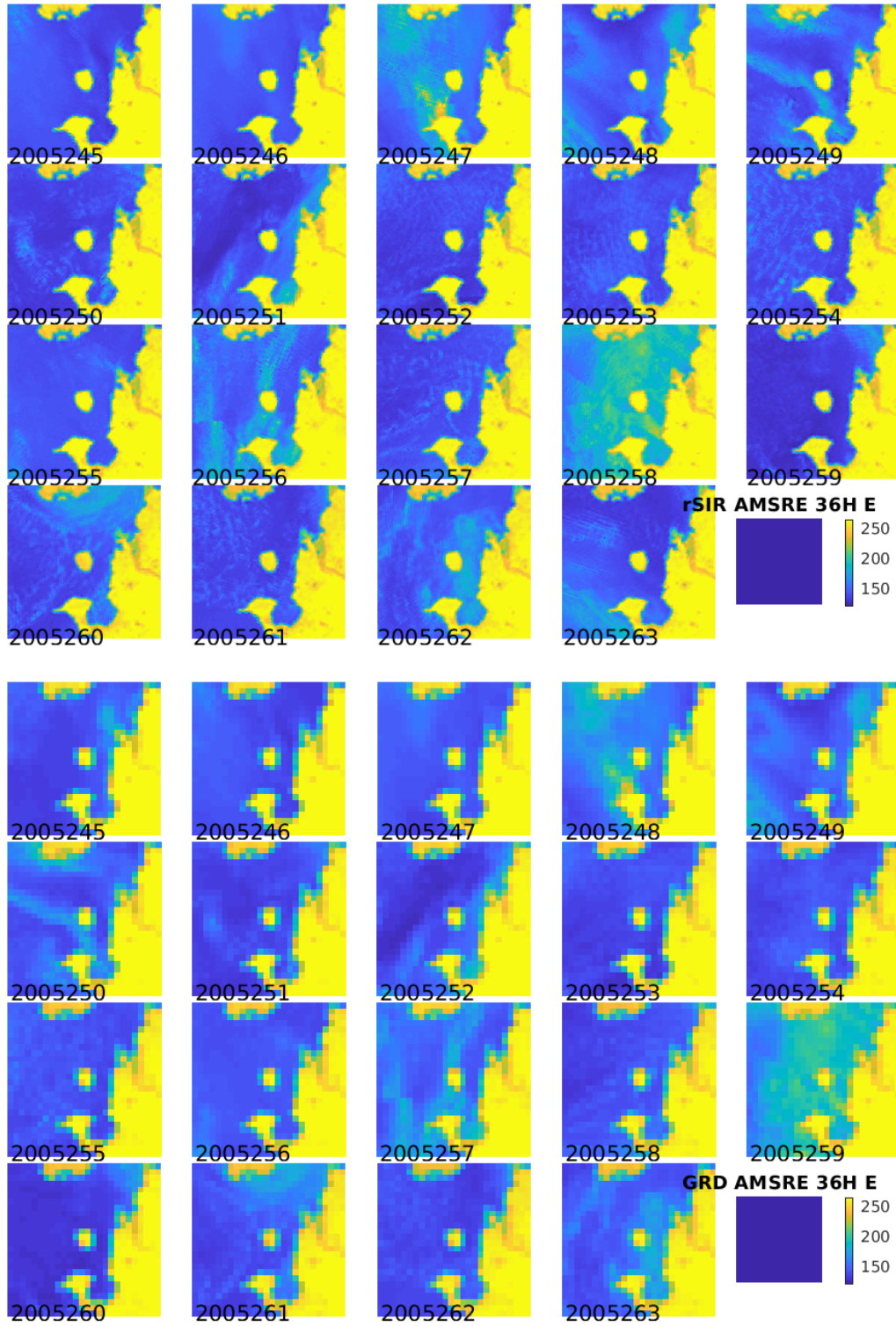


Figure 140: Time series of (top) rSIR and (bottom) GRD  $T_B$  images over the study area. Image dates are labeled on the image.



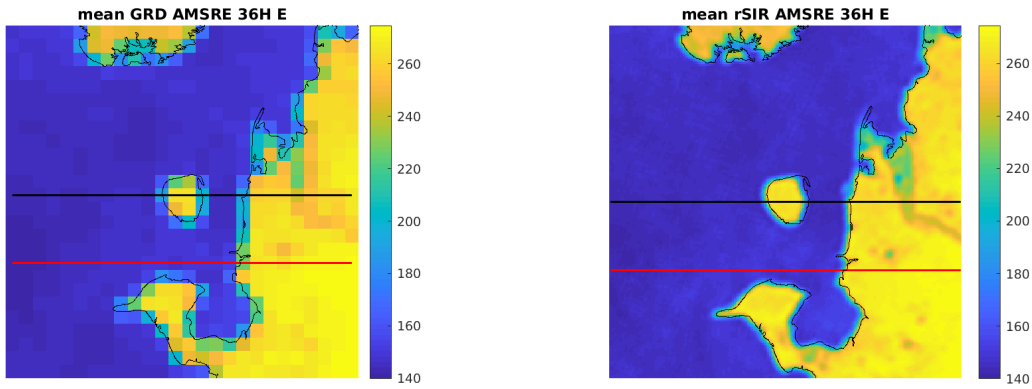


Figure 141: Average of daily  $T_B$  images over the study area. (left) 25-km GRD. (right) 3.125-km rSIR. The thick horizontal lines show the data transect locations where data is extracted from the image for analysis.

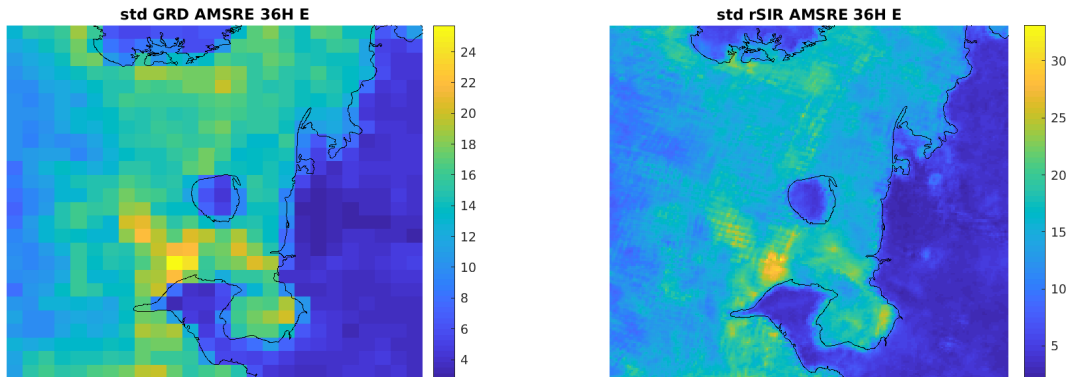


Figure 142: Standard deviation of daily  $T_B$  images over the study area. (left) 25-km GRD. (right) 3.125-km rSIR.

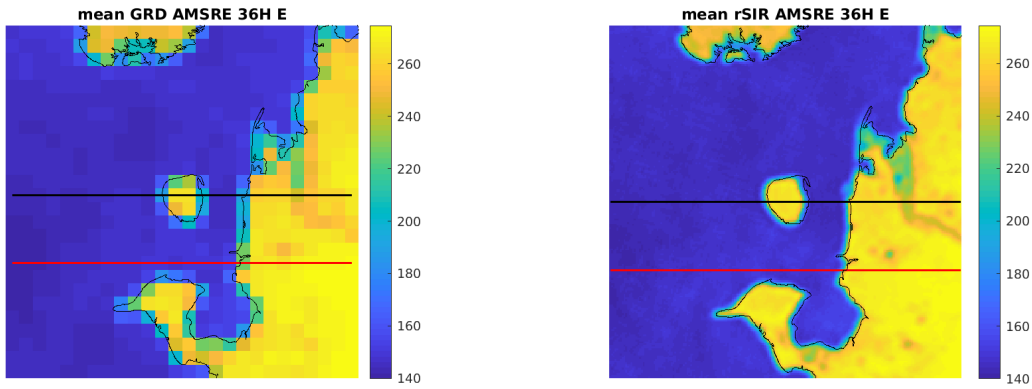


Figure 143: [Repeated] Average of daily  $T_B$  images over the study area. (left) 25-km GRD. (right) 3.125-km rSIR. The thick horizontal lines show the data transect locations where data is extracted from the image for analysis.

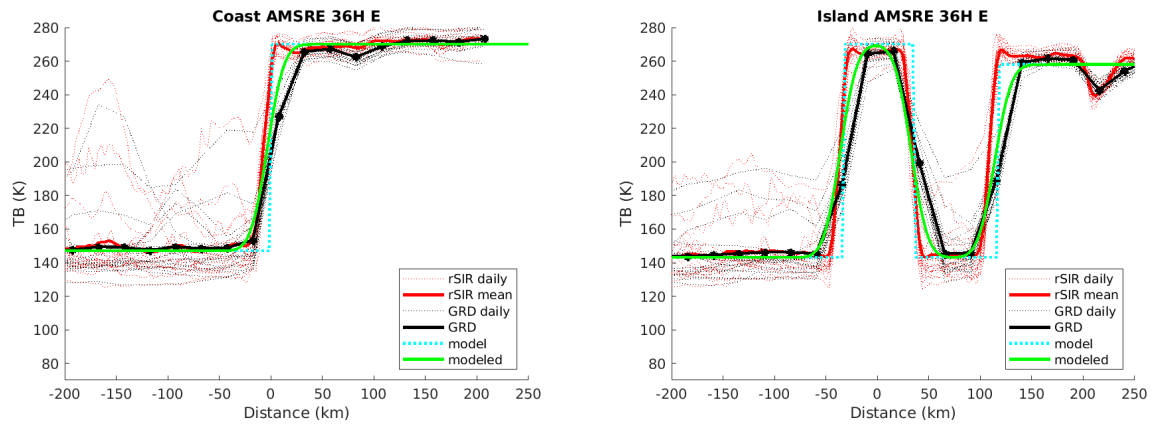


Figure 144: Plots of  $T_B$  along the two analysis case transect lines for the (left) coast-crossing and (right) island-crossing cases.

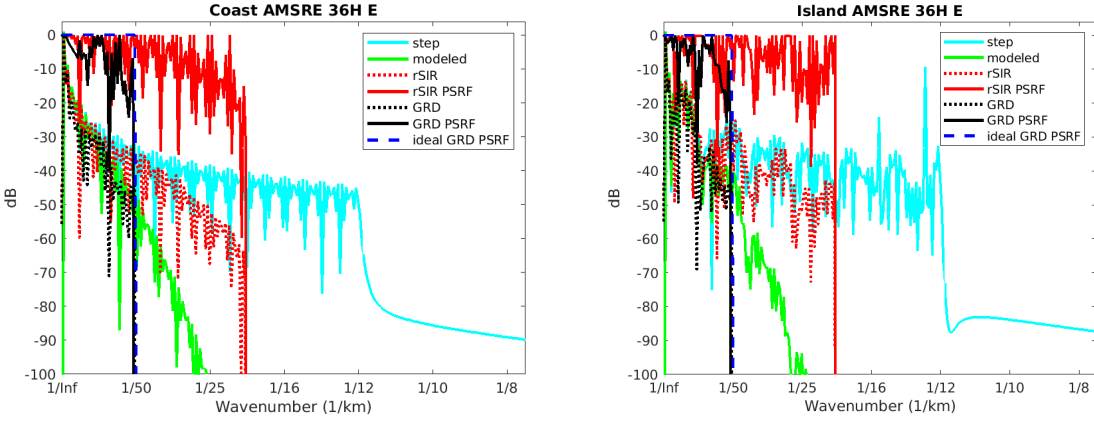


Figure 145: Wavenumber spectra of the  $T_B$  slices, the model, and the PSRF. (left) Coast-crossing case. (right) Island-crossing case.

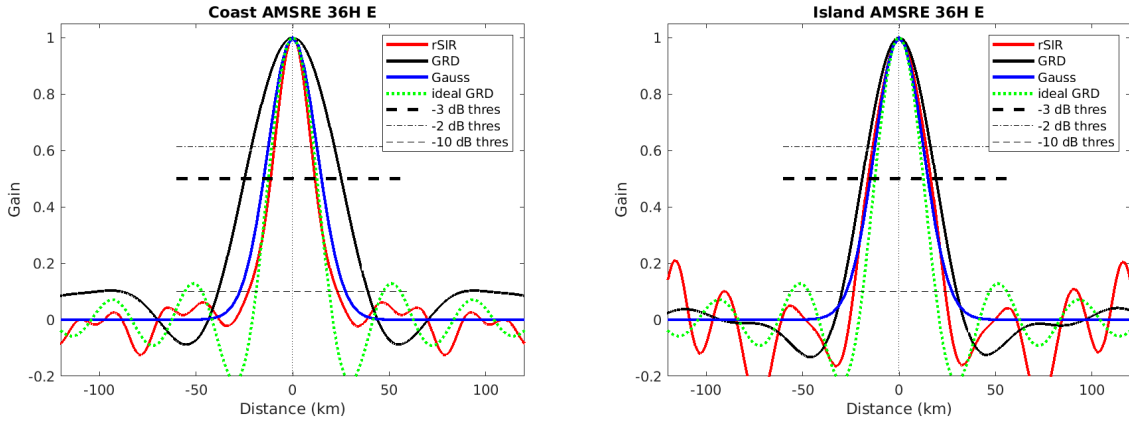


Figure 146: Derived single-pass rSIR and GRD PSRFs from the (left) coast-crossing and (right) island-crossing cases.

Table 92: Resolution estimates for AMSRE channel 36H LTOD E

Algorithm	-3 dB Thres		-2 dB Thres		-10 dB Thres	
	Coast	Island	Coast	Island	Coast	Island
Gauss	30.0	30.0	24.4	24.4	54.8	54.8
rSIR	23.0	32.7	18.6	27.0	46.0	47.4
ideal GRD	36.2	36.2	30.3	30.3	54.5	54.5
GRD	50.0	38.2	41.7	31.8	77.4	59.5

C.18 AMSRE Channel 36H M Figures

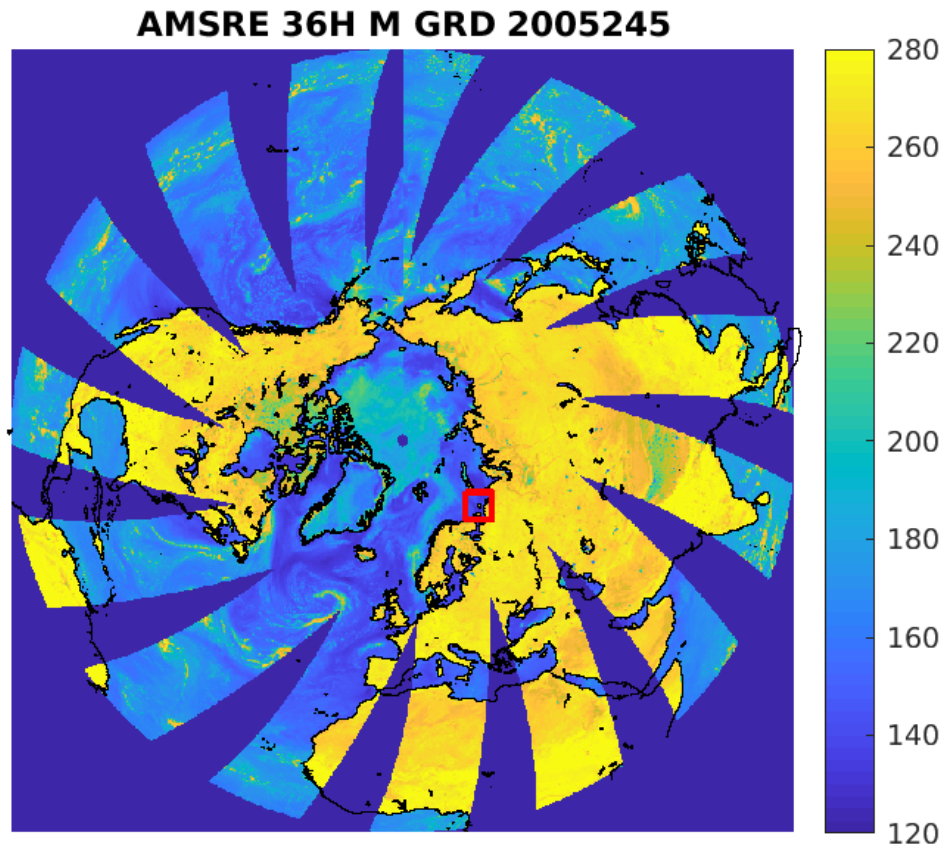


Figure 147: rSIR Northern Hemisphere view.

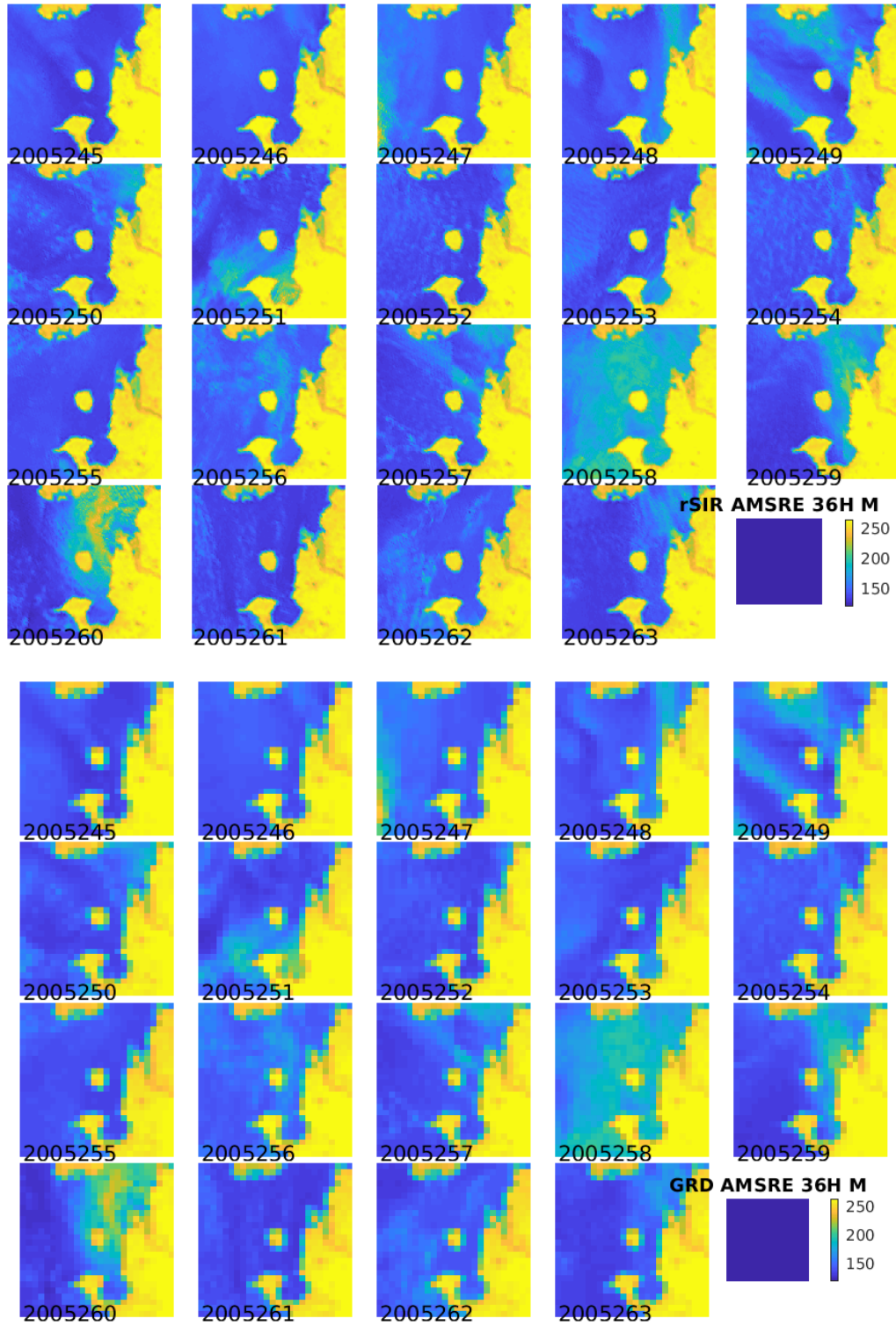


Figure 148: Time series of (top) rSIR and (bottom) GRD  $T_B$  images over the study area. Image dates are labeled on the image.

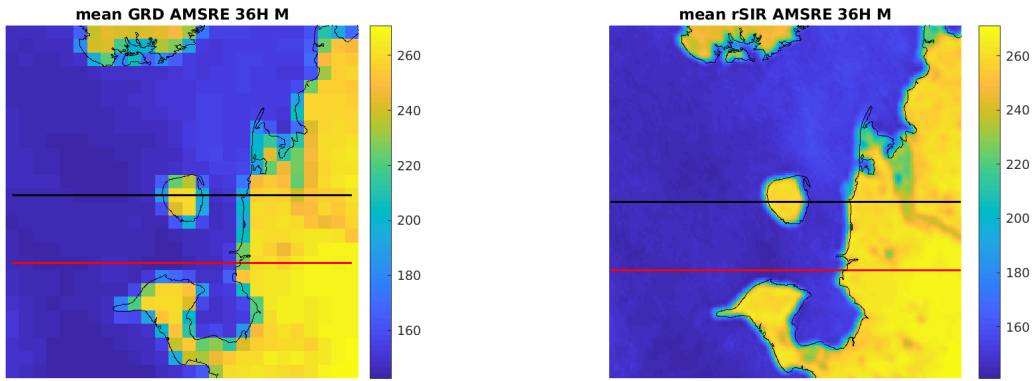


Figure 149: Average of daily  $T_B$  images over the study area. (left) 25-km GRD. (right) 3.125-km rSIR. The thick horizontal lines show the data transect locations where data is extracted from the image for analysis.

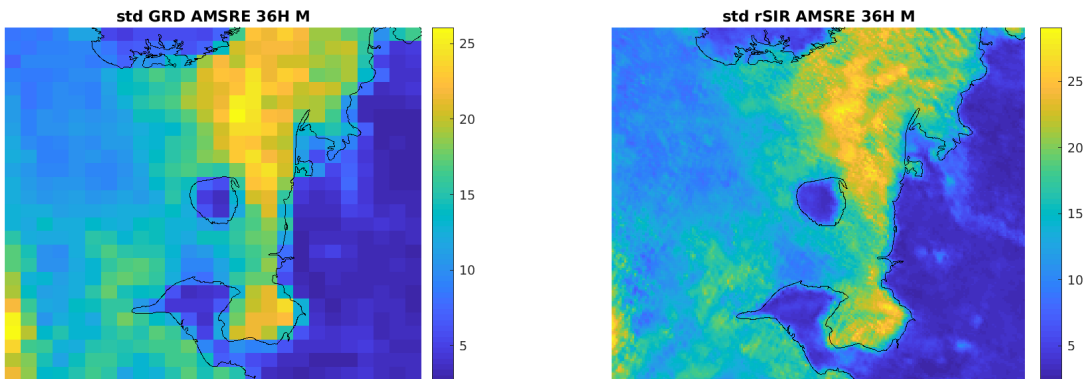


Figure 150: Standard deviation of daily  $T_B$  images over the study area. (left) 25-km GRD. (right) 3.125-km rSIR.

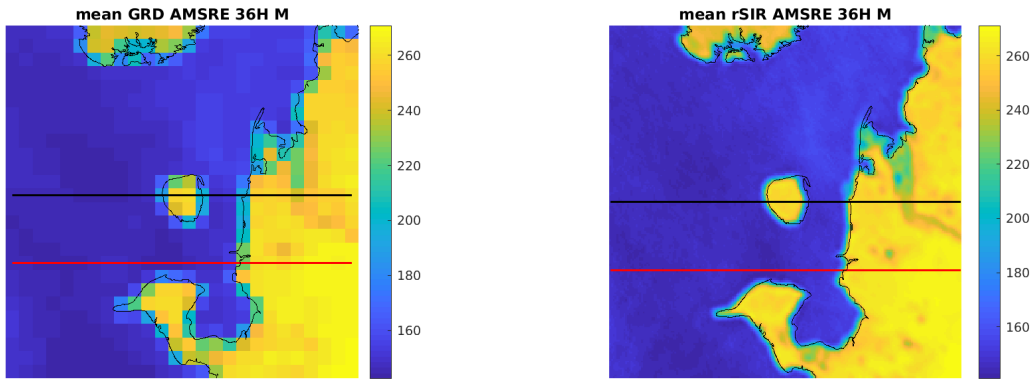


Figure 151: [Repeated] Average of daily  $T_B$  images over the study area. (left) 25-km GRD. (right) 3.125-km rSIR. The thick horizontal lines show the data transect locations where data is extracted from the image for analysis.

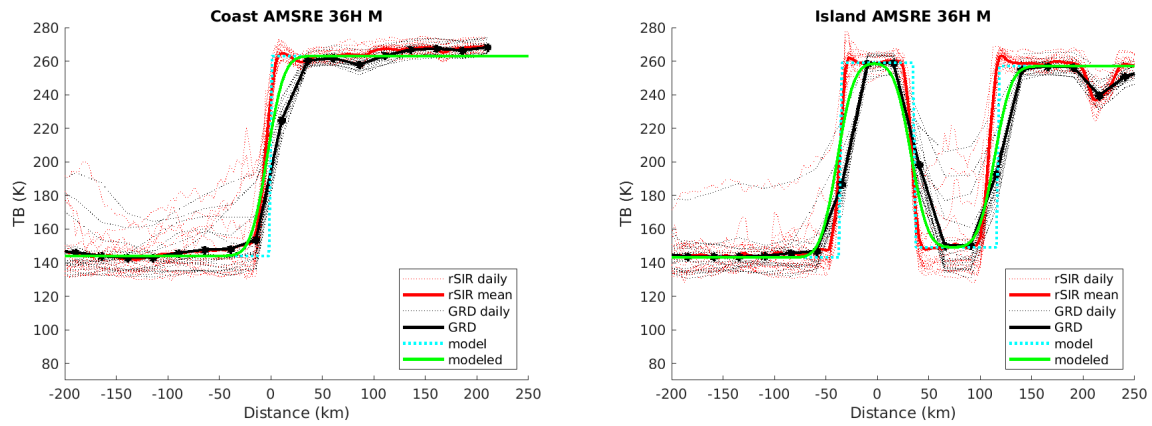


Figure 152: Plots of  $T_B$  along the two analysis case transect lines for the (left) coast-crossing and (right) island-crossing cases.

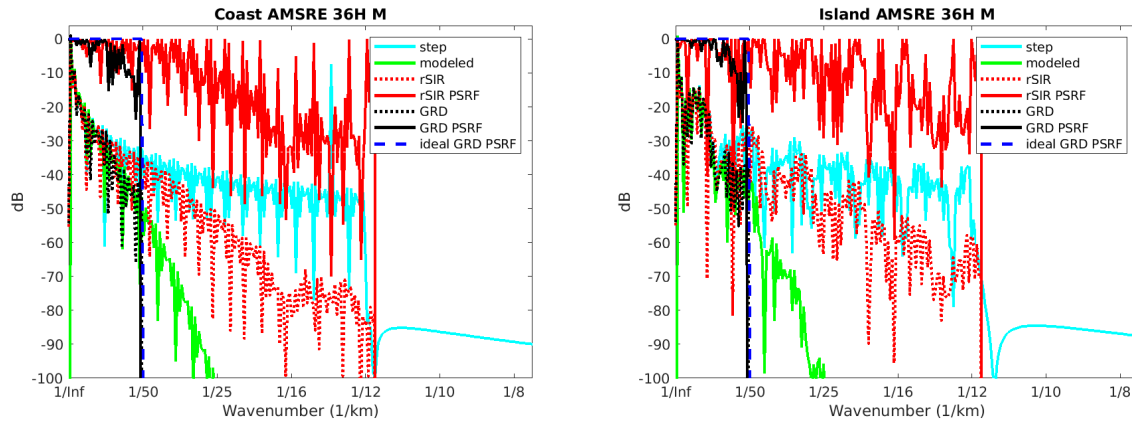


Figure 153: Wavenumber spectra of the  $T_B$  slices, the model, and the PSRF. (left) Coast-crossing case. (right) Island-crossing case.

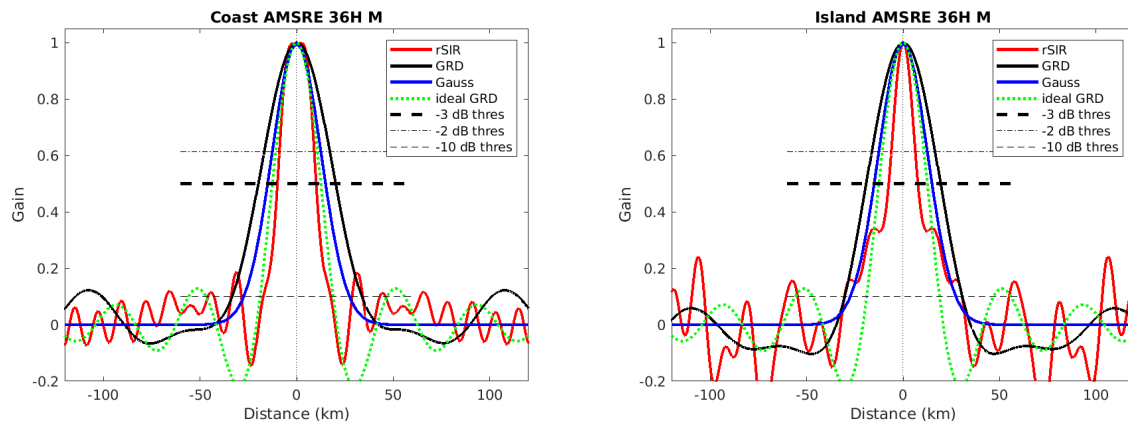


Figure 154: Derived single-pass rSIR and GRD PSRFs from the (left) coast-crossing and (right) island-crossing cases.

Table 93: Resolution estimates for AMSRE channel 36H LTOD M

Algorithm	-3 dB Thres		-2 dB Thres		-10 dB Thres	
	Coast	Island	Coast	Island	Coast	Island
Gauss	30.0	30.0	24.4	24.4	54.8	54.8
rSIR	20.1	15.1	17.7	12.0	34.9	61.1
ideal GRD	36.2	36.2	30.3	30.3	54.5	54.5
GRD	40.1	38.6	33.0	32.0	67.2	61.0



## C.19 AMSRE Channel 36V E Figures

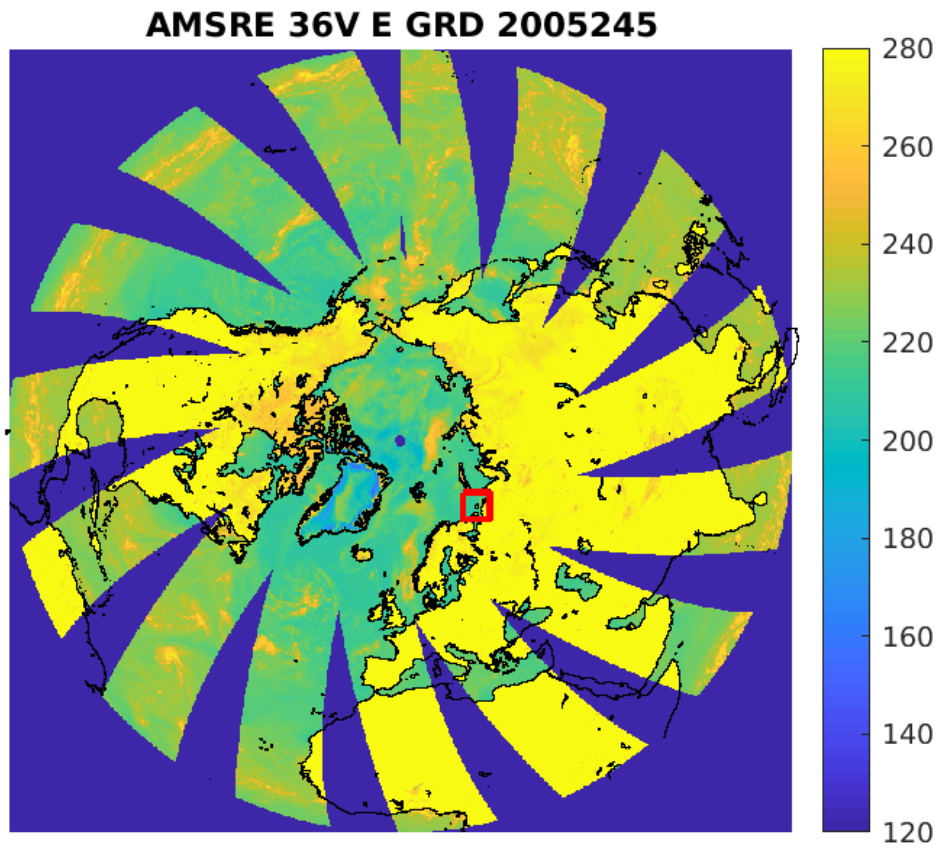


Figure 155: rSIR Northern Hemisphere view.

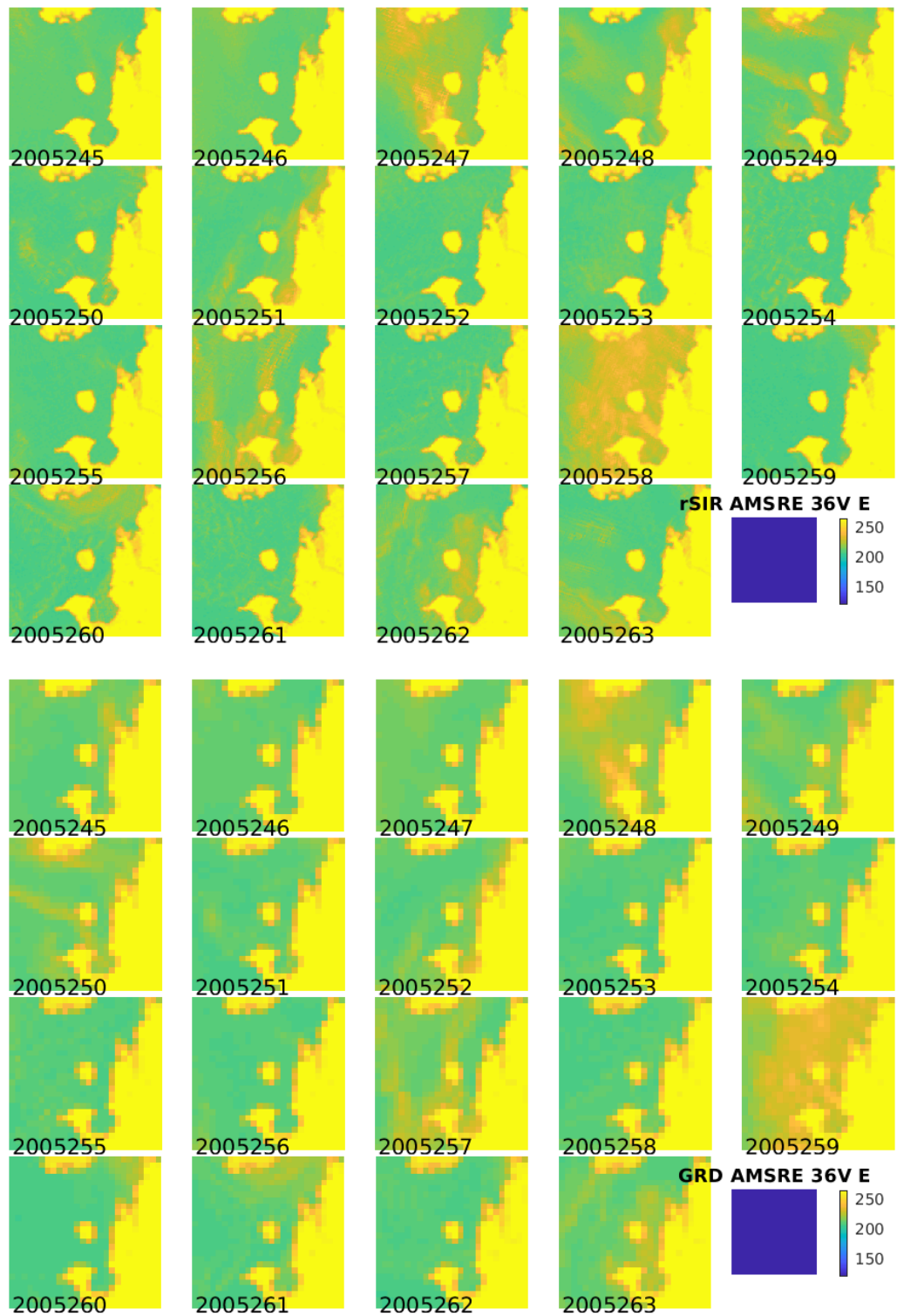


Figure 156: Time series of (top) rSIR and (bottom) GRD  $T_B$  images over the study area. Image dates are labeled on the image.

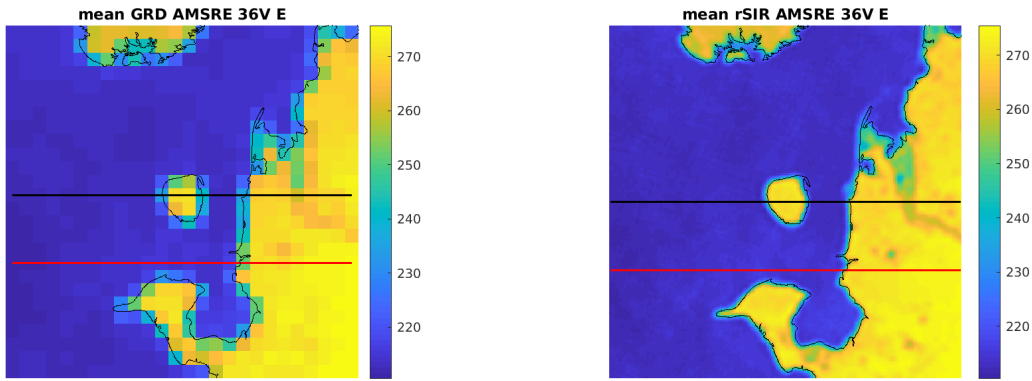


Figure 157: Average of daily  $T_B$  images over the study area. (left) 25-km GRD. (right) 3.125-km rSIR. The thick horizontal lines show the data transect locations where data is extracted from the image for analysis.

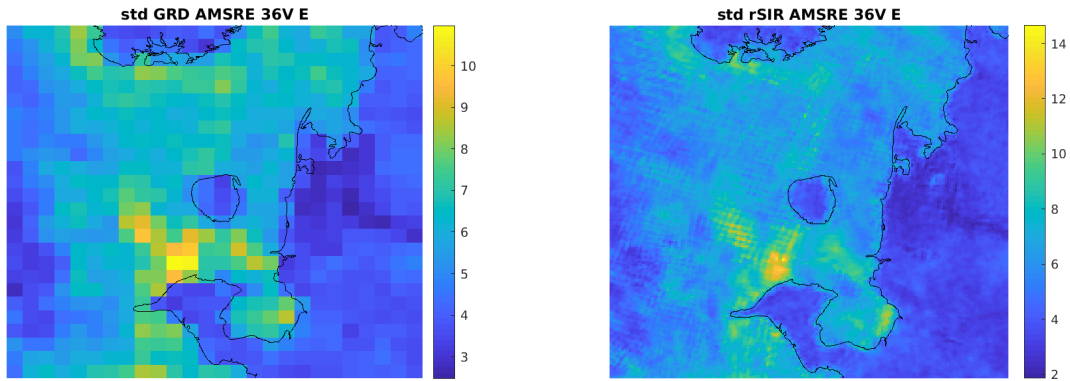


Figure 158: Standard deviation of daily  $T_B$  images over the study area. (left) 25-km GRD. (right) 3.125-km rSIR.

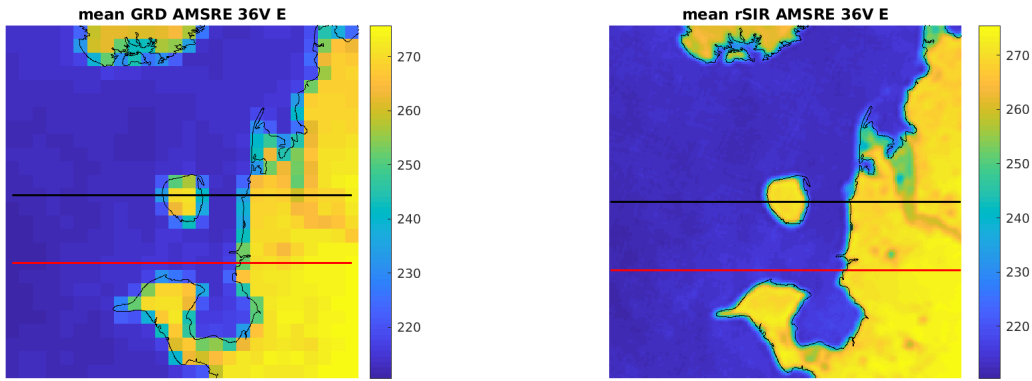


Figure 159: [Repeated] Average of daily  $T_B$  images over the study area. (left) 25-km GRD. (right) 3.125-km rSIR. The thick horizontal lines show the data transect locations where data is extracted from the image for analysis.

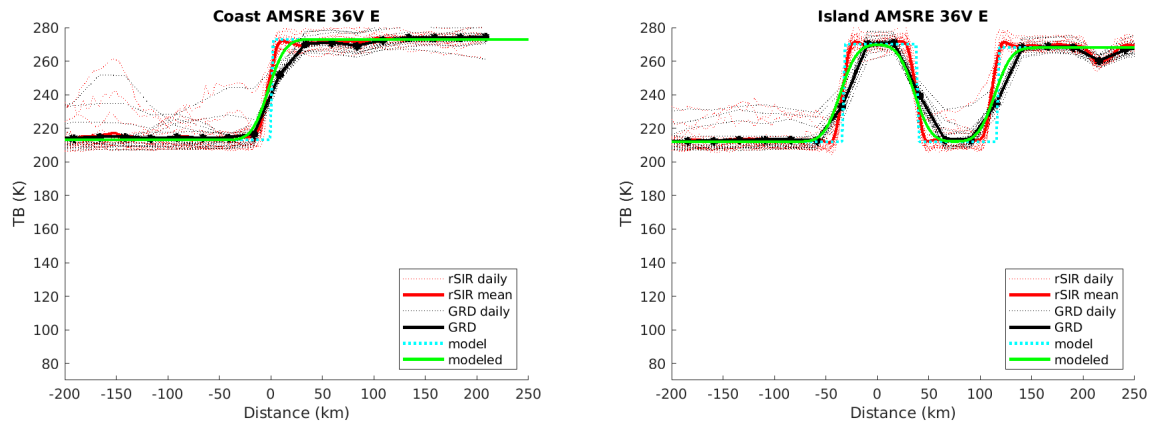


Figure 160: Plots of  $T_B$  along the two analysis case transect lines for the (left) coast-crossing and (right) island-crossing cases.

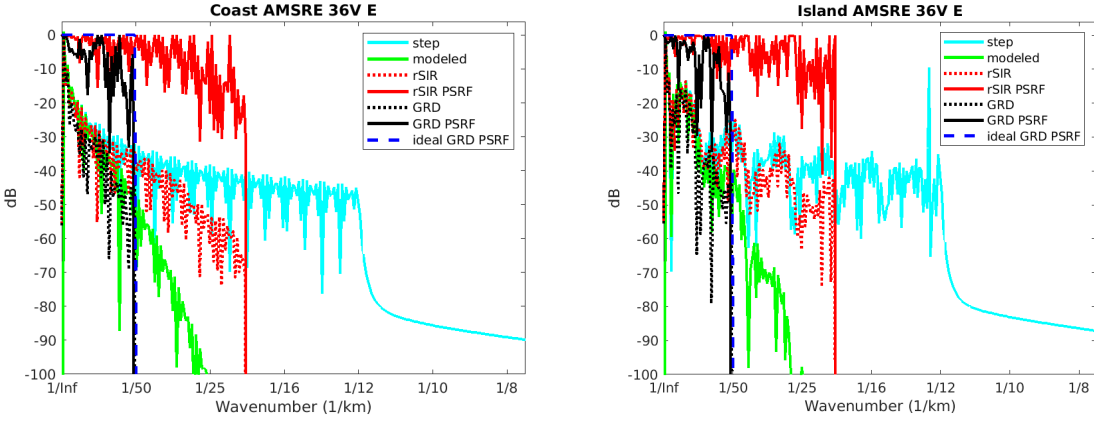


Figure 161: Wavenumber spectra of the  $T_B$  slices, the model, and the PSRF. (left) Coast-crossing case. (right) Island-crossing case.

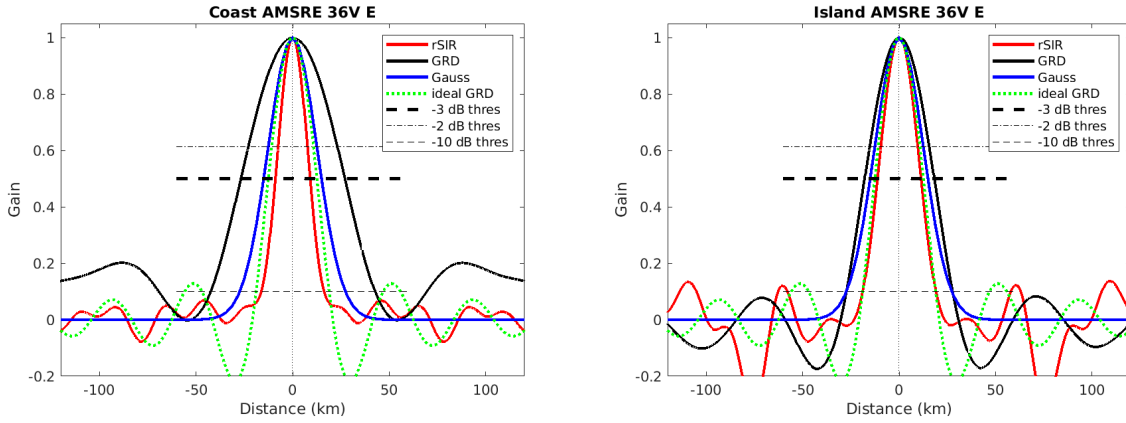


Figure 162: Derived single-pass rSIR and GRD PSRFs from the (left) coast-crossing and (right) island-crossing cases.

Table 94: Resolution estimates for AMSRE channel 36V LTOD E

Algorithm	-3 dB Thres		-2 dB Thres		-10 dB Thres	
	Coast	Island	Coast	Island	Coast	Island
Gauss	30.0	30.0	24.4	24.4	54.8	54.8
rSIR	18.0	22.6	14.8	18.6	32.5	37.9
ideal GRD	36.2	36.2	30.3	30.3	54.5	54.5
GRD	53.8	36.1	44.9	30.1	85.1	55.0

## C.20 AMSRE Channel 36V M Figures

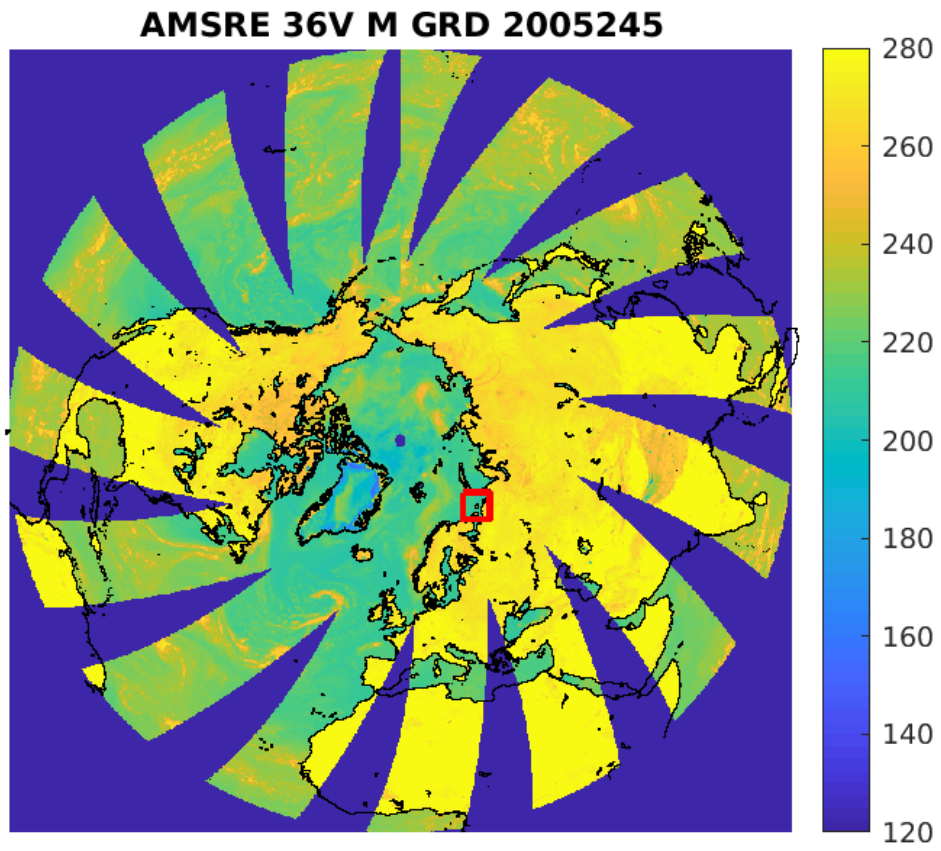


Figure 163: rSIR Northern Hemisphere view.

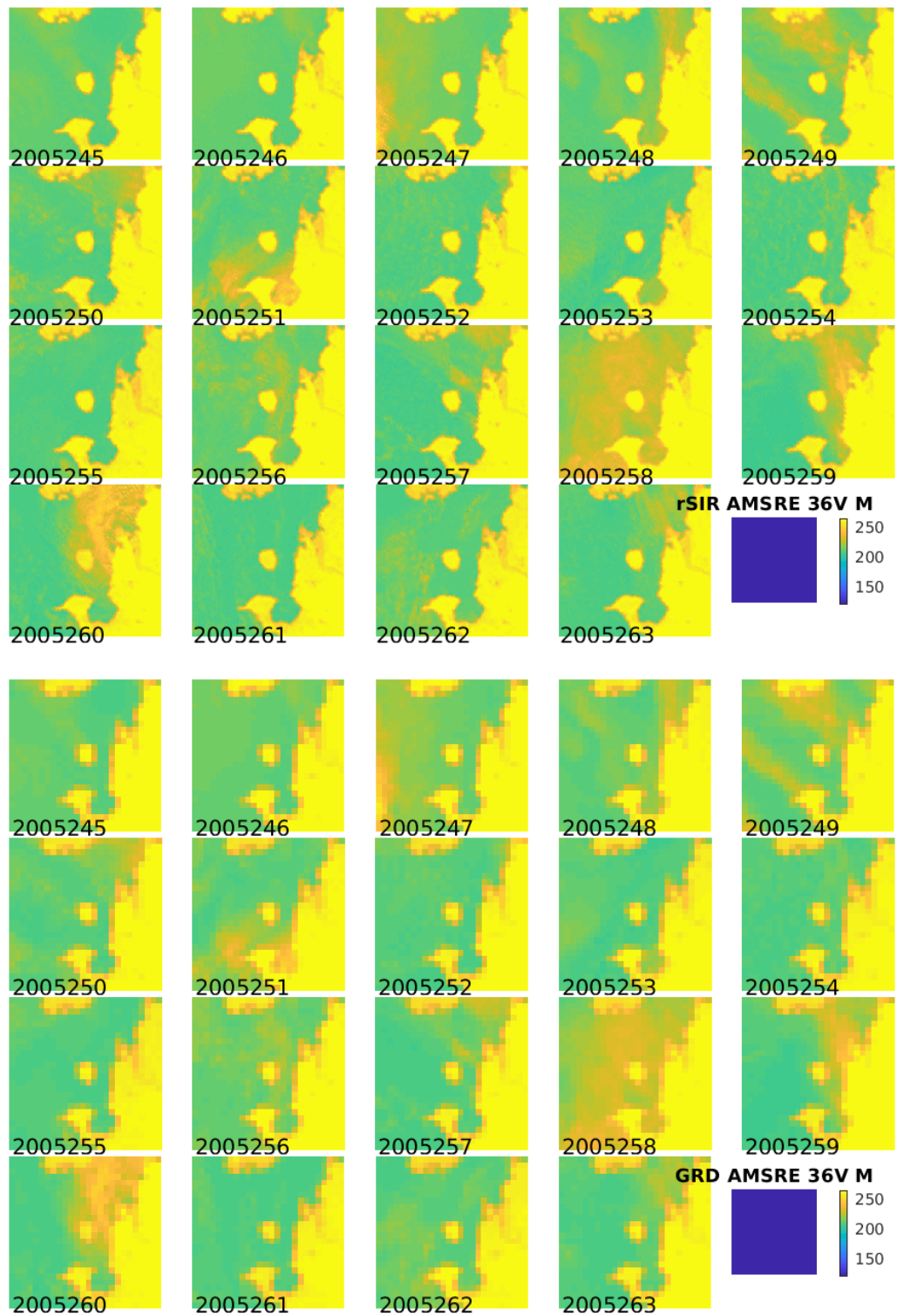


Figure 164: Time series of (top) rSIR and (bottom) GRD  $T_B$  images over the study area. Image dates are labeled on the image.

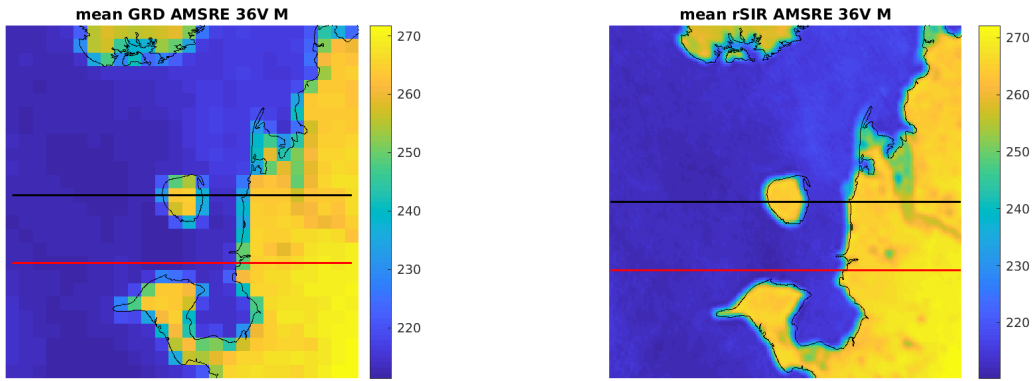


Figure 165: Average of daily  $T_B$  images over the study area. (left) 25-km GRD. (right) 3.125-km rSIR. The thick horizontal lines show the data transect locations where data is extracted from the image for analysis.

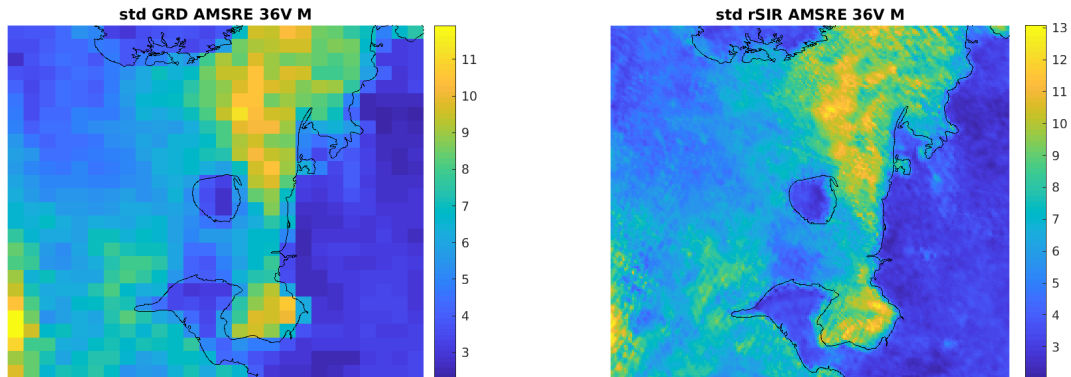


Figure 166: Standard deviation of daily  $T_B$  images over the study area. (left) 25-km GRD. (right) 3.125-km rSIR.



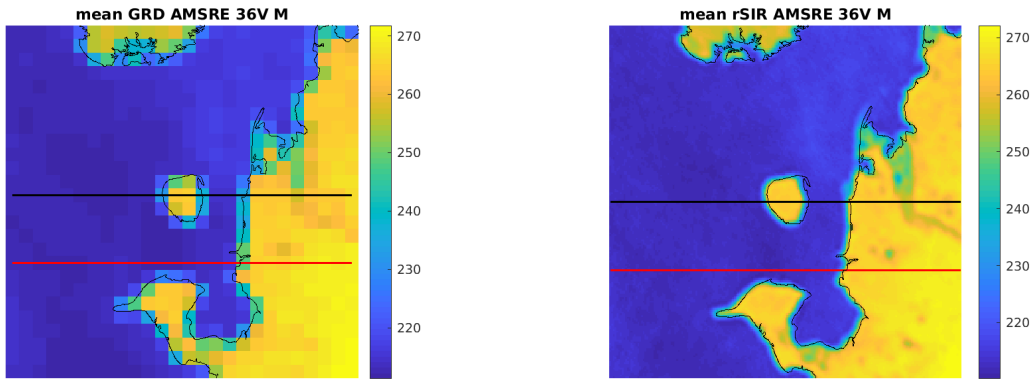


Figure 167: [Repeated] Average of daily  $T_B$  images over the study area. (left) 25-km GRD. (right) 3.125-km rSIR. The thick horizontal lines show the data transect locations where data is extracted from the image for analysis.

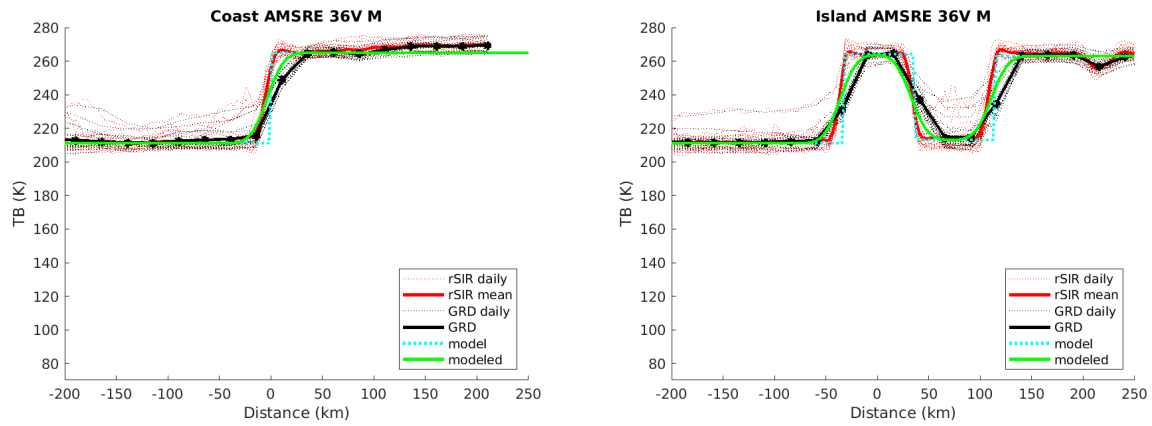


Figure 168: Plots of  $T_B$  along the two analysis case transect lines for the (left) coast-crossing and (right) island-crossing cases.

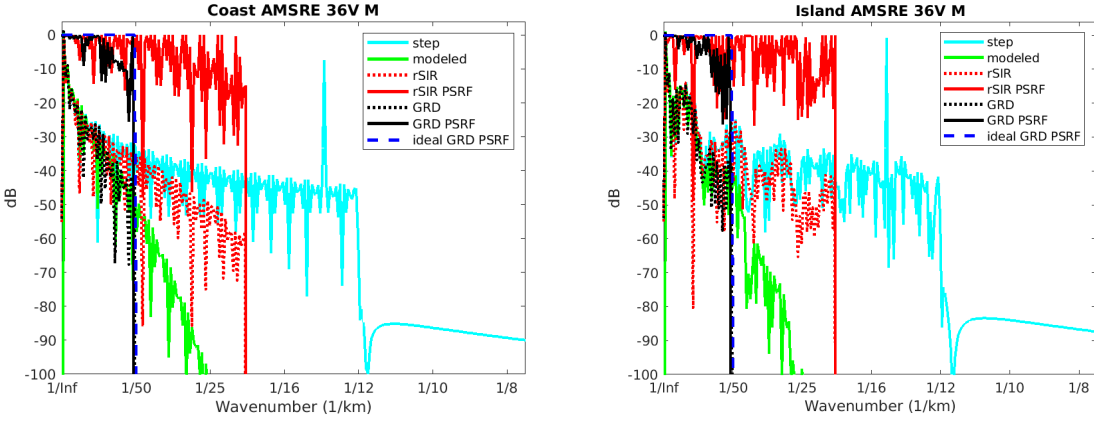


Figure 169: Wavenumber spectra of the  $T_B$  slices, the model, and the PSRF. (left) Coast-crossing case. (right) Island-crossing case.

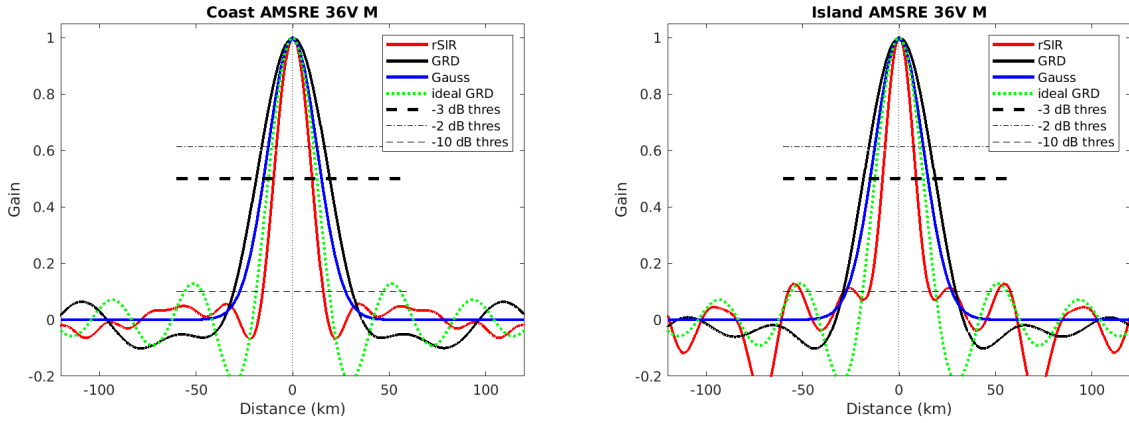


Figure 170: Derived single-pass rSIR and GRD PSRFs from the (left) coast-crossing and (right) island-crossing cases.

Table 95: Resolution estimates for AMSRE channel 36V LTOD M

Algorithm	-3 dB Thres		-2 dB Thres		-10 dB Thres	
	Coast	Island	Coast	Island	Coast	Island
Gauss	30.0	30.0	24.4	24.4	54.8	54.8
rSIR	19.9	17.4	16.6	14.3	31.3	31.5
ideal GRD	36.2	36.2	30.3	30.3	54.5	54.5
GRD	38.1	37.1	31.5	30.8	61.4	58.4

## C.21 AMSRE Channel 89H E Figures

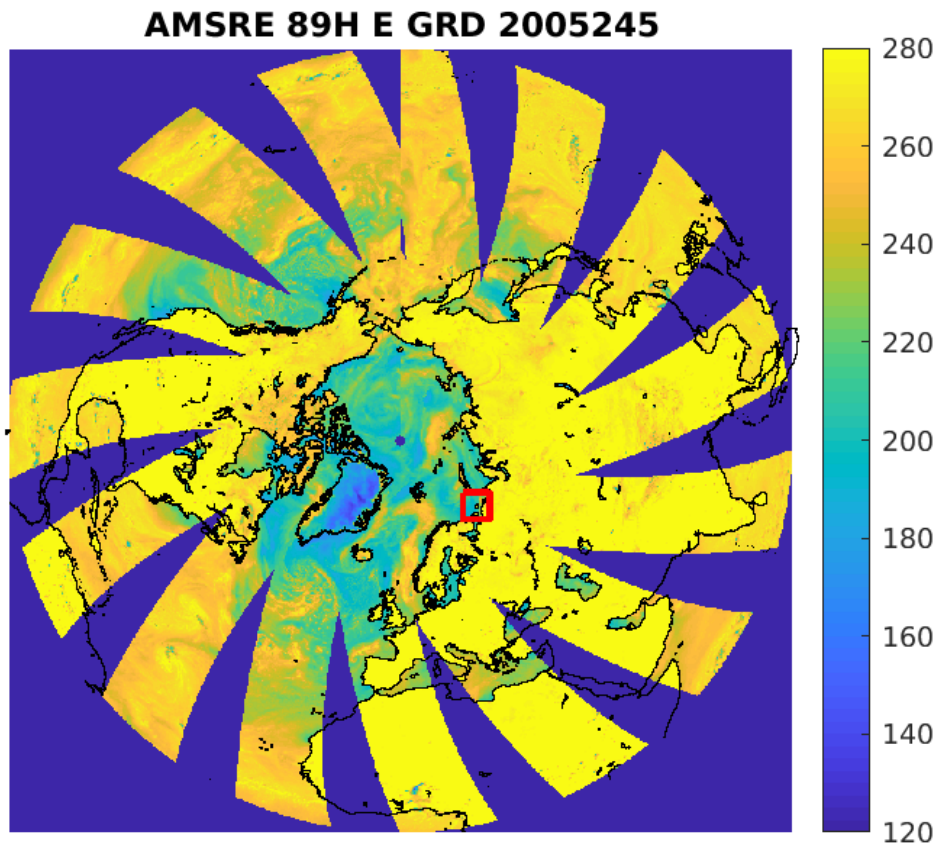


Figure 171: rSIR Northern Hemisphere view.

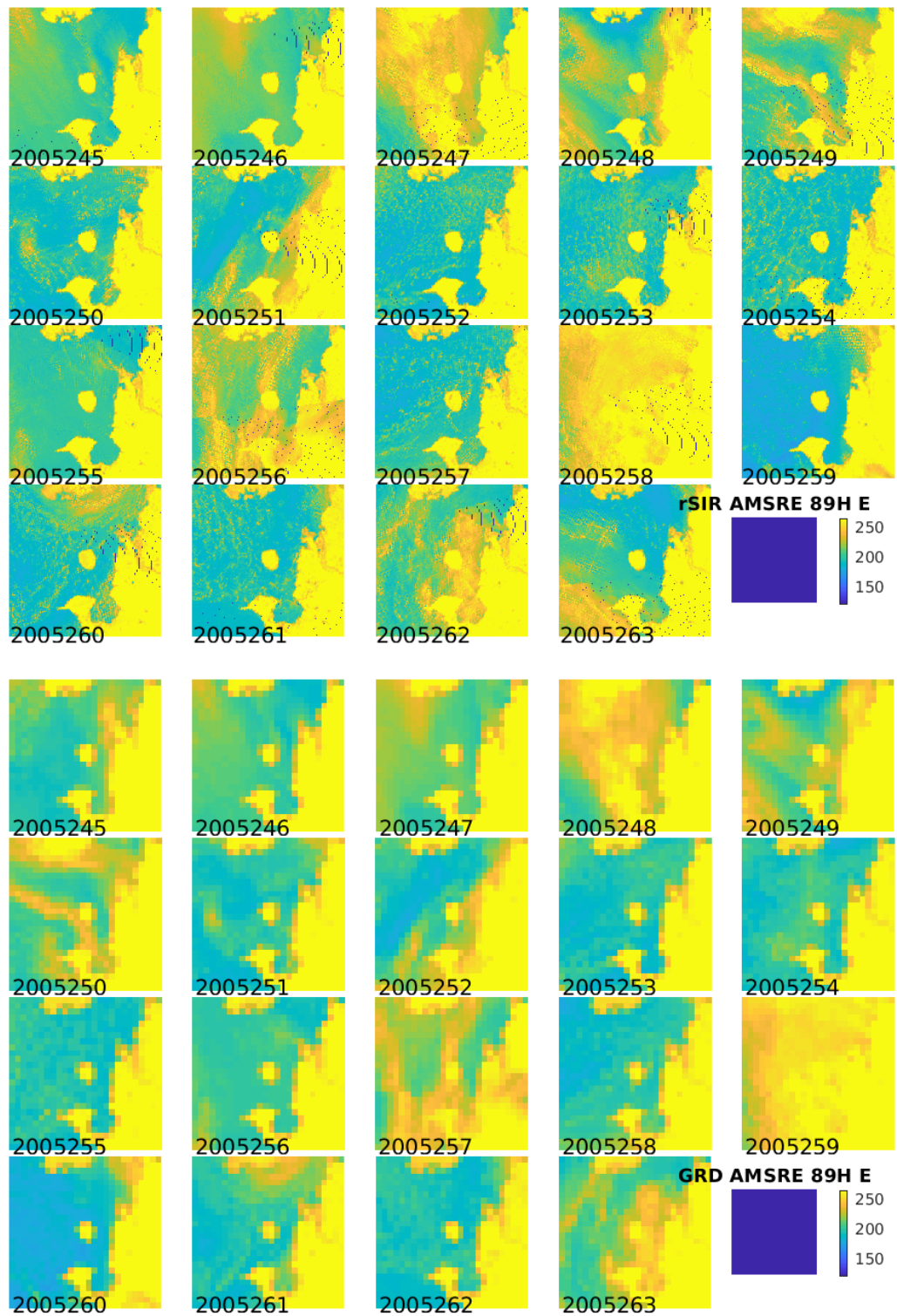


Figure 172: Time series of (top) rSIR and (bottom) GRD  $T_B$  images over the study area. Image dates are labeled on the image.

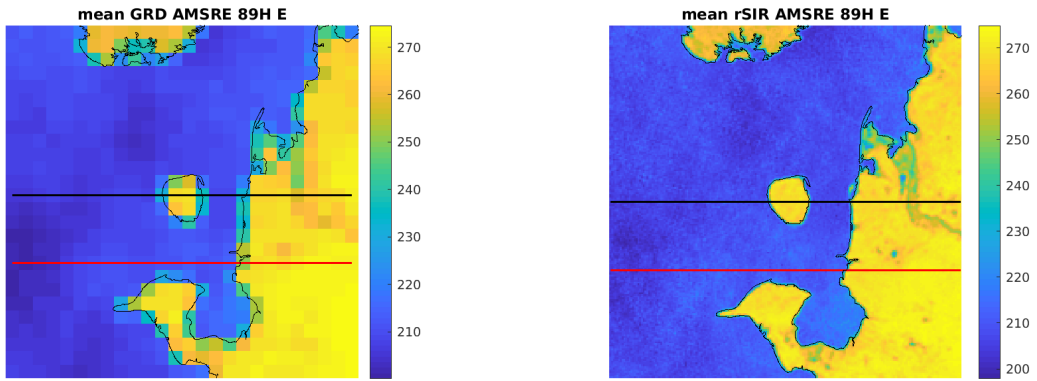


Figure 173: Average of daily  $T_B$  images over the study area. (left) 25-km GRD. (right) 3.125-km rSIR. The thick horizontal lines show the data transect locations where data is extracted from the image for analysis.

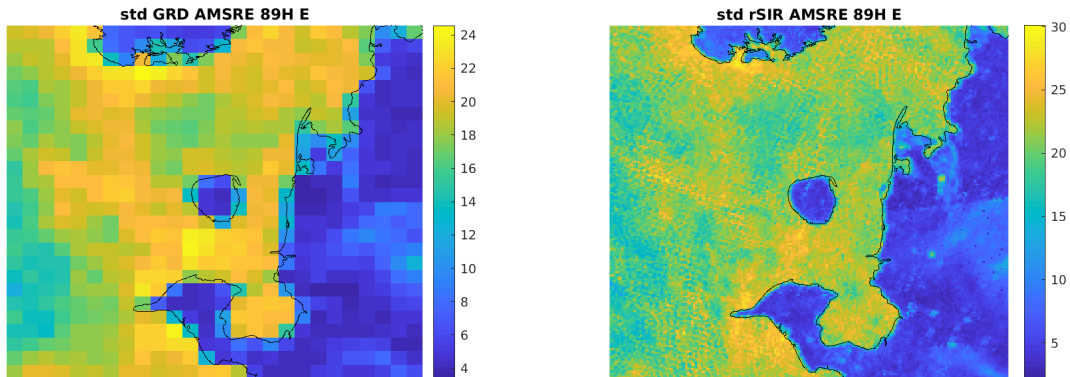


Figure 174: Standard deviation of daily  $T_B$  images over the study area. (left) 25-km GRD. (right) 3.125-km rSIR.

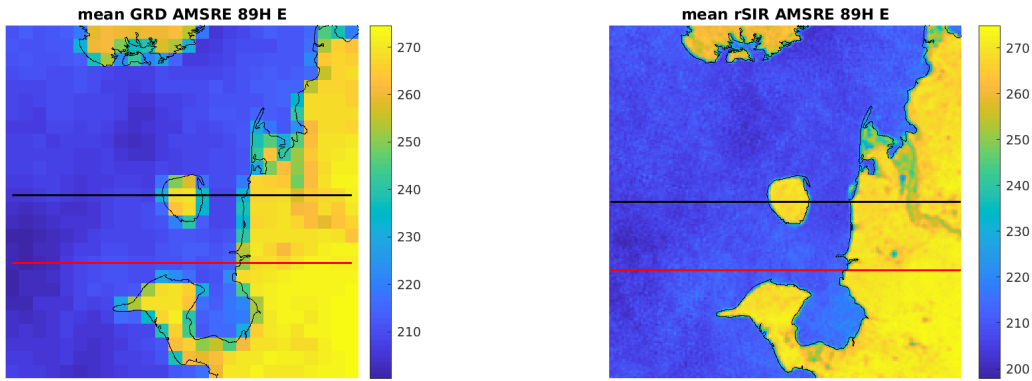


Figure 175: [Repeated] Average of daily  $T_B$  images over the study area. (left) 25-km GRD. (right) 3.125-km rSIR. The thick horizontal lines show the data transect locations where data is extracted from the image for analysis.

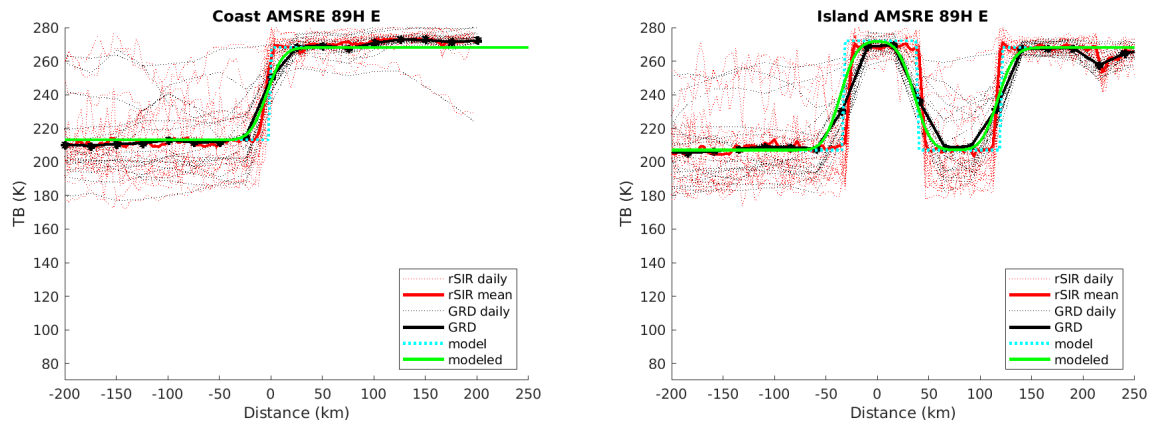


Figure 176: Plots of  $T_B$  along the two analysis case transect lines for the (left) coast-crossing and (right) island-crossing cases.

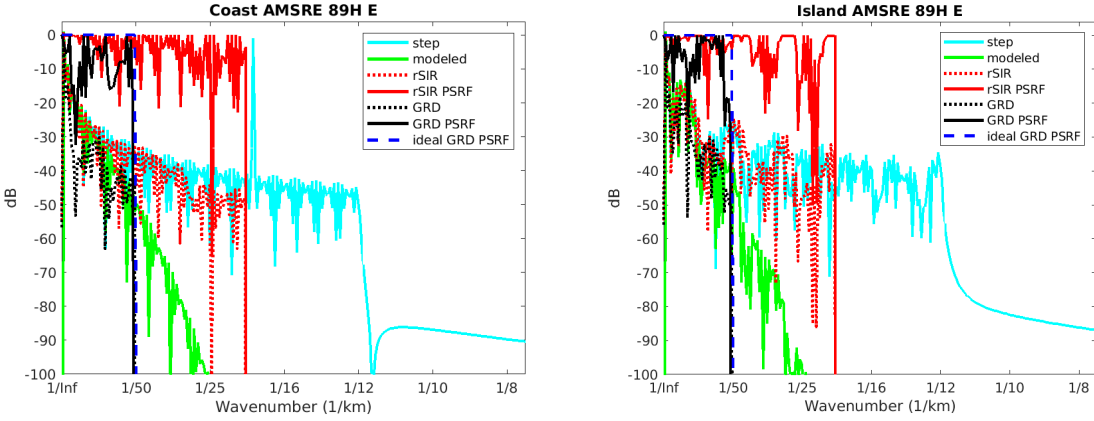


Figure 177: Wavenumber spectra of the  $T_B$  slices, the model, and the PSRF. (left) Coast-crossing case. (right) Island-crossing case.

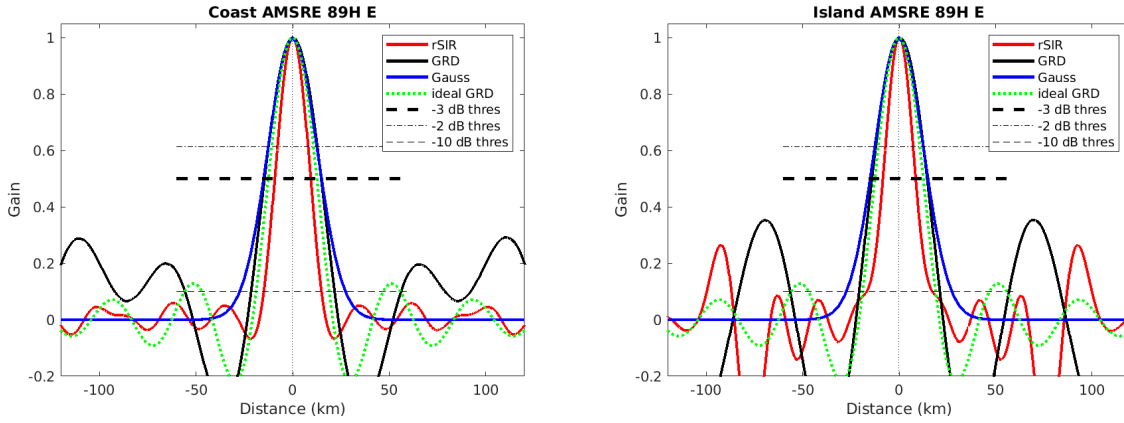


Figure 178: Derived single-pass rSIR and GRD PSRFs from the (left) coast-crossing and (right) island-crossing cases.

Table 96: Resolution estimates for AMSRE channel 89H LTOD E

Algorithm	-3 dB Thres		-2 dB Thres		-10 dB Thres	
	Coast	Island	Coast	Island	Coast	Island
Gauss	30.0	30.0	24.4	24.4	54.8	54.8
rSIR	18.6	17.0	15.4	13.9	29.8	34.1
ideal GRD	36.2	36.2	30.3	30.3	54.5	54.5
GRD	29.3	28.8	24.5	24.2	43.3	41.7

## C.22 AMSRE Channel 89H M Figures

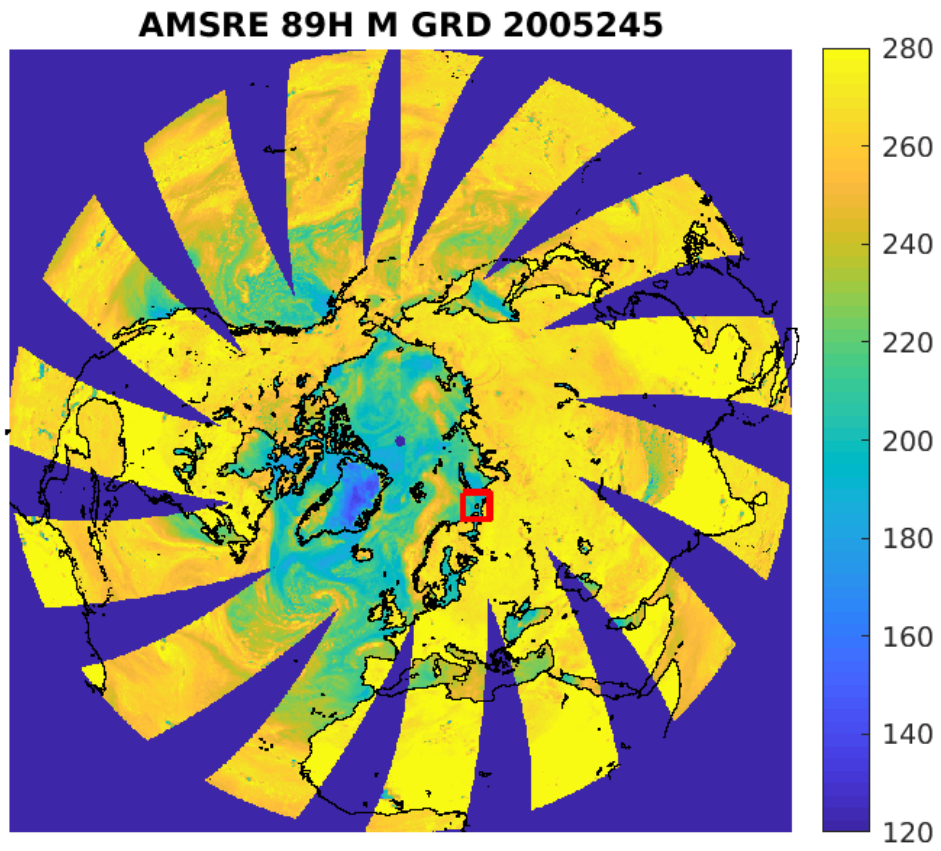


Figure 179: rSIR Northern Hemisphere view.



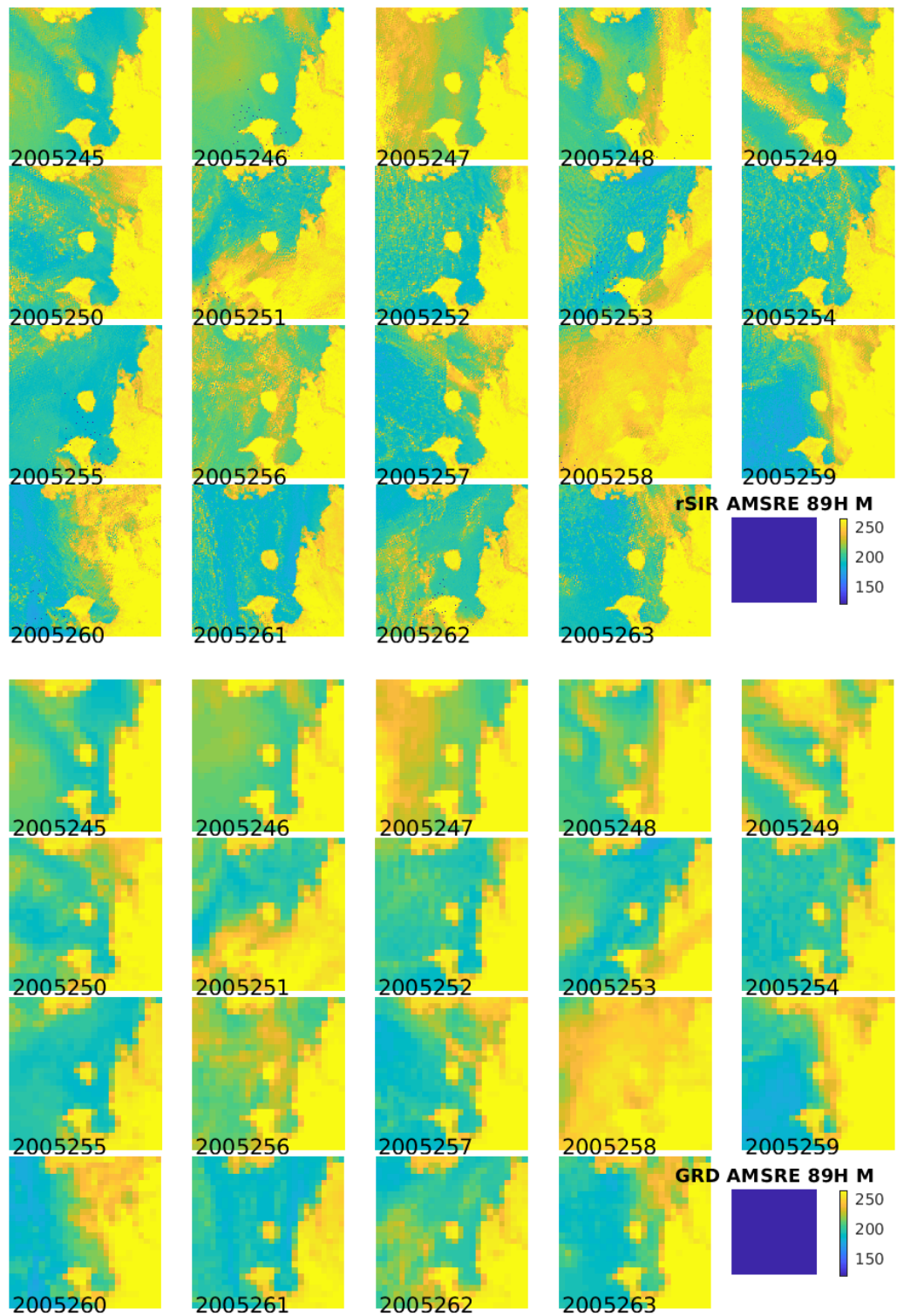


Figure 180: Time series of (top) rSIR and (bottom) GRD  $T_B$  images over the study area. Image dates are labeled on the image.

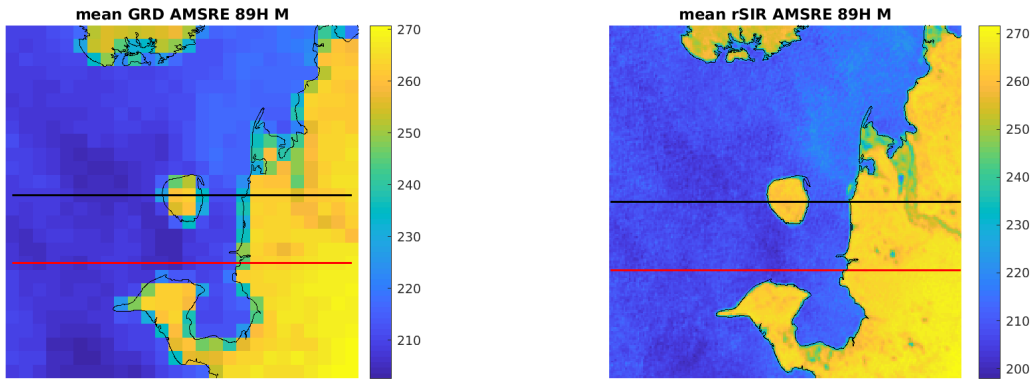


Figure 181: Average of daily  $T_B$  images over the study area. (left) 25-km GRD. (right) 3.125-km rSIR. The thick horizontal lines show the data transect locations where data is extracted from the image for analysis.

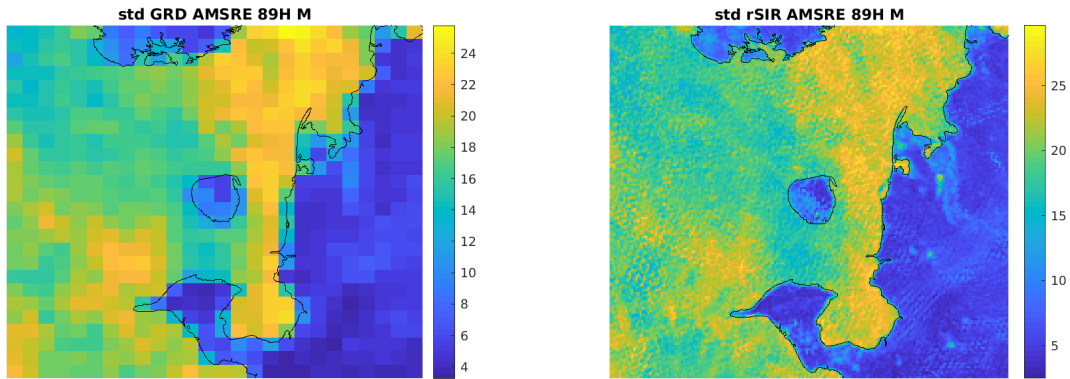


Figure 182: Standard deviation of daily  $T_B$  images over the study area. (left) 25-km GRD. (right) 3.125-km rSIR.

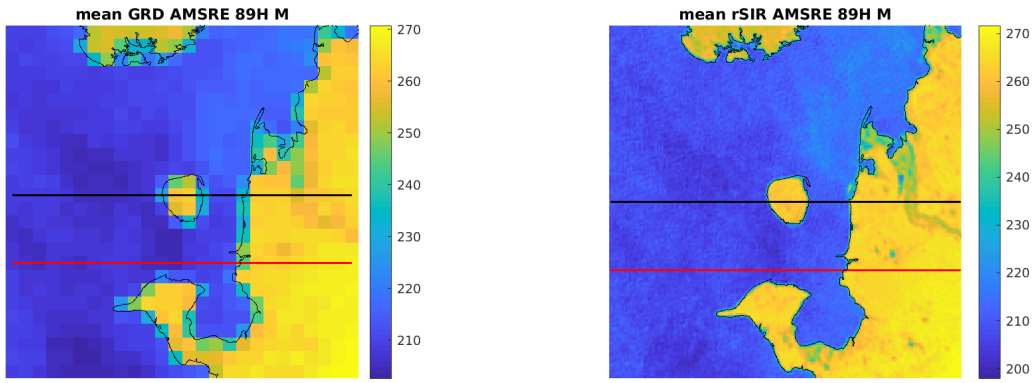


Figure 183: [Repeated] Average of daily  $T_B$  images over the study area. (left) 25-km GRD. (right) 3.125-km rSIR. The thick horizontal lines show the data transect locations where data is extracted from the image for analysis.

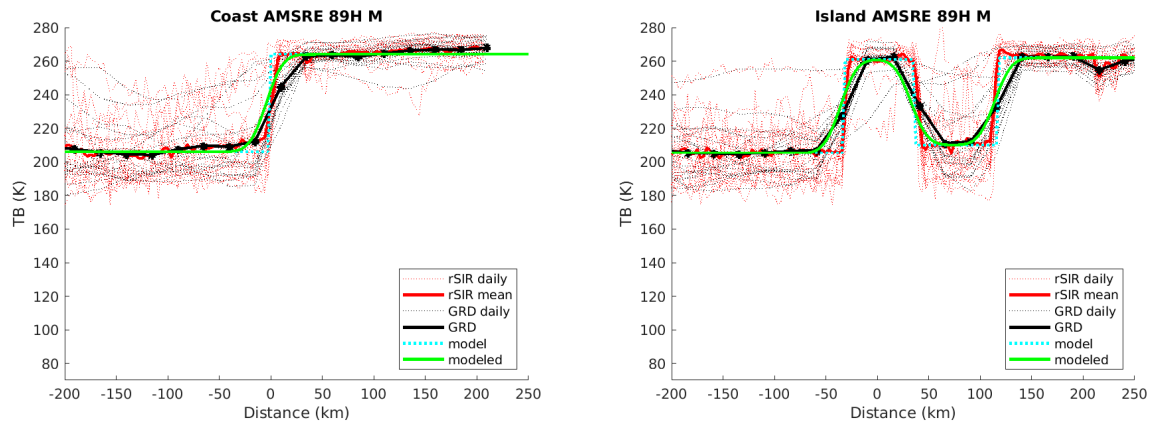


Figure 184: Plots of  $T_B$  along the two analysis case transect lines for the (left) coast-crossing and (right) island-crossing cases.

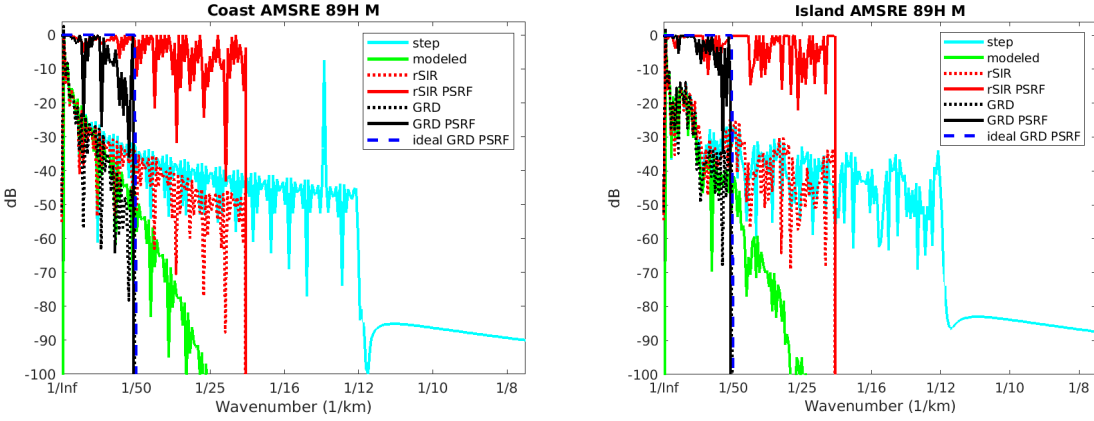


Figure 185: Wavenumber spectra of the  $T_B$  slices, the model, and the PSRF. (left) Coast-crossing case. (right) Island-crossing case.

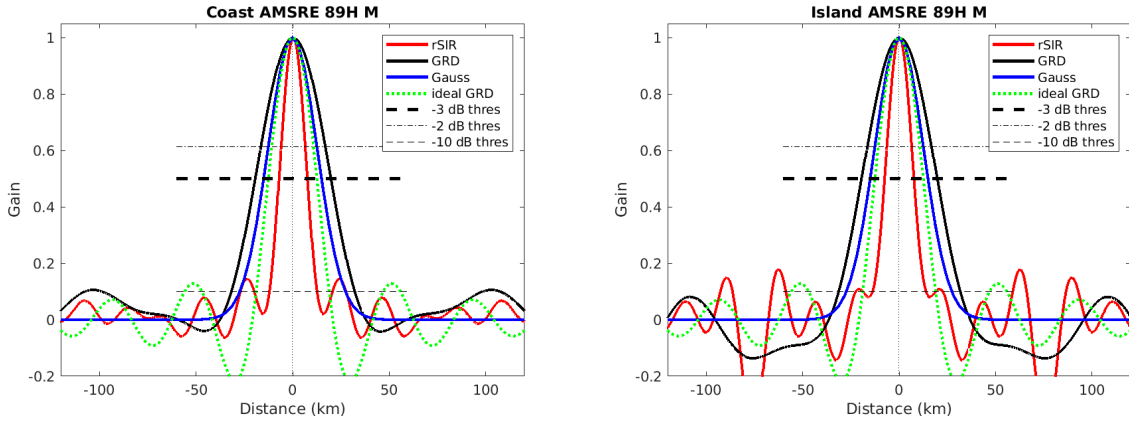


Figure 186: Derived single-pass rSIR and GRD PSRFs from the (left) coast-crossing and (right) island-crossing cases.

Table 97: Resolution estimates for AMSRE channel 89H LTOD M

Algorithm	-3 dB Thres		-2 dB Thres		-10 dB Thres	
	Coast	Island	Coast	Island	Coast	Island
Gauss	30.0	30.0	24.4	24.4	54.8	54.8
rSIR	14.8	15.2	12.2	12.5	24.6	27.9
ideal GRD	36.2	36.2	30.3	30.3	54.5	54.5
GRD	39.2	39.2	32.4	32.4	63.8	63.1

### C.23 AMSRE Channel 89V E Figures

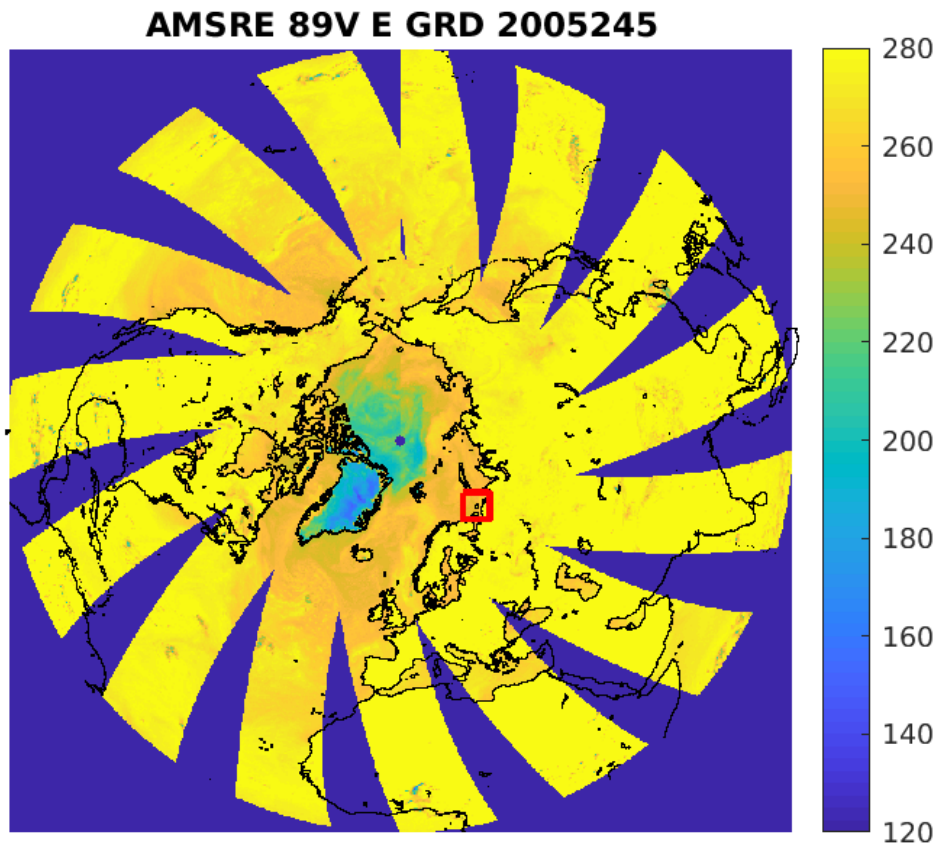


Figure 187: rSIR Northern Hemisphere view.

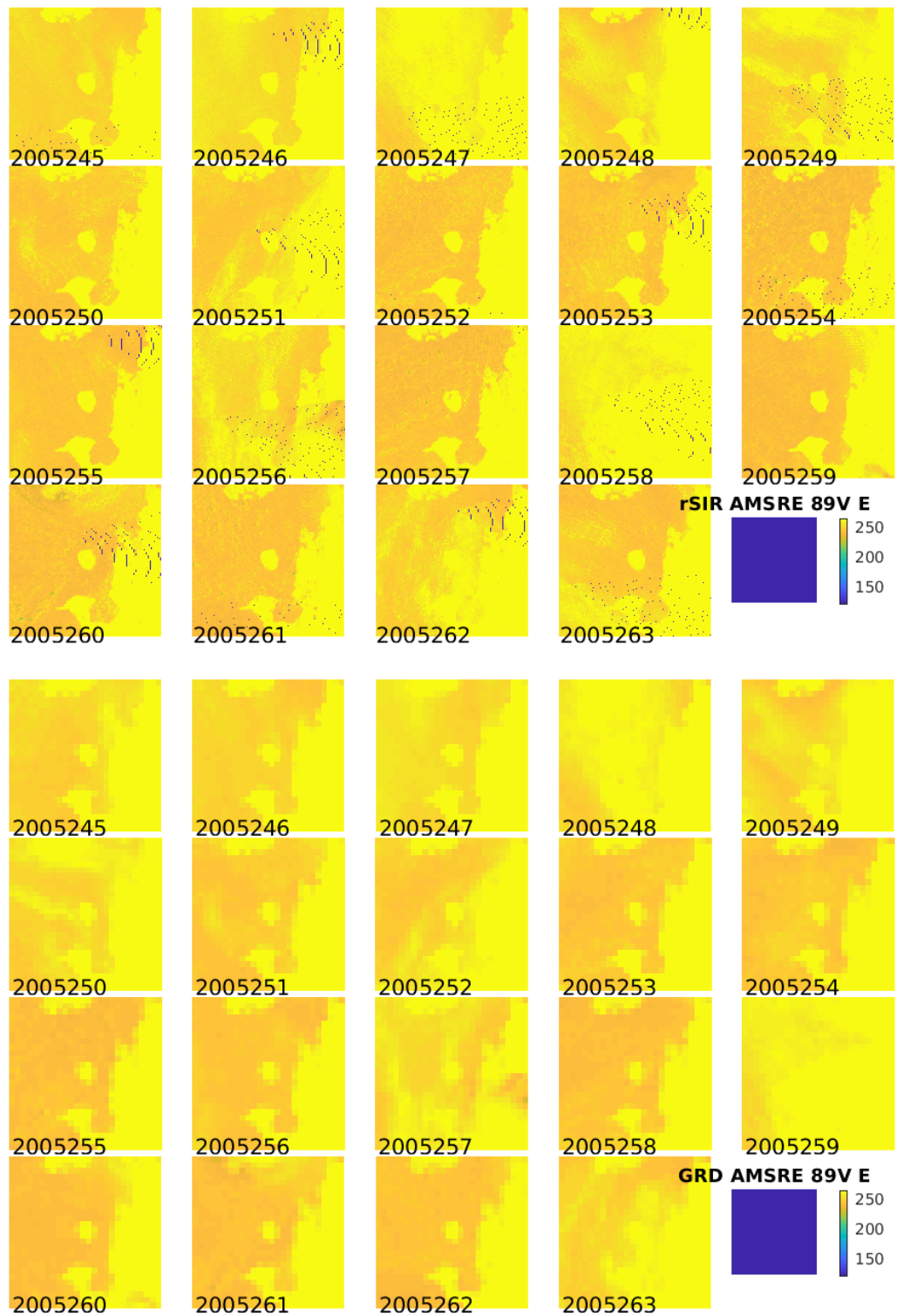


Figure 188: Time series of (top) rSIR and (bottom) GRD  $T_B$  images over the study area. Image dates are labeled on the image.

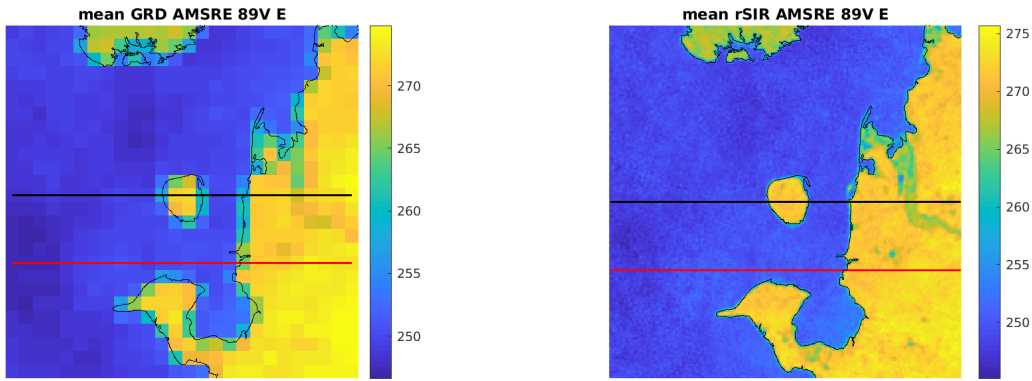


Figure 189: Average of daily  $T_B$  images over the study area. (left) 25-km GRD. (right) 3.125-km rSIR. The thick horizontal lines show the data transect locations where data is extracted from the image for analysis.

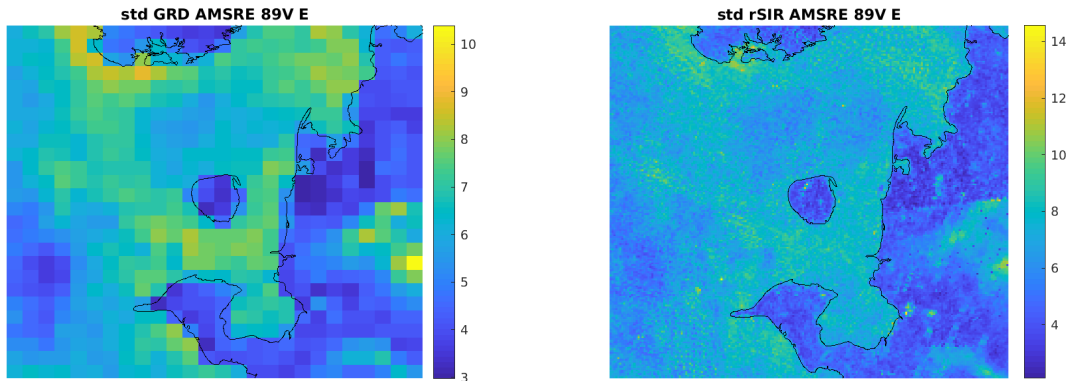


Figure 190: Standard deviation of daily  $T_B$  images over the study area. (left) 25-km GRD. (right) 3.125-km rSIR.

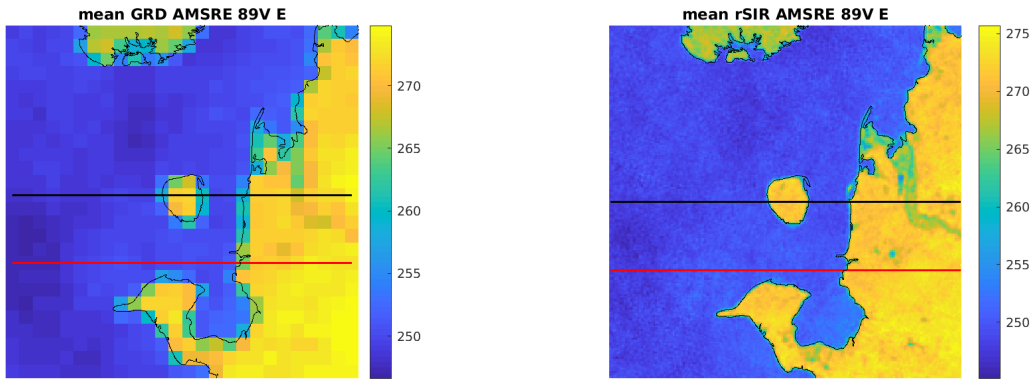


Figure 191: [Repeated] Average of daily  $T_B$  images over the study area. (left) 25-km GRD. (right) 3.125-km rSIR. The thick horizontal lines show the data transect locations where data is extracted from the image for analysis.

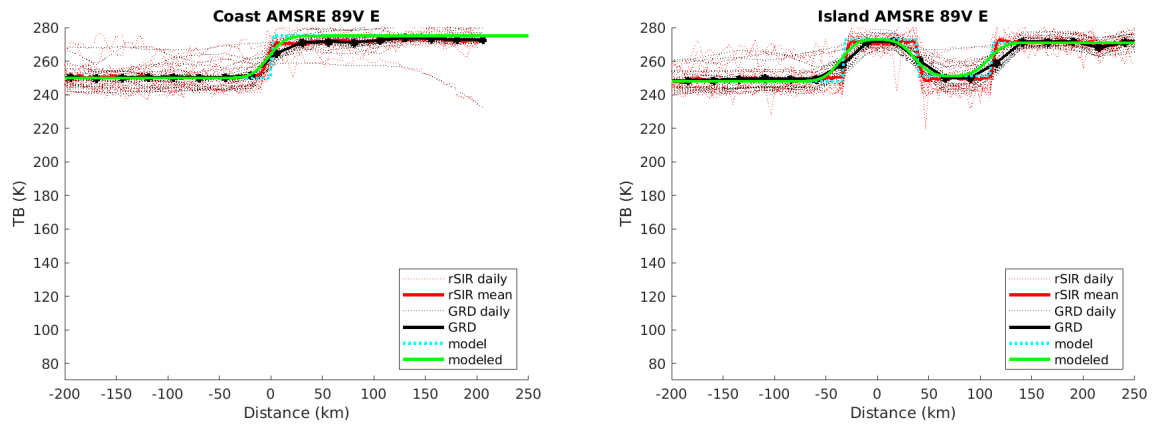


Figure 192: Plots of  $T_B$  along the two analysis case transect lines for the (left) coast-crossing and (right) island-crossing cases.



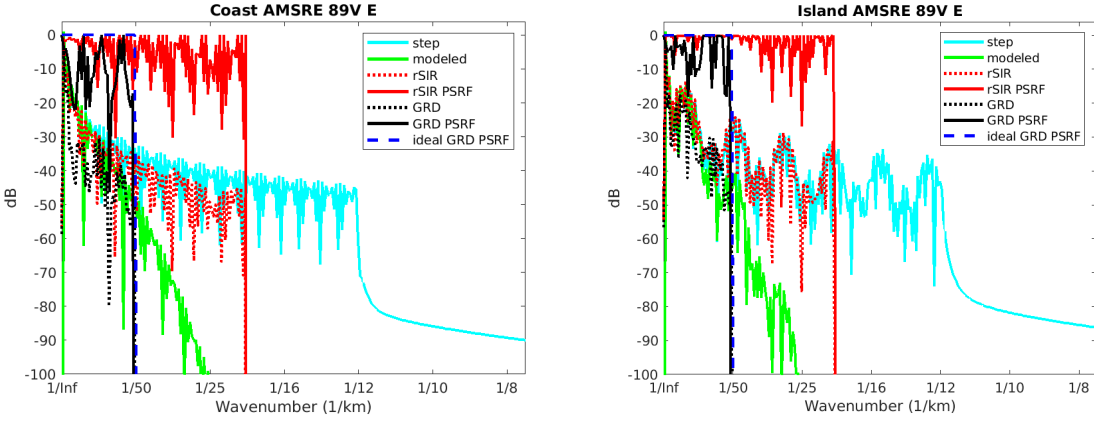


Figure 193: Wavenumber spectra of the  $T_B$  slices, the model, and the PSRF. (left) Coast-crossing case. (right) Island-crossing case.

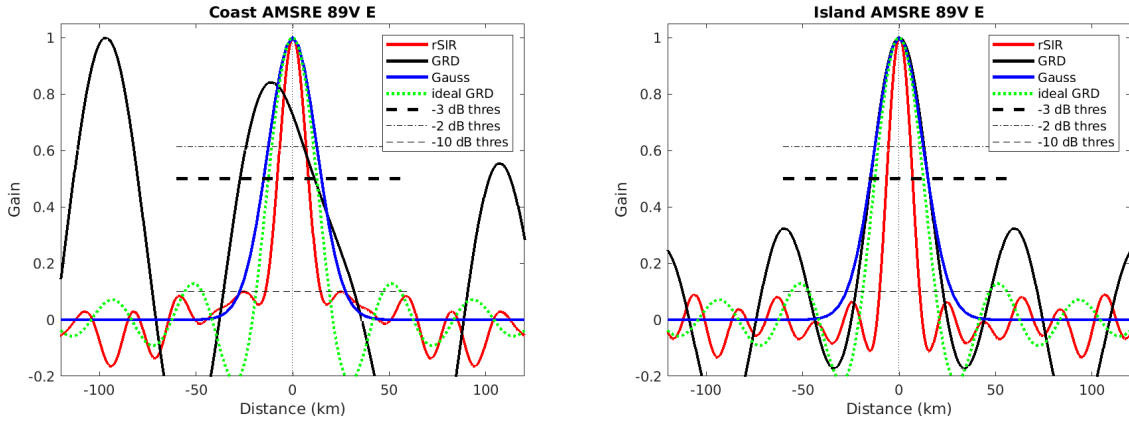


Figure 194: Derived single-pass rSIR and GRD PSRFs from the (left) coast-crossing and (right) island-crossing cases.

Table 98: Resolution estimates for AMSRE channel 89V LTOD E

Algorithm	-3 dB Thres		-2 dB Thres		-10 dB Thres	
	Coast	Island	Coast	Island	Coast	Island
Gauss	30.0	30.0	24.4	24.4	54.8	54.8
rSIR	16.2	13.4	13.3	11.2	28.5	20.8
ideal GRD	36.2	36.2	30.3	30.3	54.5	54.5
GRD	33.3	29.8	28.0	24.9	48.0	45.1

## C.24 AMSRE Channel 89V M Figures

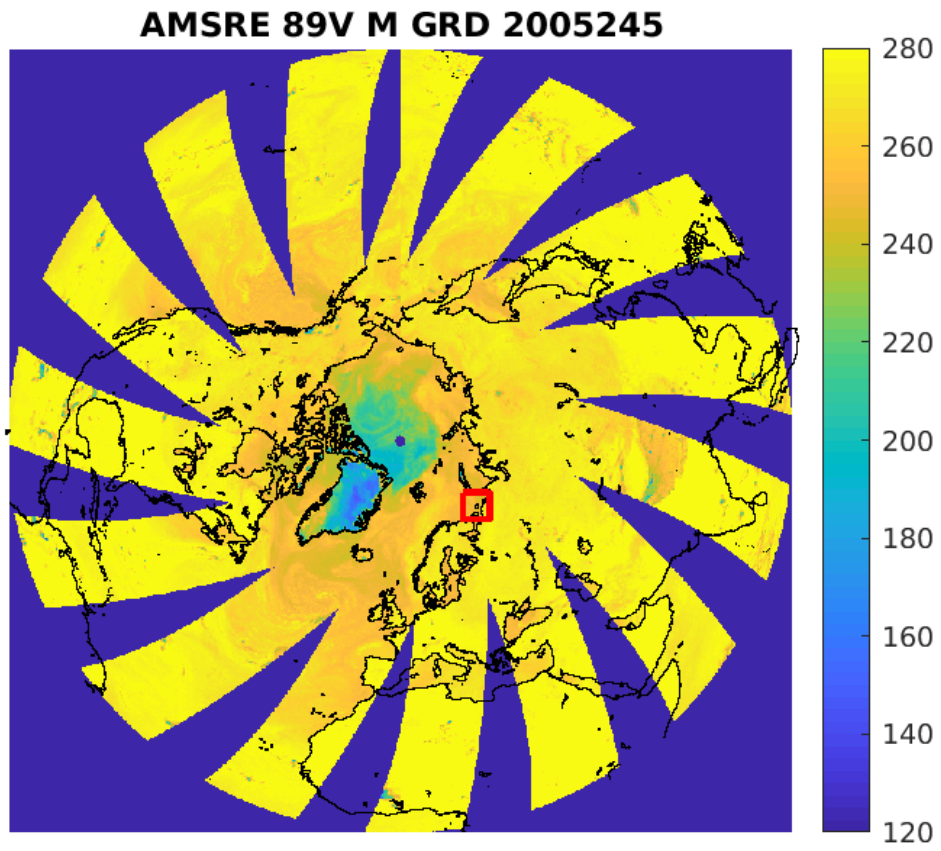


Figure 195: rSIR Northern Hemisphere view.

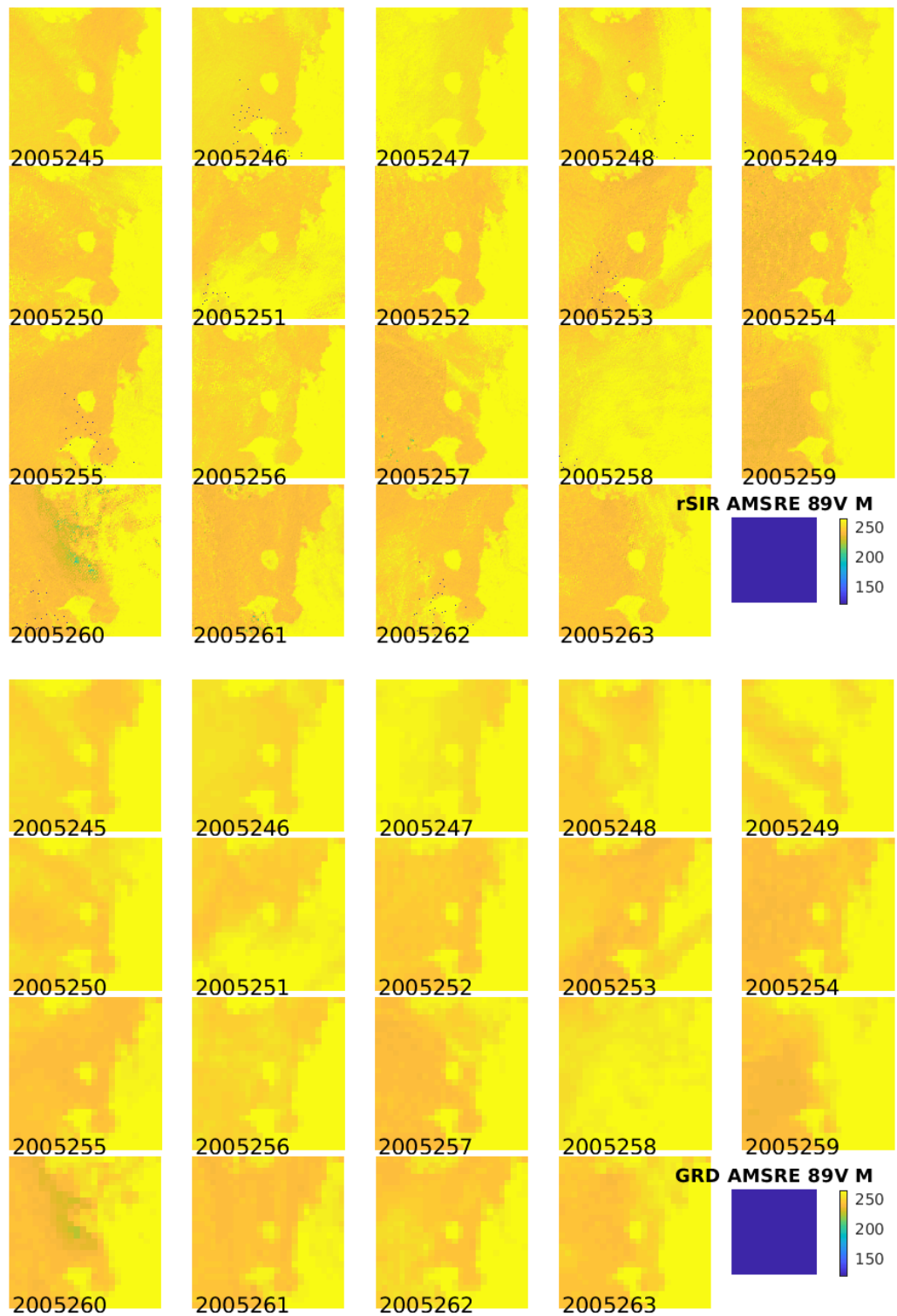


Figure 196: Time series of (top) rSIR and (bottom) GRD  $T_B$  images over the study area. Image dates are labeled on the image.

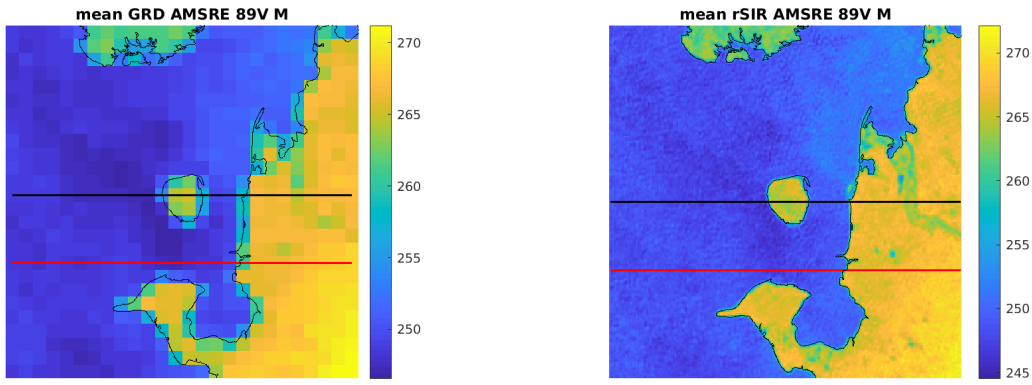


Figure 197: Average of daily  $T_B$  images over the study area. (left) 25-km GRD. (right) 3.125-km rSIR. The thick horizontal lines show the data transect locations where data is extracted from the image for analysis.

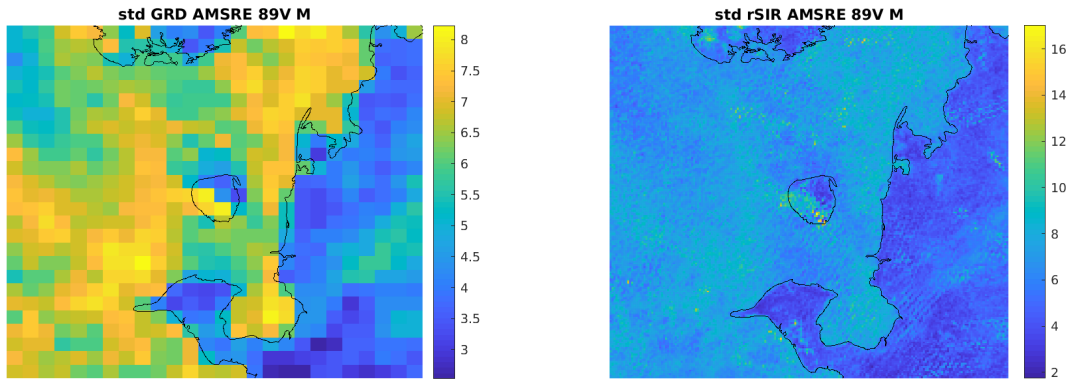


Figure 198: Standard deviation of daily  $T_B$  images over the study area. (left) 25-km GRD. (right) 3.125-km rSIR.

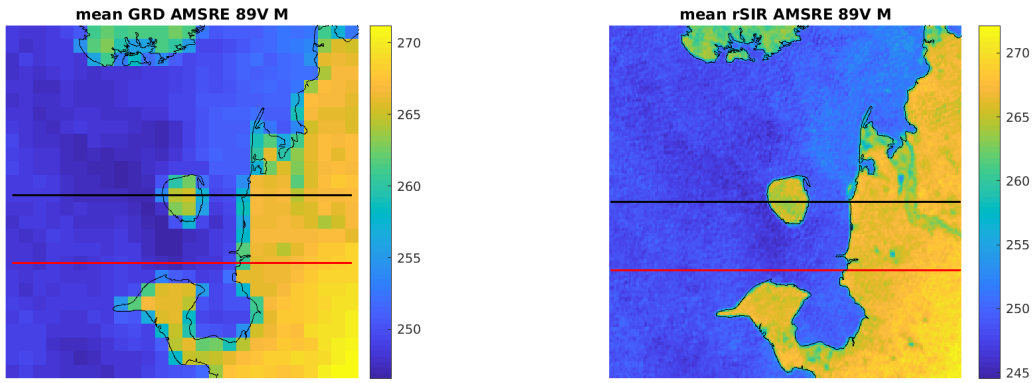


Figure 199: [Repeated] Average of daily  $T_B$  images over the study area. (left) 25-km GRD. (right) 3.125-km rSIR. The thick horizontal lines show the data transect locations where data is extracted from the image for analysis.

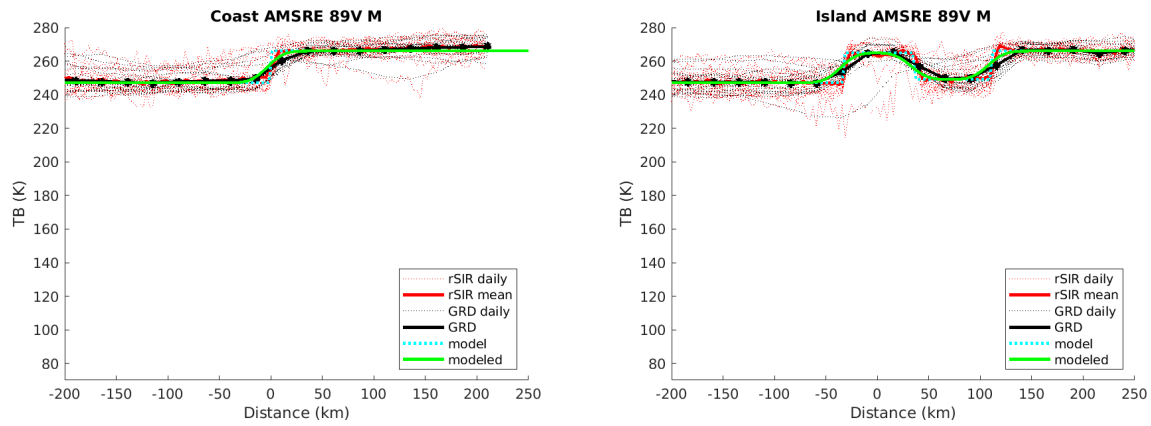


Figure 200: Plots of  $T_B$  along the two analysis case transect lines for the (left) coast-crossing and (right) island-crossing cases.

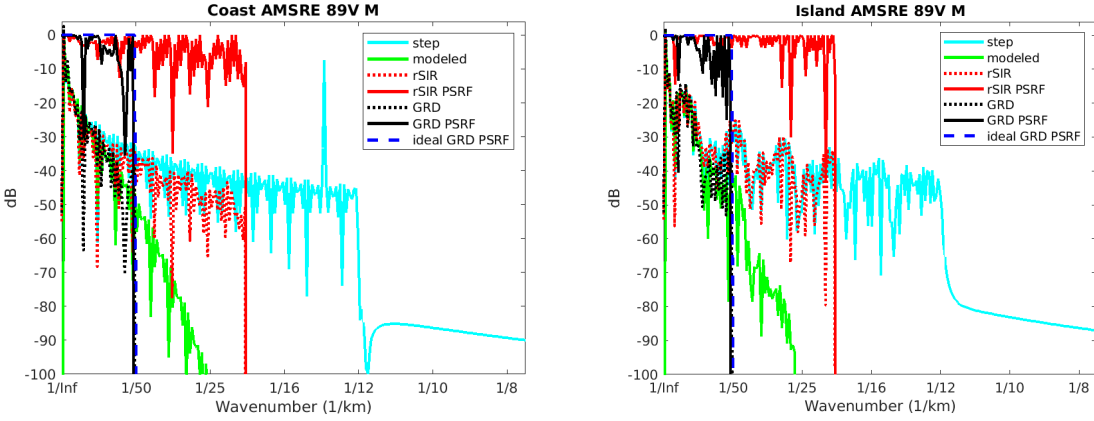


Figure 201: Wavenumber spectra of the  $T_B$  slices, the model, and the PSRF. (left) Coast-crossing case. (right) Island-crossing case.

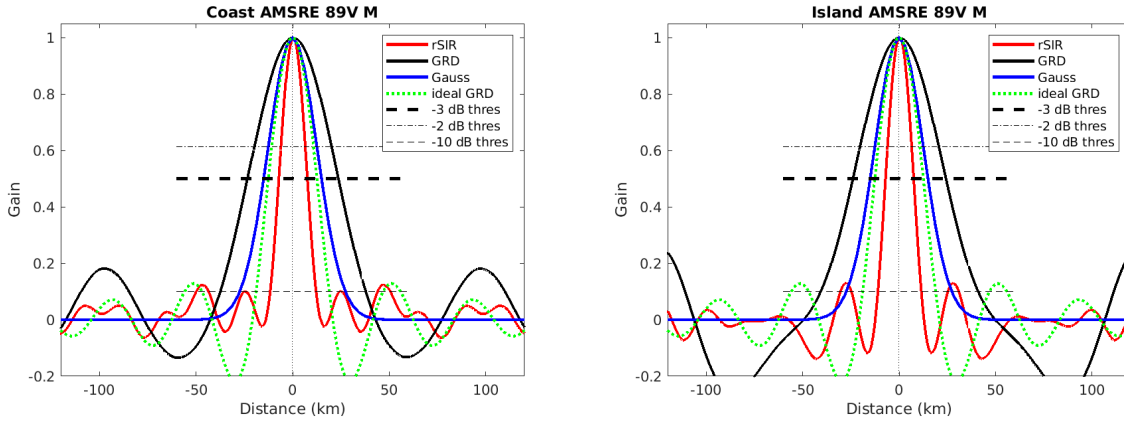


Figure 202: Derived single-pass rSIR and GRD PSRFs from the (left) coast-crossing and (right) island-crossing cases.

Table 99: Resolution estimates for AMSRE channel 89V LTOD M

Algorithm	-3 dB Thres		-2 dB Thres		-10 dB Thres	
	Coast	Island	Coast	Island	Coast	Island
Gauss	30.0	30.0	24.4	24.4	54.8	54.8
rSIR	14.7	14.6	12.2	12.1	23.8	22.6
ideal GRD	36.2	36.2	30.3	30.3	54.5	54.5
GRD	47.1	48.2	38.9	39.6	75.3	81.6

## D SMAP Figures

### D.1 SMAP Channel 1.4H E Figures

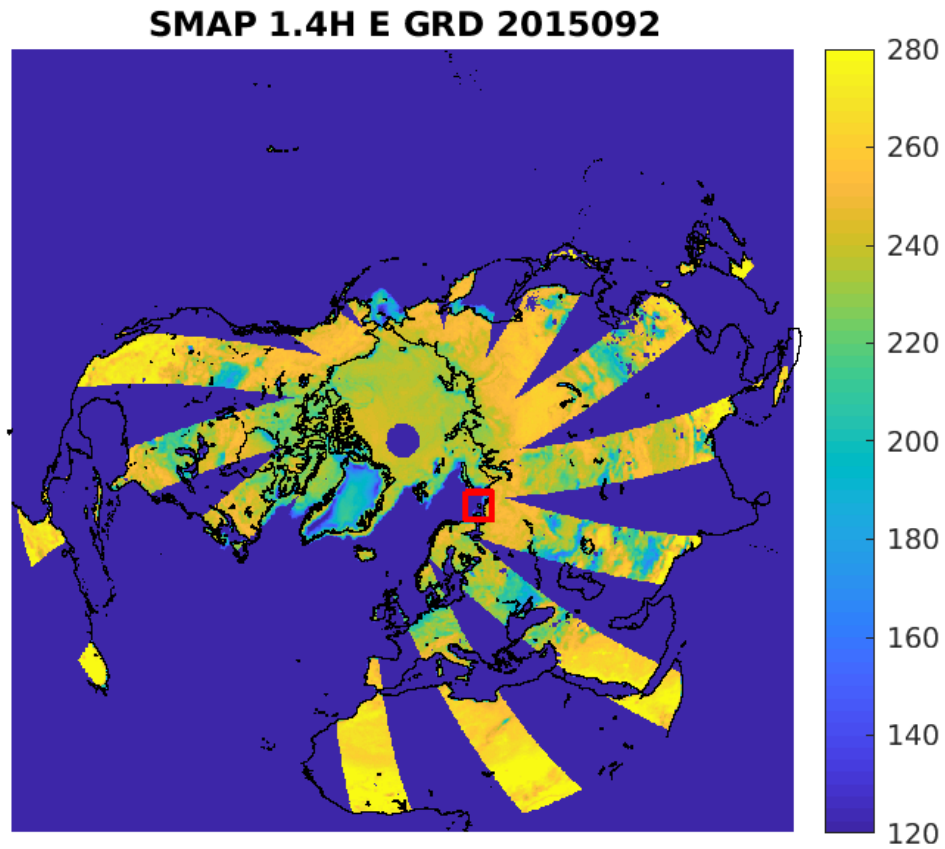


Figure 203: rSIR Northern Hemisphere view.

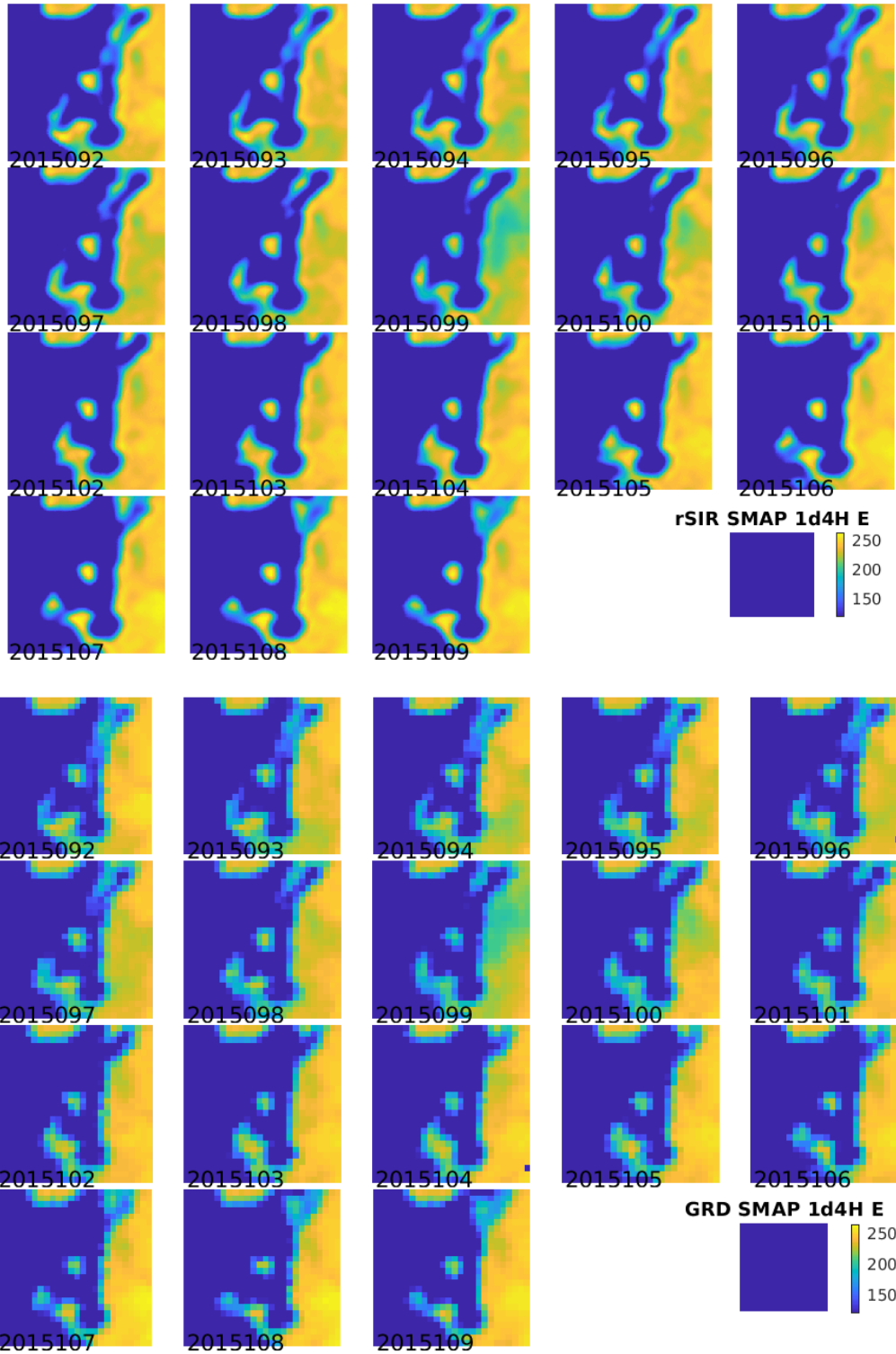


Figure 204: Time series of (top) rSIR and (bottom) GRD  $T_B$  images over the study area. Image dates are labeled on the image.



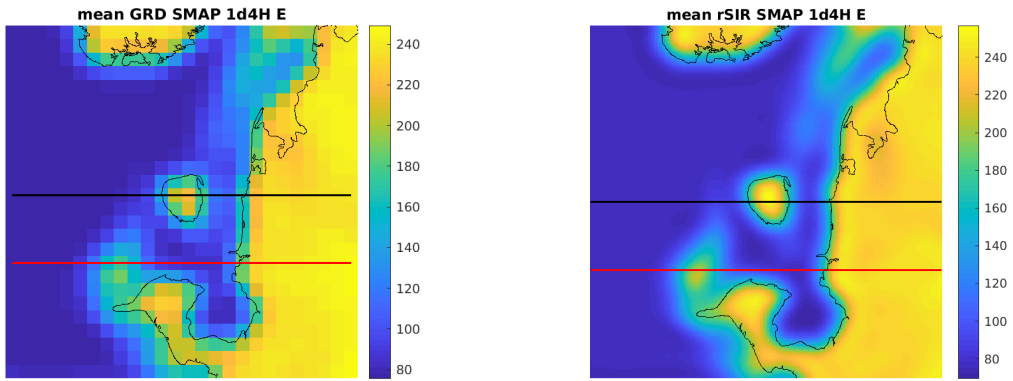


Figure 205: Average of daily  $T_B$  images over the study area. (left) 25-km GRD. (right) 3.125-km rSIR. The thick horizontal lines show the data transect locations where data is extracted from the image for analysis.

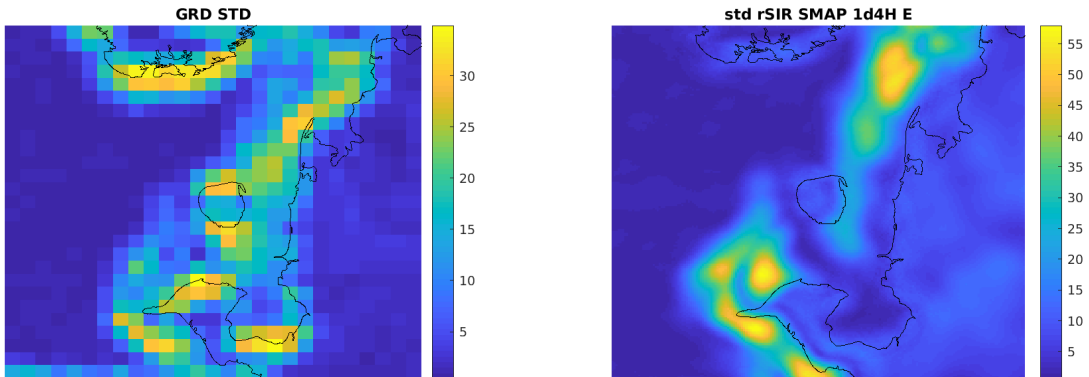


Figure 206: Standard deviation of daily  $T_B$  images over the study area. (left) 25-km GRD. (right) 3.125-km rSIR.

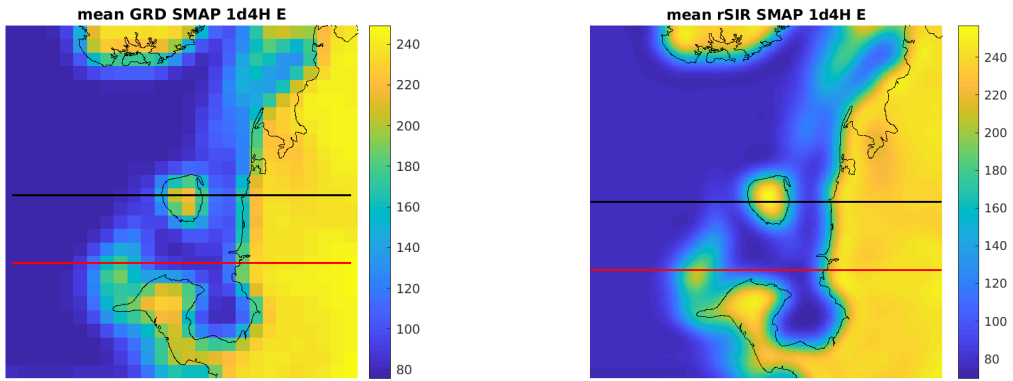


Figure 207: [Repeated] Average of daily  $T_B$  images over the study area. (left) 25-km GRD. (right) 3.125-km rSIR. The thick horizontal lines show the data transect locations where data is extracted from the image for analysis.

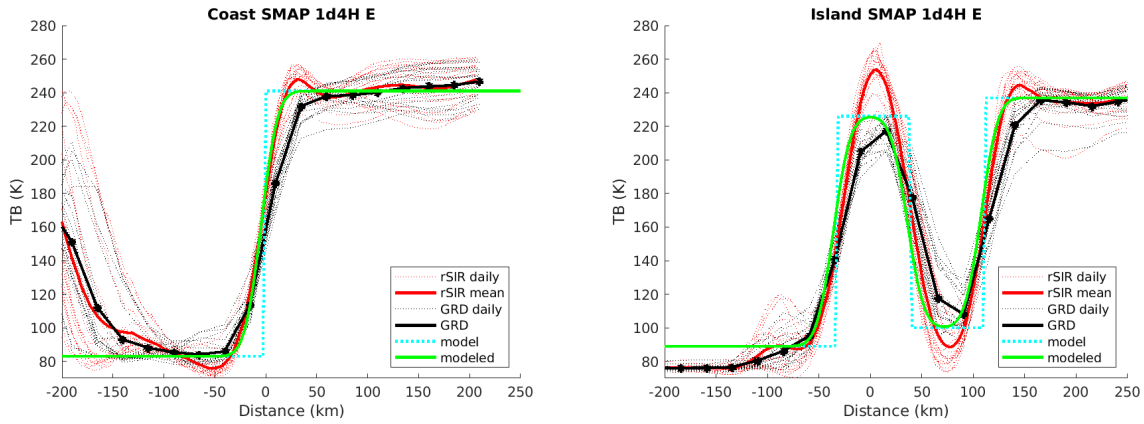


Figure 208: Plots of  $T_B$  along the two analysis case transect lines for the (left) coast-crossing and (right) island-crossing cases.

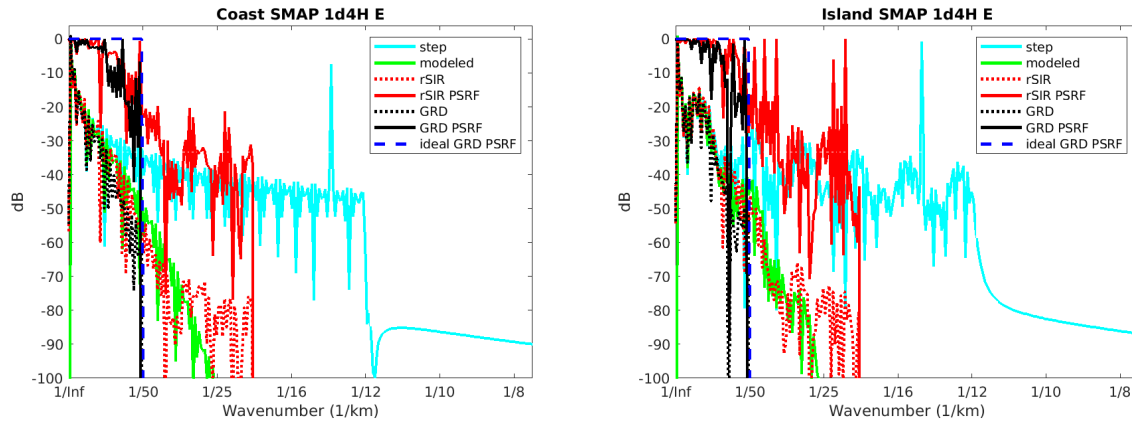


Figure 209: Wavenumber spectra of the  $T_B$  slices, the model, and the PSRF. (left) Coast-crossing case. (right) Island-crossing case.

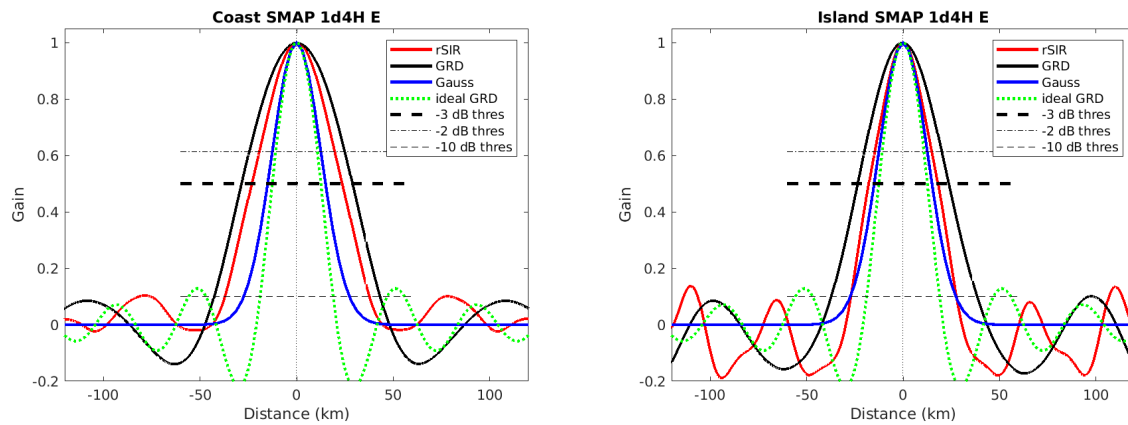


Figure 210: Derived single-pass rSIR and GRD PSRFs from the (left) coast-crossing and (right) island-crossing cases.

Table 100: Resolution estimates for SMAP channel 1.4H LTOD E

Algorithm	-3 dB Thres		-2 dB Thres		-10 dB Thres	
	Coast	Island	Coast	Island	Coast	Island
Gauss	30.0	30.0	24.4	24.4	54.8	54.8
rSIR	46.8	35.9	37.8	28.7	74.8	54.7
ideal GRD	36.2	36.2	30.3	30.3	54.5	54.5
GRD	57.4	47.2	48.2	38.9	85.9	75.6

## D.2 SMAP Channel 1.4H M Figures

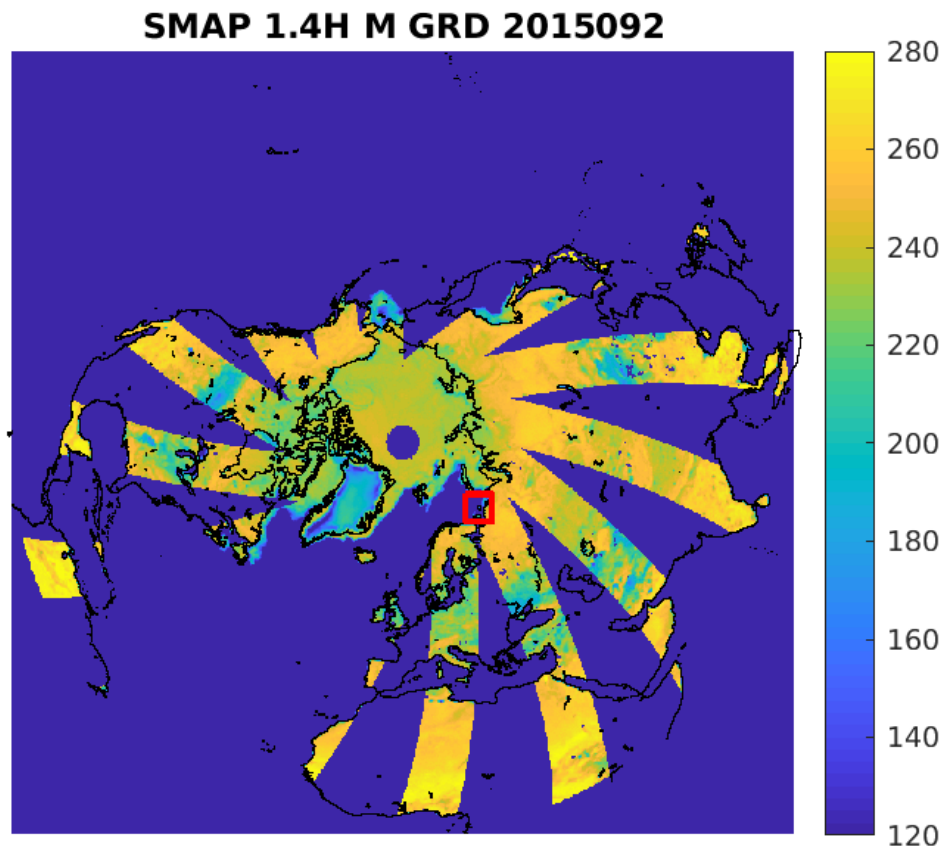


Figure 211: rSIR Northern Hemisphere view.

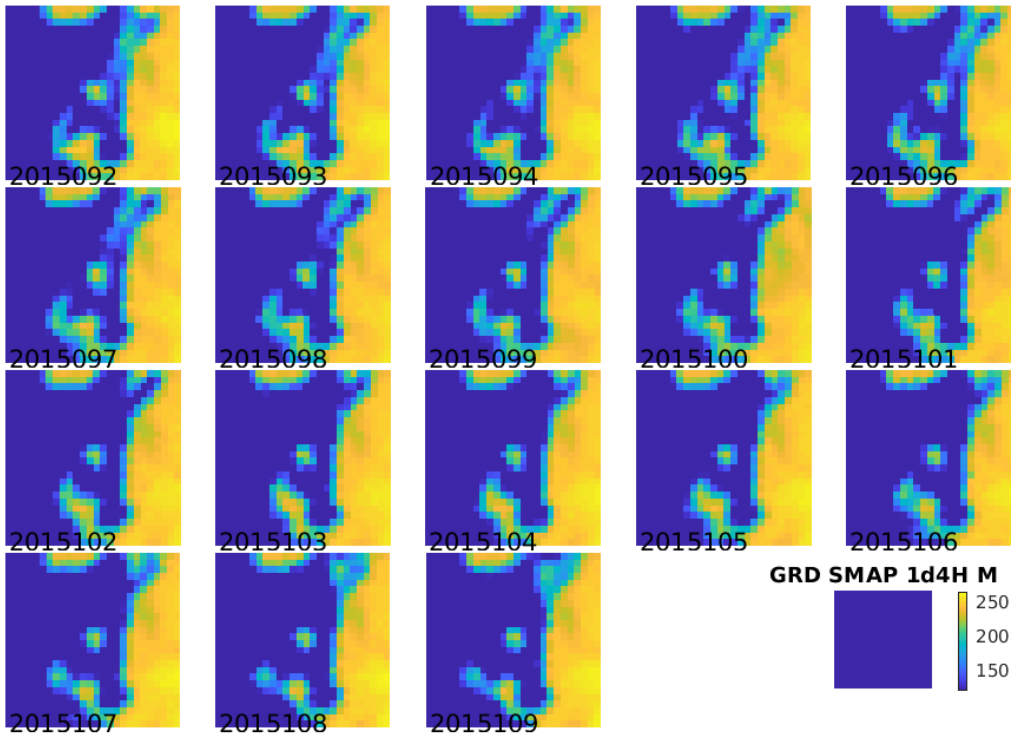
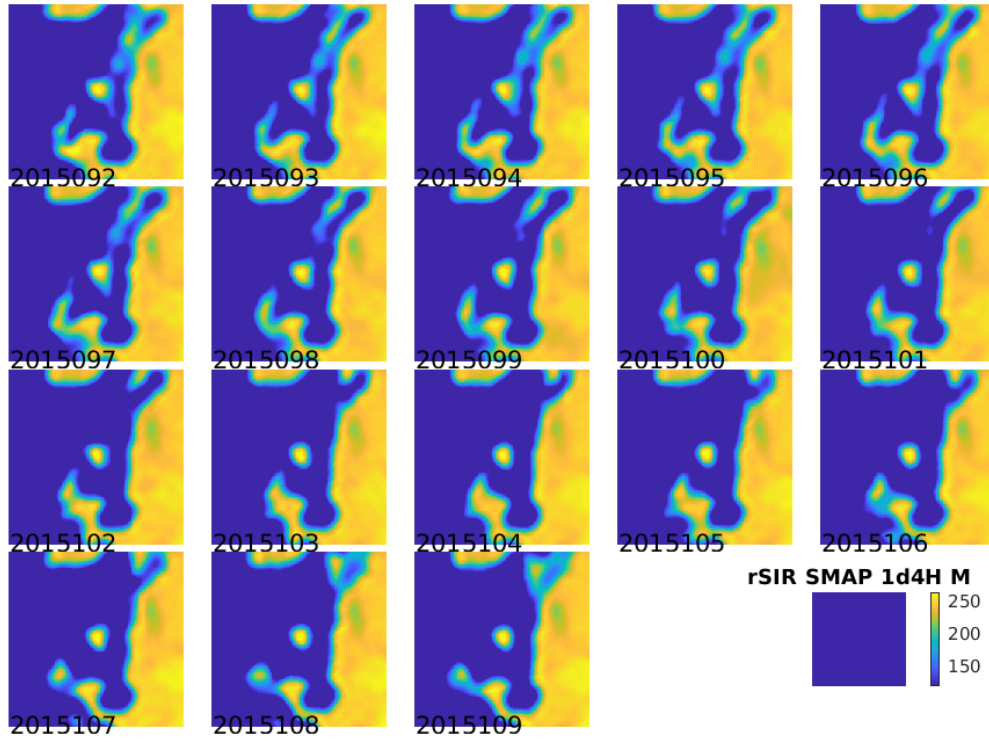


Figure 212: Time series of (top) rSIR and (bottom) GRD  $T_B$  images over the study area. Image dates are labeled on the image.

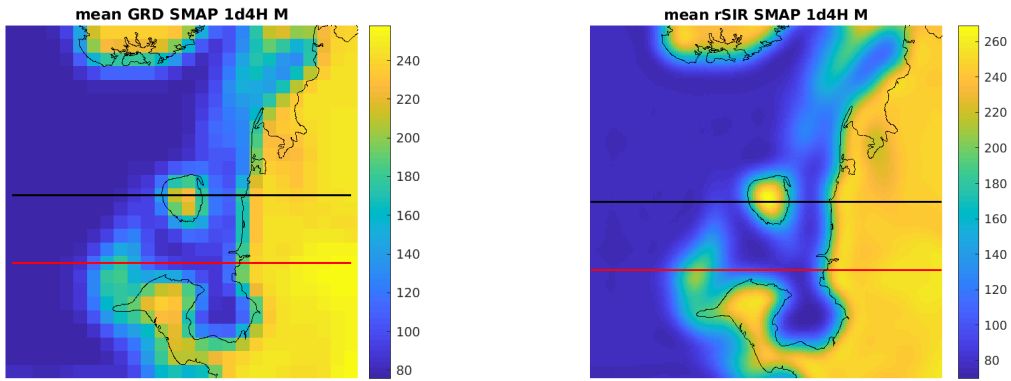


Figure 213: Average of daily  $T_B$  images over the study area. (left) 25-km GRD. (right) 3.125-km rSIR. The thick horizontal lines show the data transect locations where data is extracted from the image for analysis.

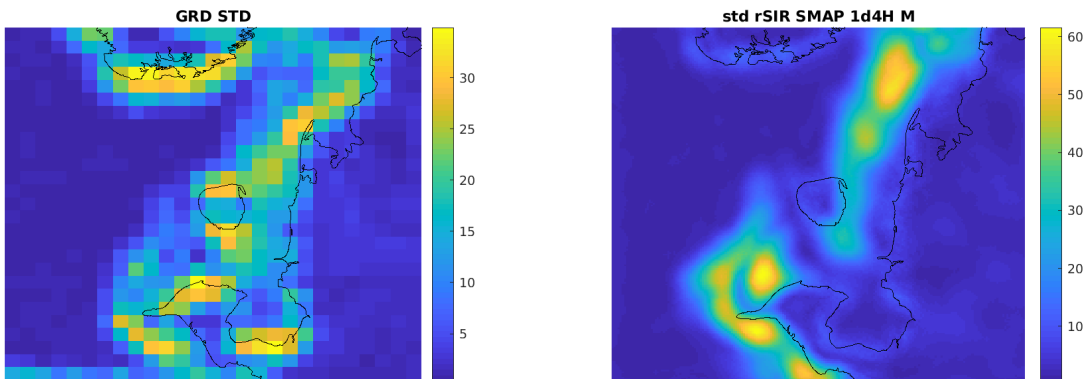


Figure 214: Standard deviation of daily  $T_B$  images over the study area. (left) 25-km GRD. (right) 3.125-km rSIR.

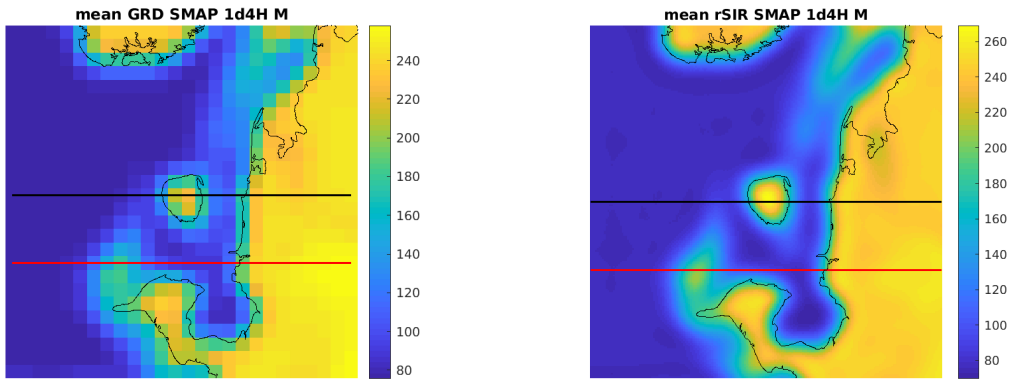


Figure 215: [Repeated] Average of daily  $T_B$  images over the study area. (left) 25-km GRD. (right) 3.125-km rSIR. The thick horizontal lines show the data transect locations where data is extracted from the image for analysis.

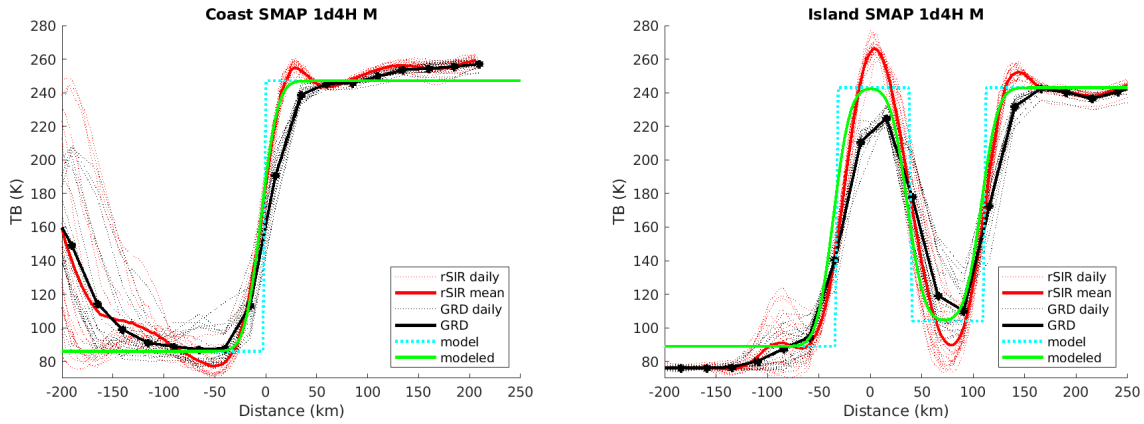


Figure 216: Plots of  $T_B$  along the two analysis case transect lines for the (left) coast-crossing and (right) island-crossing cases.

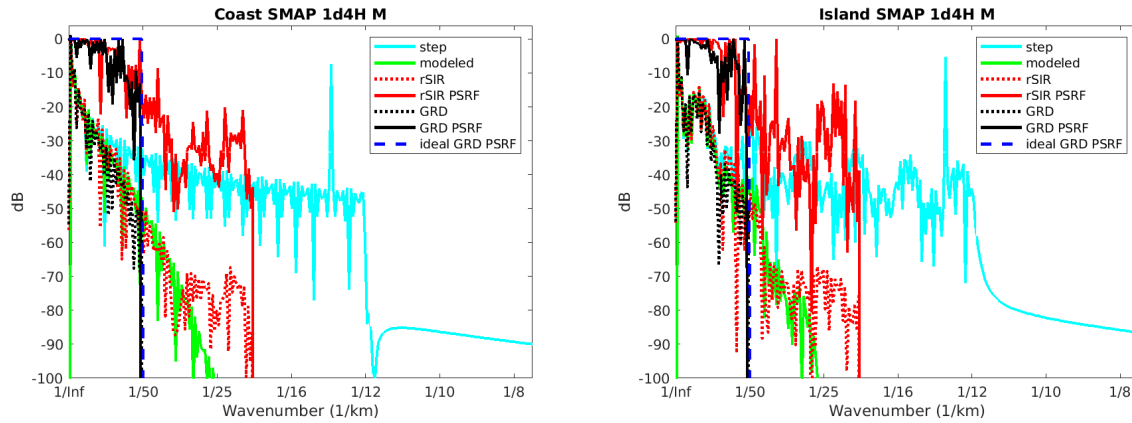


Figure 217: Wavenumber spectra of the  $T_B$  slices, the model, and the PSRF. (left) Coast-crossing case. (right) Island-crossing case.

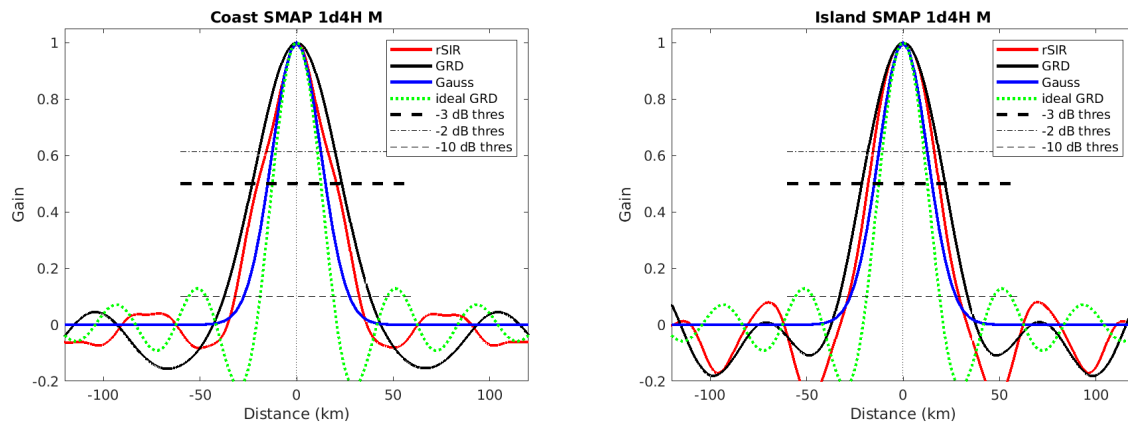


Figure 218: Derived single-pass rSIR and GRD PSRFs from the (left) coast-crossing and (right) island-crossing cases.

Table 101: Resolution estimates for SMAP channel 1.4H LTOD M

Algorithm	-3 dB Thres		-2 dB Thres		-10 dB Thres	
	Coast	Island	Coast	Island	Coast	Island
Gauss	30.0	30.0	24.4	24.4	54.8	54.8
rSIR	40.9	36.6	30.4	31.2	64.2	57.4
ideal GRD	36.2	36.2	30.3	30.3	54.5	54.5
GRD	46.5	43.1	38.4	35.9	75.5	66.5



### D.3 SMAP Channel 1.4V E Figures

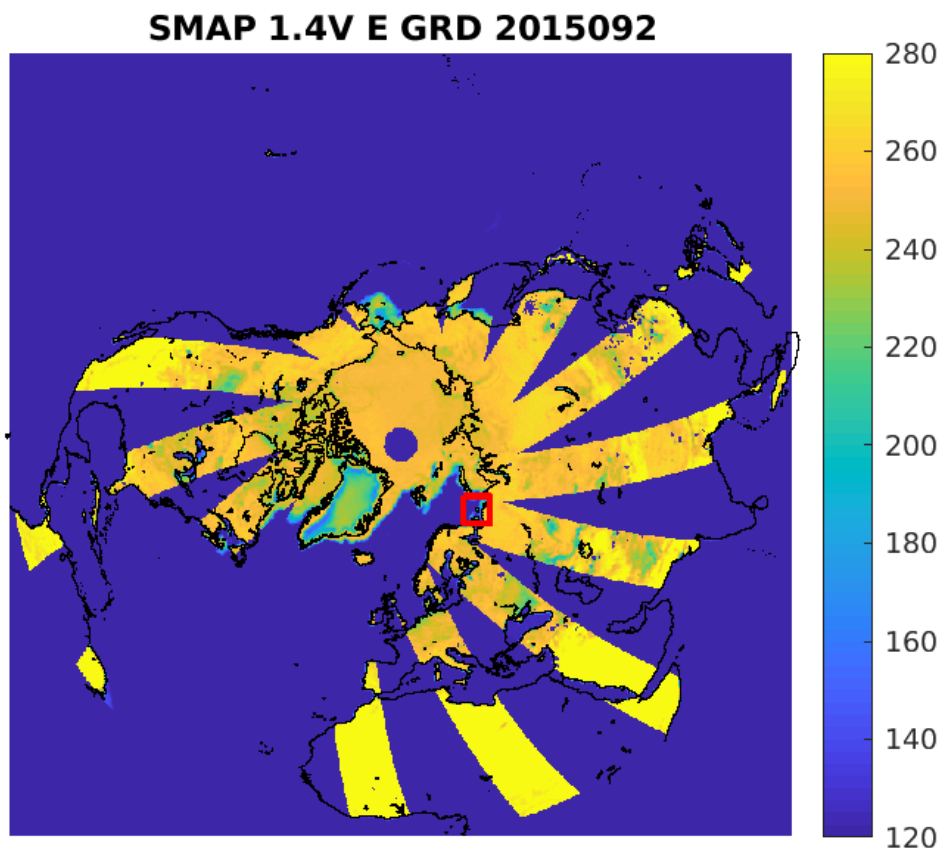


Figure 219: rSIR Northern Hemisphere view.

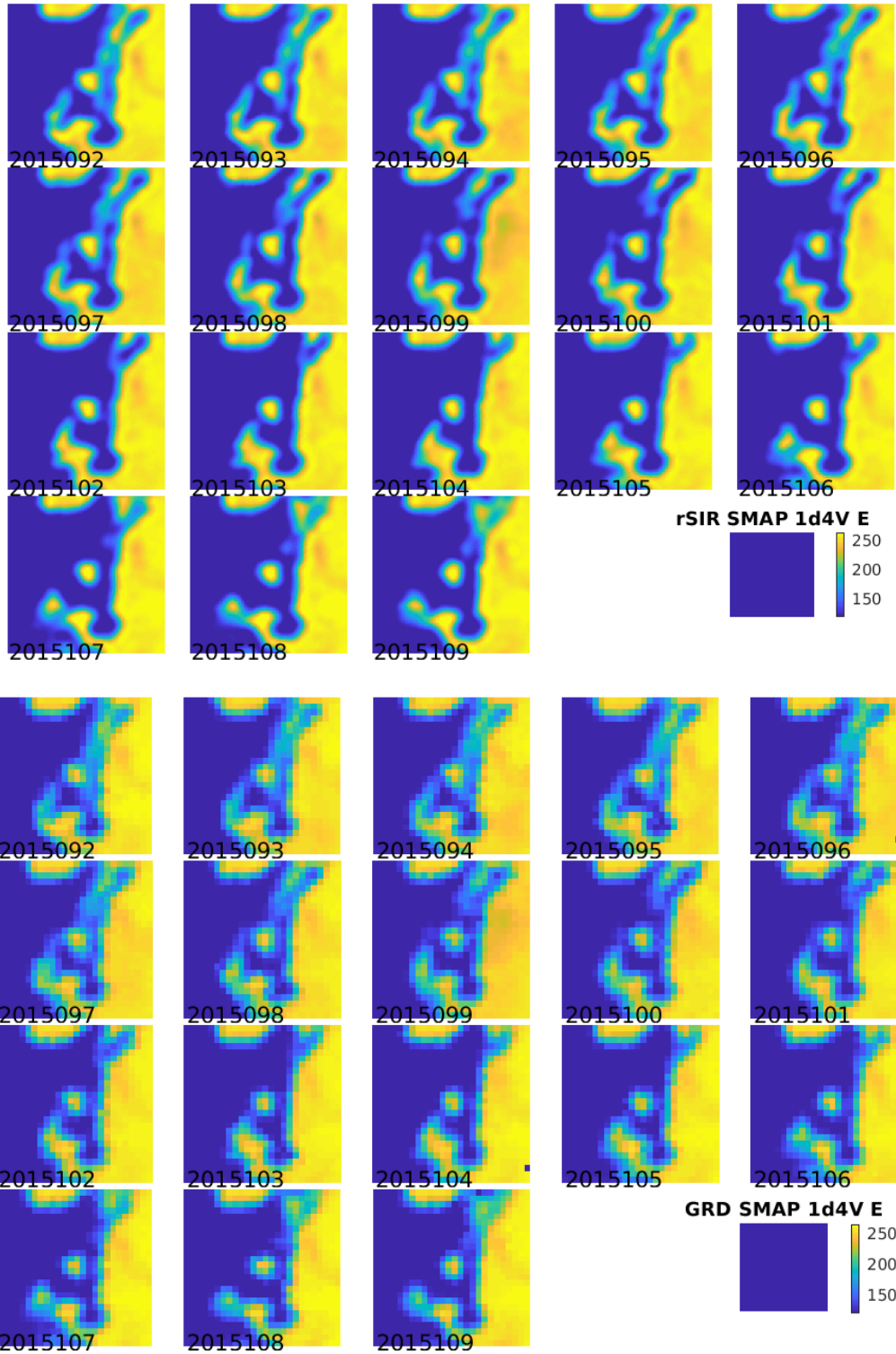


Figure 220: Time series of (top) rSIR and (bottom) GRD  $T_B$  images over the study area. Image dates are labeled on the image.

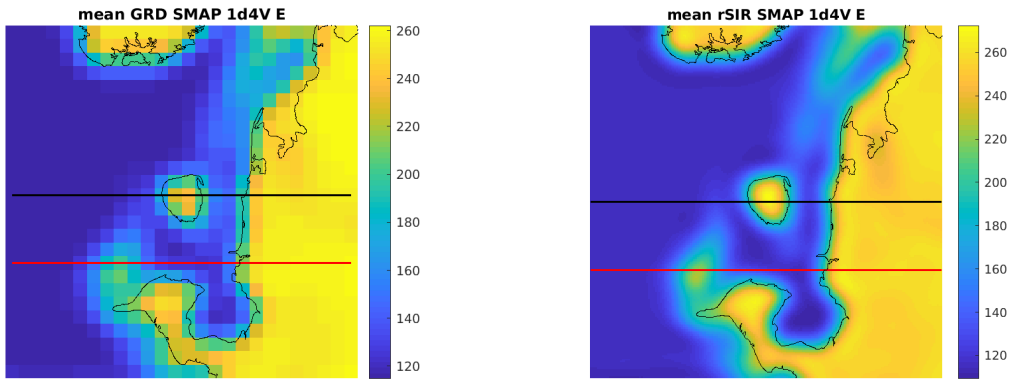


Figure 221: Average of daily  $T_B$  images over the study area. (left) 25-km GRD. (right) 3.125-km rSIR. The thick horizontal lines show the data transect locations where data is extracted from the image for analysis.

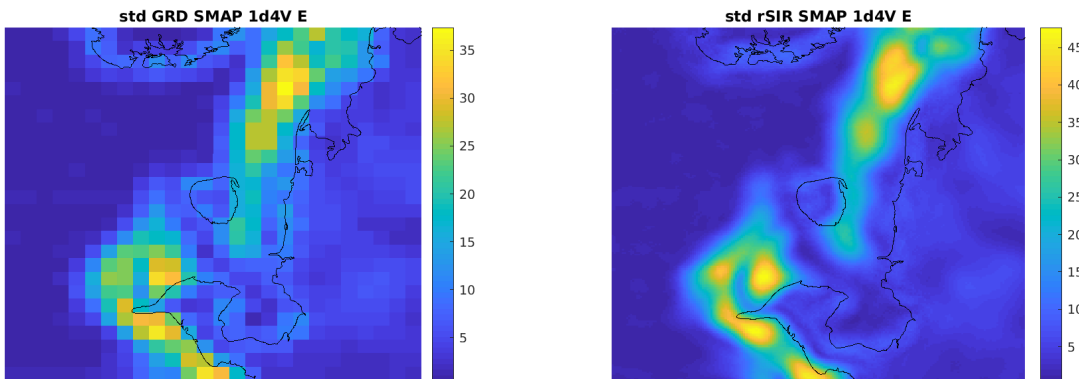


Figure 222: Standard deviation of daily  $T_B$  images over the study area. (left) 25-km GRD. (right) 3.125-km rSIR.

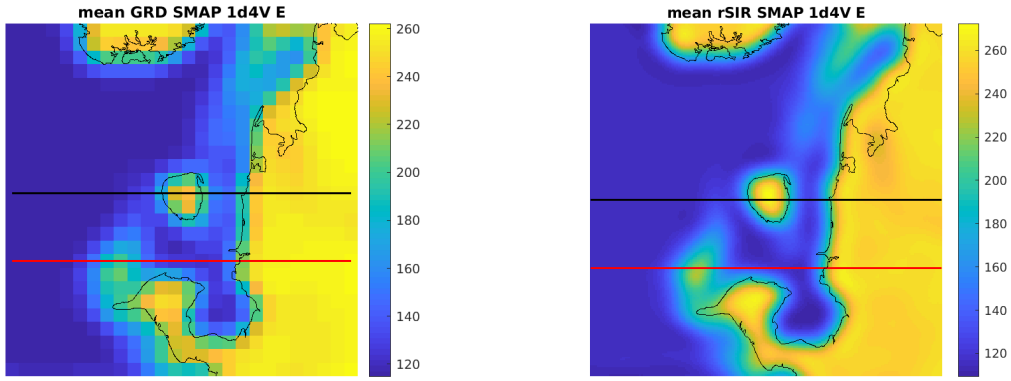


Figure 223: [Repeated] Average of daily  $T_B$  images over the study area. (left) 25-km GRD. (right) 3.125-km rSIR. The thick horizontal lines show the data transect locations where data is extracted from the image for analysis.

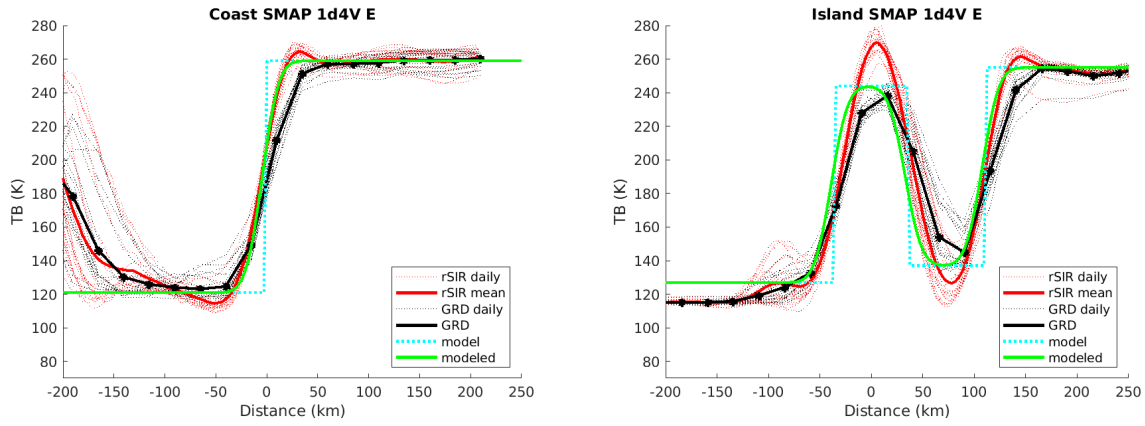


Figure 224: Plots of  $T_B$  along the two analysis case transect lines for the (left) coast-crossing and (right) island-crossing cases.

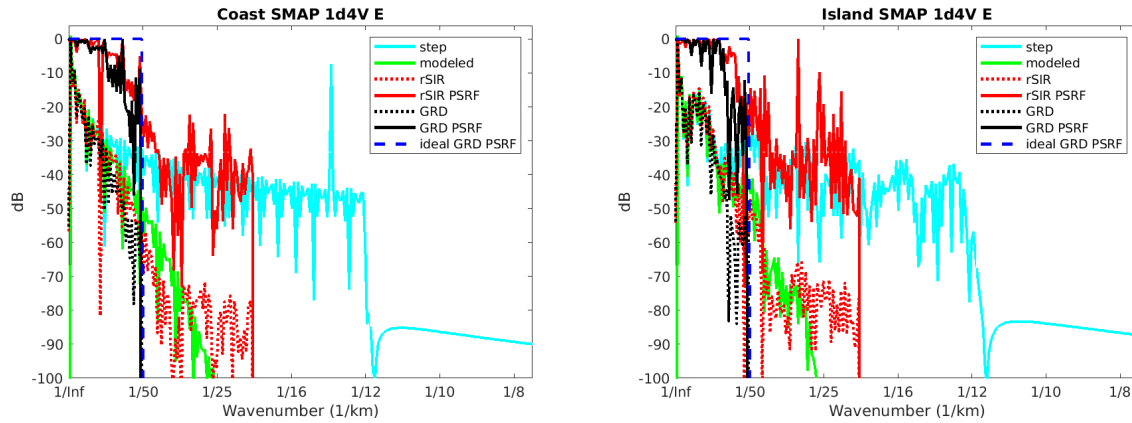


Figure 225: Wavenumber spectra of the  $T_B$  slices, the model, and the PSRF. (left) Coast-crossing case. (right) Island-crossing case.

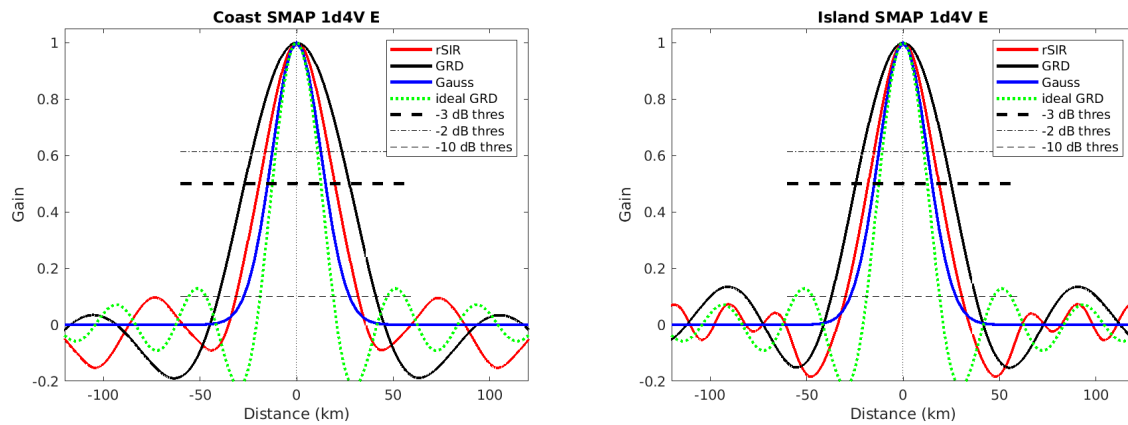


Figure 226: Derived single-pass rSIR and GRD PSRFs from the (left) coast-crossing and (right) island-crossing cases.

Table 102: Resolution estimates for SMAP channel 1.4V LTOD E

Algorithm	-3 dB Thres		-2 dB Thres		-10 dB Thres	
	Coast	Island	Coast	Island	Coast	Island
Gauss	30.0	30.0	24.4	24.4	54.8	54.8
rSIR	39.2	36.7	32.0	29.8	63.2	60.4
ideal GRD	36.2	36.2	30.3	30.3	54.5	54.5
GRD	54.3	49.4	45.4	41.3	81.6	74.7

## D.4 SMAP Channel 1.4V M Figures

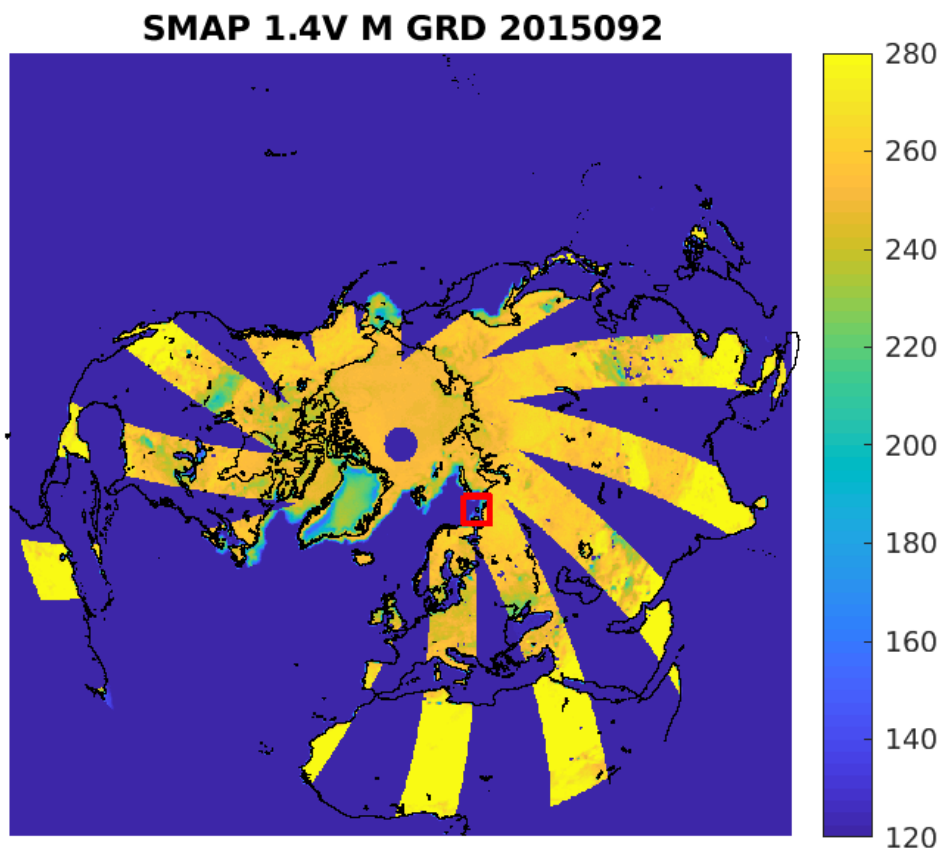


Figure 227: rSIR Northern Hemisphere view.

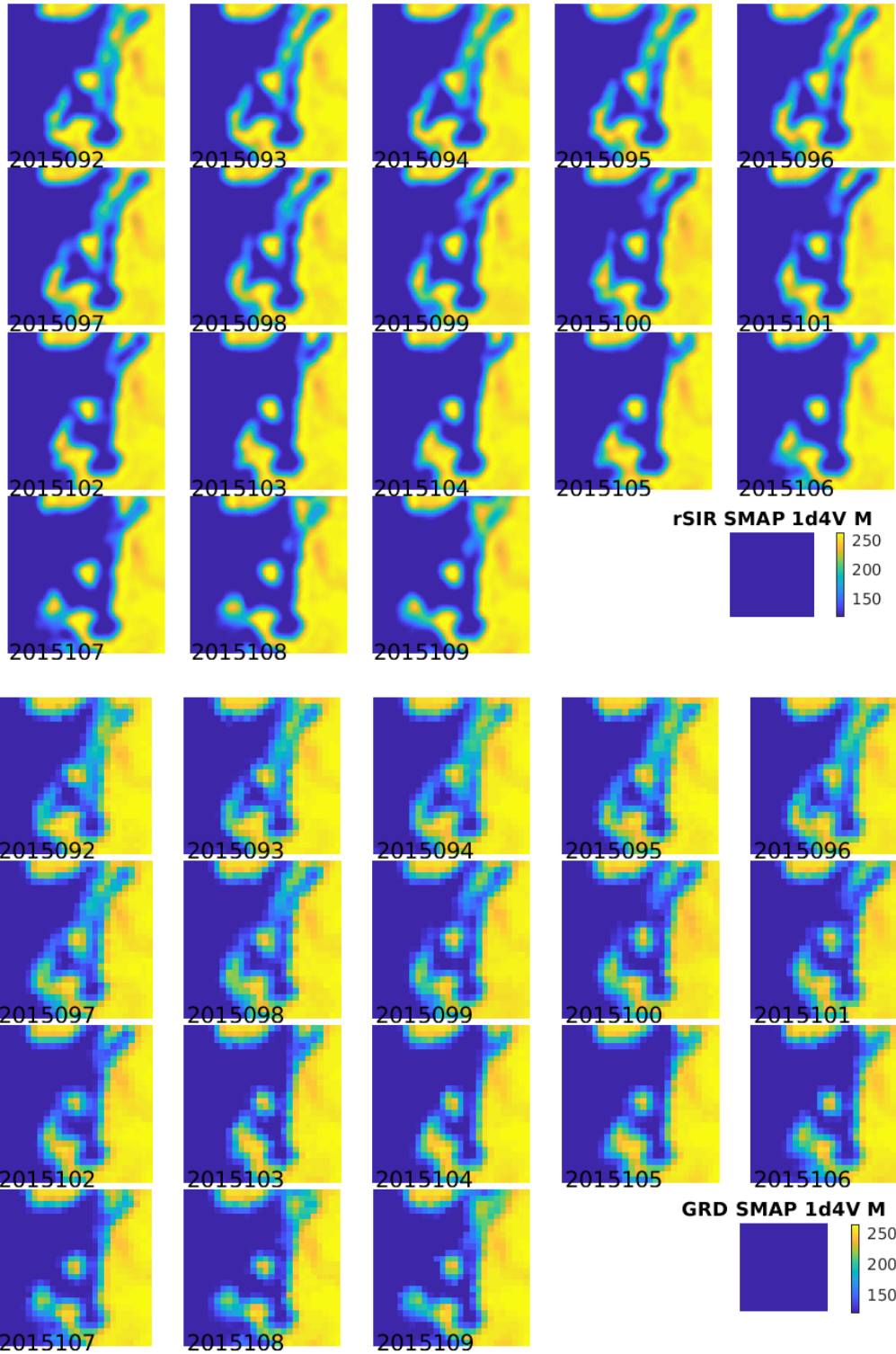


Figure 228: Time series of (top) rSIR and (bottom) GRD  $T_B$  images over the study area. Image dates are labeled on the image.

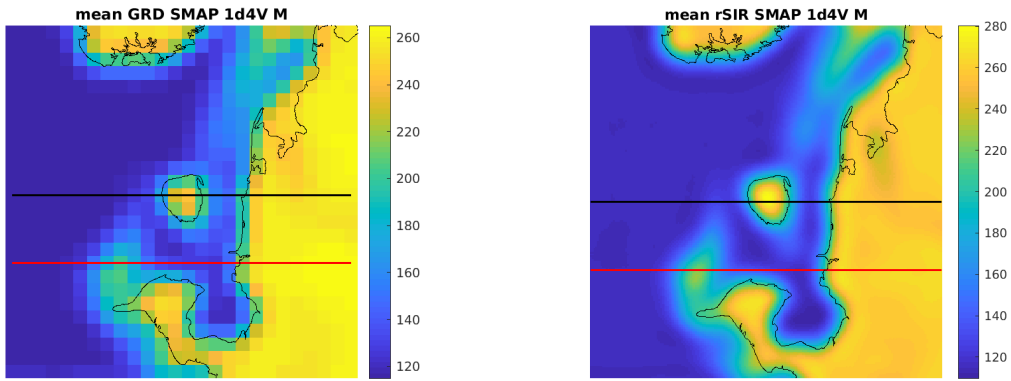


Figure 229: Average of daily  $T_B$  images over the study area. (left) 25-km GRD. (right) 3.125-km rSIR. The thick horizontal lines show the data transect locations where data is extracted from the image for analysis.

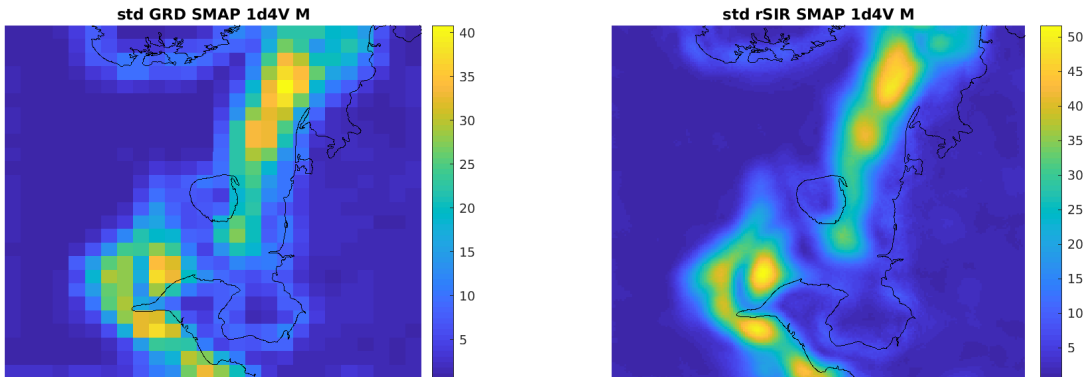


Figure 230: Standard deviation of daily  $T_B$  images over the study area. (left) 25-km GRD. (right) 3.125-km rSIR.



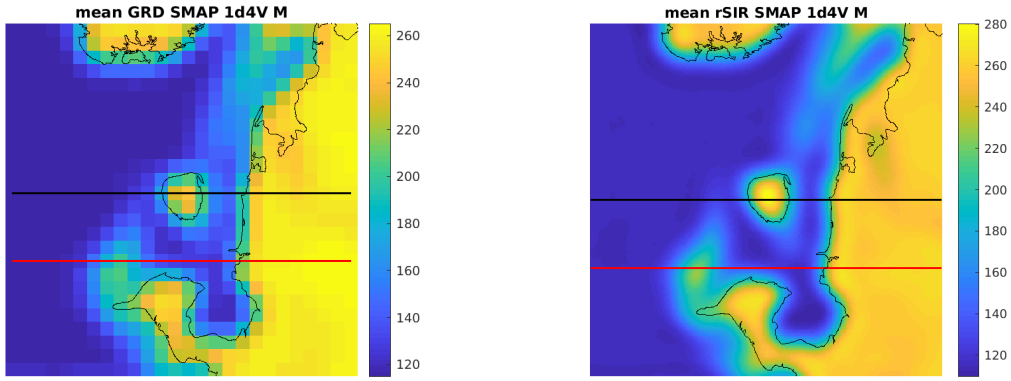


Figure 231: [Repeated] Average of daily  $T_B$  images over the study area. (left) 25-km GRD. (right) 3.125-km rSIR. The thick horizontal lines show the data transect locations where data is extracted from the image for analysis.

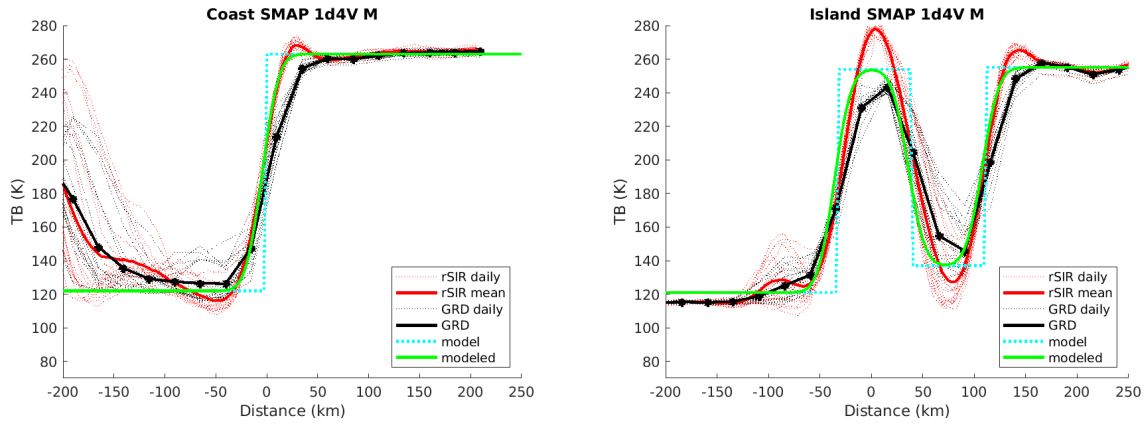


Figure 232: Plots of  $T_B$  along the two analysis case transect lines for the (left) coast-crossing and (right) island-crossing cases.

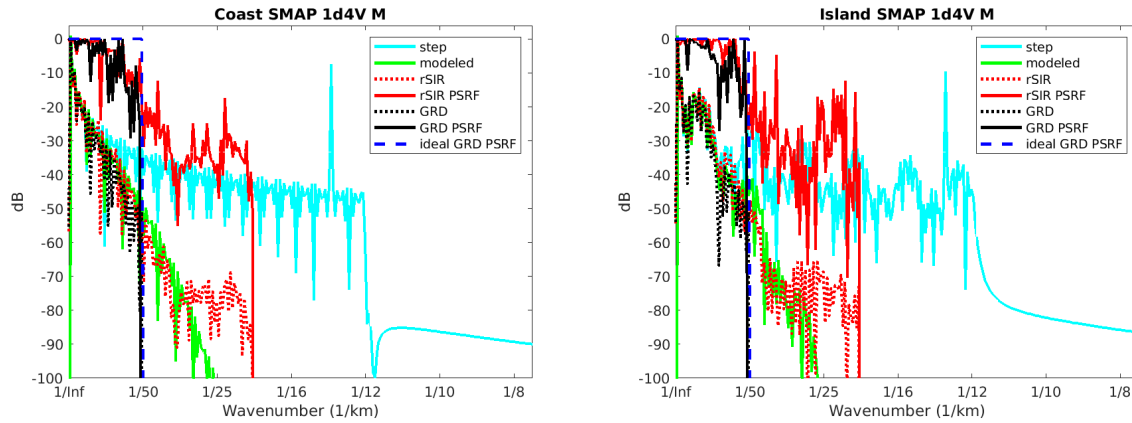


Figure 233: Wavenumber spectra of the  $T_B$  slices, the model, and the PSRF. (left) Coast-crossing case. (right) Island-crossing case.

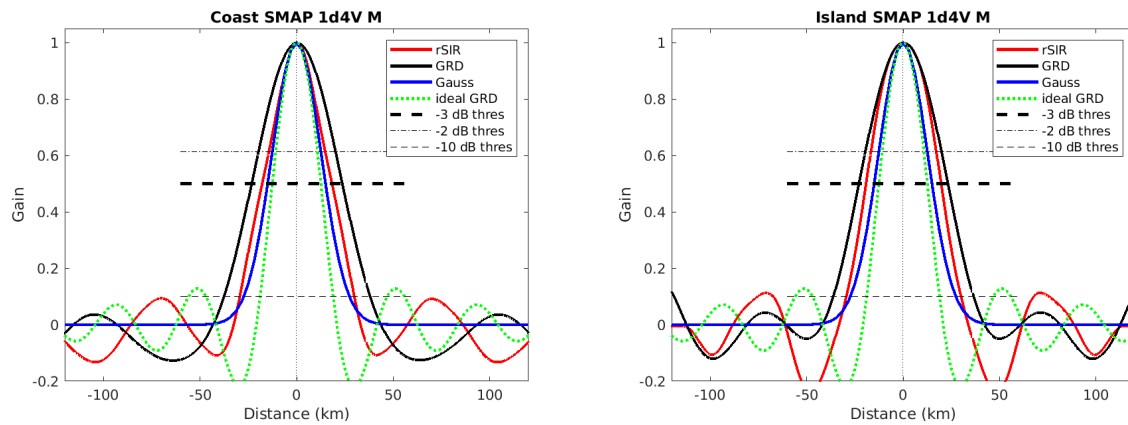


Figure 234: Derived single-pass rSIR and GRD PSRFs from the (left) coast-crossing and (right) island-crossing cases.

Table 103: Resolution estimates for SMAP channel 1.4V LTOD M

Algorithm	-3 dB Thres		-2 dB Thres		-10 dB Thres	
	Coast	Island	Coast	Island	Coast	Island
Gauss	30.0	30.0	24.4	24.4	54.8	54.8
rSIR	36.1	38.8	28.0	33.2	59.2	59.5
ideal GRD	36.2	36.2	30.3	30.3	54.5	54.5
GRD	47.0	46.1	38.8	38.3	75.7	72.7

## E SMMR Figures

### E.1 SMMR Channel 06H E Figures

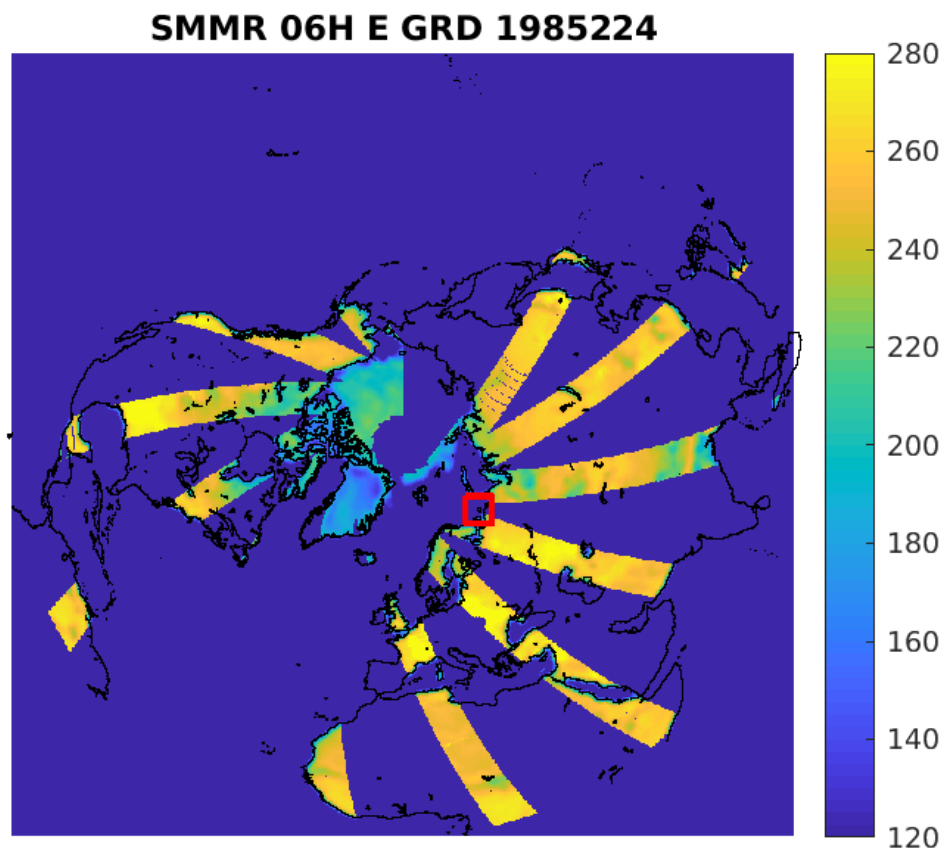


Figure 235: rSIR Northern Hemisphere view.

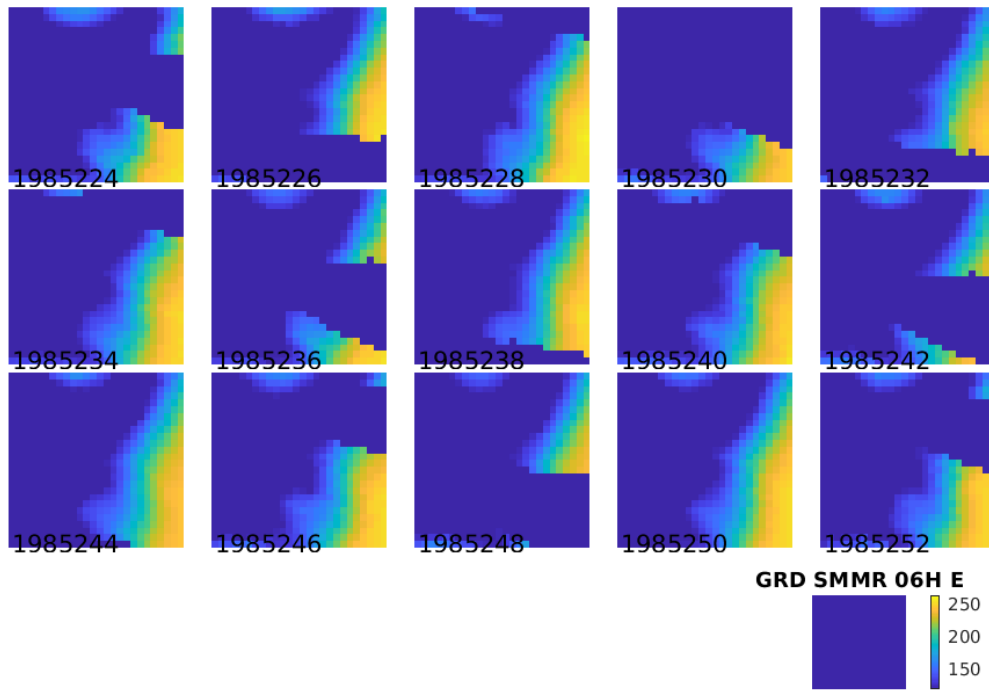
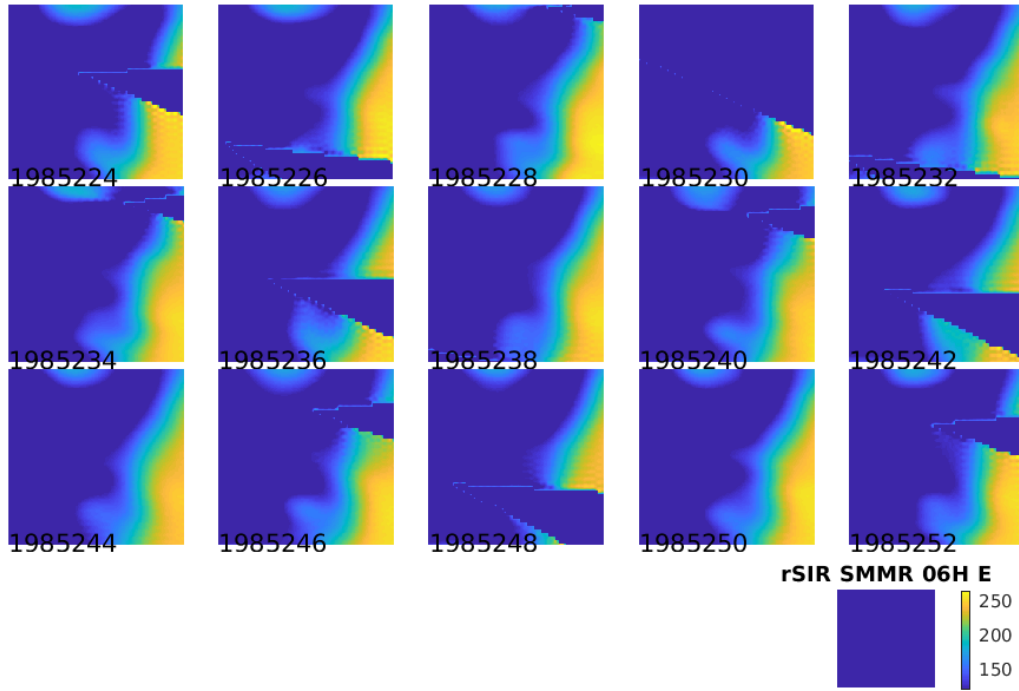


Figure 236: Time series of (top) rSIR and (bottom) GRD  $T_B$  images over the study area. Image dates are labeled on the image.

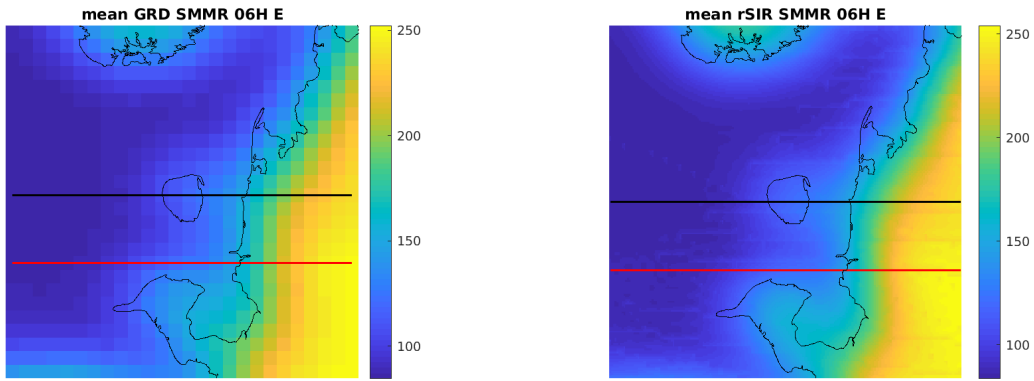


Figure 237: Average of daily  $T_B$  images over the study area. (left) 25-km GRD. (right) 3.125-km rSIR. The thick horizontal lines show the data transect locations where data is extracted from the image for analysis.

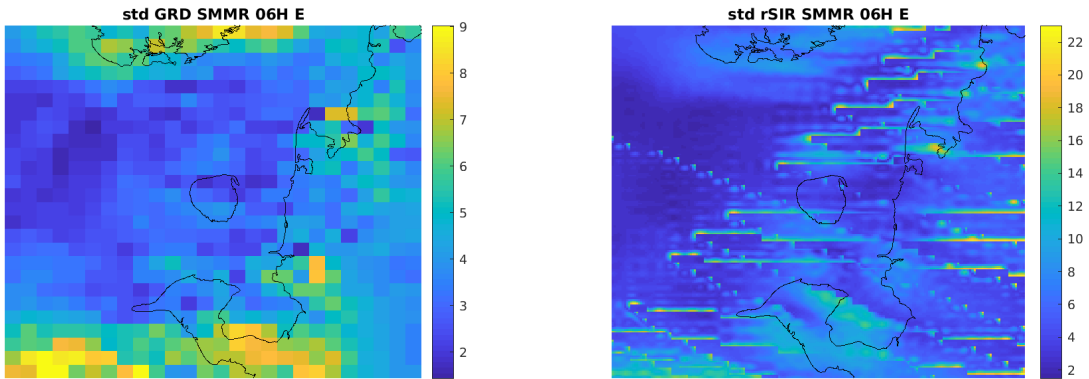


Figure 238: Standard deviation of daily  $T_B$  images over the study area. (left) 25-km GRD. (right) 3.125-km rSIR.

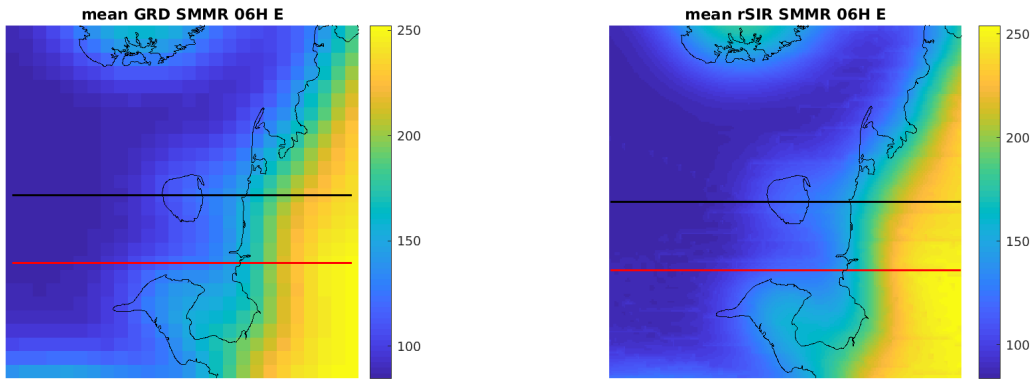


Figure 239: [Repeated] Average of daily  $T_B$  images over the study area. (left) 25-km GRD. (right) 3.125-km rSIR. The thick horizontal lines show the data transect locations where data is extracted from the image for analysis.

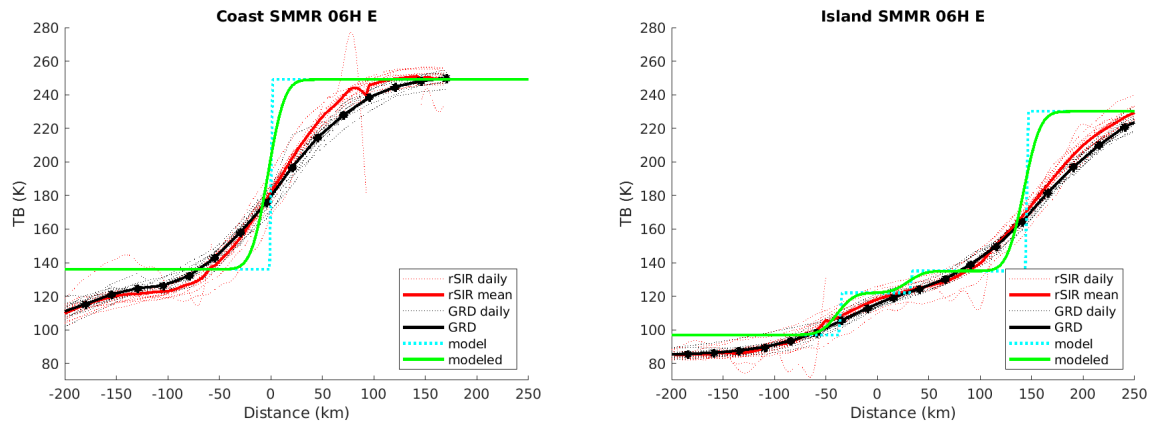


Figure 240: Plots of  $T_B$  along the two analysis case transect lines for the (left) coast-crossing and (right) island-crossing cases.

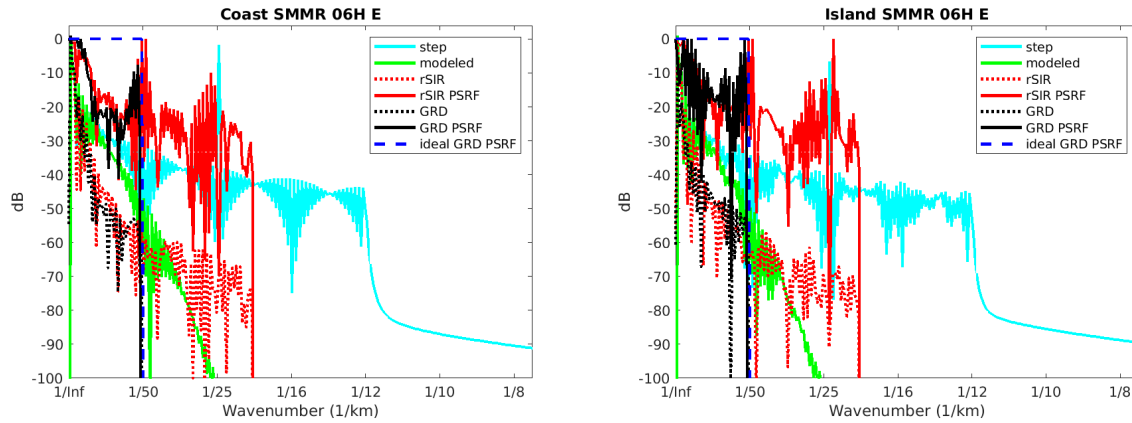


Figure 241: Wavenumber spectra of the  $T_B$  slices, the model, and the PSRF. (left) Coast-crossing case. (right) Island-crossing case.

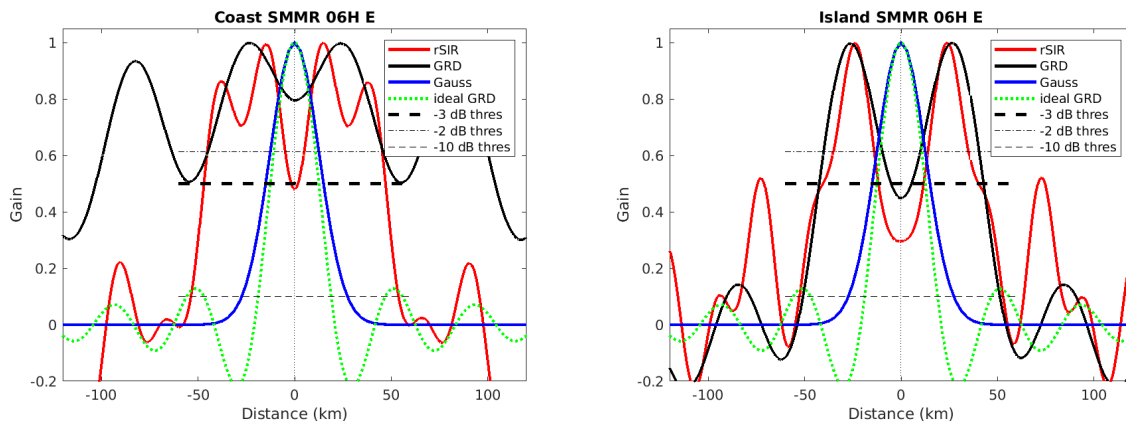


Figure 242: Derived single-pass rSIR and GRD PSRFs from the (left) coast-crossing and (right) island-crossing cases.

Table 104: Resolution estimates for SMMR channel 06H LTOD E

Algorithm	-3 dB Thres		-2 dB Thres		-10 dB Thres	
	Coast	Island	Coast	Island	Coast	Island
Gauss	30.0	30.0	24.4	24.4	54.8	54.8
rSIR	45.3	28.4	39.8	20.3	107.5	105.5
ideal GRD	36.2	36.2	30.3	30.3	54.5	54.5
GRD	206.7	32.1	89.2	26.7	324.6	49.9

## E.2 SMMR Channel 06H M Figures

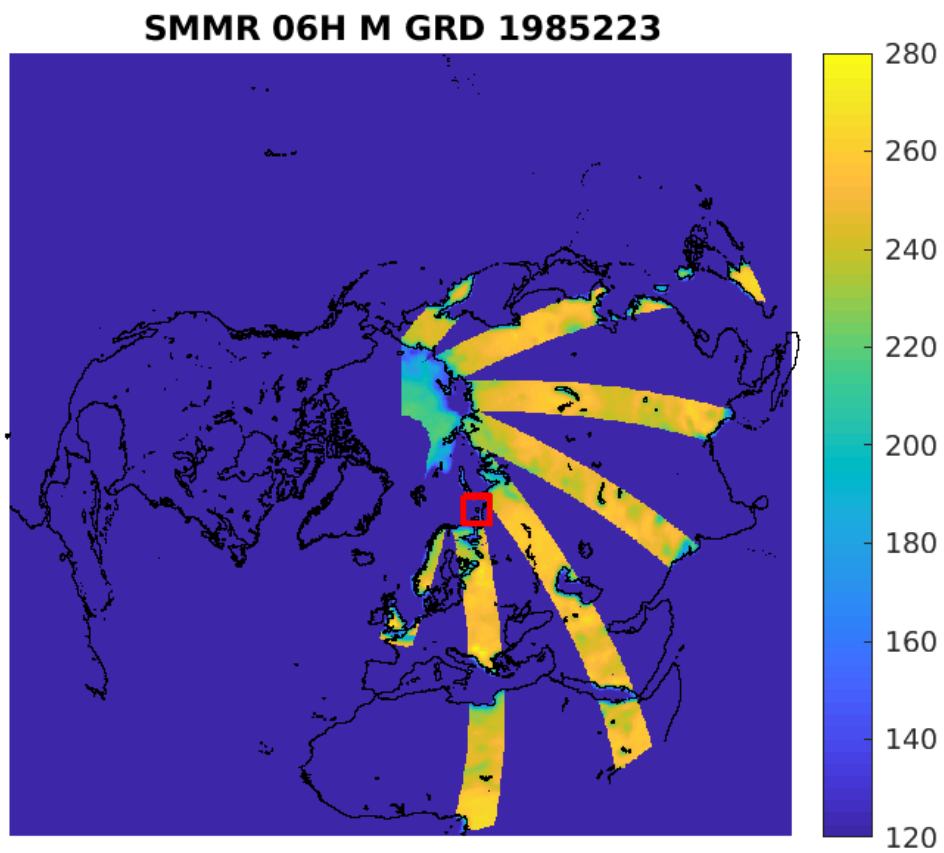


Figure 243: rSIR Northern Hemisphere view.



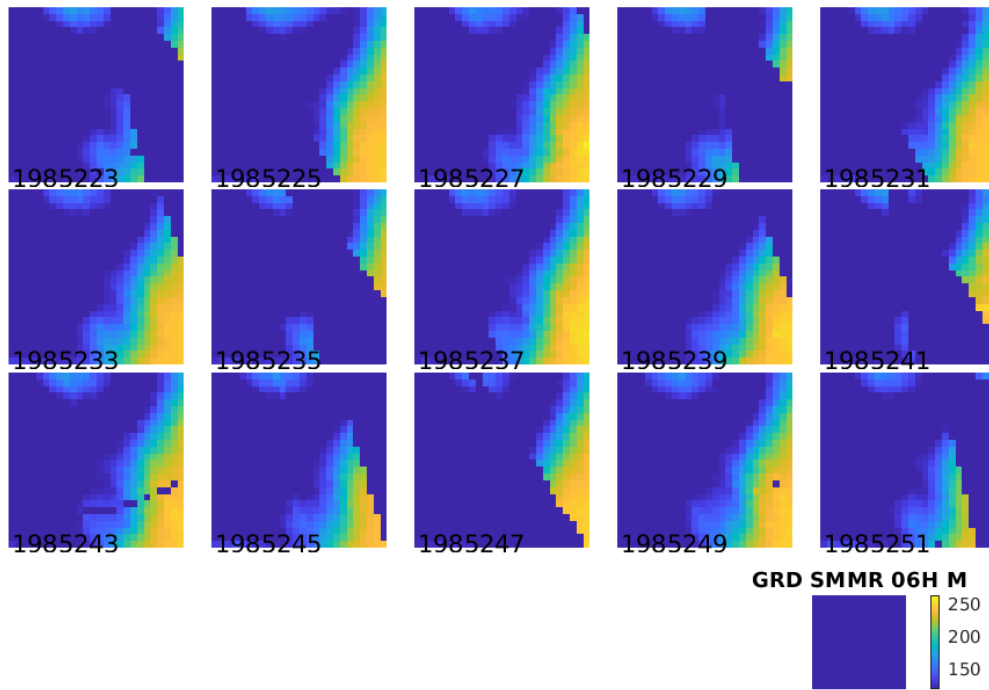
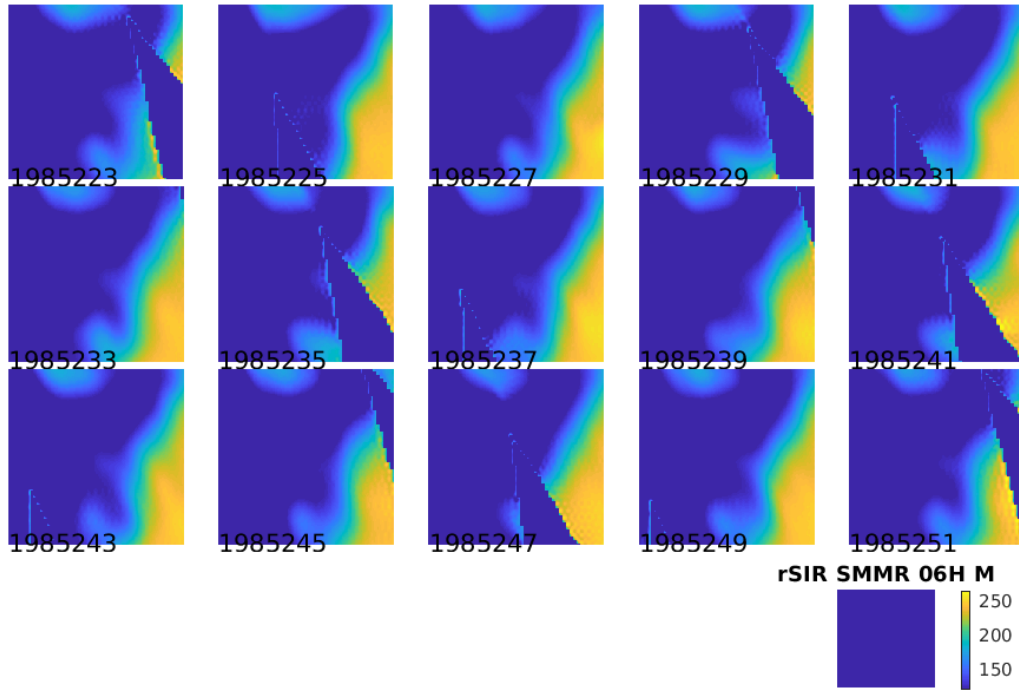


Figure 244: Time series of (top) rSIR and (bottom) GRD  $T_B$  images over the study area. Image dates are labeled on the image.

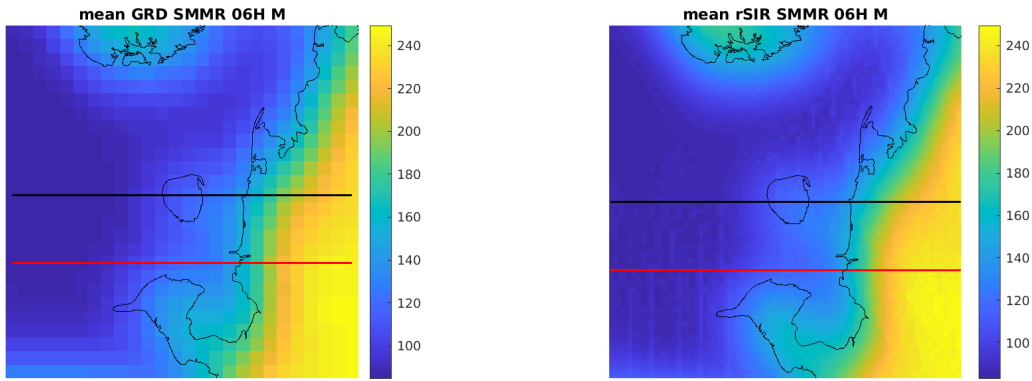


Figure 245: Average of daily  $T_B$  images over the study area. (left) 25-km GRD. (right) 3.125-km rSIR. The thick horizontal lines show the data transect locations where data is extracted from the image for analysis.

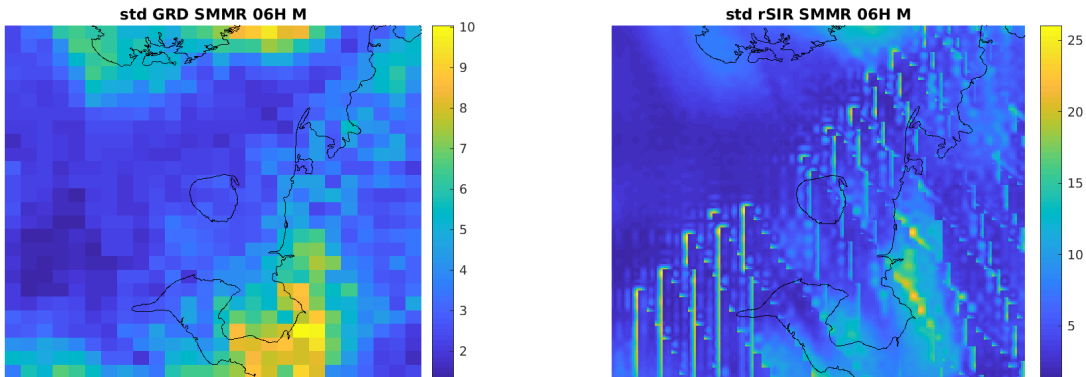


Figure 246: Standard deviation of daily  $T_B$  images over the study area. (left) 25-km GRD. (right) 3.125-km rSIR.

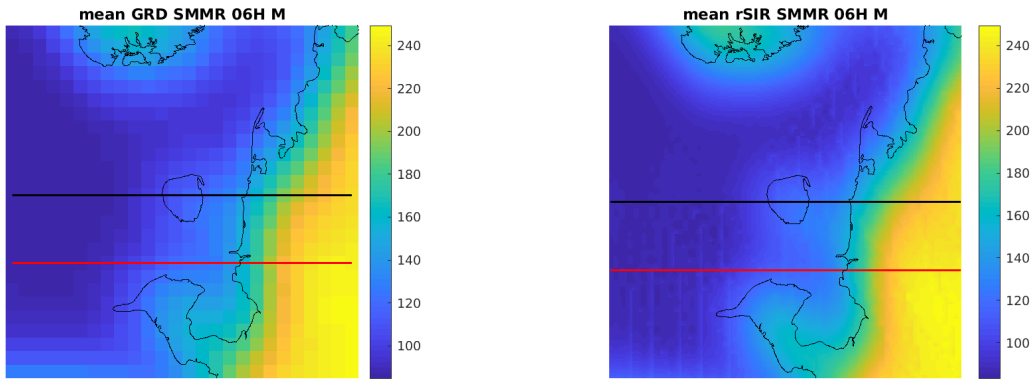


Figure 247: [Repeated] Average of daily  $T_B$  images over the study area. (left) 25-km GRD. (right) 3.125-km rSIR. The thick horizontal lines show the data transect locations where data is extracted from the image for analysis.

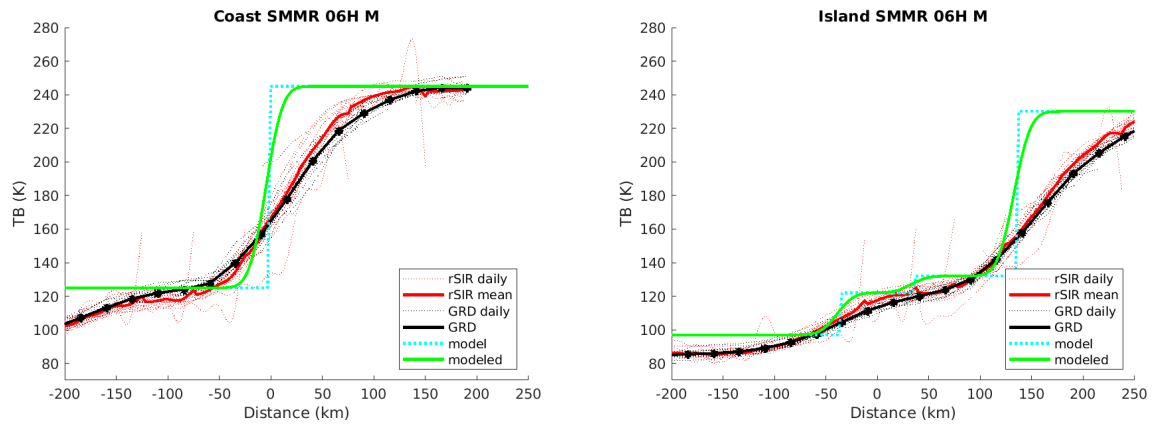


Figure 248: Plots of  $T_B$  along the two analysis case transect lines for the (left) coast-crossing and (right) island-crossing cases.

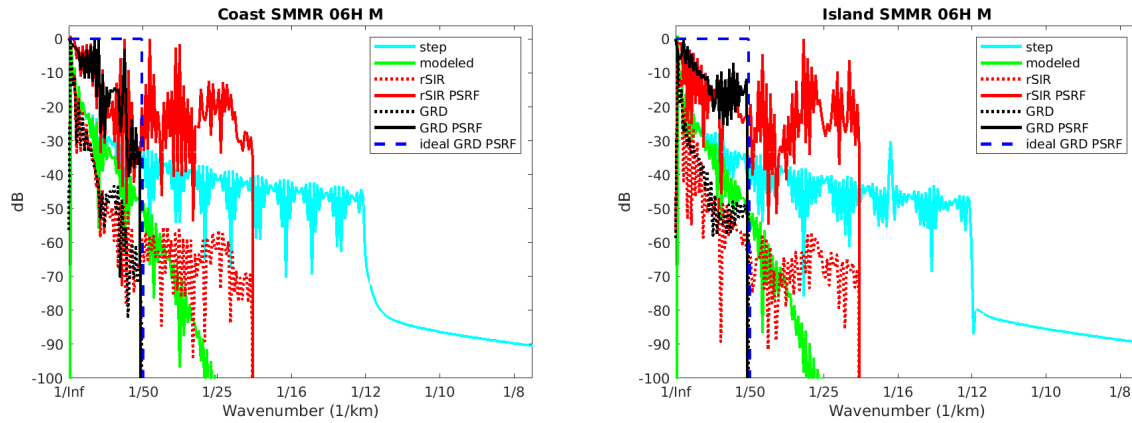


Figure 249: Wavenumber spectra of the  $T_B$  slices, the model, and the PSRF. (left) Coast-crossing case. (right) Island-crossing case.

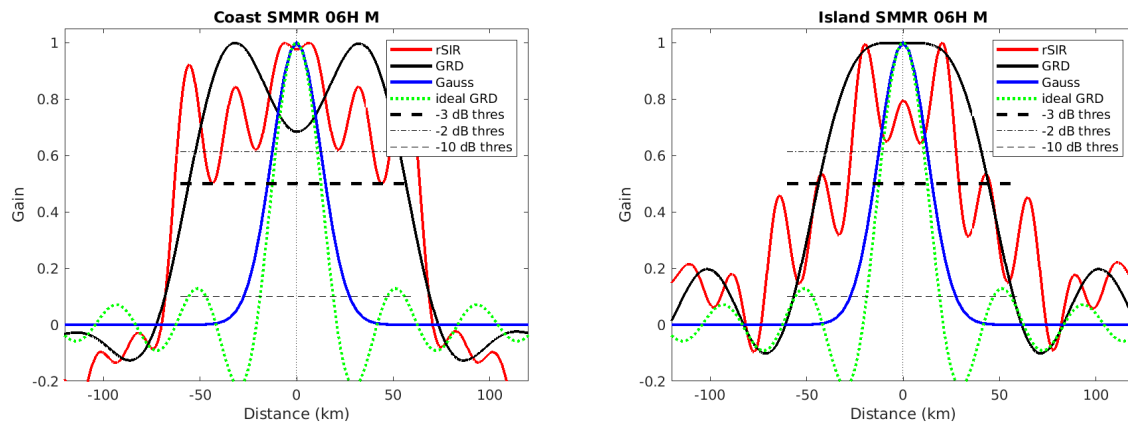


Figure 250: Derived single-pass rSIR and GRD PSRFs from the (left) coast-crossing and (right) island-crossing cases.

Table 105: Resolution estimates for SMMR channel 06H LTOD M

Algorithm	-3 dB Thres		-2 dB Thres		-10 dB Thres	
	Coast	Island	Coast	Island	Coast	Island
Gauss	30.0	30.0	24.4	24.4	54.8	54.8
rSIR	107.1	57.4	39.7	54.0	136.7	144.2
ideal GRD	36.2	36.2	30.3	30.3	54.5	54.5
GRD	112.3	88.1	104.6	79.5	137.2	113.8

### E.3 SMMR Channel 06V E Figures

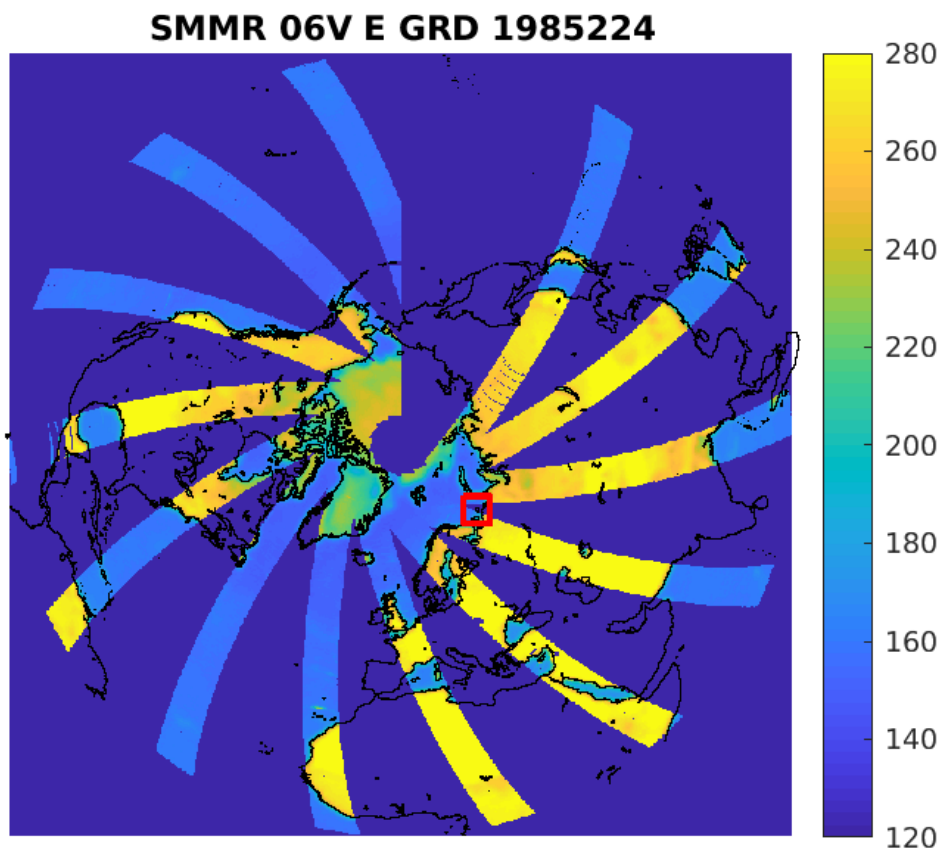


Figure 251: rSIR Northern Hemisphere view.

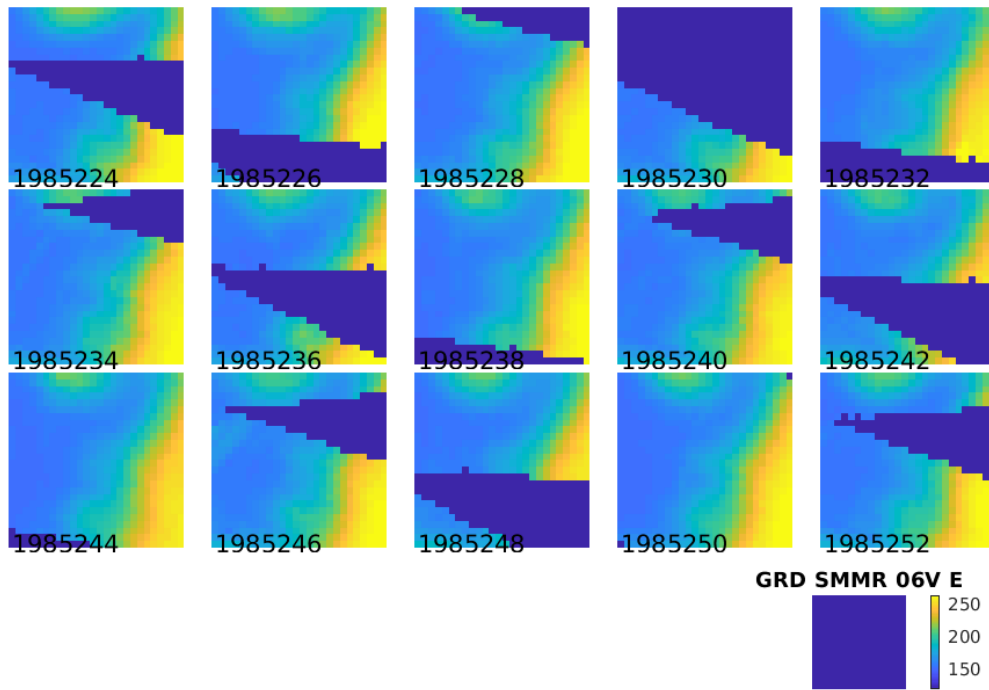
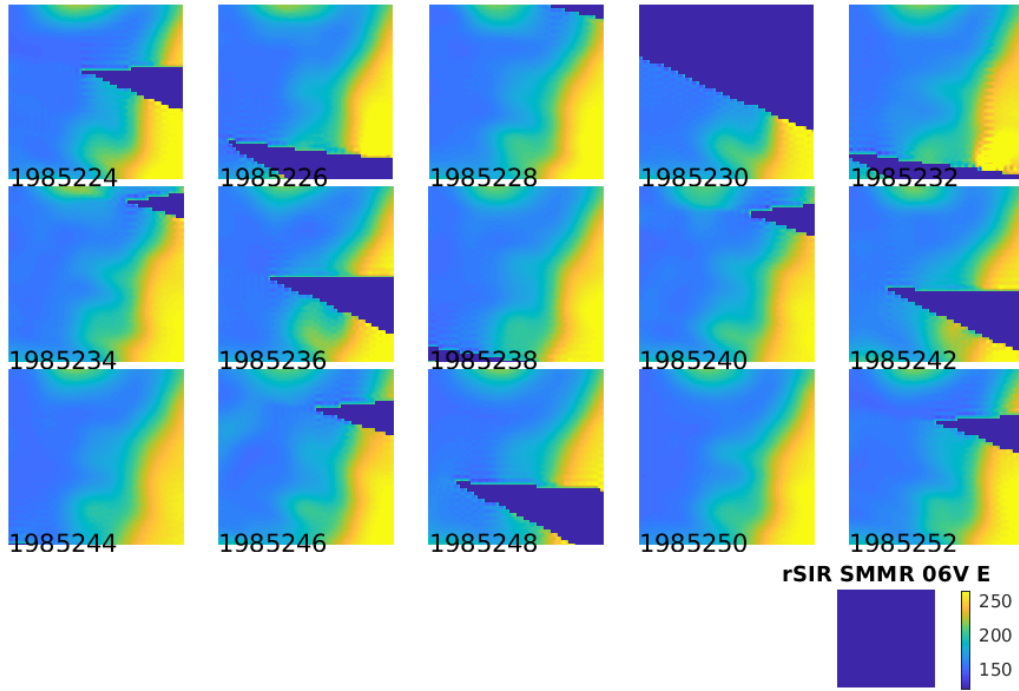


Figure 252: Time series of (top) rSIR and (bottom) GRD  $T_B$  images over the study area. Image dates are labeled on the image.

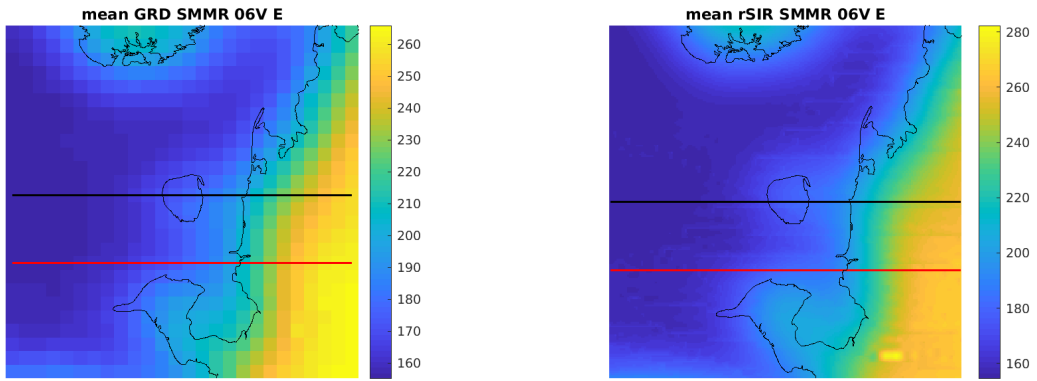


Figure 253: Average of daily  $T_B$  images over the study area. (left) 25-km GRD. (right) 3.125-km rSIR. The thick horizontal lines show the data transect locations where data is extracted from the image for analysis.

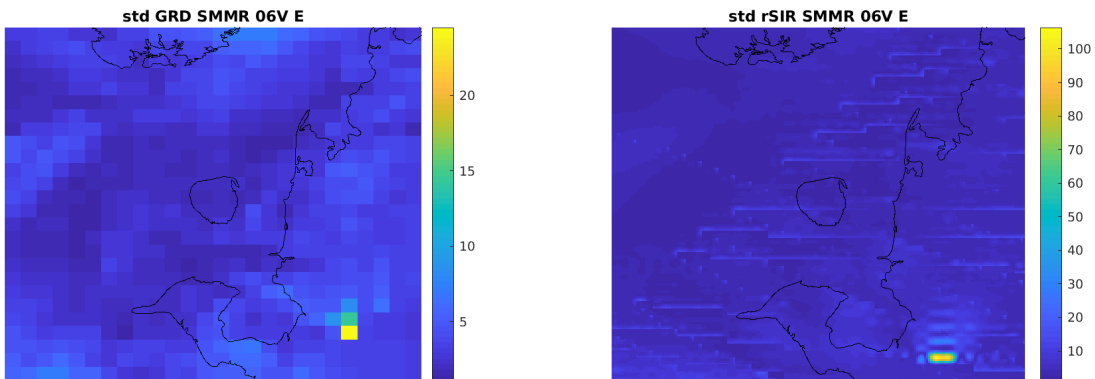


Figure 254: Standard deviation of daily  $T_B$  images over the study area. (left) 25-km GRD. (right) 3.125-km rSIR.

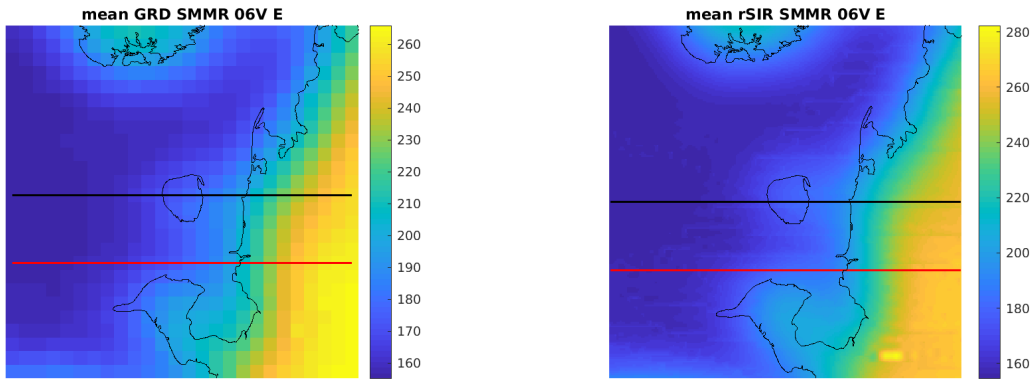


Figure 255: [Repeated] Average of daily  $T_B$  images over the study area. (left) 25-km GRD. (right) 3.125-km rSIR. The thick horizontal lines show the data transect locations where data is extracted from the image for analysis.

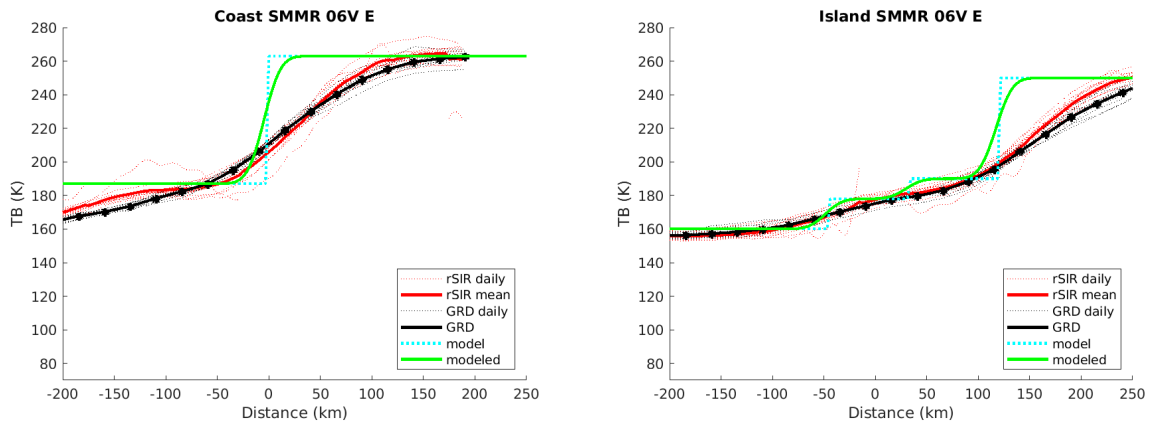


Figure 256: Plots of  $T_B$  along the two analysis case transect lines for the (left) coast-crossing and (right) island-crossing cases.



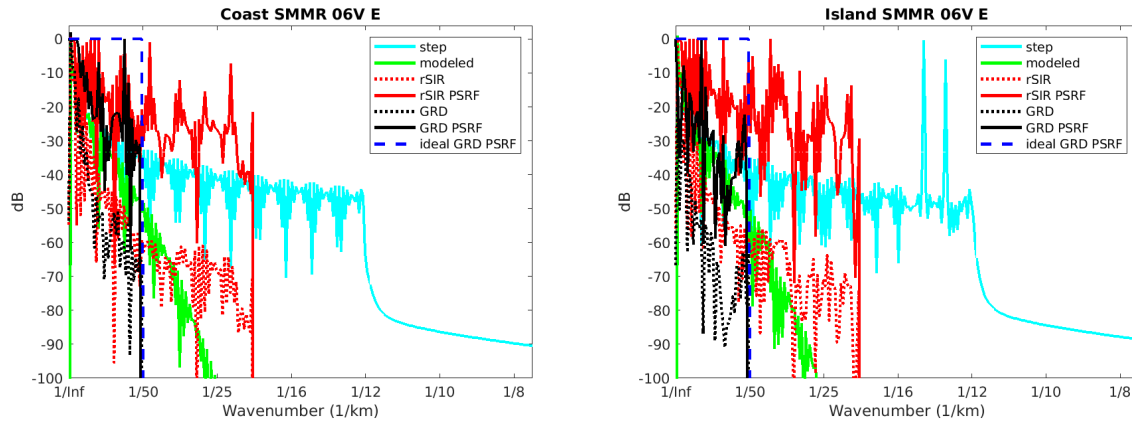


Figure 257: Wavenumber spectra of the  $T_B$  slices, the model, and the PSRF. (left) Coast-crossing case. (right) Island-crossing case.

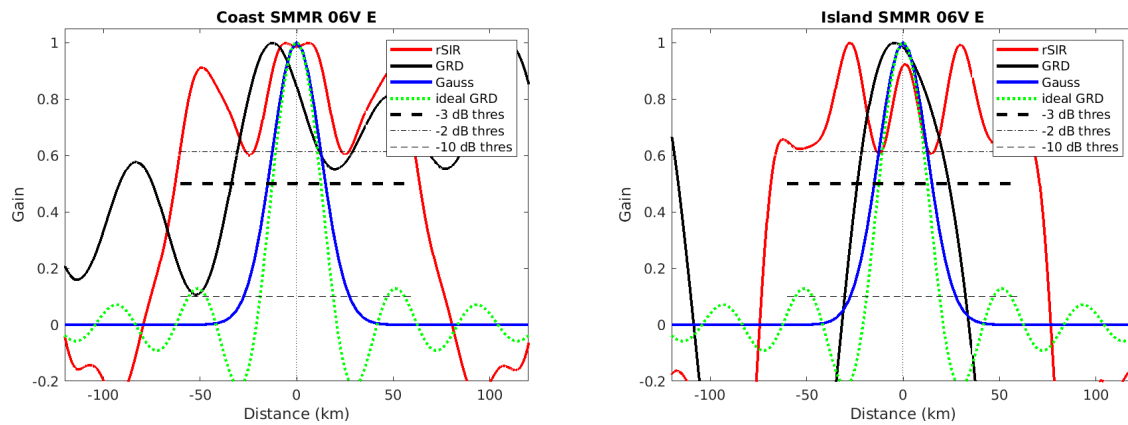


Figure 258: Derived single-pass rSIR and GRD PSRFs from the (left) coast-crossing and (right) island-crossing cases.

Table 106: Resolution estimates for SMMR channel 06V LTOD E

Algorithm	-3 dB Thres		-2 dB Thres		-10 dB Thres	
	Coast	Island	Coast	Island	Coast	Island
Gauss	30.0	30.0	24.4	24.4	54.8	54.8
rSIR	126.5	139.4	43.1	33.9	152.1	149.0
ideal GRD	36.2	36.2	30.3	30.3	54.5	54.5
GRD	164.7	47.4	40.8	40.8	446.1	62.7

## E.4 SMMR Channel 06V M Figures

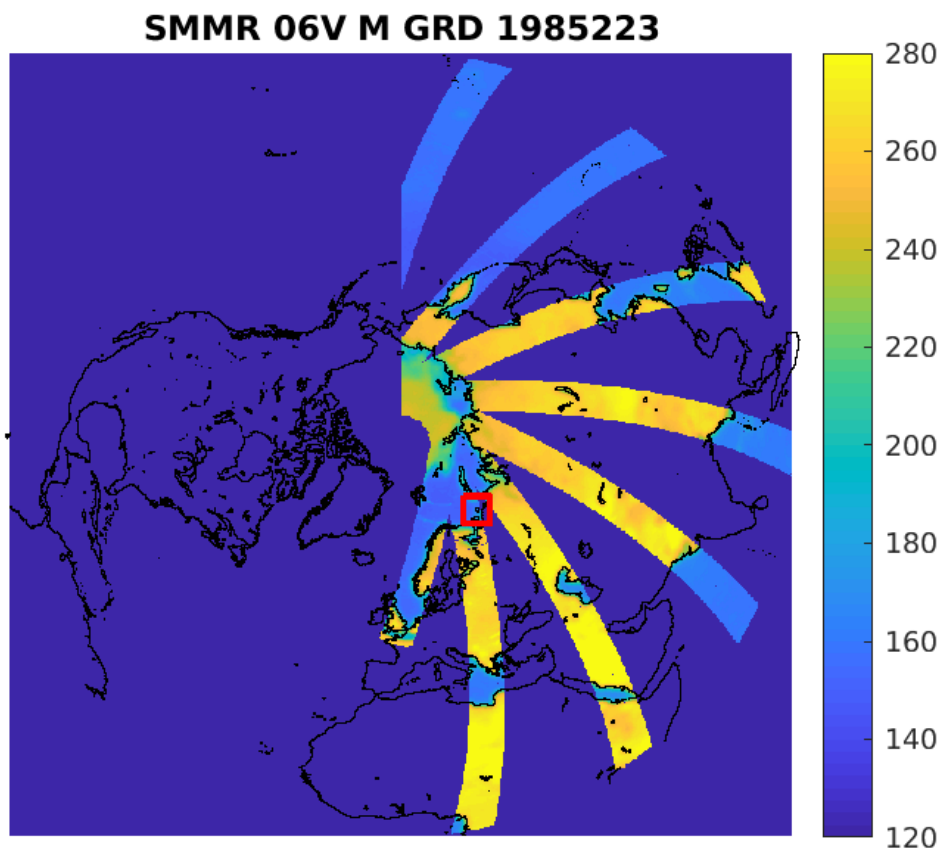


Figure 259: rSIR Northern Hemisphere view.

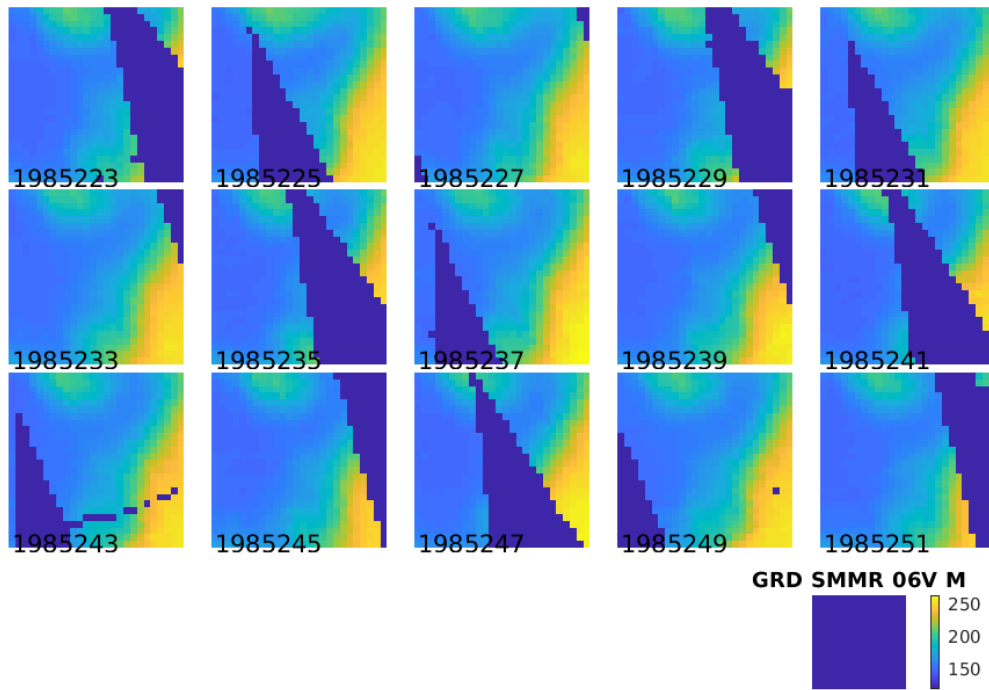
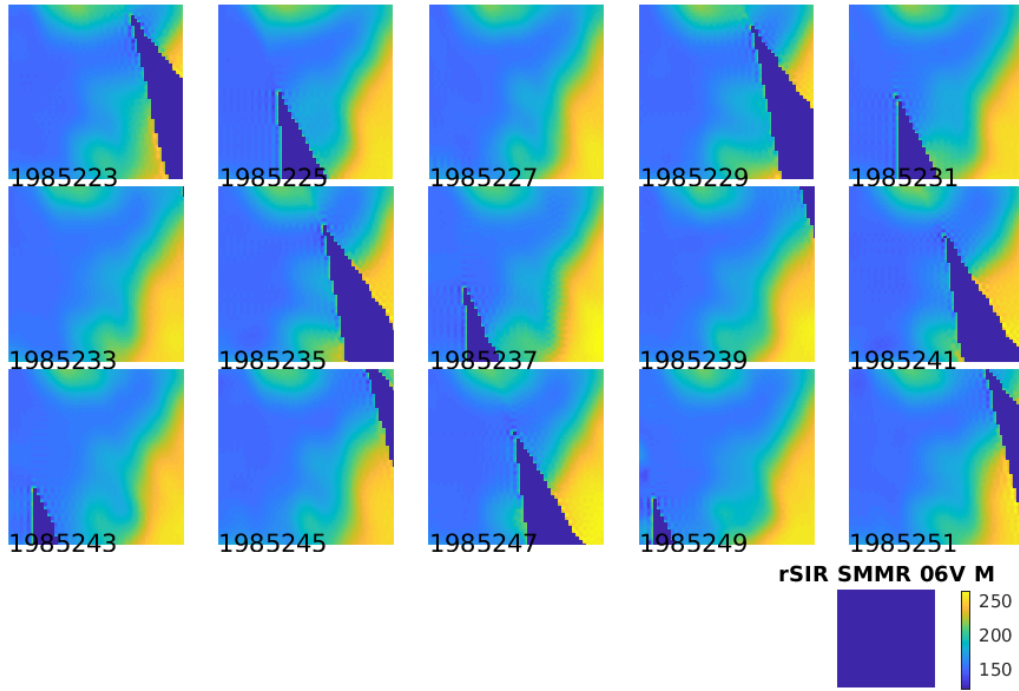


Figure 260: Time series of (top) rSIR and (bottom) GRD  $T_B$  images over the study area. Image dates are labeled on the image.

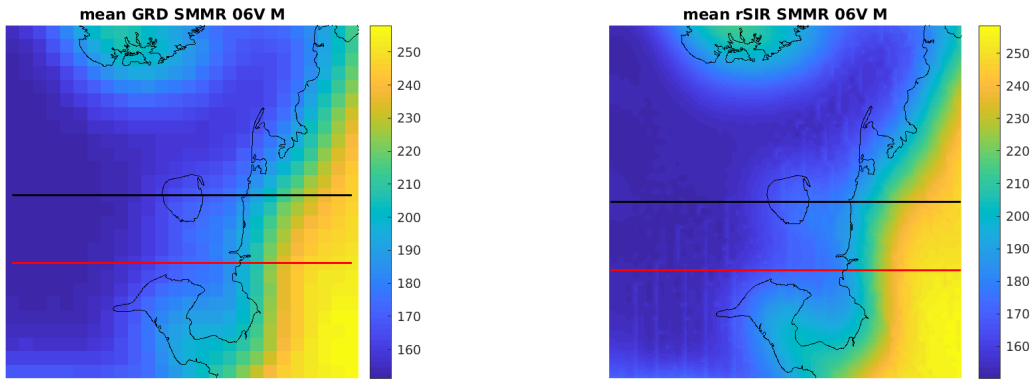


Figure 261: Average of daily  $T_B$  images over the study area. (left) 25-km GRD. (right) 3.125-km rSIR. The thick horizontal lines show the data transect locations where data is extracted from the image for analysis.

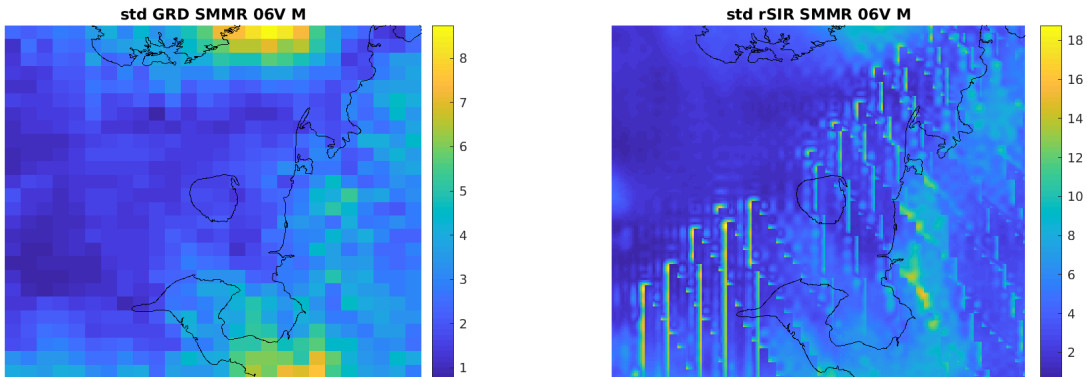


Figure 262: Standard deviation of daily  $T_B$  images over the study area. (left) 25-km GRD. (right) 3.125-km rSIR.

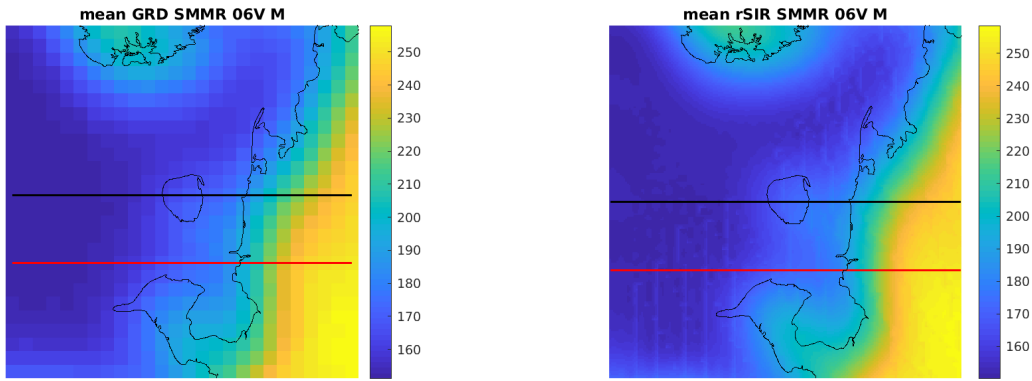


Figure 263: [Repeated] Average of daily  $T_B$  images over the study area. (left) 25-km GRD. (right) 3.125-km rSIR. The thick horizontal lines show the data transect locations where data is extracted from the image for analysis.

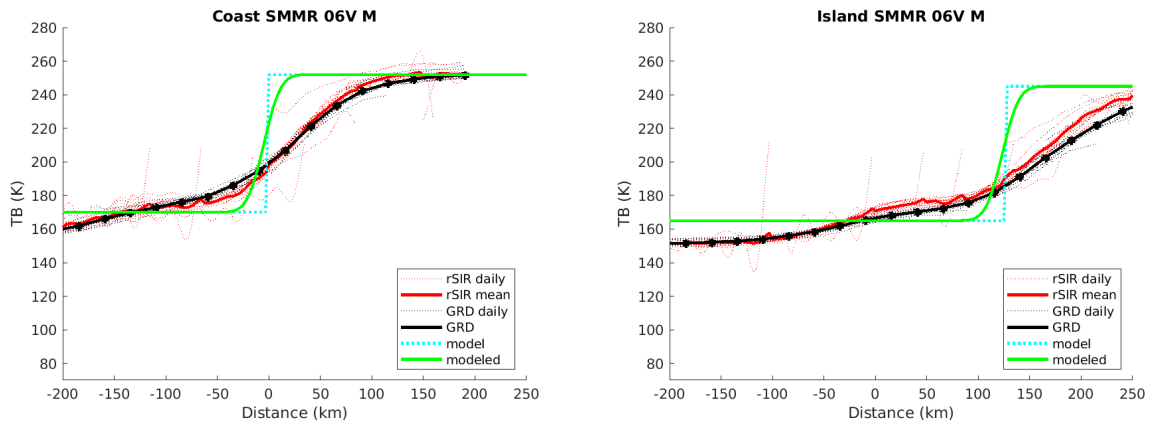


Figure 264: Plots of  $T_B$  along the two analysis case transect lines for the (left) coast-crossing and (right) island-crossing cases.

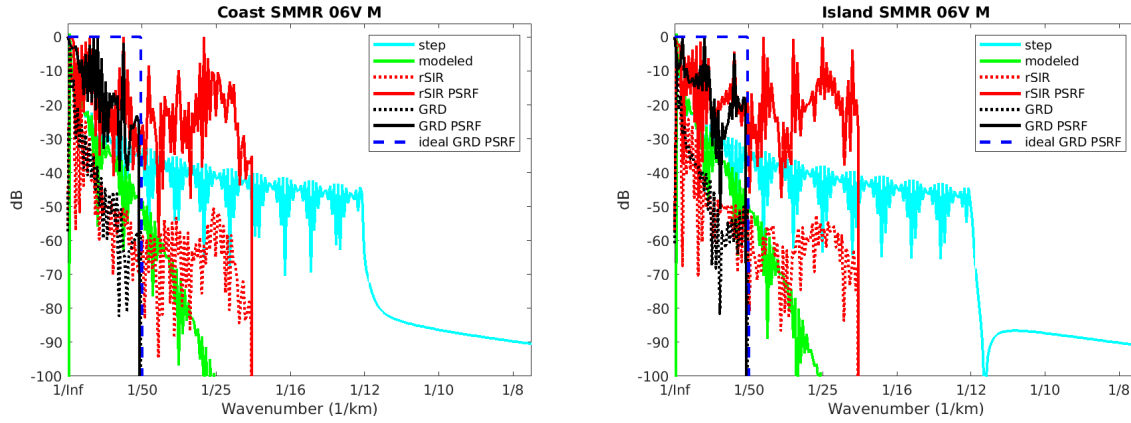


Figure 265: Wavenumber spectra of the  $T_B$  slices, the model, and the PSRF. (left) Coast-crossing case. (right) Island-crossing case.

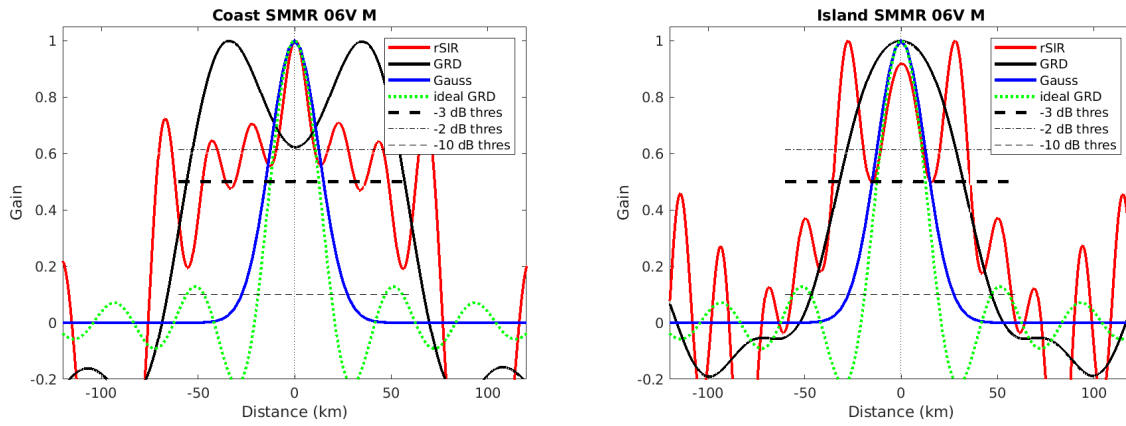


Figure 266: Derived single-pass rSIR and GRD PSRFs from the (left) coast-crossing and (right) island-crossing cases.

Table 107: Resolution estimates for SMMR channel 06V LTOD M

Algorithm	-3 dB Thres		-2 dB Thres		-10 dB Thres	
	Coast	Island	Coast	Island	Coast	Island
Gauss	30.0	30.0	24.4	24.4	54.8	54.8
rSIR	62.3	19.4	18.8	14.1	150.8	113.6
ideal GRD	36.2	36.2	30.3	30.3	54.5	54.5
GRD	112.7	64.3	49.8	55.2	132.7	93.4

## E.5 SMMR Channel 10H E Figures

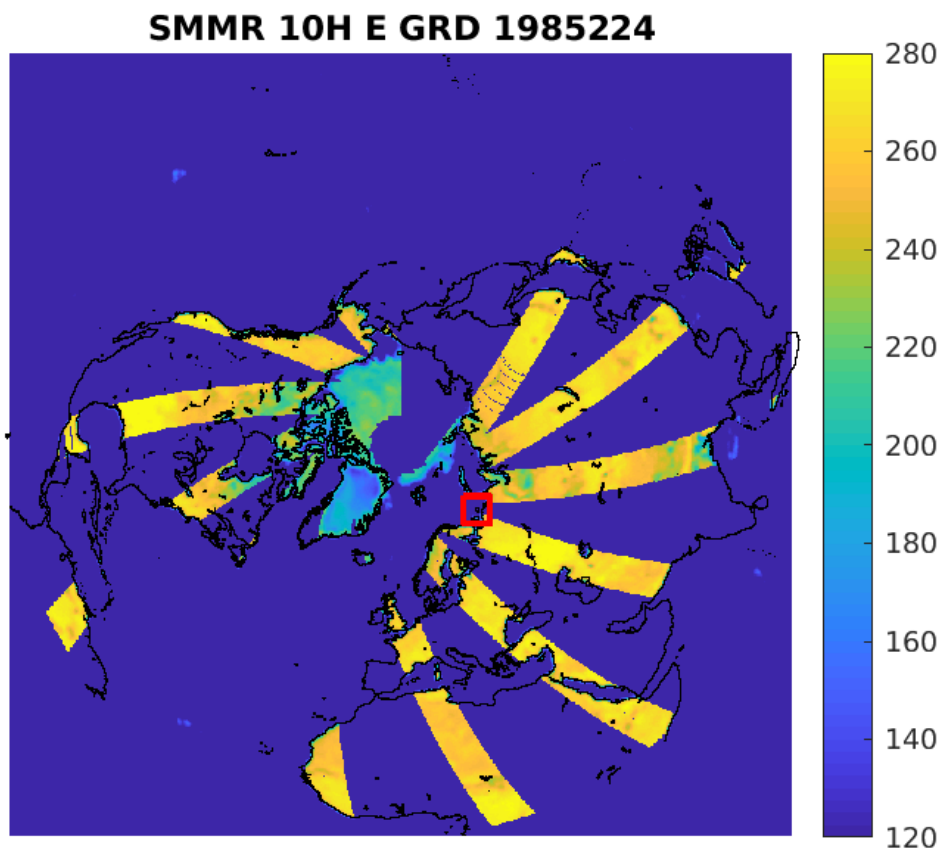


Figure 267: rSIR Northern Hemisphere view.

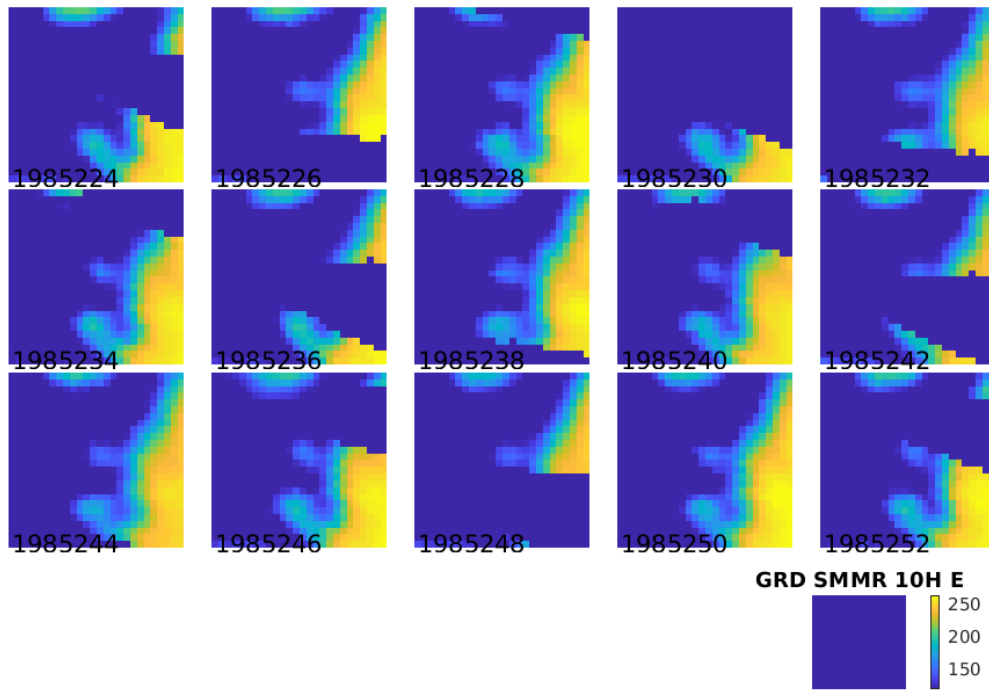
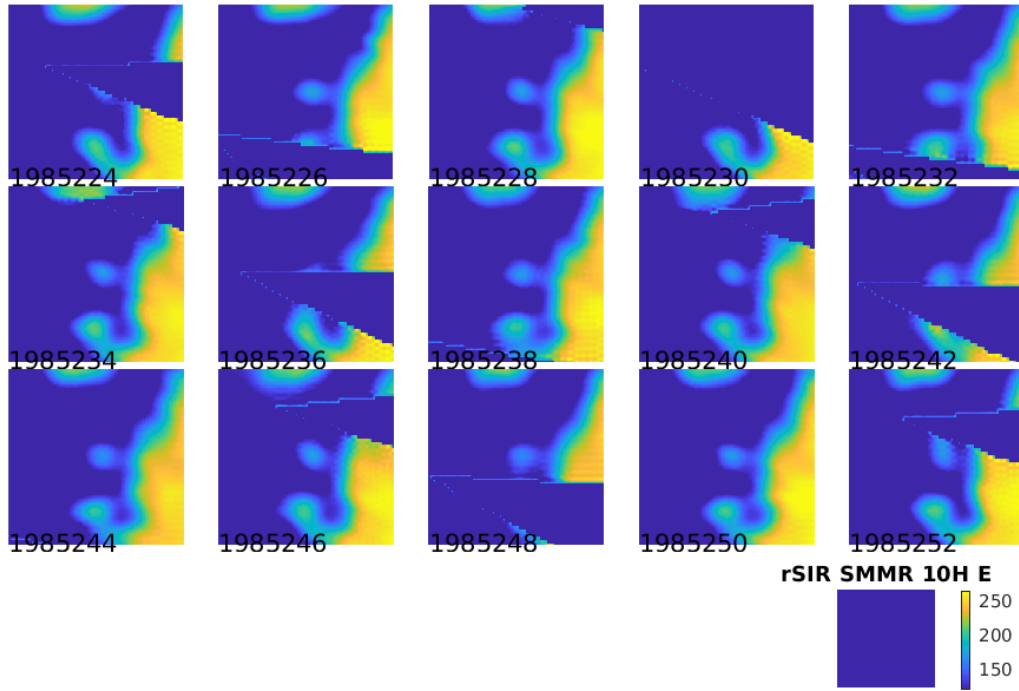


Figure 268: Time series of (top) rSIR and (bottom) GRD  $T_B$  images over the study area. Image dates are labeled on the image.



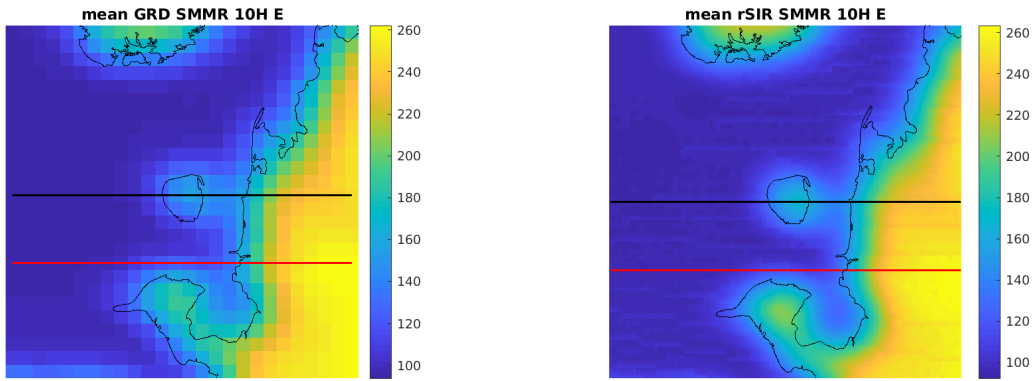


Figure 269: Average of daily  $T_B$  images over the study area. (left) 25-km GRD. (right) 3.125-km rSIR. The thick horizontal lines show the data transect locations where data is extracted from the image for analysis.

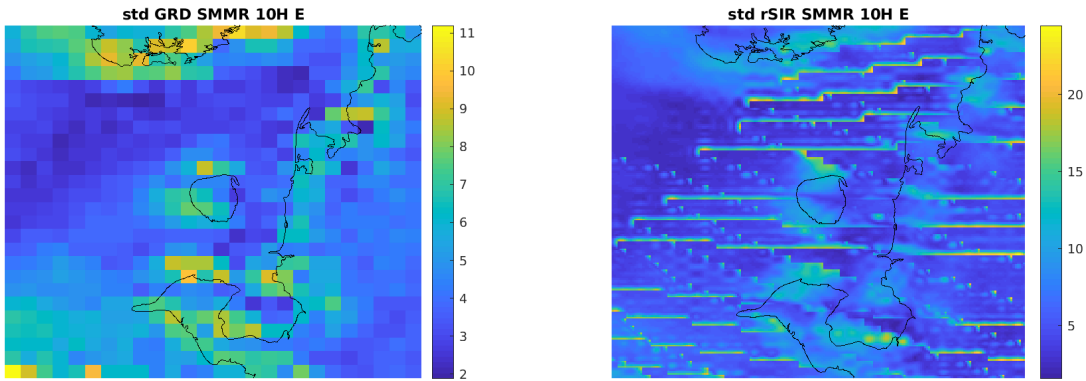


Figure 270: Standard deviation of daily  $T_B$  images over the study area. (left) 25-km GRD. (right) 3.125-km rSIR.

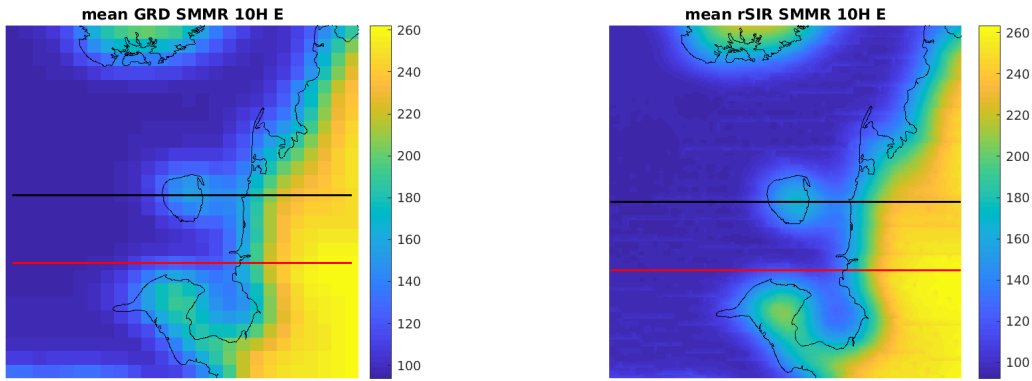


Figure 271: [Repeated] Average of daily  $T_B$  images over the study area. (left) 25-km GRD. (right) 3.125-km rSIR. The thick horizontal lines show the data transect locations where data is extracted from the image for analysis.

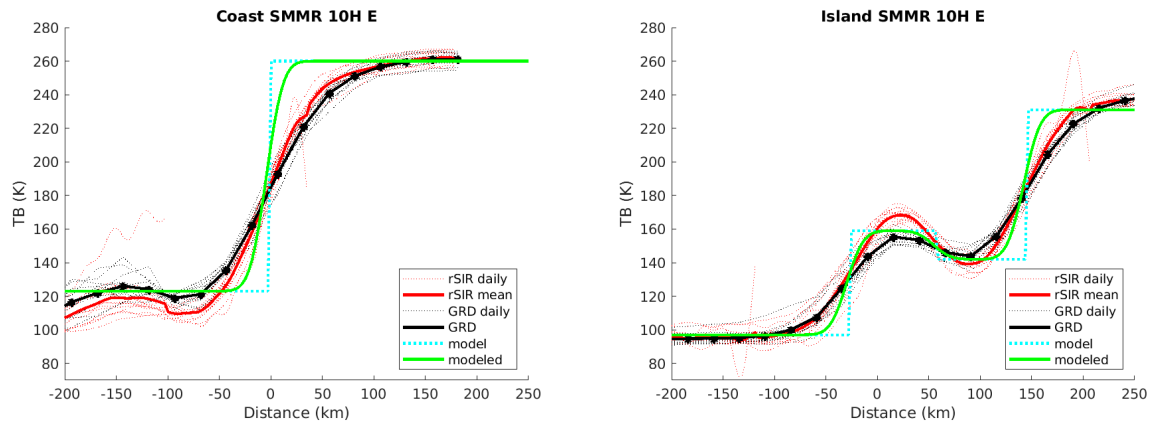


Figure 272: Plots of  $T_B$  along the two analysis case transect lines for the (left) coast-crossing and (right) island-crossing cases.

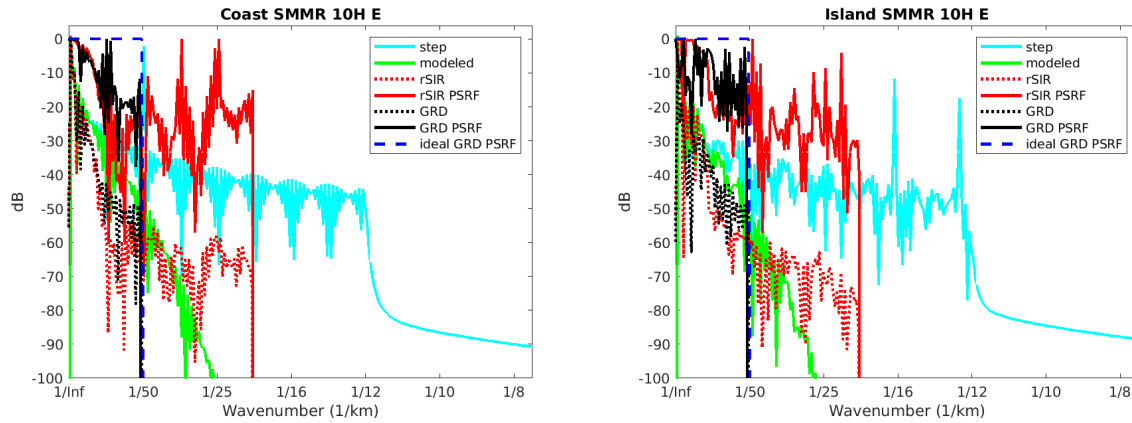


Figure 273: Wavenumber spectra of the  $T_B$  slices, the model, and the PSRF. (left) Coast-crossing case. (right) Island-crossing case.

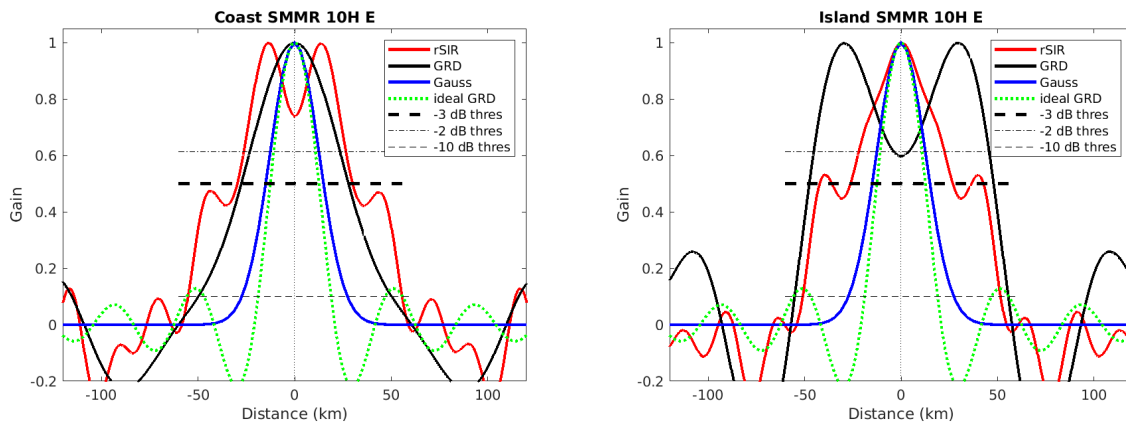


Figure 274: Derived single-pass rSIR and GRD PSRFs from the (left) coast-crossing and (right) island-crossing cases.

Table 108: Resolution estimates for SMMR channel 10H LTOD E

Algorithm	-3 dB Thres		-2 dB Thres		-10 dB Thres	
	Coast	Island	Coast	Island	Coast	Island
Gauss	30.0	30.0	24.4	24.4	54.8	54.8
rSIR	59.7	53.0	52.0	43.1	110.8	102.6
ideal GRD	36.2	36.2	30.3	30.3	54.5	54.5
GRD	55.5	35.4	45.3	30.1	100.1	50.0

## E.6 SMMR Channel 10H M Figures

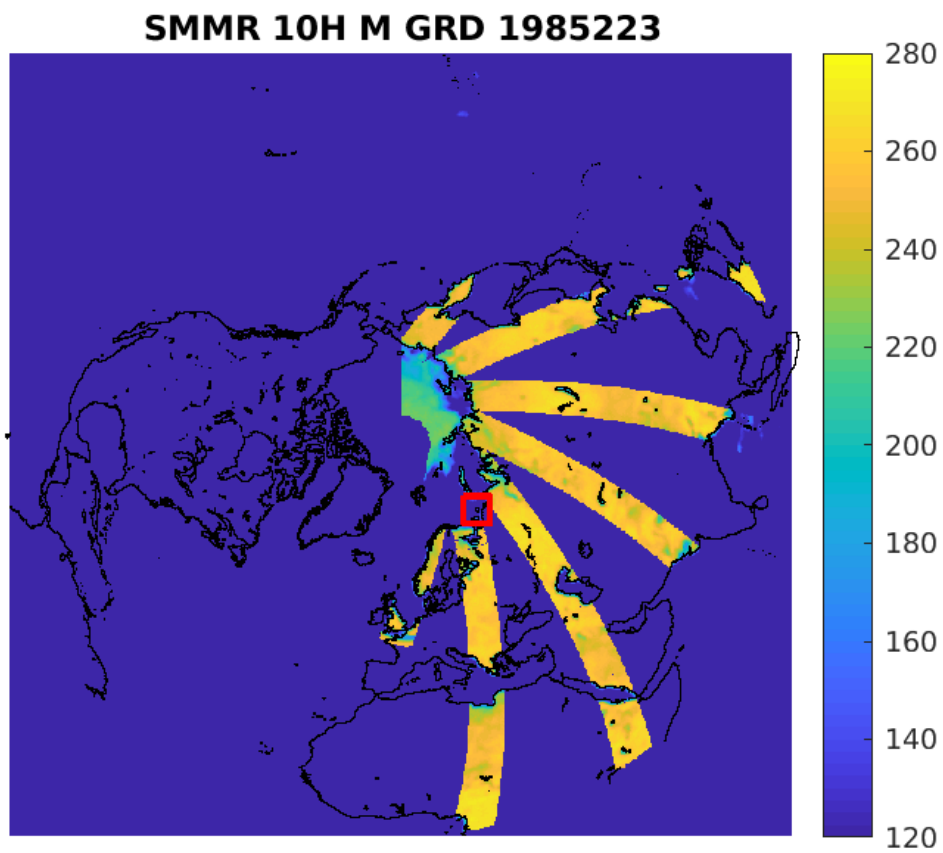


Figure 275: rSIR Northern Hemisphere view.

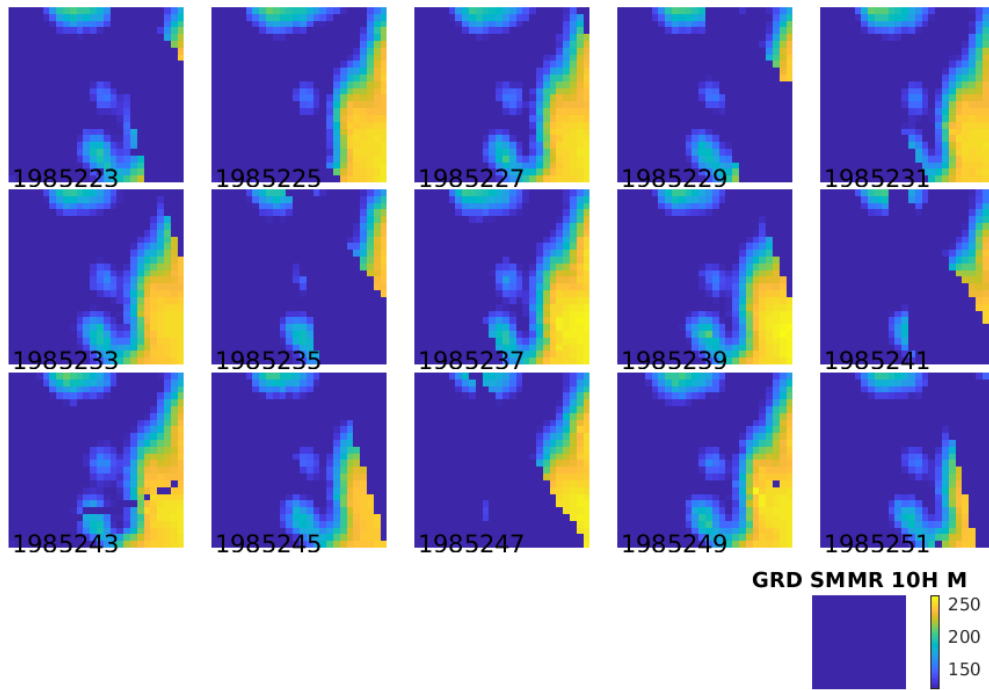
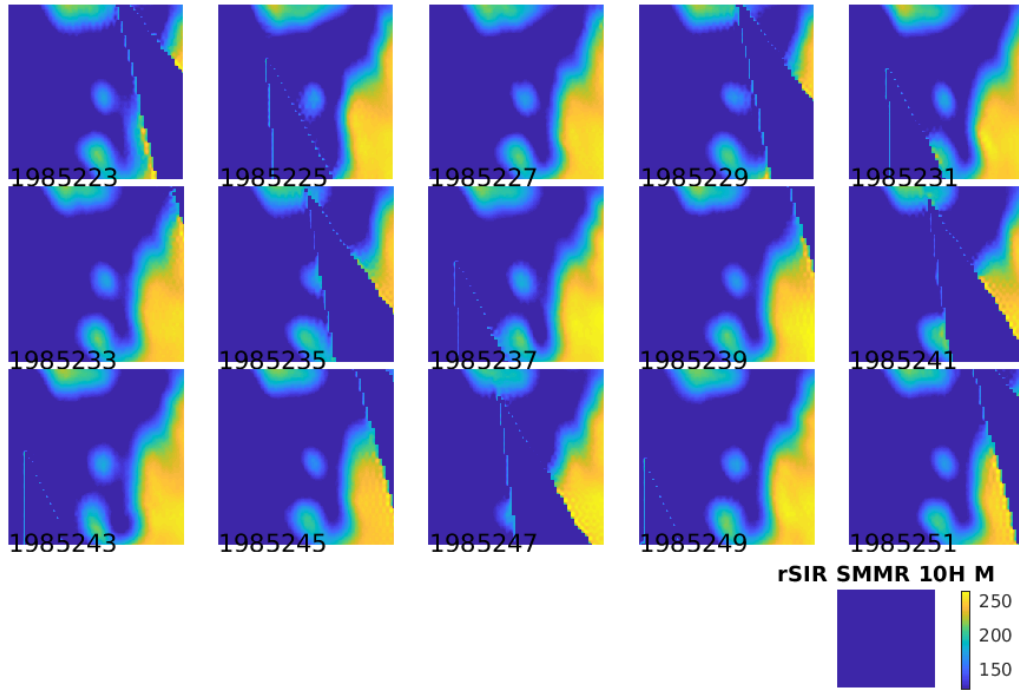


Figure 276: Time series of (top) rSIR and (bottom) GRD  $T_B$  images over the study area. Image dates are labeled on the image.

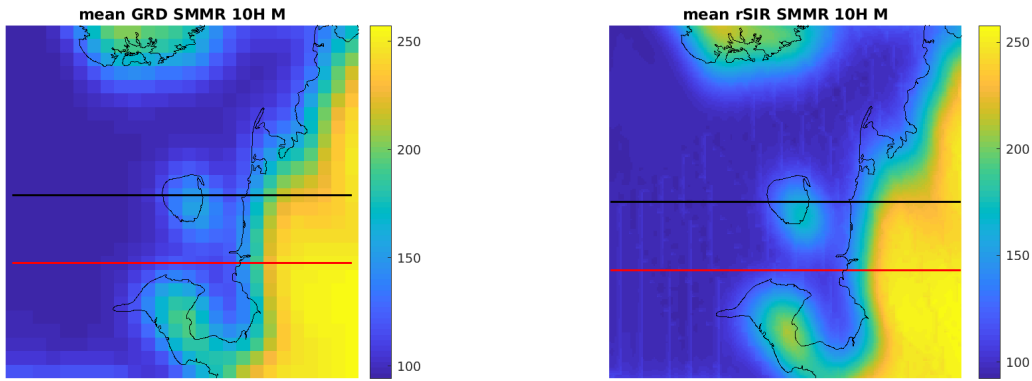


Figure 277: Average of daily  $T_B$  images over the study area. (left) 25-km GRD. (right) 3.125-km rSIR. The thick horizontal lines show the data transect locations where data is extracted from the image for analysis.

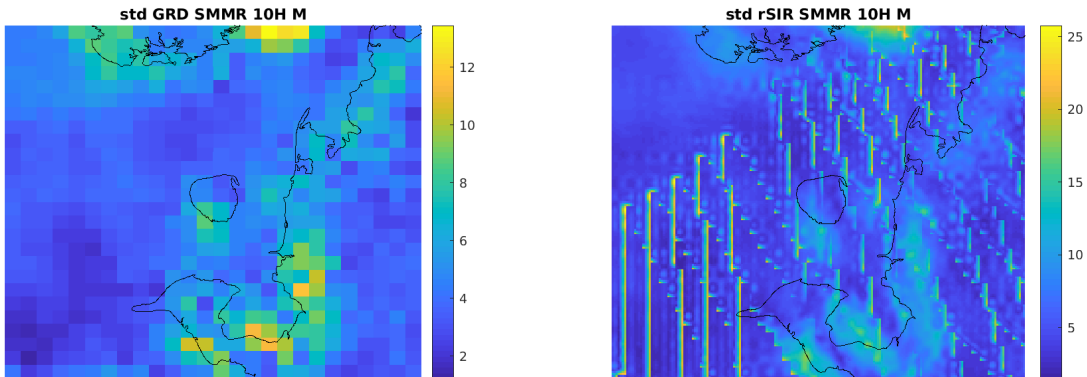


Figure 278: Standard deviation of daily  $T_B$  images over the study area. (left) 25-km GRD. (right) 3.125-km rSIR.

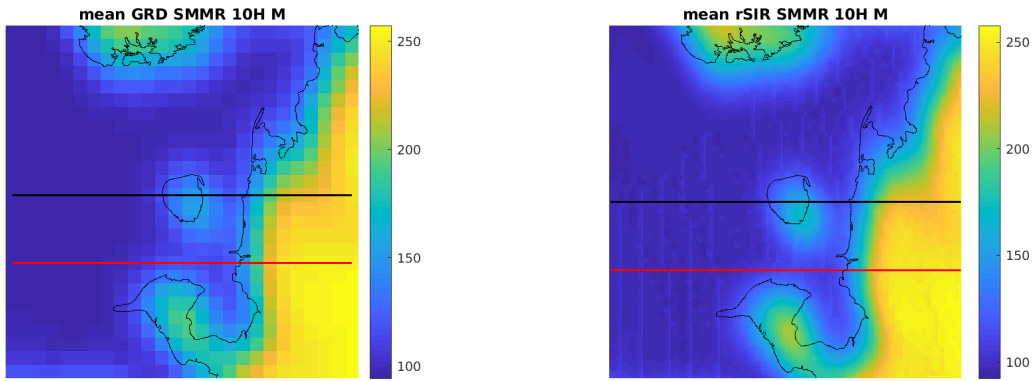


Figure 279: [Repeated] Average of daily  $T_B$  images over the study area. (left) 25-km GRD. (right) 3.125-km rSIR. The thick horizontal lines show the data transect locations where data is extracted from the image for analysis.

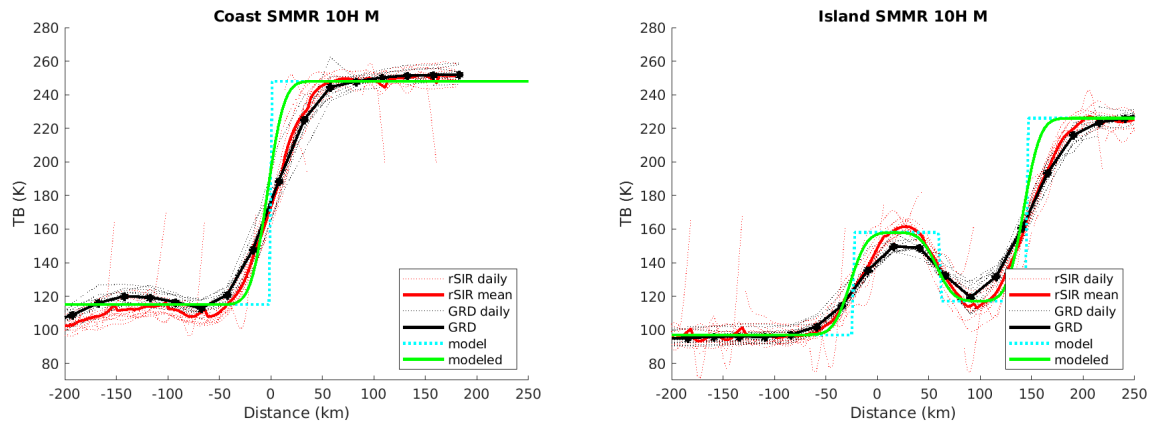


Figure 280: Plots of  $T_B$  along the two analysis case transect lines for the (left) coast-crossing and (right) island-crossing cases.

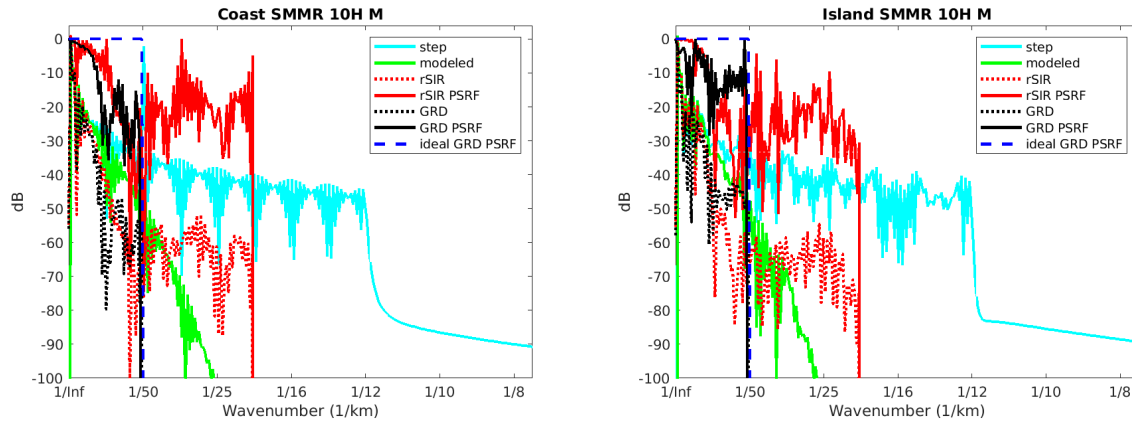


Figure 281: Wavenumber spectra of the  $T_B$  slices, the model, and the PSRF. (left) Coast-crossing case. (right) Island-crossing case.

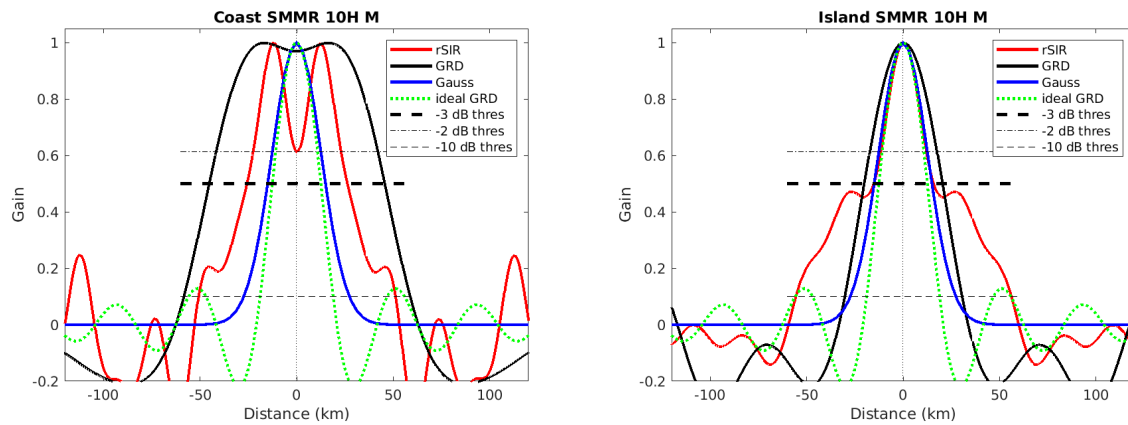


Figure 282: Derived single-pass rSIR and GRD PSRFs from the (left) coast-crossing and (right) island-crossing cases.

Table 109: Resolution estimates for SMMR channel 10H LTOD M

Algorithm	-3 dB Thres		-2 dB Thres		-10 dB Thres	
	Coast	Island	Coast	Island	Coast	Island
Gauss	30.0	30.0	24.4	24.4	54.8	54.8
rSIR	51.9	31.2	20.7	22.9	102.0	111.6
ideal GRD	36.2	36.2	30.3	30.3	54.5	54.5
GRD	90.9	40.6	82.5	34.0	117.1	60.9



## E.7 SMMR Channel 10V E Figures

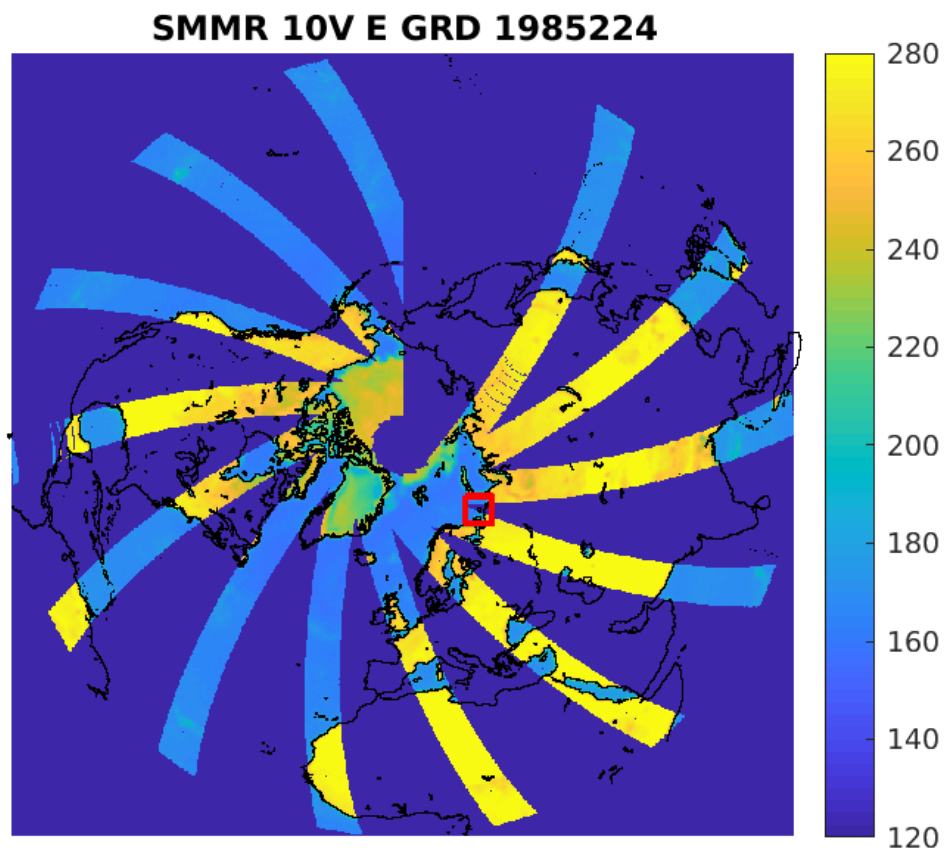


Figure 283: rSIR Northern Hemisphere view.

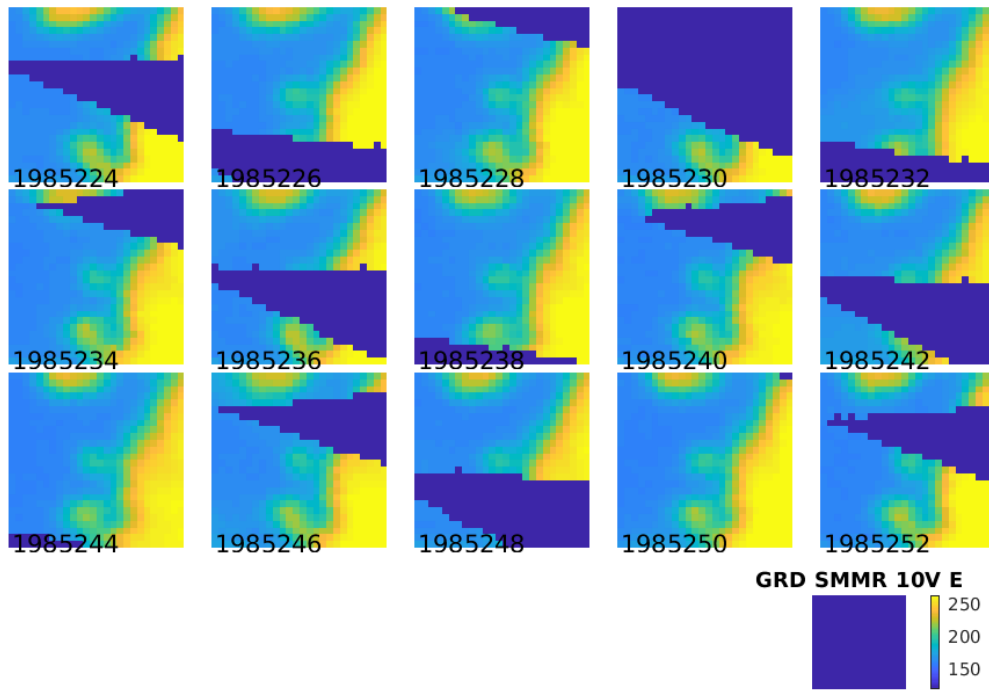
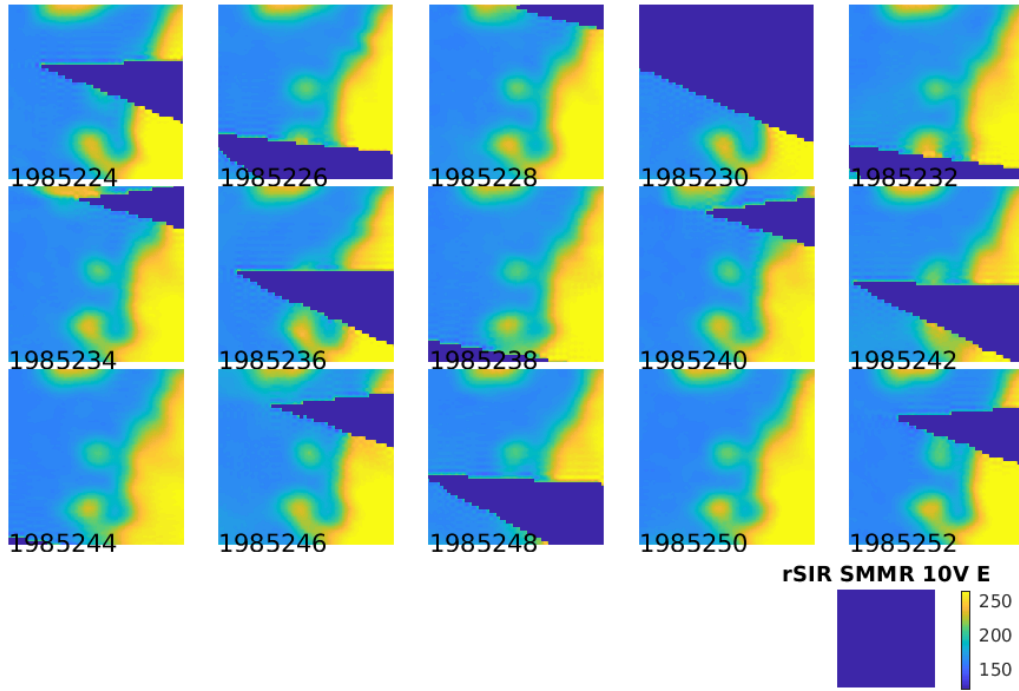


Figure 284: Time series of (top) rSIR and (bottom) GRD  $T_B$  images over the study area. Image dates are labeled on the image.

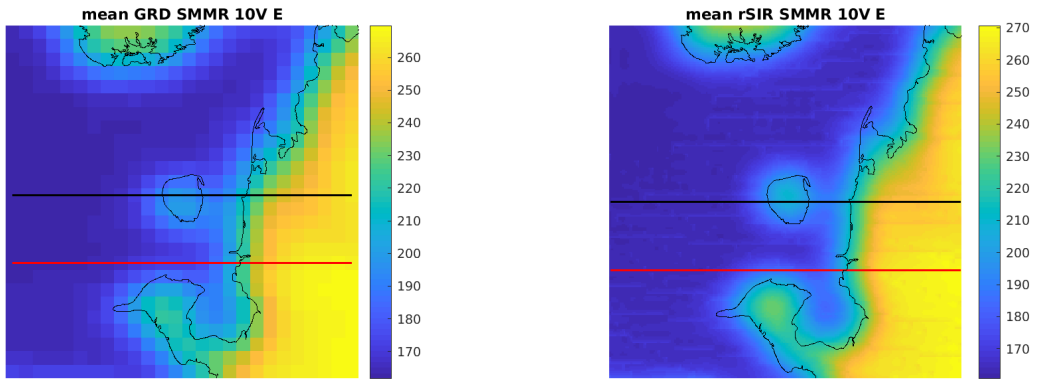


Figure 285: Average of daily  $T_B$  images over the study area. (left) 25-km GRD. (right) 3.125-km rSIR. The thick horizontal lines show the data transect locations where data is extracted from the image for analysis.

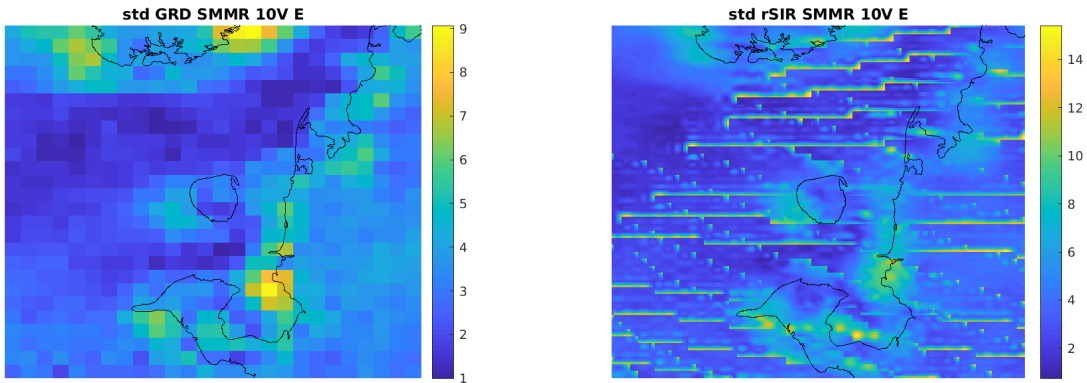


Figure 286: Standard deviation of daily  $T_B$  images over the study area. (left) 25-km GRD. (right) 3.125-km rSIR.

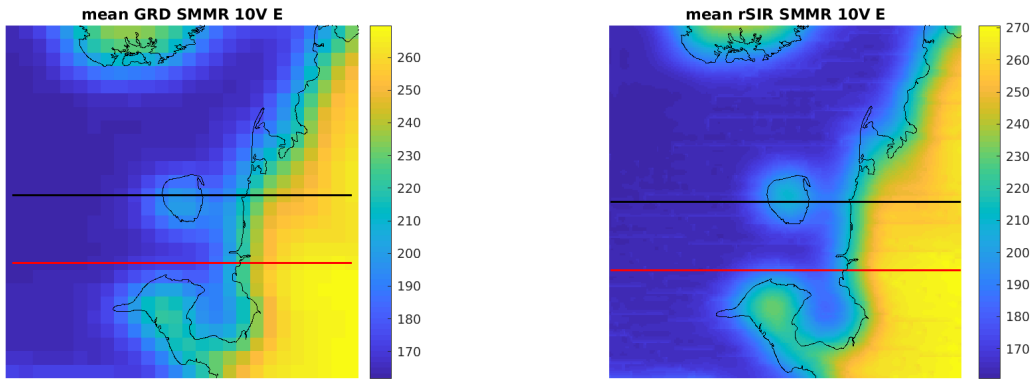


Figure 287: [Repeated] Average of daily  $T_B$  images over the study area. (left) 25-km GRD. (right) 3.125-km rSIR. The thick horizontal lines show the data transect locations where data is extracted from the image for analysis.

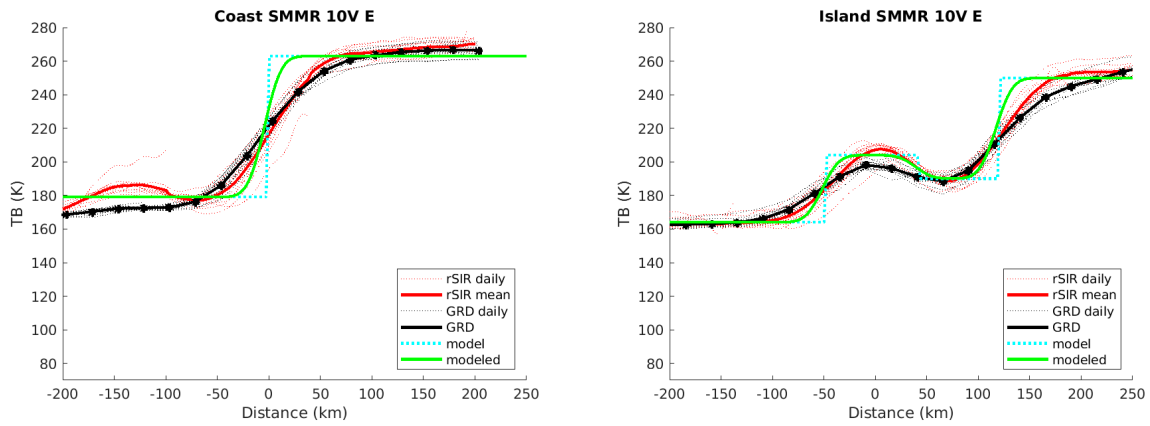


Figure 288: Plots of  $T_B$  along the two analysis case transect lines for the (left) coast-crossing and (right) island-crossing cases.

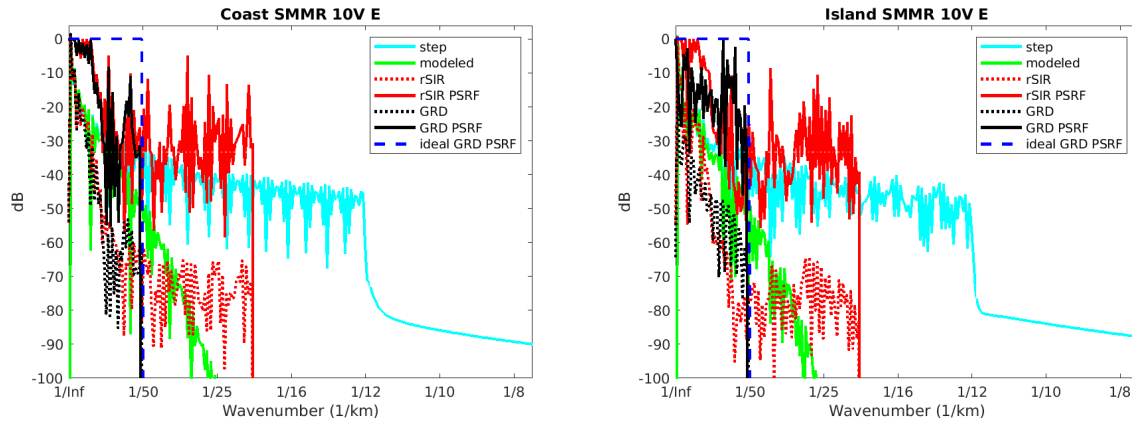


Figure 289: Wavenumber spectra of the  $T_B$  slices, the model, and the PSRF. (left) Coast-crossing case. (right) Island-crossing case.

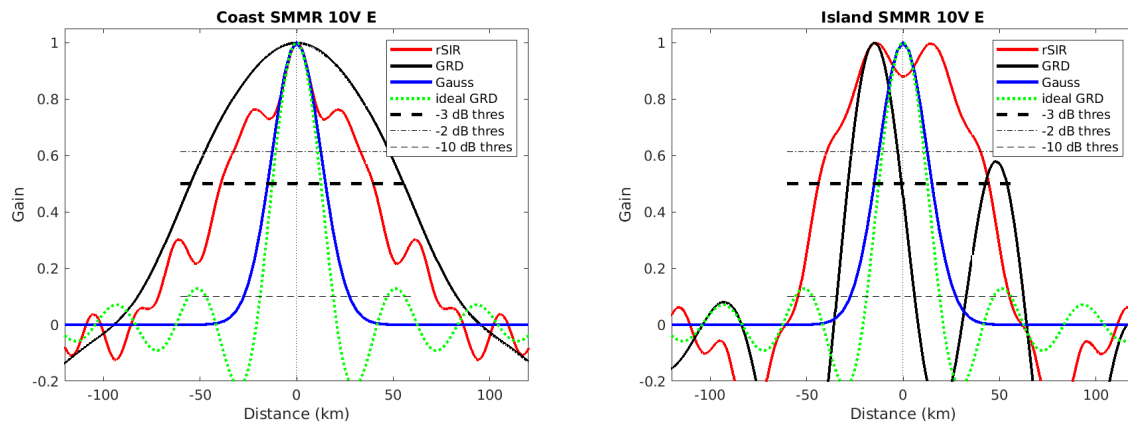


Figure 290: Derived single-pass rSIR and GRD PSRFs from the (left) coast-crossing and (right) island-crossing cases.

Table 110: Resolution estimates for SMMR channel 10V LTOD E

Algorithm	-3 dB Thres		-2 dB Thres		-10 dB Thres	
	Coast	Island	Coast	Island	Coast	Island
Gauss	30.0	30.0	24.4	24.4	54.8	54.8
rSIR	78.8	88.4	63.7	77.6	143.4	109.5
ideal GRD	36.2	36.2	30.3	30.3	54.5	54.5
GRD	110.3	27.8	93.2	23.4	165.2	40.3

## E.8 SMMR Channel 10V M Figures

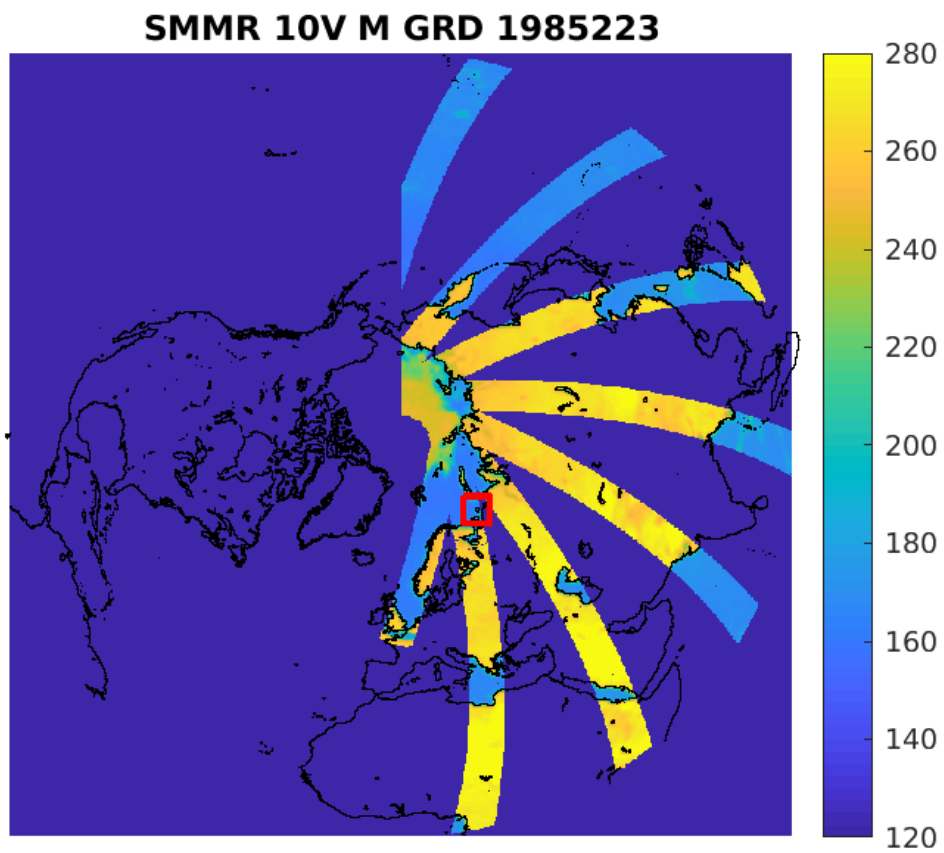


Figure 291: rSIR Northern Hemisphere view.

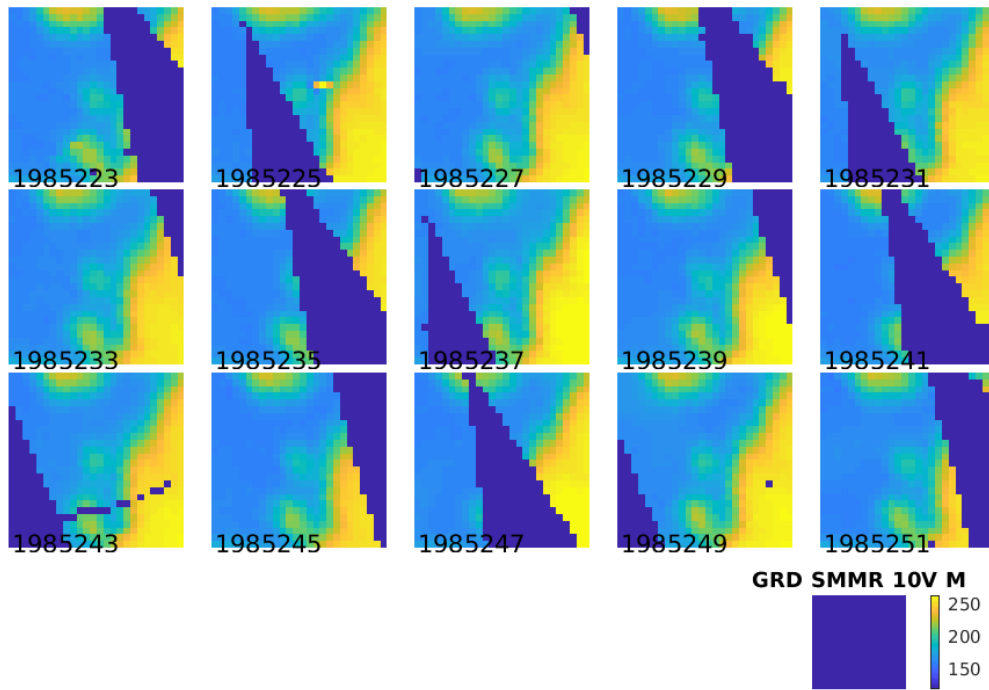
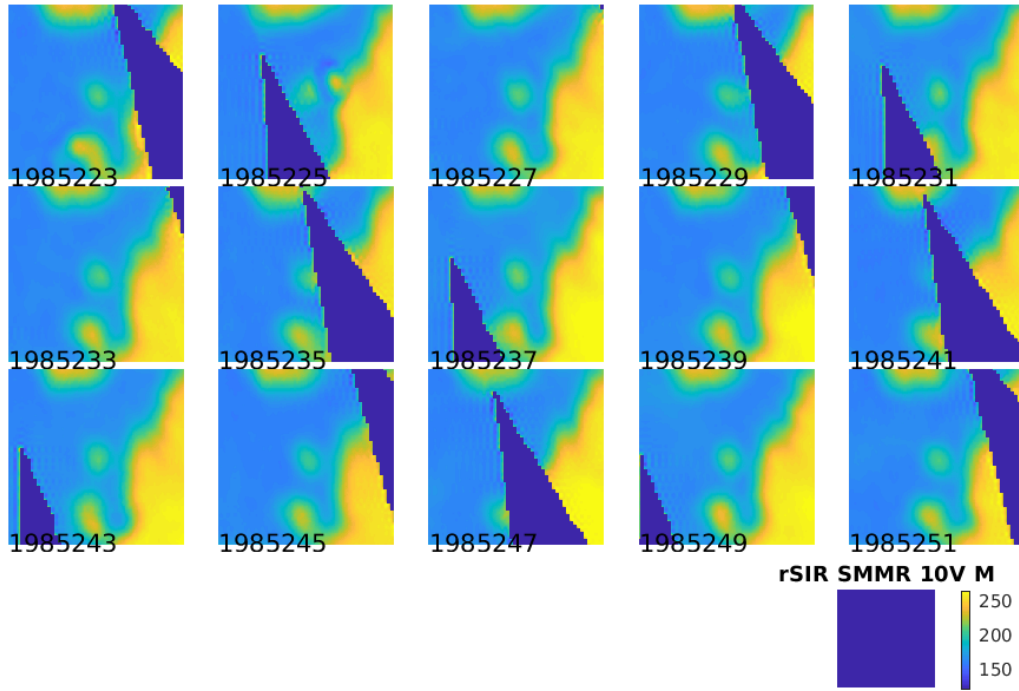


Figure 292: Time series of (top) rSIR and (bottom) GRD  $T_B$  images over the study area. Image dates are labeled on the image.

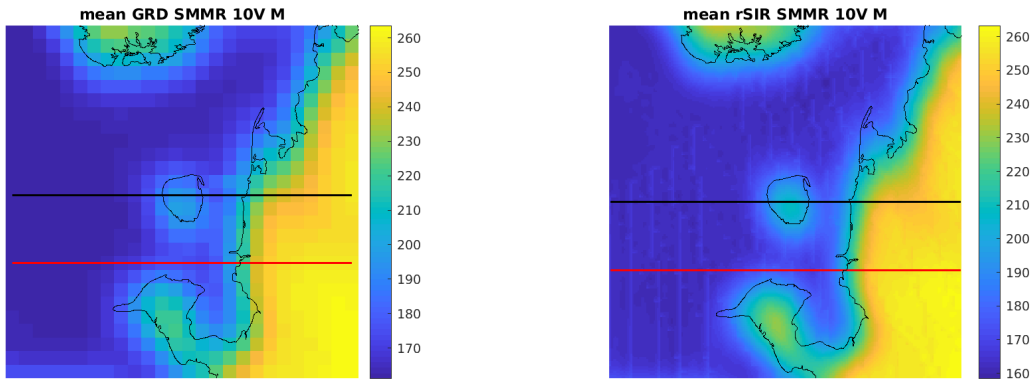


Figure 293: Average of daily  $T_B$  images over the study area. (left) 25-km GRD. (right) 3.125-km rSIR. The thick horizontal lines show the data transect locations where data is extracted from the image for analysis.

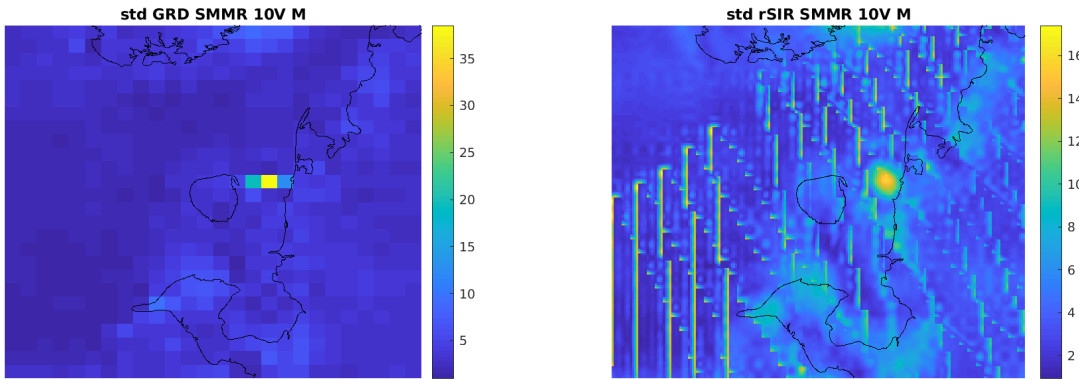


Figure 294: Standard deviation of daily  $T_B$  images over the study area. (left) 25-km GRD. (right) 3.125-km rSIR.



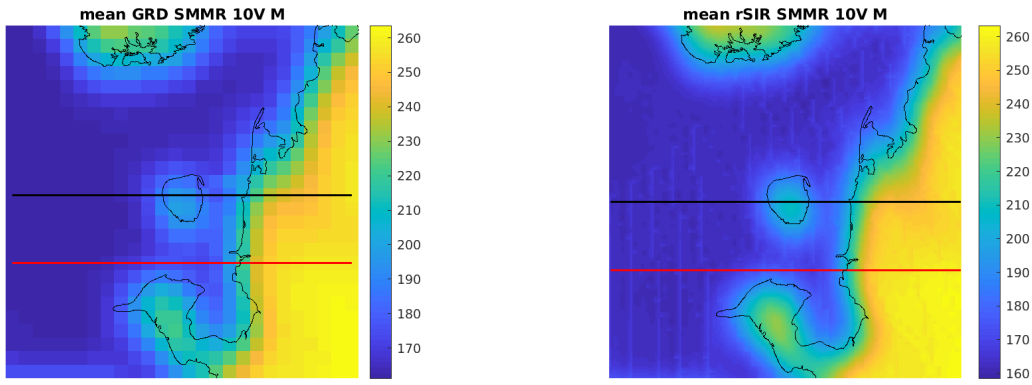


Figure 295: [Repeated] Average of daily  $T_B$  images over the study area. (left) 25-km GRD. (right) 3.125-km rSIR. The thick horizontal lines show the data transect locations where data is extracted from the image for analysis.

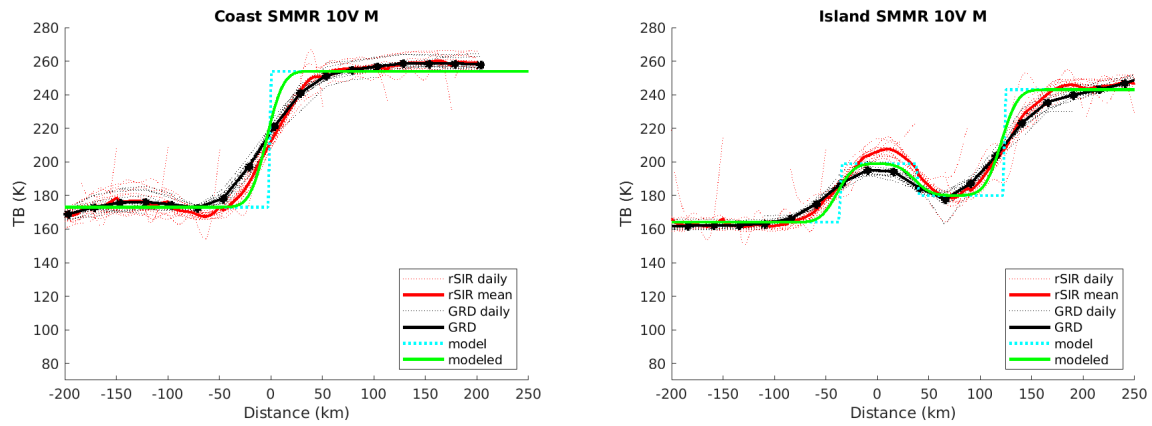


Figure 296: Plots of  $T_B$  along the two analysis case transect lines for the (left) coast-crossing and (right) island-crossing cases.

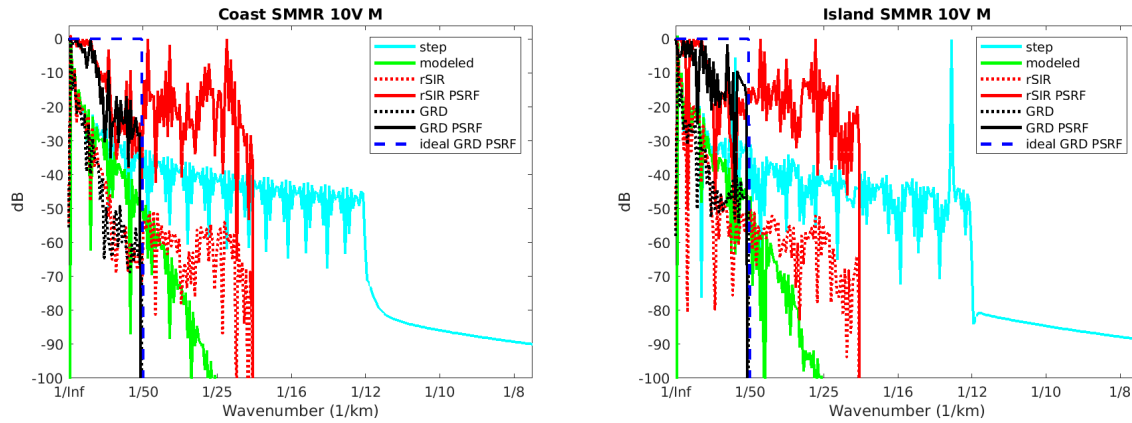


Figure 297: Wavenumber spectra of the  $T_B$  slices, the model, and the PSRF. (left) Coast-crossing case. (right) Island-crossing case.

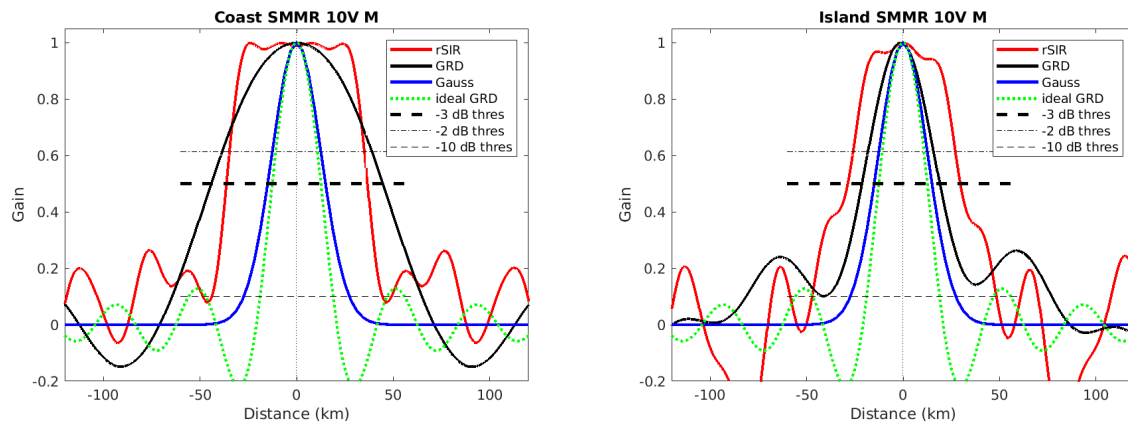


Figure 298: Derived single-pass rSIR and GRD PSRFs from the (left) coast-crossing and (right) island-crossing cases.

Table 111: Resolution estimates for SMMR channel 10V LTOD M

Algorithm	-3 dB Thres		-2 dB Thres		-10 dB Thres	
	Coast	Island	Coast	Island	Coast	Island
Gauss	30.0	30.0	24.4	24.4	54.8	54.8
rSIR	72.9	58.4	69.3	52.3	88.3	95.6
ideal GRD	36.2	36.2	30.3	30.3	54.5	54.5
GRD	88.8	40.3	75.6	33.0	129.4	158.5

## E.9 SMMR Channel 18H E Figures

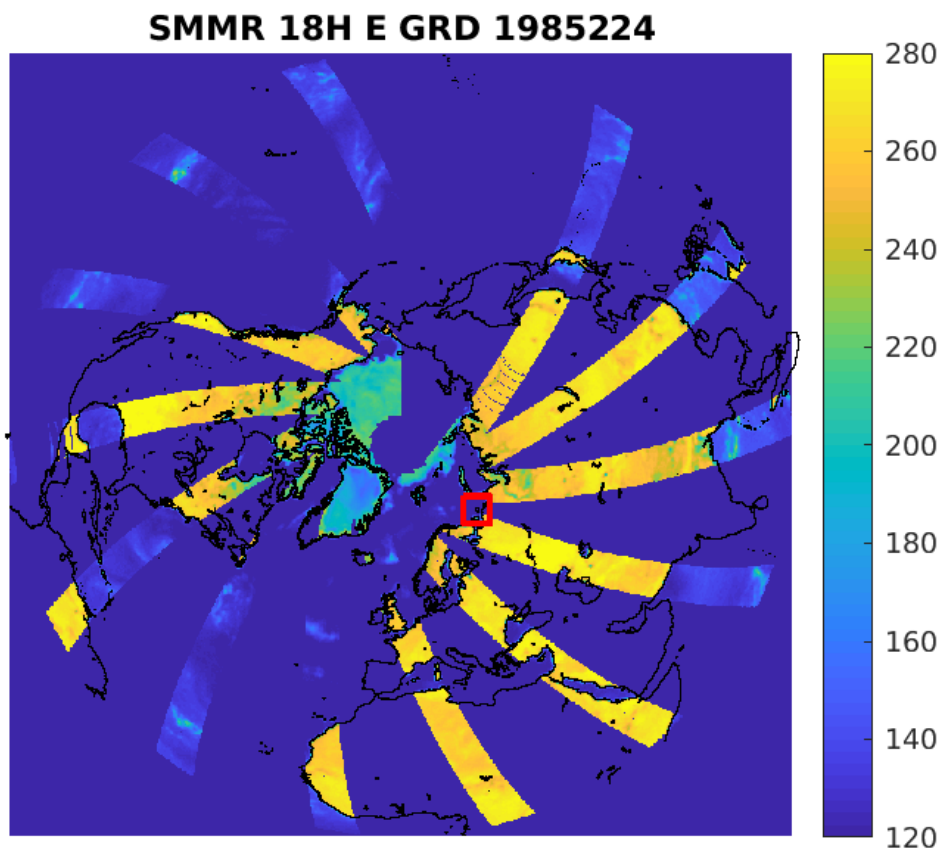


Figure 299: rSIR Northern Hemisphere view.

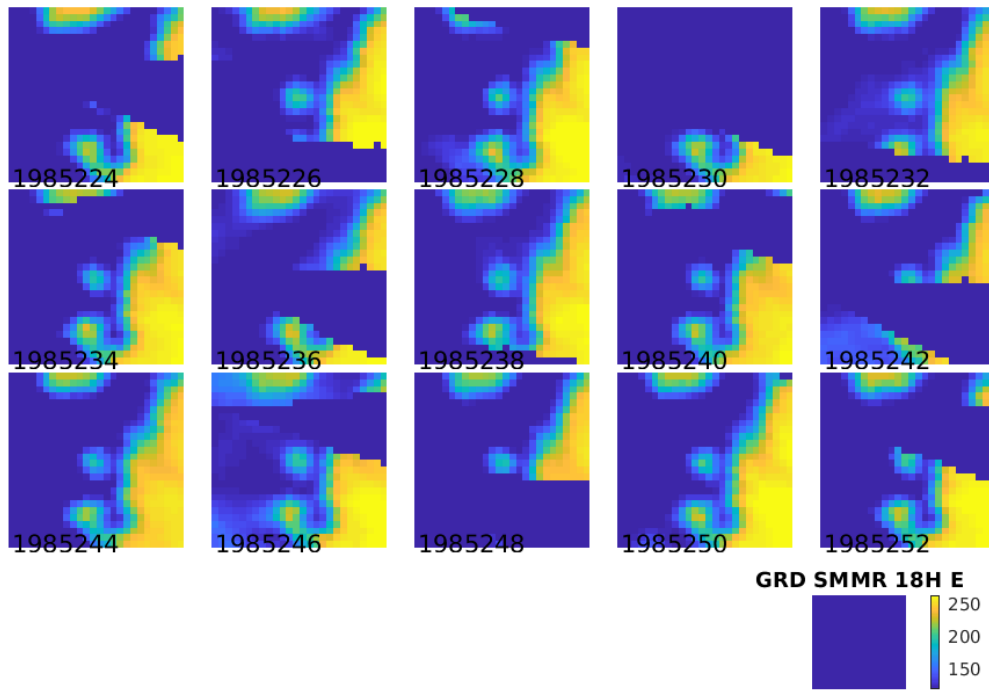
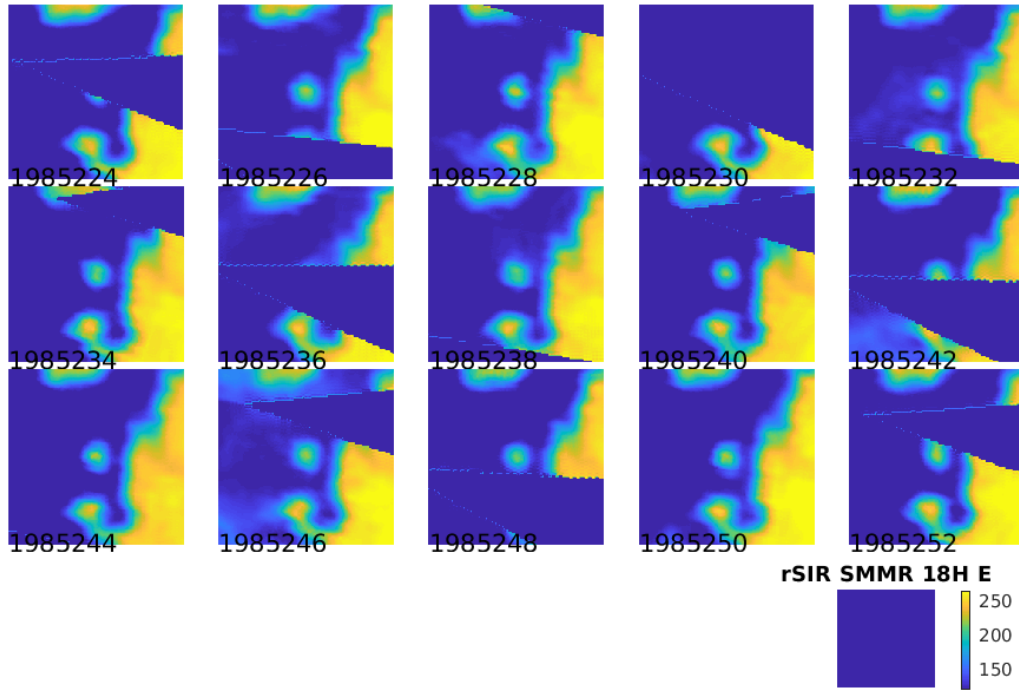


Figure 300: Time series of (top) rSIR and (bottom) GRD  $T_B$  images over the study area. Image dates are labeled on the image.

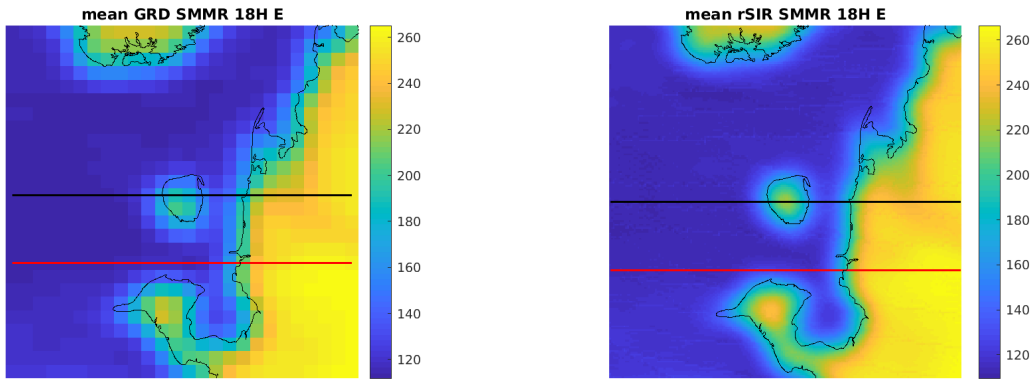


Figure 301: Average of daily  $T_B$  images over the study area. (left) 25-km GRD. (right) 3.125-km rSIR. The thick horizontal lines show the data transect locations where data is extracted from the image for analysis.

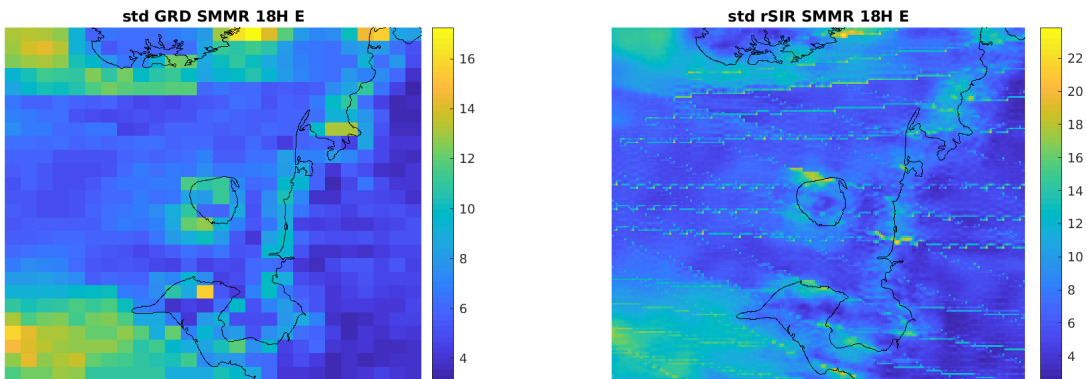


Figure 302: Standard deviation of daily  $T_B$  images over the study area. (left) 25-km GRD. (right) 3.125-km rSIR.

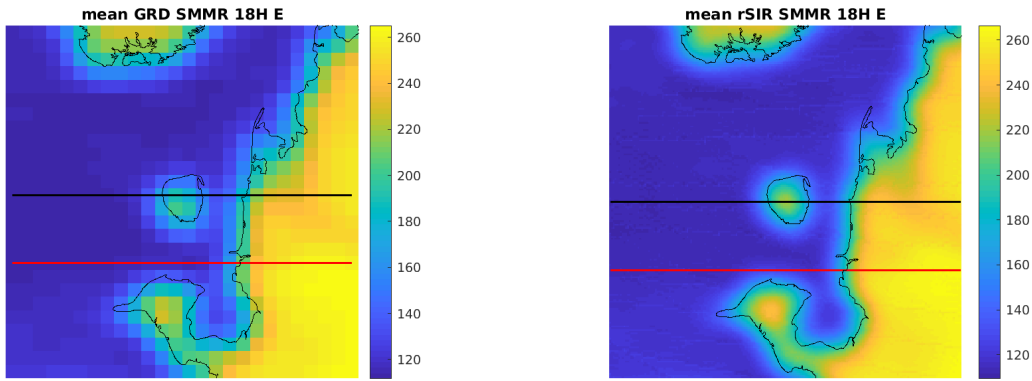


Figure 303: [Repeated] Average of daily  $T_B$  images over the study area. (left) 25-km GRD. (right) 3.125-km rSIR. The thick horizontal lines show the data transect locations where data is extracted from the image for analysis.

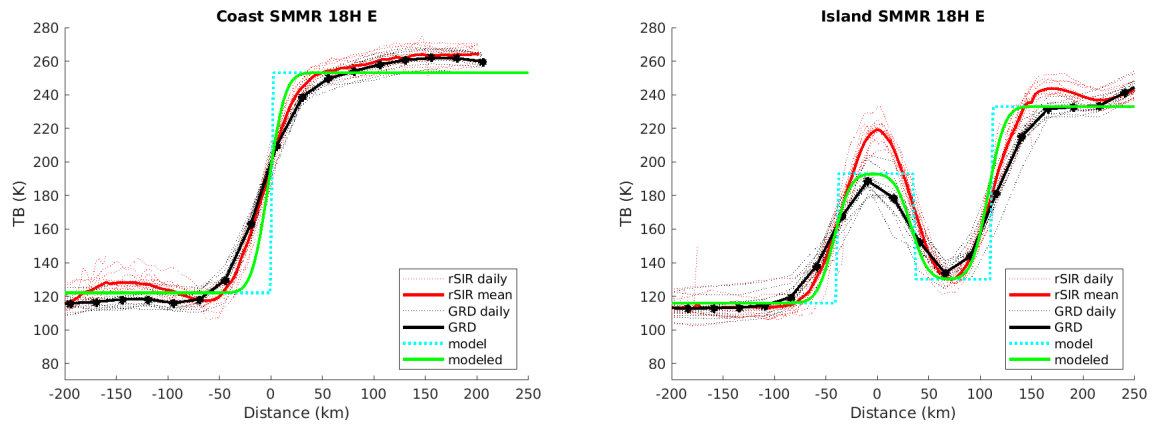


Figure 304: Plots of  $T_B$  along the two analysis case transect lines for the (left) coast-crossing and (right) island-crossing cases.

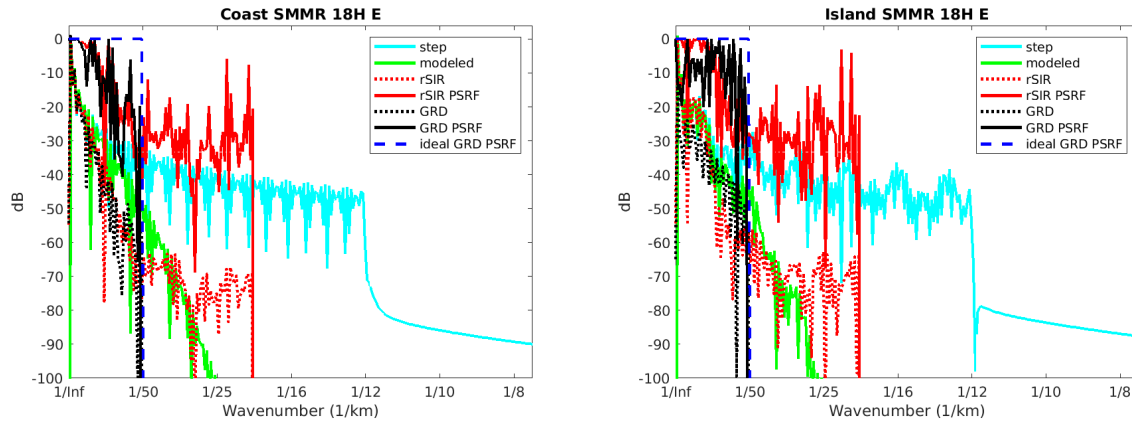


Figure 305: Wavenumber spectra of the  $T_B$  slices, the model, and the PSRF. (left) Coast-crossing case. (right) Island-crossing case.

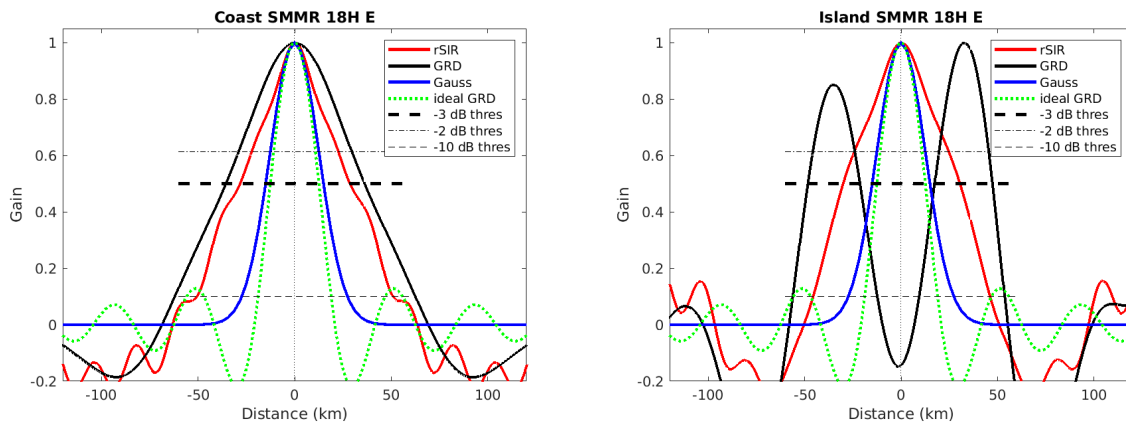


Figure 306: Derived single-pass rSIR and GRD PSRFs from the (left) coast-crossing and (right) island-crossing cases.

Table 112: Resolution estimates for SMMR channel 18H LTOD E

Algorithm	-3 dB Thres		-2 dB Thres		-10 dB Thres	
	Coast	Island	Coast	Island	Coast	Island
Gauss	30.0	30.0	24.4	24.4	54.8	54.8
rSIR	56.8	60.6	43.1	46.9	101.5	91.8
ideal GRD	36.2	36.2	30.3	30.3	54.5	54.5
GRD	71.8	30.0	56.6	25.2	124.5	44.3

## E.10 SMMR Channel 18H M Figures

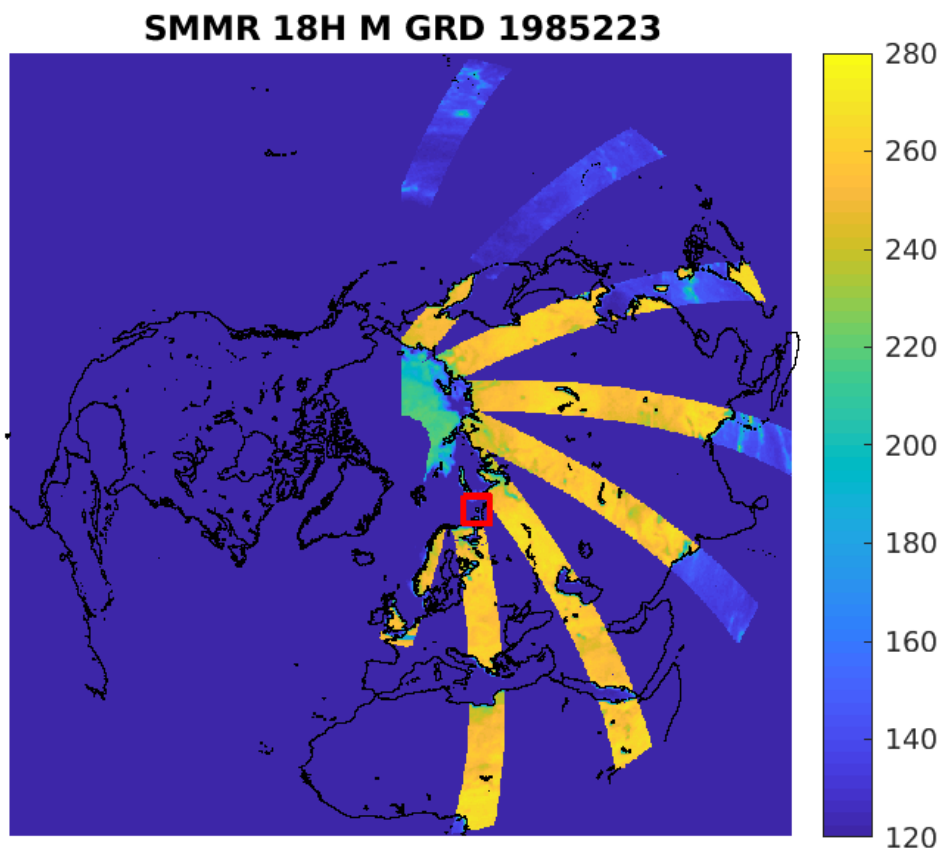


Figure 307: rSIR Northern Hemisphere view.



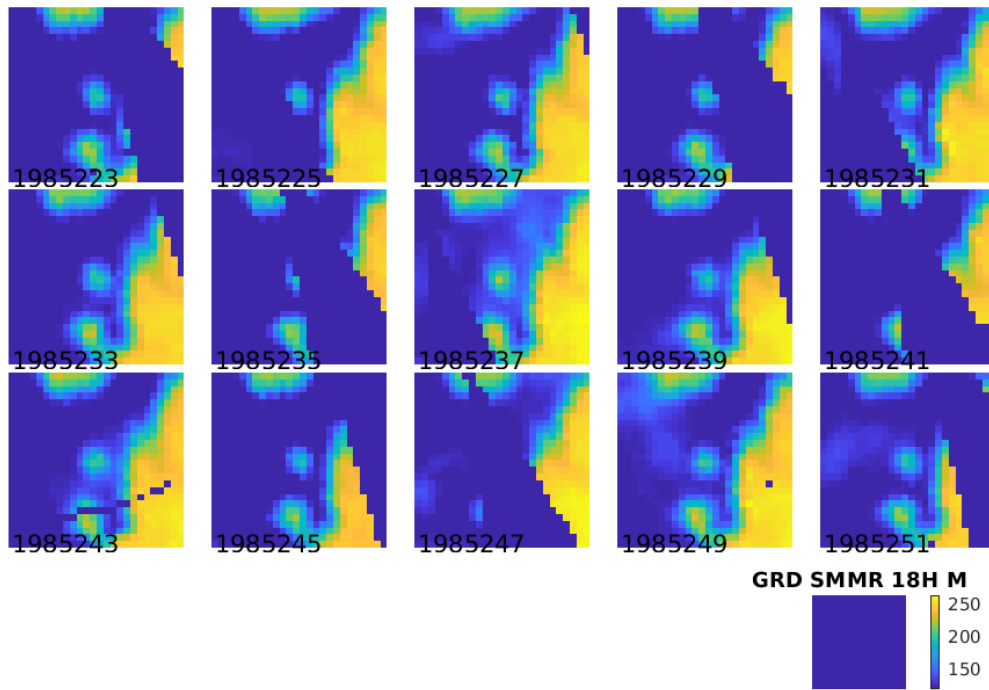
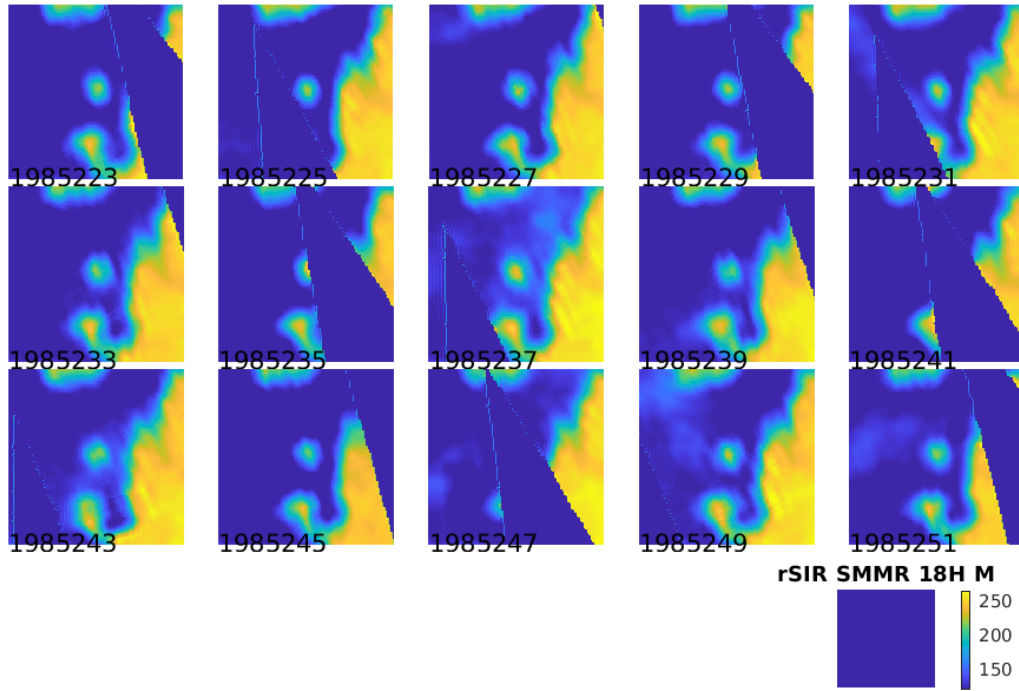


Figure 308: Time series of (top) rSIR and (bottom) GRD  $T_B$  images over the study area. Image dates are labeled on the image.

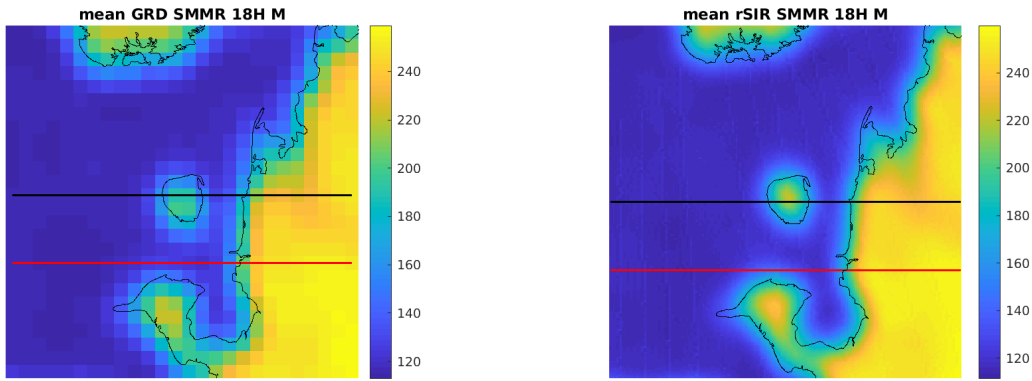


Figure 309: Average of daily  $T_B$  images over the study area. (left) 25-km GRD. (right) 3.125-km rSIR. The thick horizontal lines show the data transect locations where data is extracted from the image for analysis.

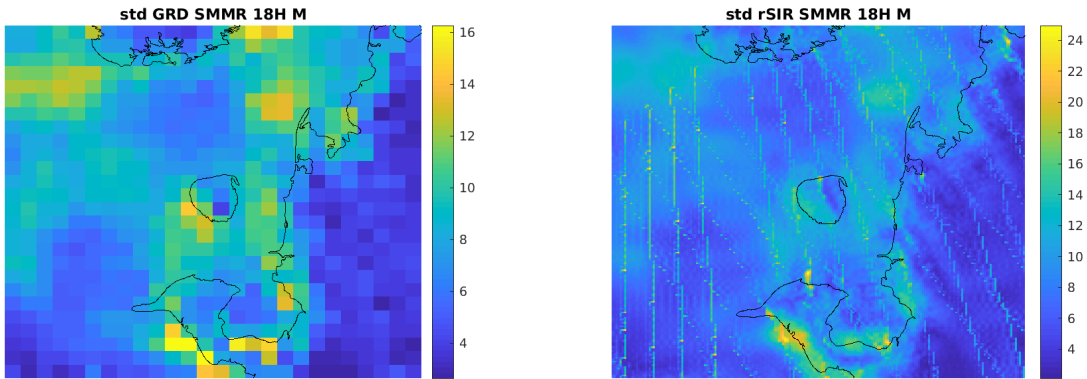


Figure 310: Standard deviation of daily  $T_B$  images over the study area. (left) 25-km GRD. (right) 3.125-km rSIR.

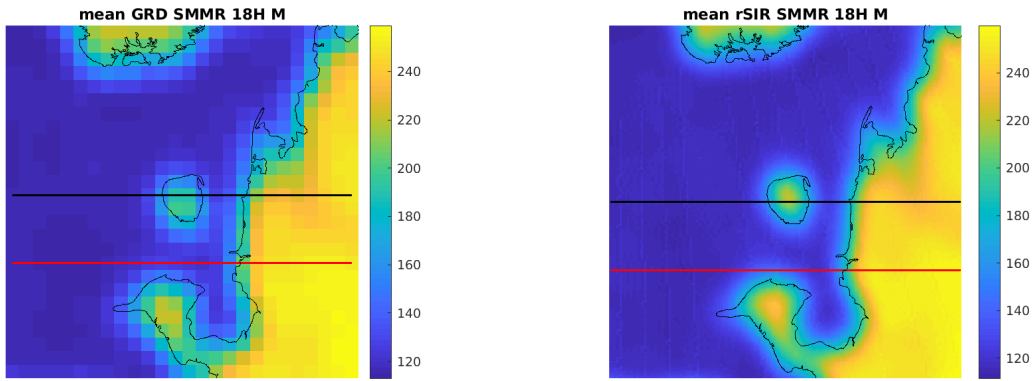


Figure 311: [Repeated] Average of daily  $T_B$  images over the study area. (left) 25-km GRD. (right) 3.125-km rSIR. The thick horizontal lines show the data transect locations where data is extracted from the image for analysis.

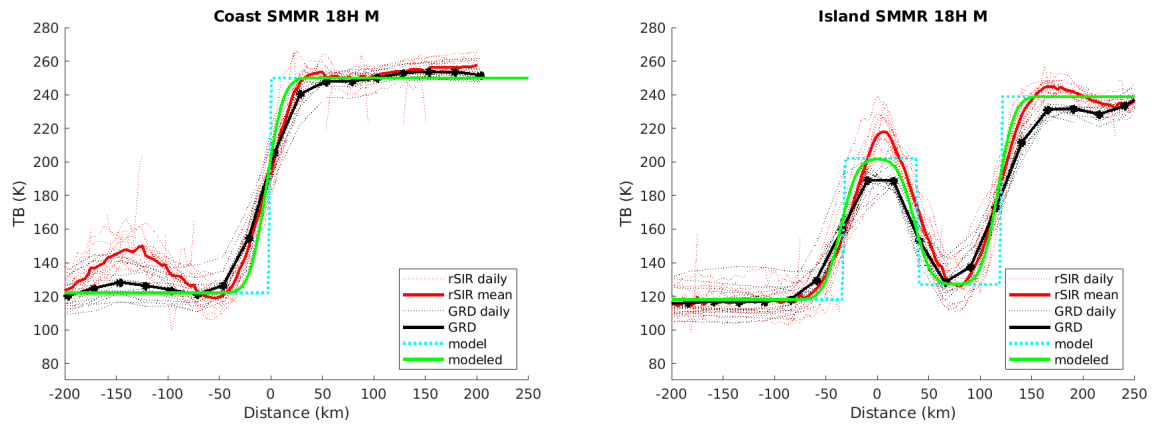


Figure 312: Plots of  $T_B$  along the two analysis case transect lines for the (left) coast-crossing and (right) island-crossing cases.

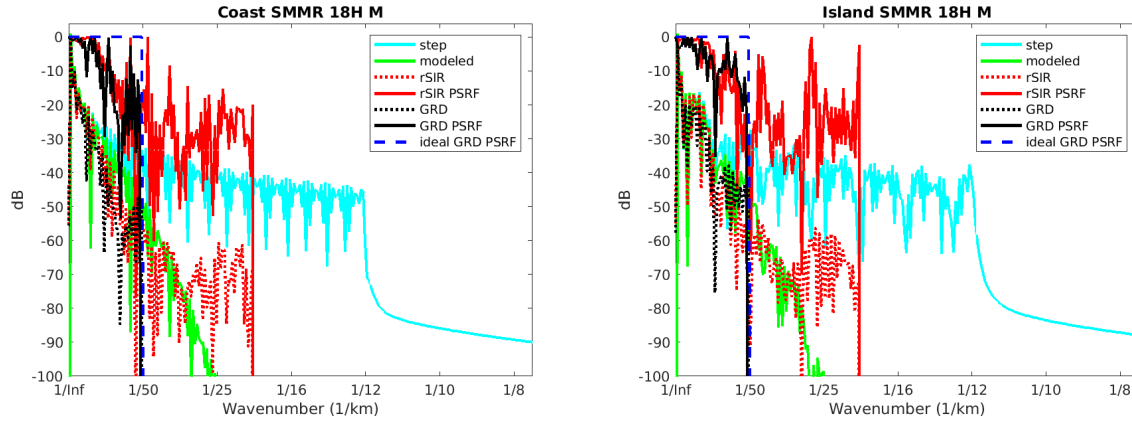


Figure 313: Wavenumber spectra of the  $T_B$  slices, the model, and the PSRF. (left) Coast-crossing case. (right) Island-crossing case.

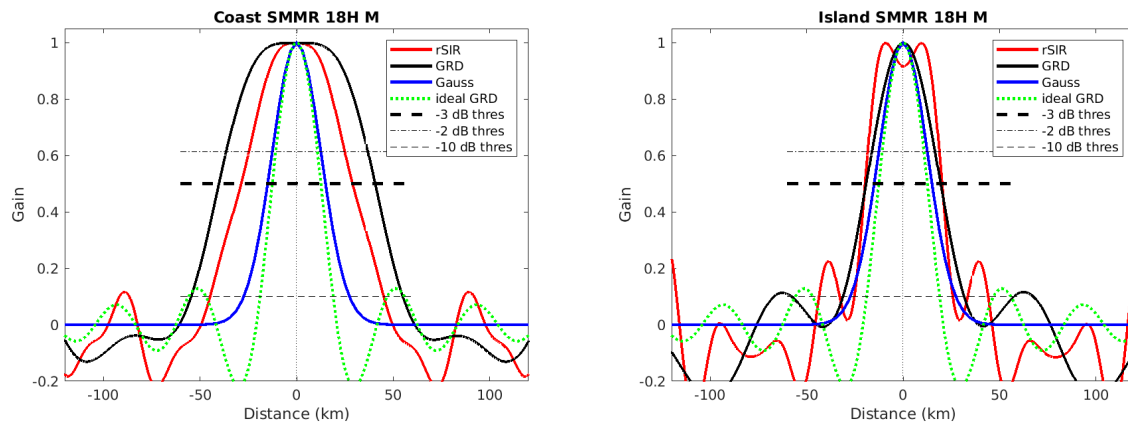


Figure 314: Derived single-pass rSIR and GRD PSRFs from the (left) coast-crossing and (right) island-crossing cases.

Table 113: Resolution estimates for SMMR channel 18H LTOD M

Algorithm	-3 dB Thres		-2 dB Thres		-10 dB Thres	
	Coast	Island	Coast	Island	Coast	Island
Gauss	30.0	30.0	24.4	24.4	54.8	54.8
rSIR	57.7	39.8	48.4	36.6	89.9	51.0
ideal GRD	36.2	36.2	30.3	30.3	54.5	54.5
GRD	80.8	38.6	72.1	31.9	109.5	62.9

## E.11 SMMR Channel 18V E Figures

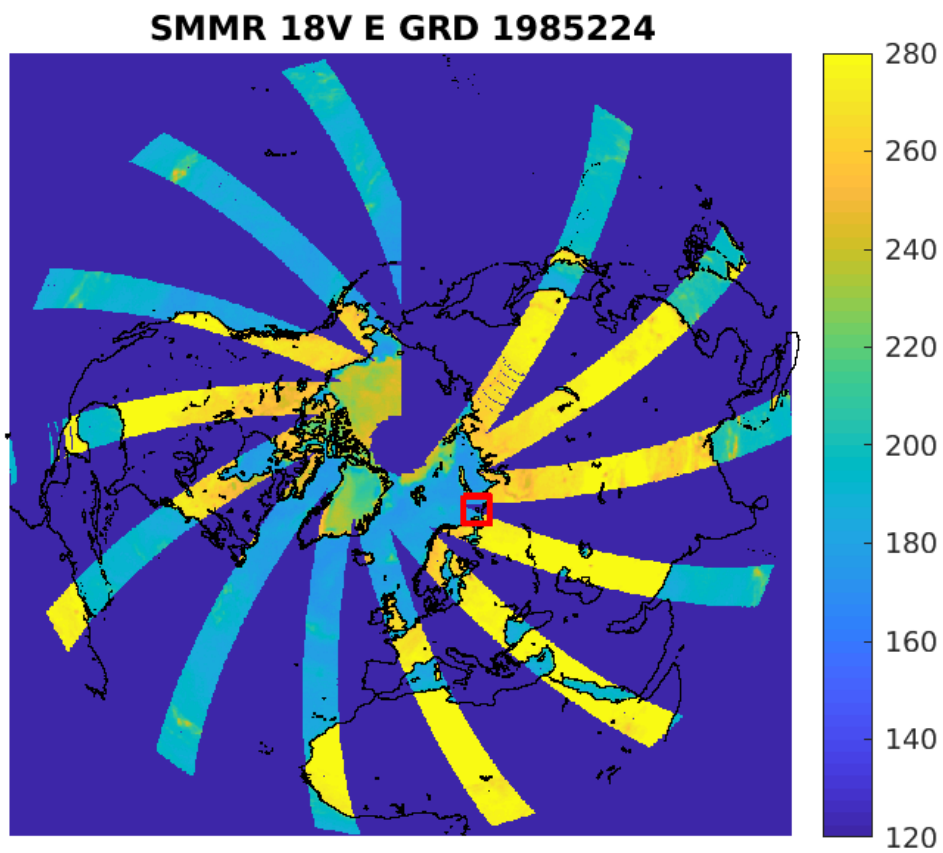


Figure 315: rSIR Northern Hemisphere view.

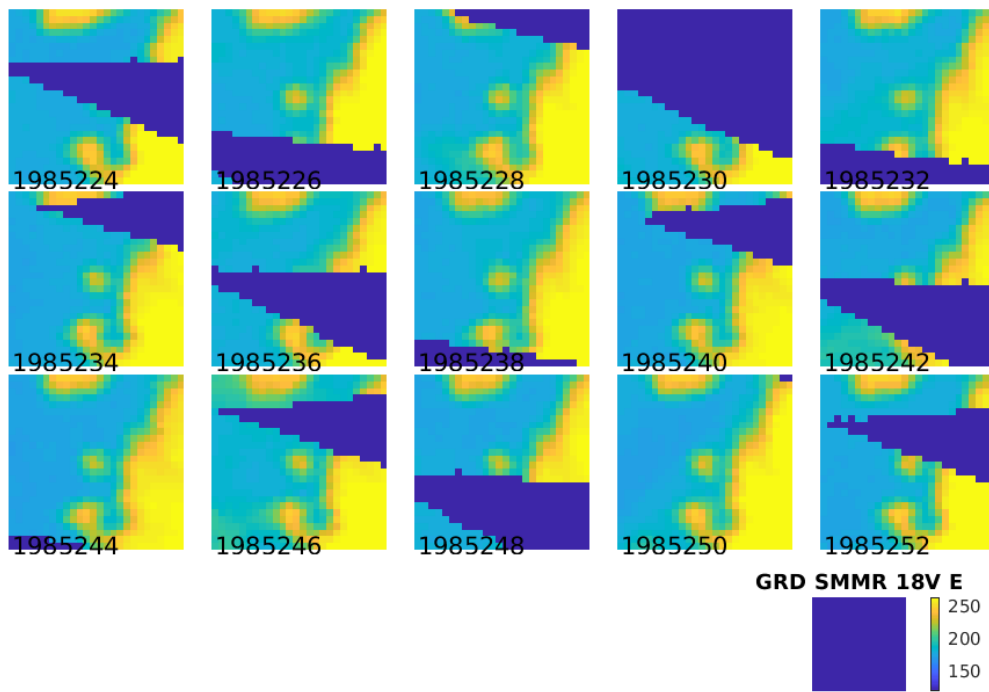
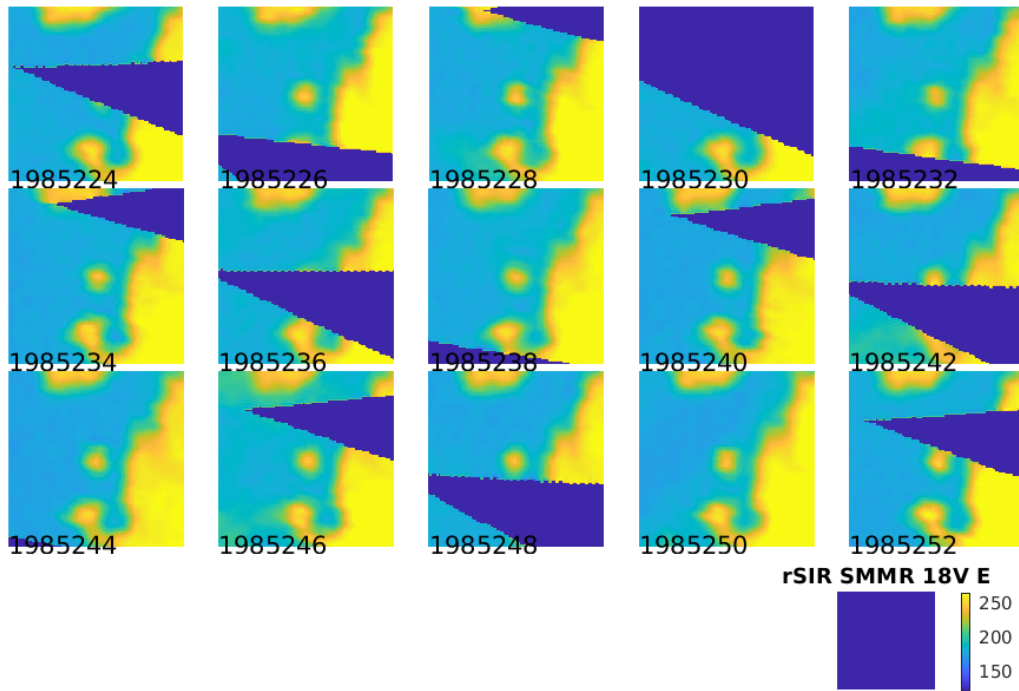


Figure 316: Time series of (top) rSIR and (bottom) GRD  $T_B$  images over the study area. Image dates are labeled on the image.

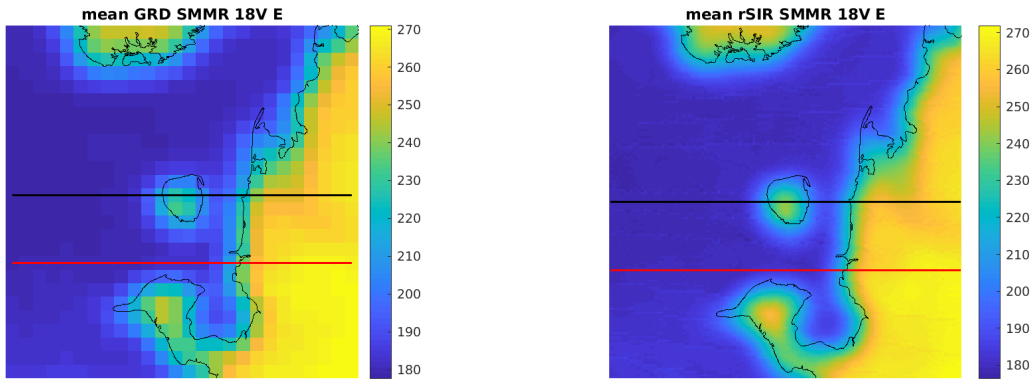


Figure 317: Average of daily  $T_B$  images over the study area. (left) 25-km GRD. (right) 3.125-km rSIR. The thick horizontal lines show the data transect locations where data is extracted from the image for analysis.

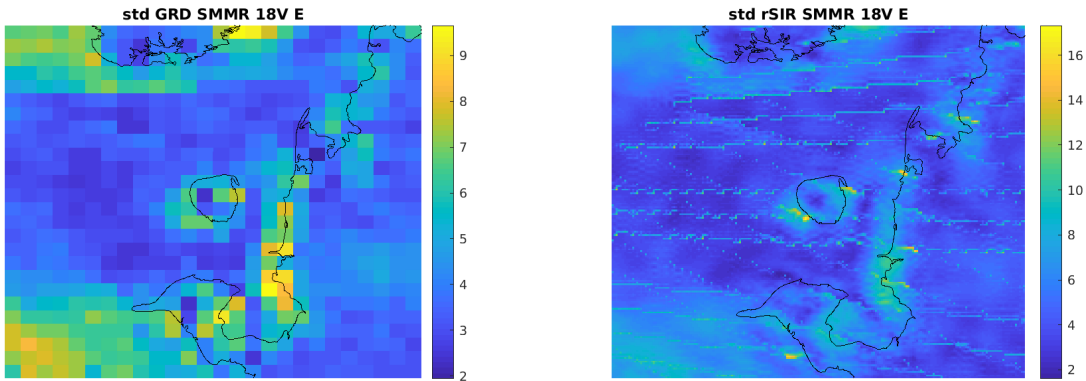


Figure 318: Standard deviation of daily  $T_B$  images over the study area. (left) 25-km GRD. (right) 3.125-km rSIR.

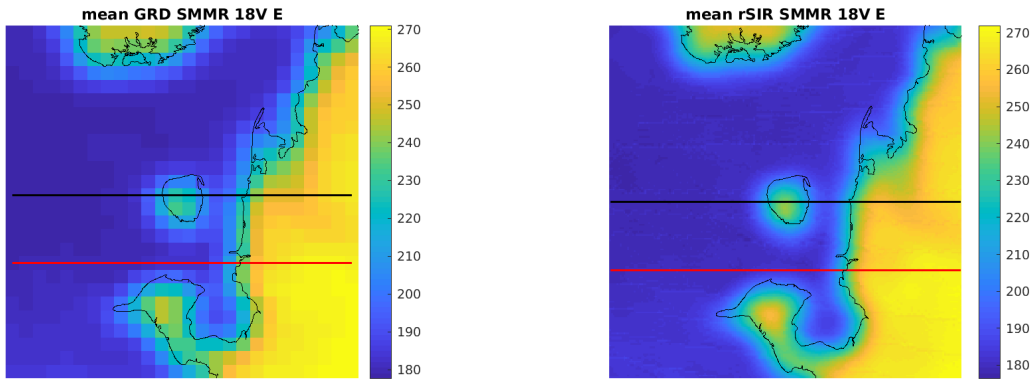


Figure 319: [Repeated] Average of daily  $T_B$  images over the study area. (left) 25-km GRD. (right) 3.125-km rSIR. The thick horizontal lines show the data transect locations where data is extracted from the image for analysis.

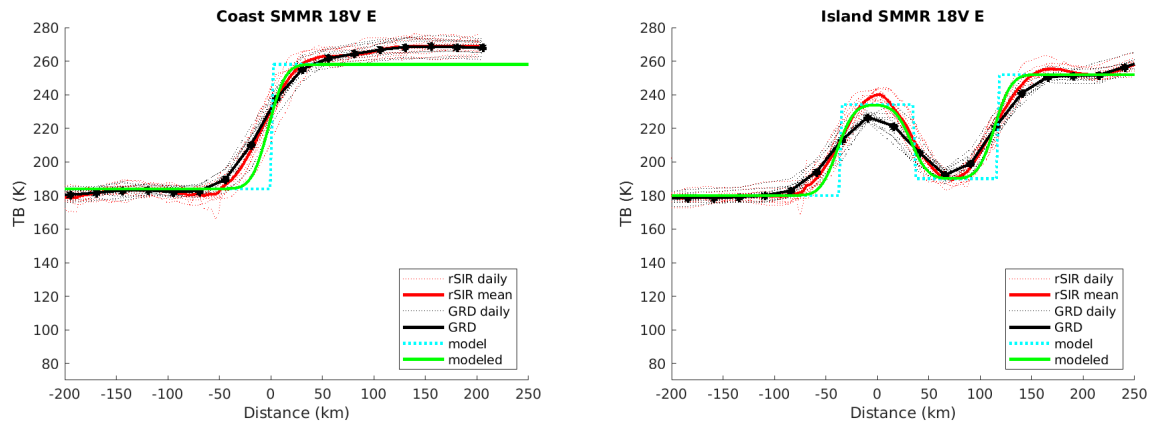


Figure 320: Plots of  $T_B$  along the two analysis case transect lines for the (left) coast-crossing and (right) island-crossing cases.



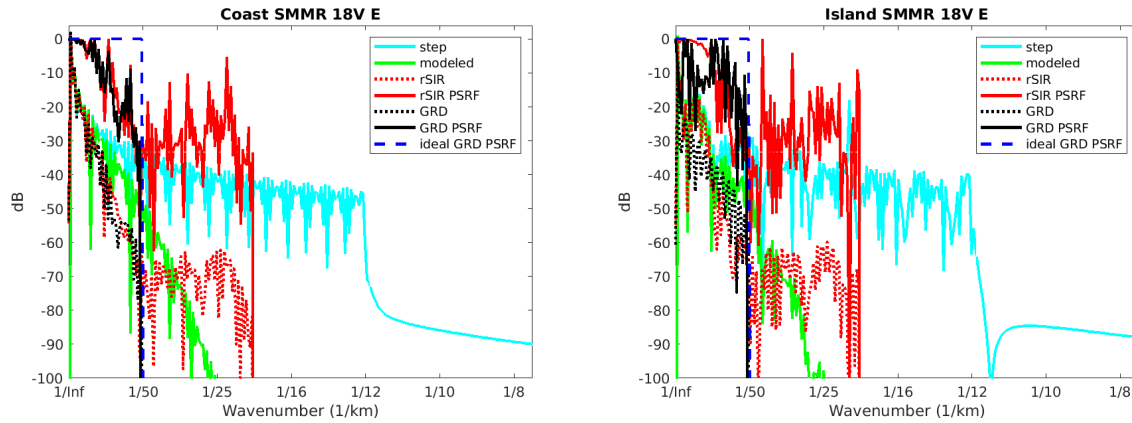


Figure 321: Wavenumber spectra of the  $T_B$  slices, the model, and the PSRF. (left) Coast-crossing case. (right) Island-crossing case.

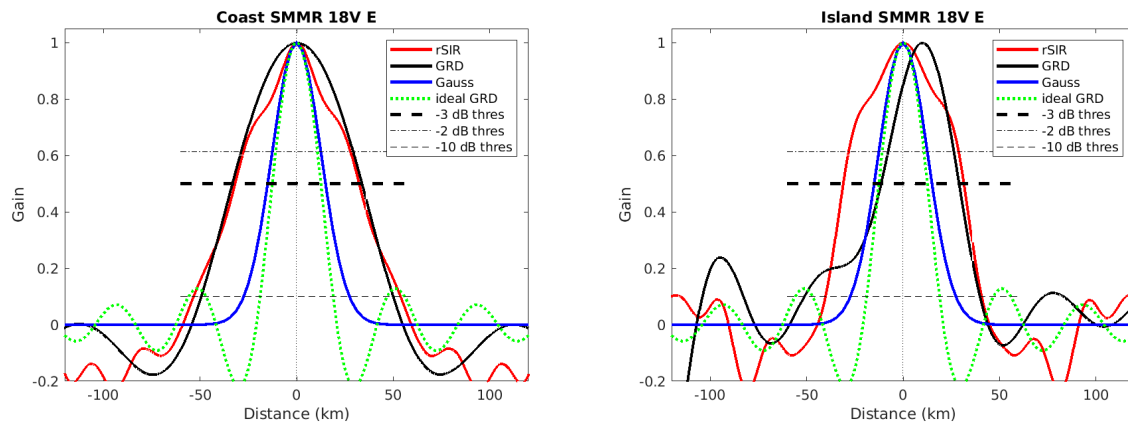


Figure 322: Derived single-pass rSIR and GRD PSRFs from the (left) coast-crossing and (right) island-crossing cases.

Table 114: Resolution estimates for SMMR channel 18V LTOD E

Algorithm	-3 dB Thres		-2 dB Thres		-10 dB Thres	
	Coast	Island	Coast	Island	Coast	Island
Gauss	30.0	30.0	24.4	24.4	54.8	54.8
rSIR	64.1	62.6	53.8	56.0	107.1	80.9
ideal GRD	36.2	36.2	30.3	30.3	54.5	54.5
GRD	67.0	40.4	56.4	33.1	99.3	91.0

## E.12 SMMR Channel 18V M Figures

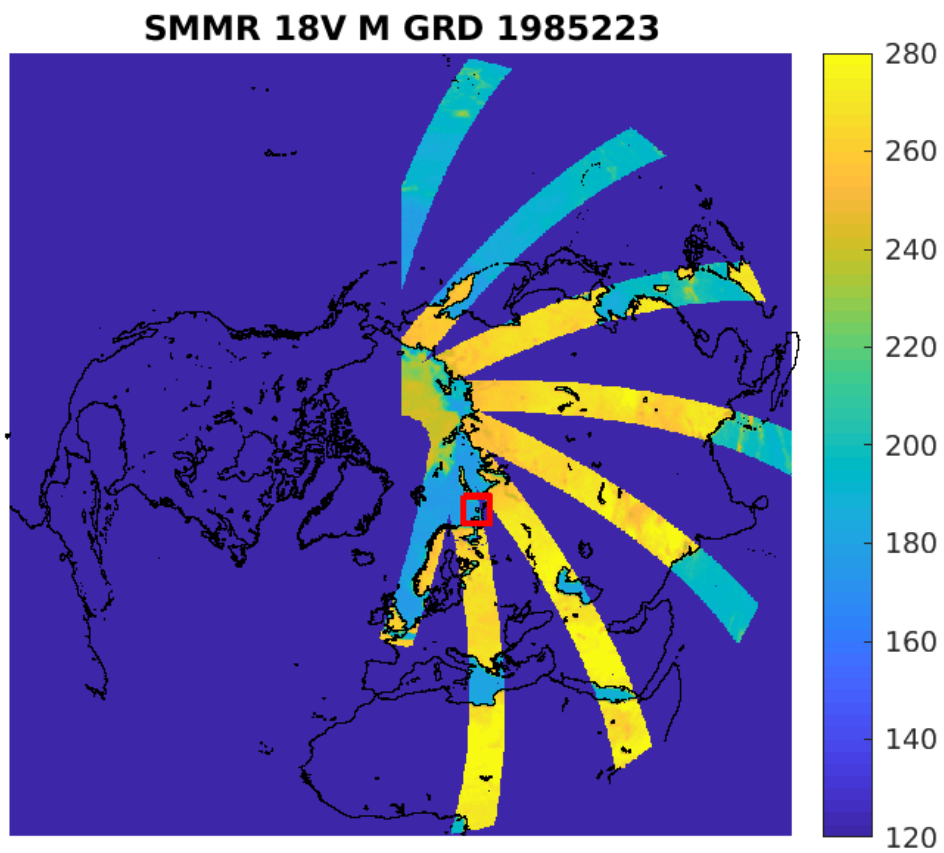


Figure 323: rSIR Northern Hemisphere view.

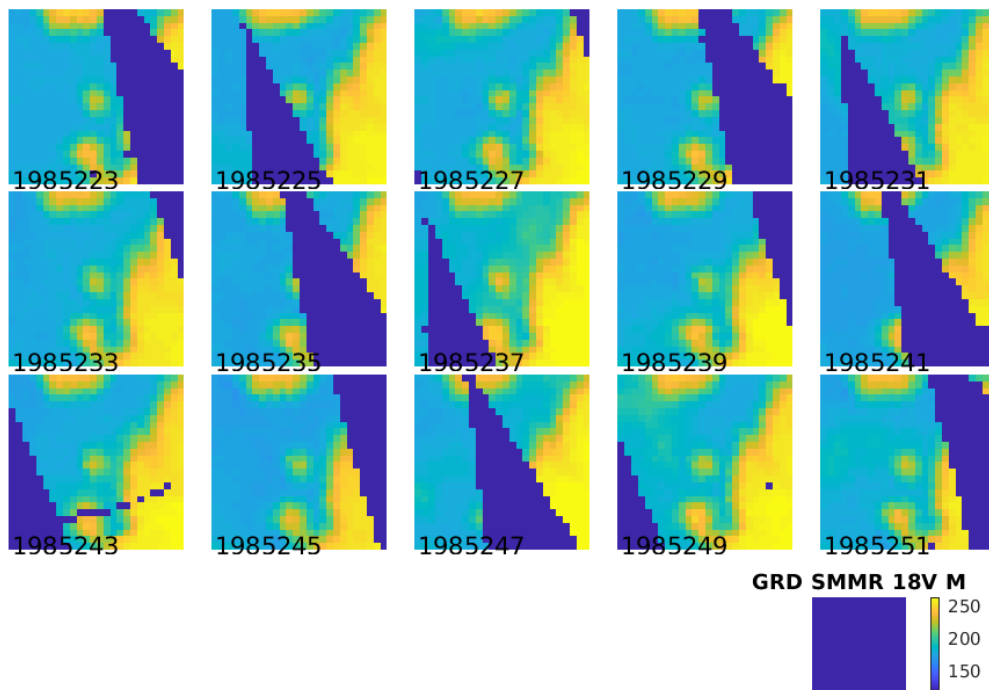
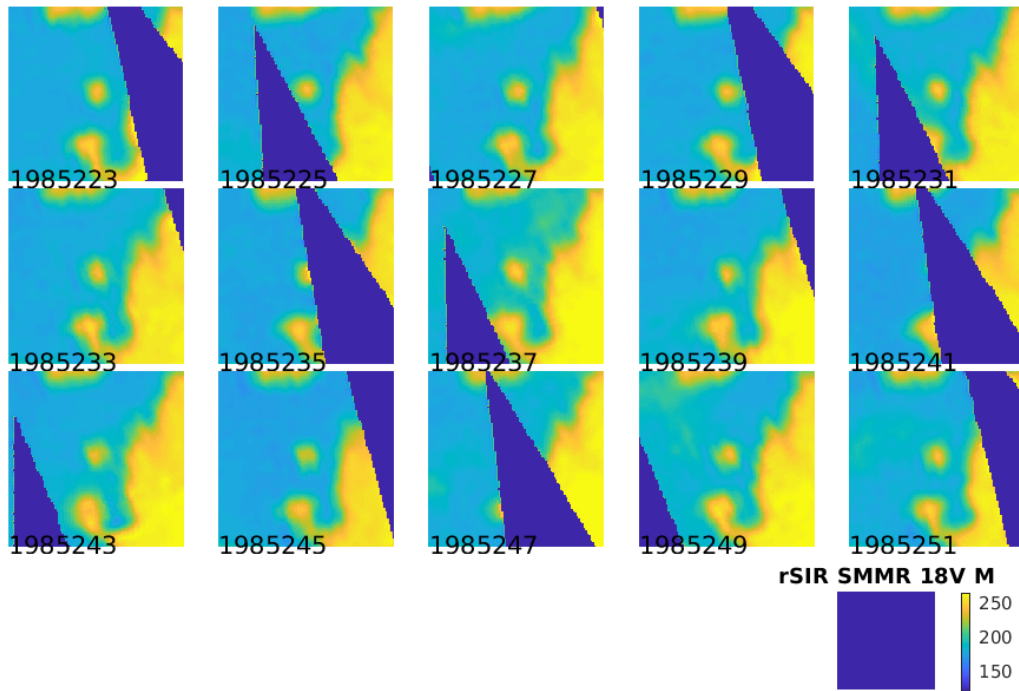


Figure 324: Time series of (top) rSIR and (bottom) GRD  $T_B$  images over the study area. Image dates are labeled on the image.

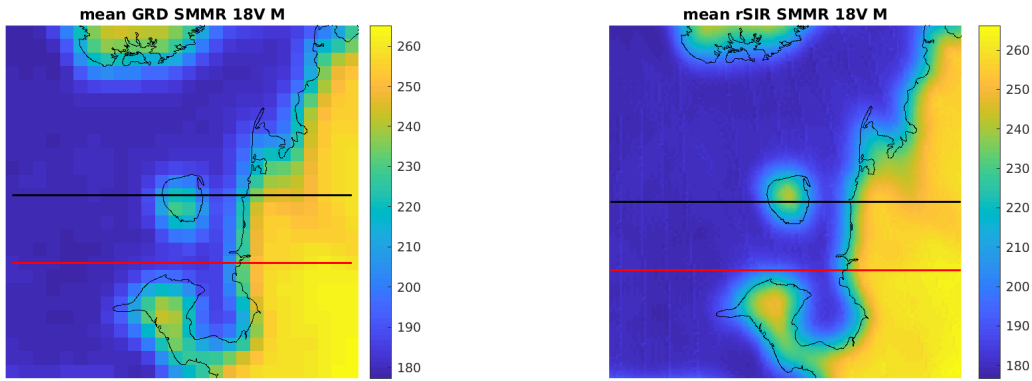


Figure 325: Average of daily  $T_B$  images over the study area. (left) 25-km GRD. (right) 3.125-km rSIR. The thick horizontal lines show the data transect locations where data is extracted from the image for analysis.

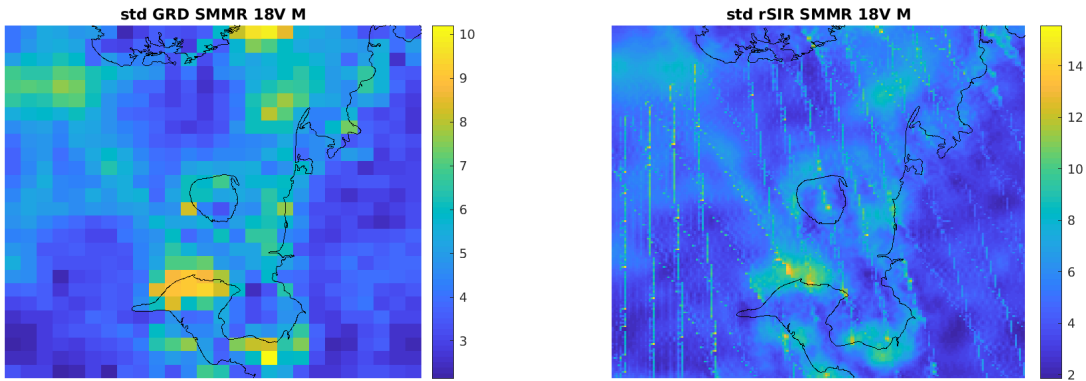


Figure 326: Standard deviation of daily  $T_B$  images over the study area. (left) 25-km GRD. (right) 3.125-km rSIR.

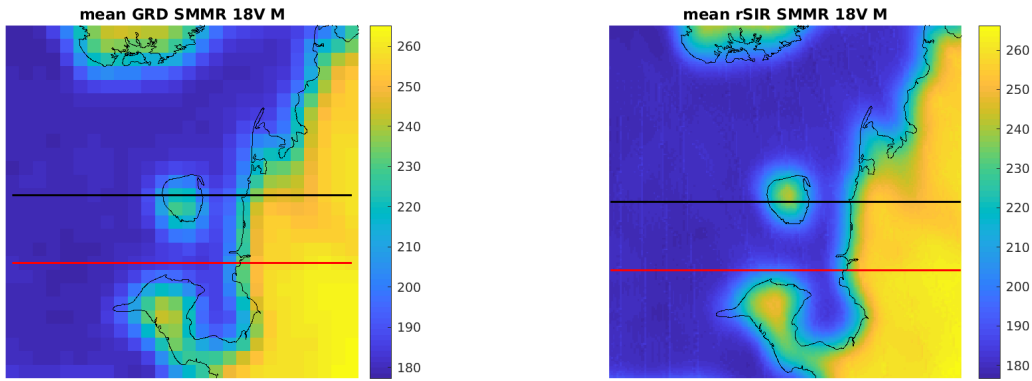


Figure 327: [Repeated] Average of daily  $T_B$  images over the study area. (left) 25-km GRD. (right) 3.125-km rSIR. The thick horizontal lines show the data transect locations where data is extracted from the image for analysis.

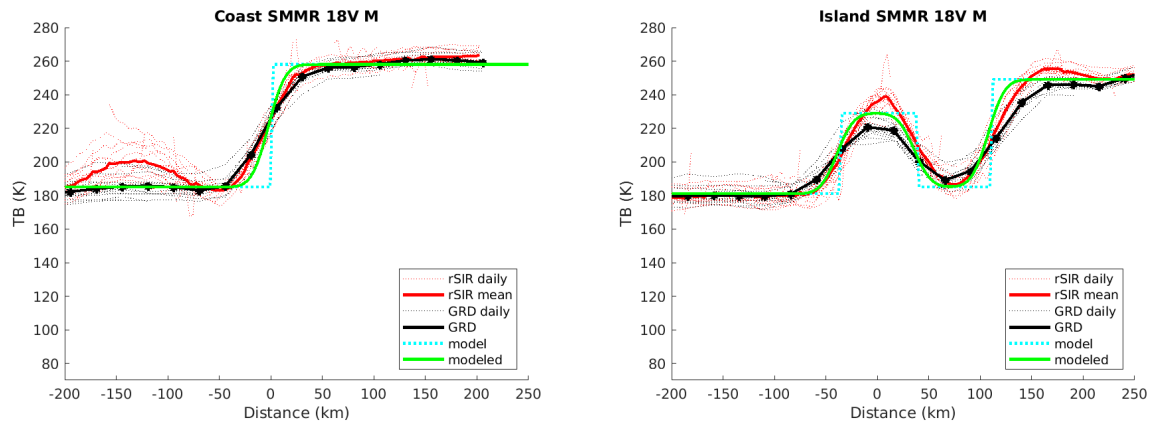


Figure 328: Plots of  $T_B$  along the two analysis case transect lines for the (left) coast-crossing and (right) island-crossing cases.

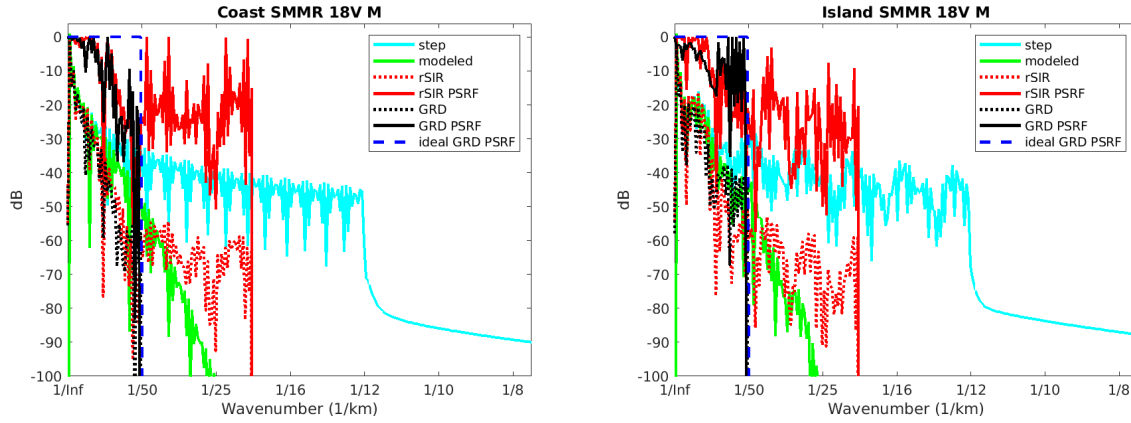


Figure 329: Wavenumber spectra of the  $T_B$  slices, the model, and the PSRF. (left) Coast-crossing case. (right) Island-crossing case.

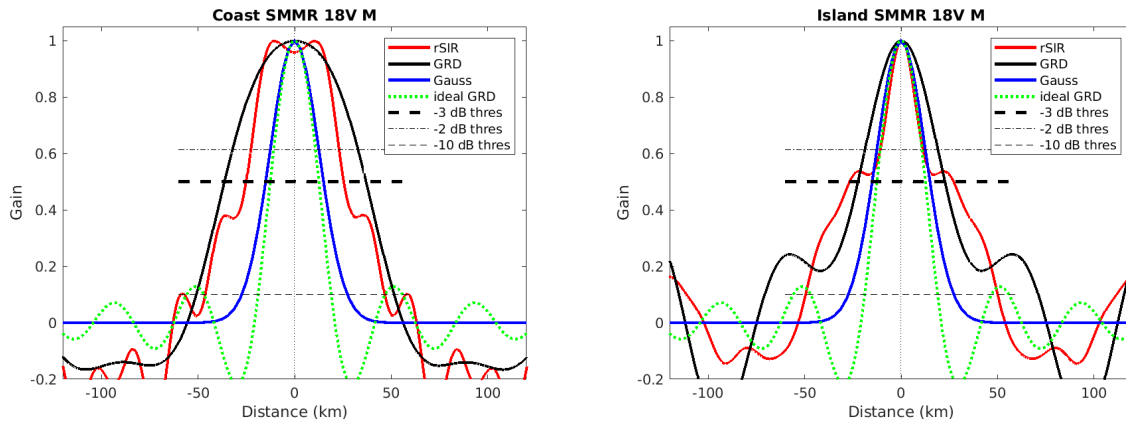


Figure 330: Derived single-pass rSIR and GRD PSRFs from the (left) coast-crossing and (right) island-crossing cases.

Table 115: Resolution estimates for SMMR channel 18V LTOD M

Algorithm	-3 dB Thres		-2 dB Thres		-10 dB Thres	
	Coast	Island	Coast	Island	Coast	Island
Gauss	30.0	30.0	24.4	24.4	54.8	54.8
rSIR	50.5	53.9	45.1	21.2	92.8	99.7
ideal GRD	36.2	36.2	30.3	30.3	54.5	54.5
GRD	73.3	45.0	63.6	36.7	102.4	141.8

### E.13 SMMR Channel 21H E Figures

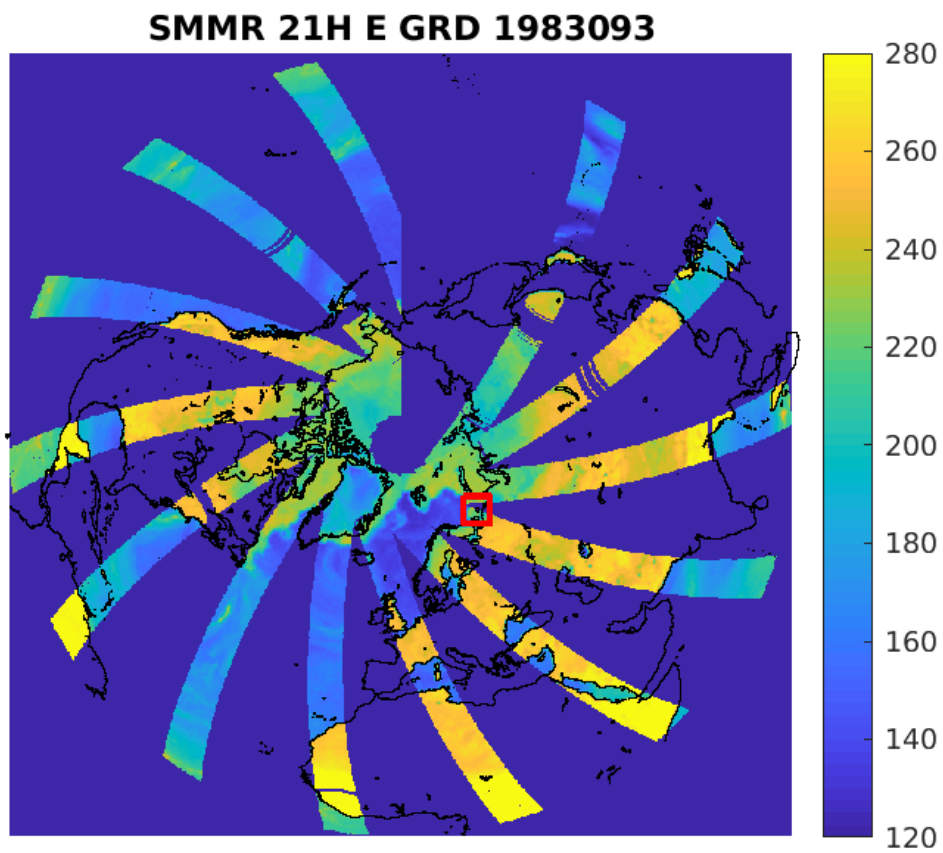


Figure 331: rSIR Northern Hemisphere view.

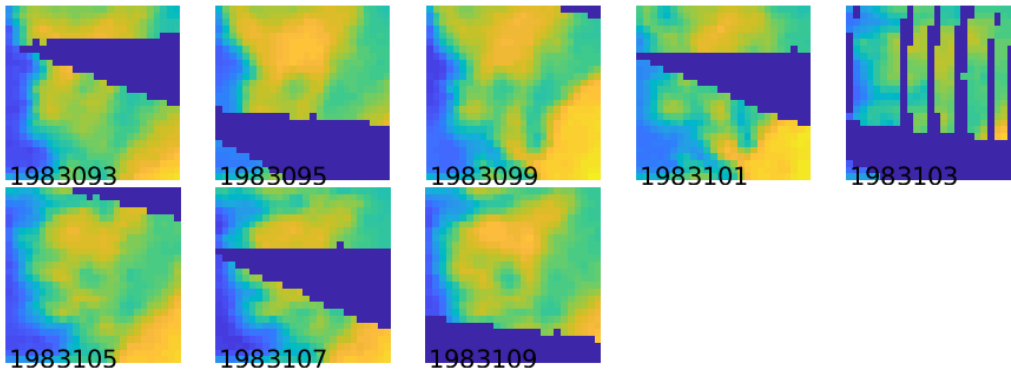
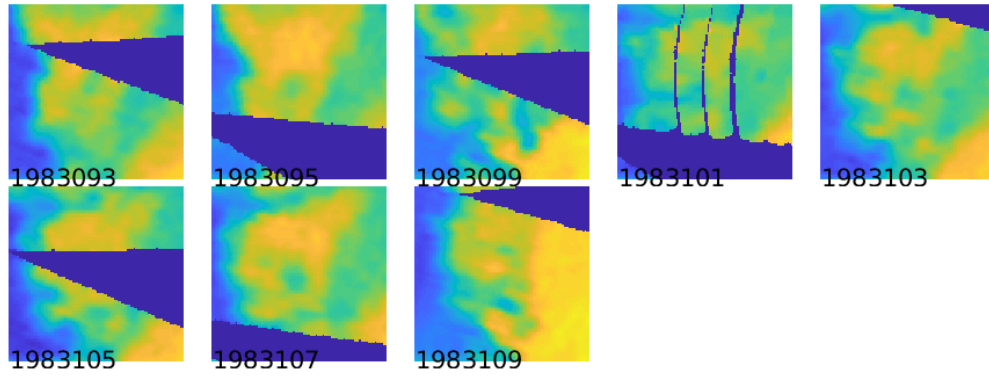


Figure 332: Time series of (top) rSIR and (bottom) GRD  $T_B$  images over the study area. Image dates are labeled on the image.



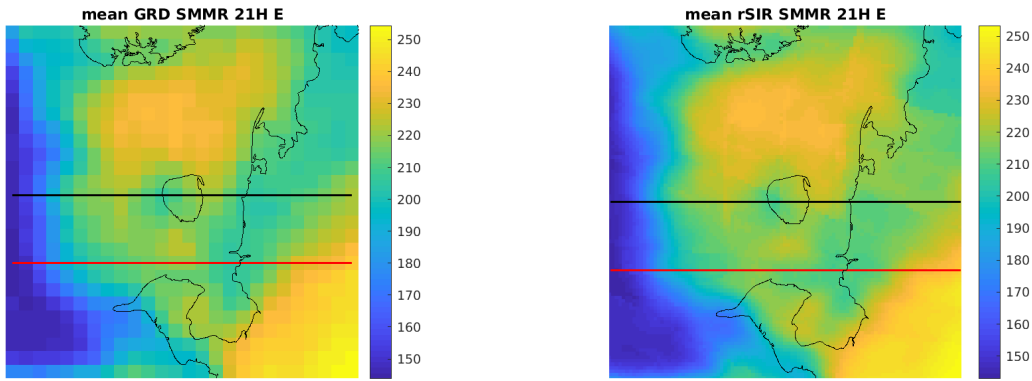


Figure 333: Average of daily  $T_B$  images over the study area. (left) 25-km GRD. (right) 3.125-km rSIR. The thick horizontal lines show the data transect locations where data is extracted from the image for analysis.

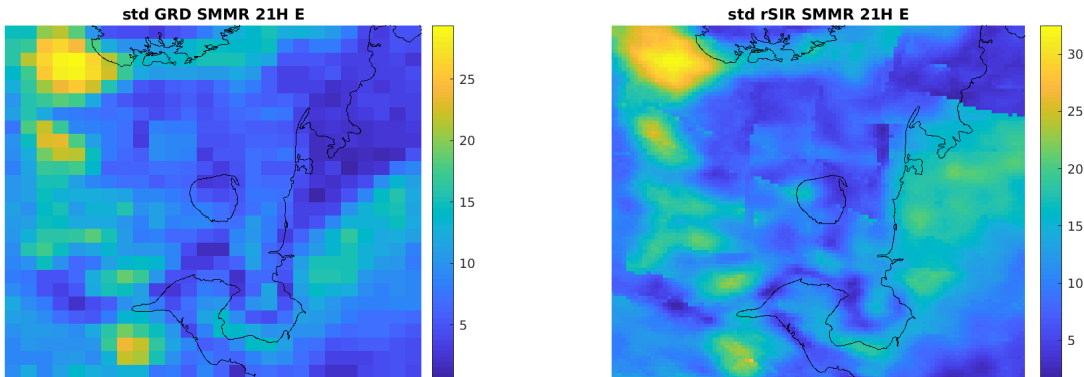


Figure 334: Standard deviation of daily  $T_B$  images over the study area. (left) 25-km GRD. (right) 3.125-km rSIR.

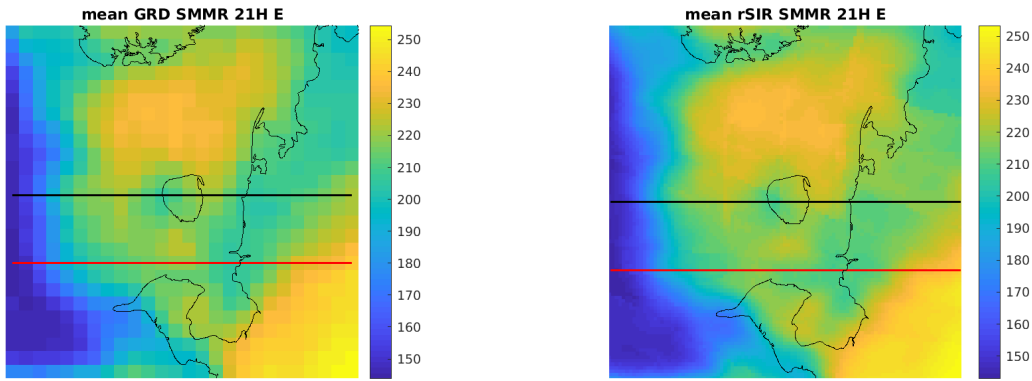


Figure 335: [Repeated] Average of daily  $T_B$  images over the study area. (left) 25-km GRD. (right) 3.125-km rSIR. The thick horizontal lines show the data transect locations where data is extracted from the image for analysis.

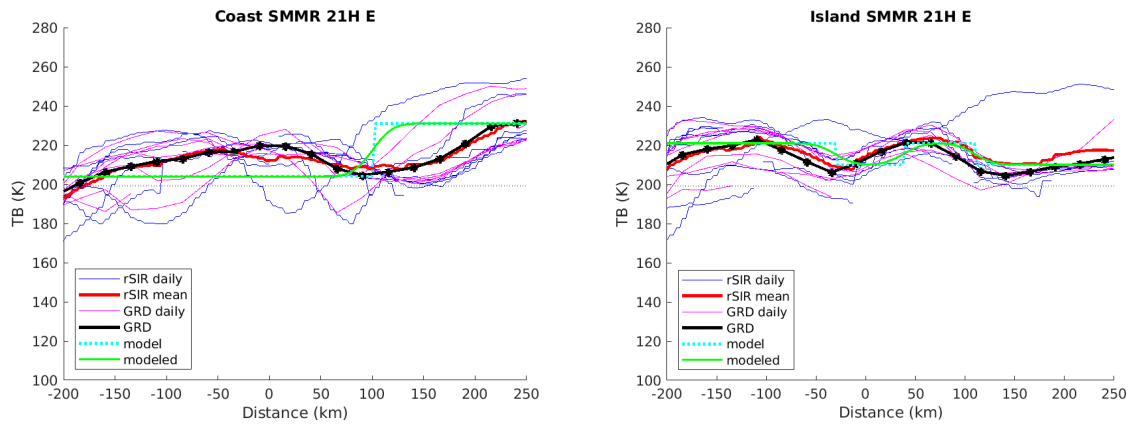


Figure 336: Plots of  $T_B$  along the two analysis case transect lines for the (left) coast-crossing and (right) island-crossing cases.

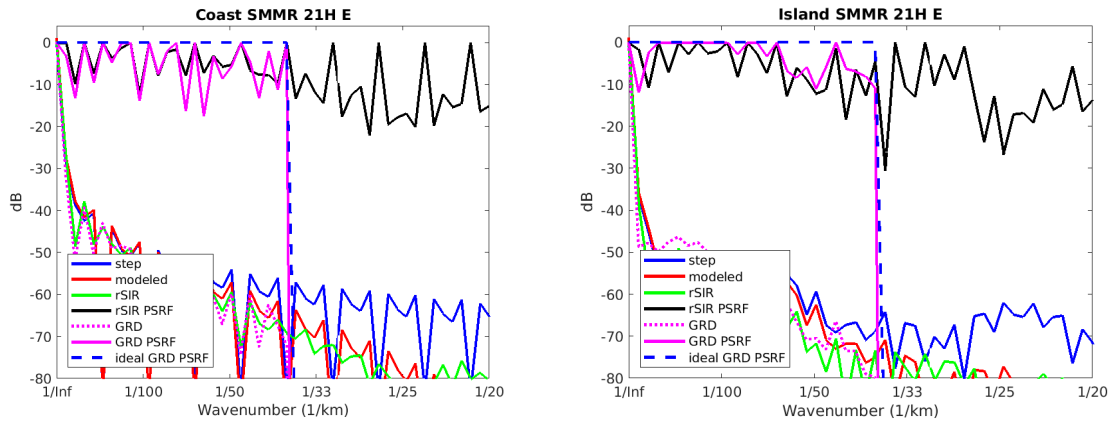


Figure 337: Wavenumber spectra of the  $T_B$  slices, the model, and the PSRF. (left) Coast-crossing case. (right) Island-crossing case.

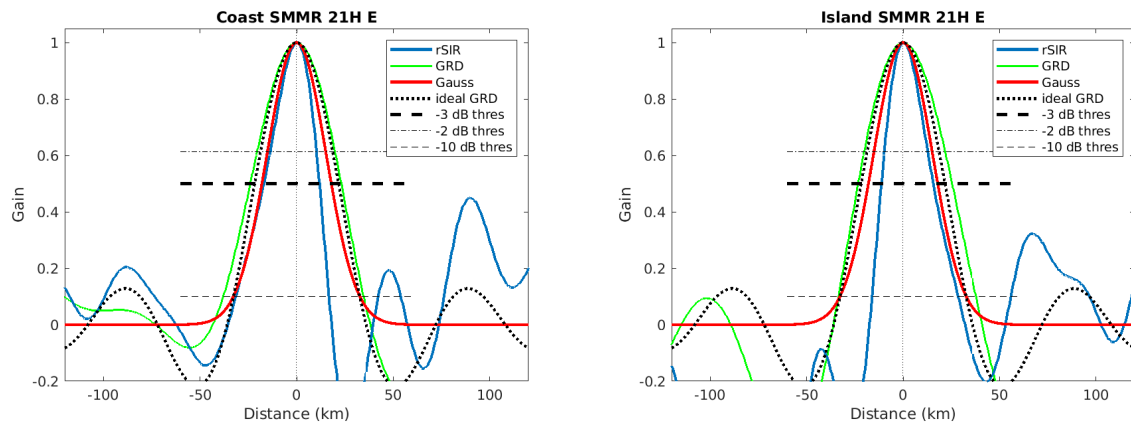


Figure 338: Derived single-pass rSIR and GRD PSRFs from the (left) coast-crossing and (right) island-crossing cases.

Table 116: Resolution estimates for SMMR channel 21H LTOD E

Algorithm	-3 dB Thres		-2 dB Thres		-10 dB Thres	
	Coast	Island	Coast	Island	Coast	Island
Gauss	35.9	35.9	29.3	29.3	65.5	65.5
rSIR	28.8	26.8	23.3	21.9	48.3	44.7
ideal GRD	43.4	43.4	36.3	36.3	65.4	65.4
GRD	47.1	48.8	39.2	40.9	72.7	71.2

## E.14 SMMR Channel 21H M Figures

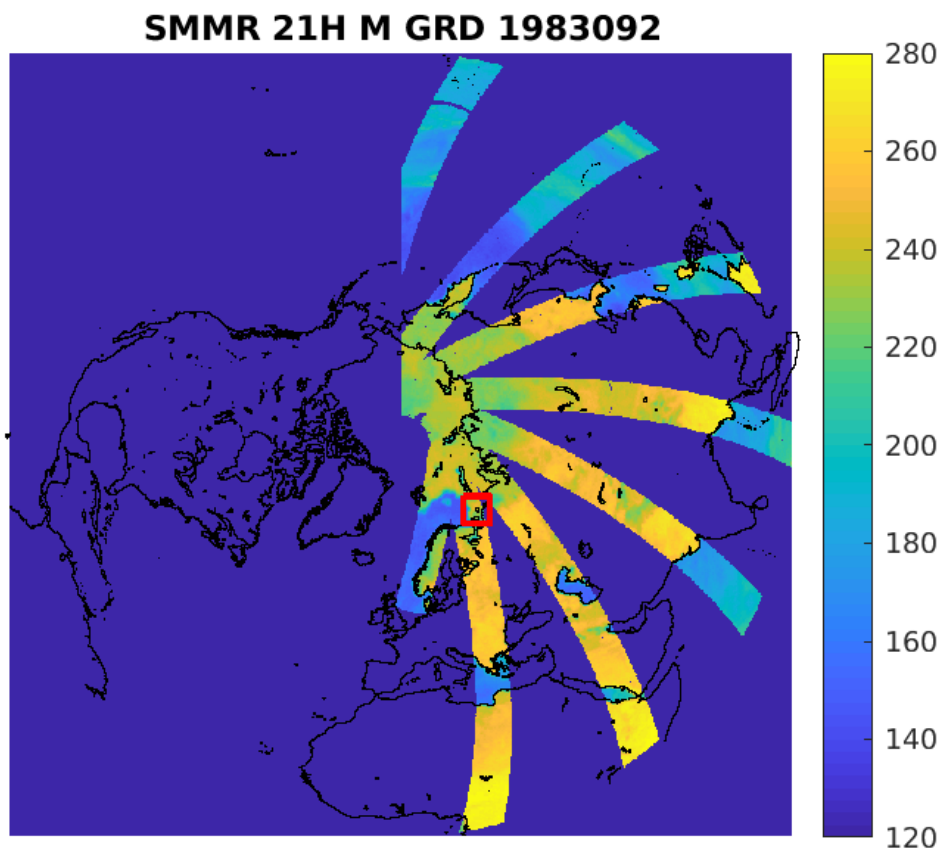


Figure 339: rSIR Northern Hemisphere view.

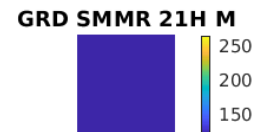
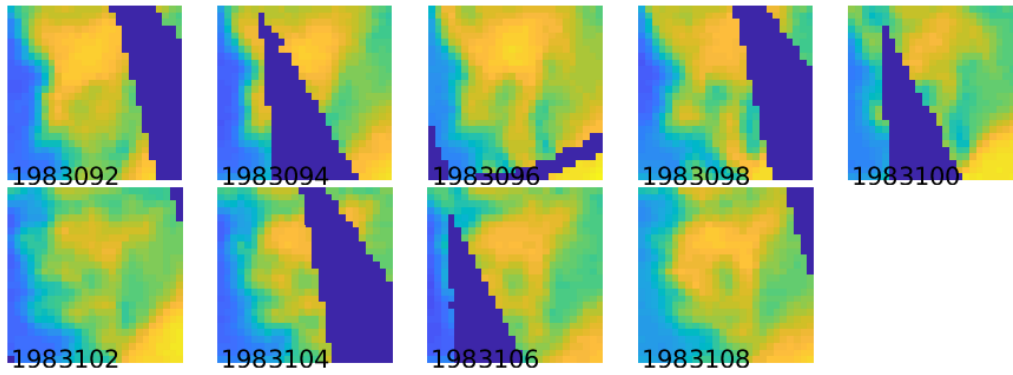
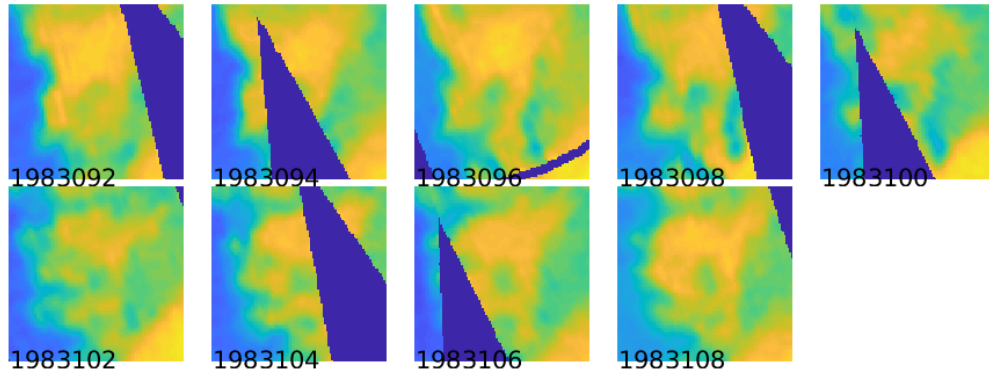


Figure 340: Time series of (top) rSIR and (bottom) GRD  $T_B$  images over the study area. Image dates are labeled on the image.

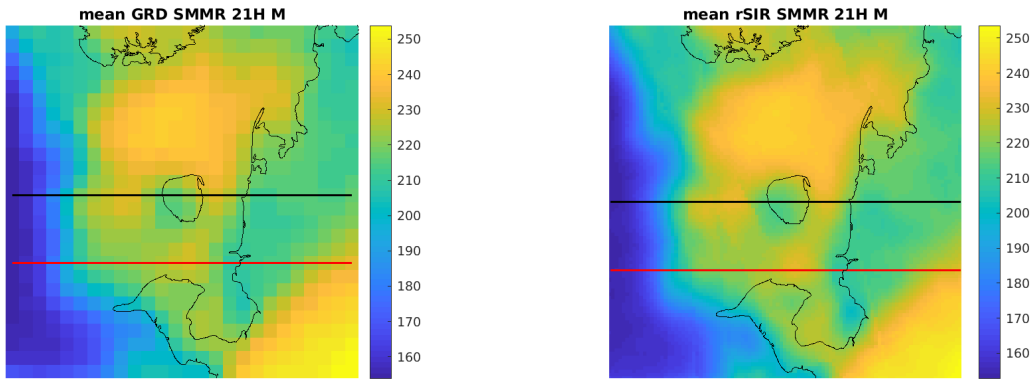


Figure 341: Average of daily  $T_B$  images over the study area. (left) 25-km GRD. (right) 3.125-km rSIR. The thick horizontal lines show the data transect locations where data is extracted from the image for analysis.

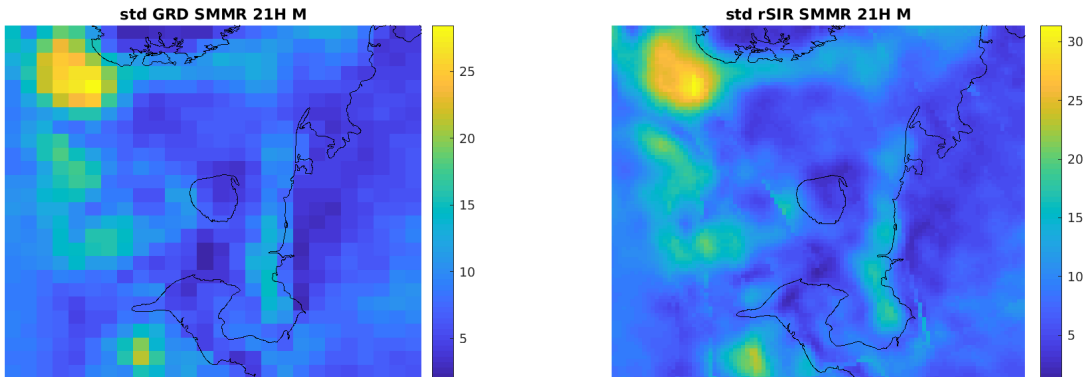


Figure 342: Standard deviation of daily  $T_B$  images over the study area. (left) 25-km GRD. (right) 3.125-km rSIR.

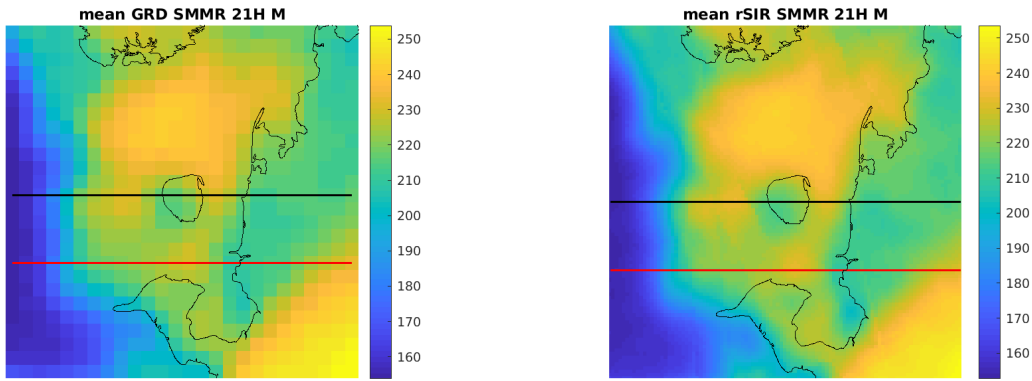


Figure 343: [Repeated] Average of daily  $T_B$  images over the study area. (left) 25-km GRD. (right) 3.125-km rSIR. The thick horizontal lines show the data transect locations where data is extracted from the image for analysis.

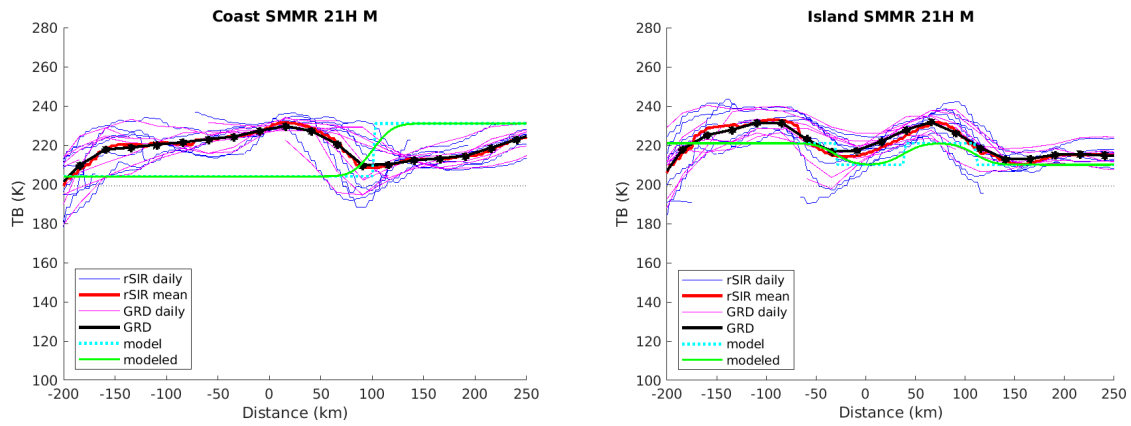


Figure 344: Plots of  $T_B$  along the two analysis case transect lines for the (left) coast-crossing and (right) island-crossing cases.

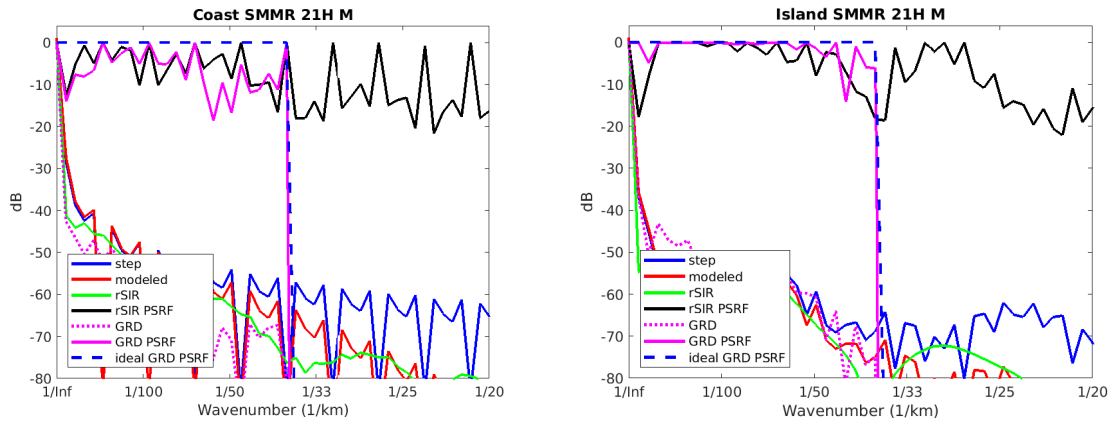


Figure 345: Wavenumber spectra of the  $T_B$  slices, the model, and the PSRF. (left) Coast-crossing case. (right) Island-crossing case.

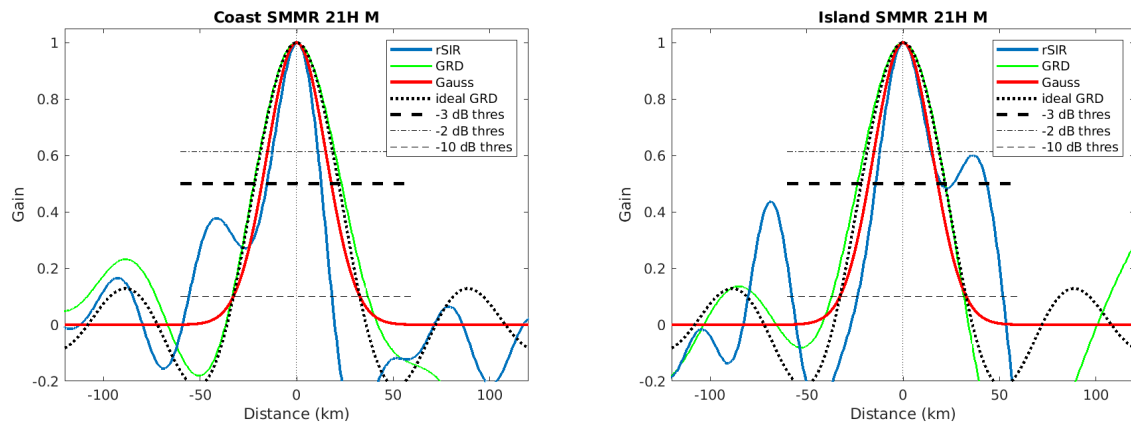


Figure 346: Derived single-pass rSIR and GRD PSRFs from the (left) coast-crossing and (right) island-crossing cases.

Table 117: Resolution estimates for SMMR channel 21H LTOD M

Algorithm	-3 dB Thres		-2 dB Thres		-10 dB Thres	
	Coast	Island	Coast	Island	Coast	Island
Gauss	35.9	35.9	29.3	29.3	65.5	65.5
rSIR	28.0	34.0	22.9	25.7	74.1	75.4
ideal GRD	43.4	43.4	36.3	36.3	65.4	65.4
GRD	45.4	45.5	37.8	38.1	70.2	68.6



## E.15 SMMR Channel 21V E Figures

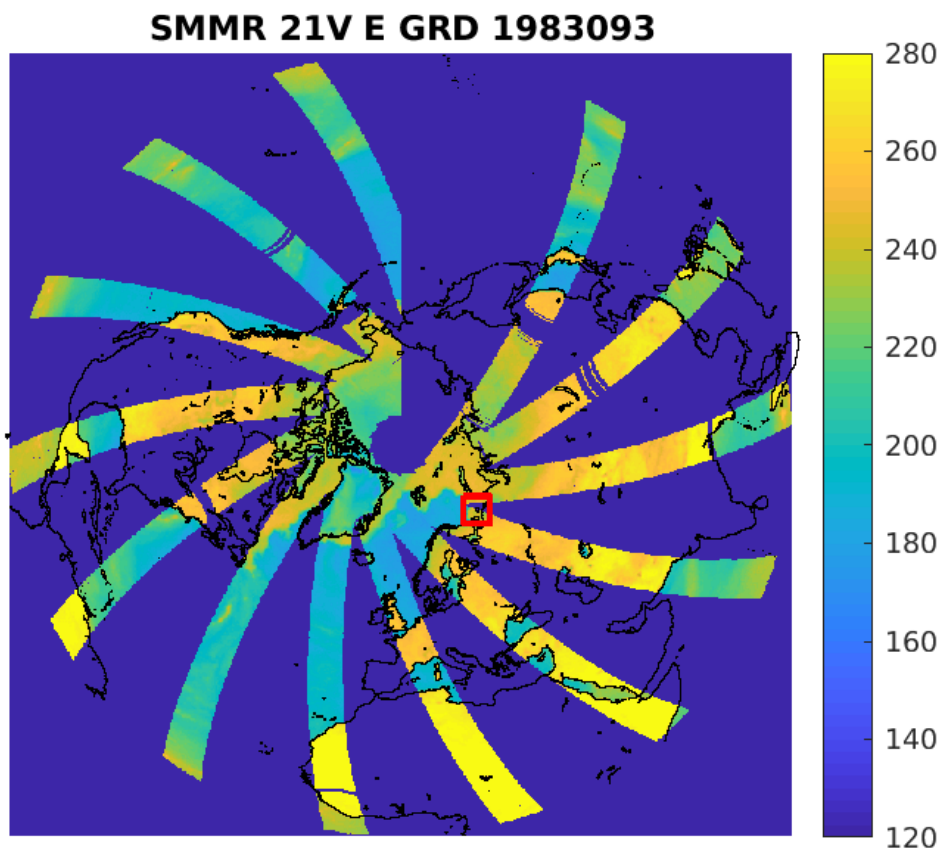


Figure 347: rSIR Northern Hemisphere view.

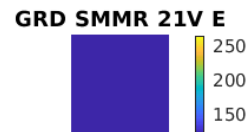
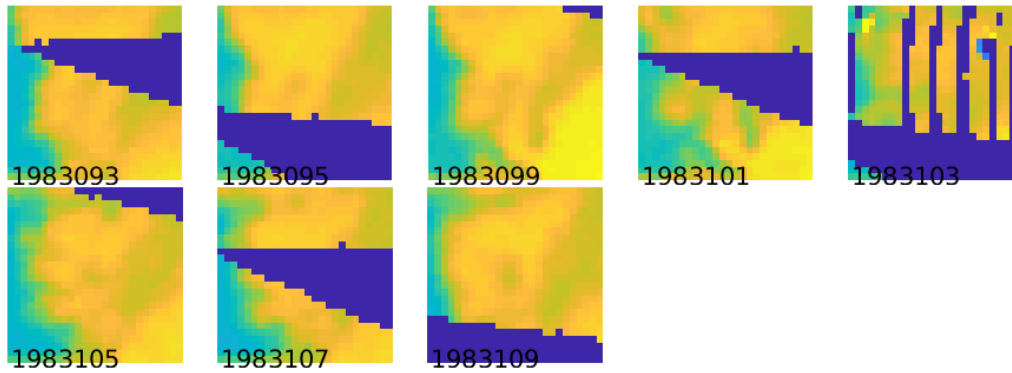
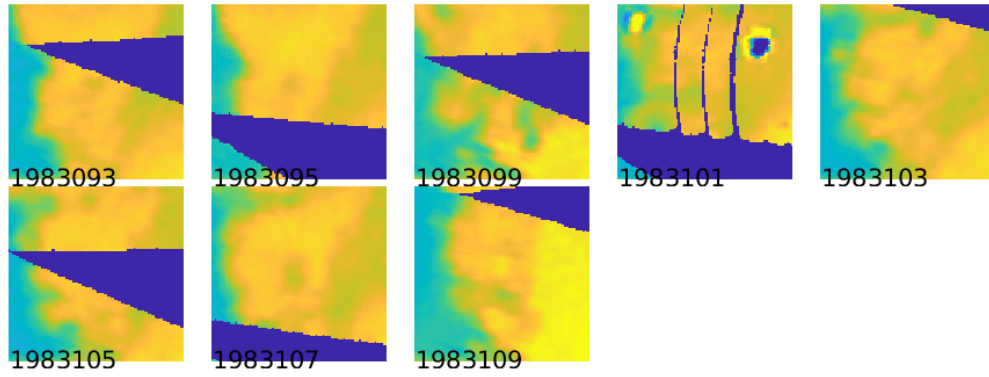


Figure 348: Time series of (top) rSIR and (bottom) GRD  $T_B$  images over the study area. Image dates are labeled on the image.

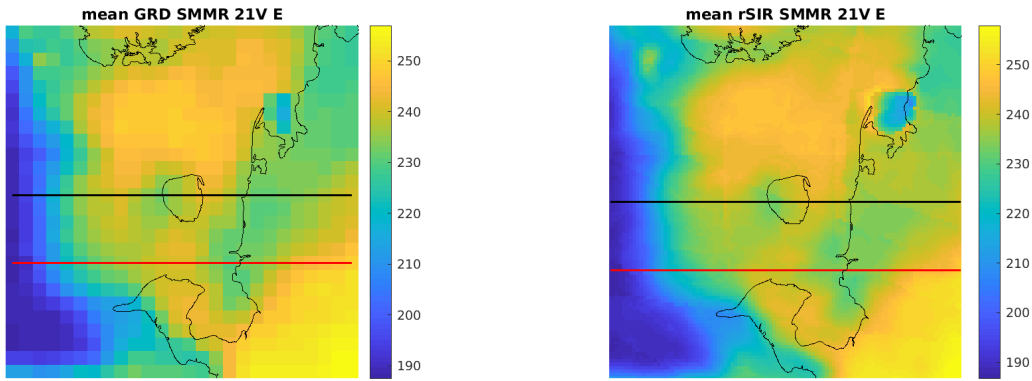


Figure 349: Average of daily  $T_B$  images over the study area. (left) 25-km GRD. (right) 3.125-km rSIR. The thick horizontal lines show the data transect locations where data is extracted from the image for analysis.

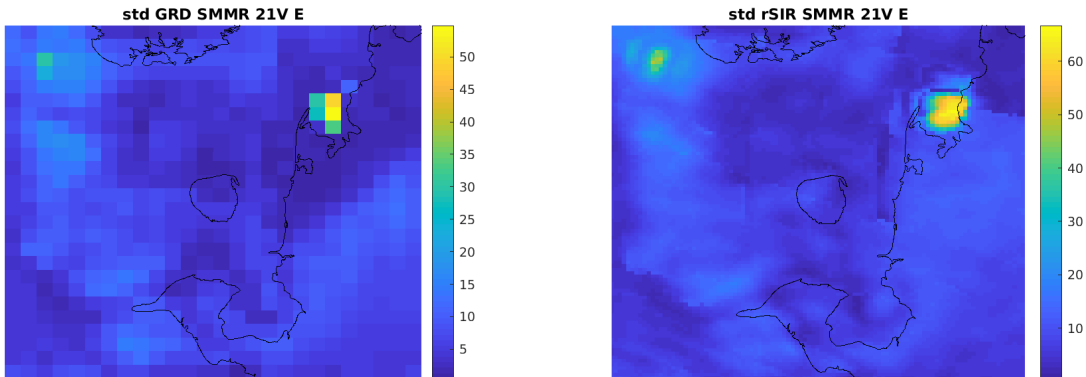


Figure 350: Standard deviation of daily  $T_B$  images over the study area. (left) 25-km GRD. (right) 3.125-km rSIR.

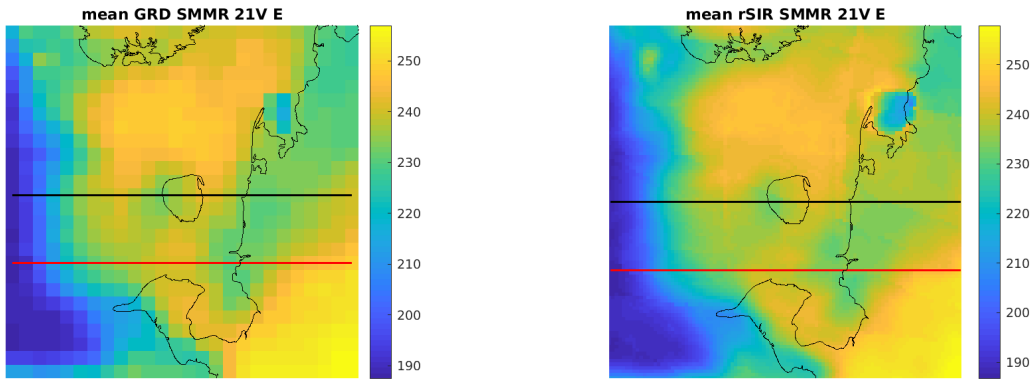


Figure 351: [Repeated] Average of daily  $T_B$  images over the study area. (left) 25-km GRD. (right) 3.125-km rSIR. The thick horizontal lines show the data transect locations where data is extracted from the image for analysis.

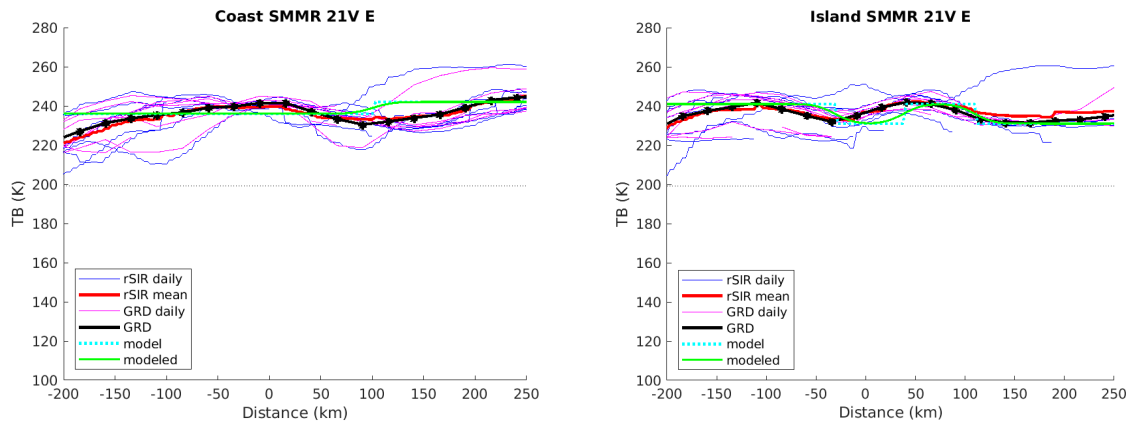


Figure 352: Plots of  $T_B$  along the two analysis case transect lines for the (left) coast-crossing and (right) island-crossing cases.

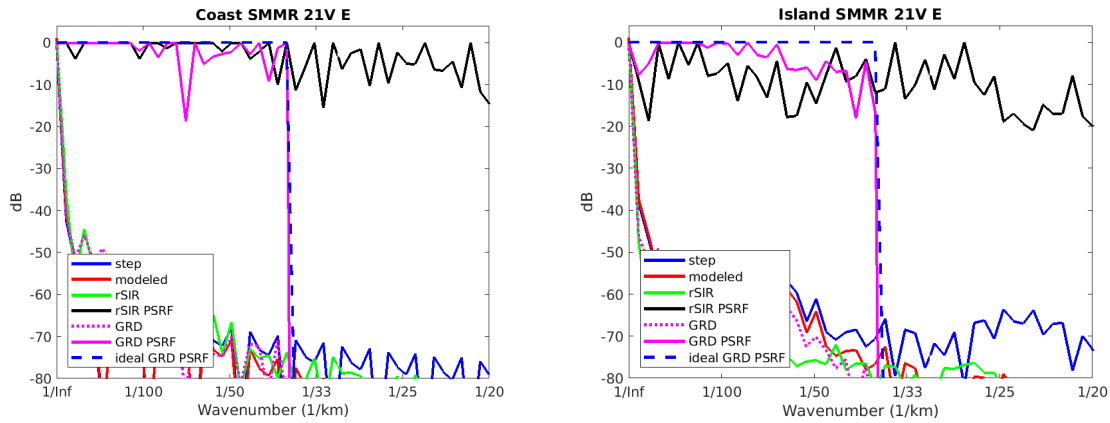


Figure 353: Wavenumber spectra of the  $T_B$  slices, the model, and the PSRF. (left) Coast-crossing case. (right) Island-crossing case.

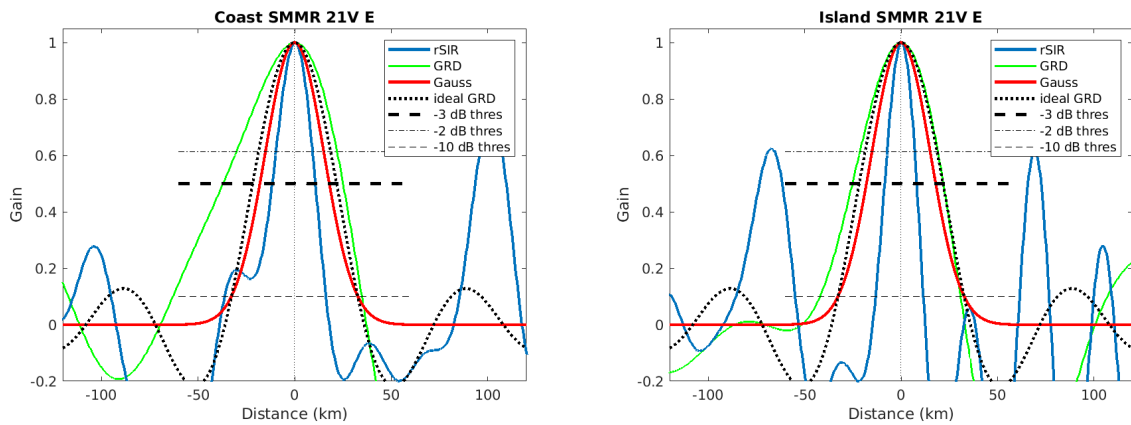


Figure 354: Derived single-pass rSIR and GRD PSRFs from the (left) coast-crossing and (right) island-crossing cases.

Table 118: Resolution estimates for SMMR channel 21V LTOD E

Algorithm	-3 dB Thres		-2 dB Thres		-10 dB Thres	
	Coast	Island	Coast	Island	Coast	Island
Gauss	35.9	35.9	29.3	29.3	65.5	65.5
rSIR	22.3	16.7	18.4	14.0	52.4	24.8
ideal GRD	43.4	43.4	36.3	36.3	65.4	65.4
GRD	62.1	47.2	50.5	39.4	97.8	72.9

## E.16 SMMR Channel 21V M Figures

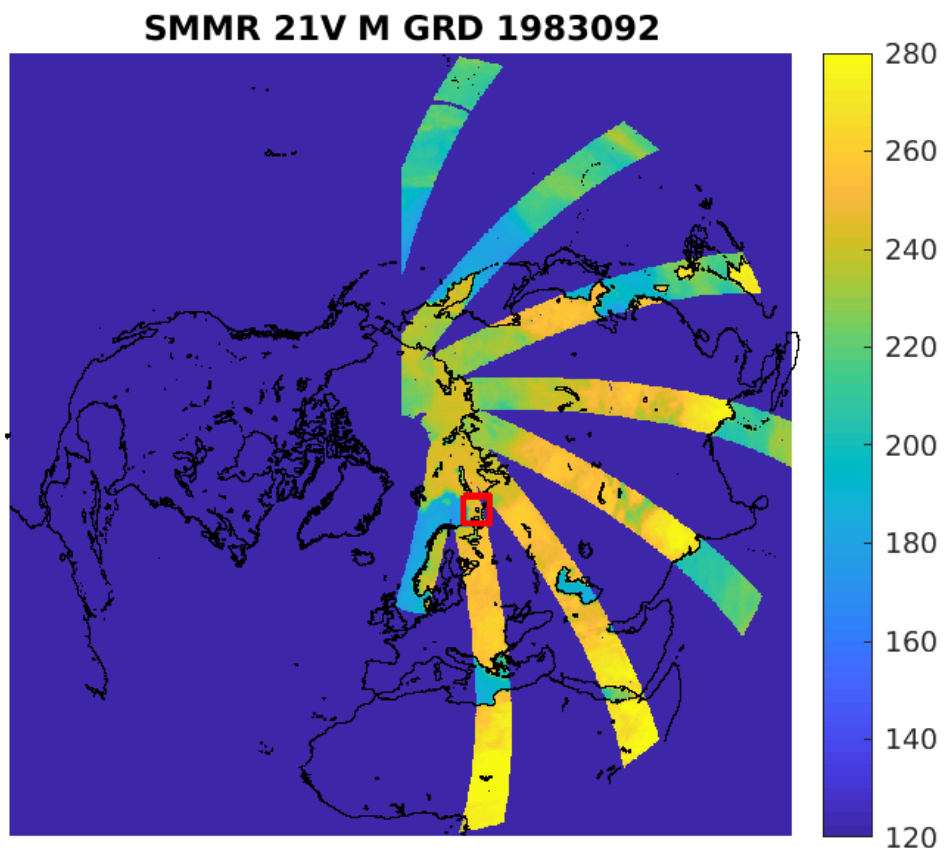


Figure 355: rSIR Northern Hemisphere view.

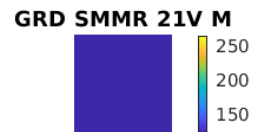
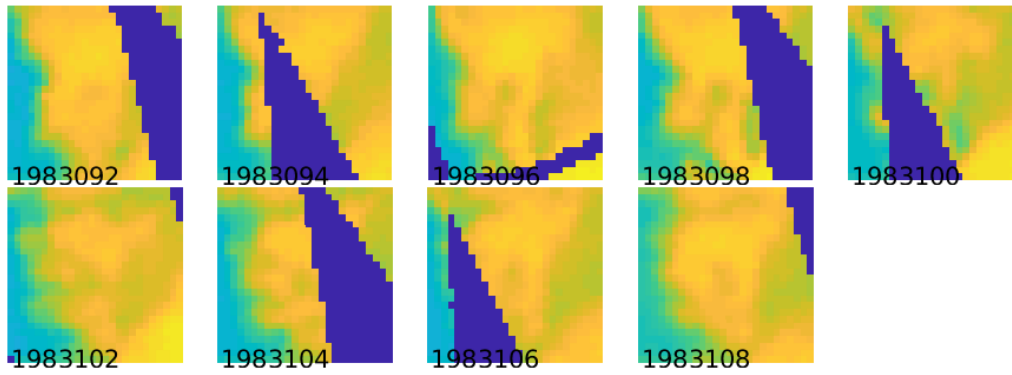
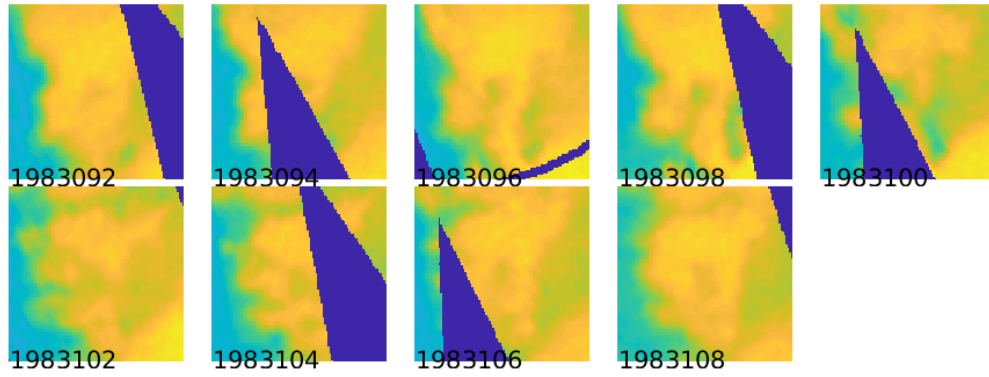


Figure 356: Time series of (top) rSIR and (bottom) GRD  $T_B$  images over the study area. Image dates are labeled on the image.

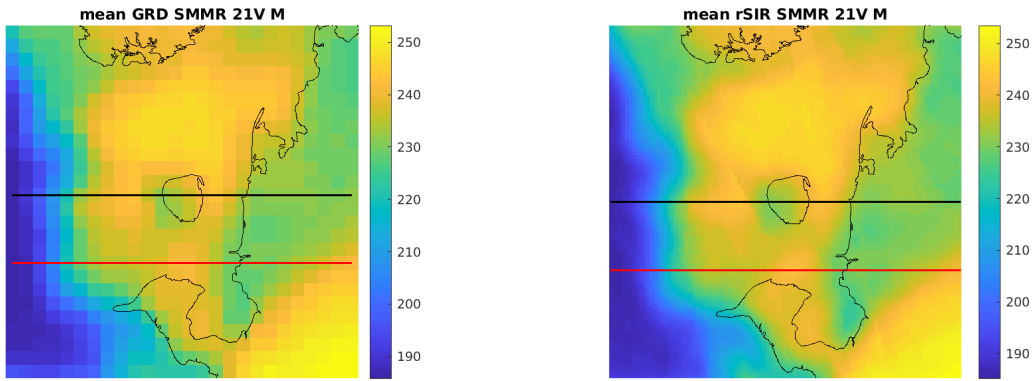


Figure 357: Average of daily  $T_B$  images over the study area. (left) 25-km GRD. (right) 3.125-km rSIR. The thick horizontal lines show the data transect locations where data is extracted from the image for analysis.

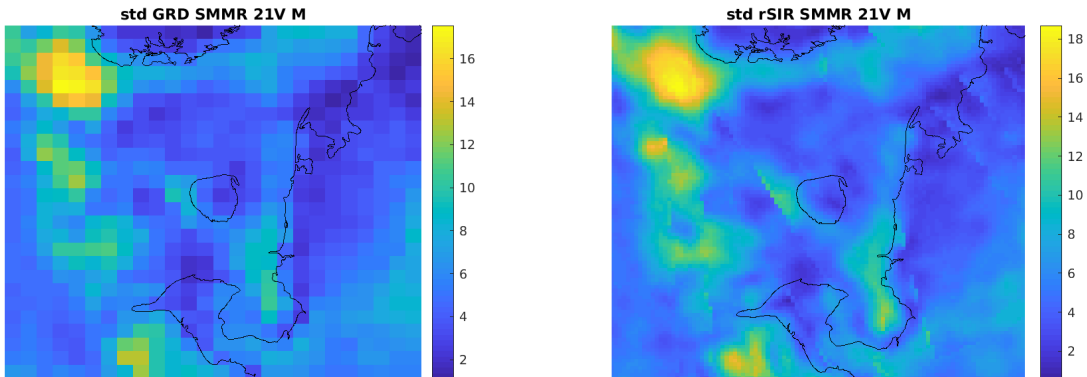


Figure 358: Standard deviation of daily  $T_B$  images over the study area. (left) 25-km GRD. (right) 3.125-km rSIR.



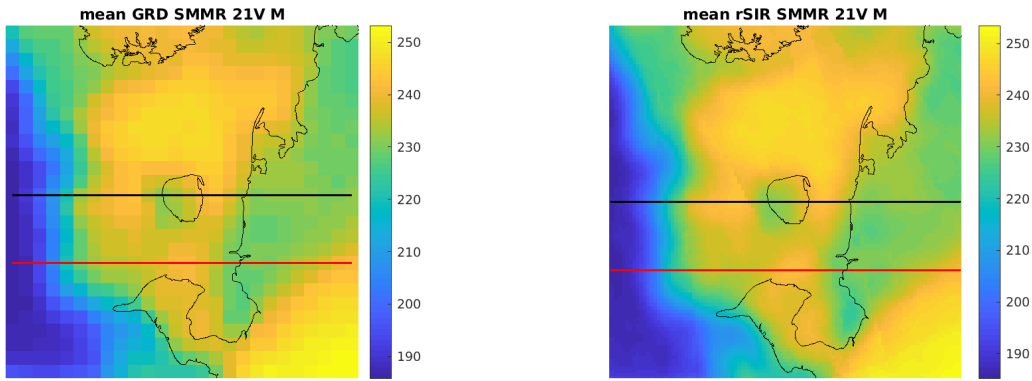


Figure 359: [Repeated] Average of daily  $T_B$  images over the study area. (left) 25-km GRD. (right) 3.125-km rSIR. The thick horizontal lines show the data transect locations where data is extracted from the image for analysis.

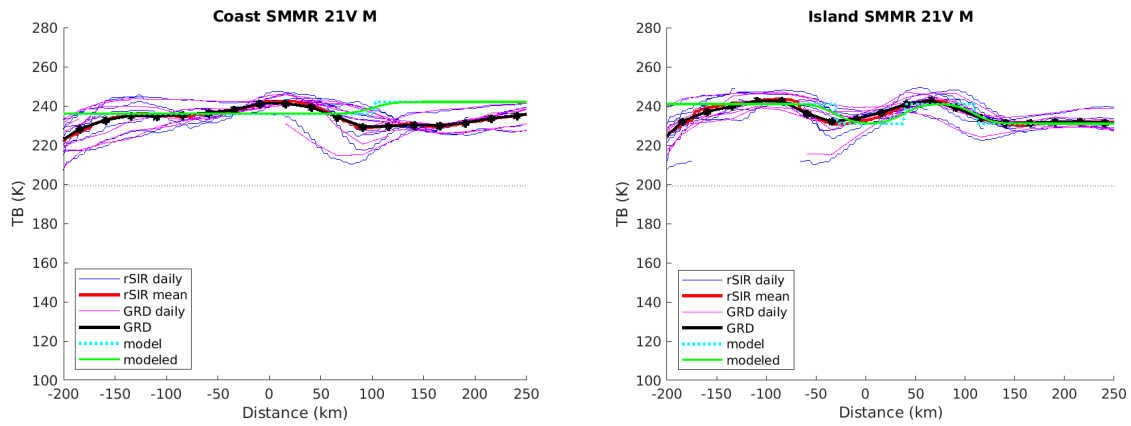


Figure 360: Plots of  $T_B$  along the two analysis case transect lines for the (left) coast-crossing and (right) island-crossing cases.

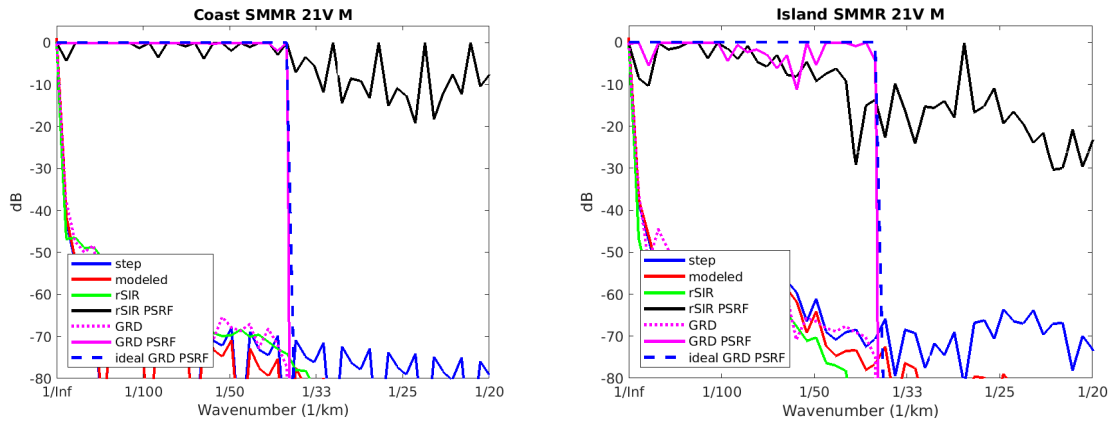


Figure 361: Wavenumber spectra of the  $T_B$  slices, the model, and the PSRF. (left) Coast-crossing case. (right) Island-crossing case.

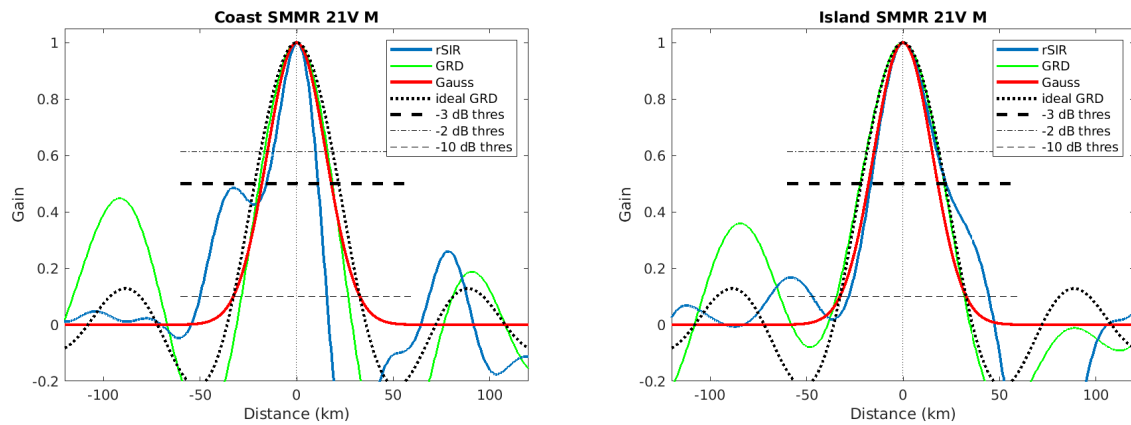


Figure 362: Derived single-pass rSIR and GRD PSRFs from the (left) coast-crossing and (right) island-crossing cases.

Table 119: Resolution estimates for SMMR channel 21V LTOD M

Algorithm	-3 dB Thres		-2 dB Thres		-10 dB Thres	
	Coast	Island	Coast	Island	Coast	Island
Gauss	35.9	35.9	29.3	29.3	65.5	65.5
rSIR	26.8	39.1	21.2	30.8	65.7	72.7
ideal GRD	43.4	43.4	36.3	36.3	65.4	65.4
GRD	38.0	43.6	31.9	36.4	55.2	66.3

## E.17 SMMR Channel 37H E Figures

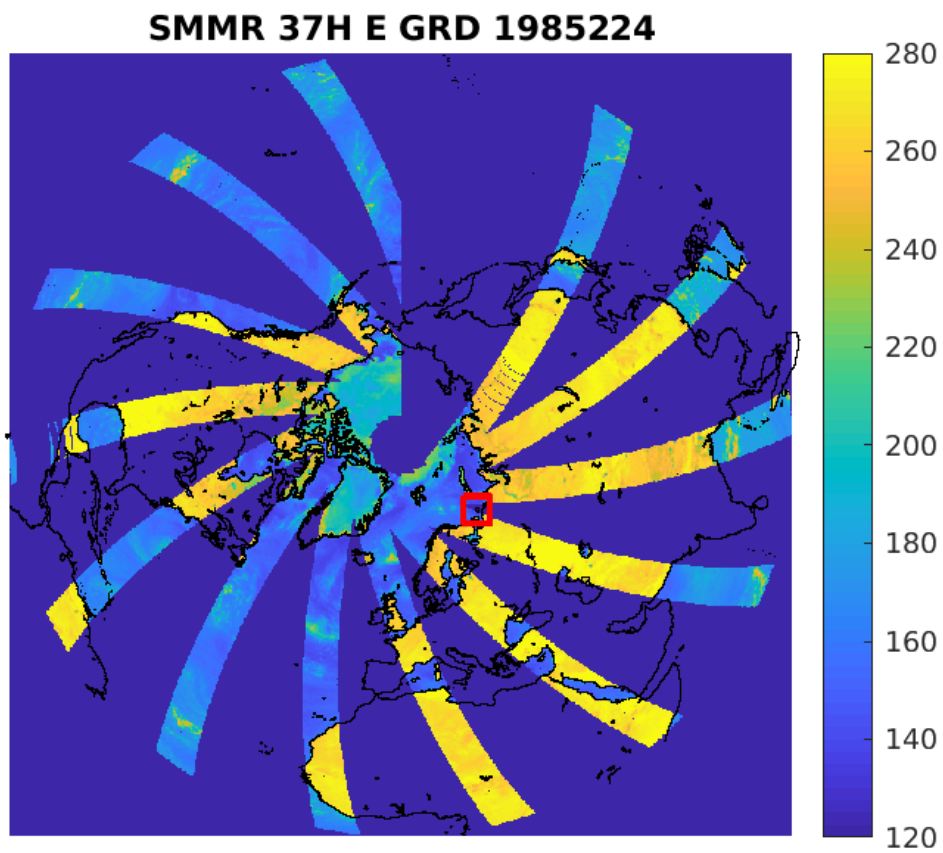


Figure 363: rSIR Northern Hemisphere view.

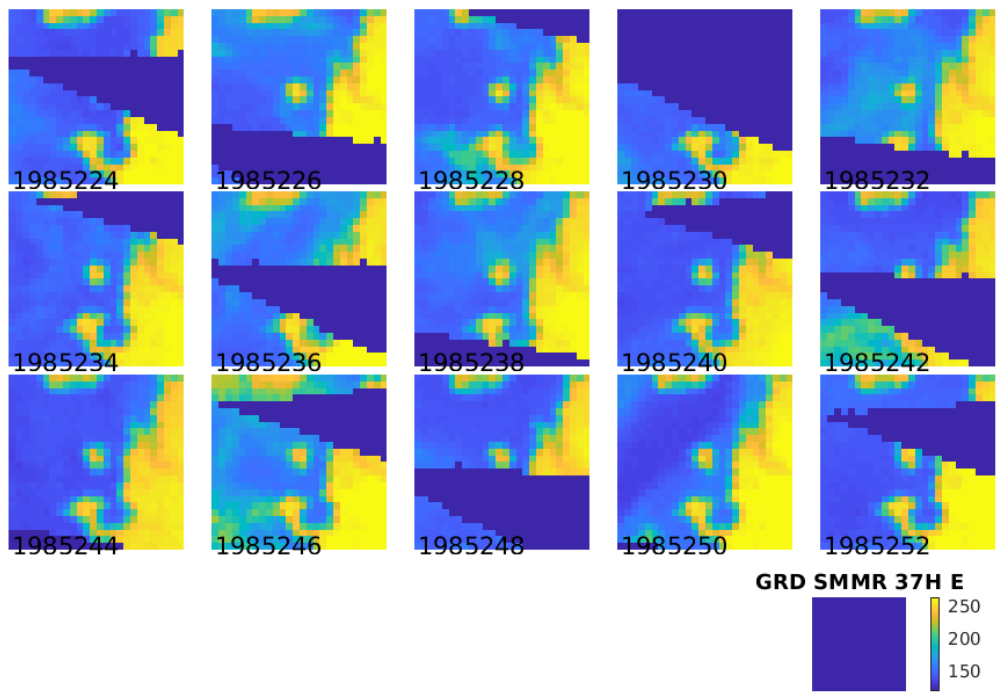
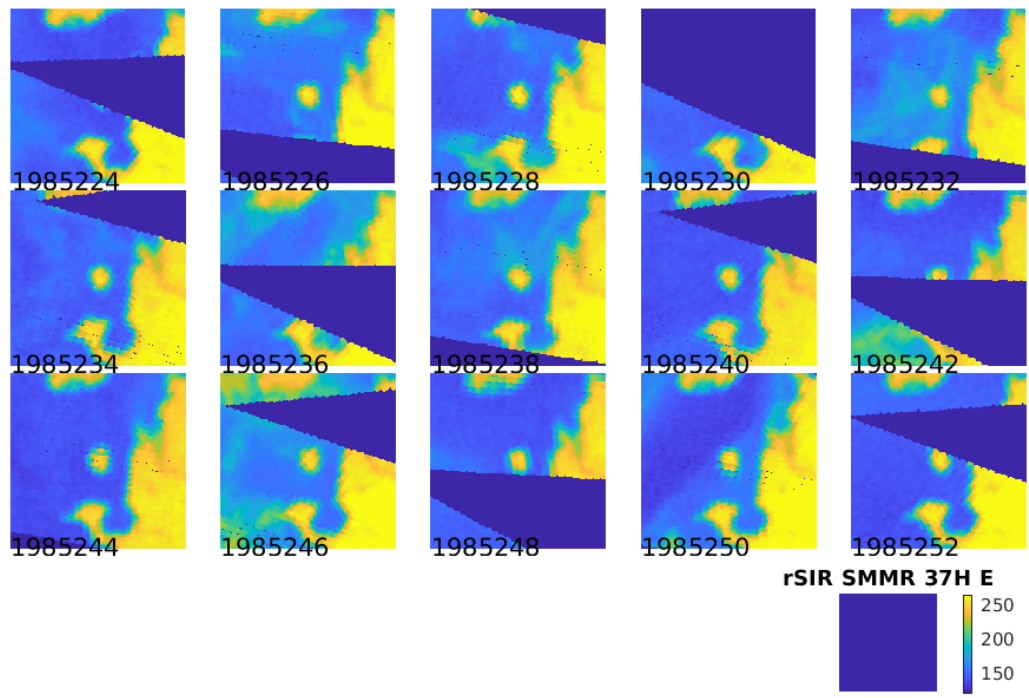


Figure 364: Time series of (top) rSIR and (bottom) GRD  $T_B$  images over the study area. Image dates are labeled on the image.

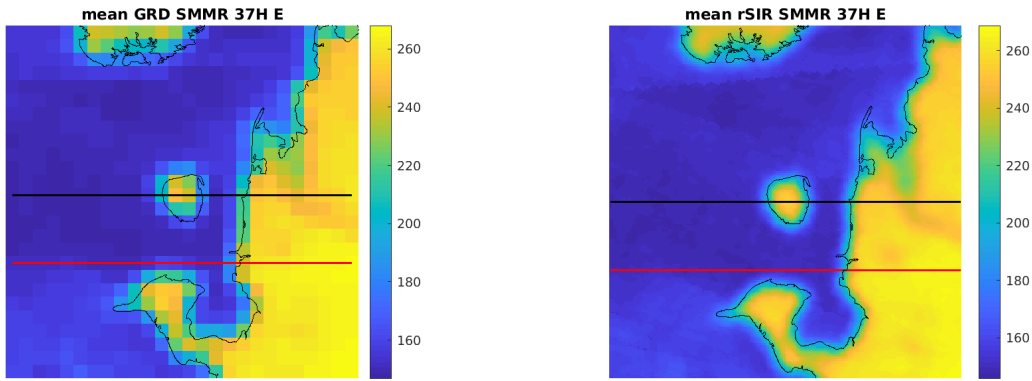


Figure 365: Average of daily  $T_B$  images over the study area. (left) 25-km GRD. (right) 3.125-km rSIR. The thick horizontal lines show the data transect locations where data is extracted from the image for analysis.

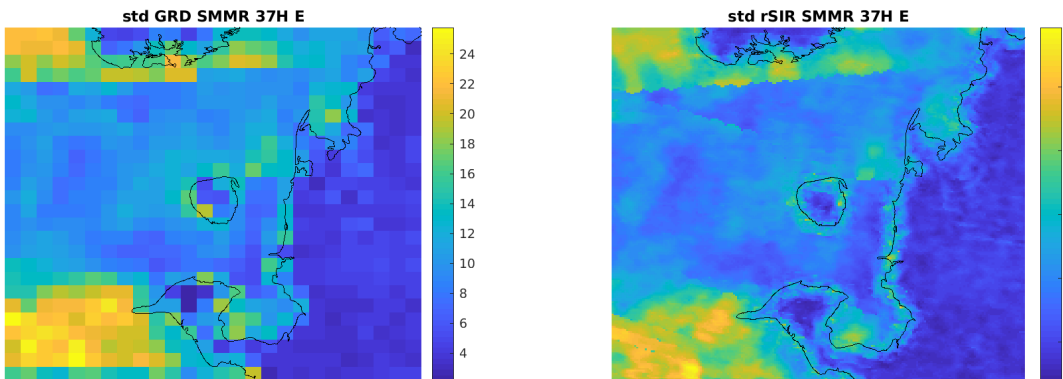


Figure 366: Standard deviation of daily  $T_B$  images over the study area. (left) 25-km GRD. (right) 3.125-km rSIR.

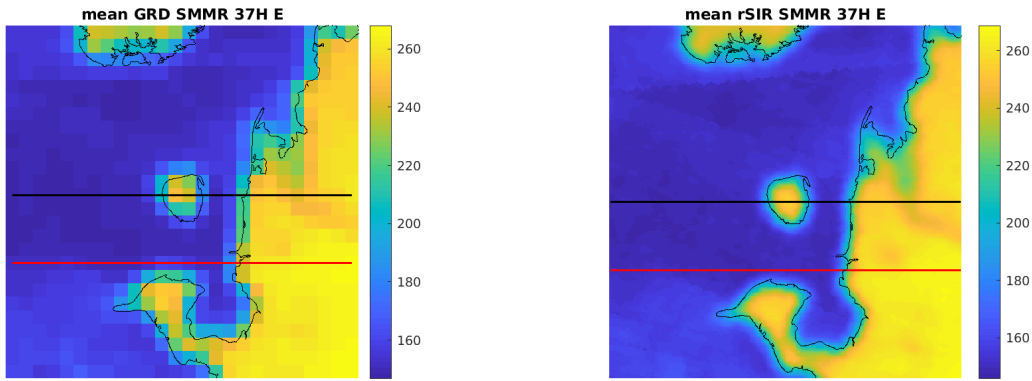


Figure 367: [Repeated] Average of daily  $T_B$  images over the study area. (left) 25-km GRD. (right) 3.125-km rSIR. The thick horizontal lines show the data transect locations where data is extracted from the image for analysis.

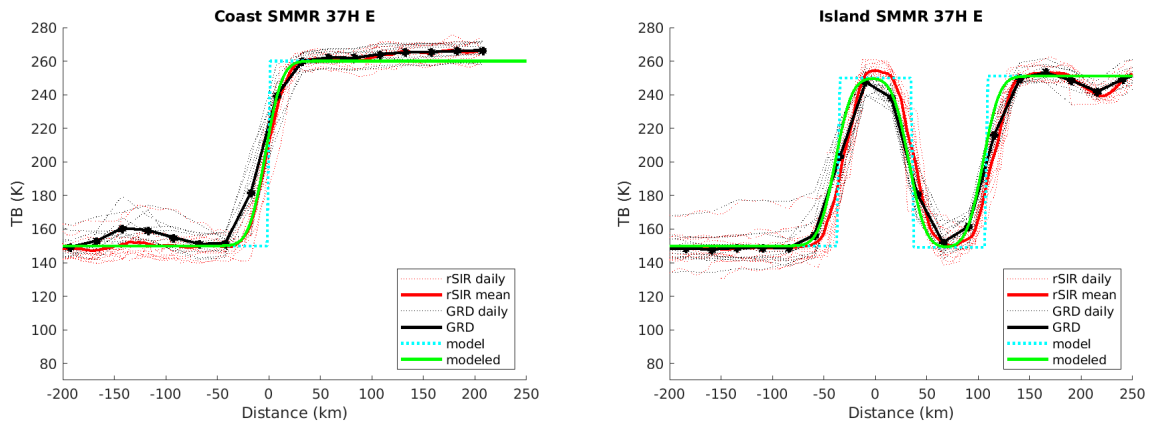


Figure 368: Plots of  $T_B$  along the two analysis case transect lines for the (left) coast-crossing and (right) island-crossing cases.

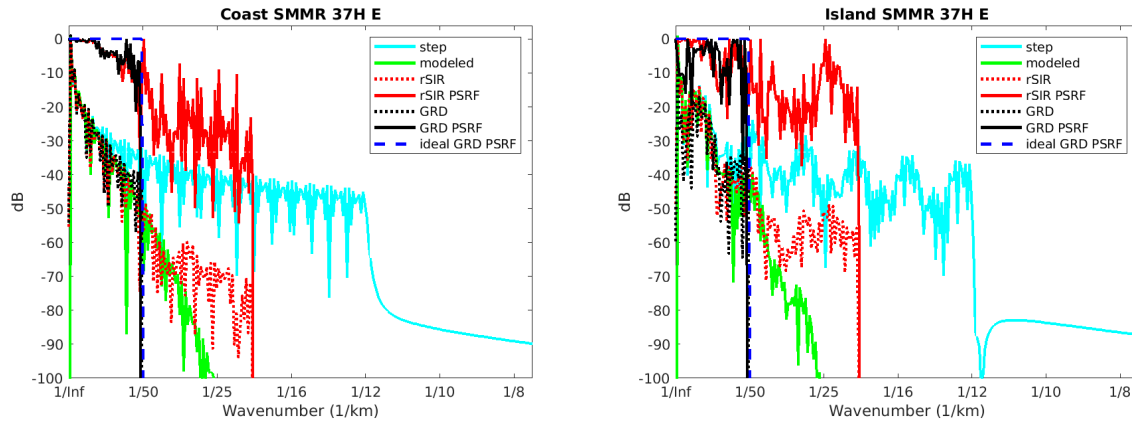


Figure 369: Wavenumber spectra of the  $T_B$  slices, the model, and the PSRF. (left) Coast-crossing case. (right) Island-crossing case.

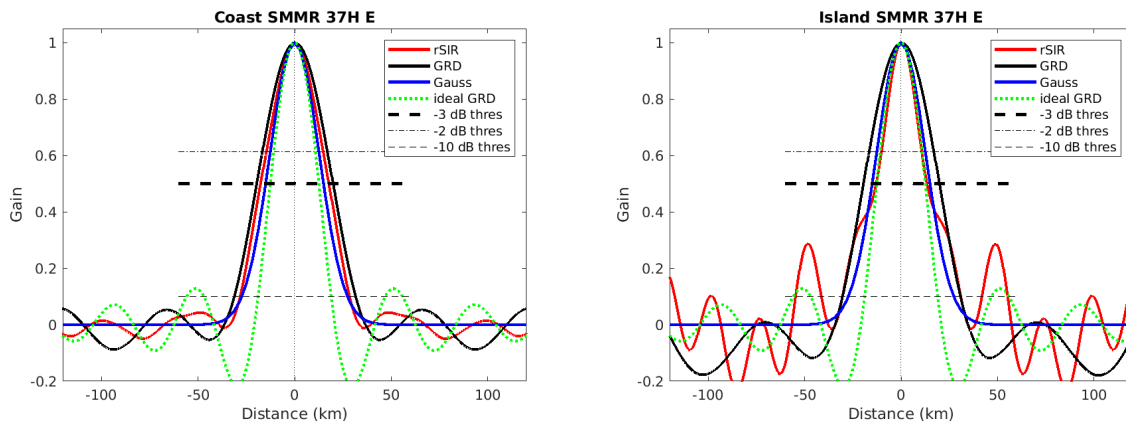


Figure 370: Derived single-pass rSIR and GRD PSRFs from the (left) coast-crossing and (right) island-crossing cases.

Table 120: Resolution estimates for SMMR channel 37H LTOD E

Algorithm	-3 dB Thres		-2 dB Thres		-10 dB Thres	
	Coast	Island	Coast	Island	Coast	Island
Gauss	30.0	30.0	24.4	24.4	54.8	54.8
rSIR	35.3	26.4	28.5	20.2	56.7	61.4
ideal GRD	36.2	36.2	30.3	30.3	54.5	54.5
GRD	39.5	39.3	32.7	32.7	62.9	61.2

## E.18 SMMR Channel 37H M Figures

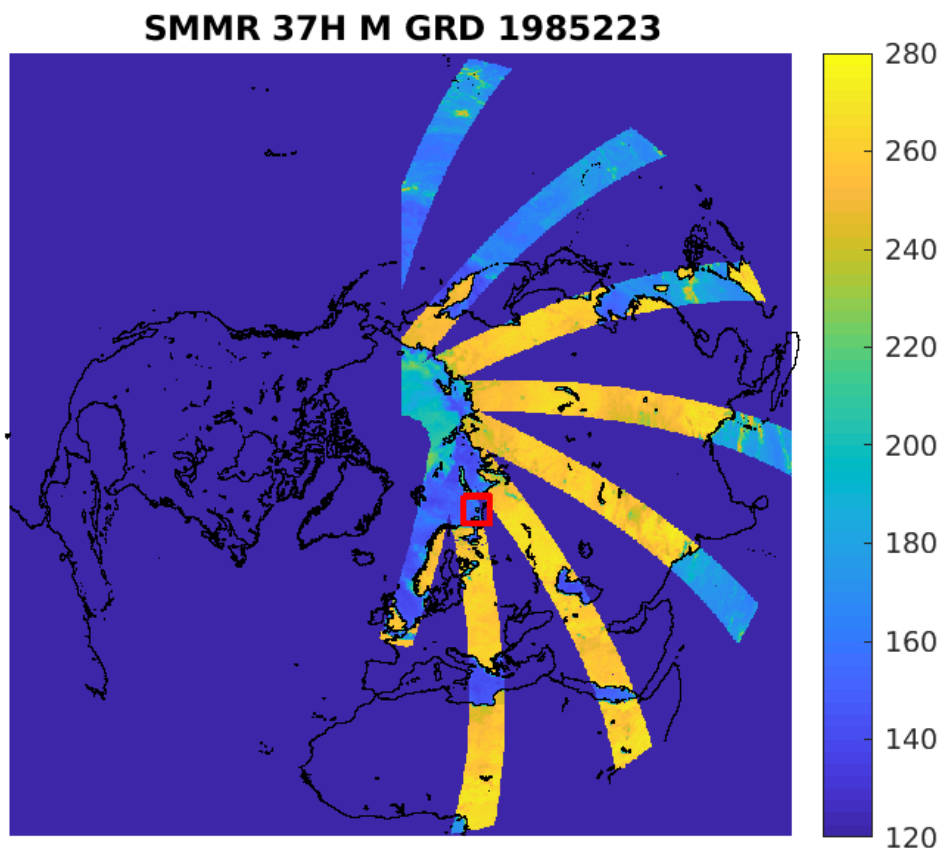


Figure 371: rSIR Northern Hemisphere view.



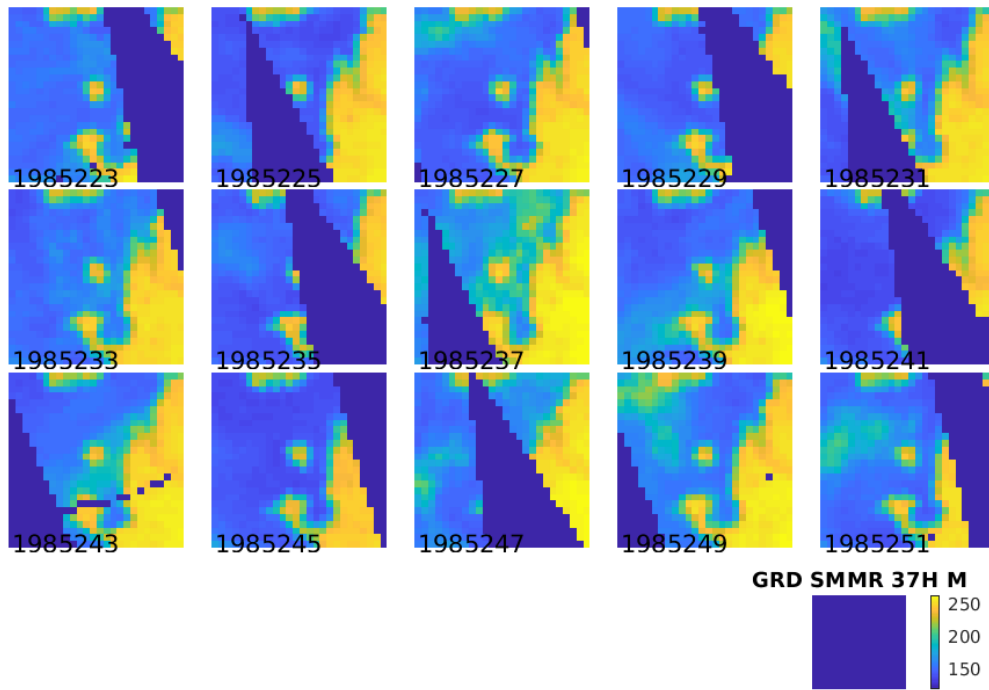
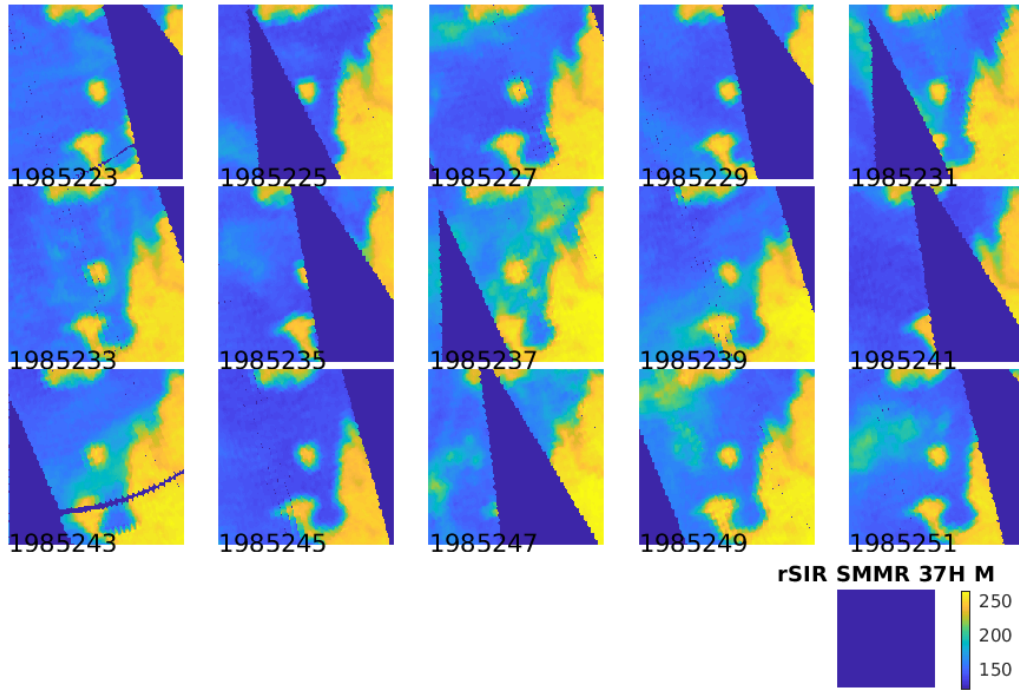


Figure 372: Time series of (top) rSIR and (bottom) GRD  $T_B$  images over the study area. Image dates are labeled on the image.

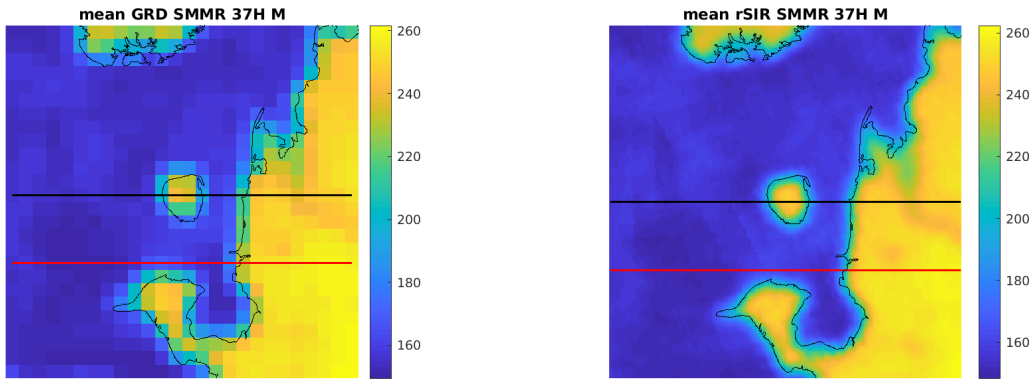


Figure 373: Average of daily  $T_B$  images over the study area. (left) 25-km GRD. (right) 3.125-km rSIR. The thick horizontal lines show the data transect locations where data is extracted from the image for analysis.

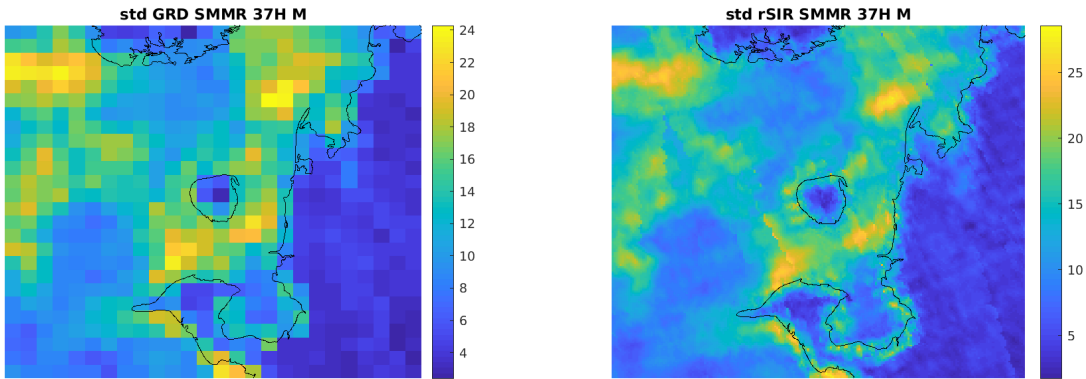


Figure 374: Standard deviation of daily  $T_B$  images over the study area. (left) 25-km GRD. (right) 3.125-km rSIR.

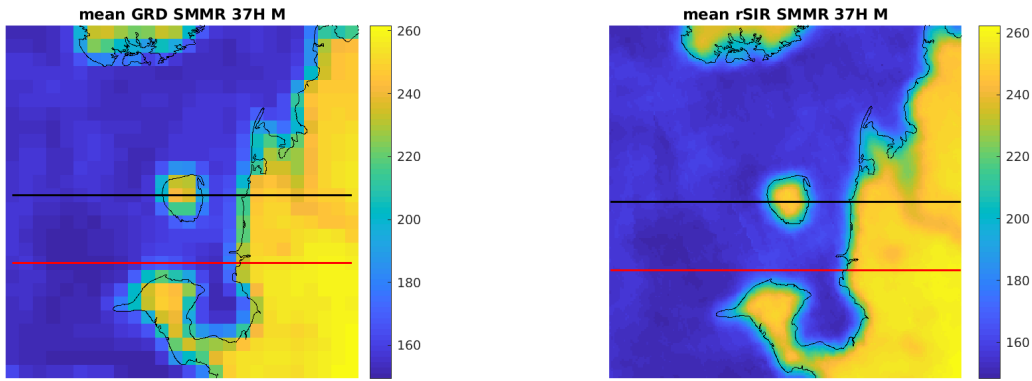


Figure 375: [Repeated] Average of daily  $T_B$  images over the study area. (left) 25-km GRD. (right) 3.125-km rSIR. The thick horizontal lines show the data transect locations where data is extracted from the image for analysis.

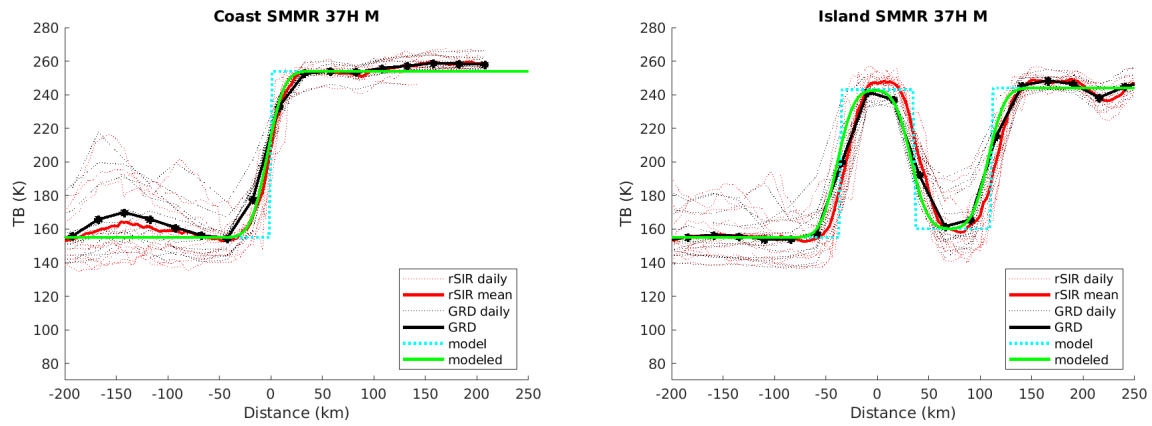


Figure 376: Plots of  $T_B$  along the two analysis case transect lines for the (left) coast-crossing and (right) island-crossing cases.

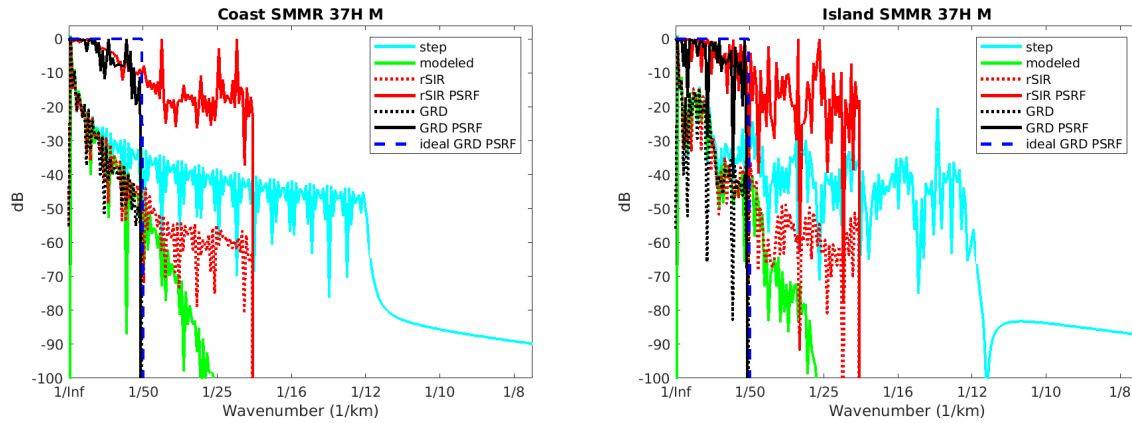


Figure 377: Wavenumber spectra of the  $T_B$  slices, the model, and the PSRF. (left) Coast-crossing case. (right) Island-crossing case.

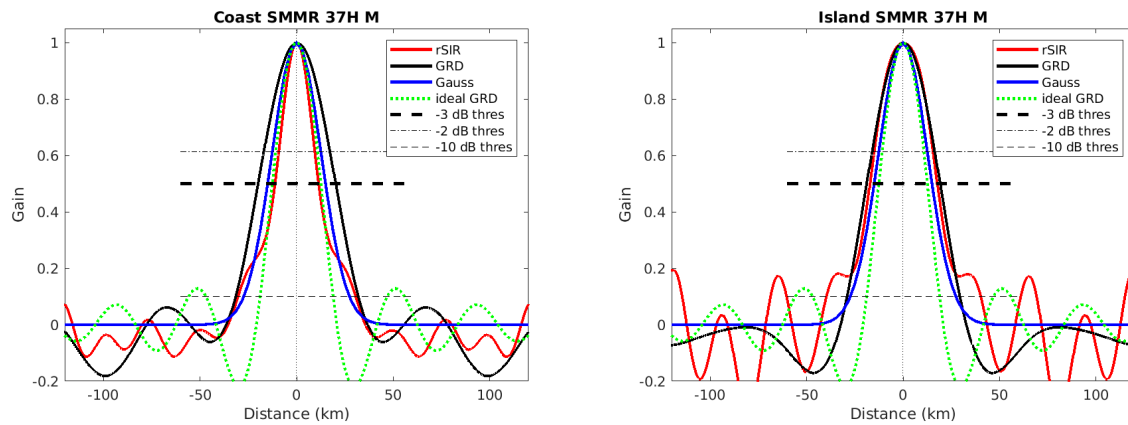


Figure 378: Derived single-pass rSIR and GRD PSRFs from the (left) coast-crossing and (right) island-crossing cases.

Table 121: Resolution estimates for SMMR channel 37H LTOD M

Algorithm	-3 dB Thres		-2 dB Thres		-10 dB Thres	
	Coast	Island	Coast	Island	Coast	Island
Gauss	30.0	30.0	24.4	24.4	54.8	54.8
rSIR	22.6	34.9	18.0	29.9	60.9	79.9
ideal GRD	36.2	36.2	30.3	30.3	54.5	54.5
GRD	40.1	38.0	33.3	31.7	63.5	58.5

## E.19 SMMR Channel 37V E Figures

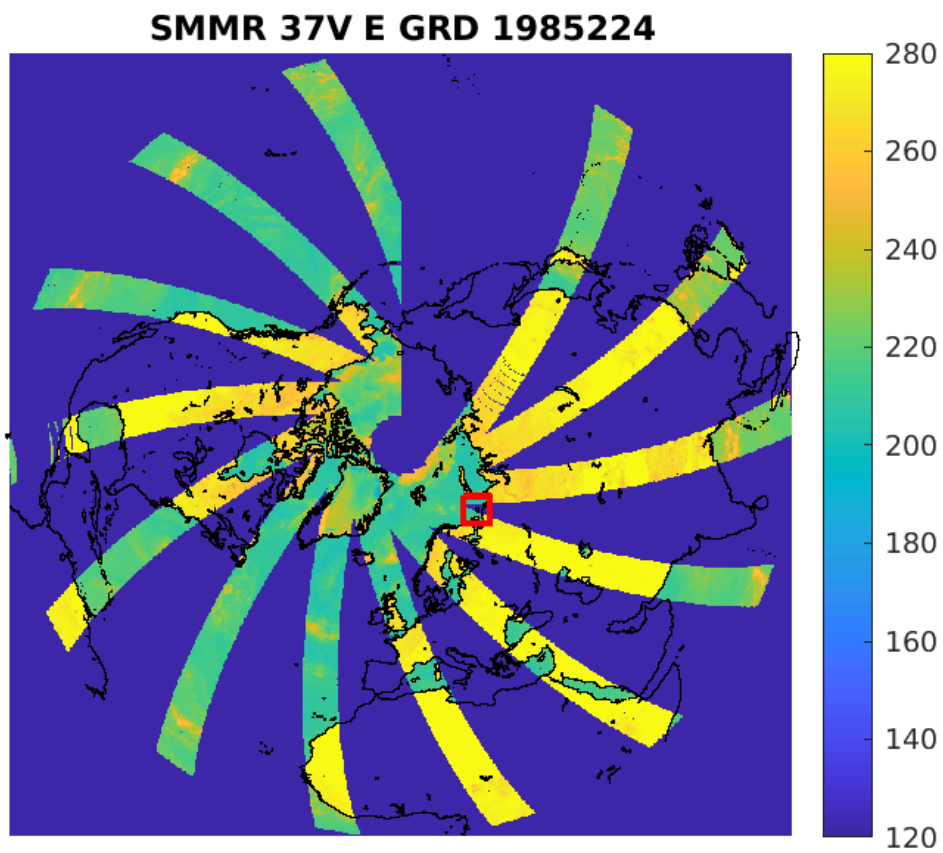


Figure 379: rSIR Northern Hemisphere view.

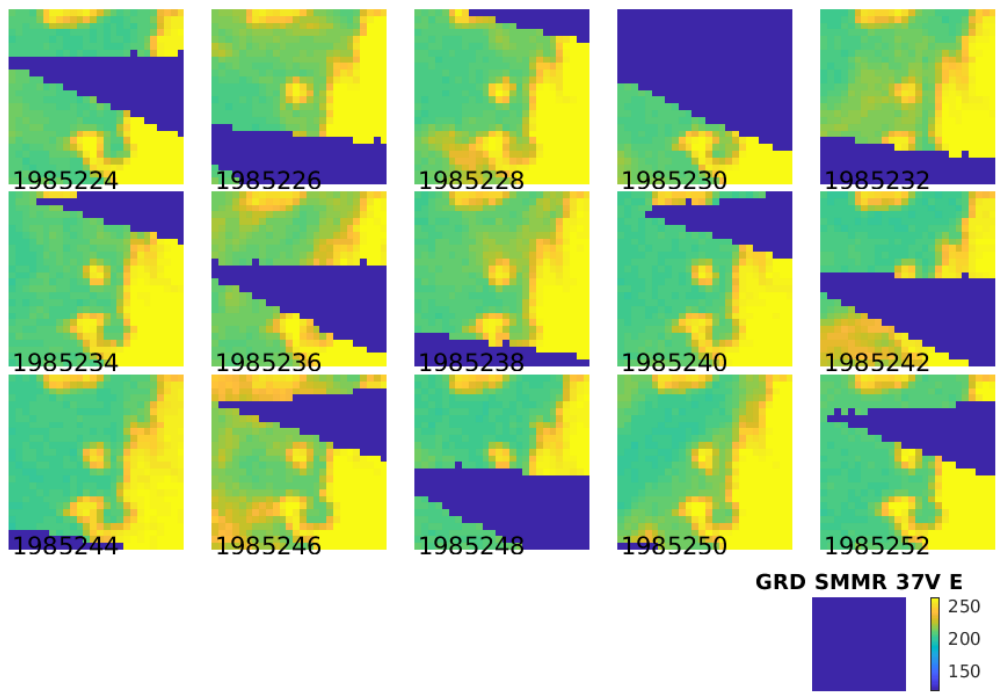
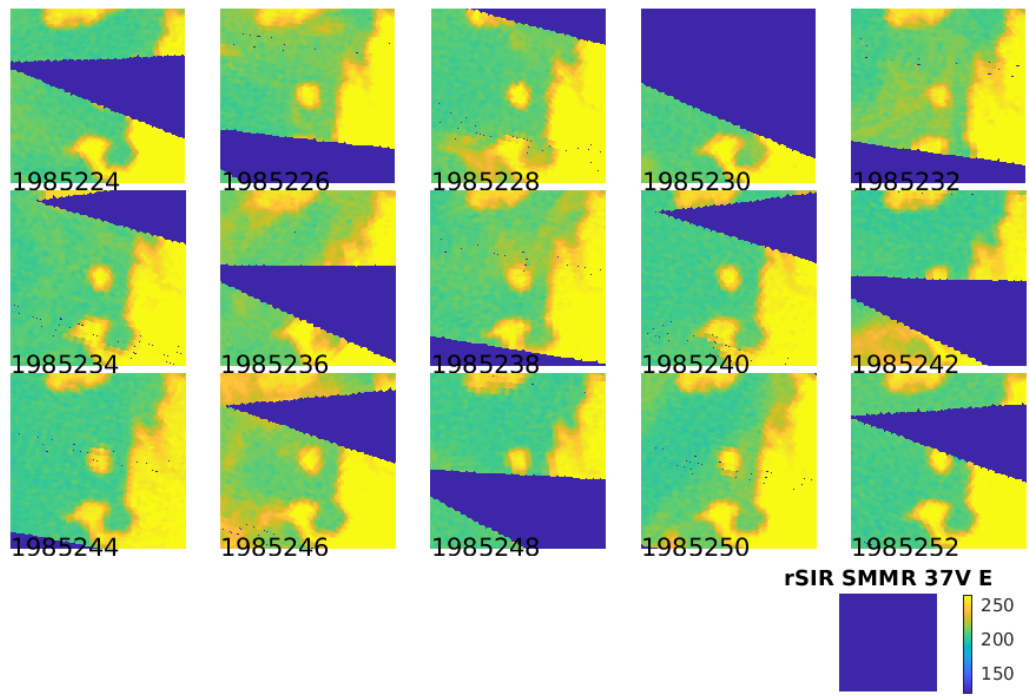


Figure 380: Time series of (top) rSIR and (bottom) GRD  $T_B$  images over the study area. Image dates are labeled on the image.

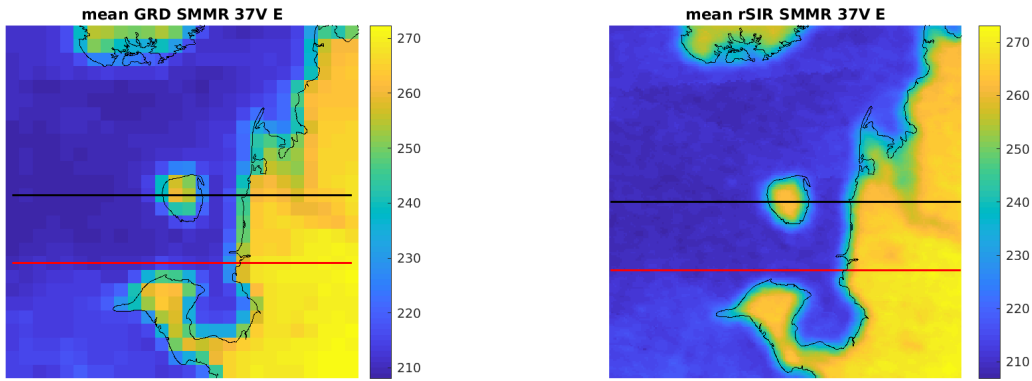


Figure 381: Average of daily  $T_B$  images over the study area. (left) 25-km GRD. (right) 3.125-km rSIR. The thick horizontal lines show the data transect locations where data is extracted from the image for analysis.

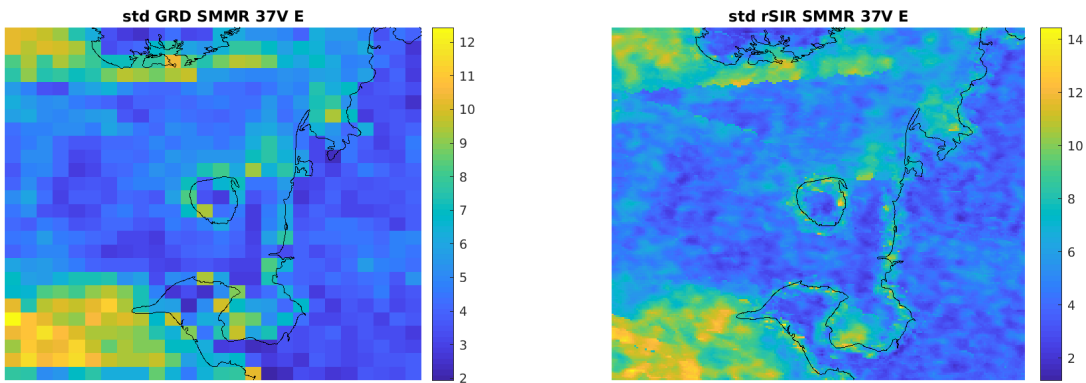


Figure 382: Standard deviation of daily  $T_B$  images over the study area. (left) 25-km GRD. (right) 3.125-km rSIR.

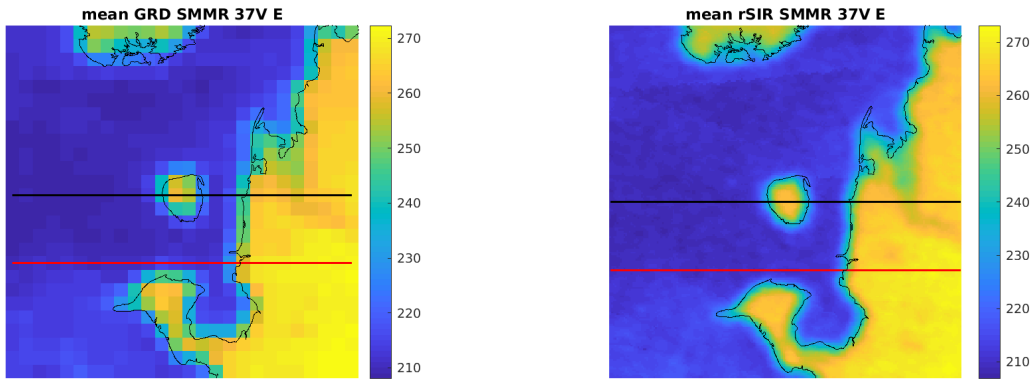


Figure 383: [Repeated] Average of daily  $T_B$  images over the study area. (left) 25-km GRD. (right) 3.125-km rSIR. The thick horizontal lines show the data transect locations where data is extracted from the image for analysis.

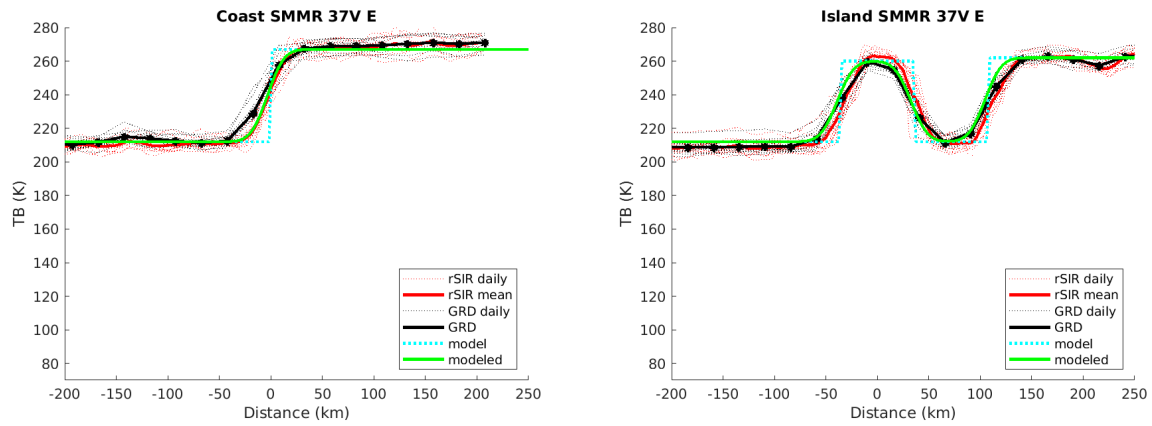


Figure 384: Plots of  $T_B$  along the two analysis case transect lines for the (left) coast-crossing and (right) island-crossing cases.



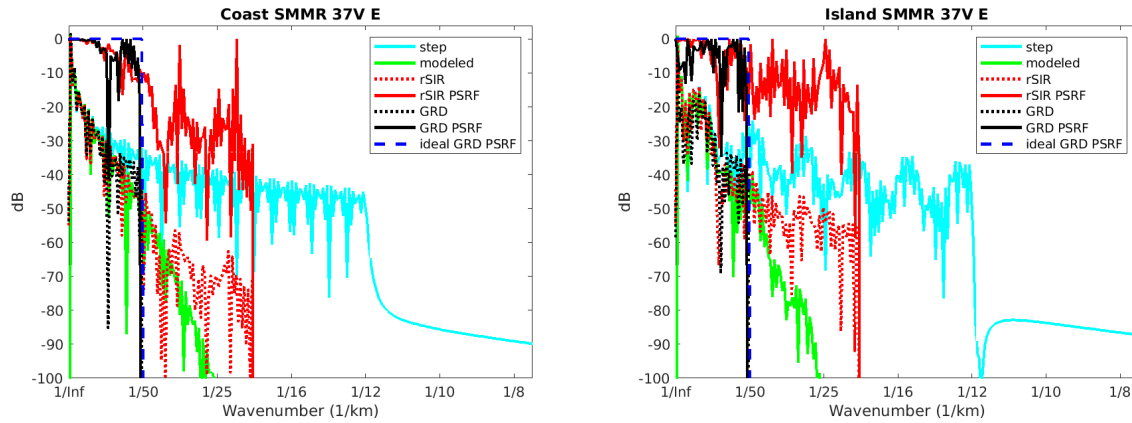


Figure 385: Wavenumber spectra of the  $T_B$  slices, the model, and the PSRF. (left) Coast-crossing case. (right) Island-crossing case.

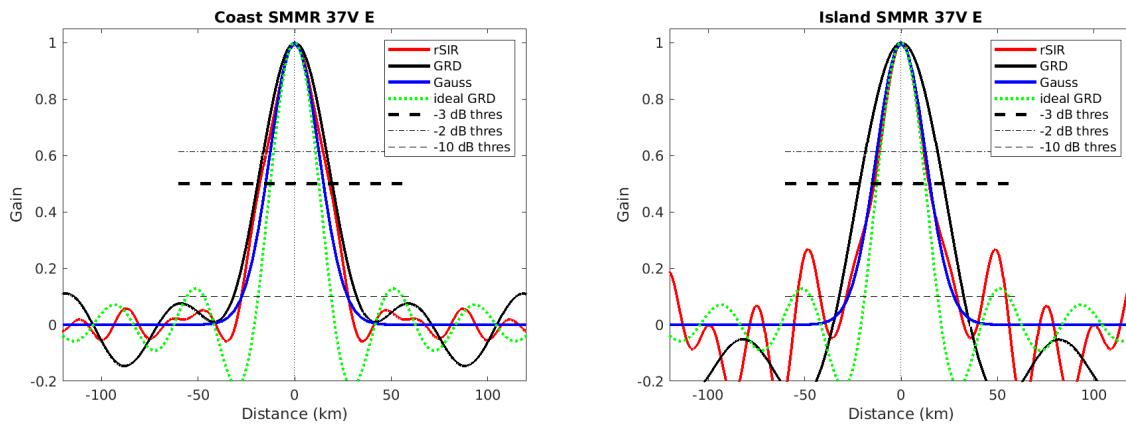


Figure 386: Derived single-pass rSIR and GRD PSRFs from the (left) coast-crossing and (right) island-crossing cases.

Table 122: Resolution estimates for SMMR channel 37V LTOD E

Algorithm	-3 dB Thres		-2 dB Thres		-10 dB Thres	
	Coast	Island	Coast	Island	Coast	Island
Gauss	30.0	30.0	24.4	24.4	54.8	54.8
rSIR	36.2	28.4	28.3	22.4	55.4	57.4
ideal GRD	36.2	36.2	30.3	30.3	54.5	54.5
GRD	38.5	43.4	31.8	36.3	63.8	64.7

## E.20 SMMR Channel 37V M Figures

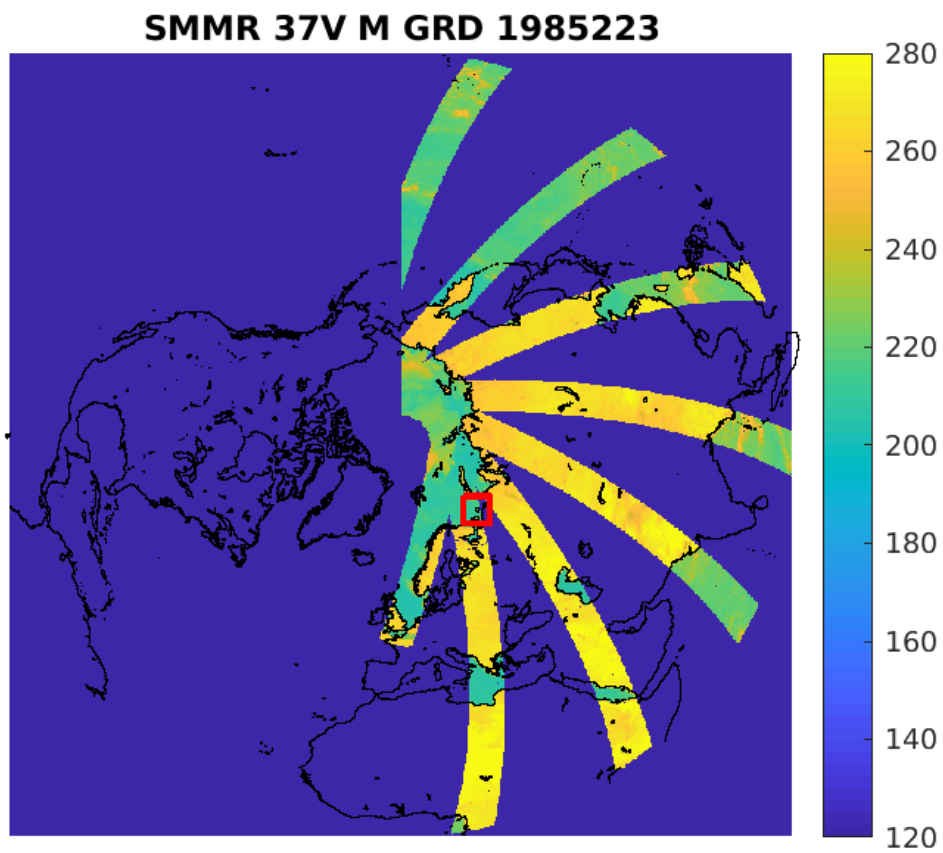


Figure 387: rSIR Northern Hemisphere view.

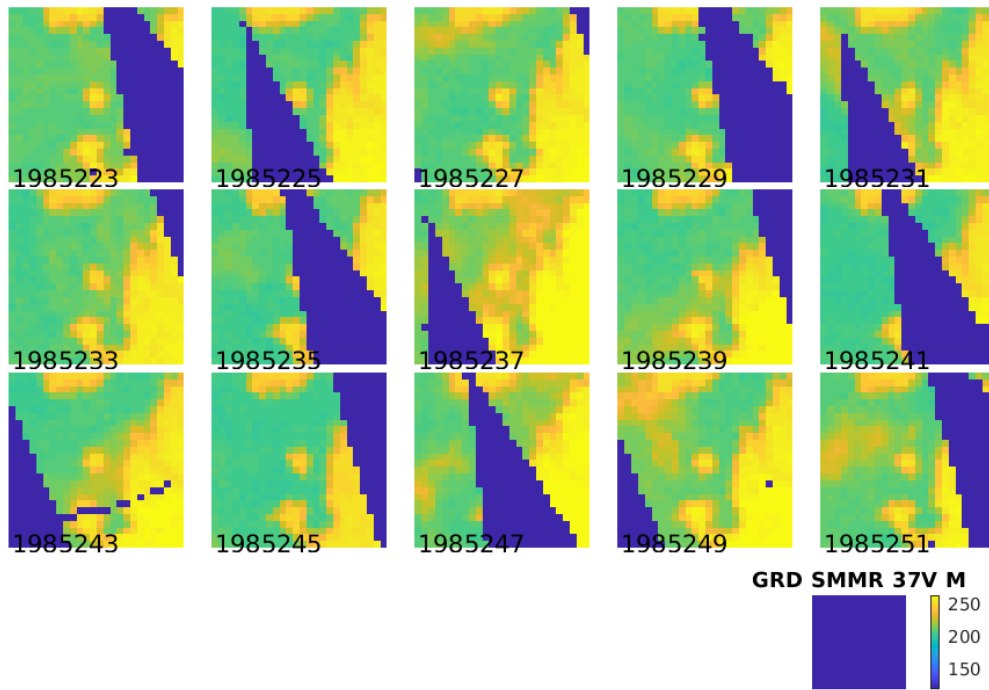
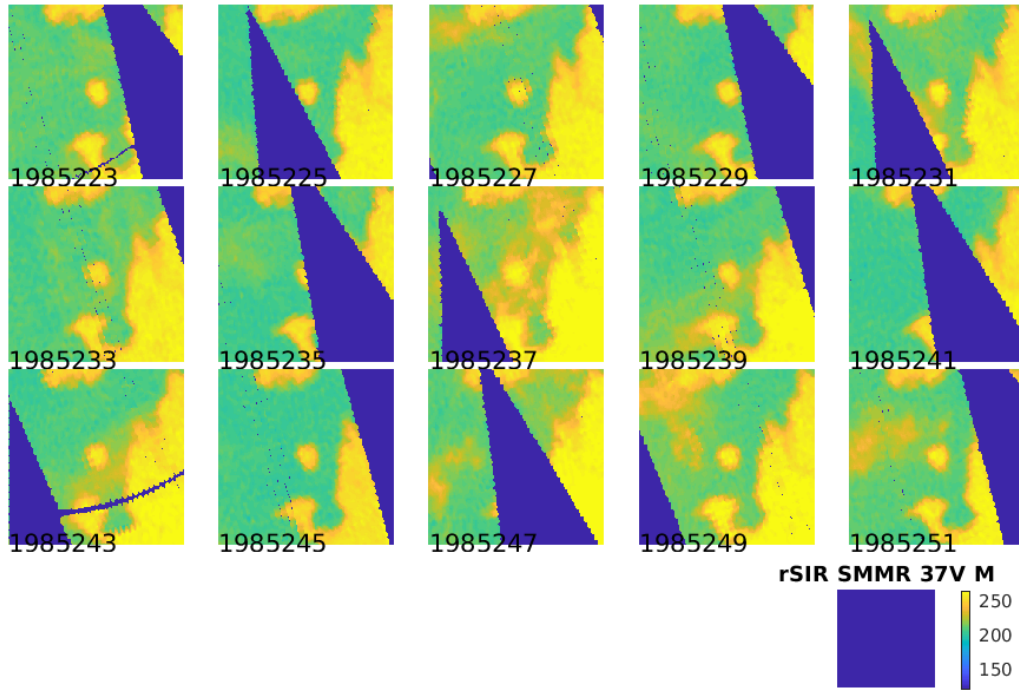


Figure 388: Time series of (top) rSIR and (bottom) GRD  $T_B$  images over the study area. Image dates are labeled on the image.

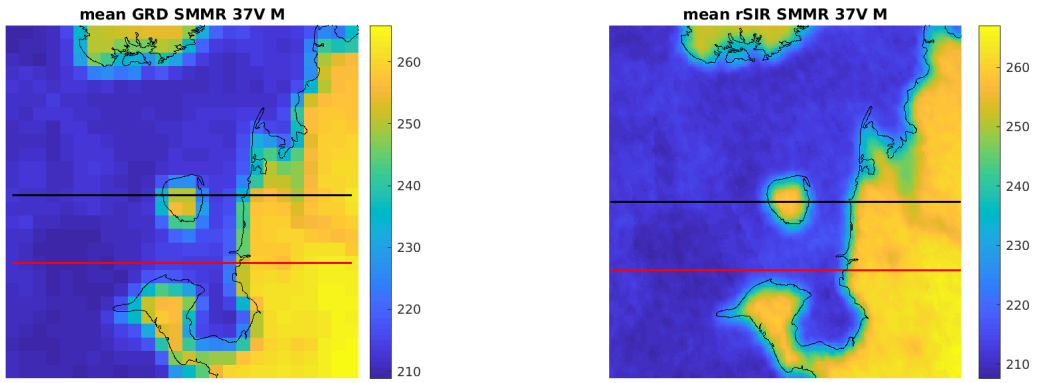


Figure 389: Average of daily  $T_B$  images over the study area. (left) 25-km GRD. (right) 3.125-km rSIR. The thick horizontal lines show the data transect locations where data is extracted from the image for analysis.

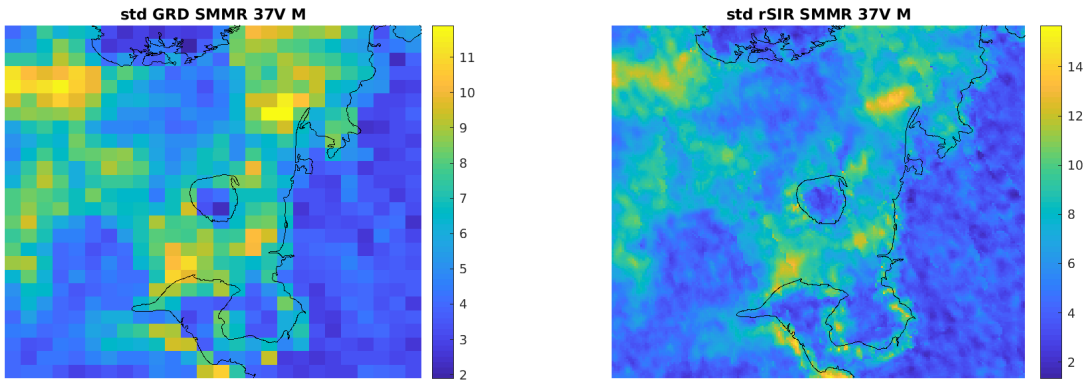


Figure 390: Standard deviation of daily  $T_B$  images over the study area. (left) 25-km GRD. (right) 3.125-km rSIR.

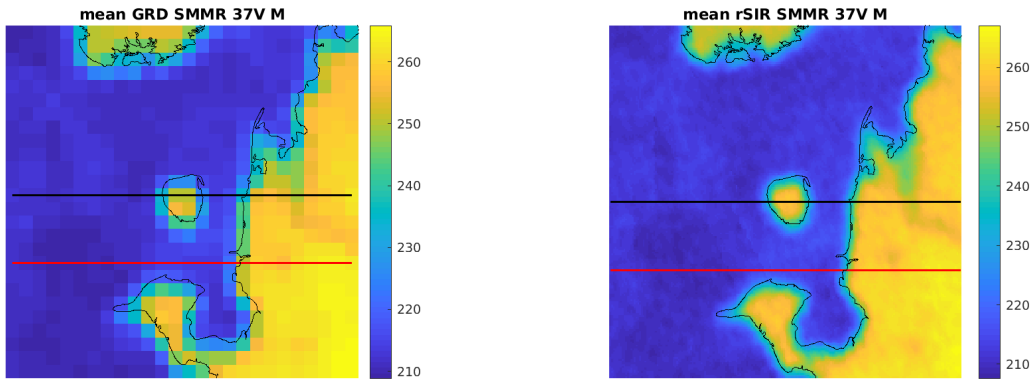


Figure 391: [Repeated] Average of daily  $T_B$  images over the study area. (left) 25-km GRD. (right) 3.125-km rSIR. The thick horizontal lines show the data transect locations where data is extracted from the image for analysis.

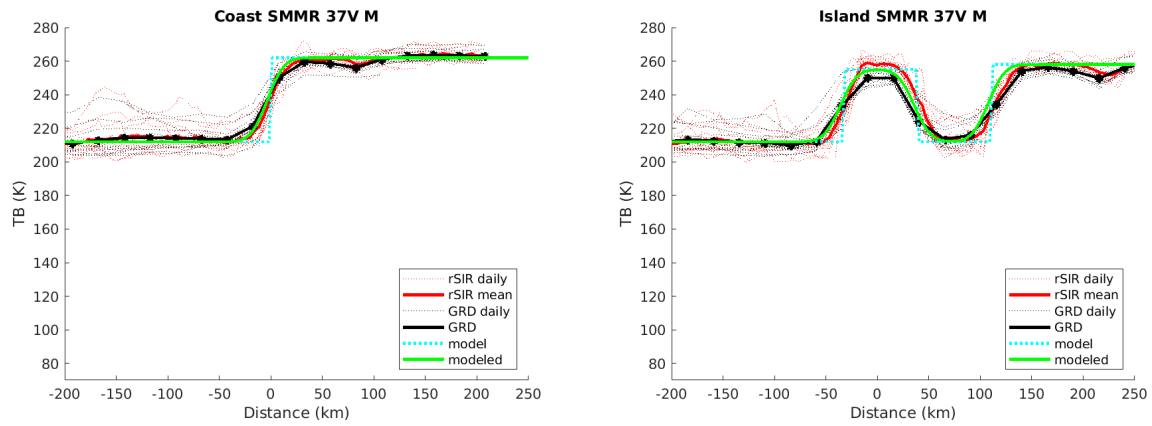


Figure 392: Plots of  $T_B$  along the two analysis case transect lines for the (left) coast-crossing and (right) island-crossing cases.

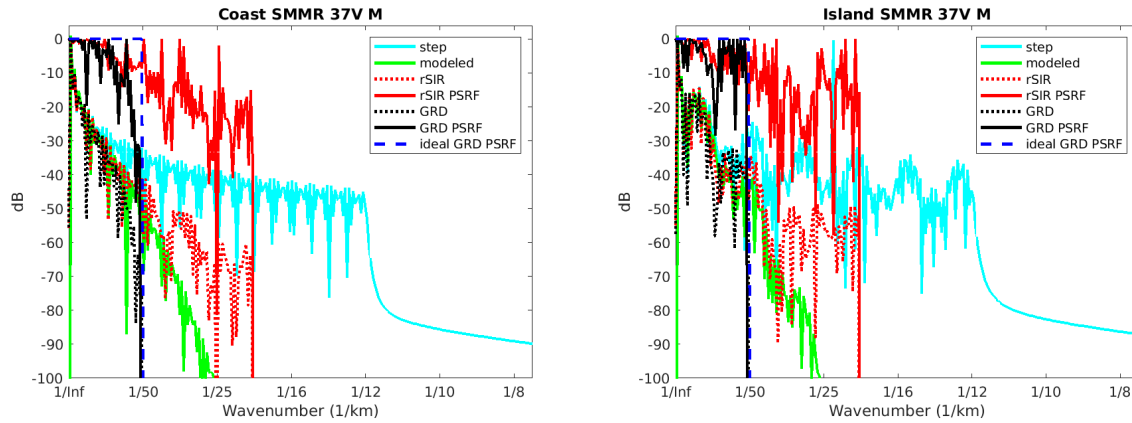


Figure 393: Wavenumber spectra of the  $T_B$  slices, the model, and the PSRF. (left) Coast-crossing case. (right) Island-crossing case.

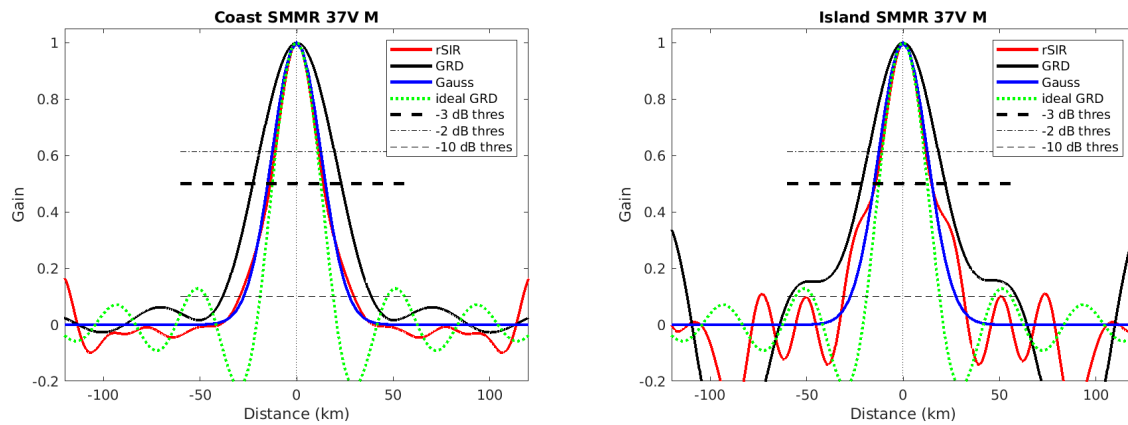


Figure 394: Derived single-pass rSIR and GRD PSRFs from the (left) coast-crossing and (right) island-crossing cases.

Table 123: Resolution estimates for SMMR channel 37V LTOD M

Algorithm	-3 dB Thres		-2 dB Thres		-10 dB Thres	
	Coast	Island	Coast	Island	Coast	Island
Gauss	30.0	30.0	24.4	24.4	54.8	54.8
rSIR	27.5	29.2	21.8	22.4	59.1	62.4
ideal GRD	36.2	36.2	30.3	30.3	54.5	54.5
GRD	45.7	43.2	37.7	35.2	76.9	117.2

## F SSMIS Figures

### F.1 SSMIS Channel 19H E Figures

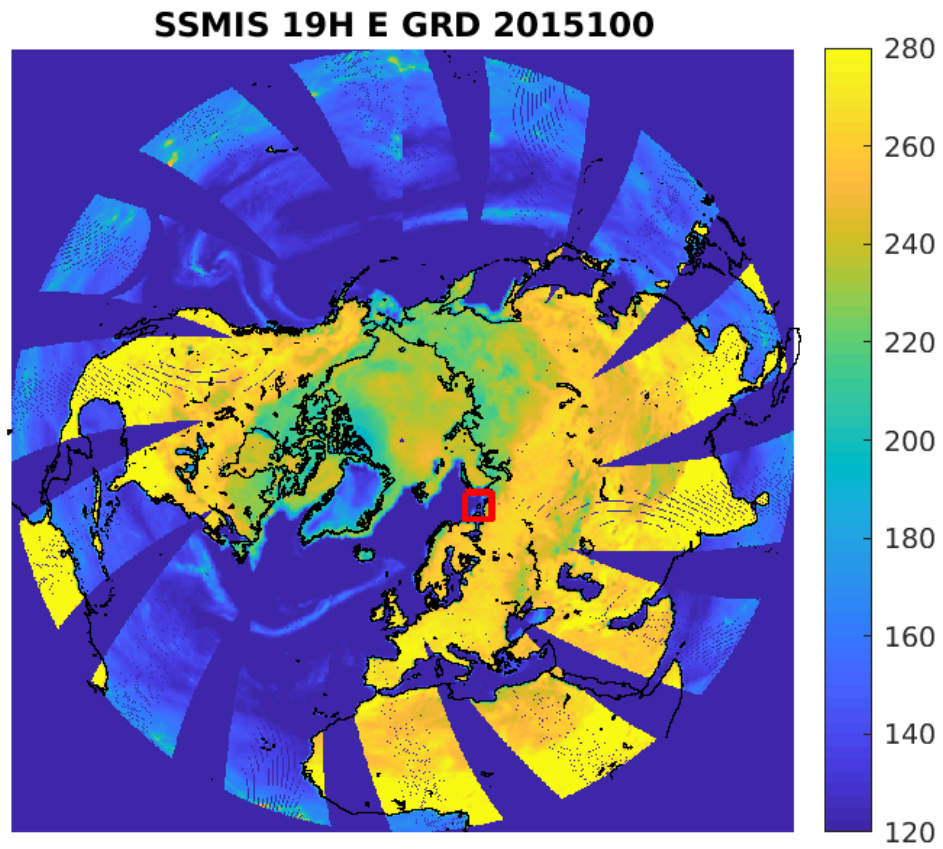


Figure 395: rSIR Northern Hemisphere view.

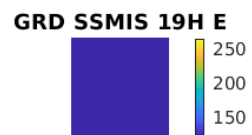
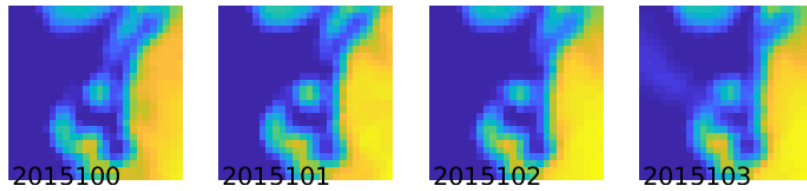
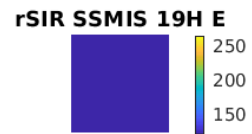
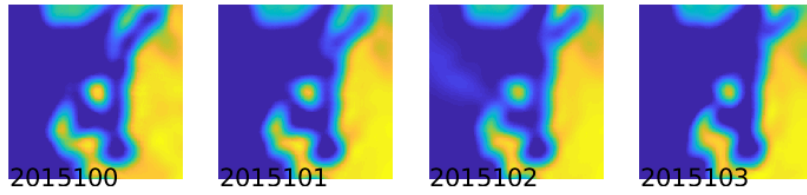


Figure 396: Time series of (top) rSIR and (bottom) GRD  $T_B$  images over the study area. Image dates are labeled on the image.



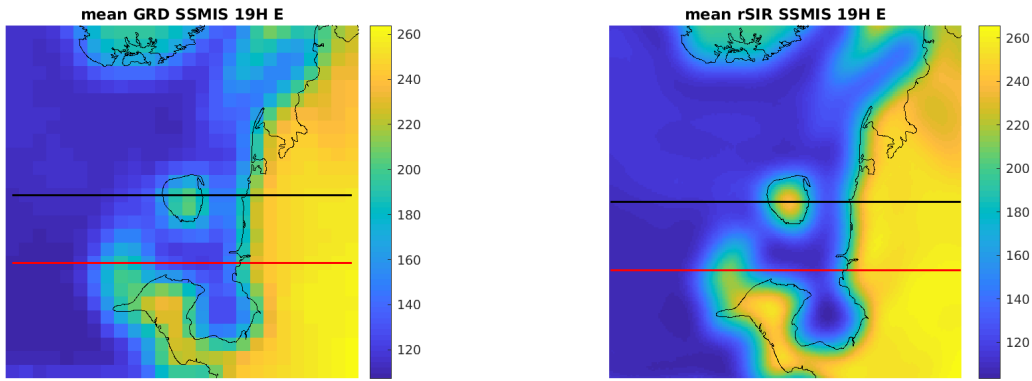


Figure 397: Average of daily  $T_B$  images over the study area. (left) 25-km GRD. (right) 3.125-km rSIR. The thick horizontal lines show the data transect locations where data is extracted from the image for analysis.

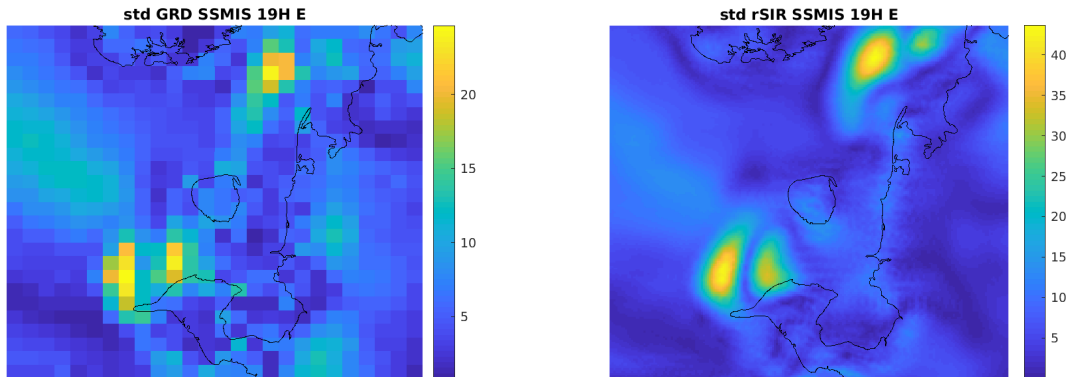


Figure 398: Standard deviation of daily  $T_B$  images over the study area. (left) 25-km GRD. (right) 3.125-km rSIR.

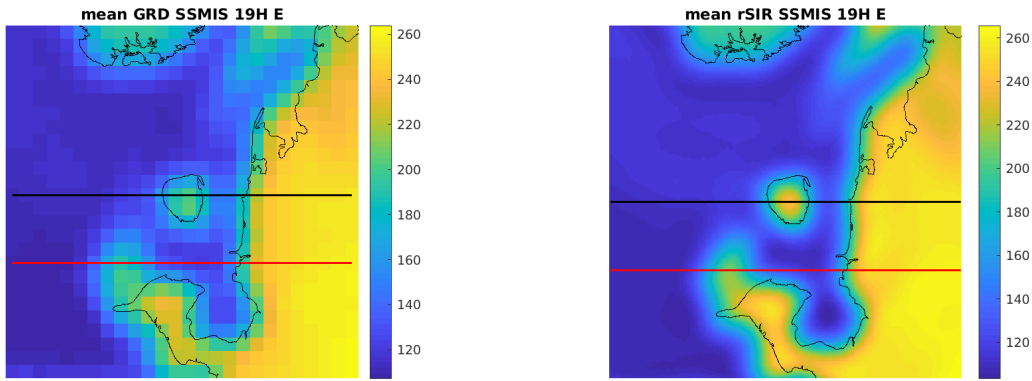


Figure 399: [Repeated] Average of daily  $T_B$  images over the study area. (left) 25-km GRD. (right) 3.125-km rSIR. The thick horizontal lines show the data transect locations where data is extracted from the image for analysis.

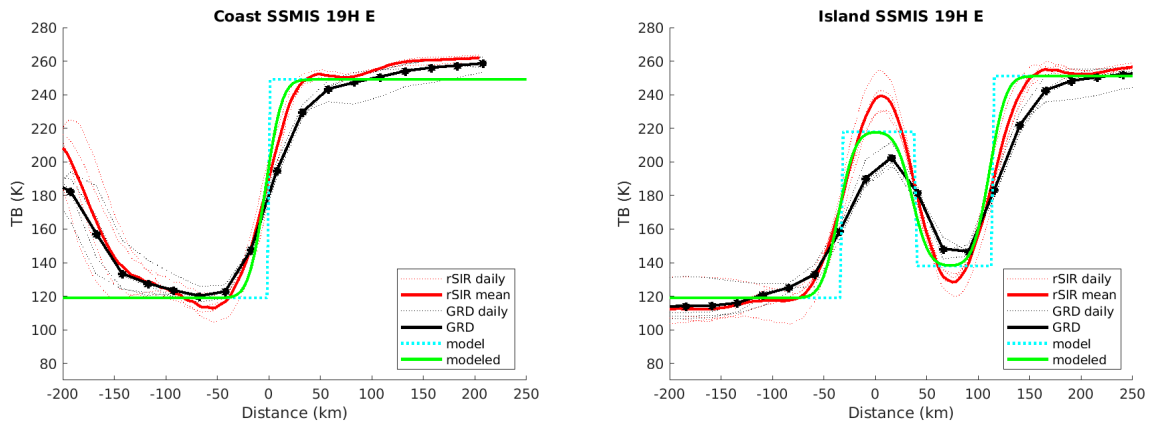


Figure 400: Plots of  $T_B$  along the two analysis case transect lines for the (left) coast-crossing and (right) island-crossing cases.

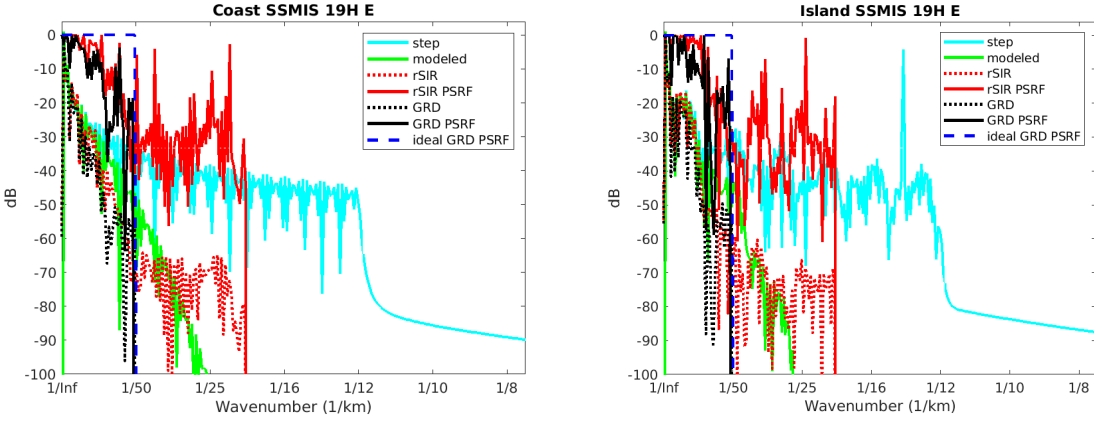


Figure 401: Wavenumber spectra of the  $T_B$  slices, the model, and the PSRF. (left) Coast-crossing case. (right) Island-crossing case.

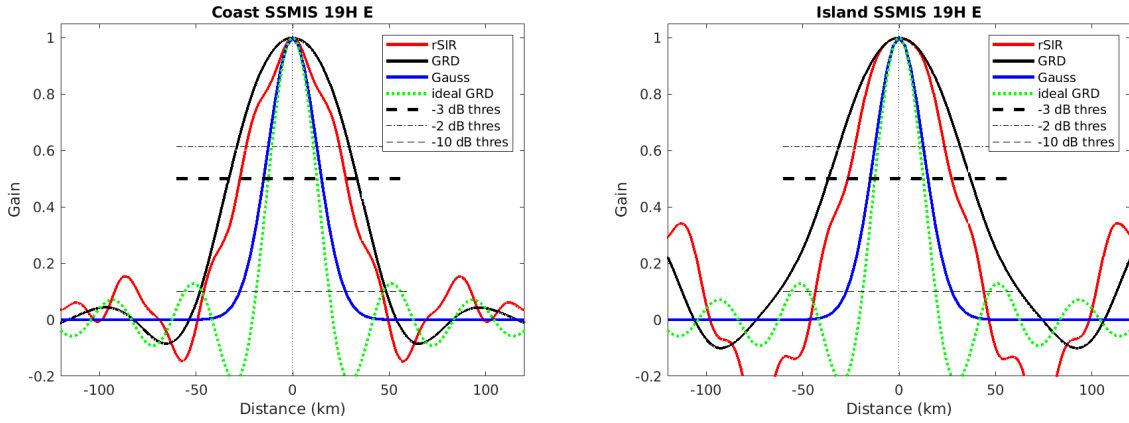


Figure 402: Derived single-pass rSIR and GRD PSRFs from the (left) coast-crossing and (right) island-crossing cases.

Table 124: Resolution estimates for SSMIS channel 19H LTOD E

Algorithm	-3 dB Thres		-2 dB Thres		-10 dB Thres	
	Coast	Island	Coast	Island	Coast	Island
Gauss	30.0	30.0	24.4	24.4	54.8	54.8
rSIR	54.8	53.8	47.3	45.4	92.3	87.3
ideal GRD	36.2	36.2	30.3	30.3	54.5	54.5
GRD	66.5	73.6	56.9	61.4	96.4	125.0

## F.2 SSMIS Channel 19H M Figures

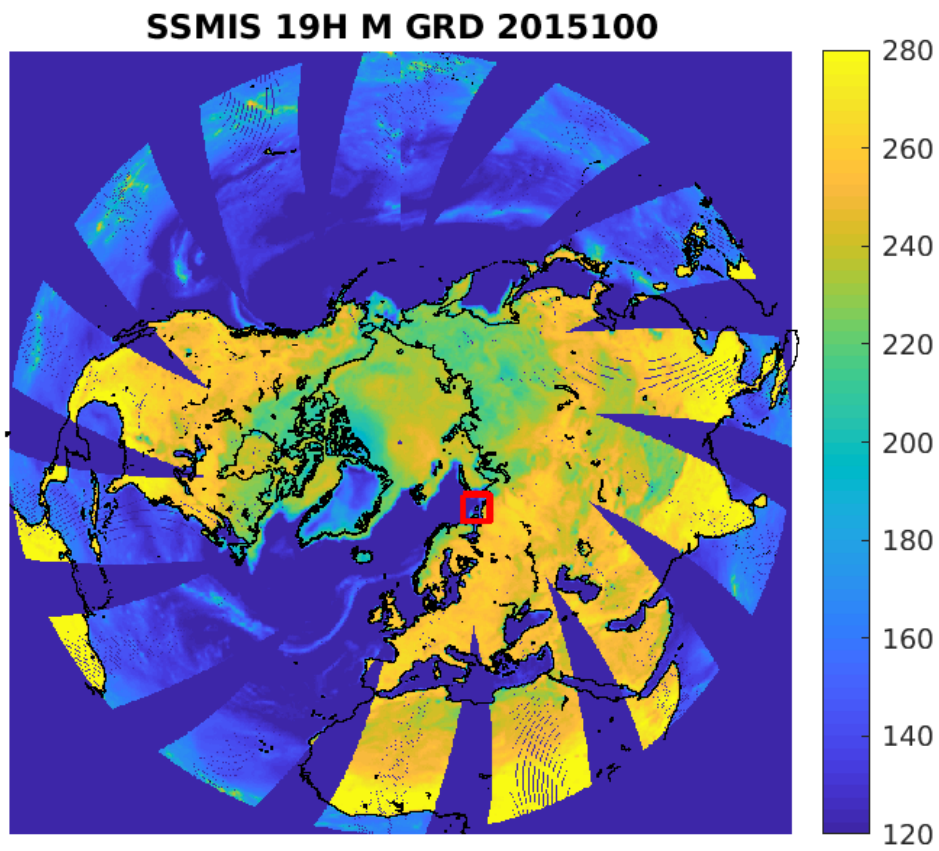


Figure 403: rSIR Northern Hemisphere view.

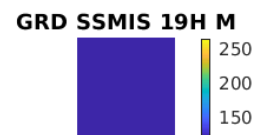
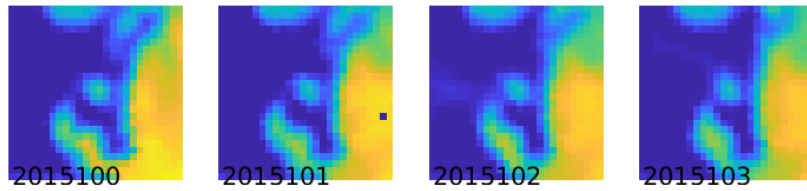
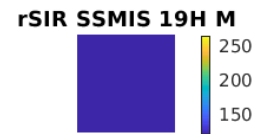
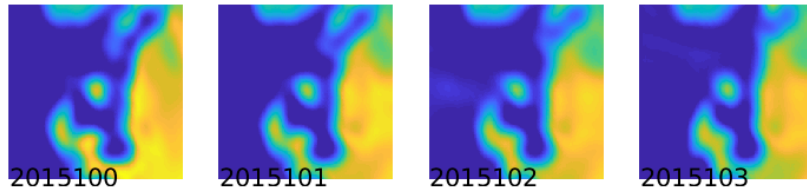


Figure 404: Time series of (top) rSIR and (bottom) GRD  $T_B$  images over the study area. Image dates are labeled on the image.

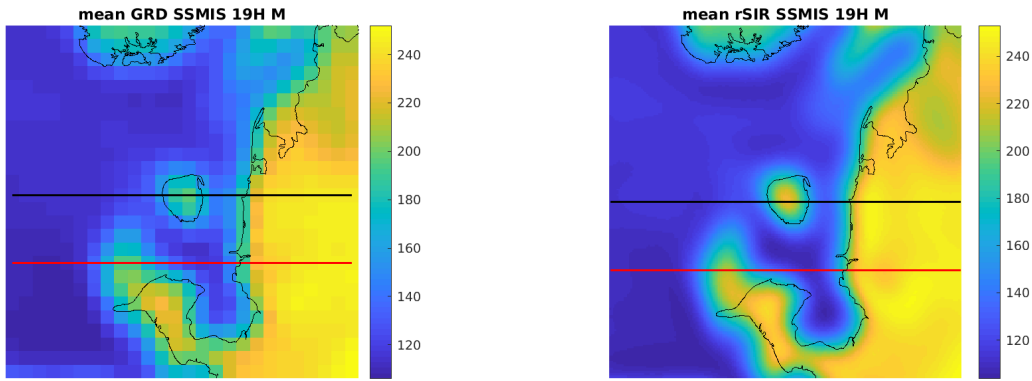


Figure 405: Average of daily  $T_B$  images over the study area. (left) 25-km GRD. (right) 3.125-km rSIR. The thick horizontal lines show the data transect locations where data is extracted from the image for analysis.

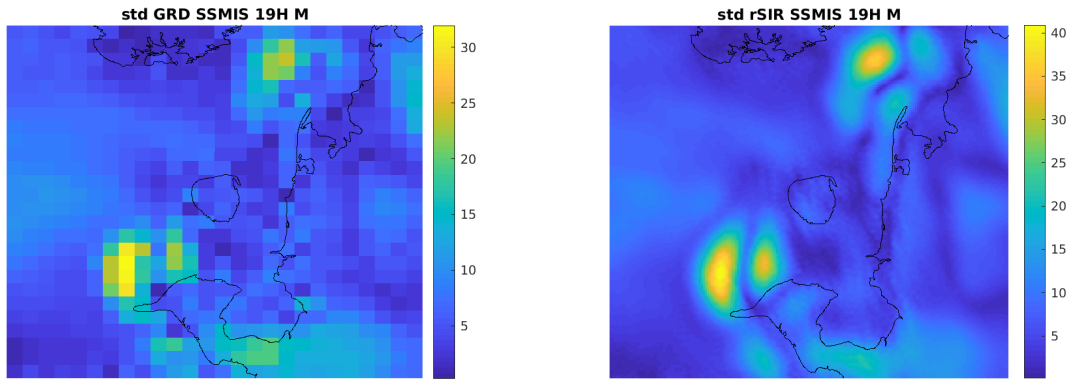


Figure 406: Standard deviation of daily  $T_B$  images over the study area. (left) 25-km GRD. (right) 3.125-km rSIR.

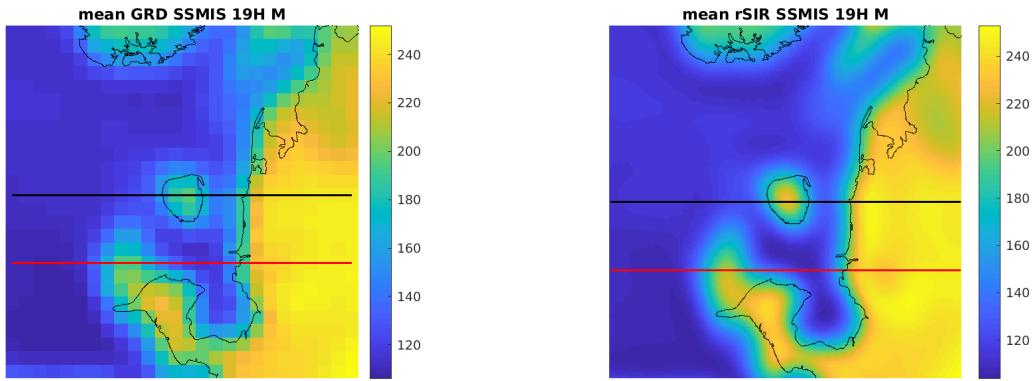


Figure 407: [Repeated] Average of daily  $T_B$  images over the study area. (left) 25-km GRD. (right) 3.125-km rSIR. The thick horizontal lines show the data transect locations where data is extracted from the image for analysis.

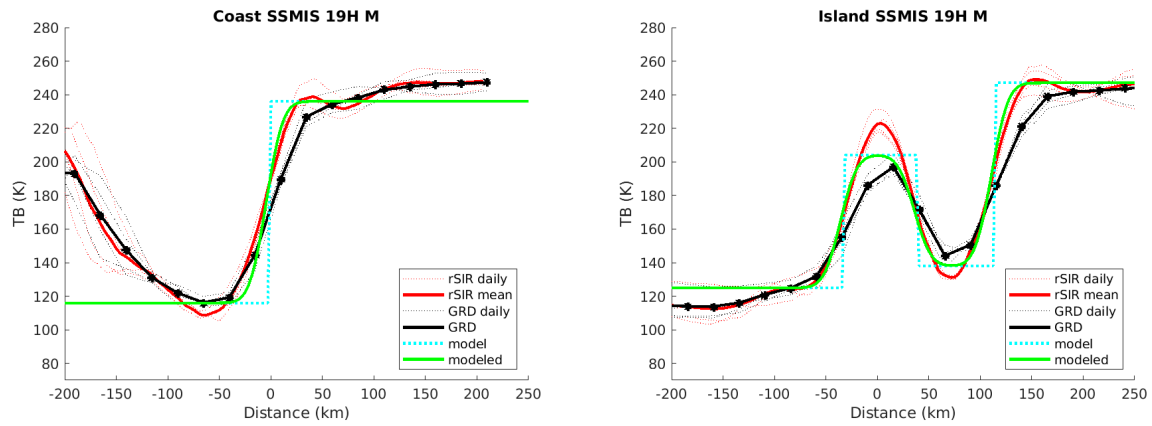


Figure 408: Plots of  $T_B$  along the two analysis case transect lines for the (left) coast-crossing and (right) island-crossing cases.

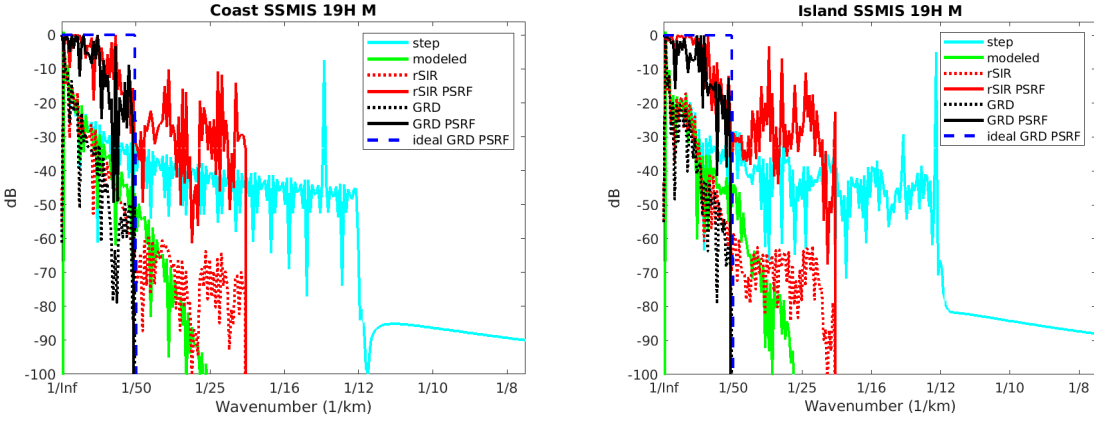


Figure 409: Wavenumber spectra of the  $T_B$  slices, the model, and the PSRF. (left) Coast-crossing case. (right) Island-crossing case.

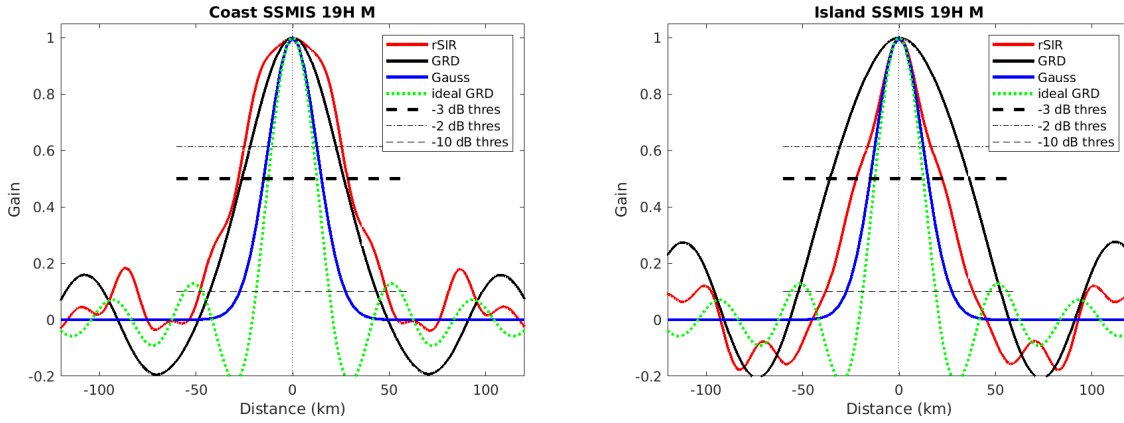


Figure 410: Derived single-pass rSIR and GRD PSRFs from the (left) coast-crossing and (right) island-crossing cases.

Table 125: Resolution estimates for SSMIS channel 19H LTOD M

Algorithm	-3 dB Thres		-2 dB Thres		-10 dB Thres	
	Coast	Island	Coast	Island	Coast	Island
Gauss	30.0	30.0	24.4	24.4	54.8	54.8
rSIR	56.5	44.4	49.7	31.3	96.5	76.4
ideal GRD	36.2	36.2	30.3	30.3	54.5	54.5
GRD	52.8	72.2	43.3	60.3	86.4	104.9



### F.3 SSMIS Channel 19V E Figures

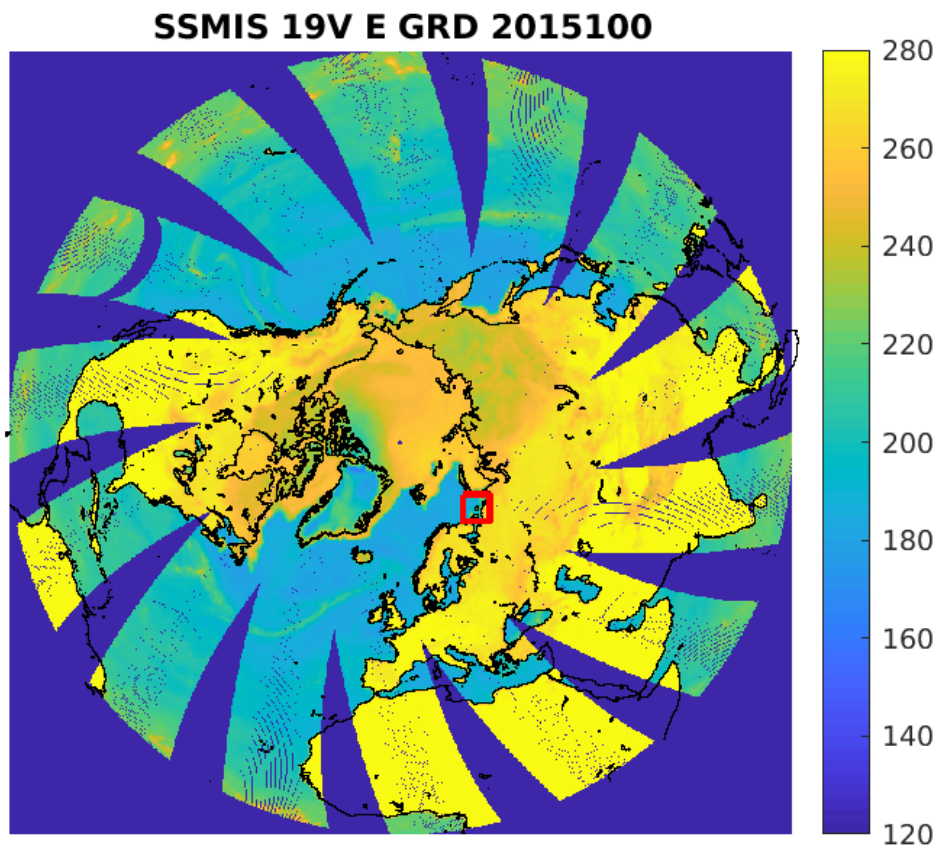


Figure 411: rSIR Northern Hemisphere view.

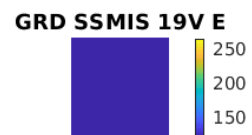
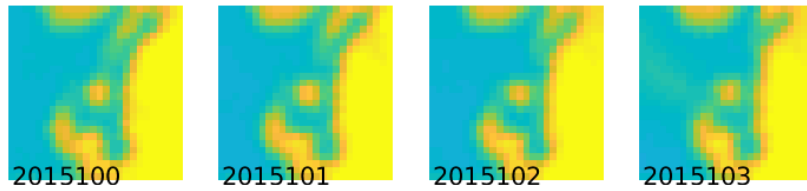
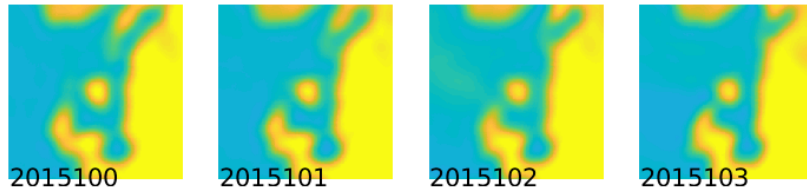


Figure 412: Time series of (top) rSIR and (bottom) GRD  $T_B$  images over the study area. Image dates are labeled on the image.

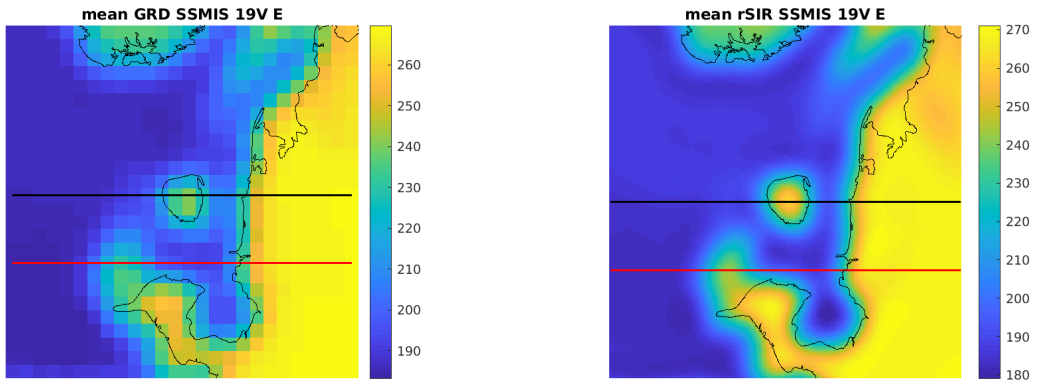


Figure 413: Average of daily  $T_B$  images over the study area. (left) 25-km GRD. (right) 3.125-km rSIR. The thick horizontal lines show the data transect locations where data is extracted from the image for analysis.

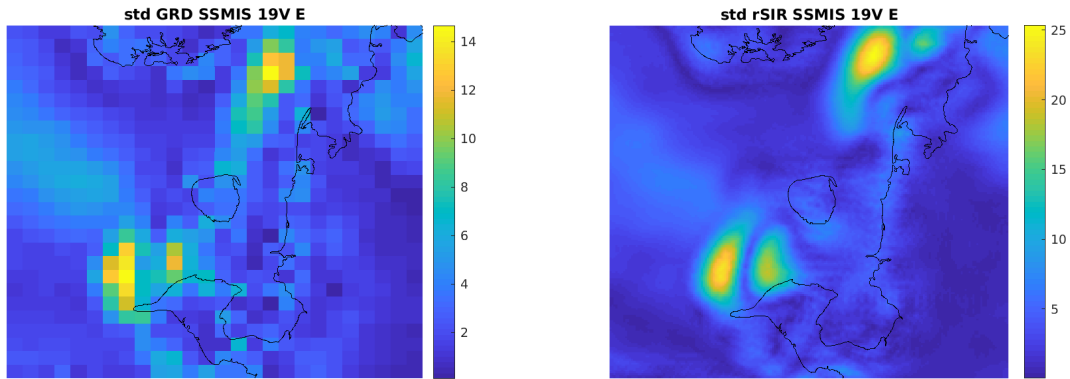


Figure 414: Standard deviation of daily  $T_B$  images over the study area. (left) 25-km GRD. (right) 3.125-km rSIR.

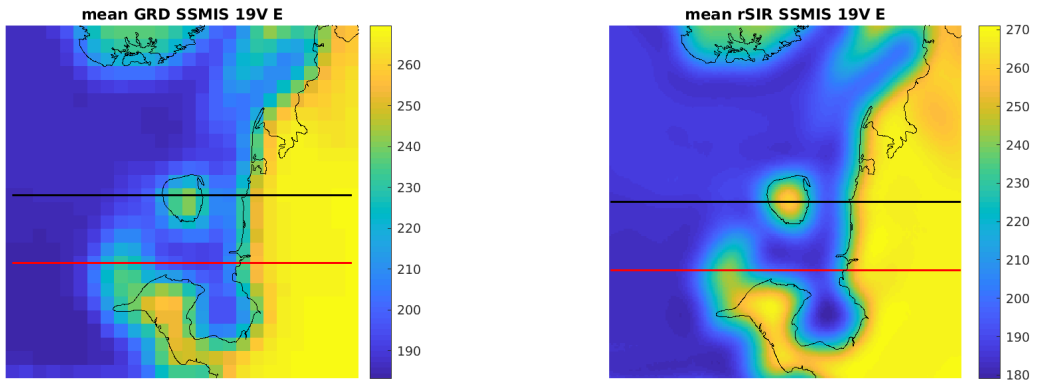


Figure 415: [Repeated] Average of daily  $T_B$  images over the study area. (left) 25-km GRD. (right) 3.125-km rSIR. The thick horizontal lines show the data transect locations where data is extracted from the image for analysis.

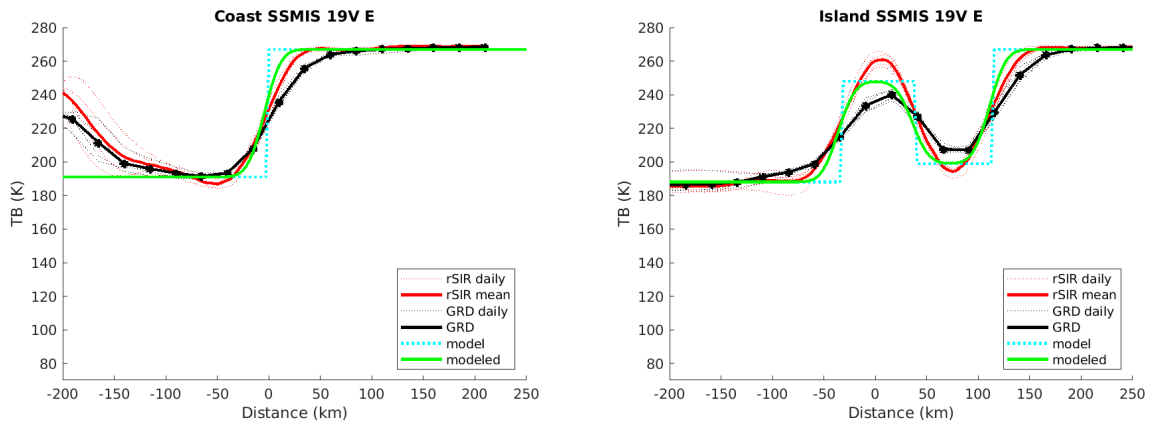


Figure 416: Plots of  $T_B$  along the two analysis case transect lines for the (left) coast-crossing and (right) island-crossing cases.

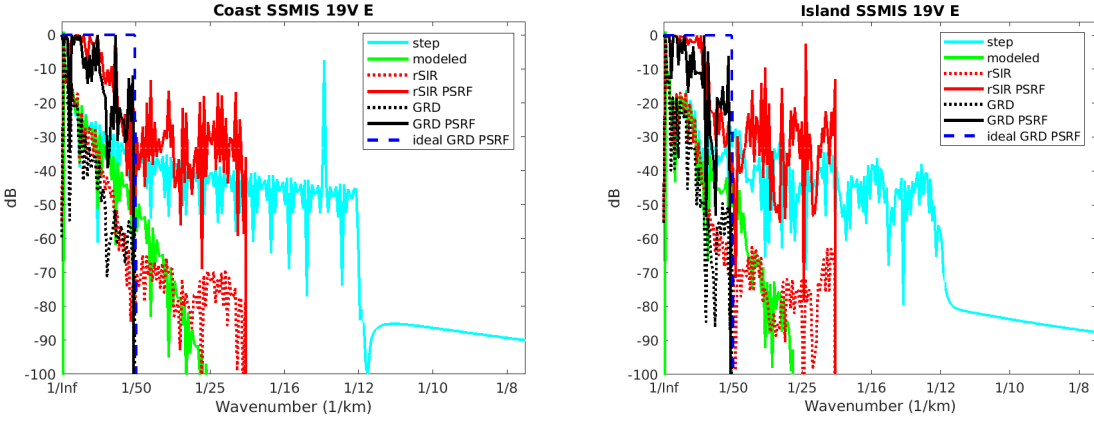


Figure 417: Wavenumber spectra of the  $T_B$  slices, the model, and the PSRF. (left) Coast-crossing case. (right) Island-crossing case.

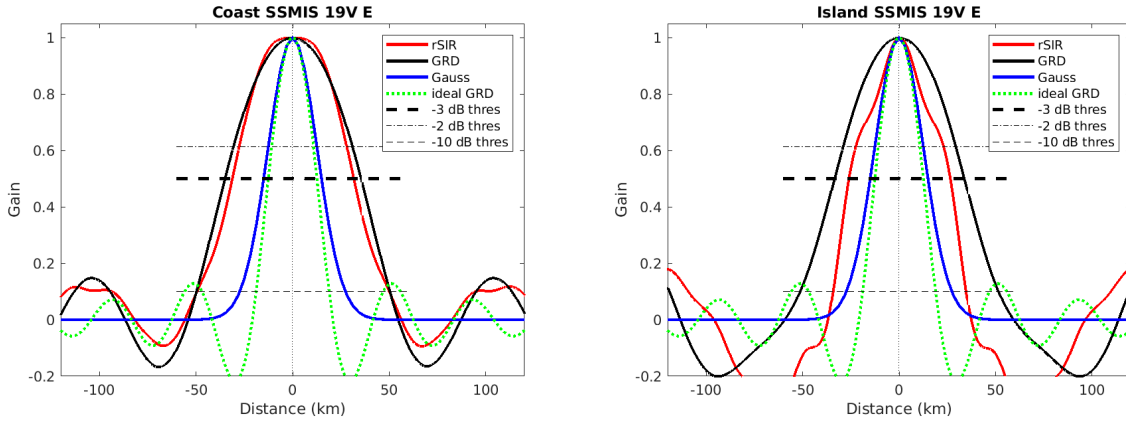


Figure 418: Derived single-pass rSIR and GRD PSRFs from the (left) coast-crossing and (right) island-crossing cases.

Table 126: Resolution estimates for SSMIS channel 19V LTOD E

Algorithm	-3 dB Thres		-2 dB Thres		-10 dB Thres	
	Coast	Island	Coast	Island	Coast	Island
Gauss	30.0	30.0	24.4	24.4	54.8	54.8
rSIR	62.8	52.5	54.5	43.9	99.5	69.0
ideal GRD	36.2	36.2	30.3	30.3	54.5	54.5
GRD	70.4	67.3	60.1	57.0	100.0	102.9

## F.4 SSMIS Channel 19V M Figures

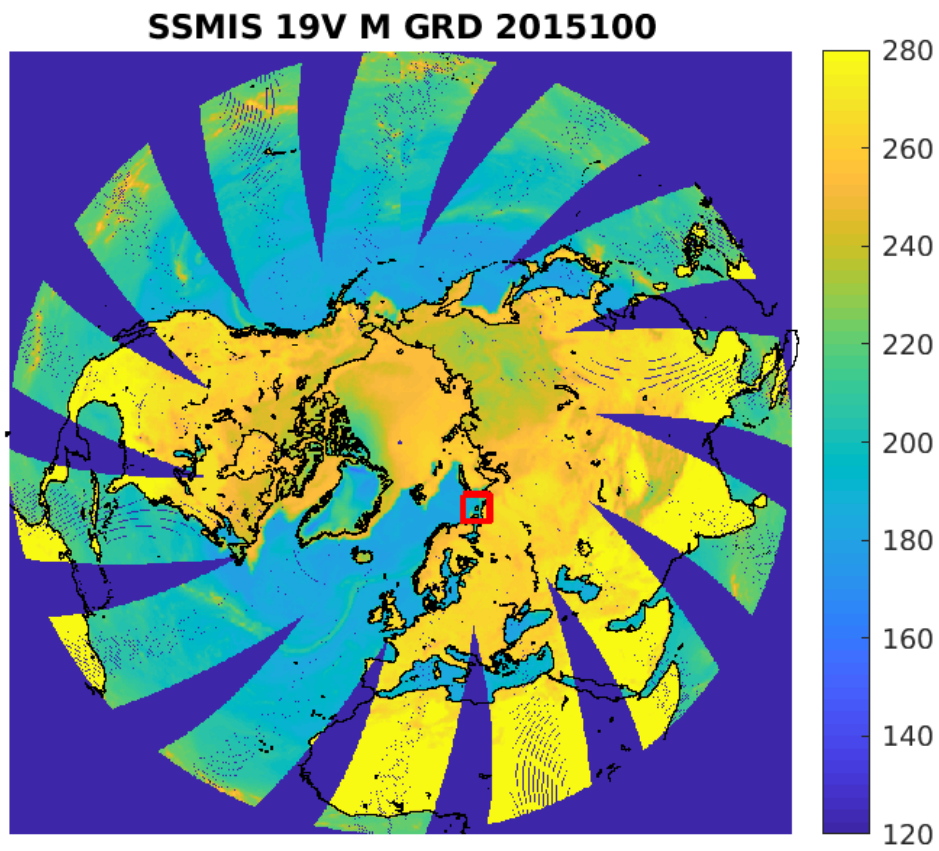


Figure 419: rSIR Northern Hemisphere view.

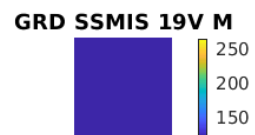
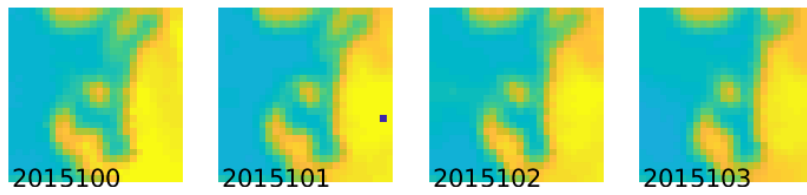
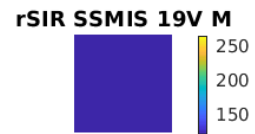
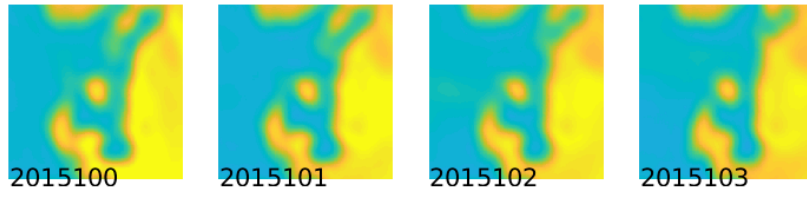


Figure 420: Time series of (top) rSIR and (bottom) GRD  $T_B$  images over the study area. Image dates are labeled on the image.

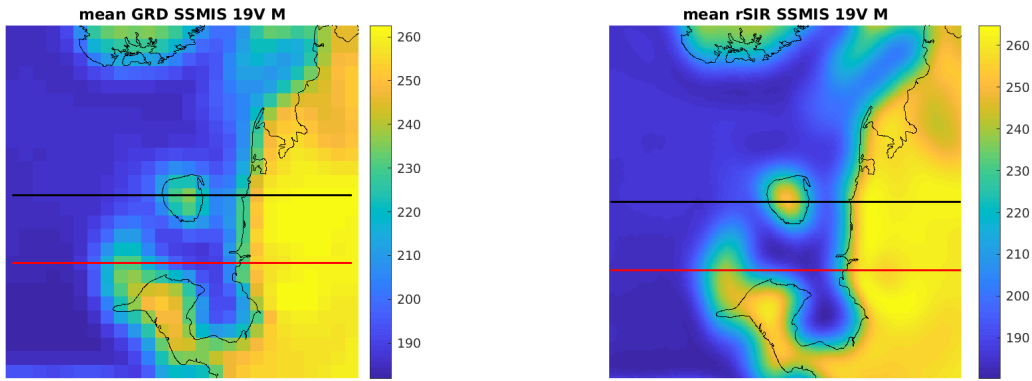


Figure 421: Average of daily  $T_B$  images over the study area. (left) 25-km GRD. (right) 3.125-km rSIR. The thick horizontal lines show the data transect locations where data is extracted from the image for analysis.

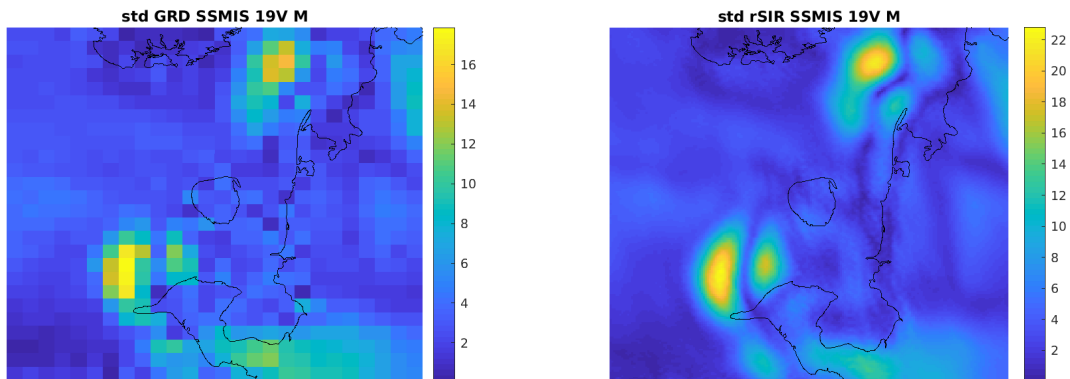


Figure 422: Standard deviation of daily  $T_B$  images over the study area. (left) 25-km GRD. (right) 3.125-km rSIR.



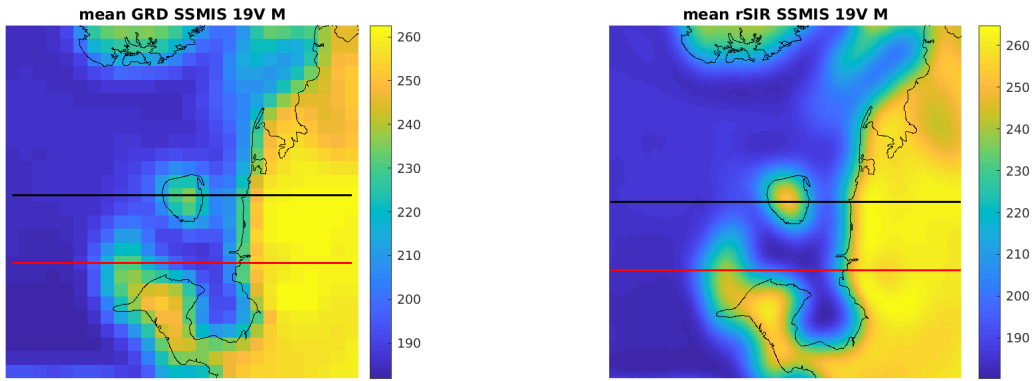


Figure 423: [Repeated] Average of daily  $T_B$  images over the study area. (left) 25-km GRD. (right) 3.125-km rSIR. The thick horizontal lines show the data transect locations where data is extracted from the image for analysis.

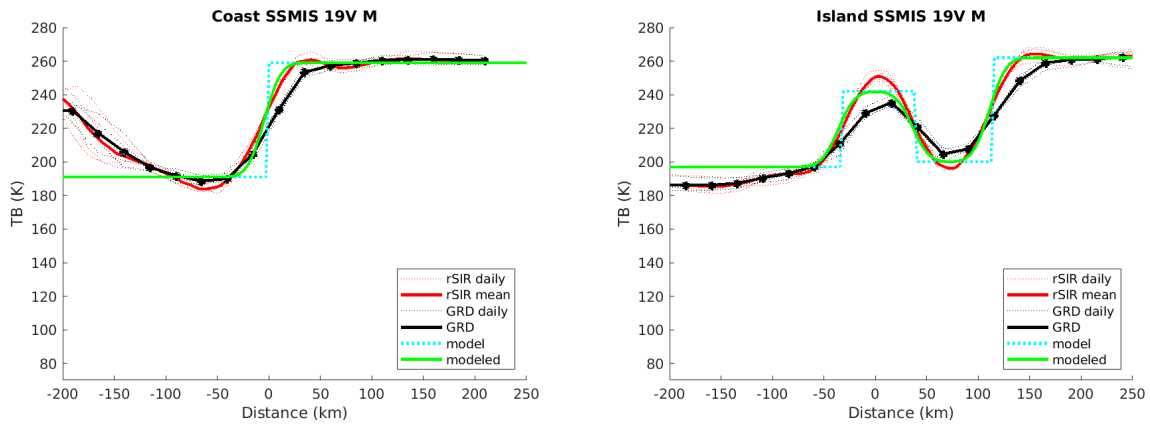


Figure 424: Plots of  $T_B$  along the two analysis case transect lines for the (left) coast-crossing and (right) island-crossing cases.

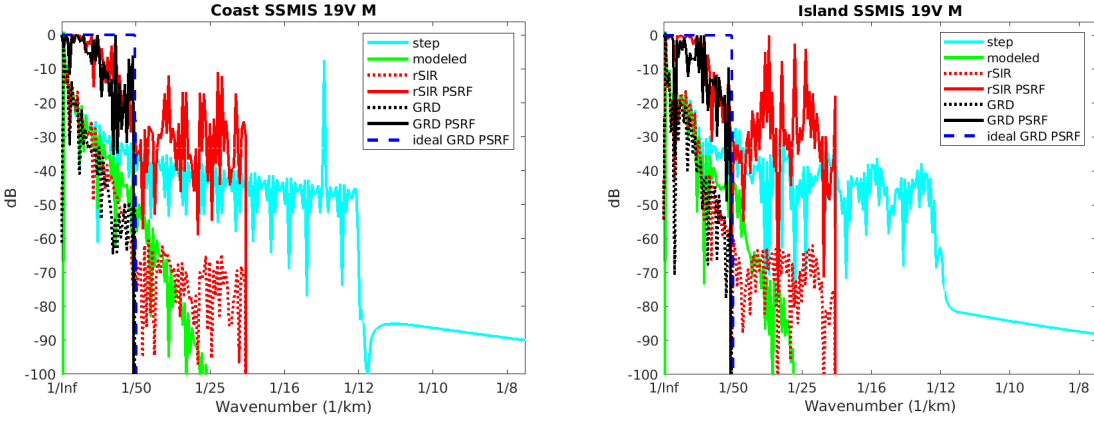


Figure 425: Wavenumber spectra of the  $T_B$  slices, the model, and the PSRF. (left) Coast-crossing case. (right) Island-crossing case.

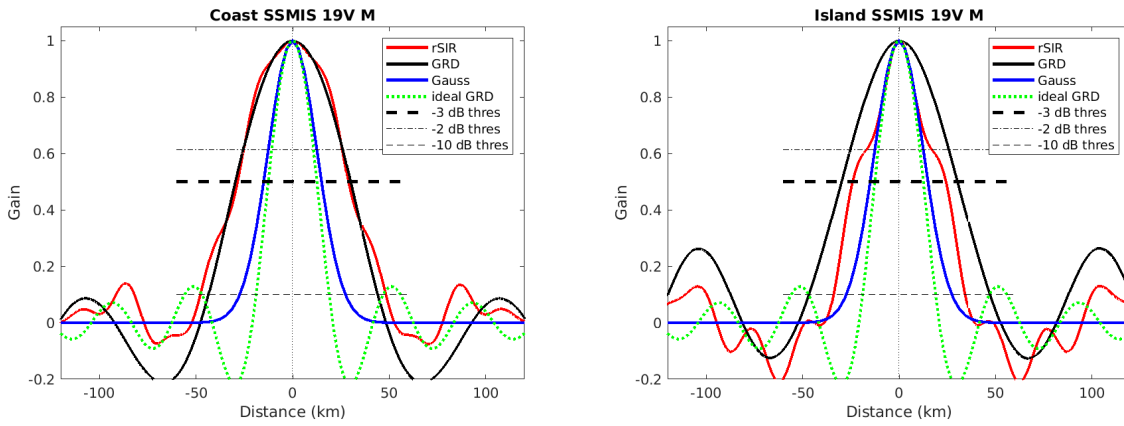


Figure 426: Derived single-pass rSIR and GRD PSRFs from the (left) coast-crossing and (right) island-crossing cases.

Table 127: Resolution estimates for SSMIS channel 19V LTOD M

Algorithm	-3 dB Thres		-2 dB Thres		-10 dB Thres	
	Coast	Island	Coast	Island	Coast	Island
Gauss	30.0	30.0	24.4	24.4	54.8	54.8
rSIR	57.3	48.3	50.1	30.8	95.9	68.3
ideal GRD	36.2	36.2	30.3	30.3	54.5	54.5
GRD	59.6	60.1	50.2	49.7	87.6	93.9

## F.5 SSMIS Channel 22V E Figures

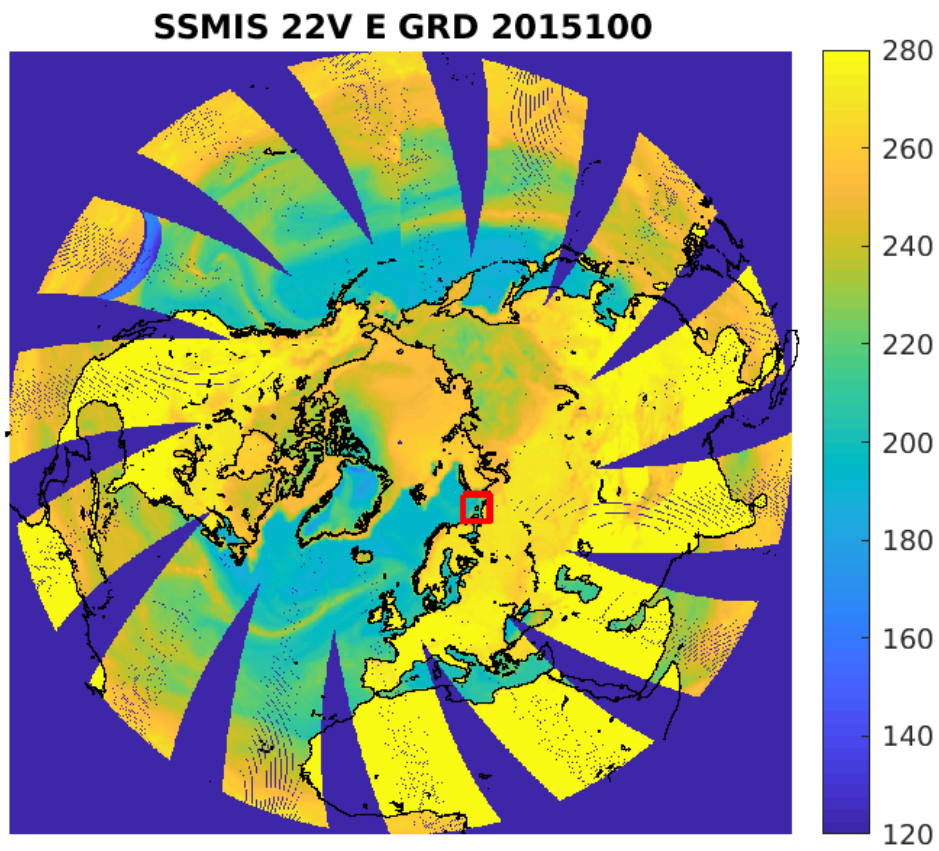


Figure 427: rSIR Northern Hemisphere view.

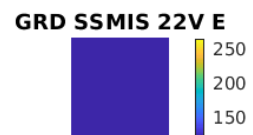
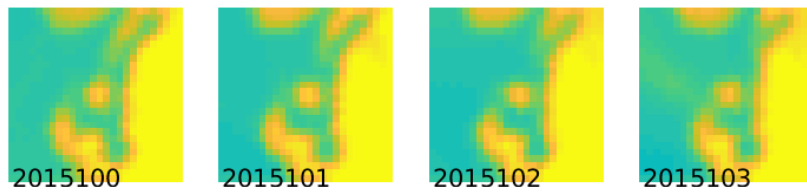
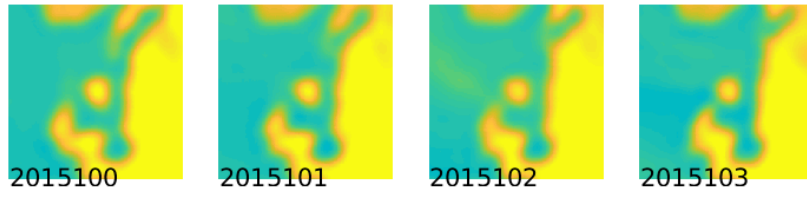


Figure 428: Time series of (top) rSIR and (bottom) GRD  $T_B$  images over the study area. Image dates are labeled on the image.

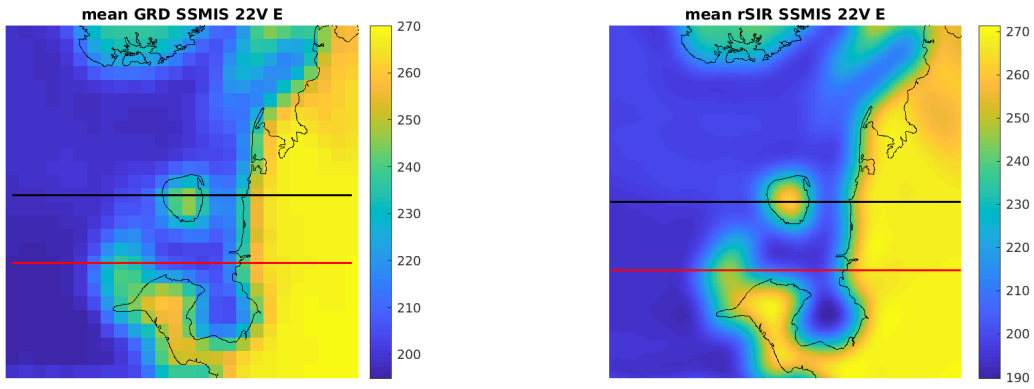


Figure 429: Average of daily  $T_B$  images over the study area. (left) 25-km GRD. (right) 3.125-km rSIR. The thick horizontal lines show the data transect locations where data is extracted from the image for analysis.

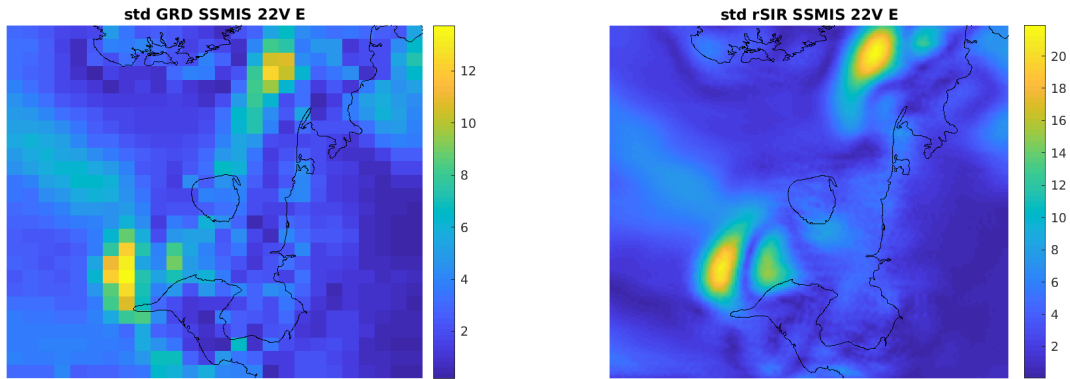


Figure 430: Standard deviation of daily  $T_B$  images over the study area. (left) 25-km GRD. (right) 3.125-km rSIR.

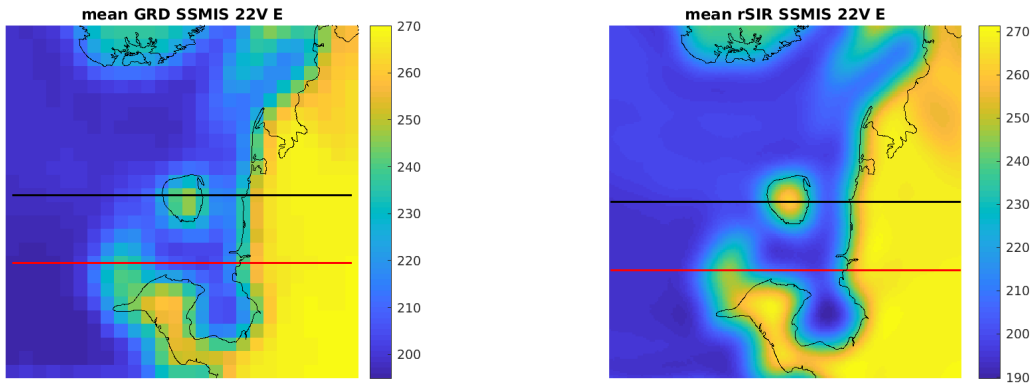


Figure 431: [Repeated] Average of daily  $T_B$  images over the study area. (left) 25-km GRD. (right) 3.125-km rSIR. The thick horizontal lines show the data transect locations where data is extracted from the image for analysis.

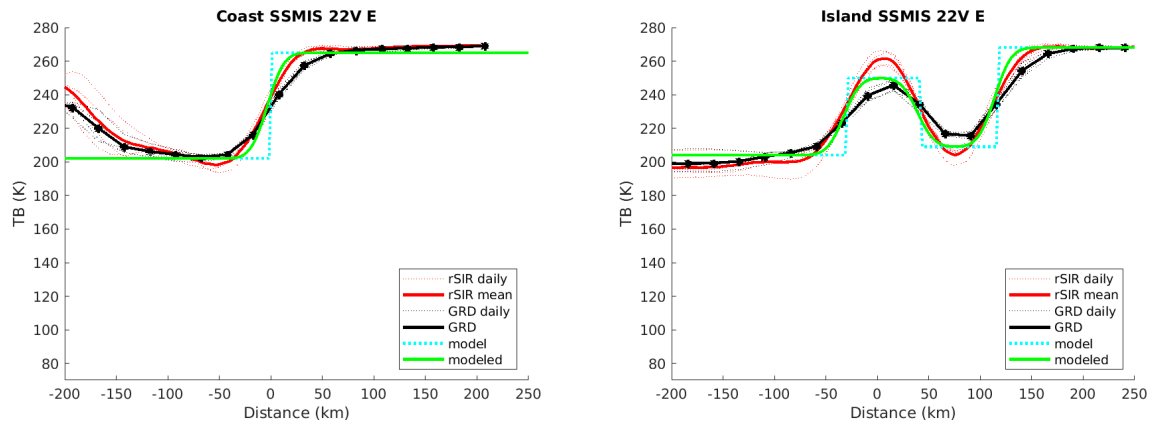


Figure 432: Plots of  $T_B$  along the two analysis case transect lines for the (left) coast-crossing and (right) island-crossing cases.

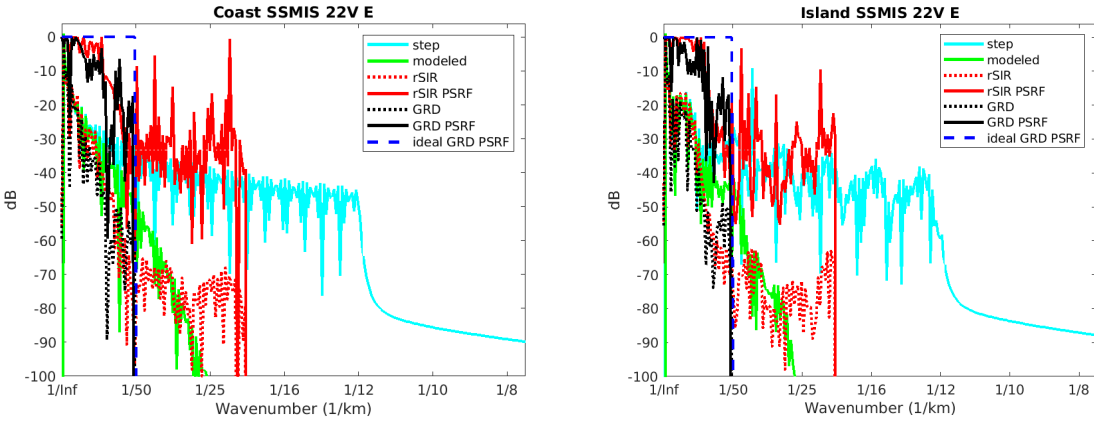


Figure 433: Wavenumber spectra of the  $T_B$  slices, the model, and the PSRF. (left) Coast-crossing case. (right) Island-crossing case.

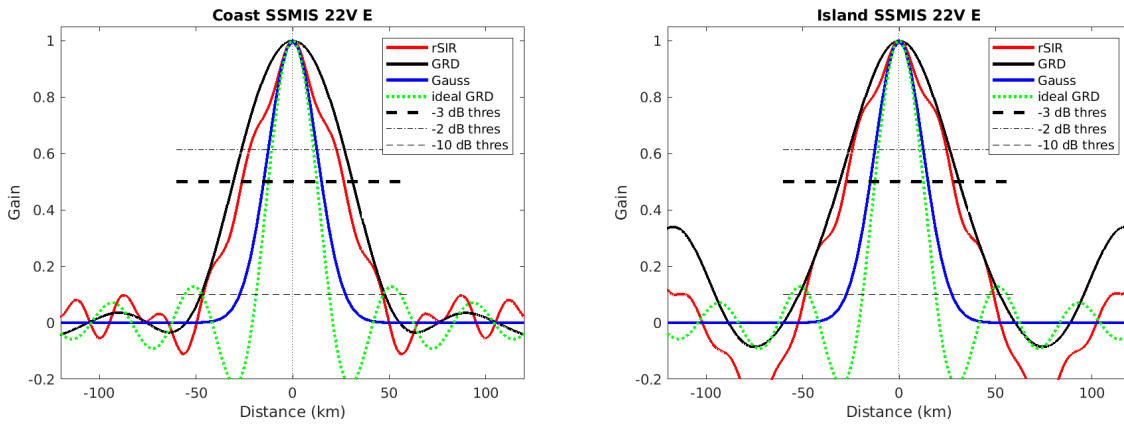


Figure 434: Derived single-pass rSIR and GRD PSRFs from the (left) coast-crossing and (right) island-crossing cases.

Table 128: Resolution estimates for SSMIS channel 22V LTOD E

Algorithm	-3 dB Thres		-2 dB Thres		-10 dB Thres	
	Coast	Island	Coast	Island	Coast	Island
Gauss	30.0	30.0	24.4	24.4	54.8	54.8
rSIR	52.7	55.4	43.5	47.8	92.8	97.8
ideal GRD	36.2	36.2	30.3	30.3	54.5	54.5
GRD	61.8	62.0	51.9	50.7	95.2	104.0

## F.6 SSMIS Channel 22V M Figures

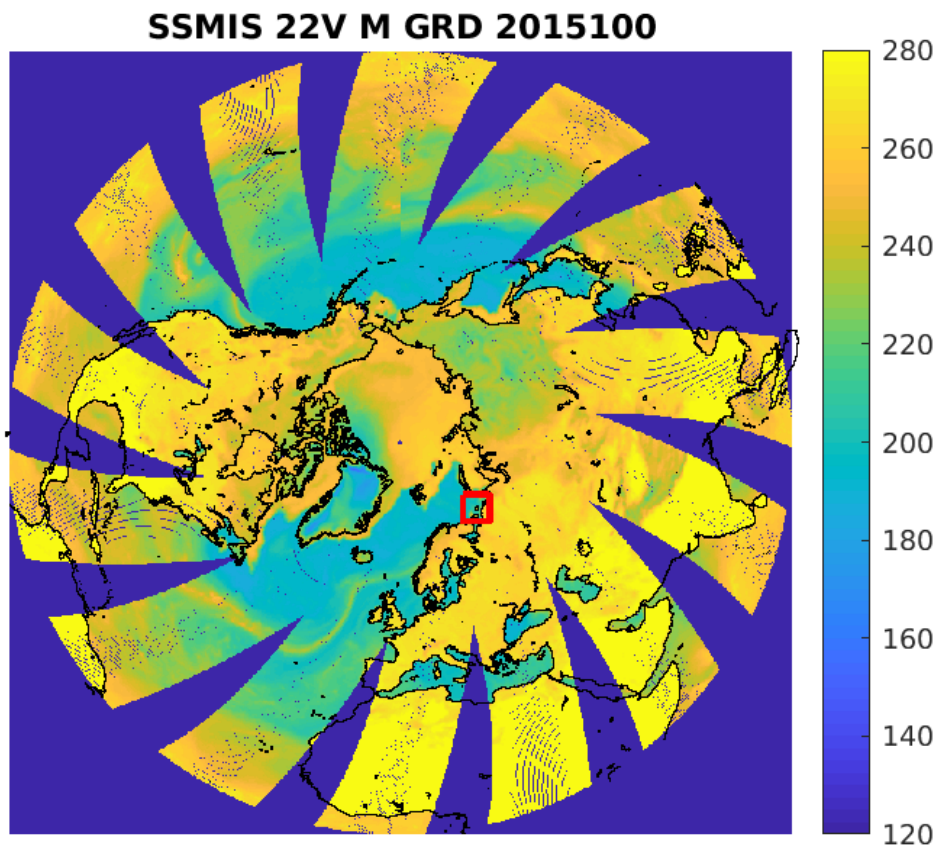


Figure 435: rSIR Northern Hemisphere view.



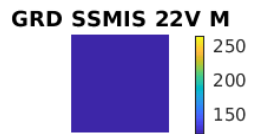
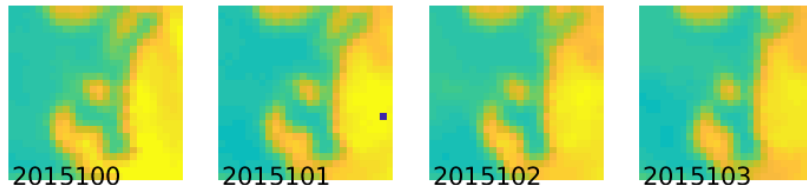
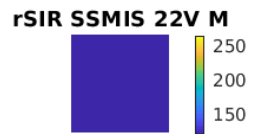
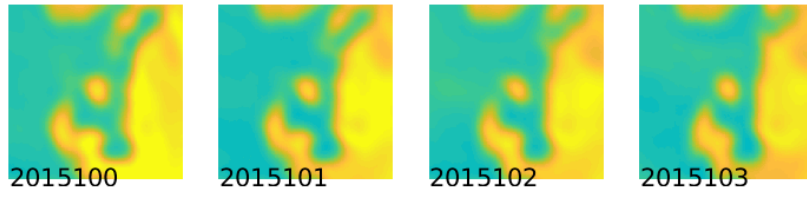


Figure 436: Time series of (top) rSIR and (bottom) GRD  $T_B$  images over the study area. Image dates are labeled on the image.

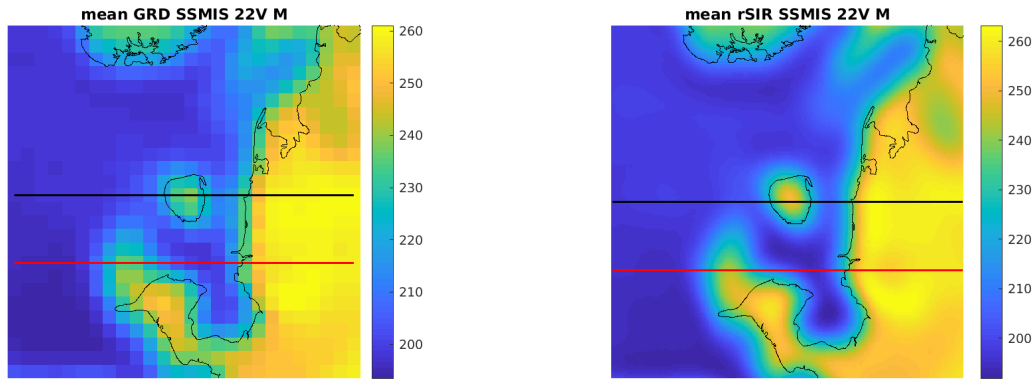


Figure 437: Average of daily  $T_B$  images over the study area. (left) 25-km GRD. (right) 3.125-km rSIR. The thick horizontal lines show the data transect locations where data is extracted from the image for analysis.

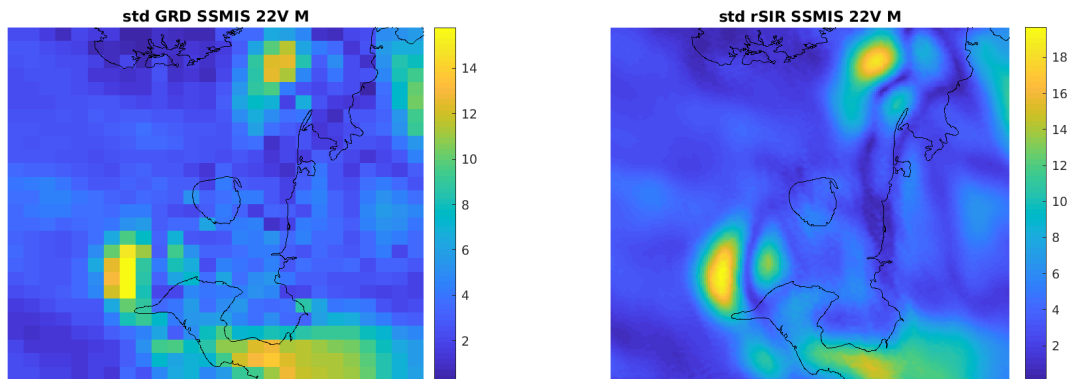


Figure 438: Standard deviation of daily  $T_B$  images over the study area. (left) 25-km GRD. (right) 3.125-km rSIR.

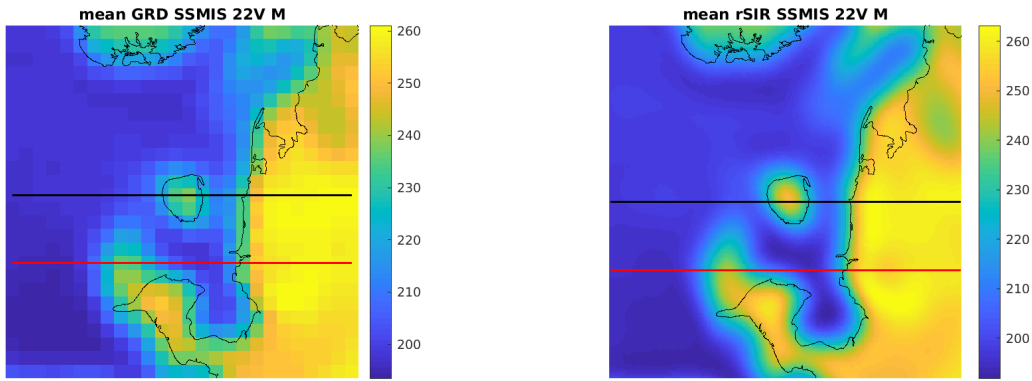


Figure 439: [Repeated] Average of daily  $T_B$  images over the study area. (left) 25-km GRD. (right) 3.125-km rSIR. The thick horizontal lines show the data transect locations where data is extracted from the image for analysis.

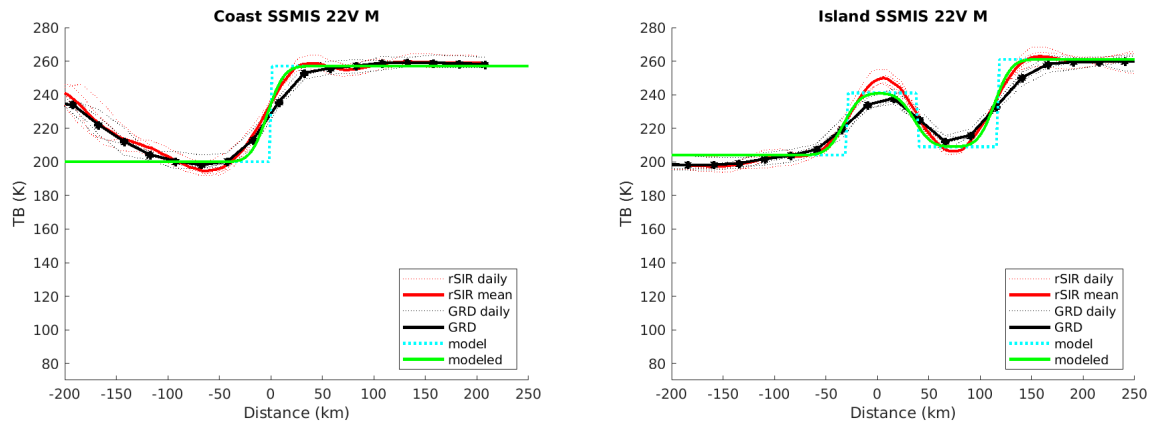


Figure 440: Plots of  $T_B$  along the two analysis case transect lines for the (left) coast-crossing and (right) island-crossing cases.

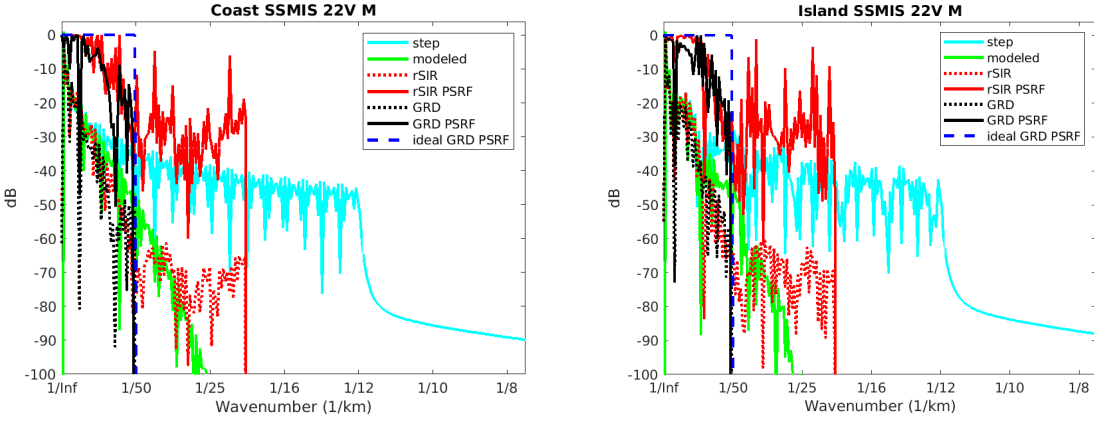


Figure 441: Wavenumber spectra of the  $T_B$  slices, the model, and the PSRF. (left) Coast-crossing case. (right) Island-crossing case.

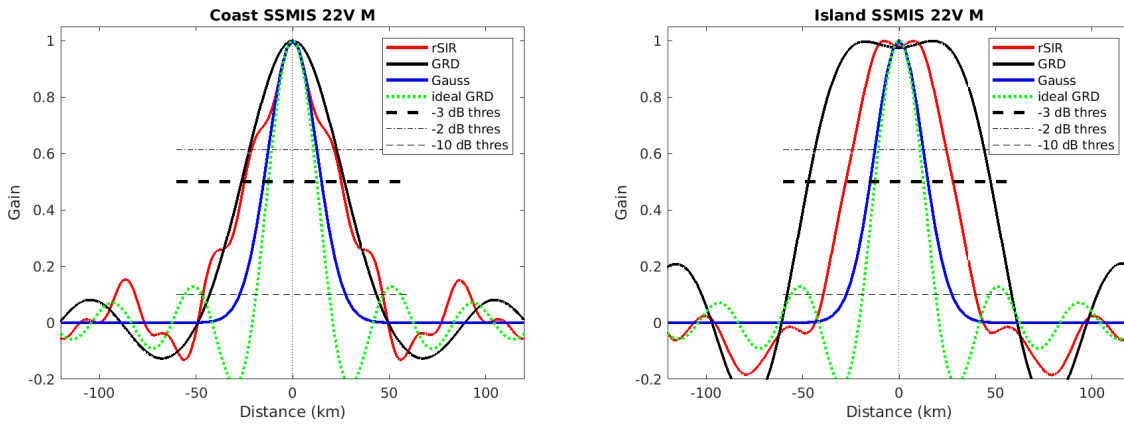


Figure 442: Derived single-pass rSIR and GRD PSRFs from the (left) coast-crossing and (right) island-crossing cases.

Table 129: Resolution estimates for SSMIS channel 22V LTOD M

Algorithm	-3 dB Thres		-2 dB Thres		-10 dB Thres	
	Coast	Island	Coast	Island	Coast	Island
Gauss	30.0	30.0	24.4	24.4	54.8	54.8
rSIR	50.1	55.6	41.1	47.5	93.1	78.8
ideal GRD	36.2	36.2	30.3	30.3	54.5	54.5
GRD	53.3	94.6	43.9	86.8	86.4	116.3

## F.7 SSMIS Channel 37H E Figures

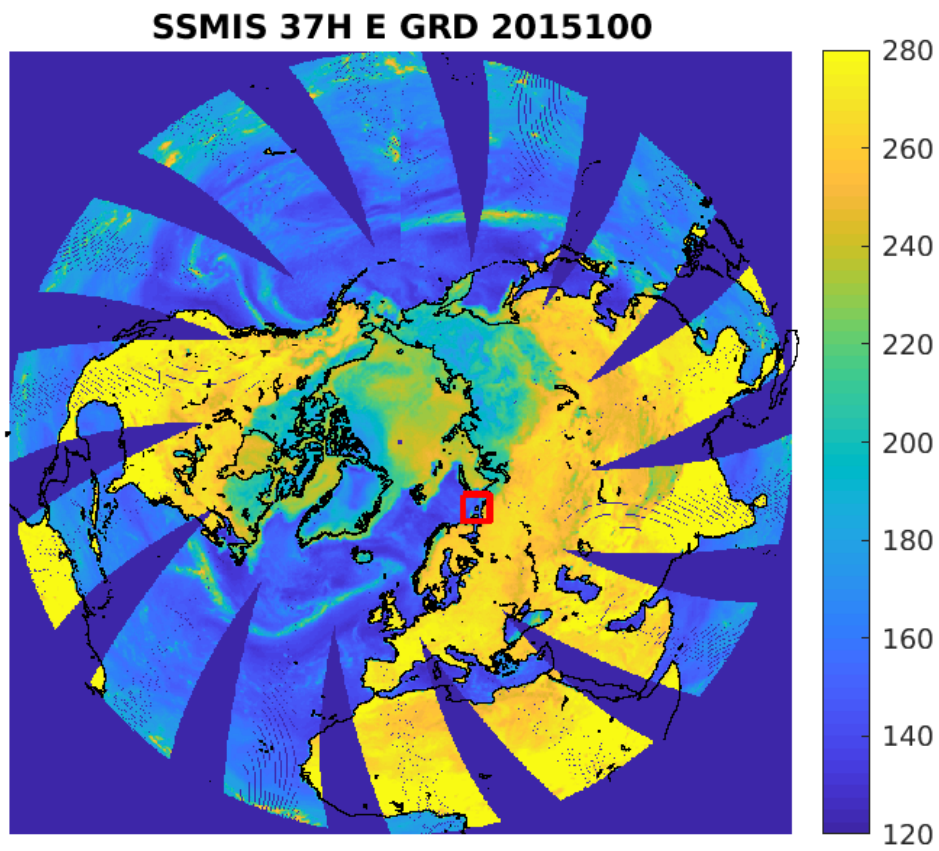


Figure 443: rSIR Northern Hemisphere view.

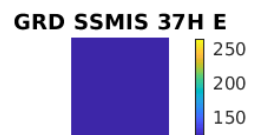
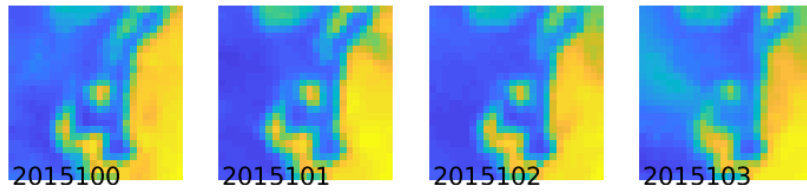
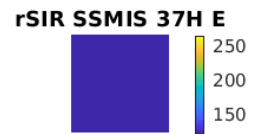
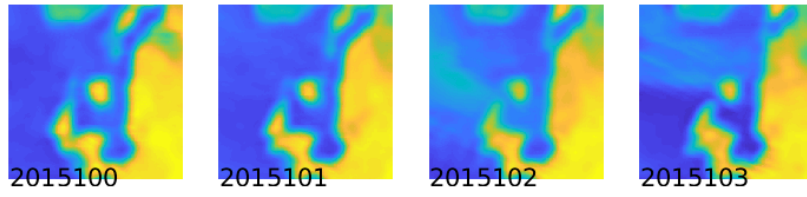


Figure 444: Time series of (top) rSIR and (bottom) GRD  $T_B$  images over the study area. Image dates are labeled on the image.

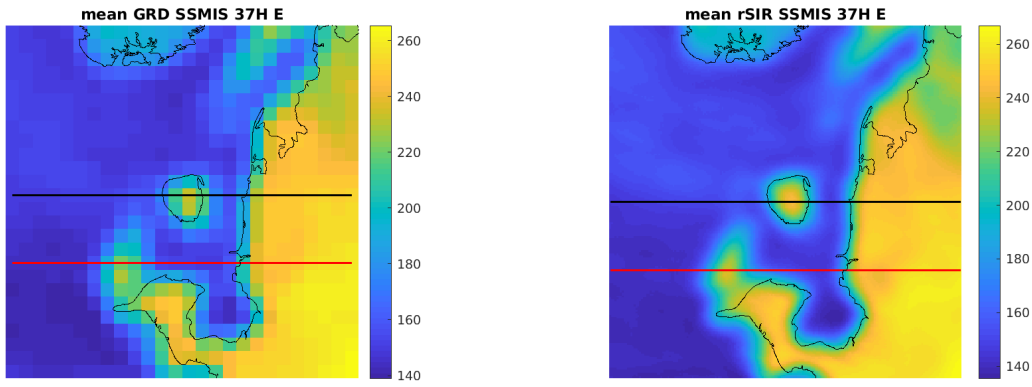


Figure 445: Average of daily  $T_B$  images over the study area. (left) 25-km GRD. (right) 3.125-km rSIR. The thick horizontal lines show the data transect locations where data is extracted from the image for analysis.

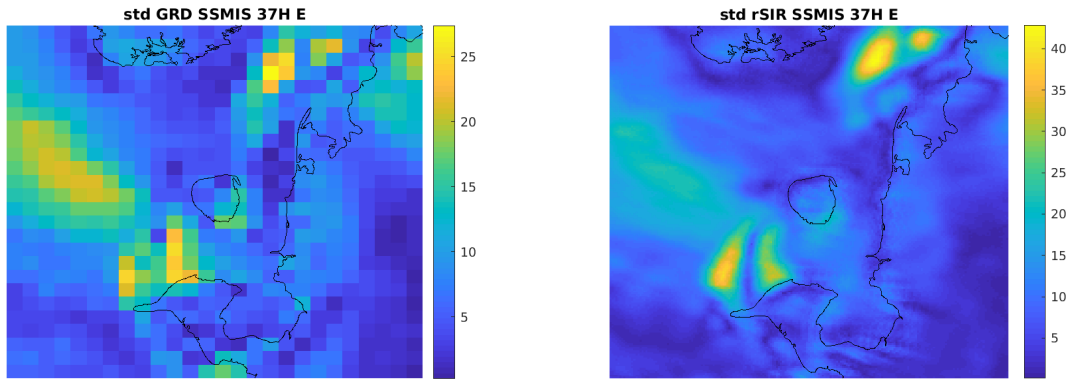


Figure 446: Standard deviation of daily  $T_B$  images over the study area. (left) 25-km GRD. (right) 3.125-km rSIR.

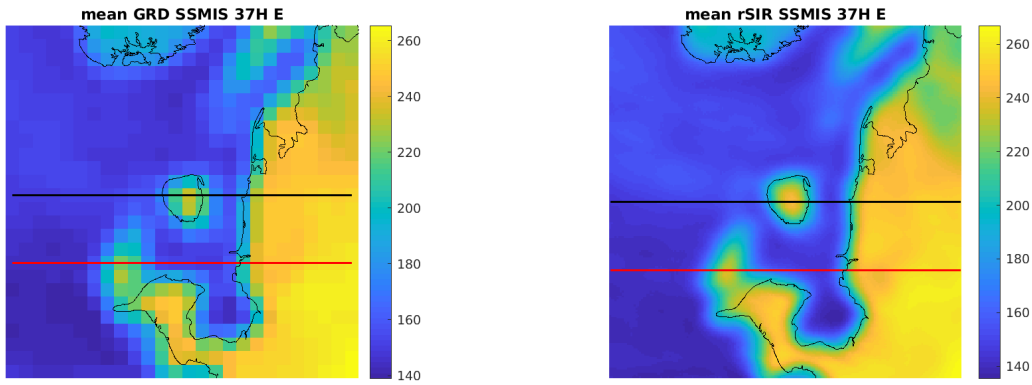


Figure 447: [Repeated] Average of daily  $T_B$  images over the study area. (left) 25-km GRD. (right) 3.125-km rSIR. The thick horizontal lines show the data transect locations where data is extracted from the image for analysis.

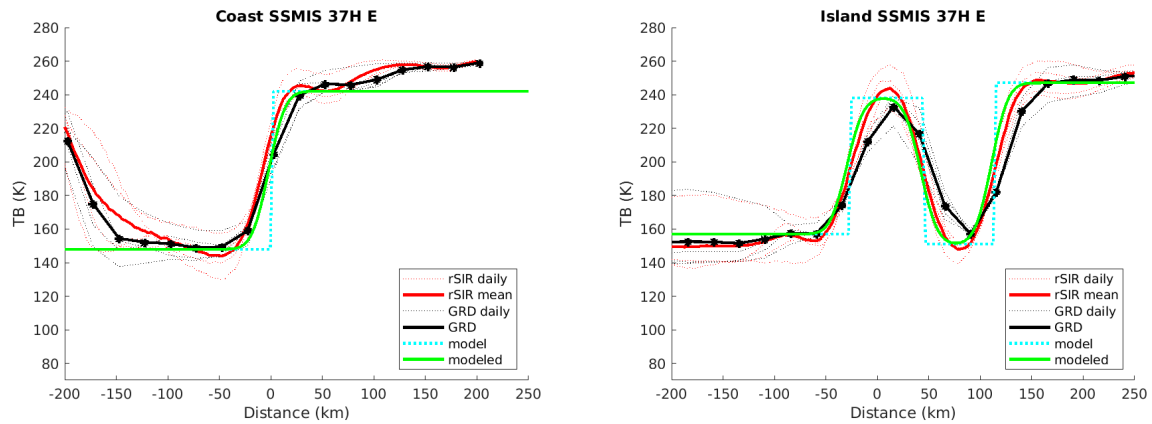


Figure 448: Plots of  $T_B$  along the two analysis case transect lines for the (left) coast-crossing and (right) island-crossing cases.



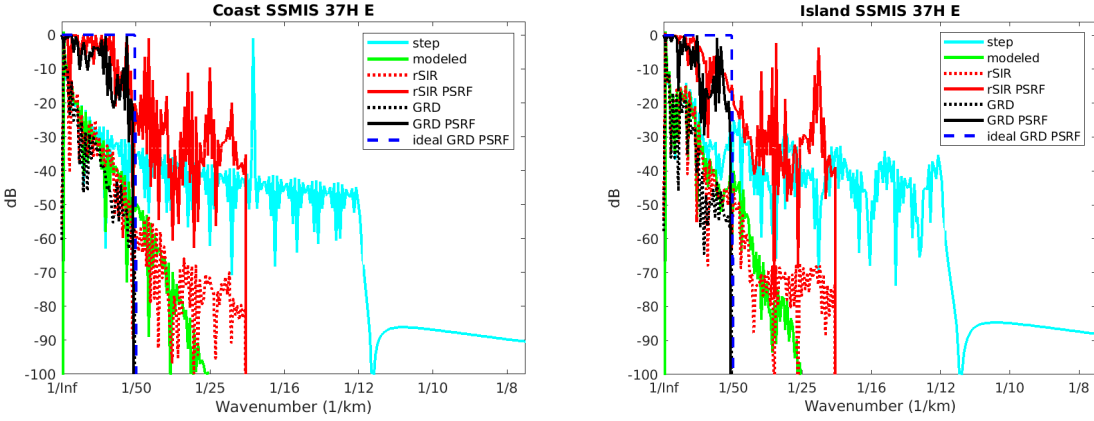


Figure 449: Wavenumber spectra of the  $T_B$  slices, the model, and the PSRF. (left) Coast-crossing case. (right) Island-crossing case.

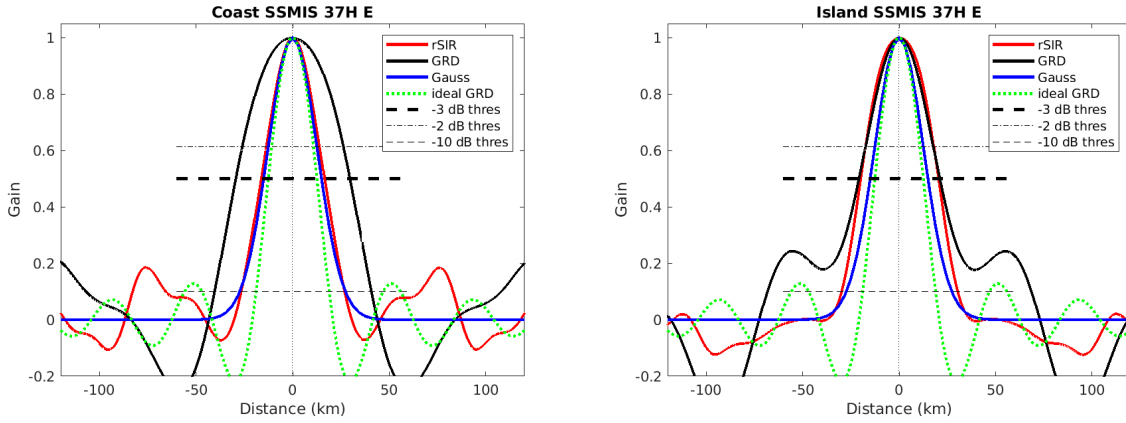


Figure 450: Derived single-pass rSIR and GRD PSRFs from the (left) coast-crossing and (right) island-crossing cases.

Table 130: Resolution estimates for SSMIS channel 37H LTOD E

Algorithm	-3 dB Thres		-2 dB Thres		-10 dB Thres	
	Coast	Island	Coast	Island	Coast	Island
Gauss	30.0	30.0	24.4	24.4	54.8	54.8
rSIR	32.8	40.3	26.7	34.6	53.5	60.3
ideal GRD	36.2	36.2	30.3	30.3	54.5	54.5
GRD	59.1	41.8	51.2	34.1	81.1	136.9

## F.8 SSMIS Channel 37H M Figures

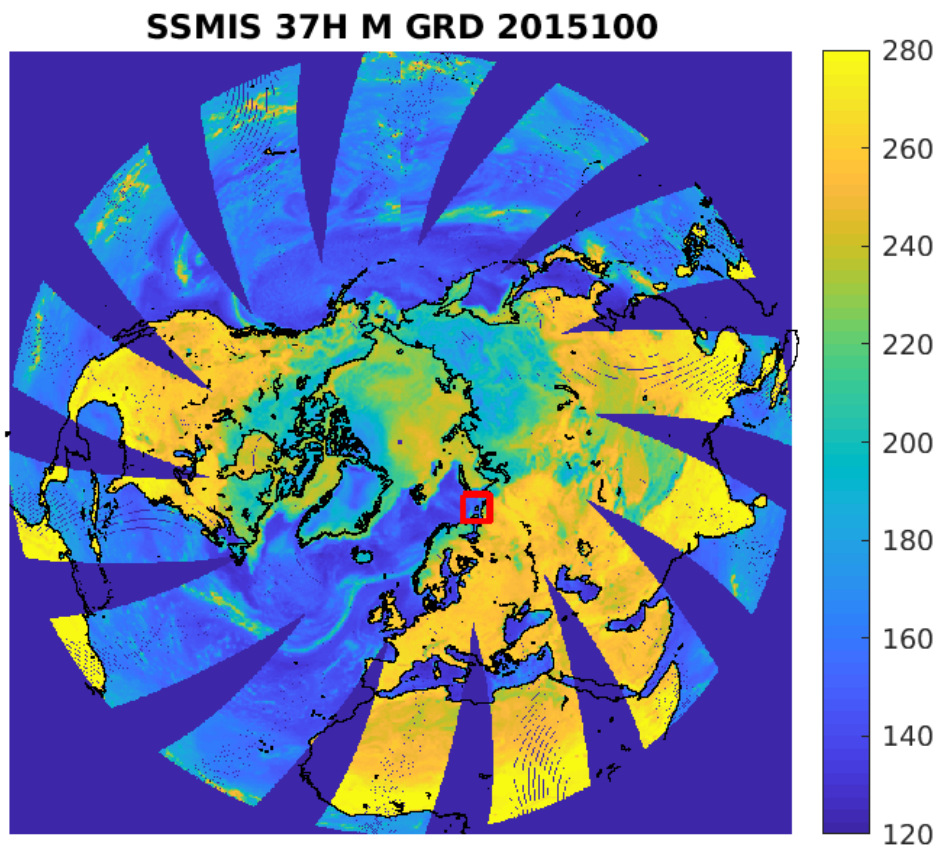


Figure 451: rSIR Northern Hemisphere view.

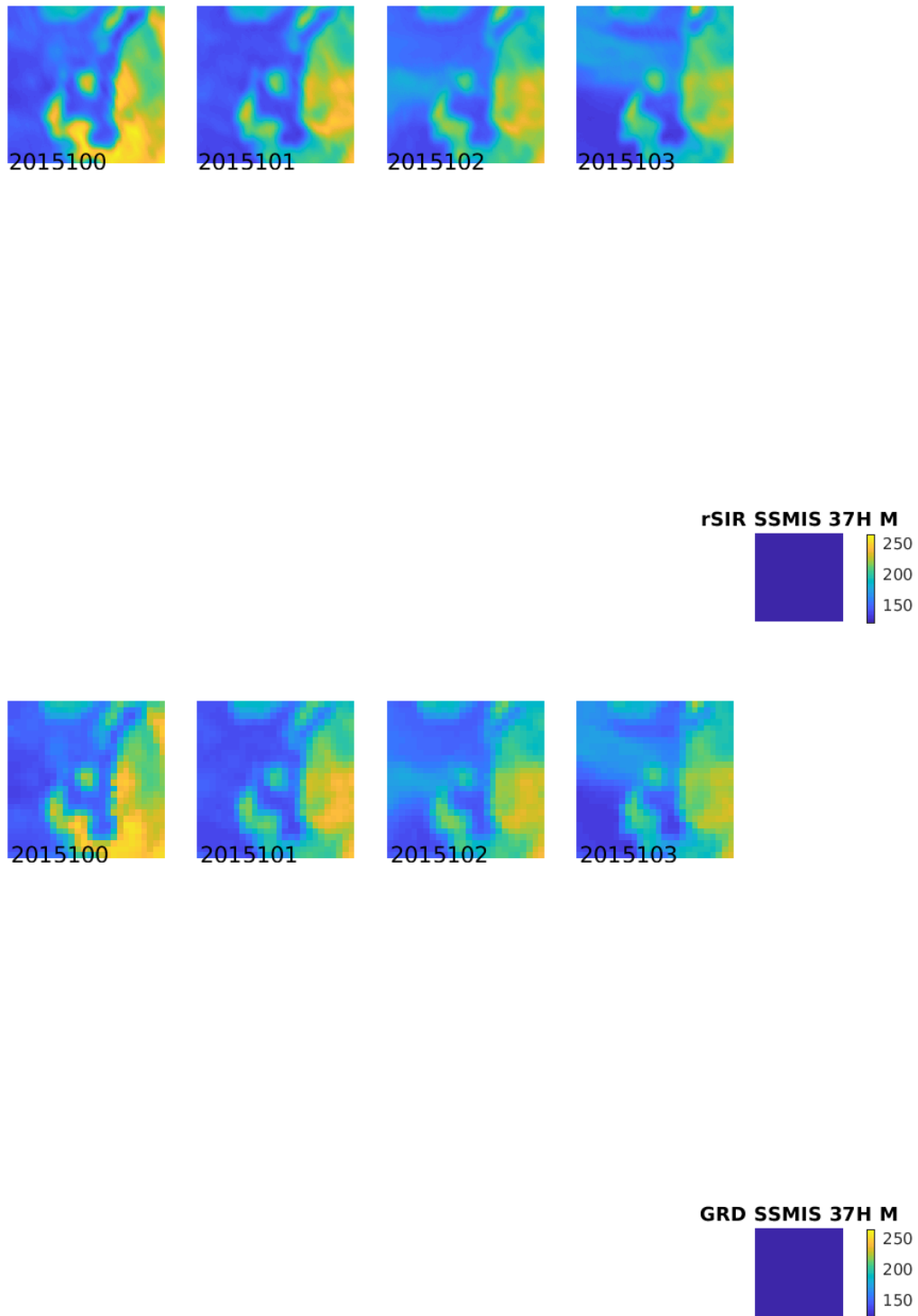


Figure 452: Time series of (top) rSIR and (bottom) GRD  $T_B$  images over the study area. Image dates are labeled on the image.

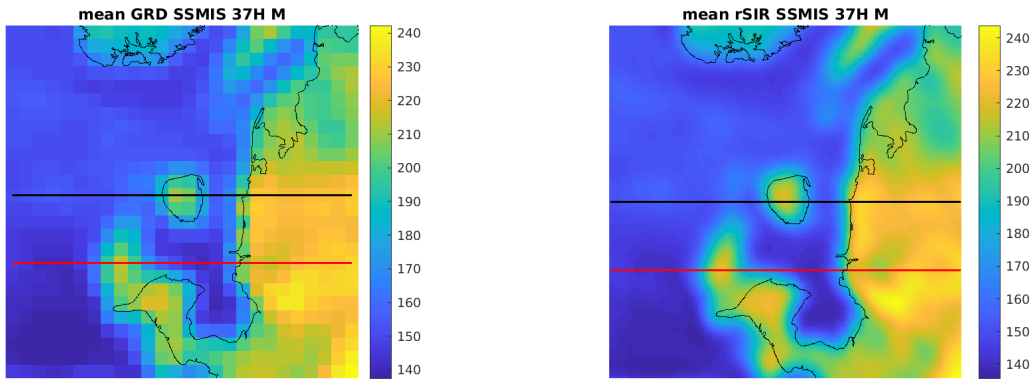


Figure 453: Average of daily  $T_B$  images over the study area. (left) 25-km GRD. (right) 3.125-km rSIR. The thick horizontal lines show the data transect locations where data is extracted from the image for analysis.

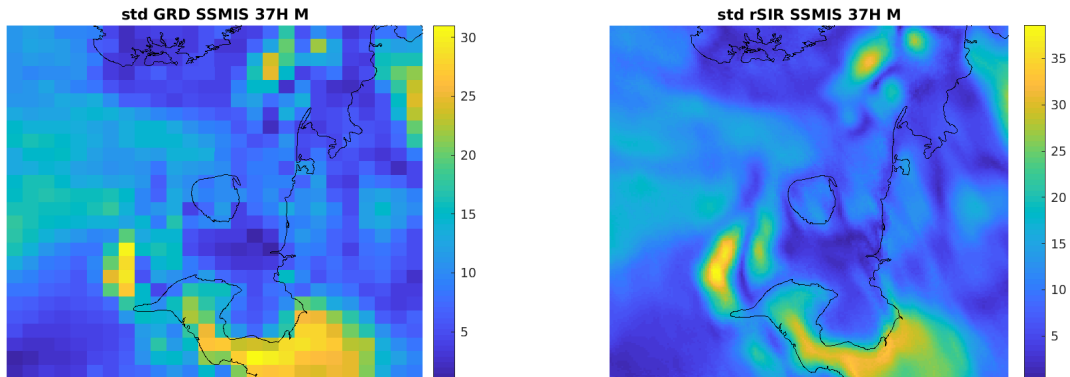


Figure 454: Standard deviation of daily  $T_B$  images over the study area. (left) 25-km GRD. (right) 3.125-km rSIR.

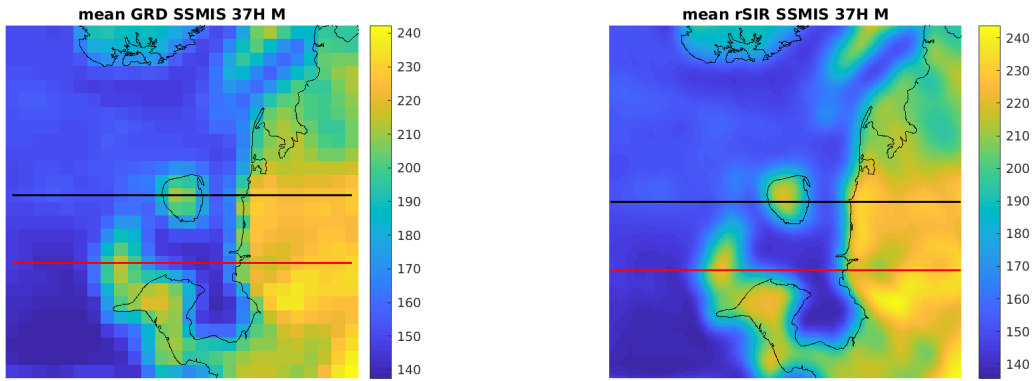


Figure 455: [Repeated] Average of daily  $T_B$  images over the study area. (left) 25-km GRD. (right) 3.125-km rSIR. The thick horizontal lines show the data transect locations where data is extracted from the image for analysis.

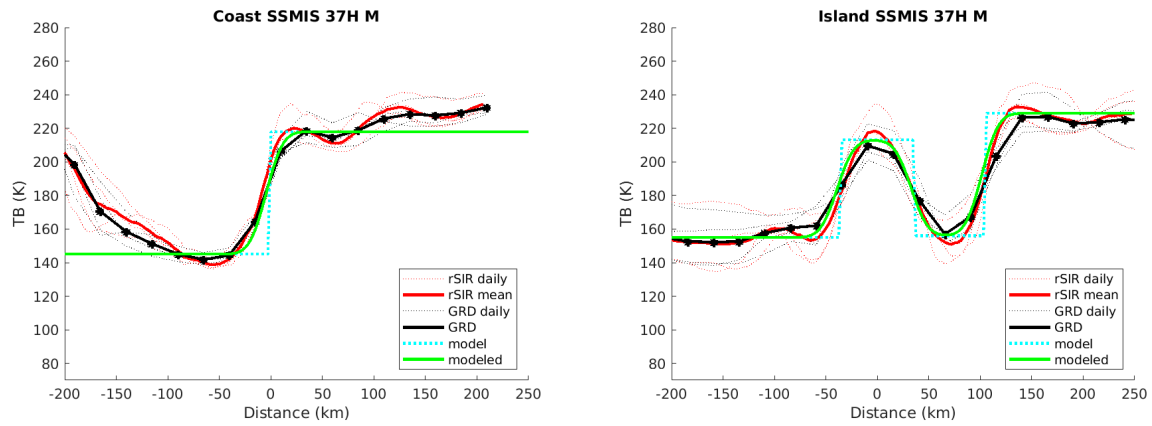


Figure 456: Plots of  $T_B$  along the two analysis case transect lines for the (left) coast-crossing and (right) island-crossing cases.

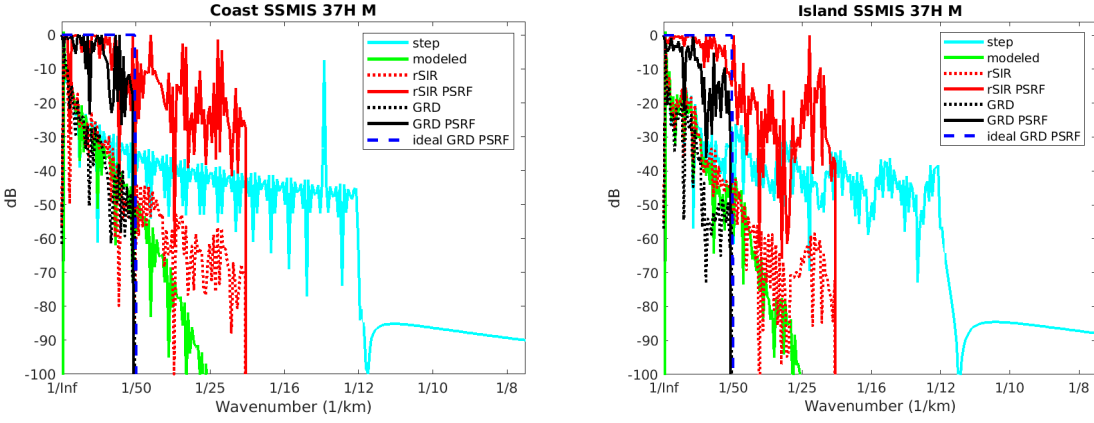


Figure 457: Wavenumber spectra of the  $T_B$  slices, the model, and the PSRF. (left) Coast-crossing case. (right) Island-crossing case.

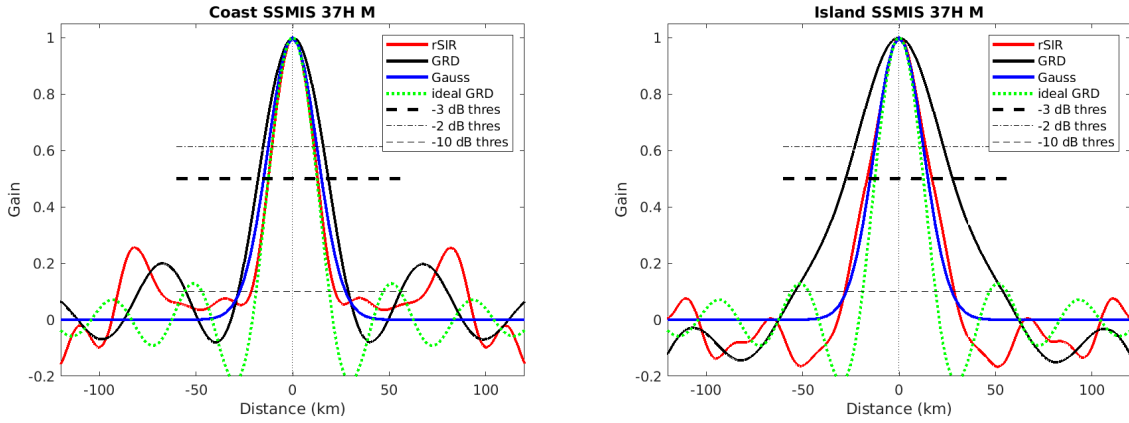


Figure 458: Derived single-pass rSIR and GRD PSRFs from the (left) coast-crossing and (right) island-crossing cases.

Table 131: Resolution estimates for SSMIS channel 37H LTOD M

Algorithm	-3 dB Thres		-2 dB Thres		-10 dB Thres	
	Coast	Island	Coast	Island	Coast	Island
Gauss	30.0	30.0	24.4	24.4	54.8	54.8
rSIR	25.4	33.8	21.1	26.2	43.5	56.8
ideal GRD	36.2	36.2	30.3	30.3	54.5	54.5
GRD	36.4	55.4	30.3	44.5	56.8	107.8

## F.9 SSMIS Channel 37V E Figures

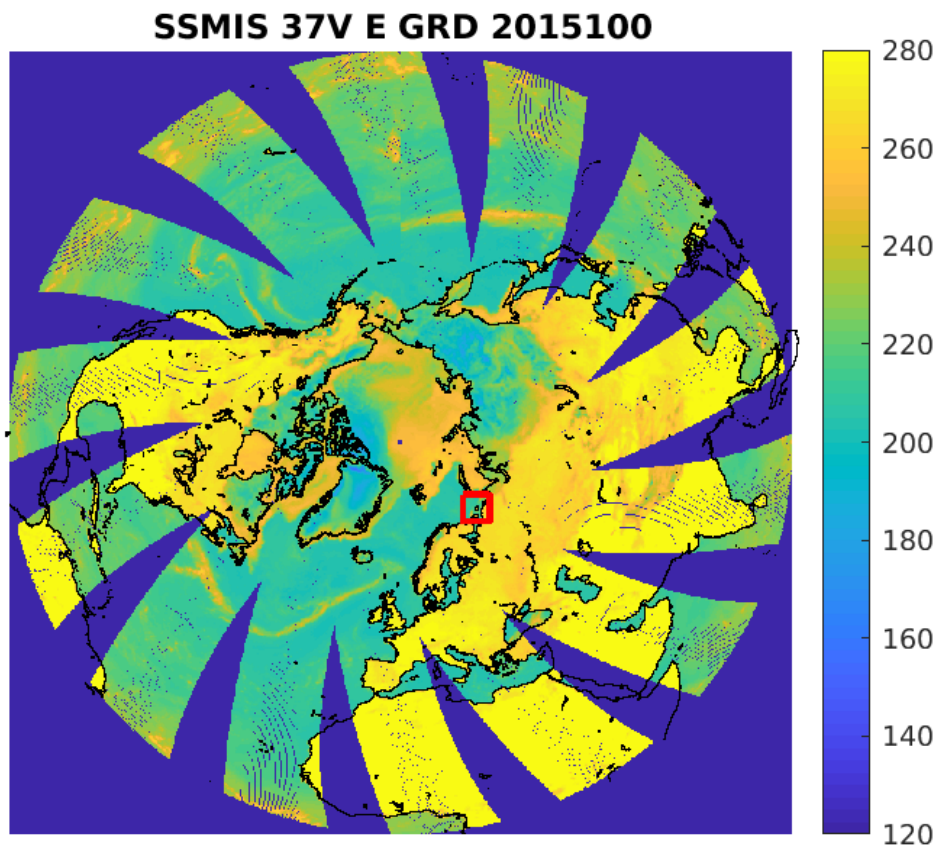


Figure 459: rSIR Northern Hemisphere view.

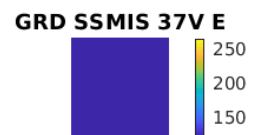
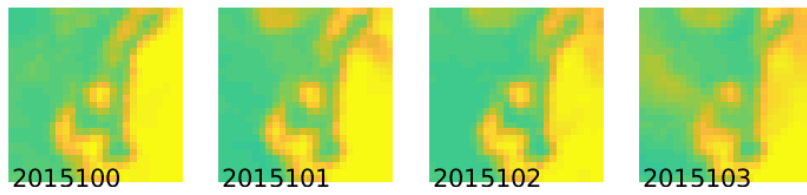
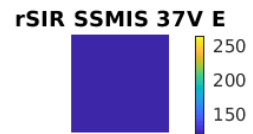
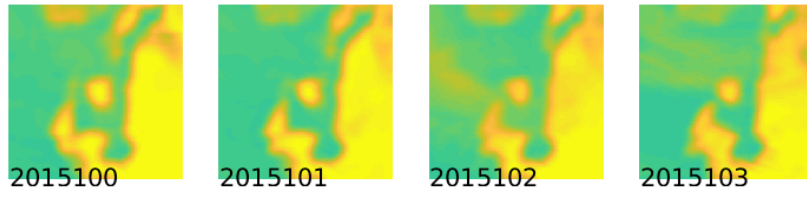


Figure 460: Time series of (top) rSIR and (bottom) GRD  $T_B$  images over the study area. Image dates are labeled on the image.



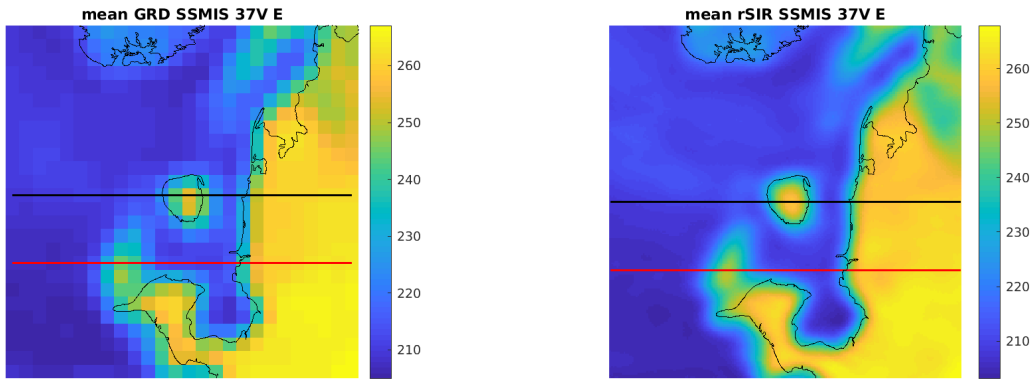


Figure 461: Average of daily  $T_B$  images over the study area. (left) 25-km GRD. (right) 3.125-km rSIR. The thick horizontal lines show the data transect locations where data is extracted from the image for analysis.

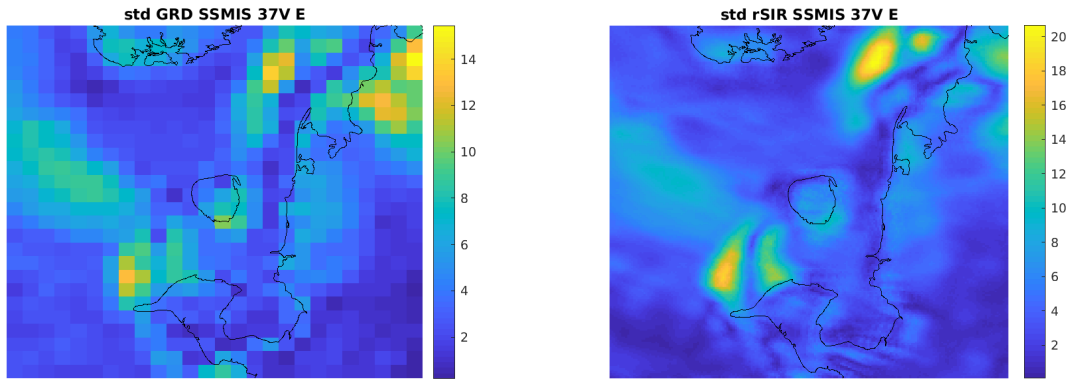


Figure 462: Standard deviation of daily  $T_B$  images over the study area. (left) 25-km GRD. (right) 3.125-km rSIR.

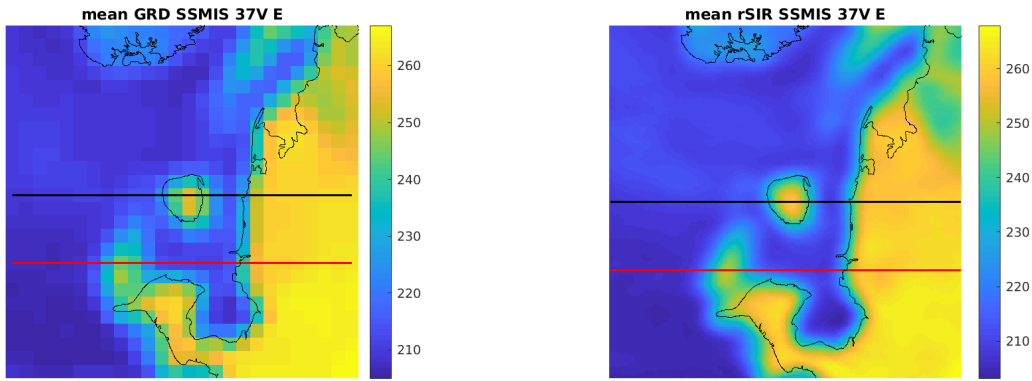


Figure 463: [Repeated] Average of daily  $T_B$  images over the study area. (left) 25-km GRD. (right) 3.125-km rSIR. The thick horizontal lines show the data transect locations where data is extracted from the image for analysis.

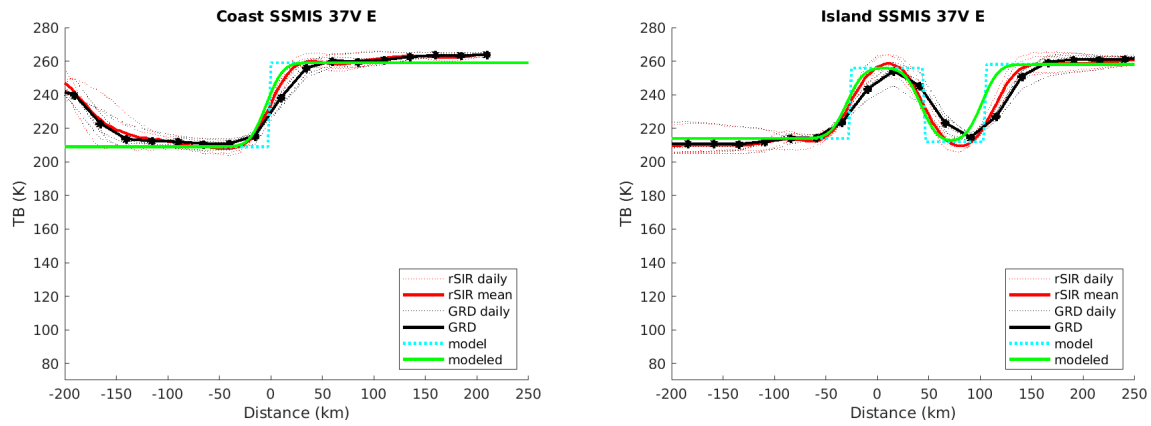


Figure 464: Plots of  $T_B$  along the two analysis case transect lines for the (left) coast-crossing and (right) island-crossing cases.

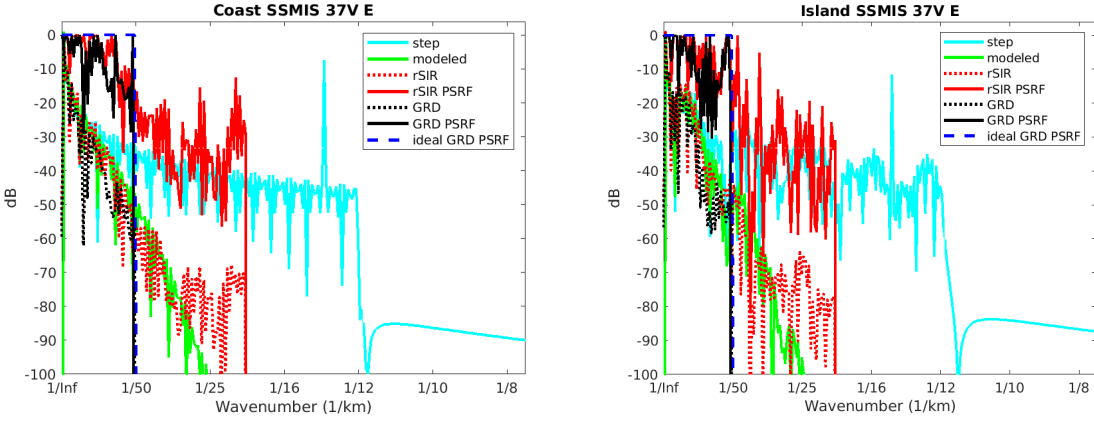


Figure 465: Wavenumber spectra of the  $T_B$  slices, the model, and the PSRF. (left) Coast-crossing case. (right) Island-crossing case.

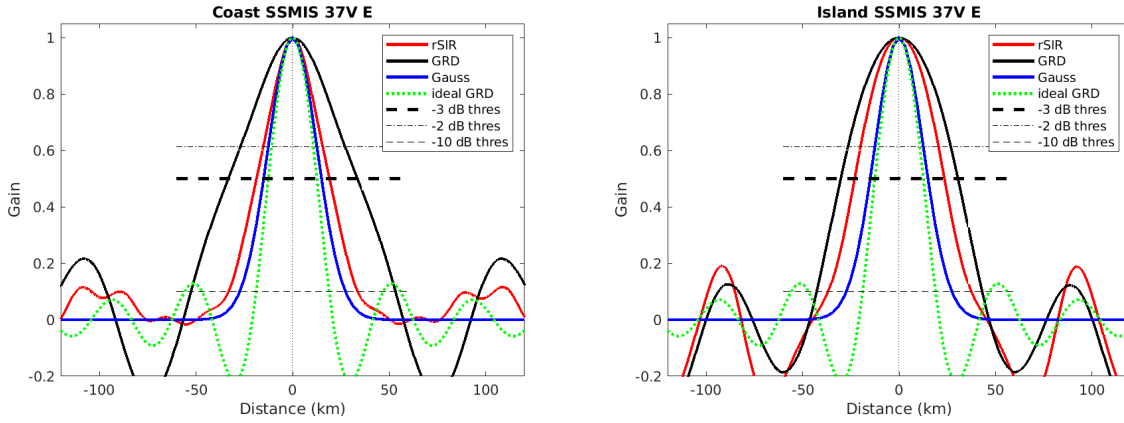


Figure 466: Derived single-pass rSIR and GRD PSRFs from the (left) coast-crossing and (right) island-crossing cases.

Table 132: Resolution estimates for SSMIS channel 37V LTOD E

Algorithm	-3 dB Thres		-2 dB Thres		-10 dB Thres	
	Coast	Island	Coast	Island	Coast	Island
Gauss	30.0	30.0	24.4	24.4	54.8	54.8
rSIR	37.8	46.5	29.6	39.3	66.8	74.2
ideal GRD	36.2	36.2	30.3	30.3	54.5	54.5
GRD	66.8	60.8	52.3	52.1	105.8	85.8

## F.10 SSMIS Channel 37V M Figures

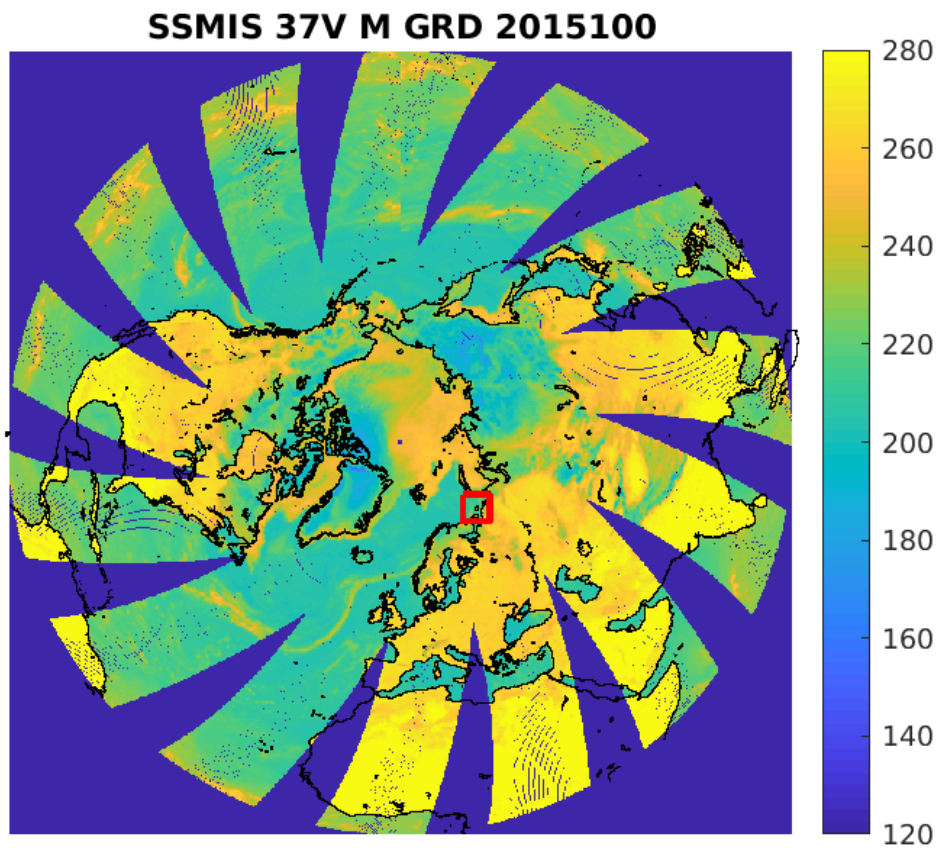


Figure 467: rSIR Northern Hemisphere view.

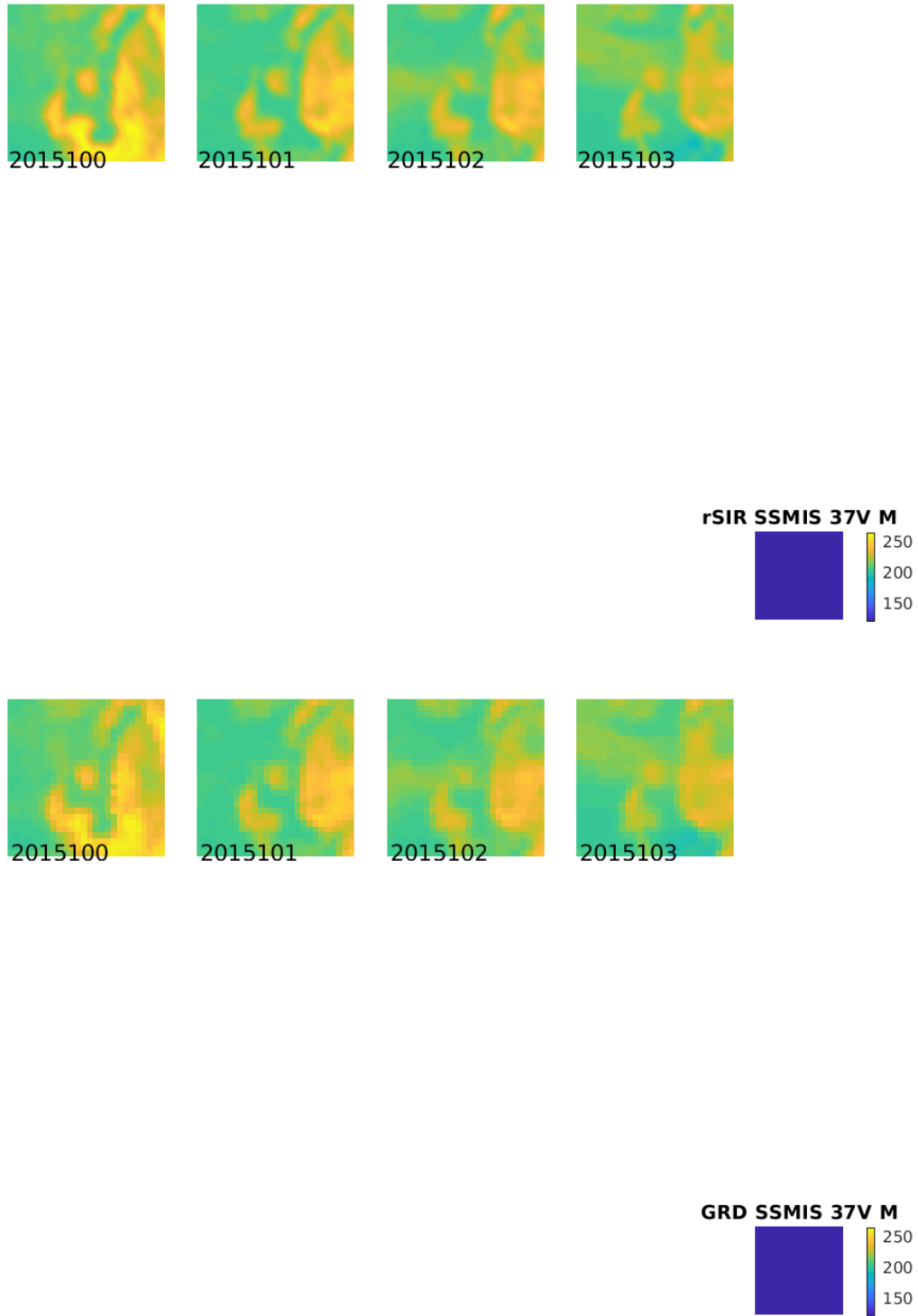


Figure 468: Time series of (top) rSIR and (bottom) GRD  $T_B$  images over the study area. Image dates are labeled on the image.

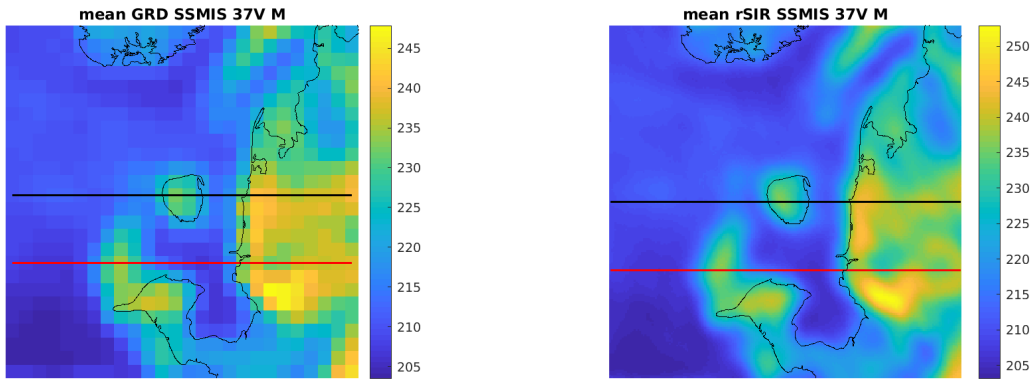


Figure 469: Average of daily  $T_B$  images over the study area. (left) 25-km GRD. (right) 3.125-km rSIR. The thick horizontal lines show the data transect locations where data is extracted from the image for analysis.

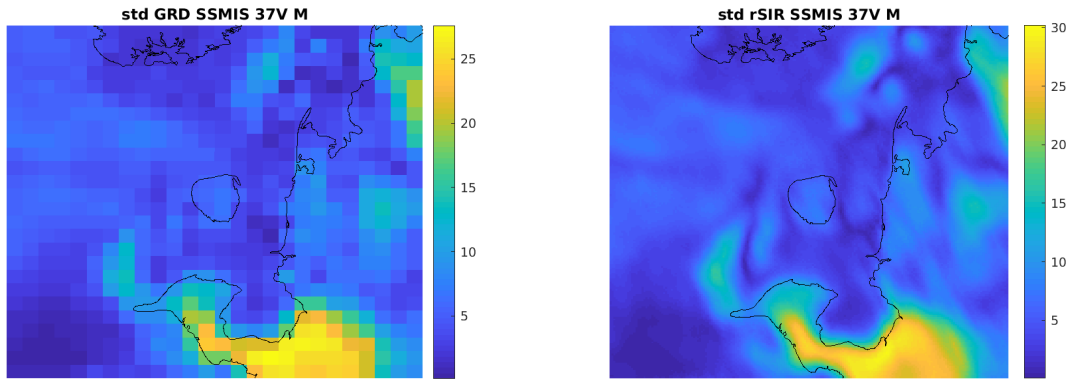


Figure 470: Standard deviation of daily  $T_B$  images over the study area. (left) 25-km GRD. (right) 3.125-km rSIR.

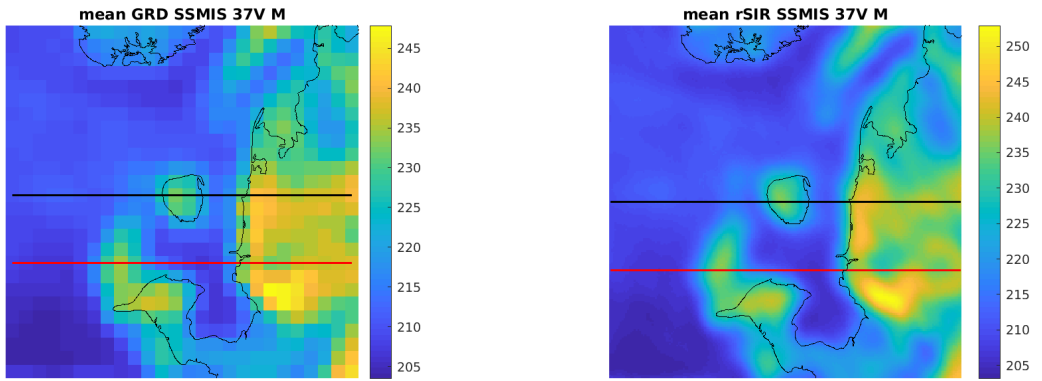


Figure 471: [Repeated] Average of daily  $T_B$  images over the study area. (left) 25-km GRD. (right) 3.125-km rSIR. The thick horizontal lines show the data transect locations where data is extracted from the image for analysis.

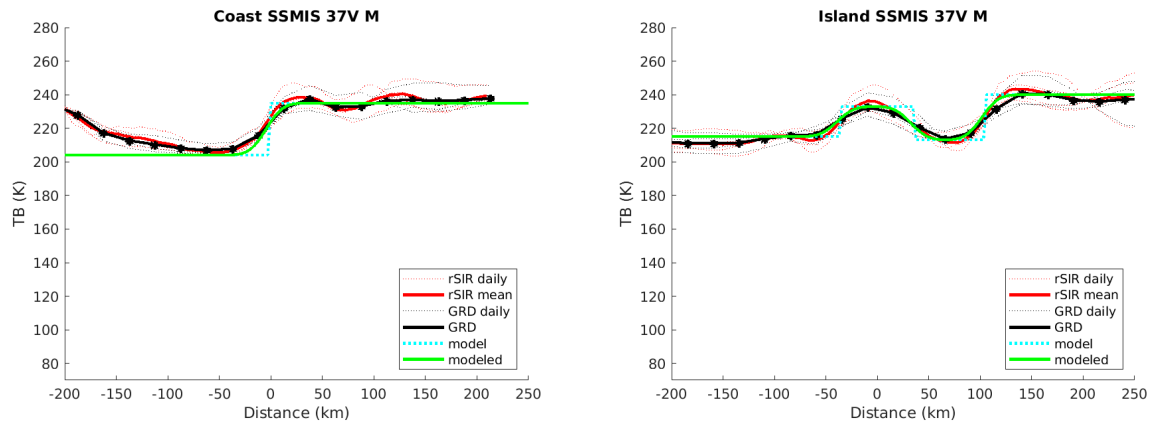


Figure 472: Plots of  $T_B$  along the two analysis case transect lines for the (left) coast-crossing and (right) island-crossing cases.

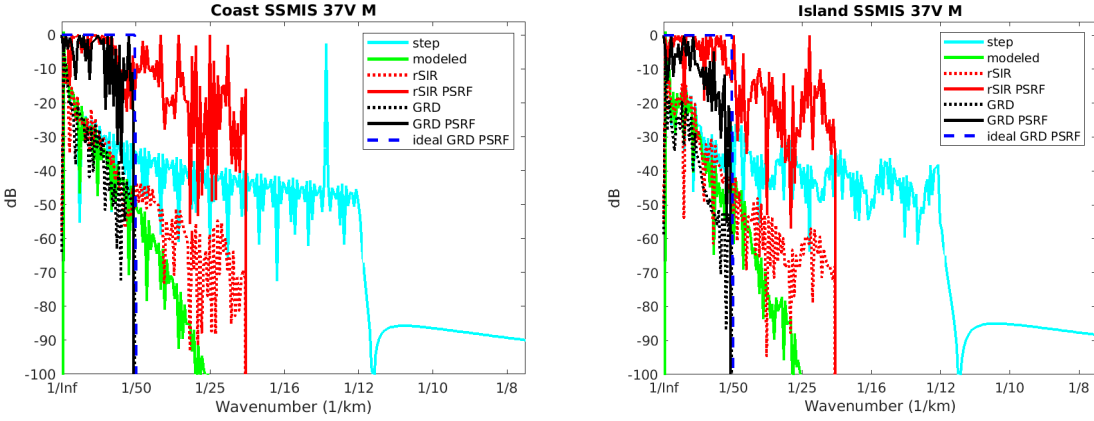


Figure 473: Wavenumber spectra of the  $T_B$  slices, the model, and the PSRF. (left) Coast-crossing case. (right) Island-crossing case.

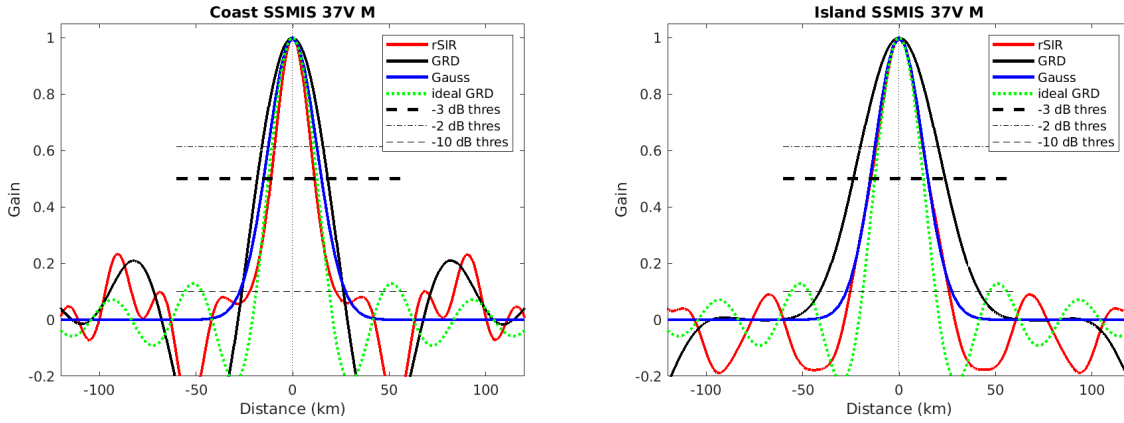


Figure 474: Derived single-pass rSIR and GRD PSRFs from the (left) coast-crossing and (right) island-crossing cases.

Table 133: Resolution estimates for SSMIS channel 37V LTOD M

Algorithm	-3 dB Thres		-2 dB Thres		-10 dB Thres	
	Coast	Island	Coast	Island	Coast	Island
Gauss	30.0	30.0	24.4	24.4	54.8	54.8
rSIR	22.6	29.7	18.3	23.5	44.6	51.2
ideal GRD	36.2	36.2	30.3	30.3	54.5	54.5
GRD	36.5	47.6	30.8	39.1	52.5	82.6



## F.11 SSMIS Channel 91H E Figures

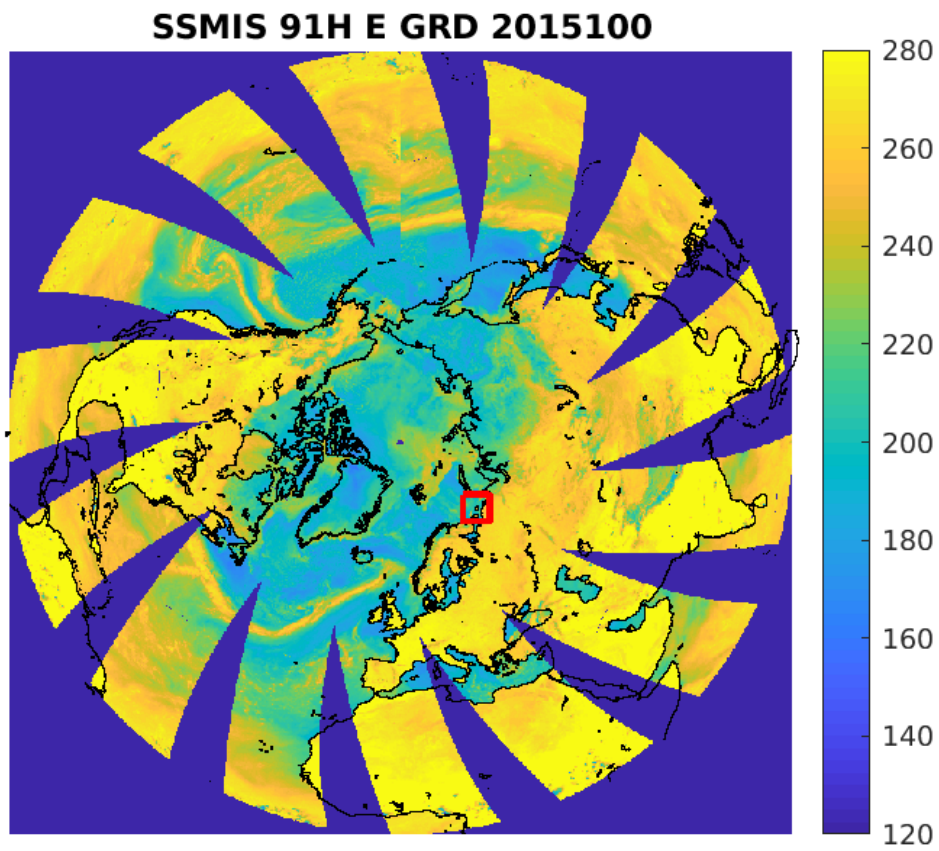


Figure 475: rSIR Northern Hemisphere view.

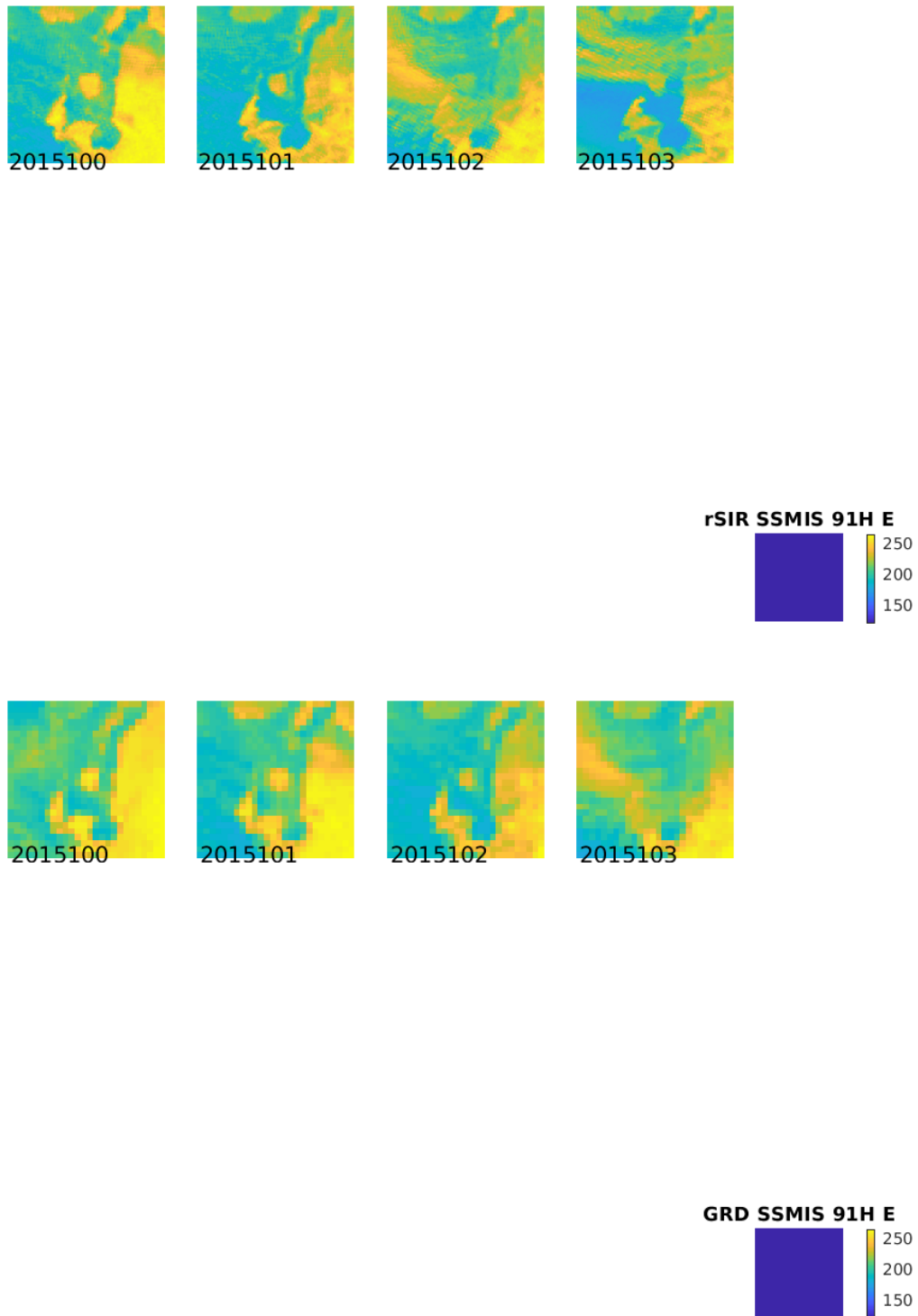


Figure 476: Time series of (top) rSIR and (bottom) GRD  $T_B$  images over the study area. Image dates are labeled on the image.

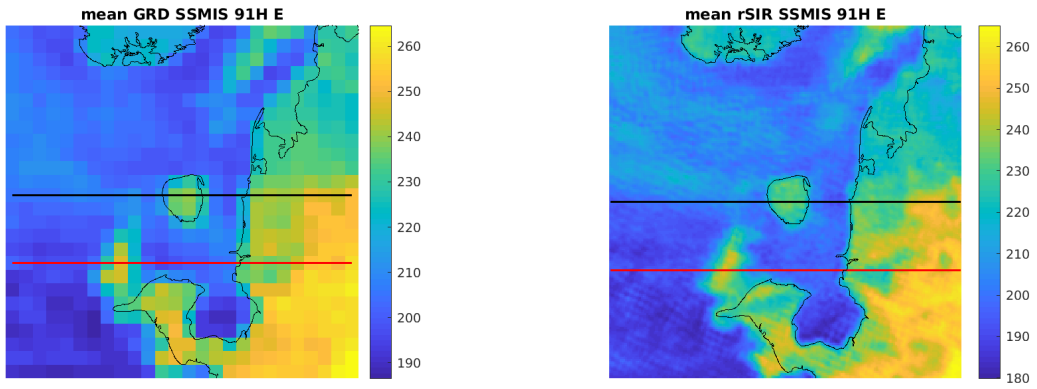


Figure 477: Average of daily  $T_B$  images over the study area. (left) 25-km GRD. (right) 3.125-km rSIR. The thick horizontal lines show the data transect locations where data is extracted from the image for analysis.

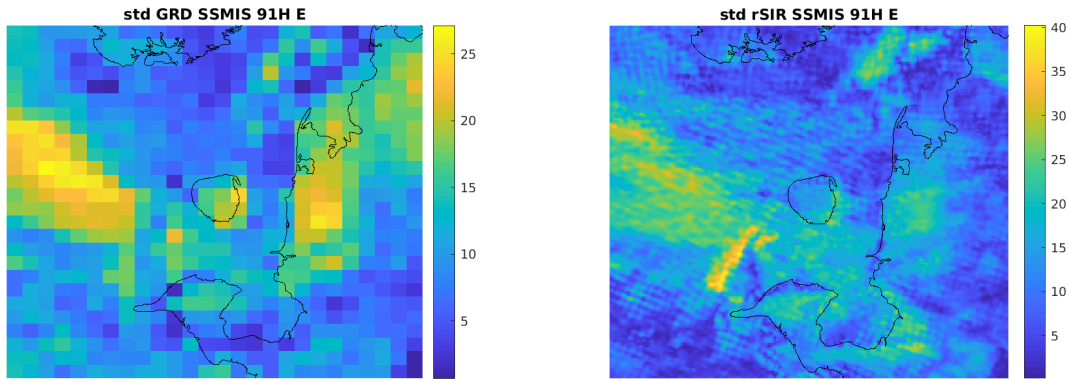


Figure 478: Standard deviation of daily  $T_B$  images over the study area. (left) 25-km GRD. (right) 3.125-km rSIR.

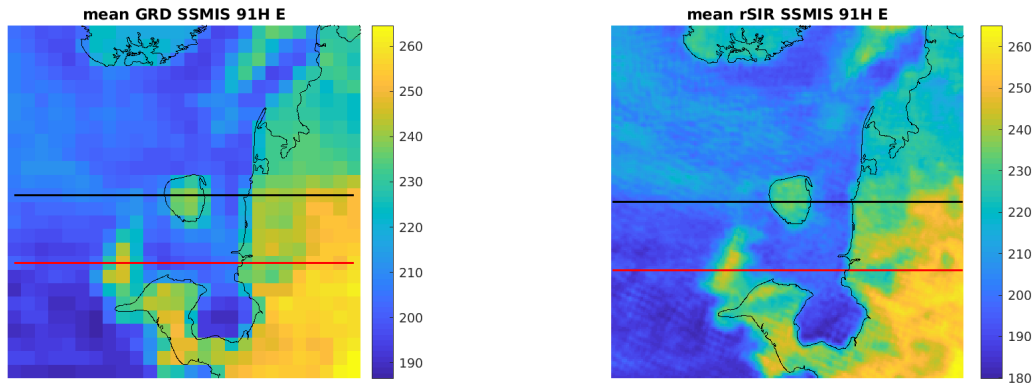


Figure 479: [Repeated] Average of daily  $T_B$  images over the study area. (left) 25-km GRD. (right) 3.125-km rSIR. The thick horizontal lines show the data transect locations where data is extracted from the image for analysis.

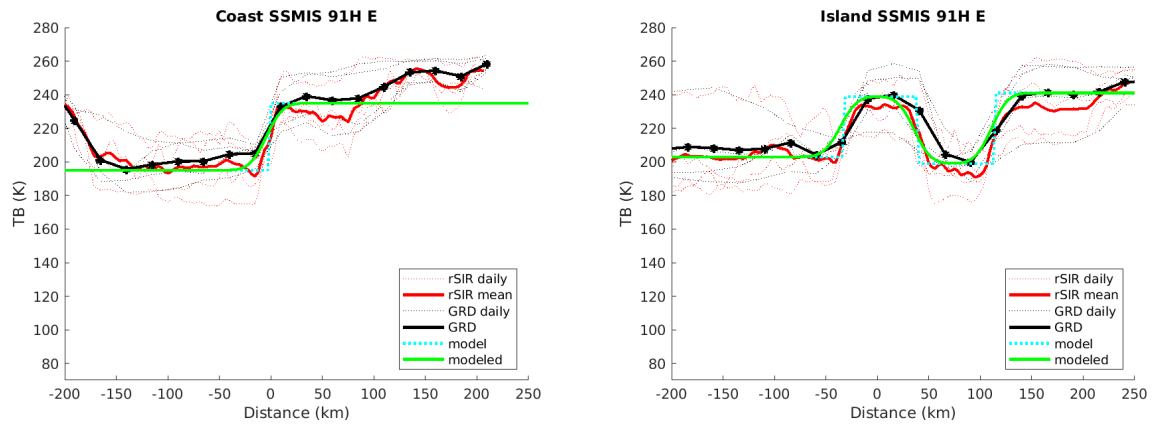


Figure 480: Plots of  $T_B$  along the two analysis case transect lines for the (left) coast-crossing and (right) island-crossing cases.

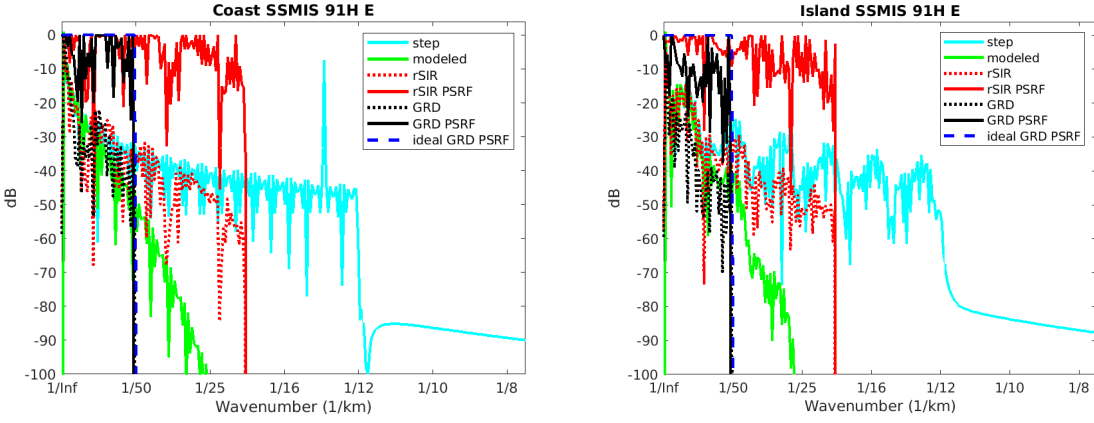


Figure 481: Wavenumber spectra of the  $T_B$  slices, the model, and the PSRF. (left) Coast-crossing case. (right) Island-crossing case.

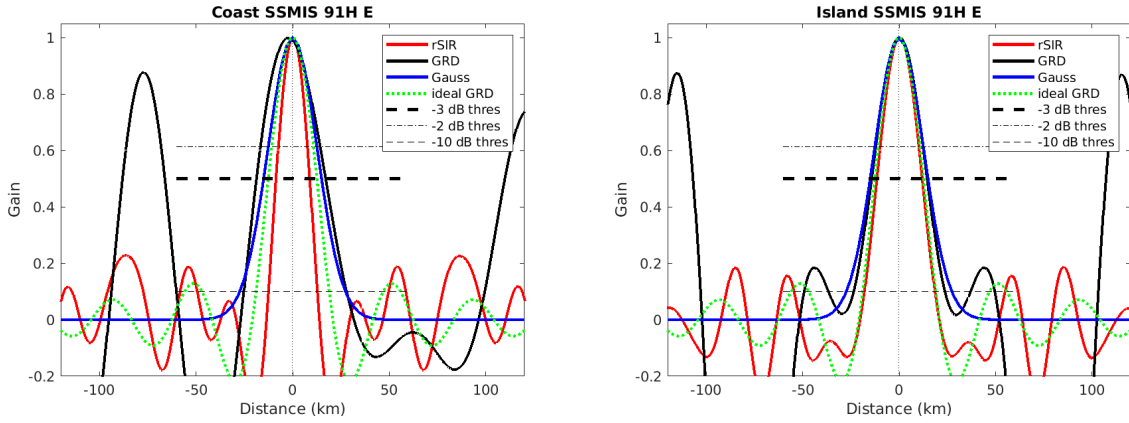


Figure 482: Derived single-pass rSIR and GRD PSRFs from the (left) coast-crossing and (right) island-crossing cases.

Table 134: Resolution estimates for SSMIS channel 91H LTOD E

Algorithm	-3 dB Thres		-2 dB Thres		-10 dB Thres	
	Coast	Island	Coast	Island	Coast	Island
Gauss	30.0	30.0	24.4	24.4	54.8	54.8
rSIR	17.4	23.5	14.7	19.5	25.2	36.5
ideal GRD	36.2	36.2	30.3	30.3	54.5	54.5
GRD	35.8	35.4	30.1	28.9	53.1	129.6

## F.12 SSMIS Channel 91H M Figures

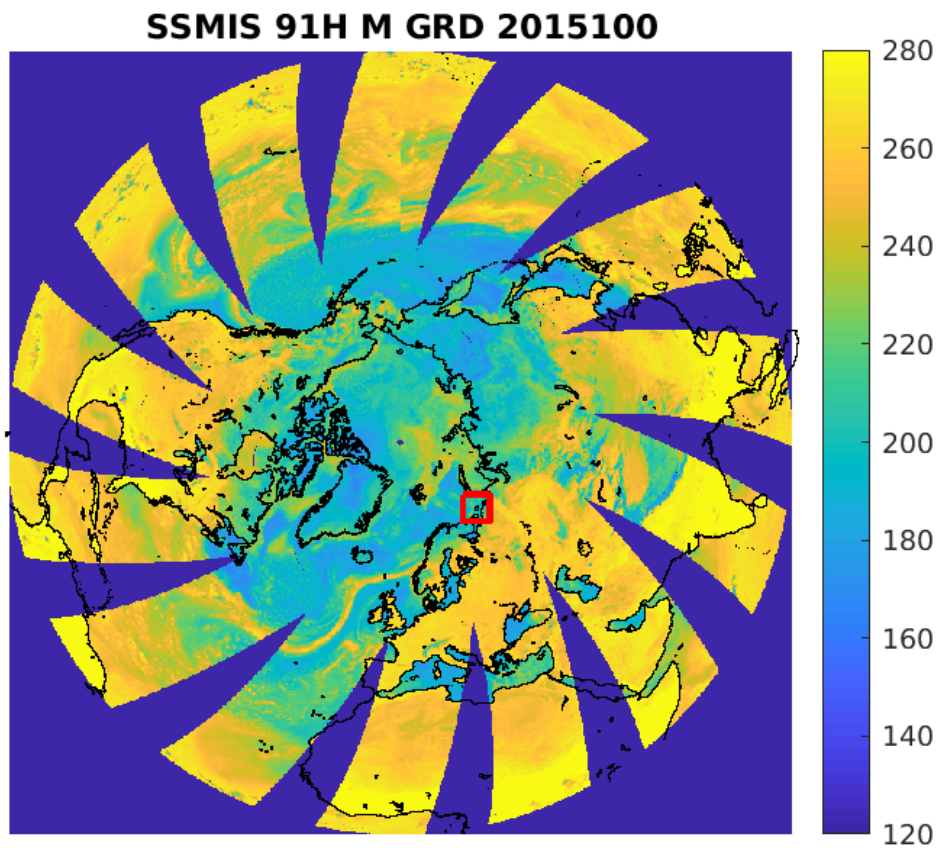


Figure 483: rSIR Northern Hemisphere view.

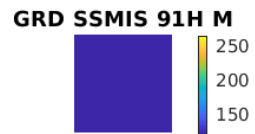
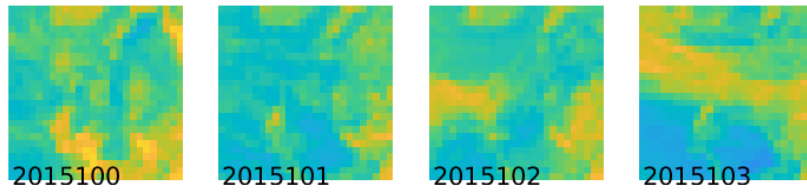
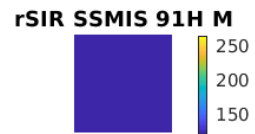
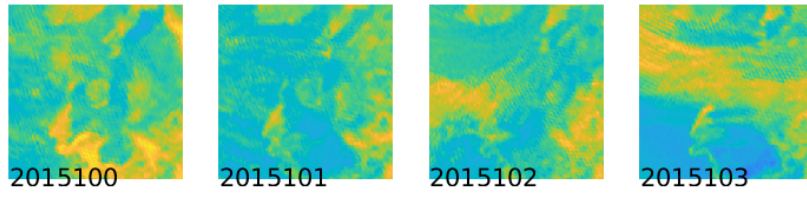


Figure 484: Time series of (top) rSIR and (bottom) GRD  $T_B$  images over the study area. Image dates are labeled on the image.

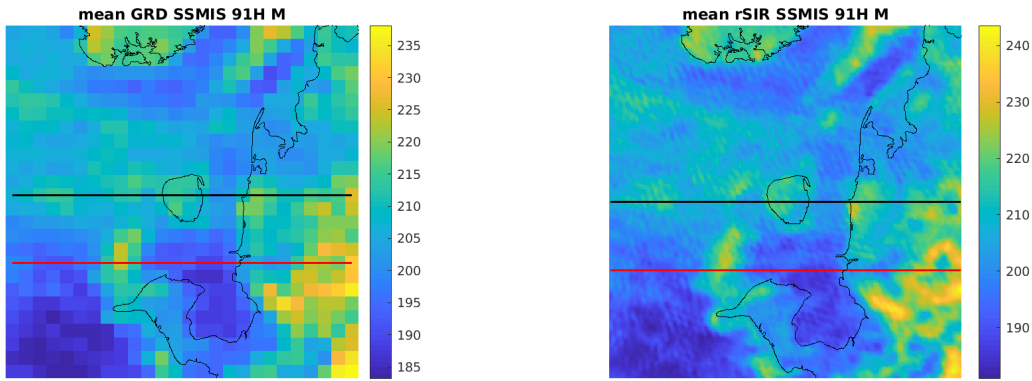


Figure 485: Average of daily  $T_B$  images over the study area. (left) 25-km GRD. (right) 3.125-km rSIR. The thick horizontal lines show the data transect locations where data is extracted from the image for analysis.

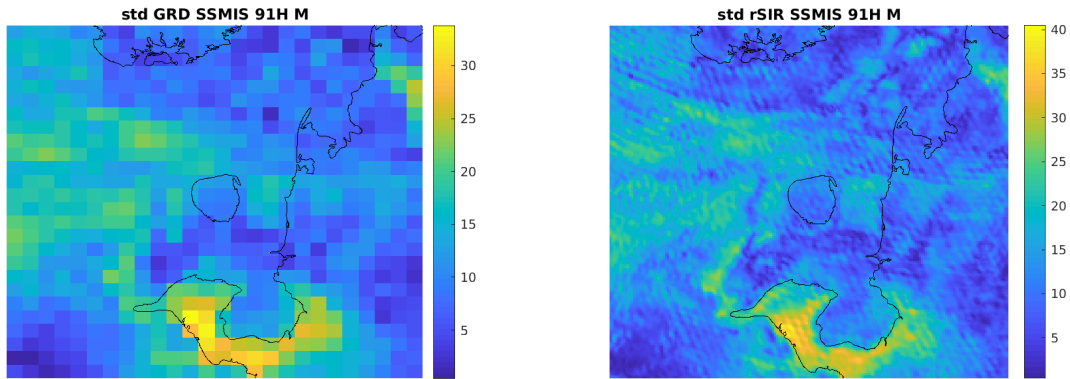


Figure 486: Standard deviation of daily  $T_B$  images over the study area. (left) 25-km GRD. (right) 3.125-km rSIR.



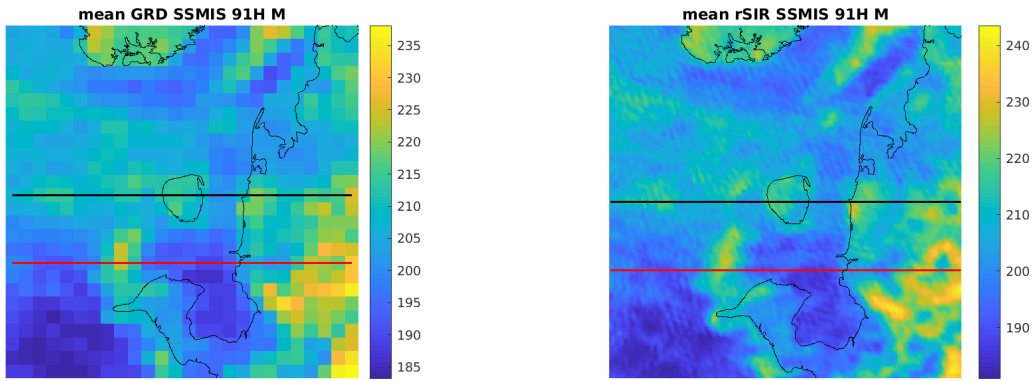


Figure 487: [Repeated] Average of daily  $T_B$  images over the study area. (left) 25-km GRD. (right) 3.125-km rSIR. The thick horizontal lines show the data transect locations where data is extracted from the image for analysis.

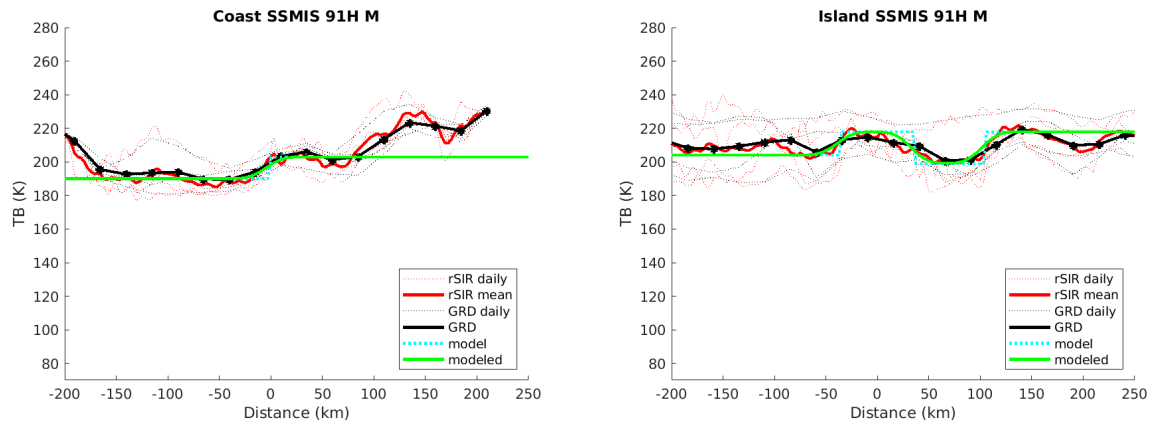


Figure 488: Plots of  $T_B$  along the two analysis case transect lines for the (left) coast-crossing and (right) island-crossing cases.

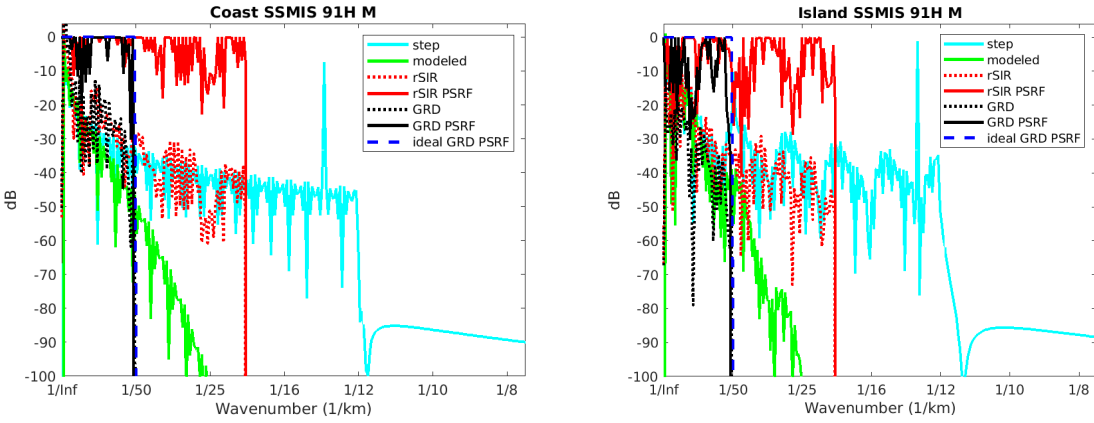


Figure 489: Wavenumber spectra of the  $T_B$  slices, the model, and the PSRF. (left) Coast-crossing case. (right) Island-crossing case.

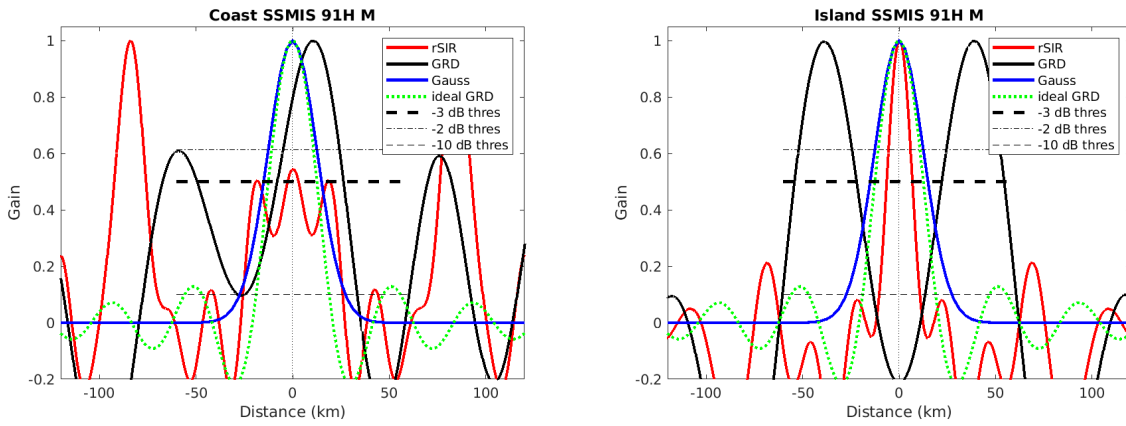


Figure 490: Derived single-pass rSIR and GRD PSRFs from the (left) coast-crossing and (right) island-crossing cases.

Table 135: Resolution estimates for SSMIS channel 91H LTOD M

Algorithm	-3 dB Thres		-2 dB Thres		-10 dB Thres	
	Coast	Island	Coast	Island	Coast	Island
Gauss	30.0	30.0	24.4	24.4	54.8	54.8
rSIR	16.5	13.3	13.5	11.0	28.3	21.1
ideal GRD	36.2	36.2	30.3	30.3	54.5	54.5
GRD	25.5	32.3	21.5	27.2	36.4	47.1

### F.13 SSMIS Channel 91V E Figures

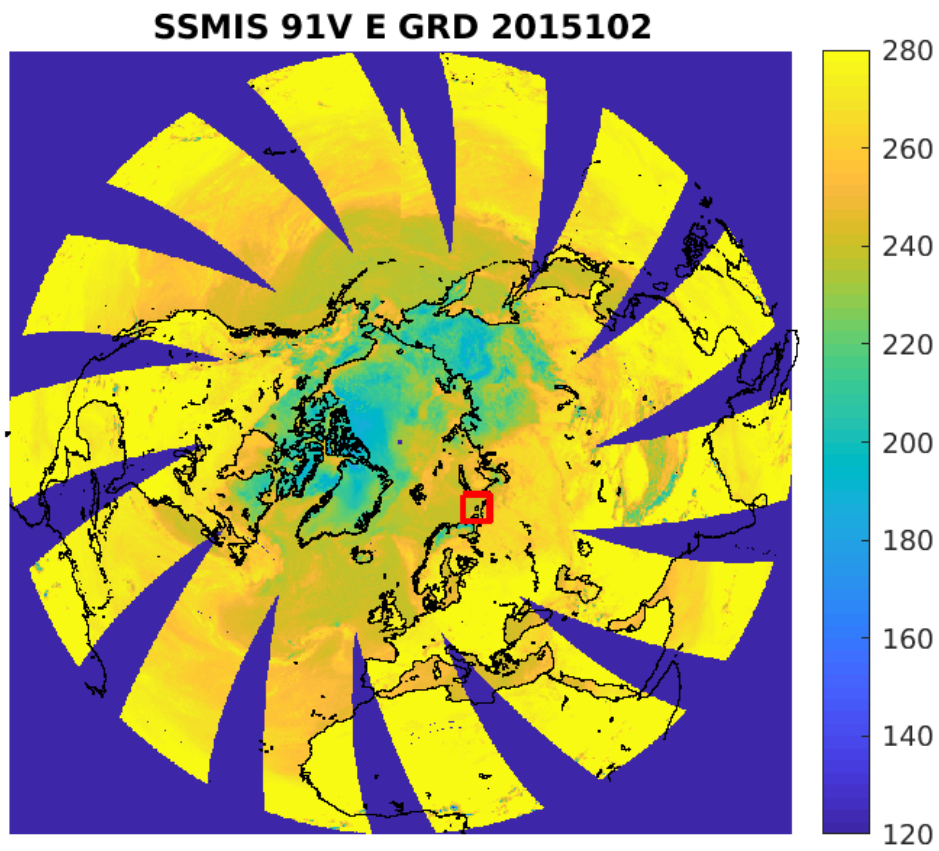


Figure 491: rSIR Northern Hemisphere view.

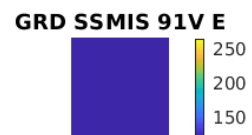
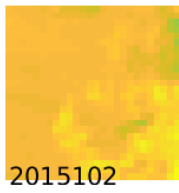
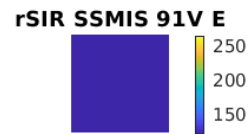
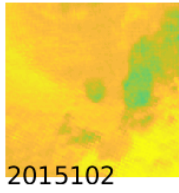


Figure 492: Time series of (top) rSIR and (bottom) GRD  $T_B$  images over the study area. Image dates are labeled on the image.

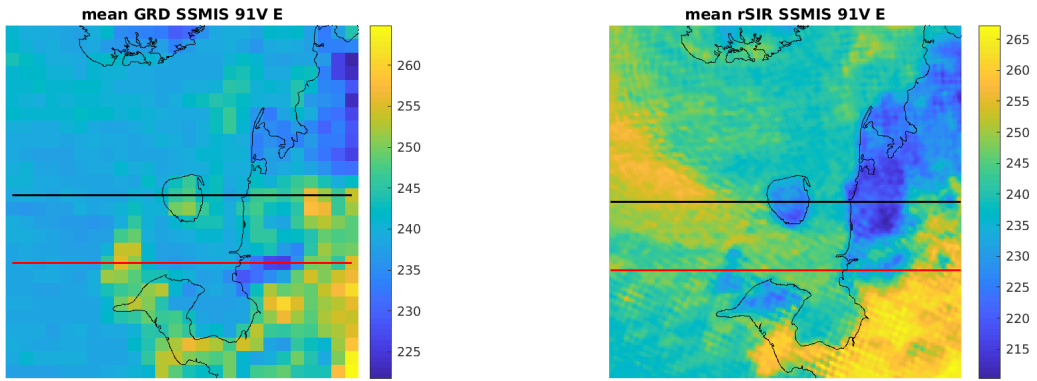


Figure 493: Average of daily  $T_B$  images over the study area. (left) 25-km GRD. (right) 3.125-km rSIR. The thick horizontal lines show the data transect locations where data is extracted from the image for analysis.

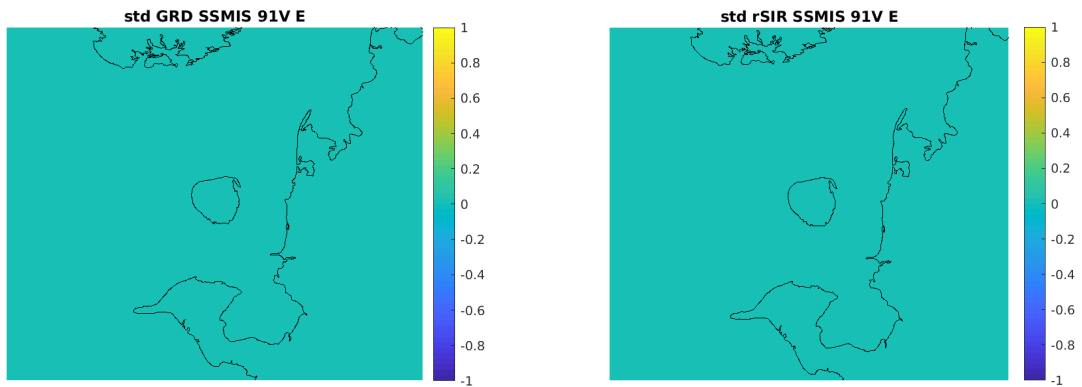


Figure 494: Standard deviation of daily  $T_B$  images over the study area. (left) 25-km GRD. (right) 3.125-km rSIR.

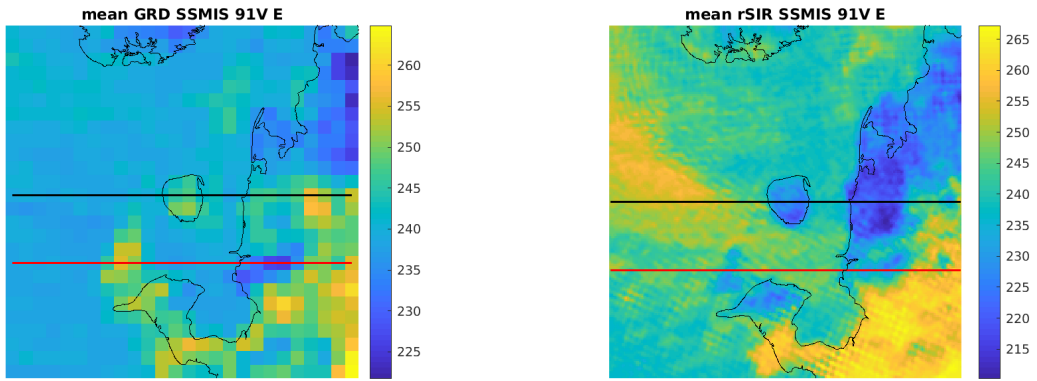


Figure 495: [Repeated] Average of daily  $T_B$  images over the study area. (left) 25-km GRD. (right) 3.125-km rSIR. The thick horizontal lines show the data transect locations where data is extracted from the image for analysis.

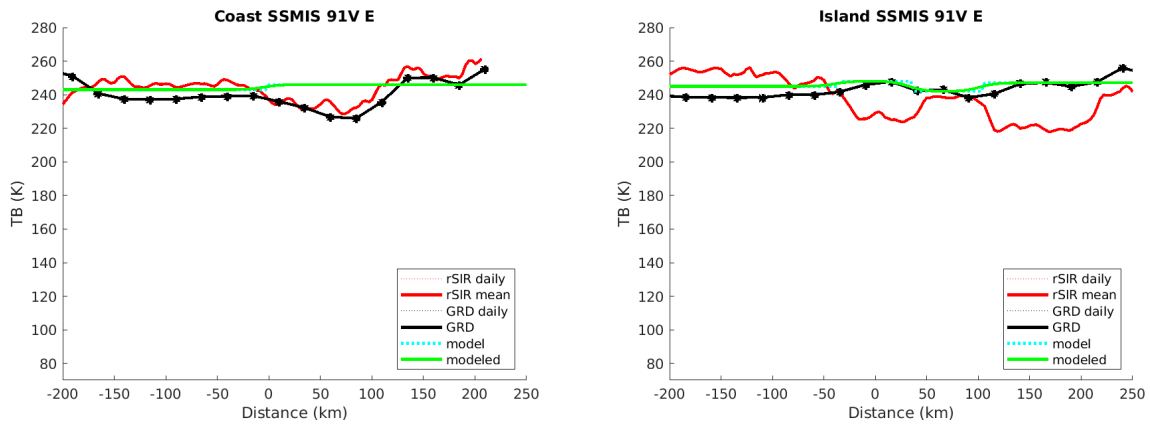


Figure 496: Plots of  $T_B$  along the two analysis case transect lines for the (left) coast-crossing and (right) island-crossing cases.

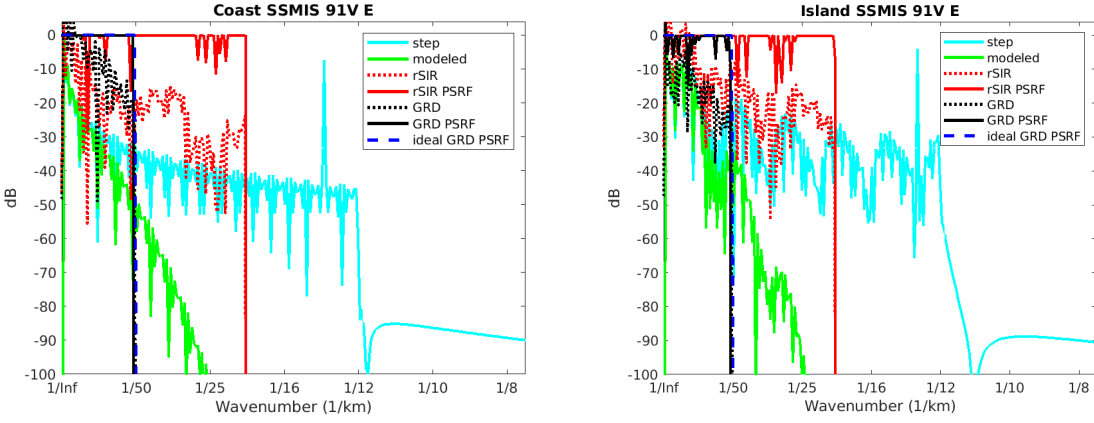


Figure 497: Wavenumber spectra of the  $T_B$  slices, the model, and the PSRF. (left) Coast-crossing case. (right) Island-crossing case.

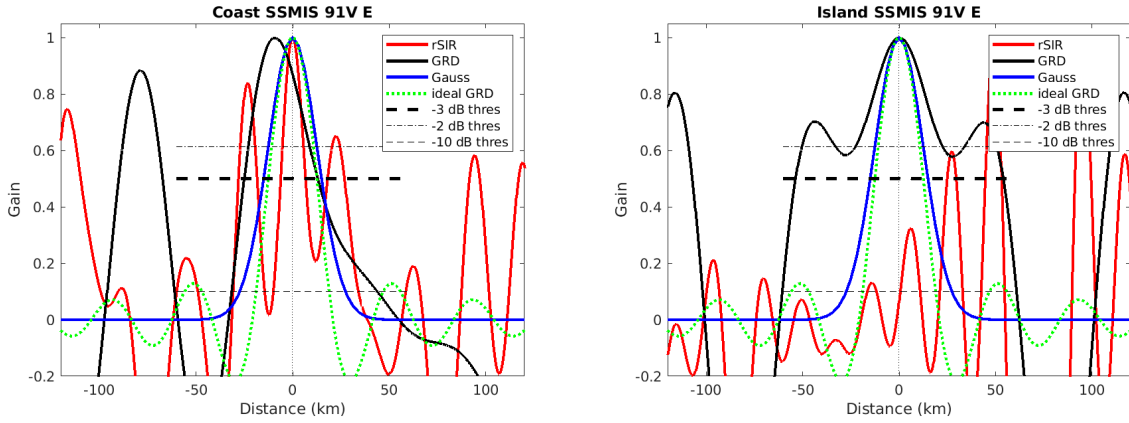


Figure 498: Derived single-pass rSIR and GRD PSRFs from the (left) coast-crossing and (right) island-crossing cases.

Table 136: Resolution estimates for SSMIS channel 91V LTOD E

Algorithm	-3 dB Thres		-2 dB Thres		-10 dB Thres	
	Coast	Island	Coast	Island	Coast	Island
Gauss	30.0	30.0	24.4	24.4	54.8	54.8
rSIR	10.7	8.4	9.0	7.1	15.6	12.1
ideal GRD	36.2	36.2	30.3	30.3	54.5	54.5
GRD	38.0	107.6	30.9	42.6	75.3	121.4

## F.14 SSMIS Channel 91V M Figures

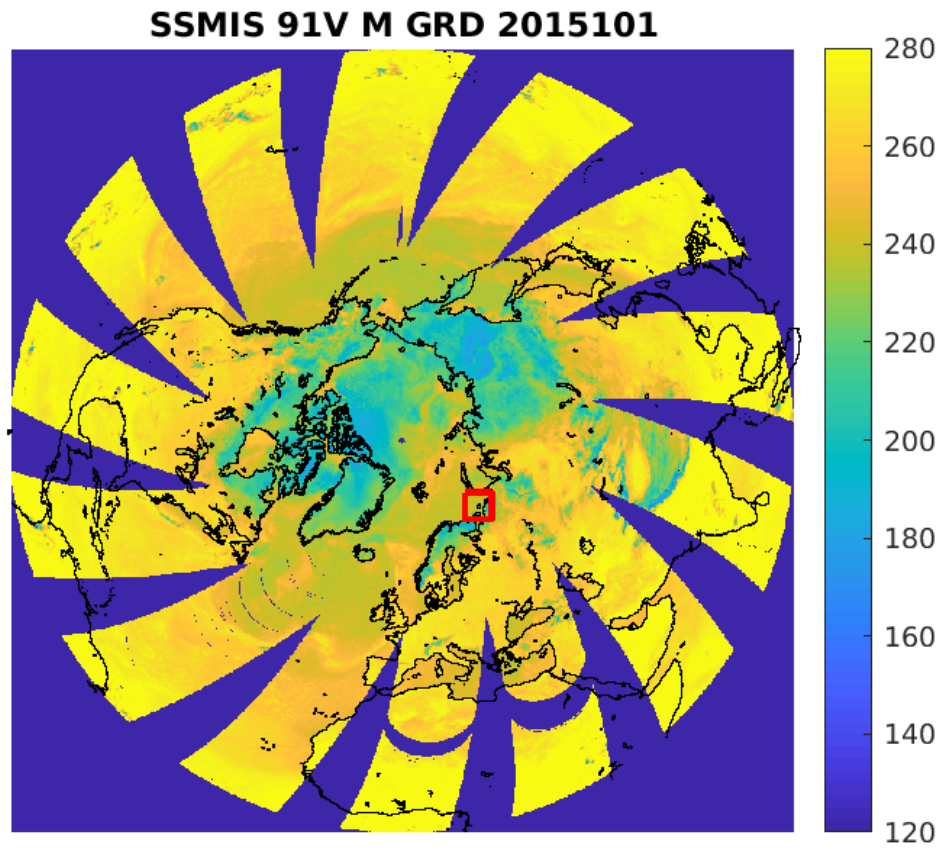


Figure 499: rSIR Northern Hemisphere view.



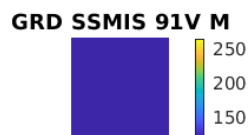
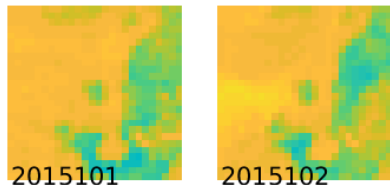
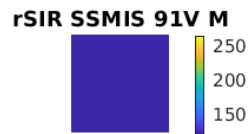
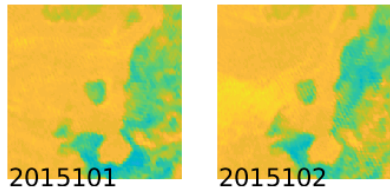


Figure 500: Time series of (top) rSIR and (bottom) GRD  $T_B$  images over the study area. Image dates are labeled on the image.

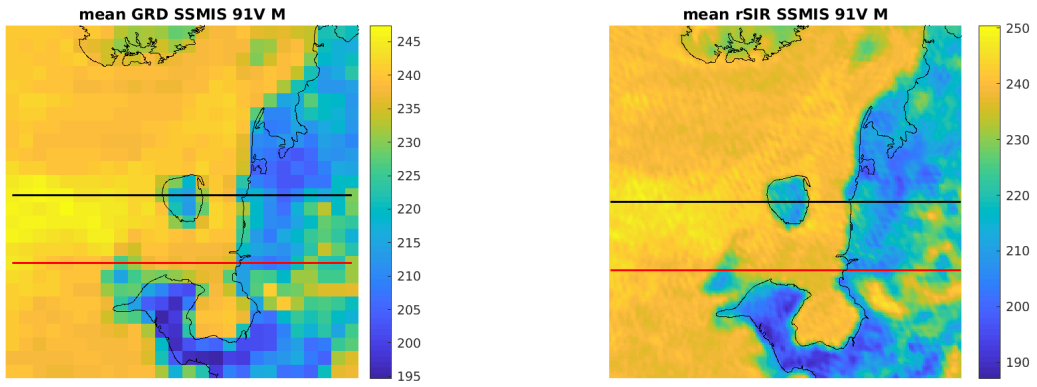


Figure 501: Average of daily  $T_B$  images over the study area. (left) 25-km GRD. (right) 3.125-km rSIR. The thick horizontal lines show the data transect locations where data is extracted from the image for analysis.

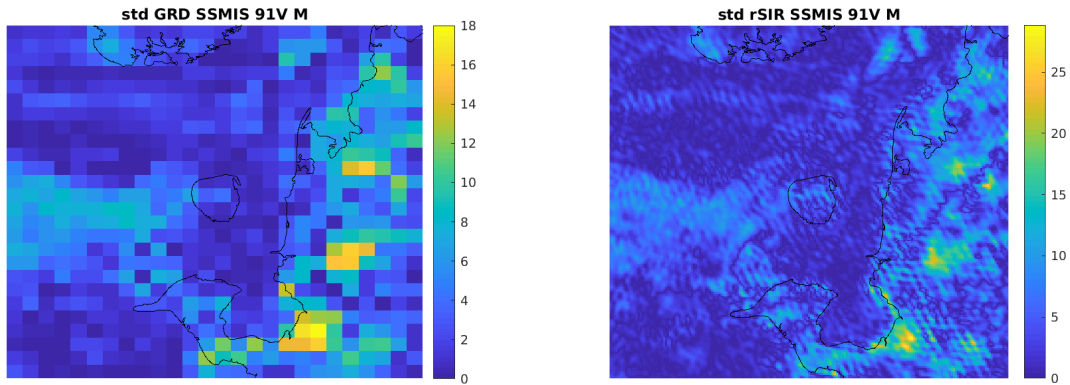


Figure 502: Standard deviation of daily  $T_B$  images over the study area. (left) 25-km GRD. (right) 3.125-km rSIR.

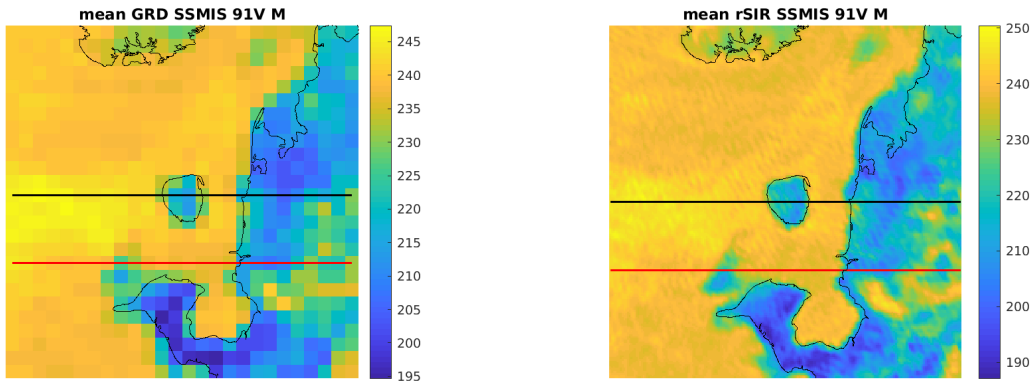


Figure 503: [Repeated] Average of daily  $T_B$  images over the study area. (left) 25-km GRD. (right) 3.125-km rSIR. The thick horizontal lines show the data transect locations where data is extracted from the image for analysis.

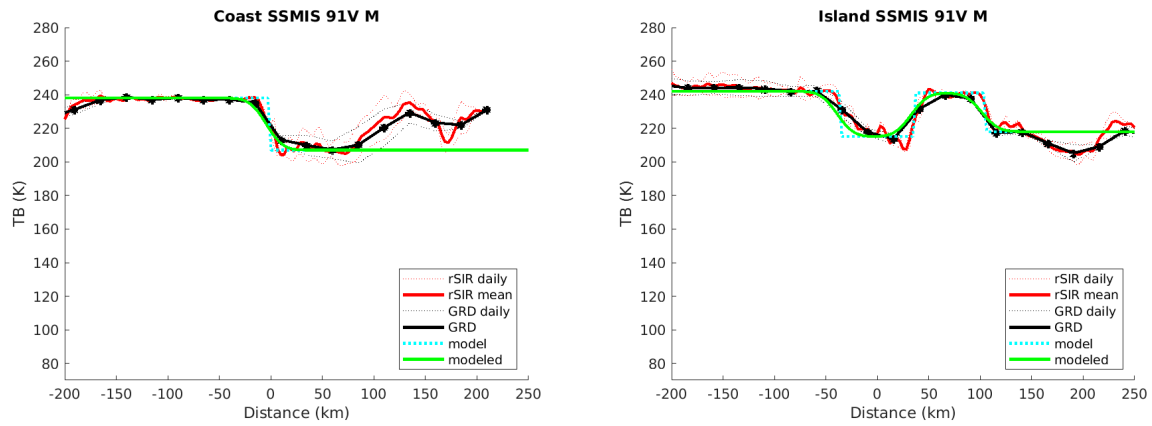


Figure 504: Plots of  $T_B$  along the two analysis case transect lines for the (left) coast-crossing and (right) island-crossing cases.

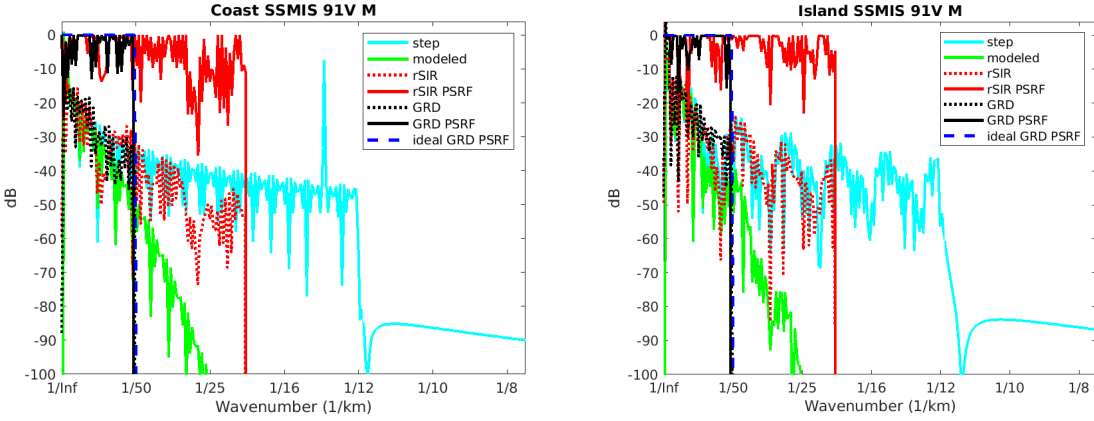


Figure 505: Wavenumber spectra of the  $T_B$  slices, the model, and the PSRF. (left) Coast-crossing case. (right) Island-crossing case.

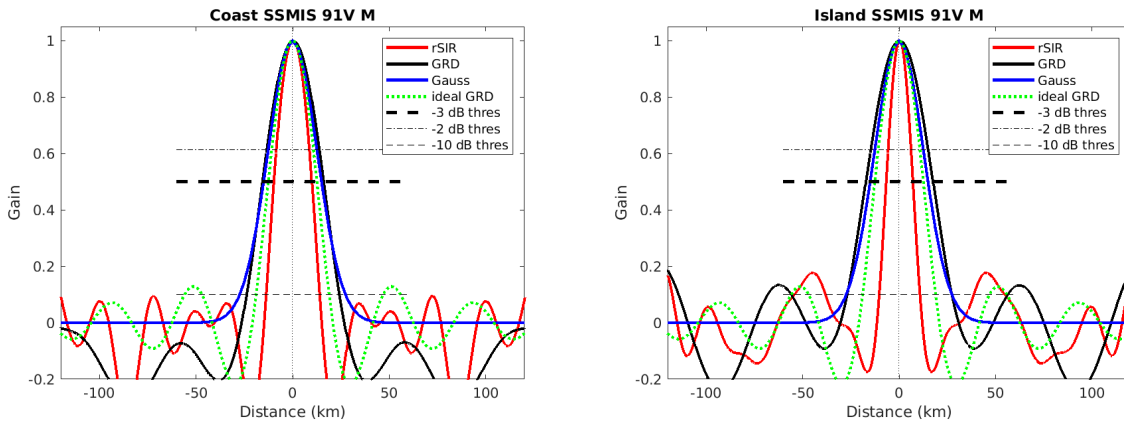


Figure 506: Derived single-pass rSIR and GRD PSRFs from the (left) coast-crossing and (right) island-crossing cases.

Table 137: Resolution estimates for SSMIS channel 91V LTOD M

Algorithm	-3 dB Thres		-2 dB Thres		-10 dB Thres	
	Coast	Island	Coast	Island	Coast	Island
Gauss	30.0	30.0	24.4	24.4	54.8	54.8
rSIR	19.6	13.8	16.7	11.5	27.6	21.2
ideal GRD	36.2	36.2	30.3	30.3	54.5	54.5
GRD	31.7	34.9	26.4	29.0	48.0	54.3

# G SSMI Figures

## G.1 SSMI Channel 19H E Figures

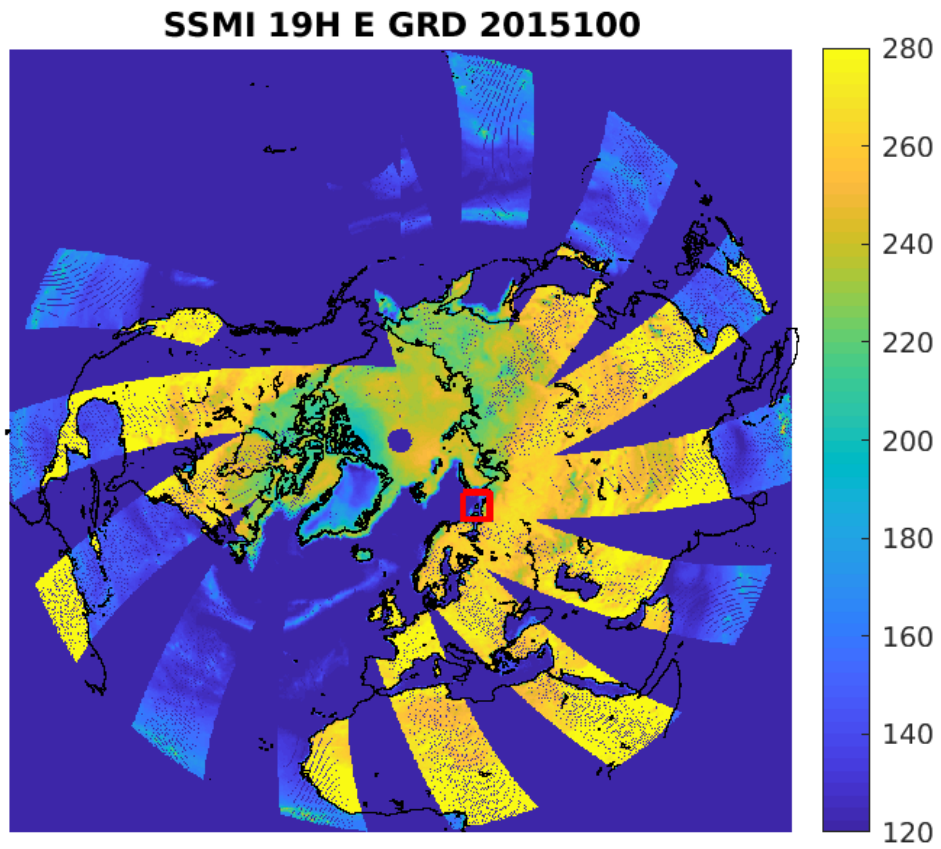


Figure 507: rSIR Northern Hemisphere view.

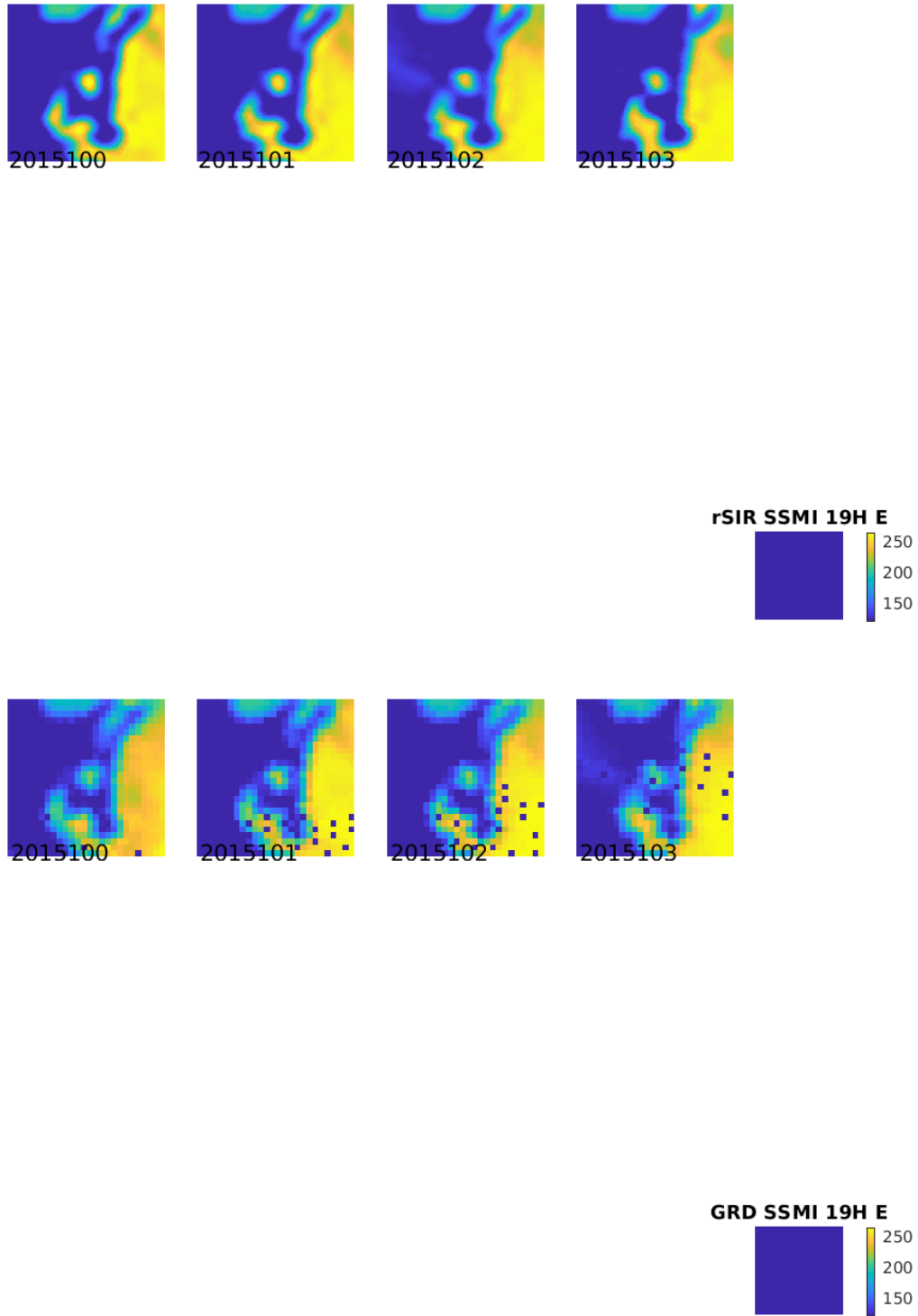


Figure 508: Time series of (top) rSIR and (bottom) GRD  $T_B$  images over the study area. Image dates are labeled on the image.

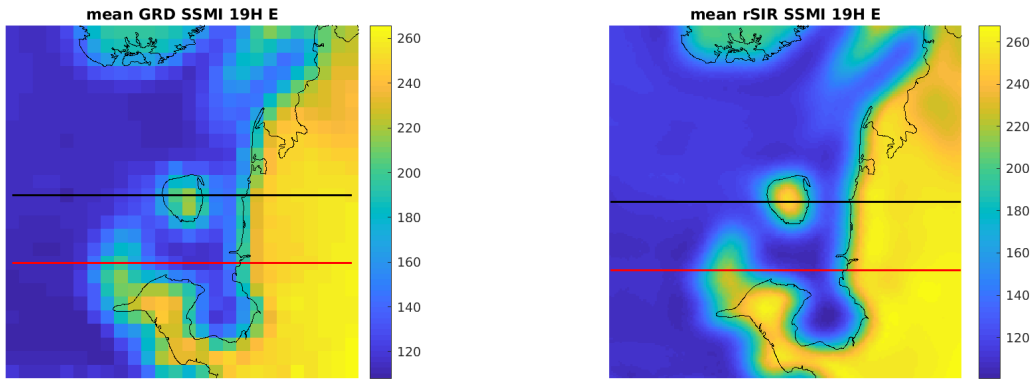


Figure 509: Average of daily  $T_B$  images over the study area. (left) 25-km GRD. (right) 3.125-km rSIR. The thick horizontal lines show the data transect locations where data is extracted from the image for analysis.

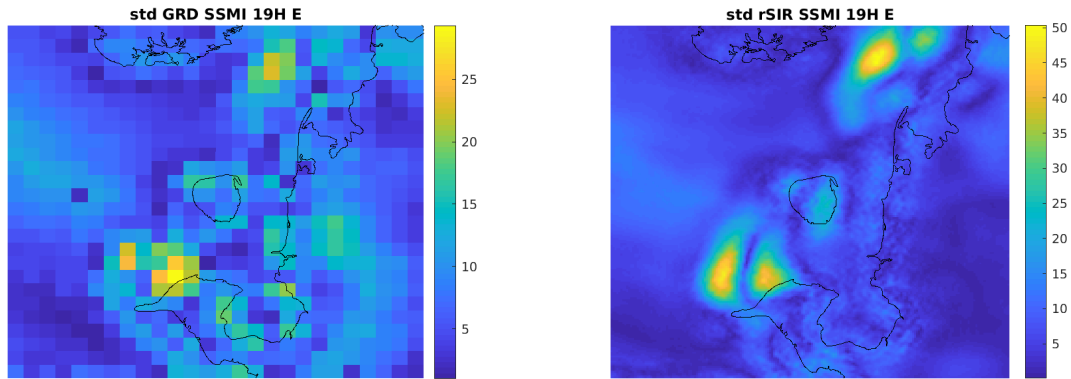


Figure 510: Standard deviation of daily  $T_B$  images over the study area. (left) 25-km GRD. (right) 3.125-km rSIR.

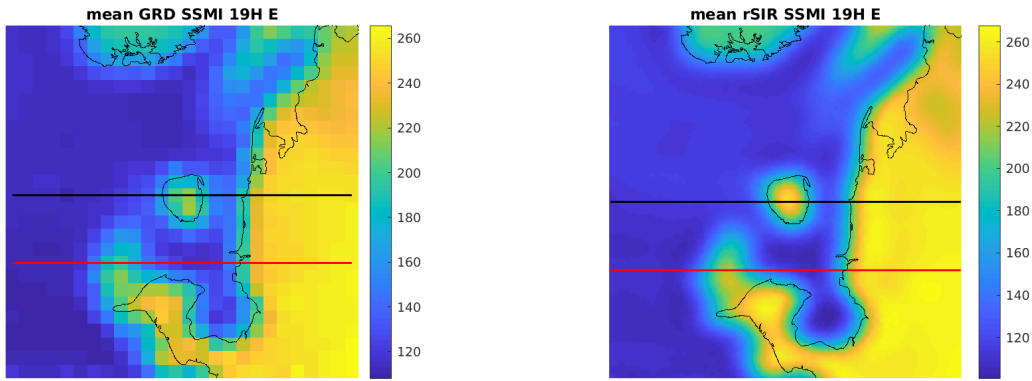


Figure 511: [Repeated] Average of daily  $T_B$  images over the study area. (left) 25-km GRD. (right) 3.125-km rSIR. The thick horizontal lines show the data transect locations where data is extracted from the image for analysis.

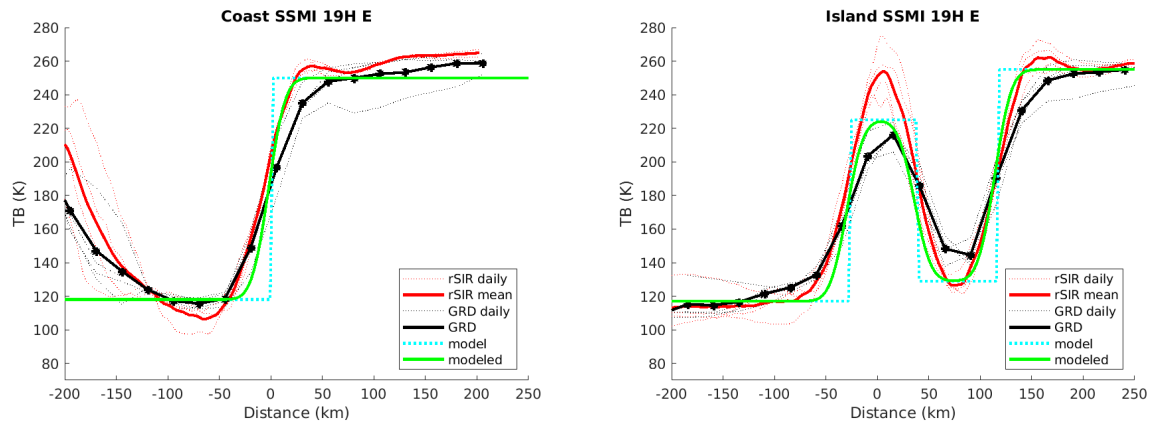


Figure 512: Plots of  $T_B$  along the two analysis case transect lines for the (left) coast-crossing and (right) island-crossing cases.



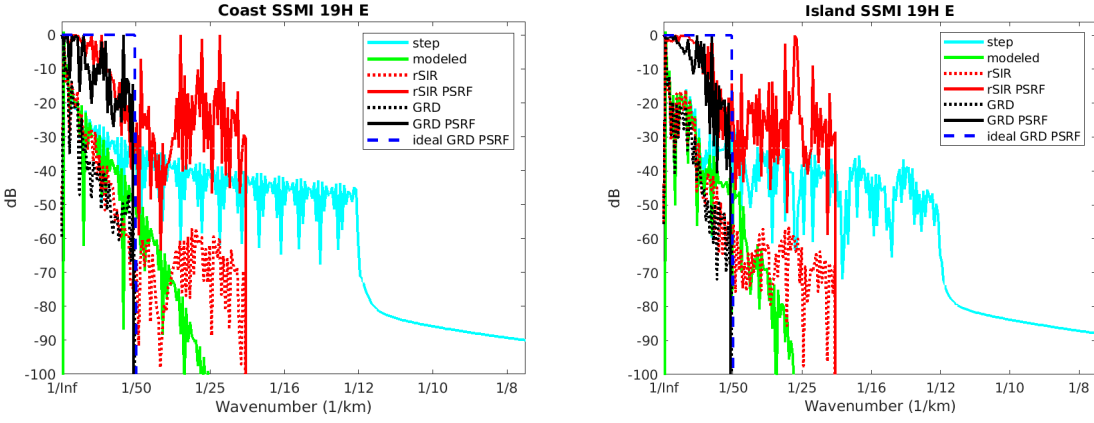


Figure 513: Wavenumber spectra of the  $T_B$  slices, the model, and the PSRF. (left) Coast-crossing case. (right) Island-crossing case.

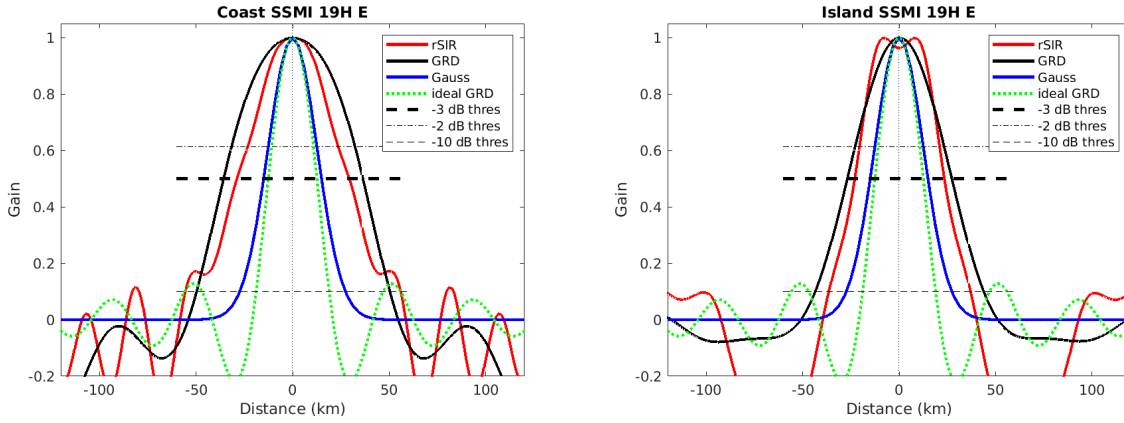


Figure 514: Derived single-pass rSIR and GRD PSRFs from the (left) coast-crossing and (right) island-crossing cases.

Table 138: Resolution estimates for SSMI channel 19H LTOD E

Algorithm	-3 dB Thres		-2 dB Thres		-10 dB Thres	
	Coast	Island	Coast	Island	Coast	Island
Gauss	30.0	30.0	24.4	24.4	54.8	54.8
rSIR	58.1	46.4	45.3	40.7	111.5	73.4
ideal GRD	36.2	36.2	30.3	30.3	54.5	54.5
GRD	72.1	54.2	62.5	44.8	100.0	87.3

## G.2 SSMI Channel 19H M Figures

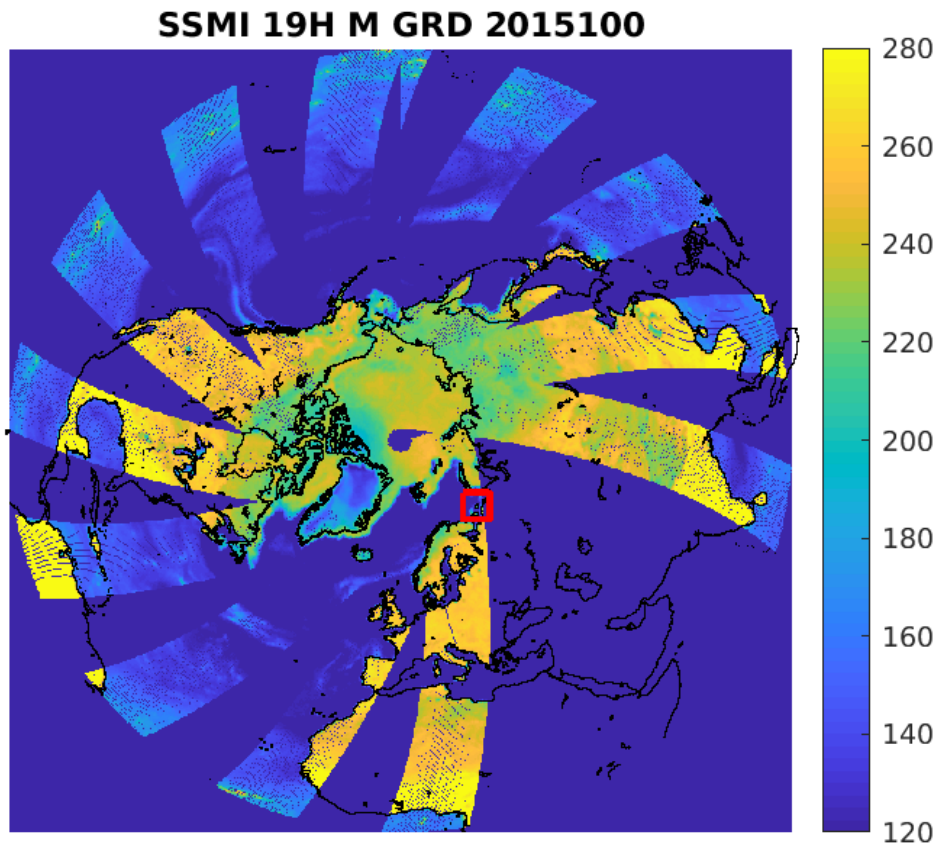


Figure 515: rSIR Northern Hemisphere view.

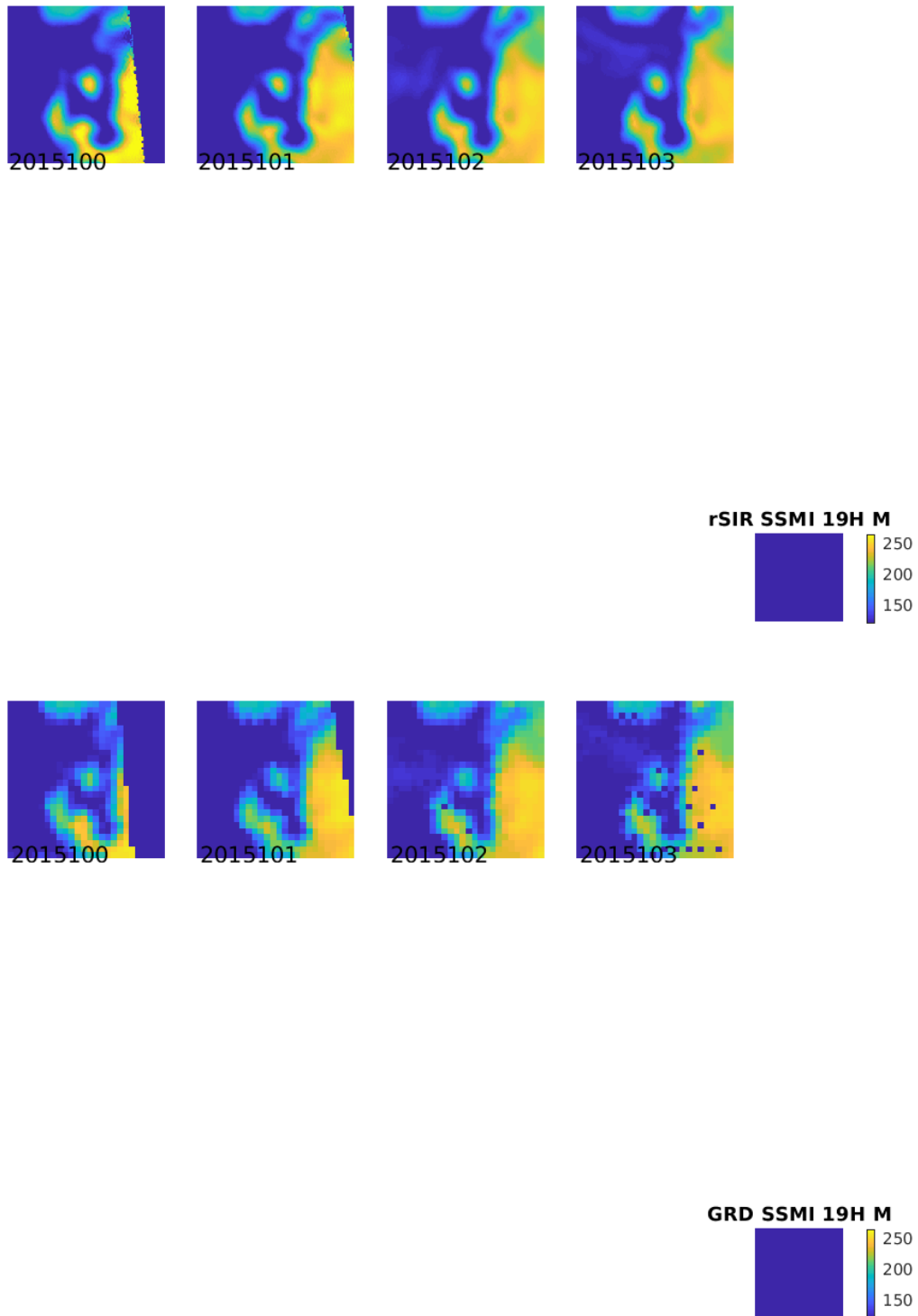


Figure 516: Time series of (top) rSIR and (bottom) GRD  $T_B$  images over the study area. Image dates are labeled on the image.

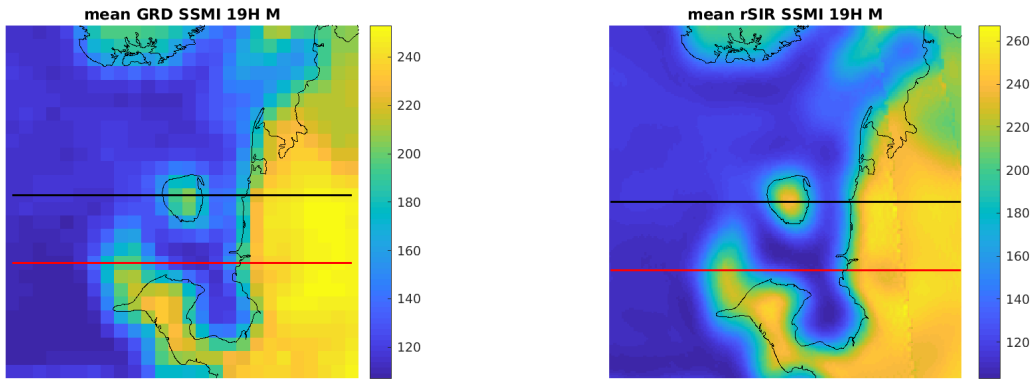


Figure 517: Average of daily  $T_B$  images over the study area. (left) 25-km GRD. (right) 3.125-km rSIR. The thick horizontal lines show the data transect locations where data is extracted from the image for analysis.

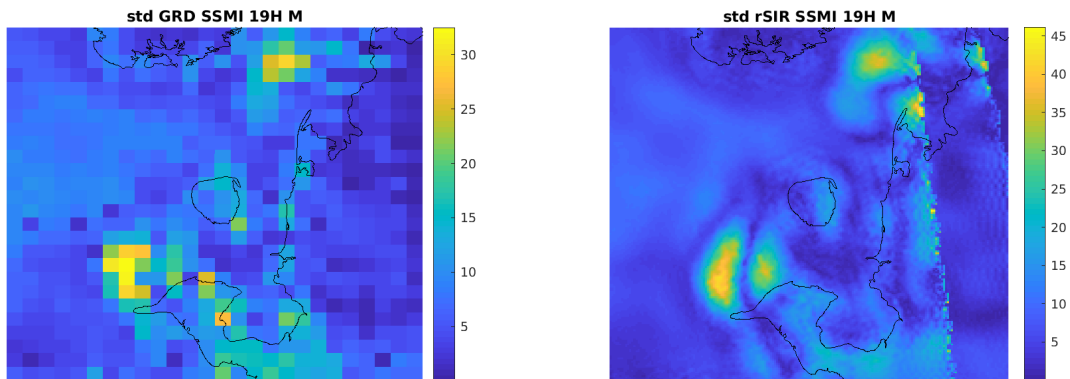


Figure 518: Standard deviation of daily  $T_B$  images over the study area. (left) 25-km GRD. (right) 3.125-km rSIR.

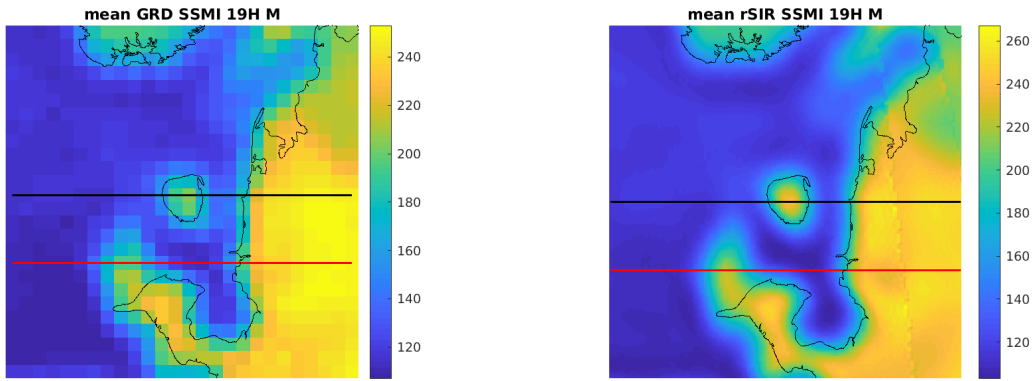


Figure 519: [Repeated] Average of daily  $T_B$  images over the study area. (left) 25-km GRD. (right) 3.125-km rSIR. The thick horizontal lines show the data transect locations where data is extracted from the image for analysis.

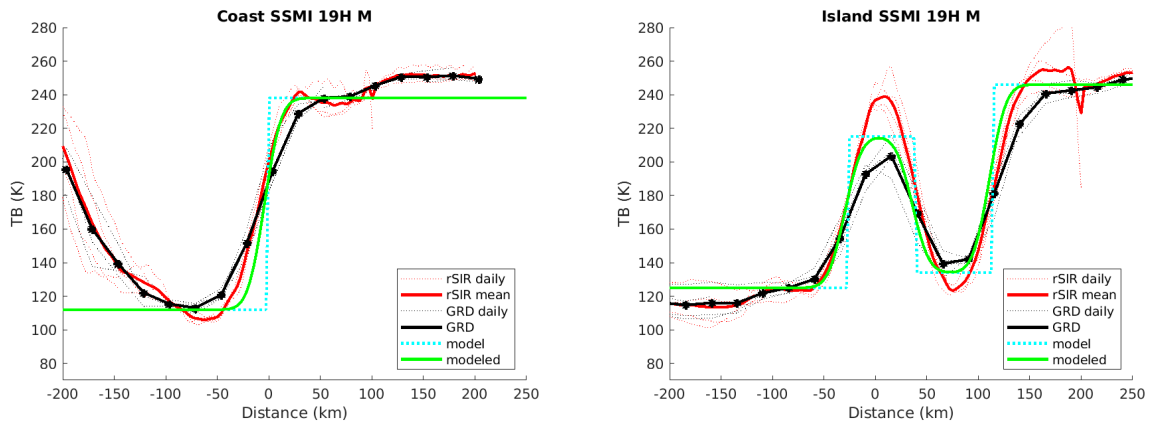


Figure 520: Plots of  $T_B$  along the two analysis case transect lines for the (left) coast-crossing and (right) island-crossing cases.

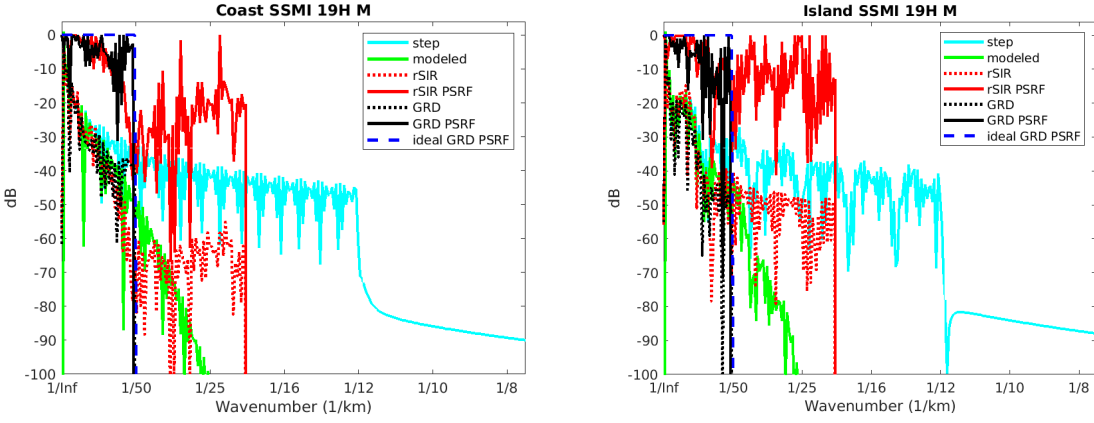


Figure 521: Wavenumber spectra of the  $T_B$  slices, the model, and the PSRF. (left) Coast-crossing case. (right) Island-crossing case.

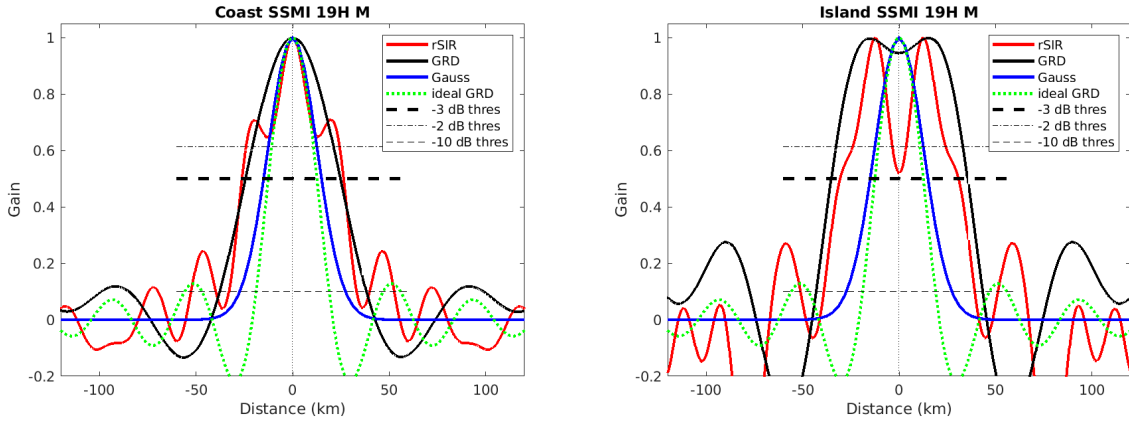


Figure 522: Derived single-pass rSIR and GRD PSRFs from the (left) coast-crossing and (right) island-crossing cases.

Table 139: Resolution estimates for SSMI channel 19H LTOD M

Algorithm	-3 dB Thres		-2 dB Thres		-10 dB Thres	
	Coast	Island	Coast	Island	Coast	Island
Gauss	30.0	30.0	24.4	24.4	54.8	54.8
rSIR	52.6	61.5	47.5	19.4	66.1	78.1
ideal GRD	36.2	36.2	30.3	30.3	54.5	54.5
GRD	49.1	70.7	40.8	65.1	75.9	86.3

### G.3 SSMI Channel 19V E Figures

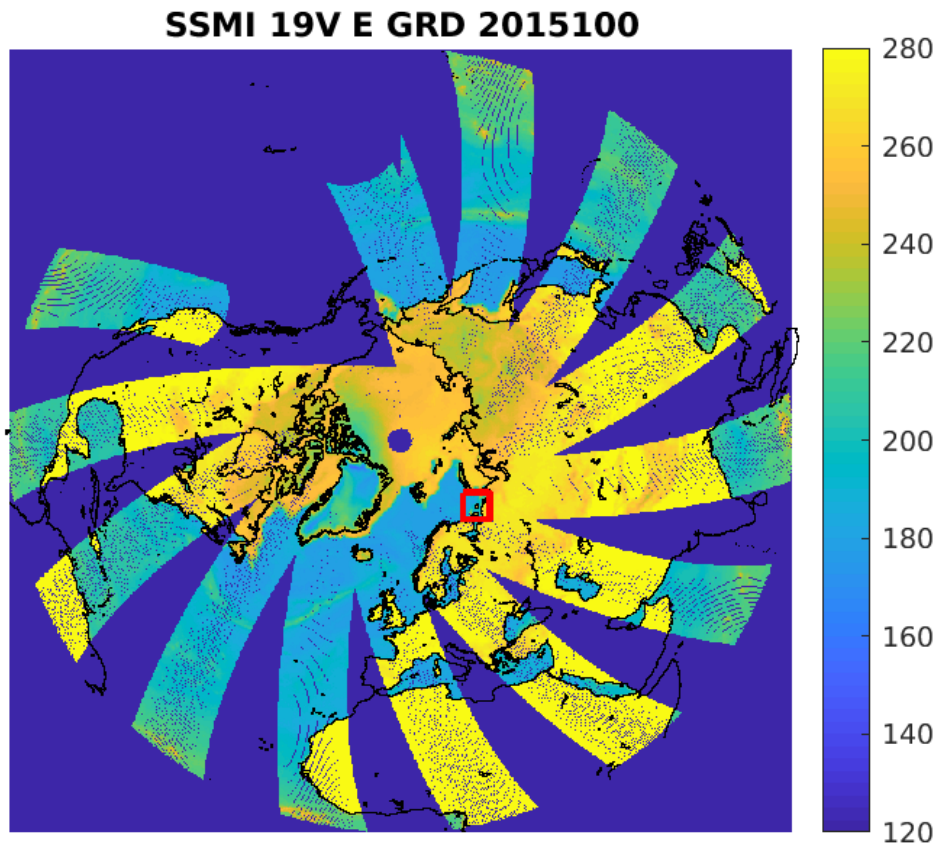


Figure 523: rSIR Northern Hemisphere view.

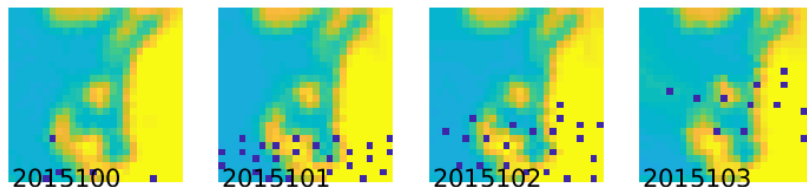
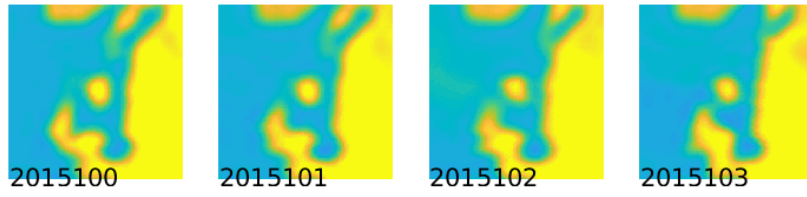


Figure 524: Time series of (top) rSIR and (bottom) GRD  $T_B$  images over the study area. Image dates are labeled on the image.



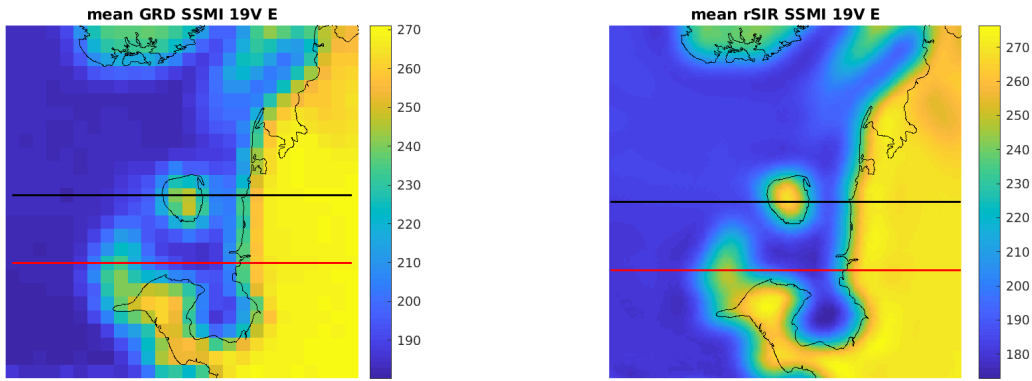


Figure 525: Average of daily  $T_B$  images over the study area. (left) 25-km GRD. (right) 3.125-km rSIR. The thick horizontal lines show the data transect locations where data is extracted from the image for analysis.

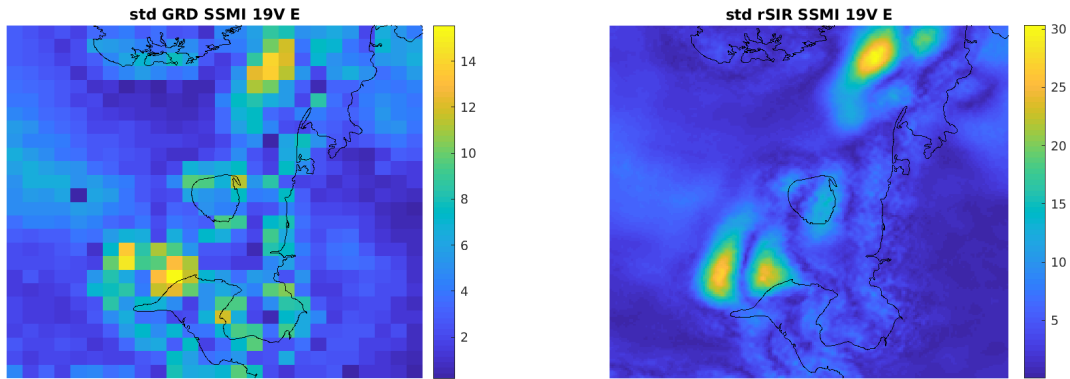


Figure 526: Standard deviation of daily  $T_B$  images over the study area. (left) 25-km GRD. (right) 3.125-km rSIR.

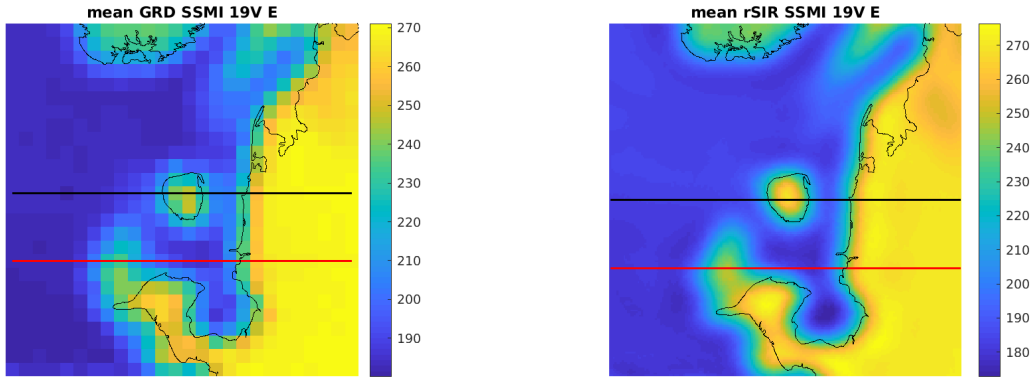


Figure 527: [Repeated] Average of daily  $T_B$  images over the study area. (left) 25-km GRD. (right) 3.125-km rSIR. The thick horizontal lines show the data transect locations where data is extracted from the image for analysis.

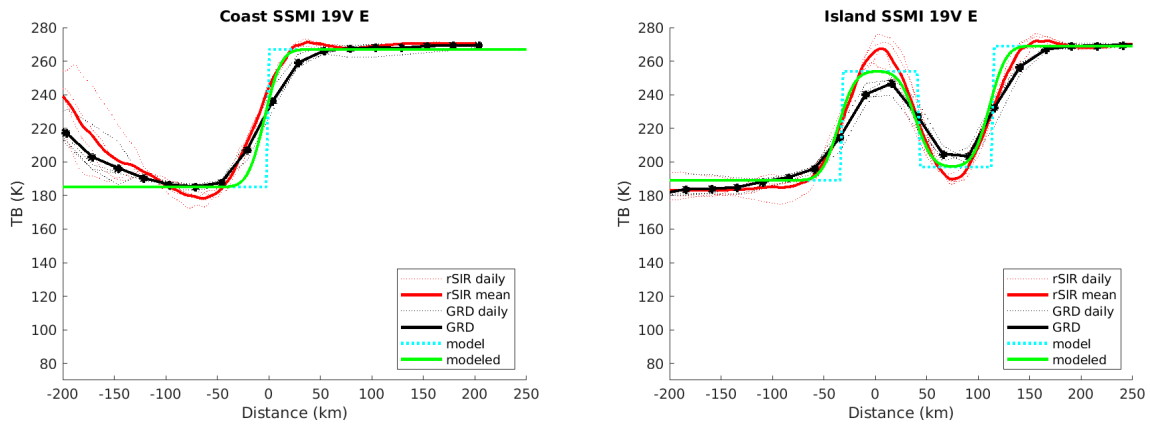


Figure 528: Plots of  $T_B$  along the two analysis case transect lines for the (left) coast-crossing and (right) island-crossing cases.

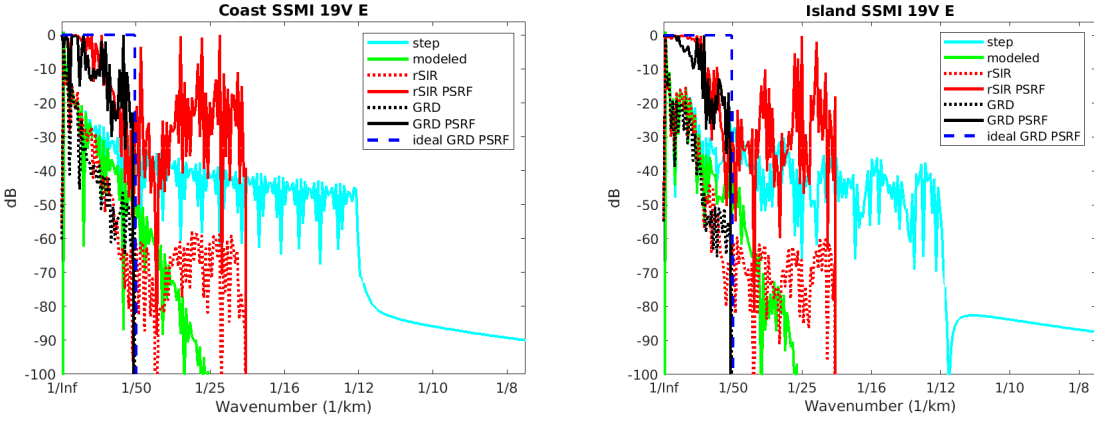


Figure 529: Wavenumber spectra of the  $T_B$  slices, the model, and the PSRF. (left) Coast-crossing case. (right) Island-crossing case.

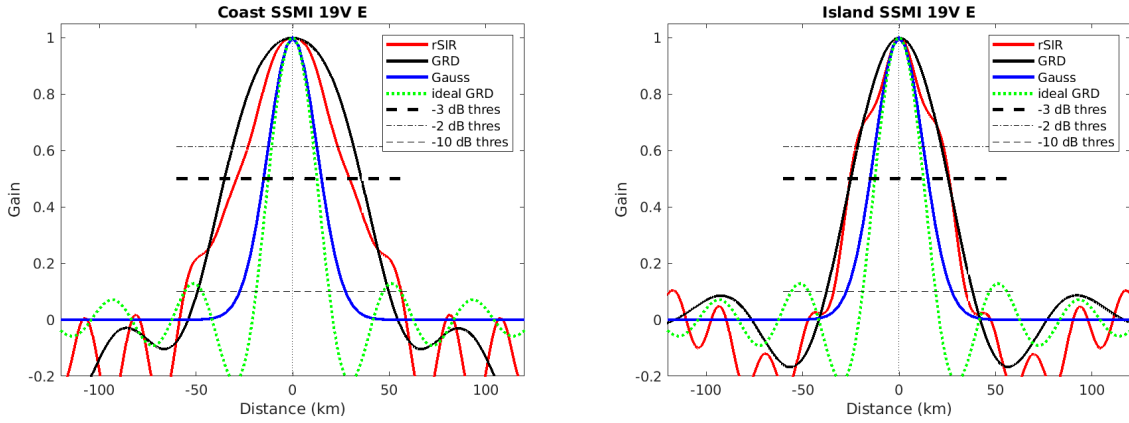


Figure 530: Derived single-pass rSIR and GRD PSRFs from the (left) coast-crossing and (right) island-crossing cases.

Table 140: Resolution estimates for SSMI channel 19V LTOD E

Algorithm	-3 dB Thres		-2 dB Thres		-10 dB Thres	
	Coast	Island	Coast	Island	Coast	Island
Gauss	30.0	30.0	24.4	24.4	54.8	54.8
rSIR	58.6	51.4	44.8	44.1	112.0	68.7
ideal GRD	36.2	36.2	30.3	30.3	54.5	54.5
GRD	70.8	50.4	61.4	42.3	99.0	75.7

## G.4 SSMI Channel 19V M Figures

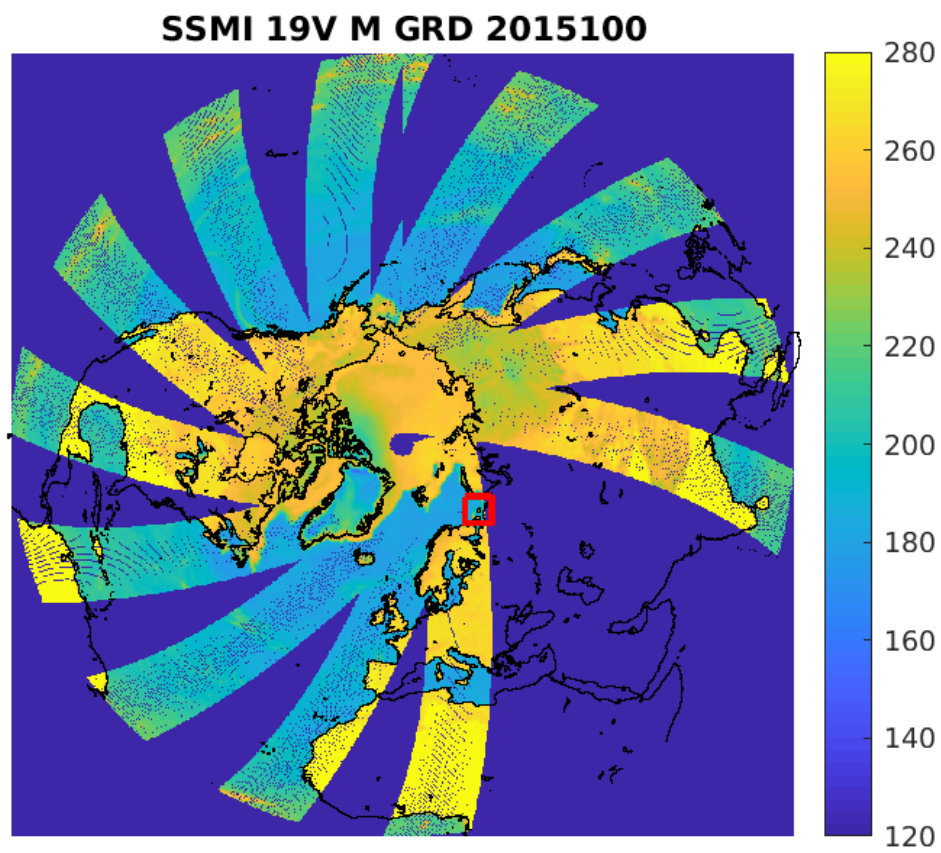


Figure 531: rSIR Northern Hemisphere view.

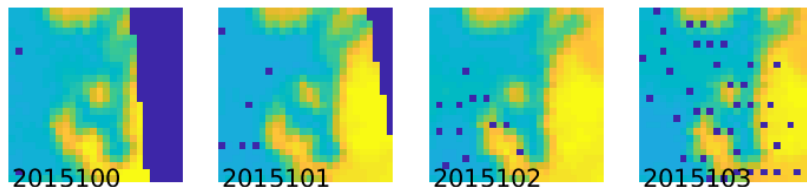
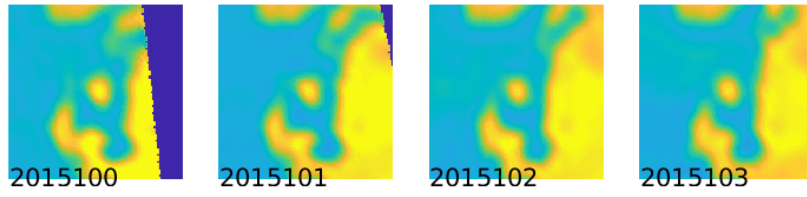


Figure 532: Time series of (top) rSIR and (bottom) GRD  $T_B$  images over the study area. Image dates are labeled on the image.

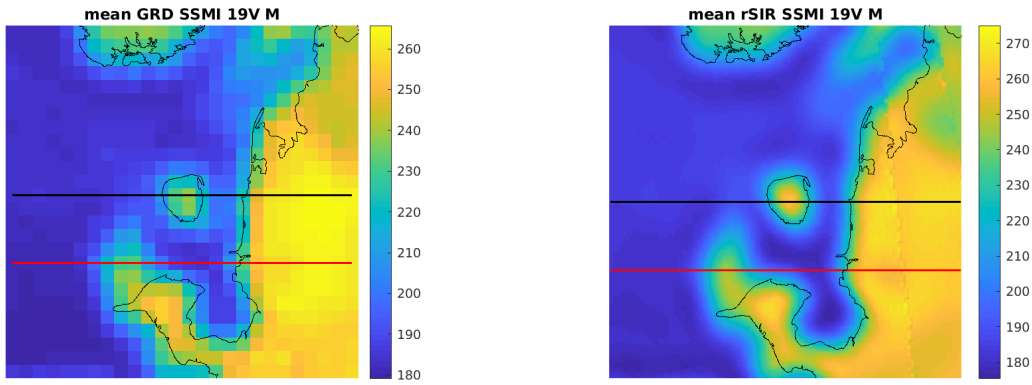


Figure 533: Average of daily  $T_B$  images over the study area. (left) 25-km GRD. (right) 3.125-km rSIR. The thick horizontal lines show the data transect locations where data is extracted from the image for analysis.

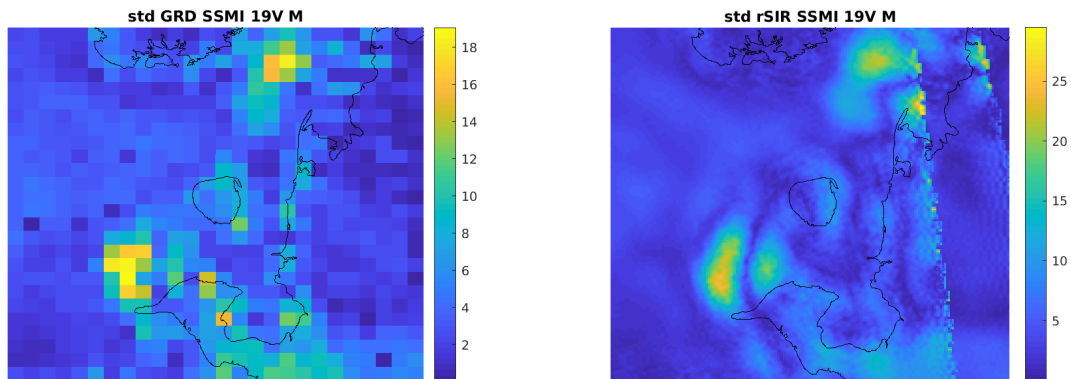


Figure 534: Standard deviation of daily  $T_B$  images over the study area. (left) 25-km GRD. (right) 3.125-km rSIR.

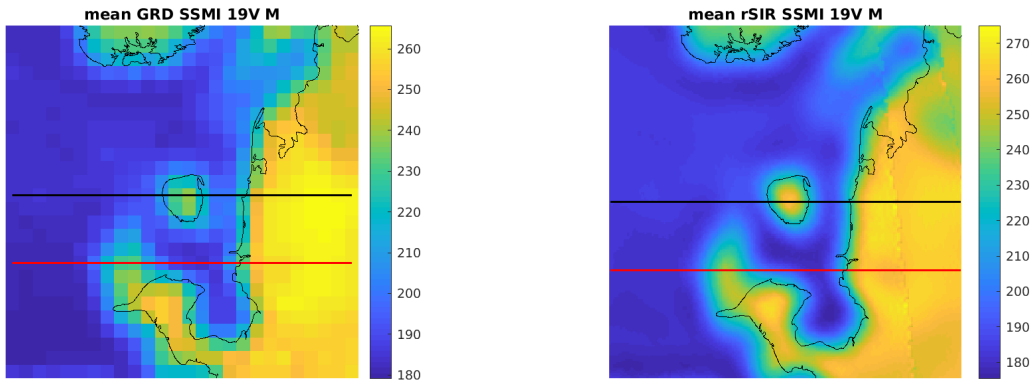


Figure 535: [Repeated] Average of daily  $T_B$  images over the study area. (left) 25-km GRD. (right) 3.125-km rSIR. The thick horizontal lines show the data transect locations where data is extracted from the image for analysis.

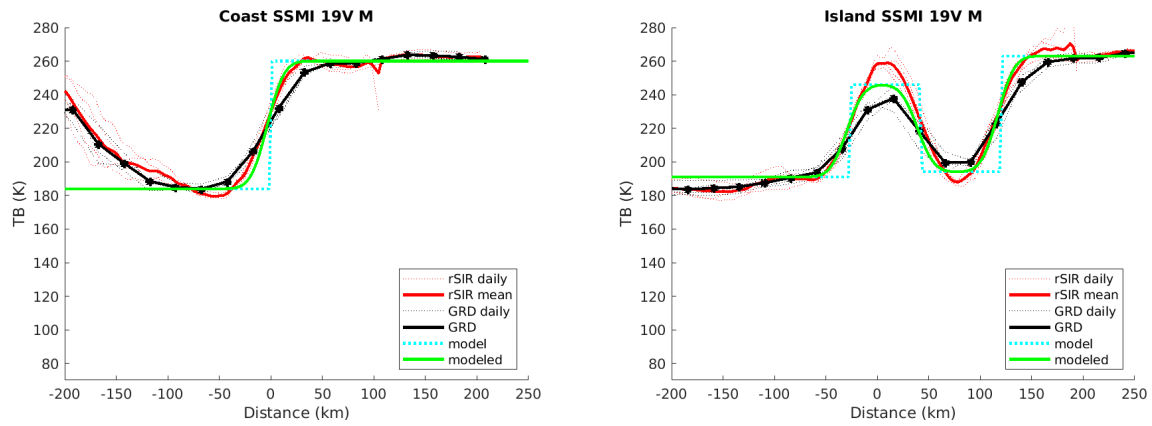


Figure 536: Plots of  $T_B$  along the two analysis case transect lines for the (left) coast-crossing and (right) island-crossing cases.

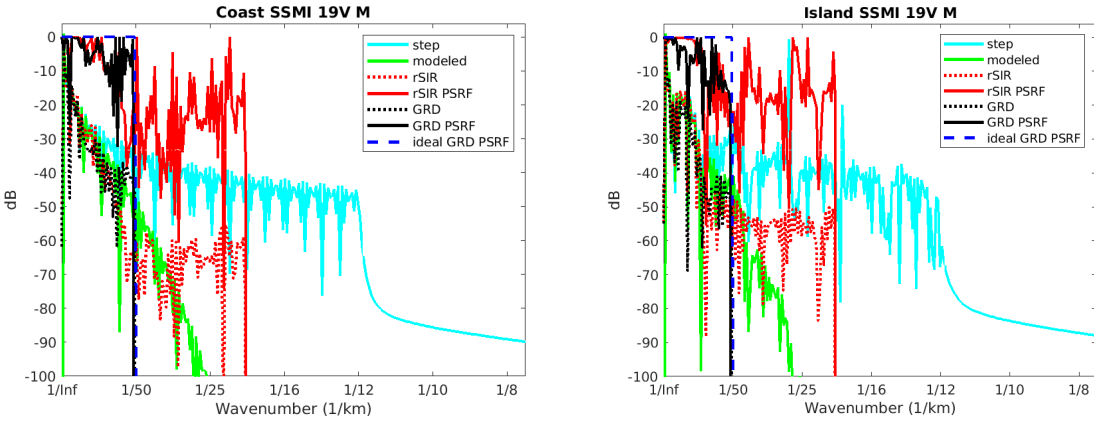


Figure 537: Wavenumber spectra of the  $T_B$  slices, the model, and the PSRF. (left) Coast-crossing case. (right) Island-crossing case.

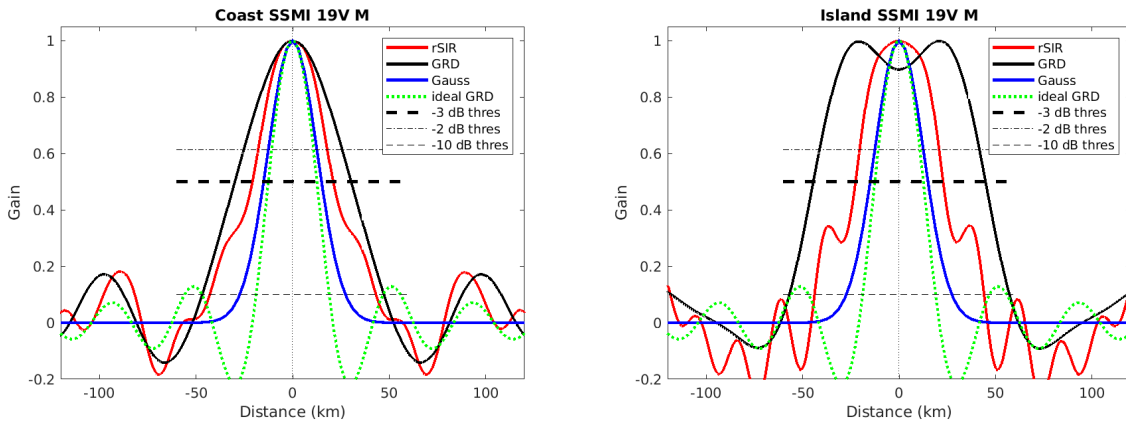


Figure 538: Derived single-pass rSIR and GRD PSRFs from the (left) coast-crossing and (right) island-crossing cases.

Table 141: Resolution estimates for SSMI channel 19V LTOD M

Algorithm	-3 dB Thres		-2 dB Thres		-10 dB Thres	
	Coast	Island	Coast	Island	Coast	Island
Gauss	30.0	30.0	24.4	24.4	54.8	54.8
rSIR	41.7	45.3	34.9	40.5	86.0	87.9
ideal GRD	36.2	36.2	30.3	30.3	54.5	54.5
GRD	60.2	89.3	49.5	81.9	94.1	114.0



## G.5 SSMI Channel 37H E Figures

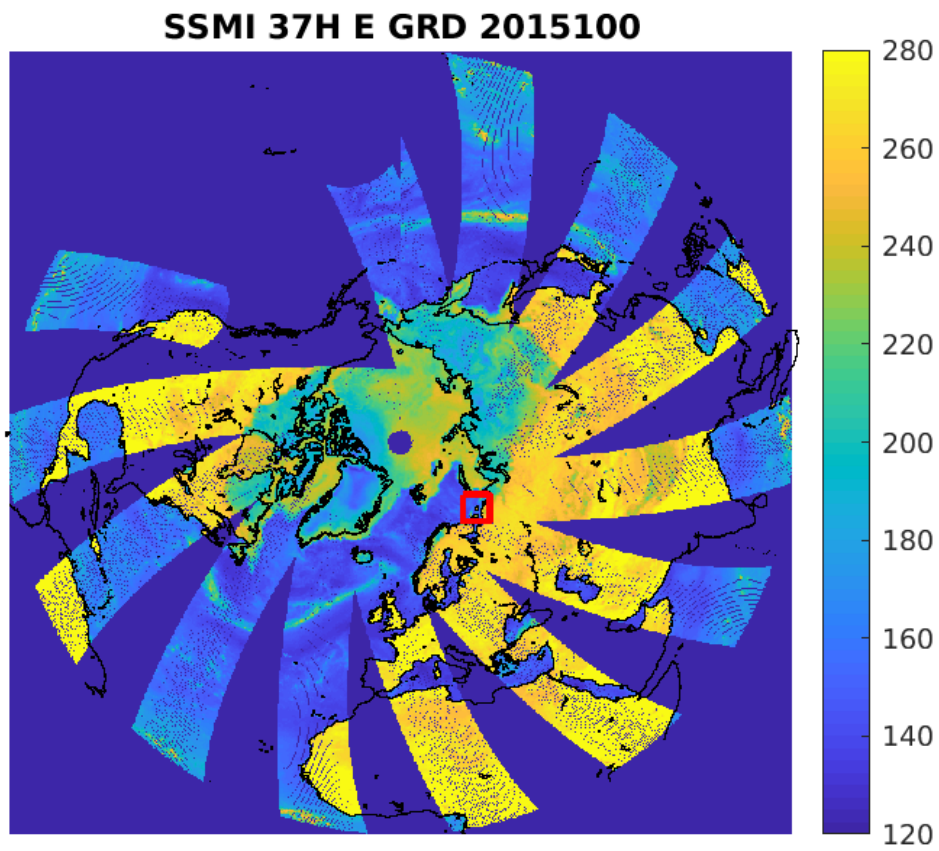


Figure 539: rSIR Northern Hemisphere view.

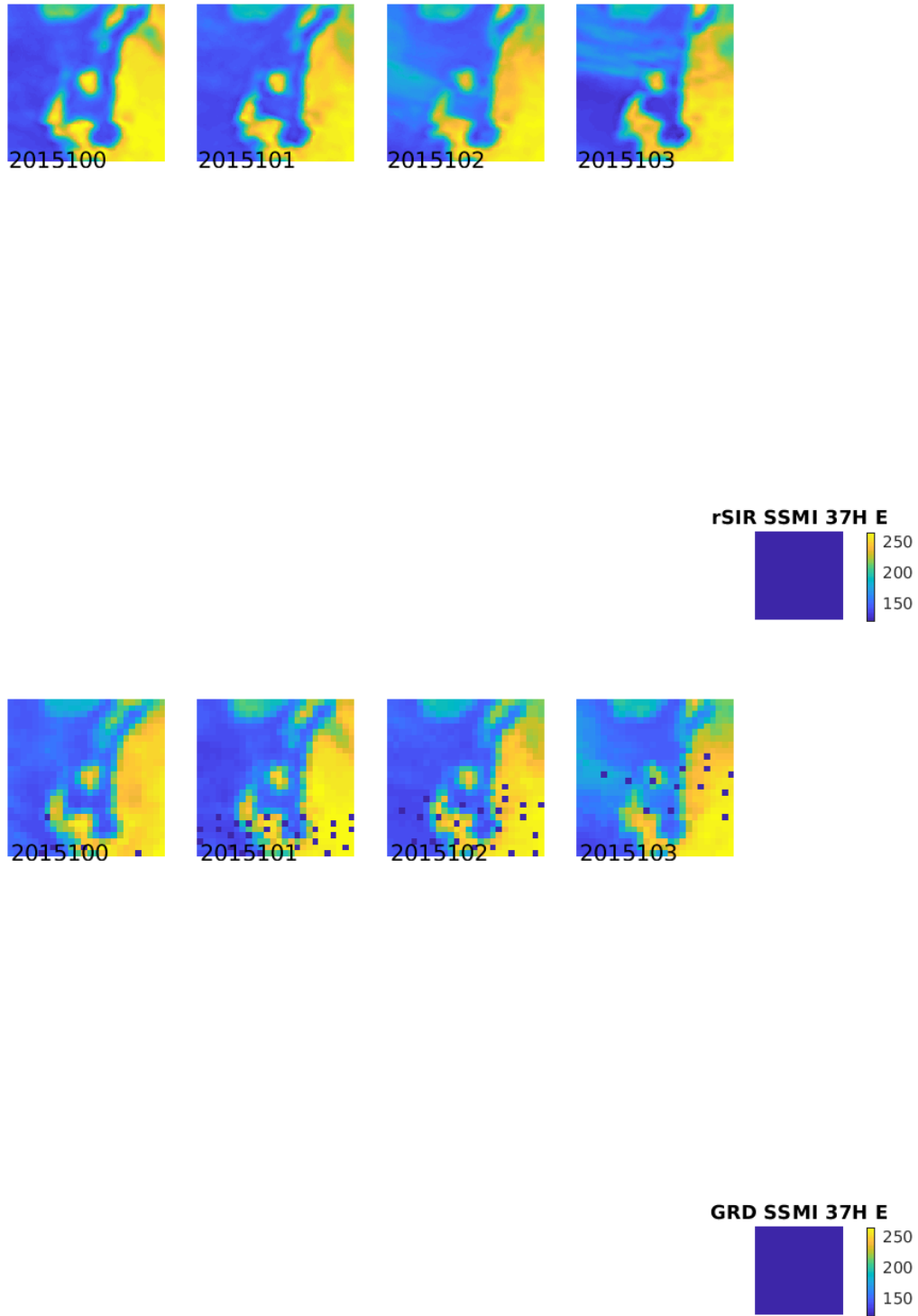


Figure 540: Time series of (top) rSIR and (bottom) GRD  $T_B$  images over the study area. Image dates are labeled on the image.

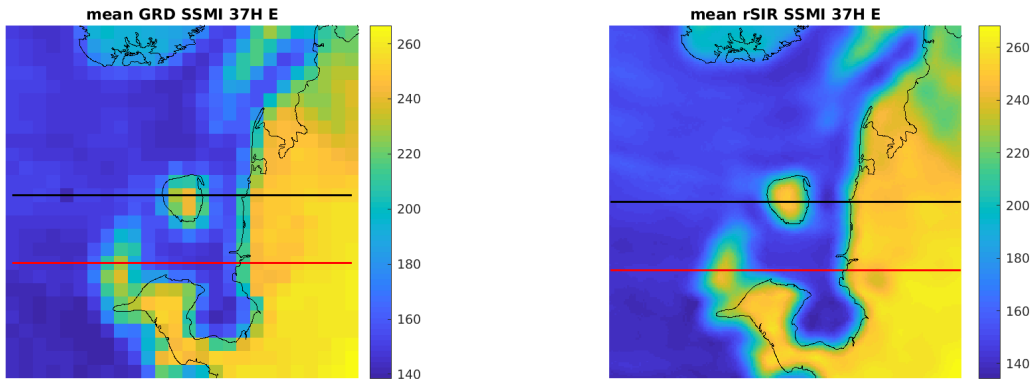


Figure 541: Average of daily  $T_B$  images over the study area. (left) 25-km GRD. (right) 3.125-km rSIR. The thick horizontal lines show the data transect locations where data is extracted from the image for analysis.

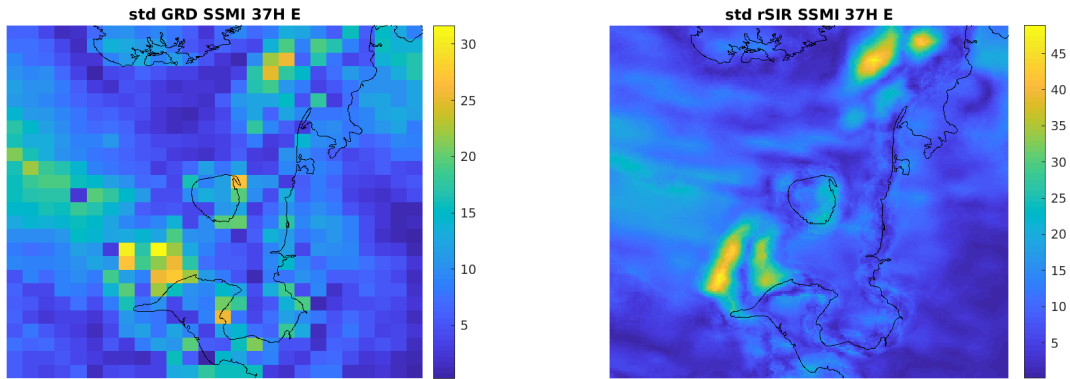


Figure 542: Standard deviation of daily  $T_B$  images over the study area. (left) 25-km GRD. (right) 3.125-km rSIR.

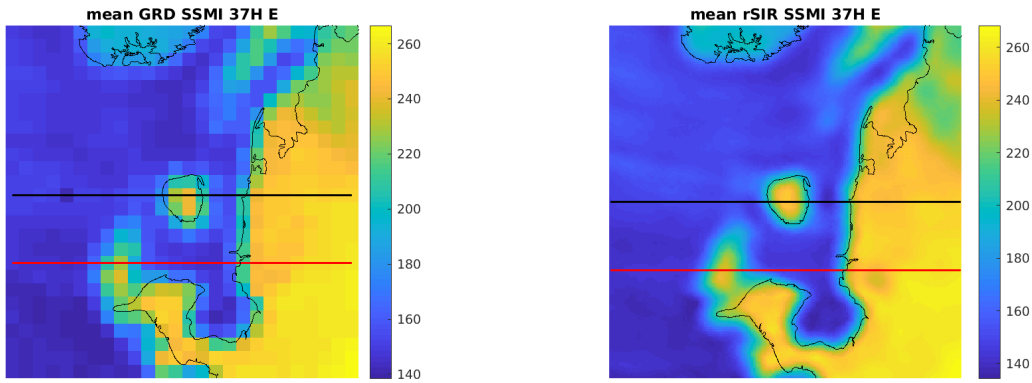


Figure 543: [Repeated] Average of daily  $T_B$  images over the study area. (left) 25-km GRD. (right) 3.125-km rSIR. The thick horizontal lines show the data transect locations where data is extracted from the image for analysis.

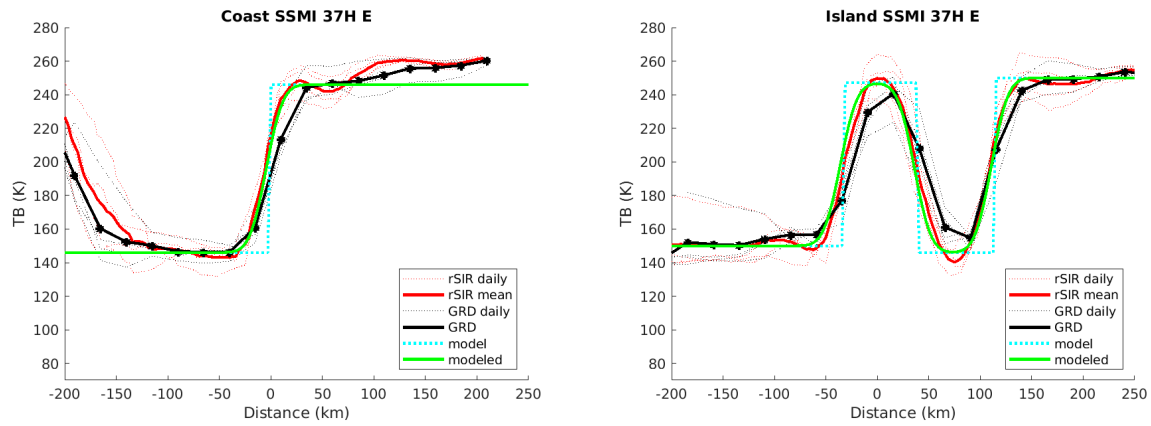


Figure 544: Plots of  $T_B$  along the two analysis case transect lines for the (left) coast-crossing and (right) island-crossing cases.

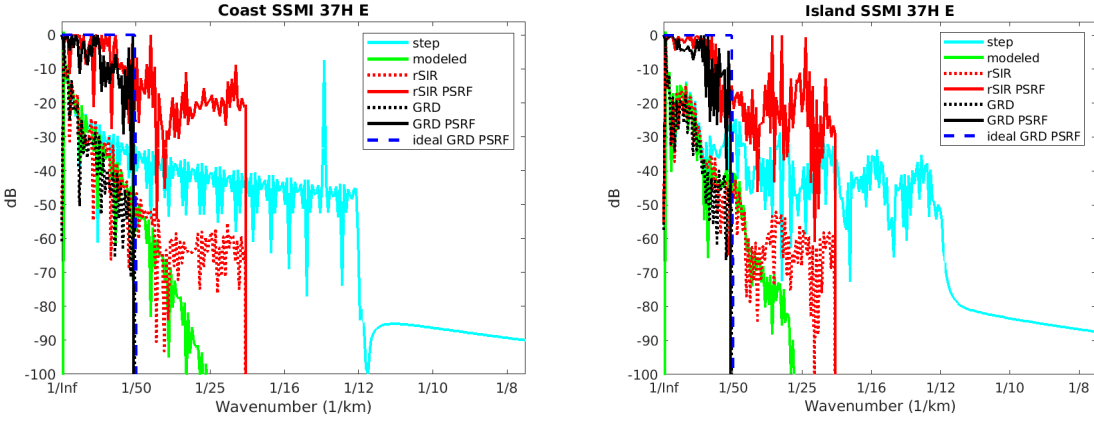


Figure 545: Wavenumber spectra of the  $T_B$  slices, the model, and the PSRF. (left) Coast-crossing case. (right) Island-crossing case.

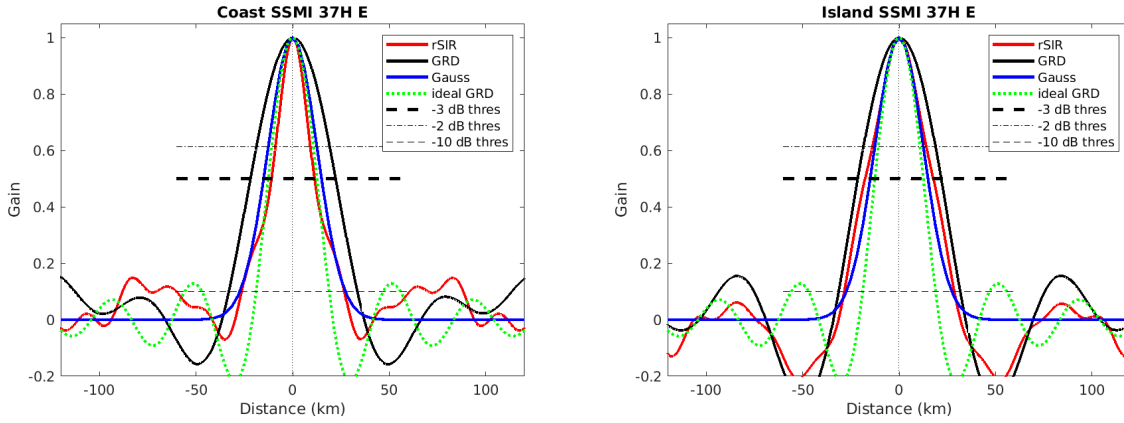


Figure 546: Derived single-pass rSIR and GRD PSRFs from the (left) coast-crossing and (right) island-crossing cases.

Table 142: Resolution estimates for SSMI channel 37H LTOD E

Algorithm	-3 dB Thres		-2 dB Thres		-10 dB Thres	
	Coast	Island	Coast	Island	Coast	Island
Gauss	30.0	30.0	24.4	24.4	54.8	54.8
rSIR	22.2	35.4	17.4	27.0	53.1	57.1
ideal GRD	36.2	36.2	30.3	30.3	54.5	54.5
GRD	44.1	43.2	37.0	36.4	66.5	63.1

## G.6 SSMI Channel 37H M Figures

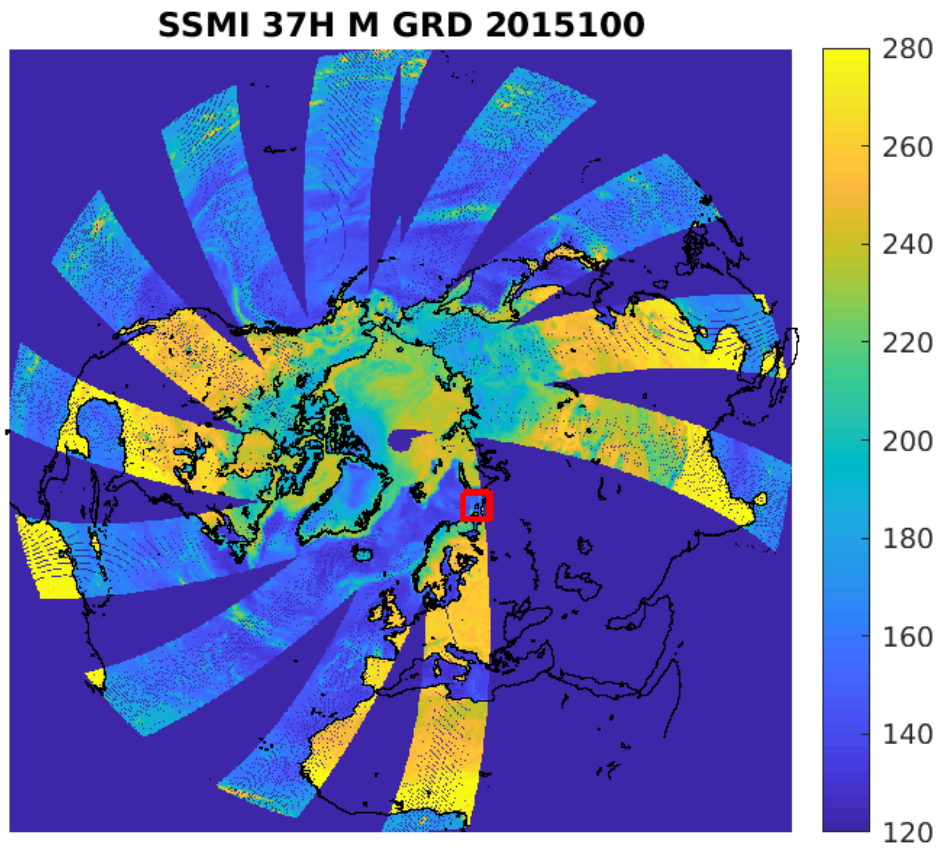


Figure 547: rSIR Northern Hemisphere view.

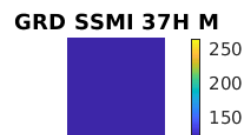
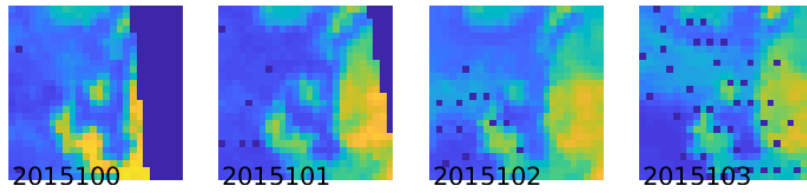
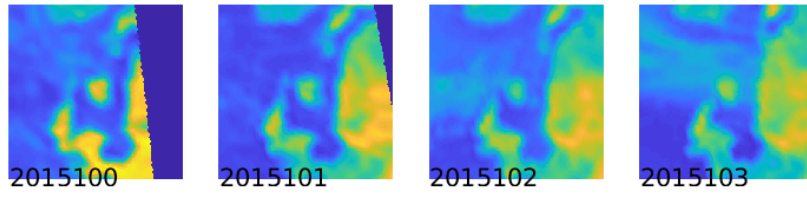


Figure 548: Time series of (top) rSIR and (bottom) GRD  $T_B$  images over the study area. Image dates are labeled on the image.

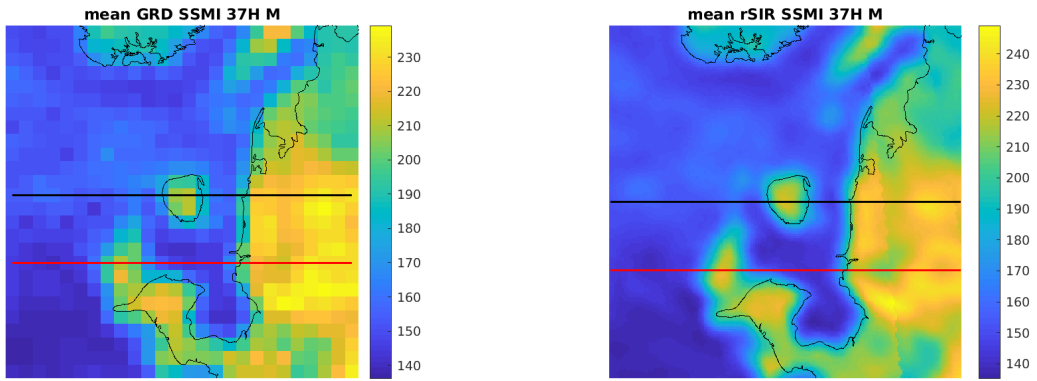


Figure 549: Average of daily  $T_B$  images over the study area. (left) 25-km GRD. (right) 3.125-km rSIR. The thick horizontal lines show the data transect locations where data is extracted from the image for analysis.

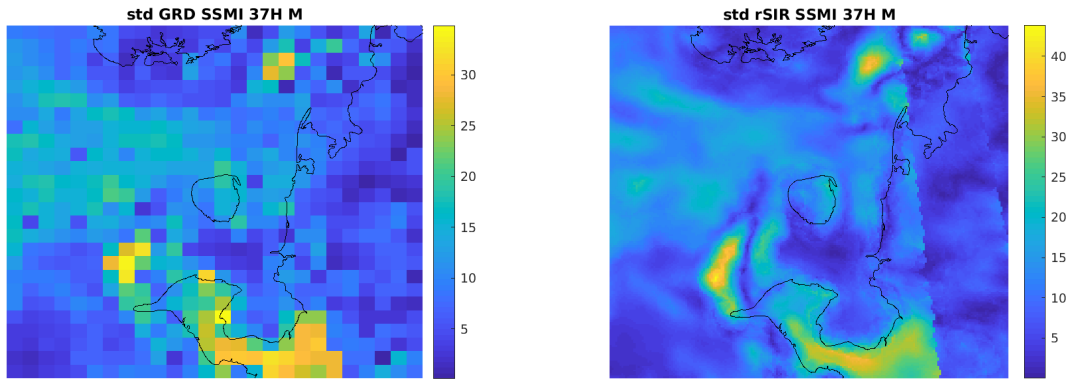


Figure 550: Standard deviation of daily  $T_B$  images over the study area. (left) 25-km GRD. (right) 3.125-km rSIR.



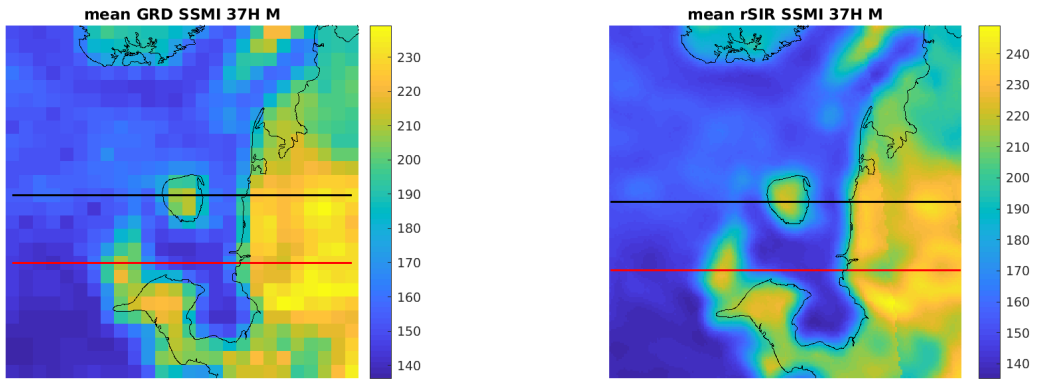


Figure 551: [Repeated] Average of daily  $T_B$  images over the study area. (left) 25-km GRD. (right) 3.125-km rSIR. The thick horizontal lines show the data transect locations where data is extracted from the image for analysis.

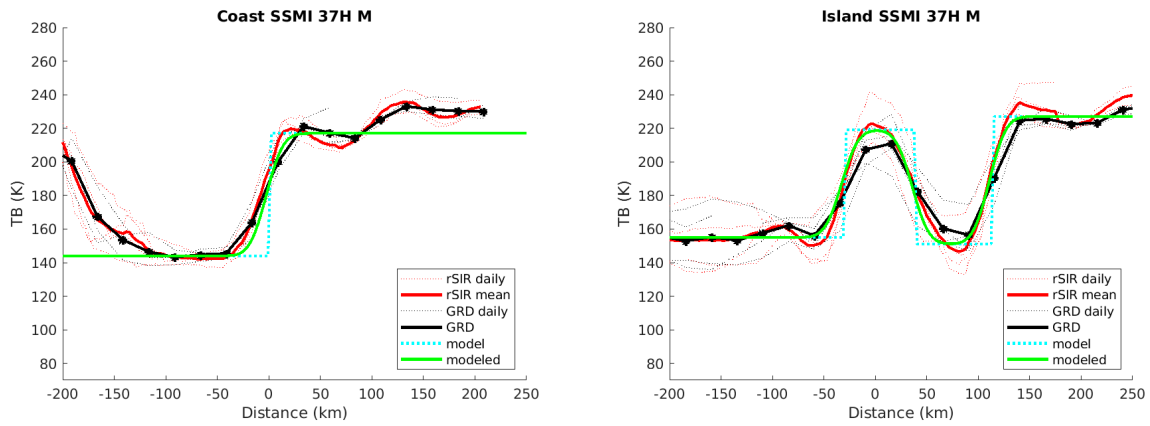


Figure 552: Plots of  $T_B$  along the two analysis case transect lines for the (left) coast-crossing and (right) island-crossing cases.

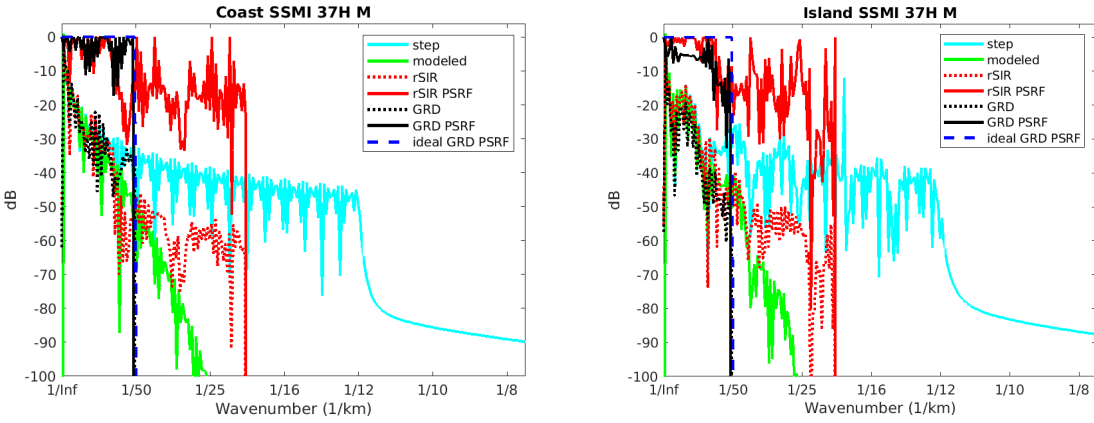


Figure 553: Wavenumber spectra of the  $T_B$  slices, the model, and the PSRF. (left) Coast-crossing case. (right) Island-crossing case.

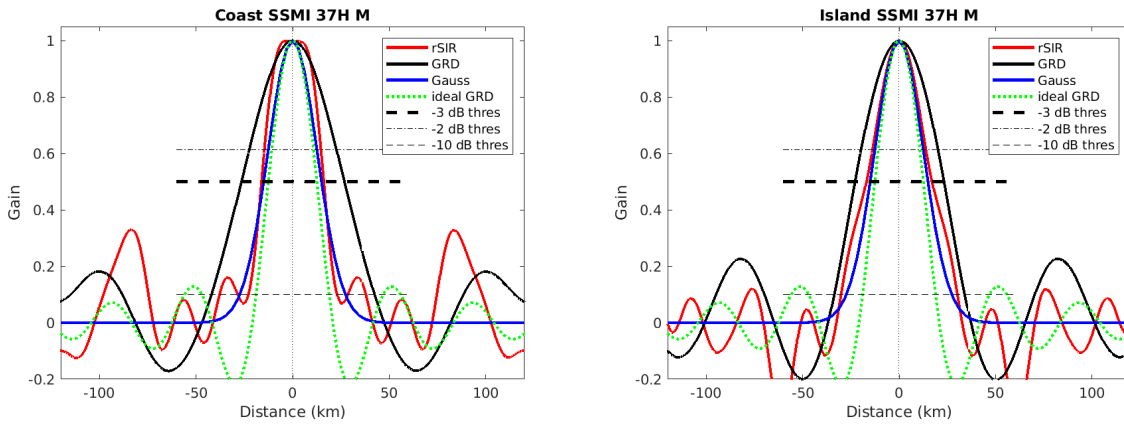


Figure 554: Derived single-pass rSIR and GRD PSRFs from the (left) coast-crossing and (right) island-crossing cases.

Table 143: Resolution estimates for SSMI channel 37H LTOD M

Algorithm	-3 dB Thres		-2 dB Thres		-10 dB Thres	
	Coast	Island	Coast	Island	Coast	Island
Gauss	30.0	30.0	24.4	24.4	54.8	54.8
rSIR	32.2	34.1	28.7	26.9	46.0	60.4
ideal GRD	36.2	36.2	30.3	30.3	54.5	54.5
GRD	53.3	46.1	43.9	38.8	84.4	67.7

## G.7 SSMI Channel 37V E Figures

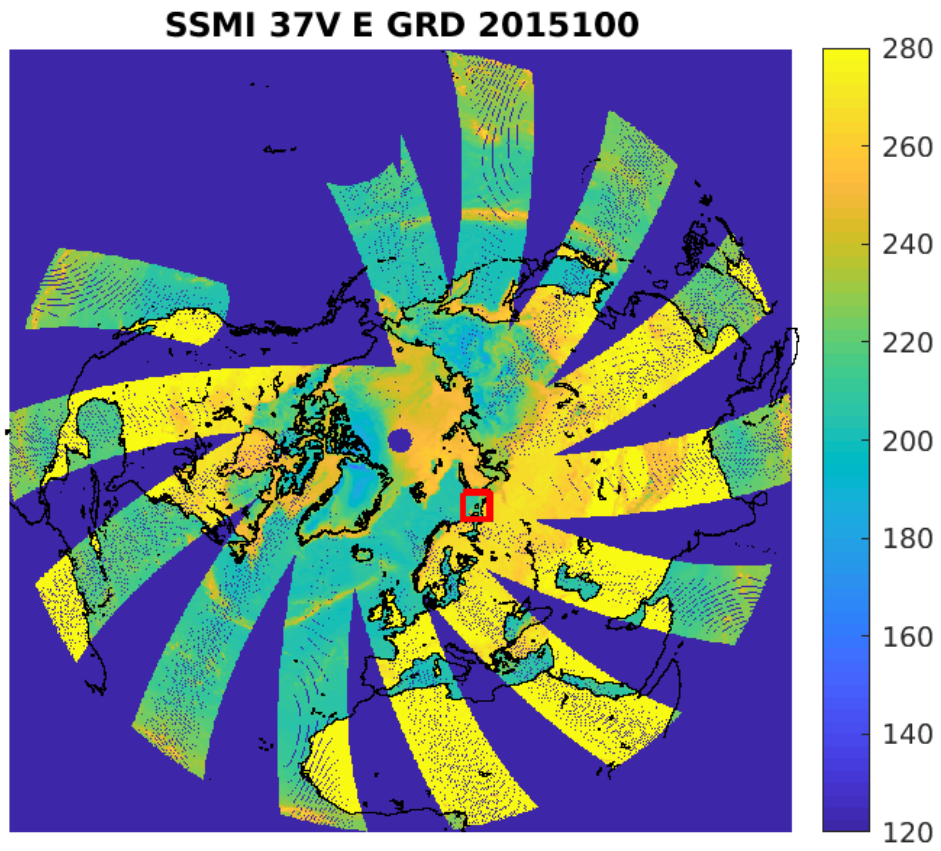


Figure 555: rSIR Northern Hemisphere view.

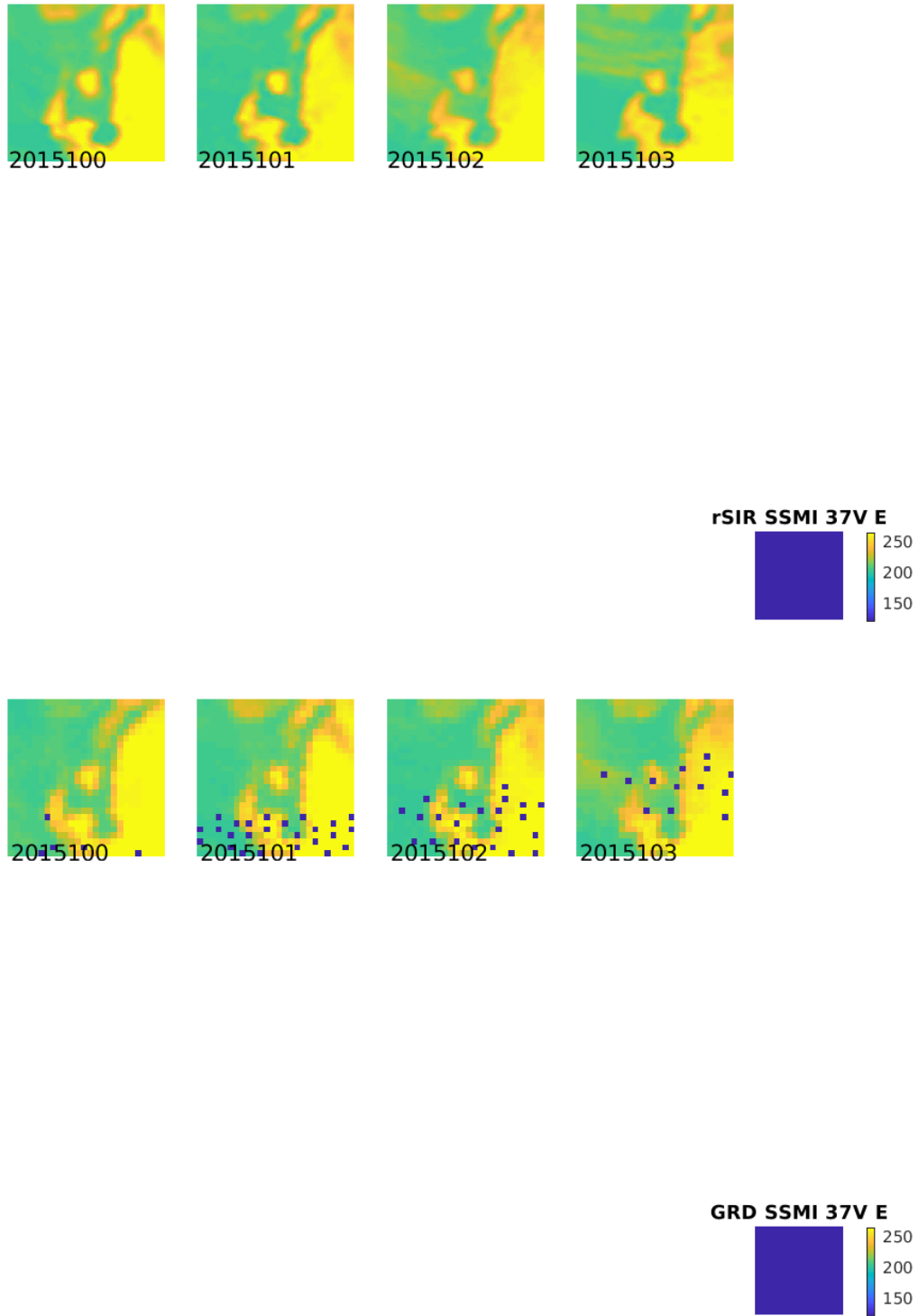


Figure 556: Time series of (top) rSIR and (bottom) GRD  $T_B$  images over the study area. Image dates are labeled on the image.

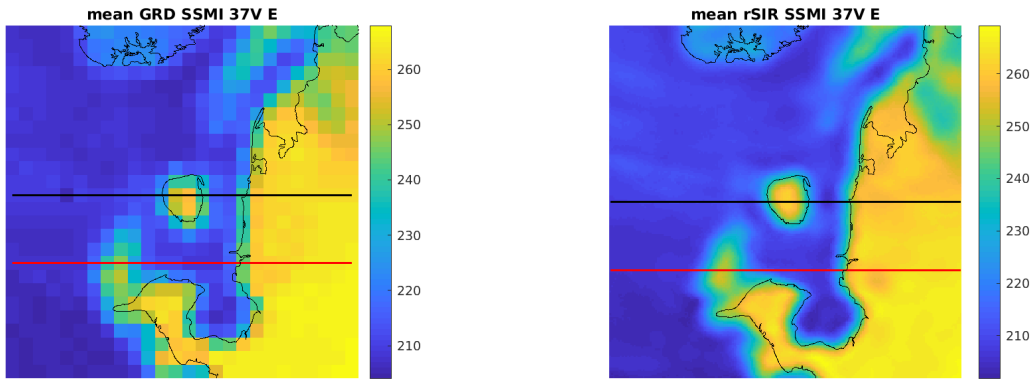


Figure 557: Average of daily  $T_B$  images over the study area. (left) 25-km GRD. (right) 3.125-km rSIR. The thick horizontal lines show the data transect locations where data is extracted from the image for analysis.

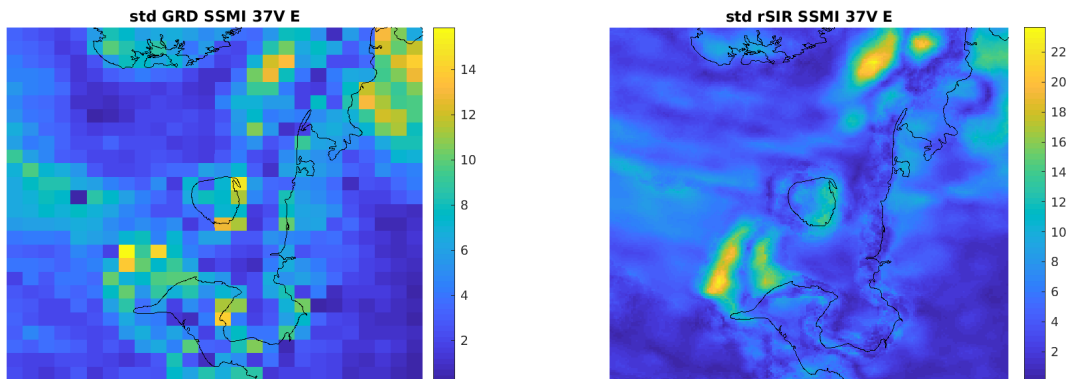


Figure 558: Standard deviation of daily  $T_B$  images over the study area. (left) 25-km GRD. (right) 3.125-km rSIR.

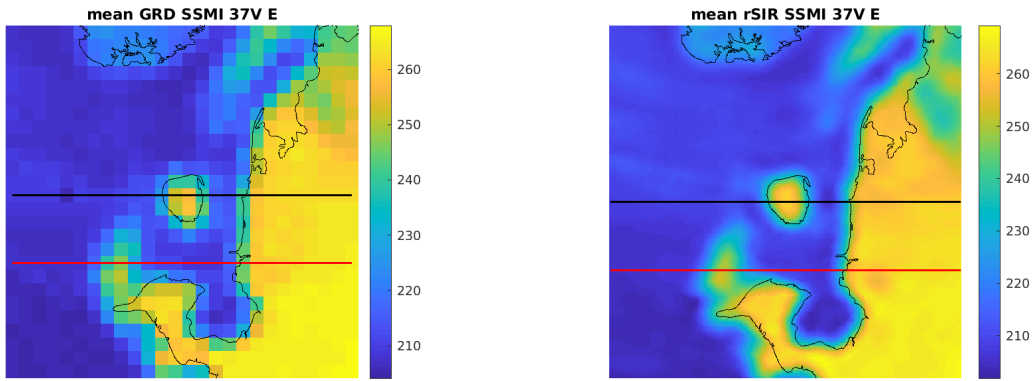


Figure 559: [Repeated] Average of daily  $T_B$  images over the study area. (left) 25-km GRD. (right) 3.125-km rSIR. The thick horizontal lines show the data transect locations where data is extracted from the image for analysis.

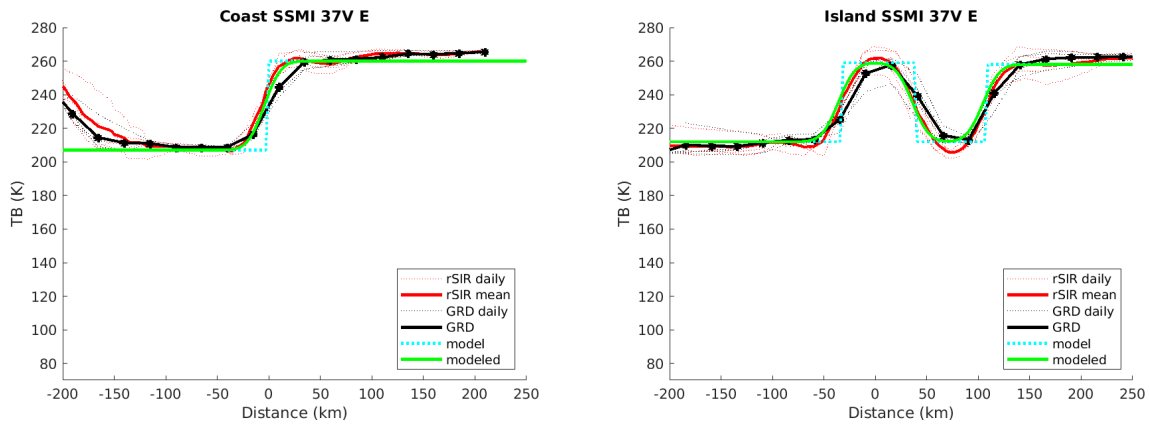


Figure 560: Plots of  $T_B$  along the two analysis case transect lines for the (left) coast-crossing and (right) island-crossing cases.

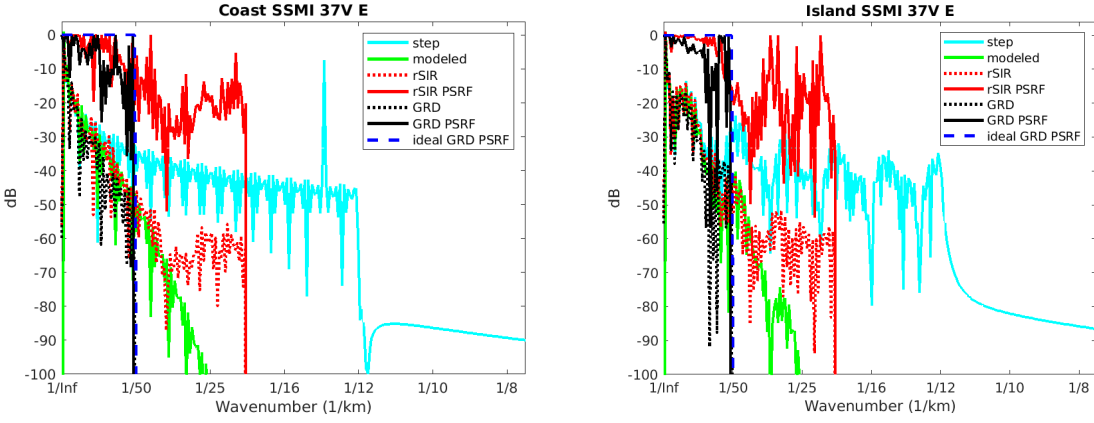


Figure 561: Wavenumber spectra of the  $T_B$  slices, the model, and the PSRF. (left) Coast-crossing case. (right) Island-crossing case.

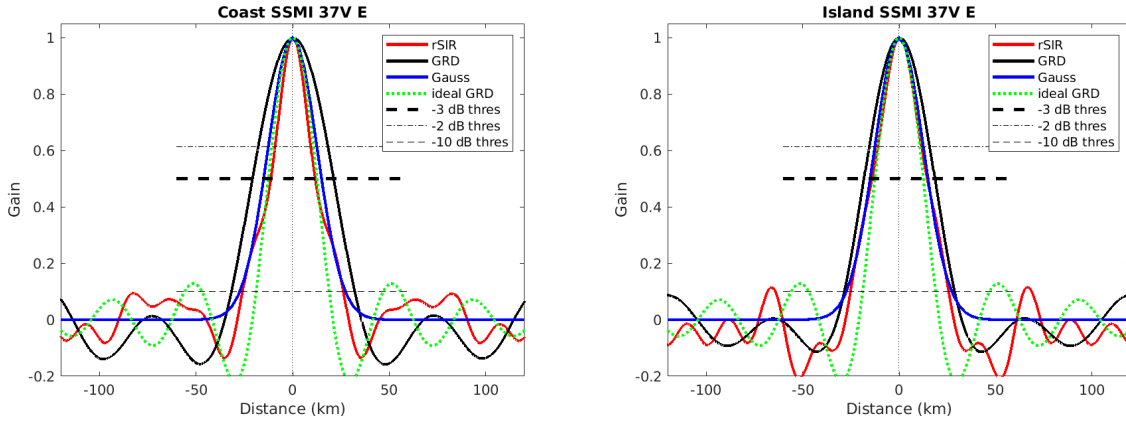


Figure 562: Derived single-pass rSIR and GRD PSRFs from the (left) coast-crossing and (right) island-crossing cases.

Table 144: Resolution estimates for SSMI channel 37V LTOD E

Algorithm	-3 dB Thres		-2 dB Thres		-10 dB Thres	
	Coast	Island	Coast	Island	Coast	Island
Gauss	30.0	30.0	24.4	24.4	54.8	54.8
rSIR	22.8	28.7	17.8	21.9	52.2	50.8
ideal GRD	36.2	36.2	30.3	30.3	54.5	54.5
GRD	42.1	36.7	35.2	30.5	63.8	57.2

## G.8 SSMI Channel 37V M Figures

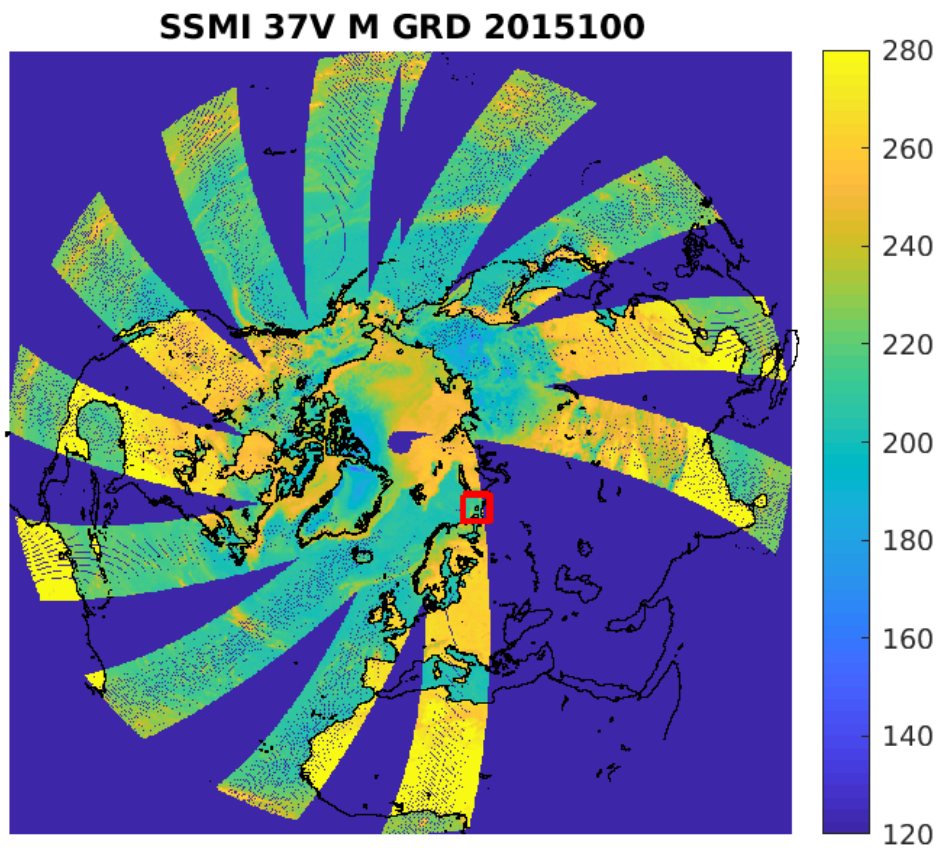


Figure 563: rSIR Northern Hemisphere view.



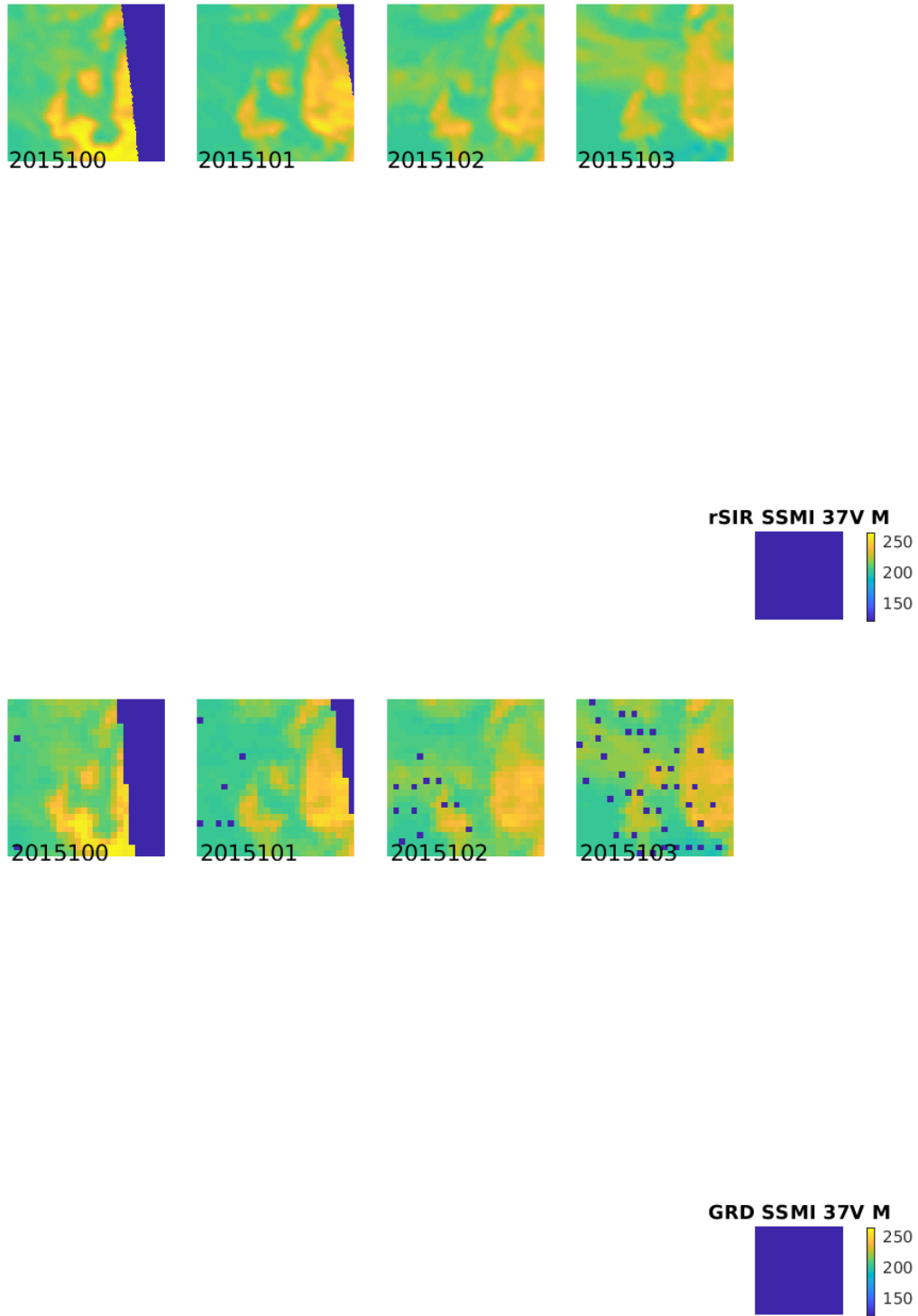


Figure 564: Time series of (top) rSIR and (bottom) GRD  $T_B$  images over the study area. Image dates are labeled on the image.

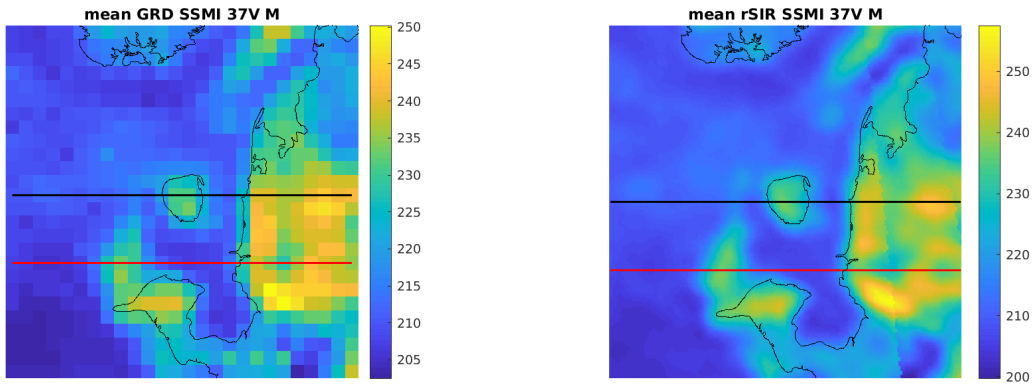


Figure 565: Average of daily  $T_B$  images over the study area. (left) 25-km GRD. (right) 3.125-km rSIR. The thick horizontal lines show the data transect locations where data is extracted from the image for analysis.

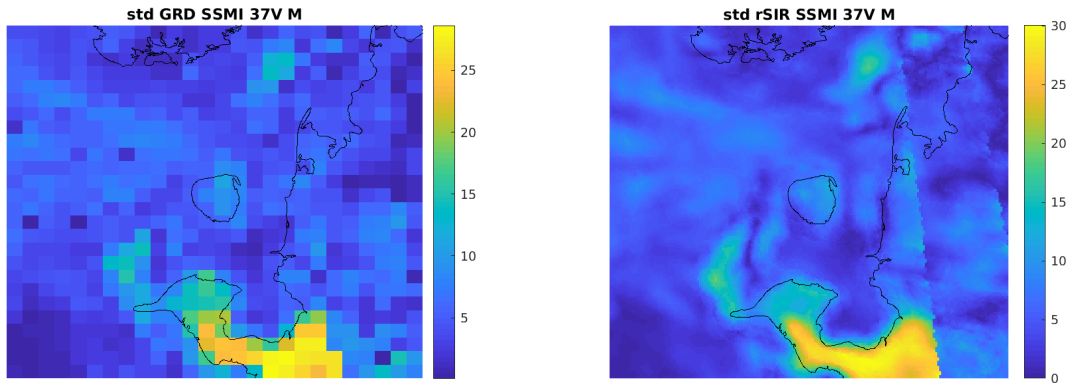


Figure 566: Standard deviation of daily  $T_B$  images over the study area. (left) 25-km GRD. (right) 3.125-km rSIR.

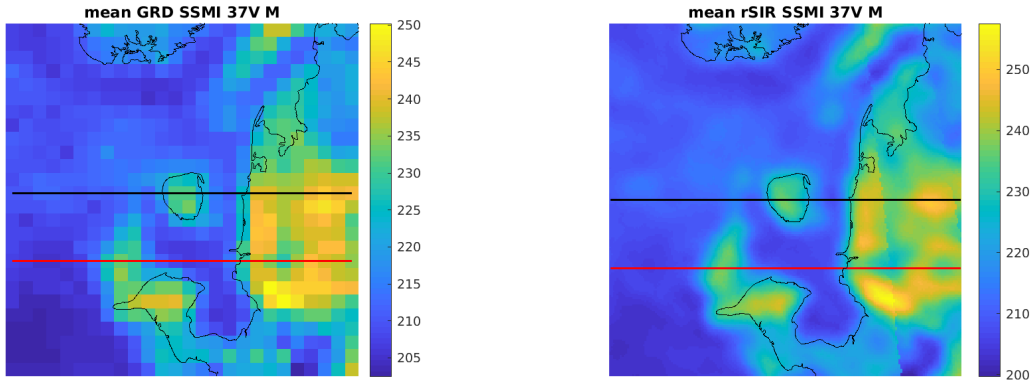


Figure 567: [Repeated] Average of daily  $T_B$  images over the study area. (left) 25-km GRD. (right) 3.125-km rSIR. The thick horizontal lines show the data transect locations where data is extracted from the image for analysis.

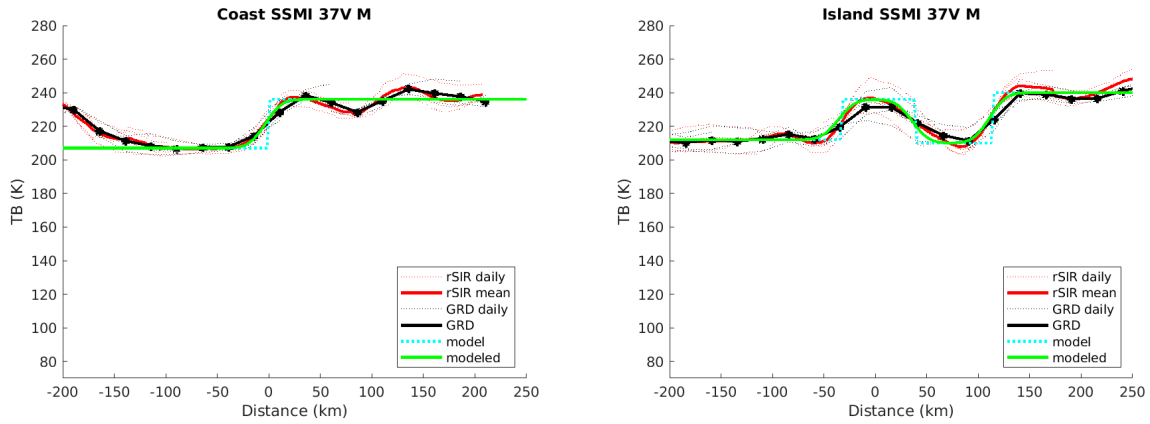


Figure 568: Plots of  $T_B$  along the two analysis case transect lines for the (left) coast-crossing and (right) island-crossing cases.

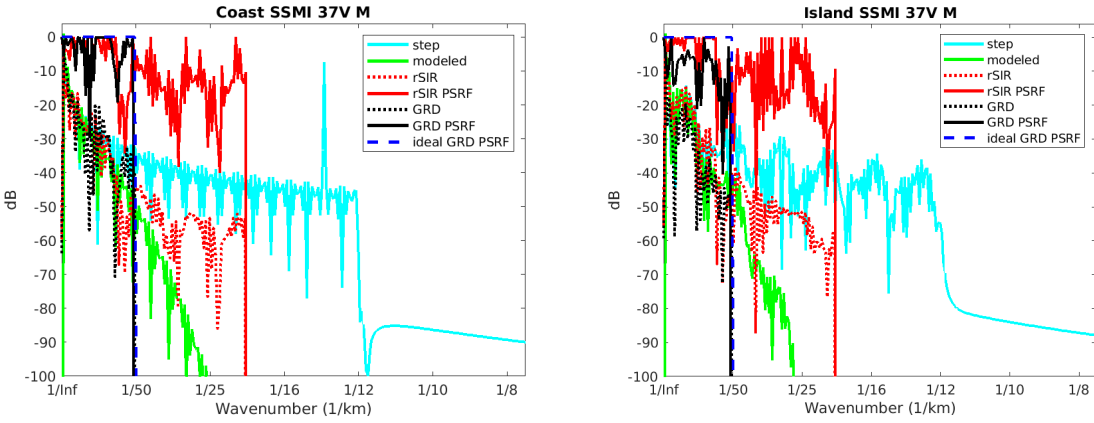


Figure 569: Wavenumber spectra of the  $T_B$  slices, the model, and the PSRF. (left) Coast-crossing case. (right) Island-crossing case.

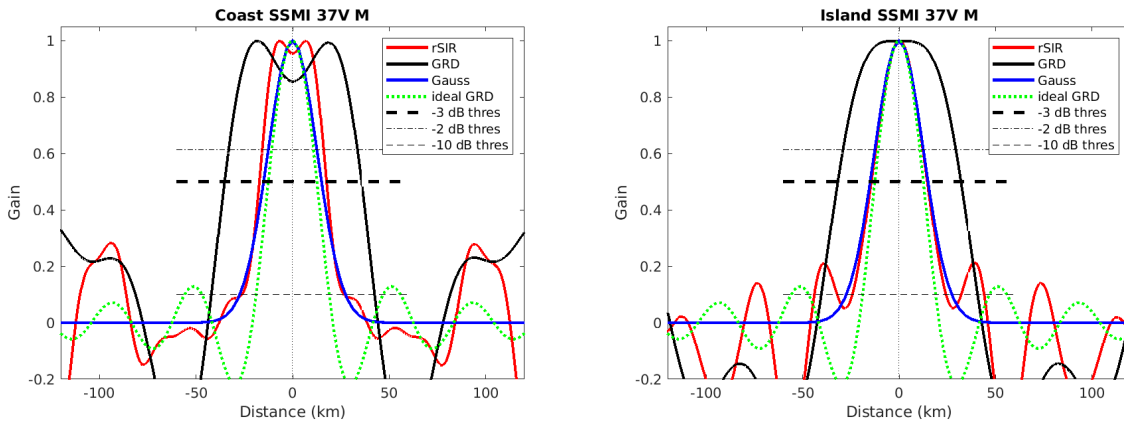


Figure 570: Derived single-pass rSIR and GRD PSRFs from the (left) coast-crossing and (right) island-crossing cases.

Table 145: Resolution estimates for SSMI channel 37V LTOD M

Algorithm	-3 dB Thres		-2 dB Thres		-10 dB Thres	
	Coast	Island	Coast	Island	Coast	Island
Gauss	30.0	30.0	24.4	24.4	54.8	54.8
rSIR	34.8	29.1	31.3	23.8	52.8	48.5
ideal GRD	36.2	36.2	30.3	30.3	54.5	54.5
GRD	70.9	63.9	65.9	57.7	84.4	80.9

## G.9 SSMI Channel 85H E Figures

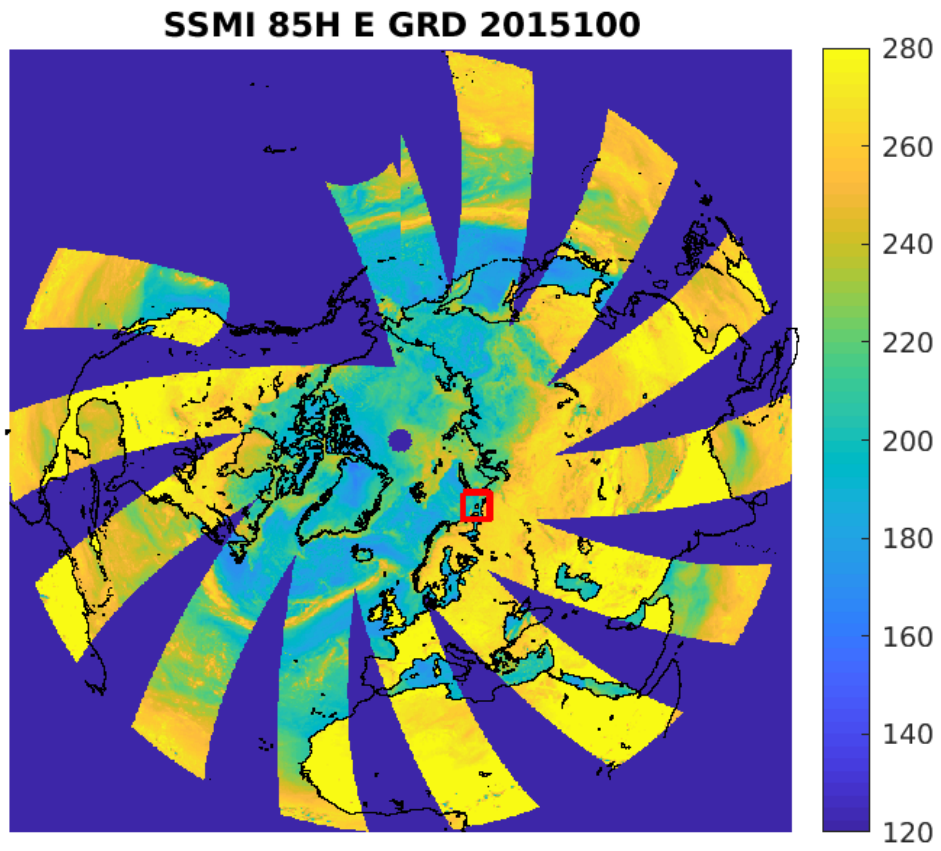


Figure 571: rSIR Northern Hemisphere view.

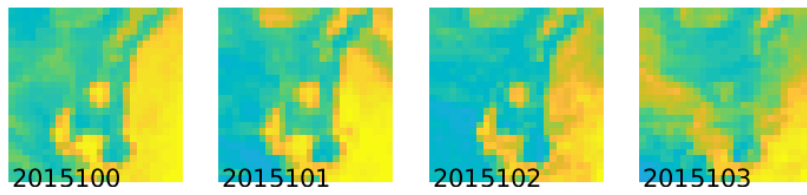
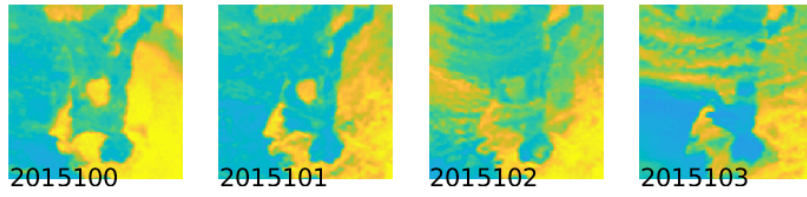


Figure 572: Time series of (top) rSIR and (bottom) GRD  $T_B$  images over the study area. Image dates are labeled on the image.

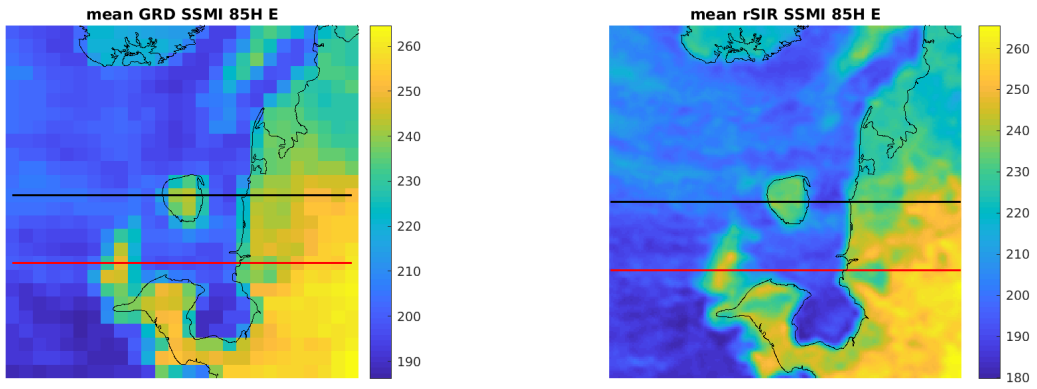


Figure 573: Average of daily  $T_B$  images over the study area. (left) 25-km GRD. (right) 3.125-km rSIR. The thick horizontal lines show the data transect locations where data is extracted from the image for analysis.

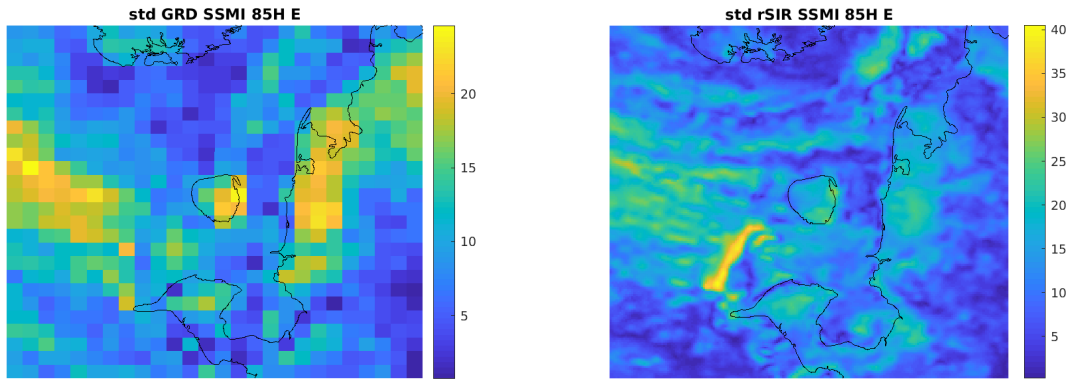


Figure 574: Standard deviation of daily  $T_B$  images over the study area. (left) 25-km GRD. (right) 3.125-km rSIR.

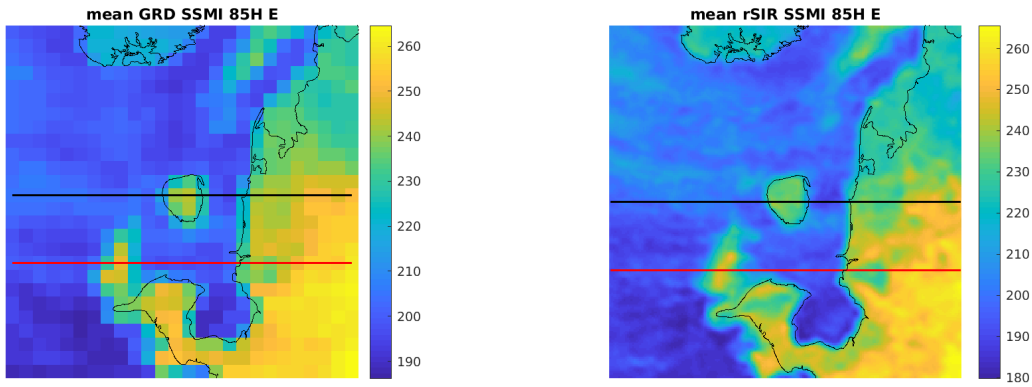


Figure 575: [Repeated] Average of daily  $T_B$  images over the study area. (left) 25-km GRD. (right) 3.125-km rSIR. The thick horizontal lines show the data transect locations where data is extracted from the image for analysis.

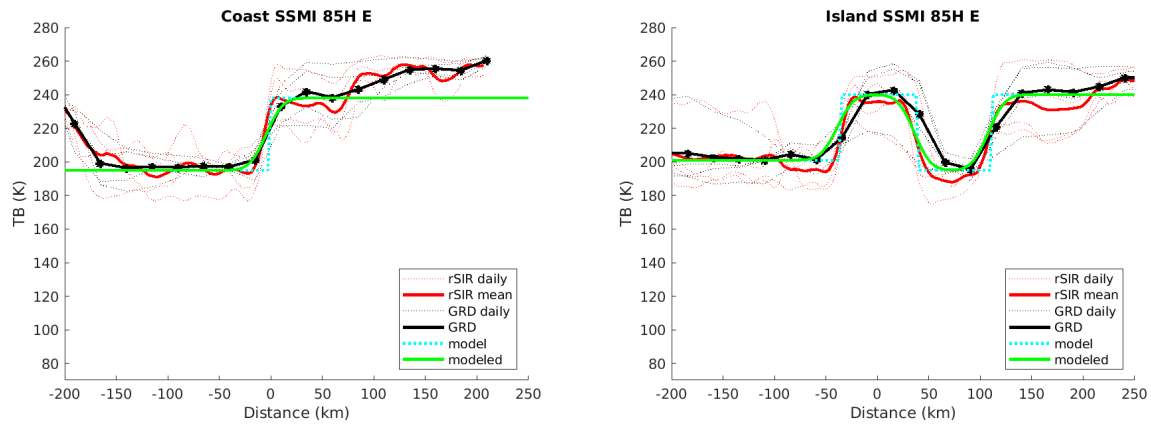


Figure 576: Plots of  $T_B$  along the two analysis case transect lines for the (left) coast-crossing and (right) island-crossing cases.



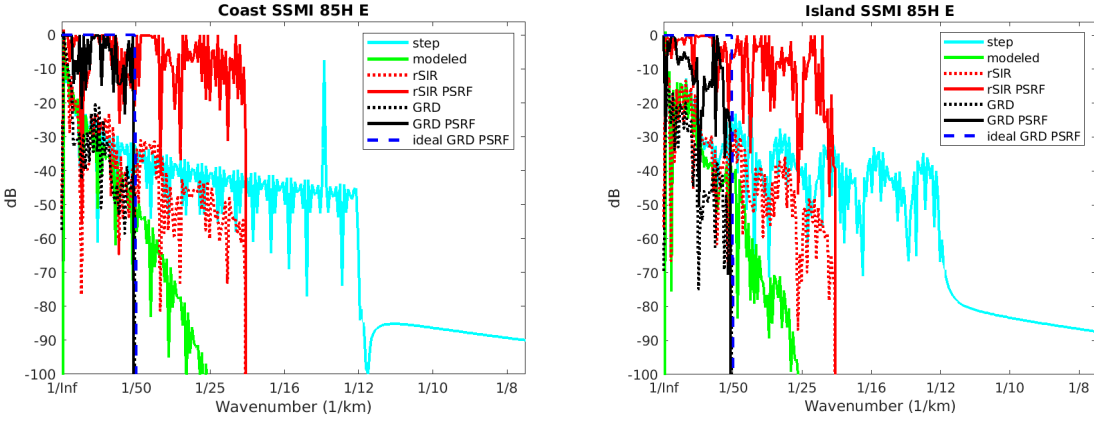


Figure 577: Wavenumber spectra of the  $T_B$  slices, the model, and the PSRF. (left) Coast-crossing case. (right) Island-crossing case.

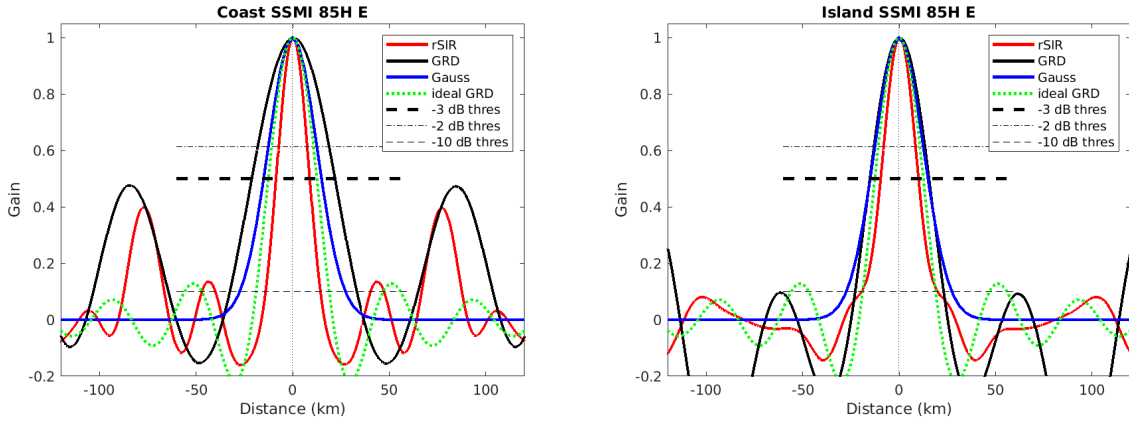


Figure 578: Derived single-pass rSIR and GRD PSRFs from the (left) coast-crossing and (right) island-crossing cases.

Table 146: Resolution estimates for SSMI channel 85H LTOD E

Algorithm	-3 dB Thres		-2 dB Thres		-10 dB Thres	
	Coast	Island	Coast	Island	Coast	Island
Gauss	30.0	30.0	24.4	24.4	54.8	54.8
rSIR	17.5	19.6	14.4	16.0	28.3	39.3
ideal GRD	36.2	36.2	30.3	30.3	54.5	54.5
GRD	43.1	30.8	36.0	25.8	65.7	45.8

## G.10 SSMI Channel 85H M Figures

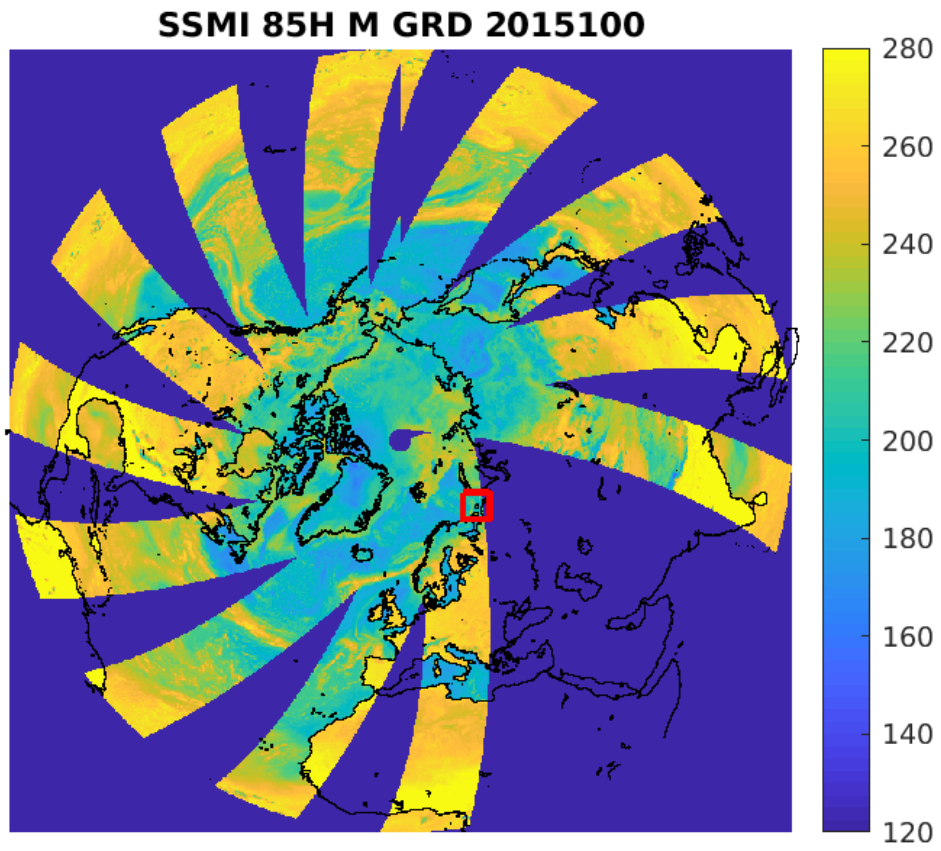


Figure 579: rSIR Northern Hemisphere view.

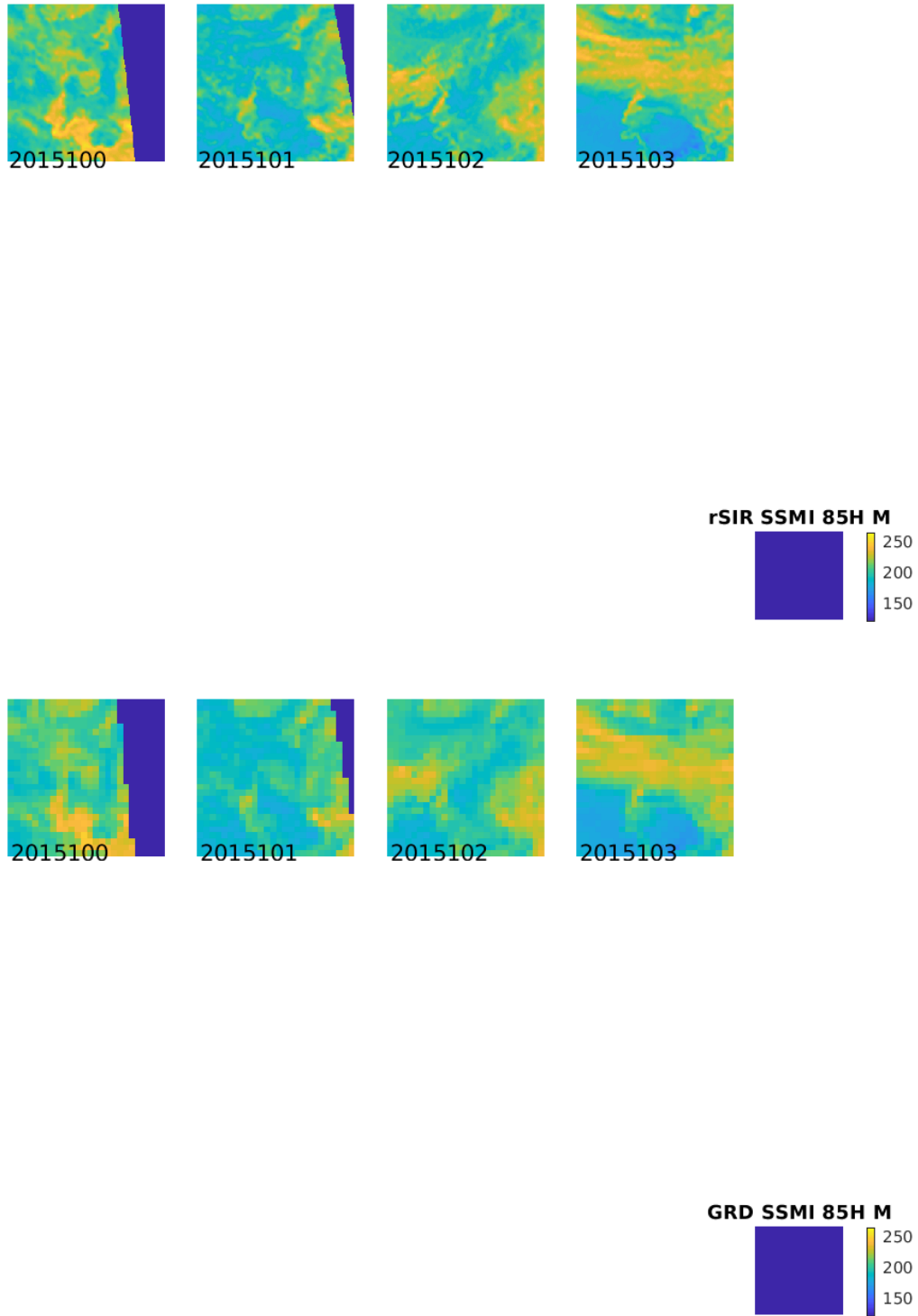


Figure 580: Time series of (top) rSIR and (bottom) GRD  $T_B$  images over the study area. Image dates are labeled on the image.

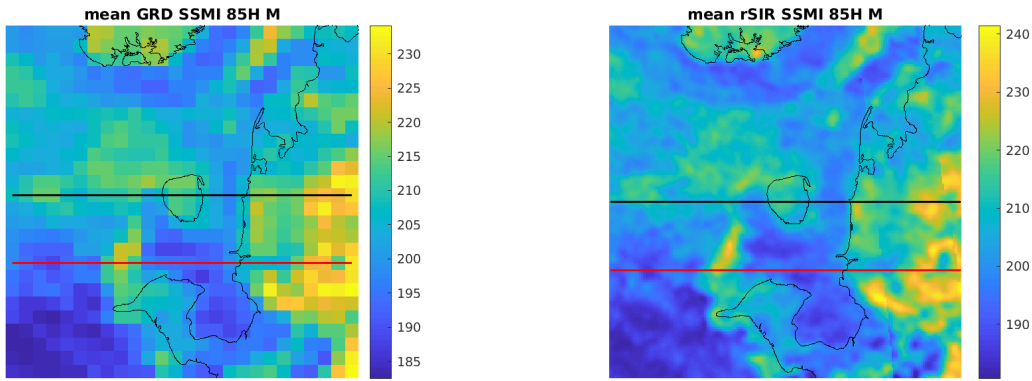


Figure 581: Average of daily  $T_B$  images over the study area. (left) 25-km GRD. (right) 3.125-km rSIR. The thick horizontal lines show the data transect locations where data is extracted from the image for analysis.

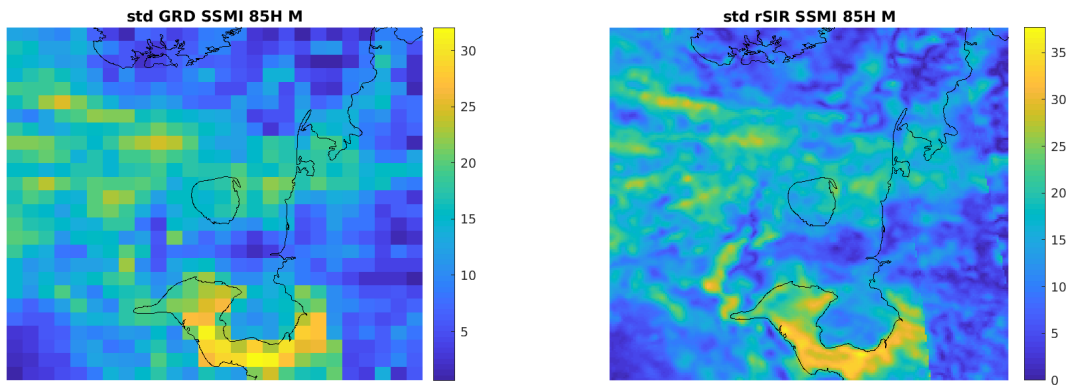


Figure 582: Standard deviation of daily  $T_B$  images over the study area. (left) 25-km GRD. (right) 3.125-km rSIR.

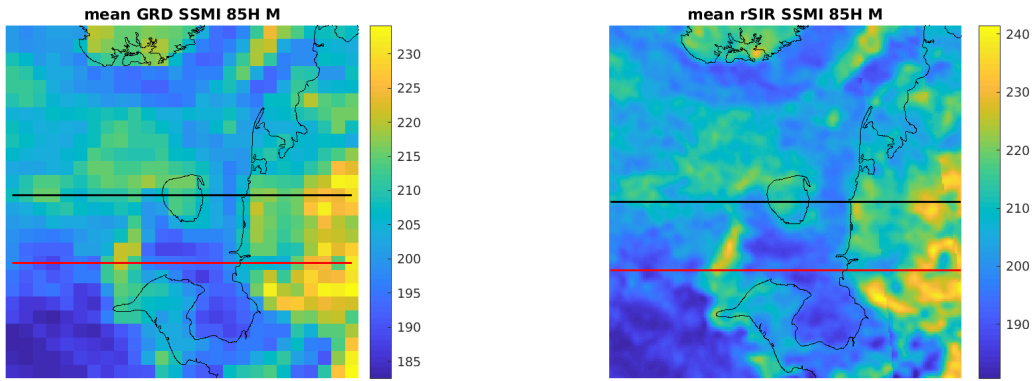


Figure 583: [Repeated] Average of daily  $T_B$  images over the study area. (left) 25-km GRD. (right) 3.125-km rSIR. The thick horizontal lines show the data transect locations where data is extracted from the image for analysis.

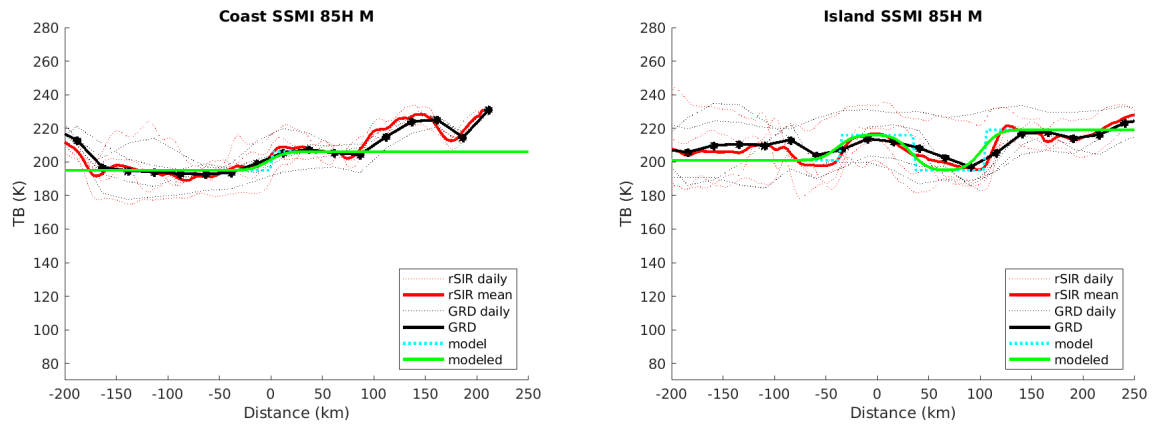


Figure 584: Plots of  $T_B$  along the two analysis case transect lines for the (left) coast-crossing and (right) island-crossing cases.

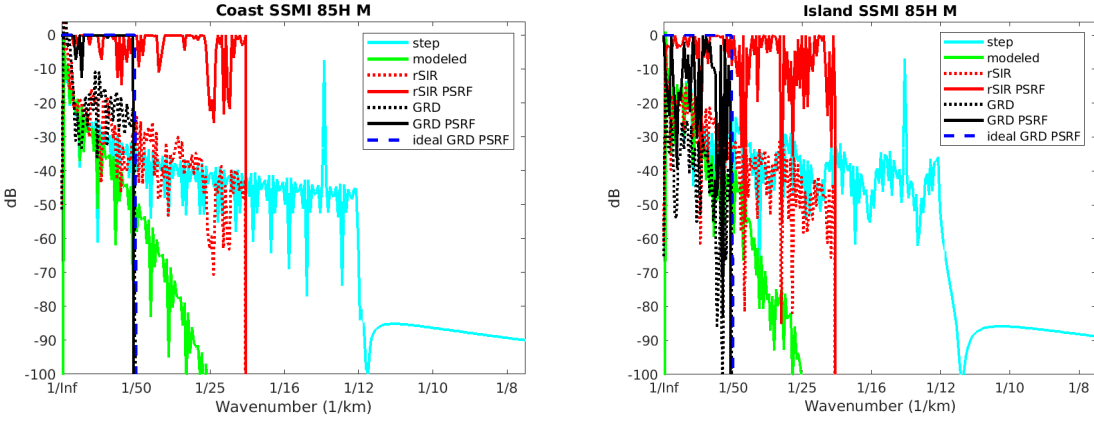


Figure 585: Wavenumber spectra of the  $T_B$  slices, the model, and the PSRF. (left) Coast-crossing case. (right) Island-crossing case.

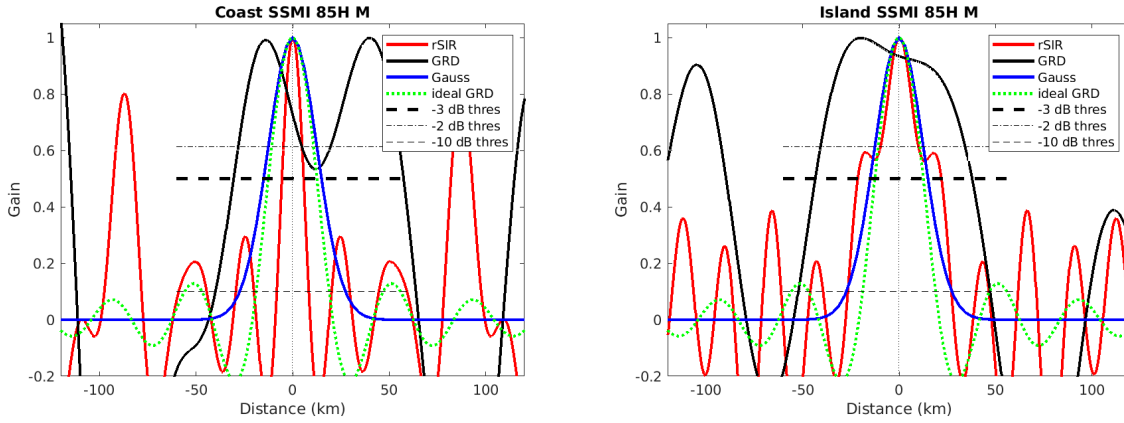


Figure 586: Derived single-pass rSIR and GRD PSRFs from the (left) coast-crossing and (right) island-crossing cases.

Table 147: Resolution estimates for SSMI channel 85H LTOD M

Algorithm	-3 dB Thres		-2 dB Thres		-10 dB Thres	
	Coast	Island	Coast	Island	Coast	Island
Gauss	30.0	30.0	24.4	24.4	54.8	54.8
rSIR	11.2	43.3	9.4	18.7	16.5	53.7
ideal GRD	36.2	36.2	30.3	30.3	54.5	54.5
GRD	24.8	26.4	20.9	22.2	35.9	37.9

## G.11 SSMI Channel 85V E Figures

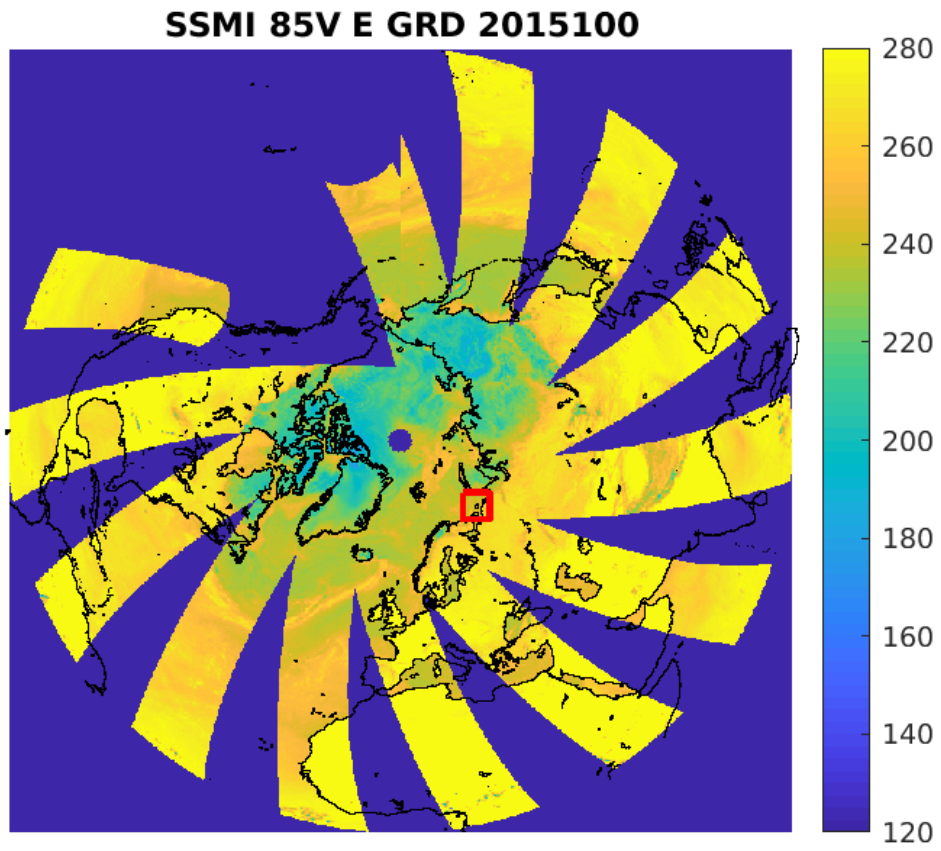


Figure 587: rSIR Northern Hemisphere view.

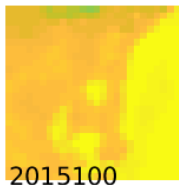
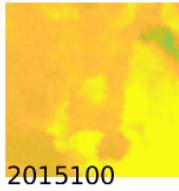


Figure 588: Time series of (top) rSIR and (bottom) GRD  $T_B$  images over the study area. Image dates are labeled on the image.



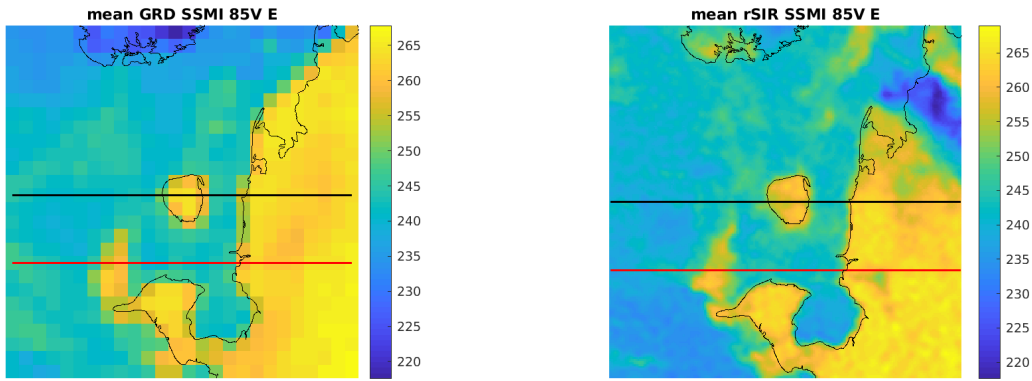


Figure 589: Average of daily  $T_B$  images over the study area. (left) 25-km GRD. (right) 3.125-km rSIR. The thick horizontal lines show the data transect locations where data is extracted from the image for analysis.

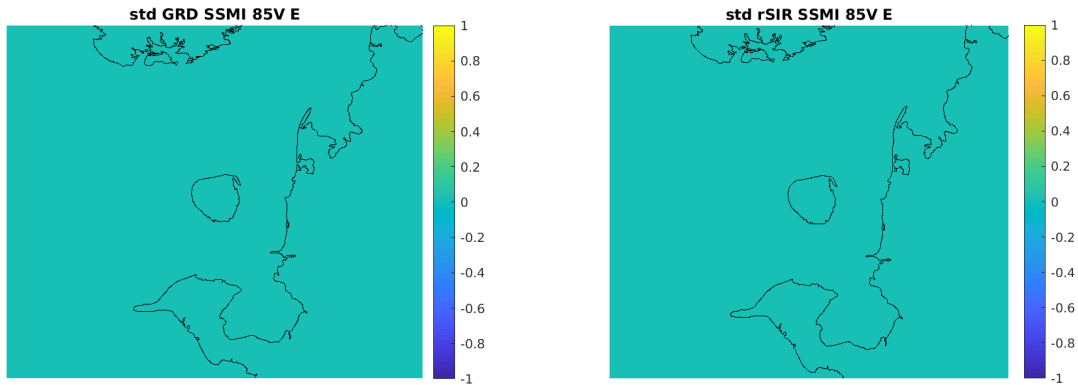


Figure 590: Standard deviation of daily  $T_B$  images over the study area. (left) 25-km GRD. (right) 3.125-km rSIR.

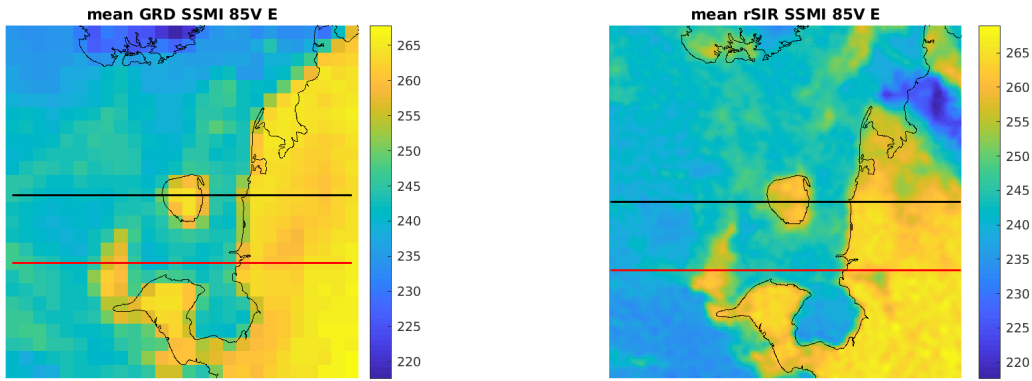


Figure 591: [Repeated] Average of daily  $T_B$  images over the study area. (left) 25-km GRD. (right) 3.125-km rSIR. The thick horizontal lines show the data transect locations where data is extracted from the image for analysis.

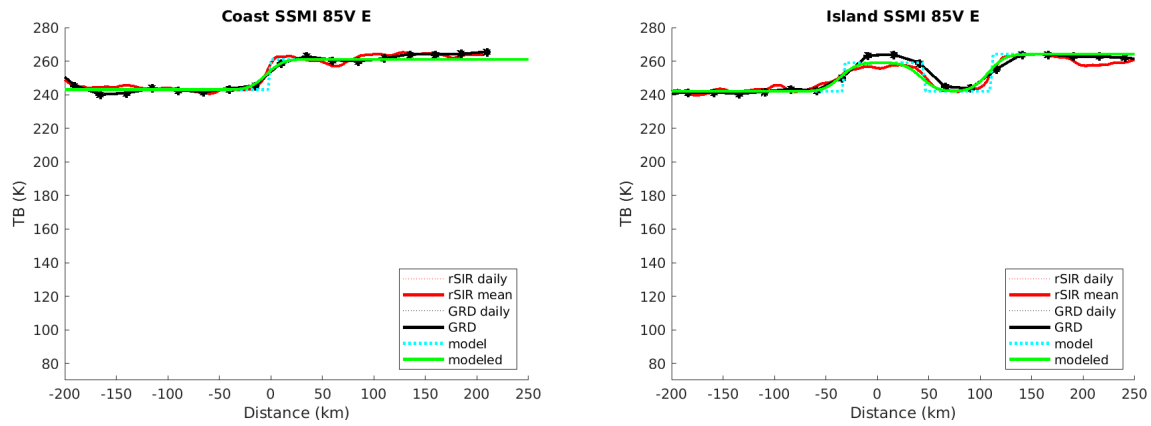


Figure 592: Plots of  $T_B$  along the two analysis case transect lines for the (left) coast-crossing and (right) island-crossing cases.

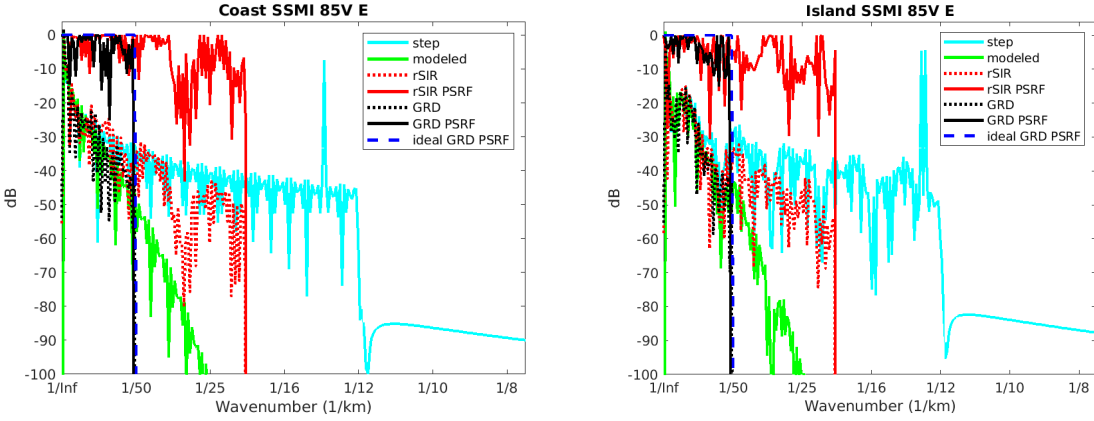


Figure 593: Wavenumber spectra of the  $T_B$  slices, the model, and the PSRF. (left) Coast-crossing case. (right) Island-crossing case.

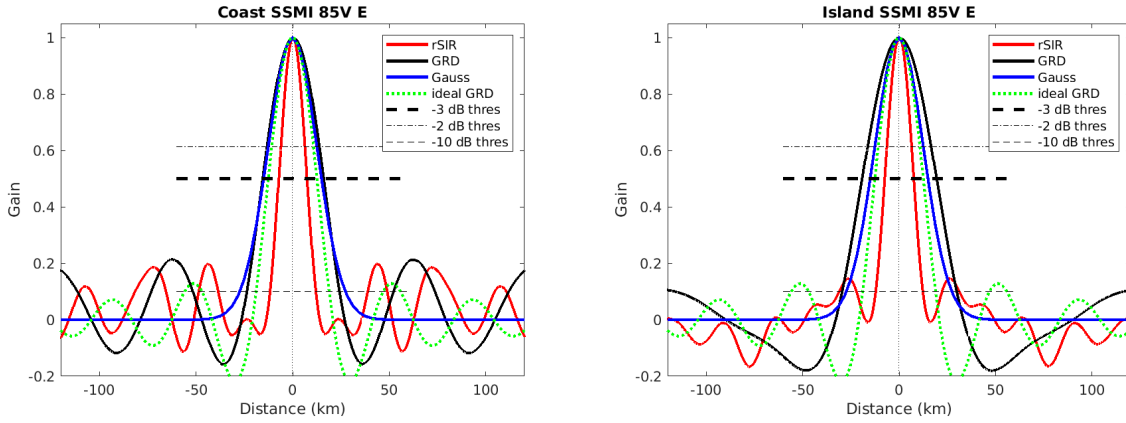


Figure 594: Derived single-pass rSIR and GRD PSRFs from the (left) coast-crossing and (right) island-crossing cases.

Table 148: Resolution estimates for SSMI channel 85V LTOD E

Algorithm	-3 dB Thres		-2 dB Thres		-10 dB Thres	
	Coast	Island	Coast	Island	Coast	Island
Gauss	30.0	30.0	24.4	24.4	54.8	54.8
rSIR	14.7	15.0	12.2	12.4	23.6	24.5
ideal GRD	36.2	36.2	30.3	30.3	54.5	54.5
GRD	31.5	38.6	26.3	32.1	48.0	59.5

## G.12 SSMI Channel 85V M Figures

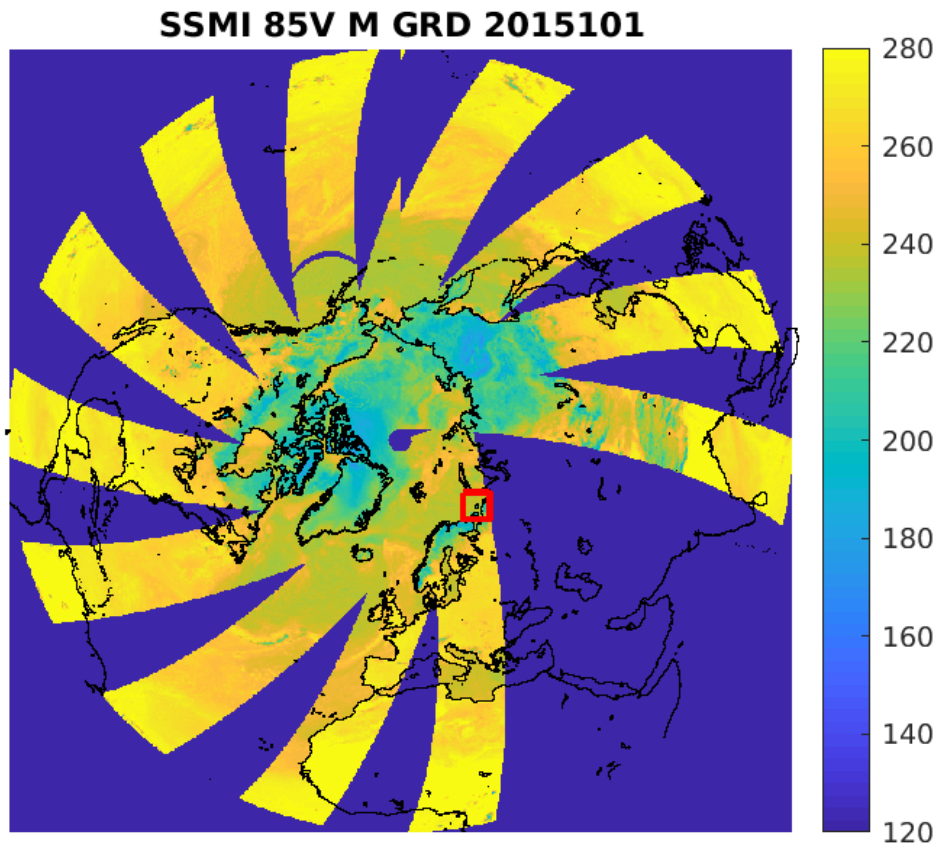


Figure 595: rSIR Northern Hemisphere view.

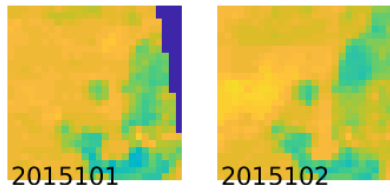
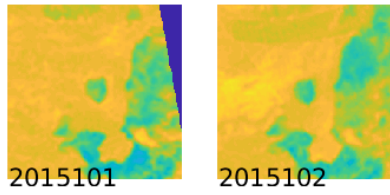


Figure 596: Time series of (top) rSIR and (bottom) GRD  $T_B$  images over the study area. Image dates are labeled on the image.

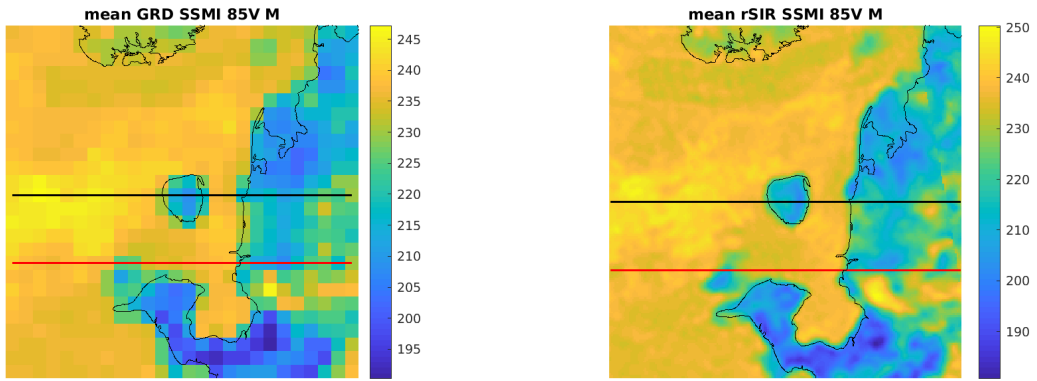


Figure 597: Average of daily  $T_B$  images over the study area. (left) 25-km GRD. (right) 3.125-km rSIR. The thick horizontal lines show the data transect locations where data is extracted from the image for analysis.

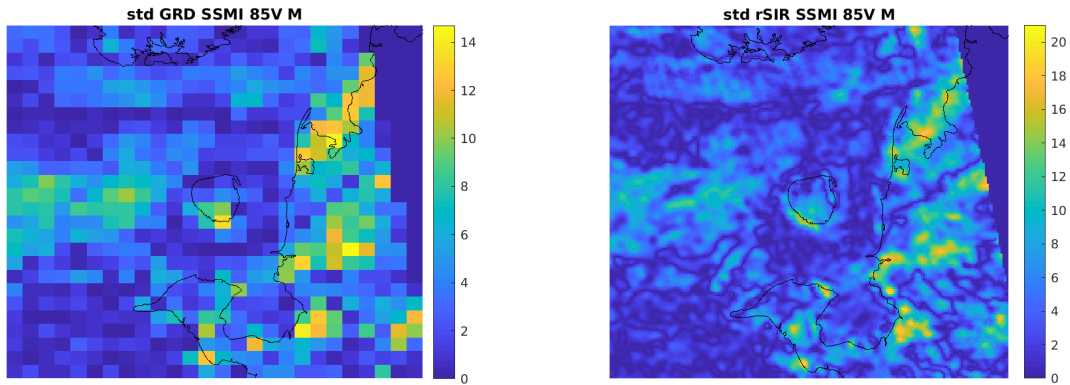


Figure 598: Standard deviation of daily  $T_B$  images over the study area. (left) 25-km GRD. (right) 3.125-km rSIR.

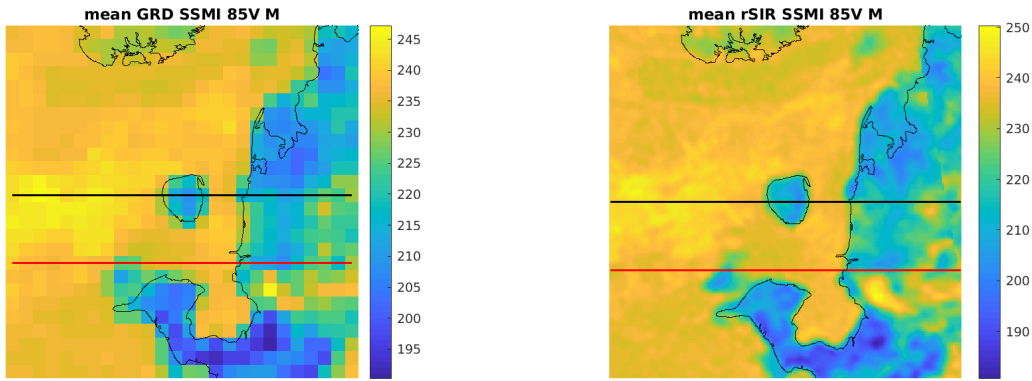


Figure 599: [Repeated] Average of daily  $T_B$  images over the study area. (left) 25-km GRD. (right) 3.125-km rSIR. The thick horizontal lines show the data transect locations where data is extracted from the image for analysis.

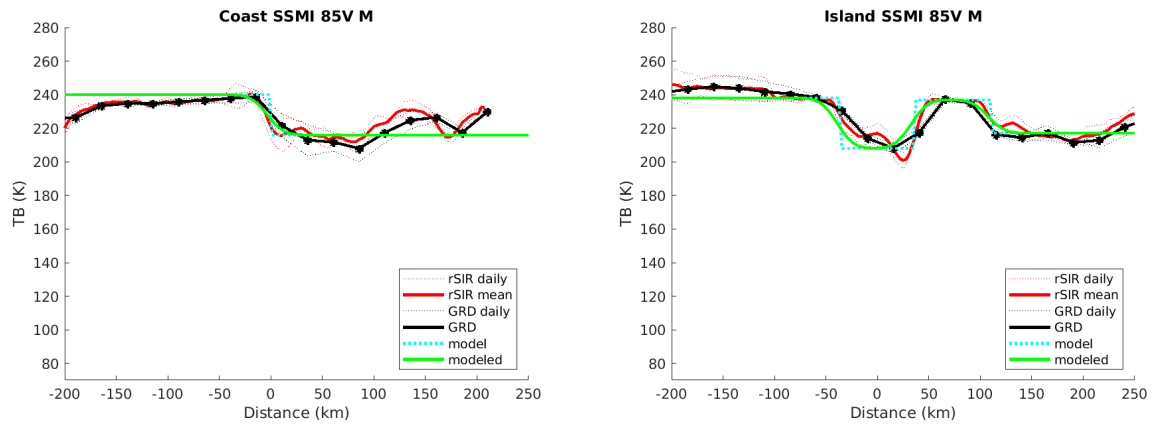


Figure 600: Plots of  $T_B$  along the two analysis case transect lines for the (left) coast-crossing and (right) island-crossing cases.

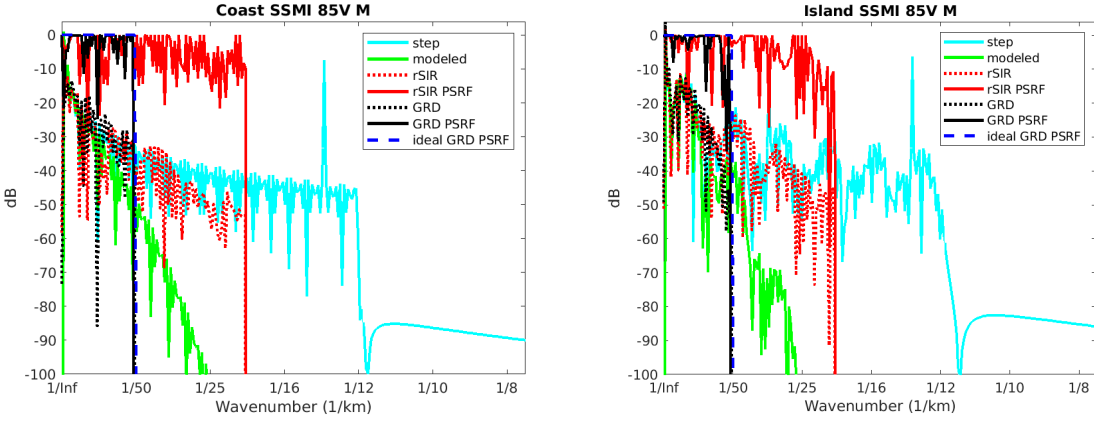


Figure 601: Wavenumber spectra of the  $T_B$  slices, the model, and the PSRF. (left) Coast-crossing case. (right) Island-crossing case.

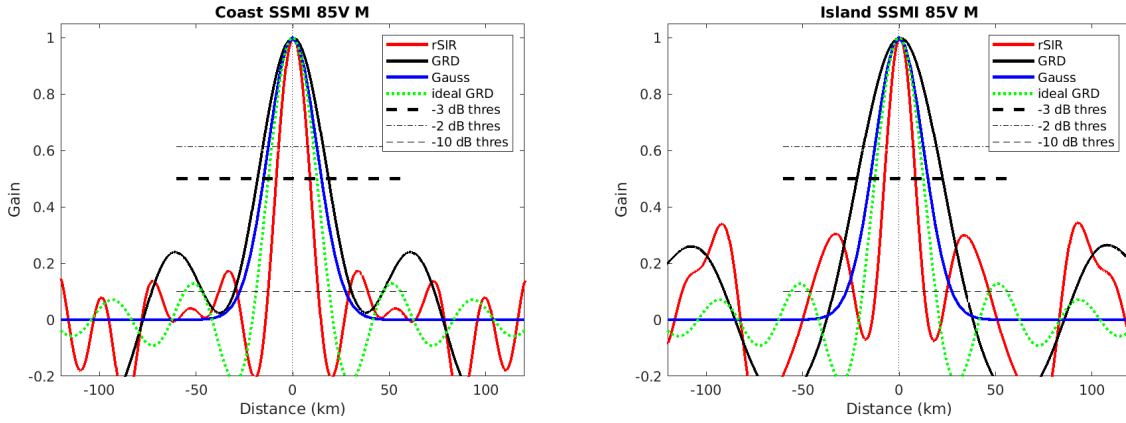


Figure 602: Derived single-pass rSIR and GRD PSRFs from the (left) coast-crossing and (right) island-crossing cases.

Table 149: Resolution estimates for SSMI channel 85V LTOD M

Algorithm	-3 dB Thres		-2 dB Thres		-10 dB Thres	
	Coast	Island	Coast	Island	Coast	Island
Gauss	30.0	30.0	24.4	24.4	54.8	54.8
rSIR	17.5	16.1	14.6	13.4	26.0	25.2
ideal GRD	36.2	36.2	30.3	30.3	54.5	54.5
GRD	36.7	44.3	30.4	36.8	60.7	68.3